This Page is Inserted by IFW Indexing and Scanning Operations and is not part of the Official Record

BEST AVAILABLE IMAGES

Defective images within this document are accurate representations of the original documents submitted by the applicant.

Defects in the images include but are not limited to the items checked:

- ☐ BLACK BORDERS
- ☐ IMAGE CUT OFF AT TOP, BOTTOM OR SIDES
- ☐ FADED TEXT OR DRAWING
- ☐ BLURRED OR ILLEGIBLE TEXT OR DRAWING
- ☐ SKEWED/SLANTED IMAGES
- ☐ COLOR OR BLACK AND WHITE PHOTOGRAPHS
- ☐ GRAY SCALE DOCUMENTS
- ☐ LINES OR MARKS ON ORIGINAL DOCUMENT
- ☐ REFERENCE(S) OR EXHIBIT(S) SUBMITTED ARE POOR QUALITY
- ☐ OTHER: _____

IMAGES ARE BEST AVAILABLE COPY.
As rescanning these documents will not correct the image problems checked, please do not report these problems to the IFW Image Problem Mailbox.

ELSEVIER

International Journal of Pharmaceutics 135 (1996) 151–160

international journal of pharmaceutics

Influence of water activity in organic solvent + water mixtures on the nature of the crystallizing drug phase. 1. Theophylline

Haijian Zhu, Ceaminia Yuen, David J.W. Grant*

Department of Pharmaceutics, College of Pharmacy, University of Minnesota, Health Science Unit F, 308 Harvard Street SE, Minneapolis, MN 55455-0343, USA

Received 6 November 1995; revised 22 January 1996; accepted 23 January 1996

Abstract

The hydration state of a hydrate depends on the water activity, a_w, in the crystallization medium. Selection of an appropriate ratio of water to cosolvent in the crystallization medium of a hydrate is critical and is often semi-empirical. This study attempts to elucidate this selection process by studying the conditions of physical stability of the solid phases of theophylline, which comprise an anhydrate and a monohydrate. A mixture of the anhydrate and the monohydrate may sometimes be obtained, if the system is not in equilibrium. The excess solid phase was characterized by powder X-ray diffractometry and the water content was measured by Karl-Fischer titrimetry. In contact with methanol + water or 2-propanol (isopropyl alcohol, IPA) + water mixtures, at $a_w < 0.25$, the anhydrate was the only solid phase at equilibrium, no matter which solid form was initially added. At $a_w > 0.25$ in either solvent mixture, the monohydrate was obtained as the most stable form at equilibrium. These results suggest (a) that water activity is the major factor determining the nature of the solid phase of theophylline which crystallizes from methanol + water or IPA + water mixtures and (b) that the system, theophylline anhydrate $\rightleftharpoons$ theophylline monohydrate, is in equilibrium at $a_w = 0.25$ and at 25°C. The solubilities of the two solid forms in each of the mixed solvent systems were also measured and are discussed. The concepts presented, tested and discussed may, in principle, be applied to any pharmaceutical system consisting of an anhydrate and a hydrate, or a lower hydrate and a higher hydrate.

Keywords: Theophylline; Anhydrate; Monohydrate; Methanol; 2-Propanol; Water activity; Crystallization; Solubility

1. Introduction

During the process of crystallization, solvent may become incorporated into the crystal structure. A hydrate forms when water is incorporated from the crystallization medium. The change in the thermodynamic activity of the drug due to hydration alters the pharmaceutically important properties, such as the solubility and the physical and chemical stability. The solubility of a drug usually influences its dissolution rate. The alter-

* Corresponding author. Tel. + 1 612 6243956; Fax. + 1 612 6250609; e-mail: grant001@maroon.tc.umn.edu

0378-5173/96/$15.00 © 1996 Elsevier Science B.V. All rights reserved
PII S0378-5173(95)04466-3

UM00012566
NOVARTIS EXHIBIT 1017
Novartis v. Regents, IPR2023-01346
Page 1312 of 4460

ation in the dissolution rate and the stability as a result of hydration may, ultimately, modify the bioavailability and product performance (Shefter and Higuchi, 1963; Haleblian, 1975; Khankari and Grant, 1995). It is, therefore, of vital importance to control the phase transformation, including the anhydrate-hydrate or lower hydrate-higher hydrate phase transition, in the development and manufacture of pharmaceutical dosage forms (De Smidt et al., 1986; Rodriguez-Hornedo et al., 1992)

The formation of hydrated crystals from anhydrous crystals (Shefter and Higuchi, 1963; Grant and Higuchi, 1990) may be represented by the following equilibrium

$$A(\text{solid}) + mH_2O \rightleftharpoons A.mH_2O(\text{solid})$$

$$K_h = \frac{a[A.mH_2O(\text{solid})]}{a[A(\text{solid})]a[H_2O]^m} \quad (1)$$

where K_h is the equilibrium constant for the process shown in Eq. 1, and $a[A.mH_2O(\text{solid})]$, $a[A(\text{solid})]$, and $a[H_2O]$ are the thermodynamic activities of the hydrate, the anhydrate, and water respectively. When $a(H_2O) = [a[A.mH_2O(\text{solid})]/\{a[A(\text{solid})]K_h\}]^{1/m}$, the anhydrate, A(solid), and water are in equilibrium with the hydrate, $A.mH_2O$(solid). When $a(H_2O) > [a[A.mH_2O(\text{solid})]/\{a[A(\text{solid})]K_h\}]^{1/m}$, the hydrate, $A.mH_2O$(solid), will be more stable than the anhydrate, A(solid). The anhydrate, A(solid), will be more stable than the hydrate, $A.mH_2O$(solid), in the inverse situation when $a(H_2O) < [a[A.mH_2O(\text{solid})]/\{a[A(\text{solid})]K_h\}]^{1/m}$. Corresponding relations also hold for the phase transitions between different hydrates of a drug. If the standard states of unit activity of A(solid) and of $A.mH_2O$(solid) are represented by their pure solid phases, Eq. 1 simplifies to give Eq. 2.

$$K_h = a[H_2O]^{-m} \quad (2)$$

where m is the number of moles of water taken up by one mole of the anhydrate (or lower hydrate) in the stoichiometric equation. Thus, the hydration state of a hydrate depends on the water activity in the surrounding medium, for example, in the crystallization medium, which may consist of water and organic solvent mixture, or in the vapor phase in which the water activity can be controlled in a relative humidity chamber.

The water activity, $a[H_2O]$, which is abbreviation to a_w, in a crystallization medium can be controlled by changing the composition of an appropriate water + organic solvent mixture. The organic co-solvent should be water-miscible, such as methanol, ethanol, 2-propanol (isopropyl alcohol, IPA), acetone, acetonitrile, or dioxan. Values of the mole fraction-based activity coefficient, γ_w, in mixtures of each of these solvents with water are known (Gölles, 1961; Gölles, 1962; Udovenko and Mazanko, 1967; Sokolova and Morachevskii, 1967; Chirikova et al., 1966; Bacarella et al., 1956). Values of a_w in mixtures of organic solvent + water can be calculated from the literature values of γ_w and the mole fraction of water, x_w, in these mixtures by Eq. 3.

$$a_w = \gamma_w \cdot x_w \quad (3)$$

Values of a_w are fitted to a polynomial in x_w, which enables a_w to be estimated at any value of x_w in the organic solvent + water mixtures employed for the crystallization of a drug. The a_w value in mixtures of organic solvent + water will be modified by the presence of the dissolved drug and a suitable means must be used to evaluate this effect. The fundamental hypotheses in the present work are that, when a drug, which can form a hydrate, is crystallized from mixtures of organic solvent + water, (a) the water activity, a_w, in the mixtures is the major factor determining the nature of the anhydrate or hydrate phase that crystallizes and, (b) that the dissolved drug in the aqueous solvent mixtures influences a_w to a much smaller extent than does the organic solvent. For this concept to be useful, the organic solvent should not form a solid solvate nor a solid solvate-hydrate phase with the drug. The above hypotheses have been previously tested in preliminary studies with nedocromil sodium ($C_{19}H_{15}NO_7Na_2$) in IPA + water mixtures (Khankari and Grant, 1993) and with ampicillin in methanol + water mixtures at 25°C (Zhu and Grant, 1994). The work reported here is part of a continuing series of studies, in which the above hypotheses are further tested using theophylline, caffeine, carbamazepine, and nedocromil magne-

UM00012567
NOVARTIS EXHIBIT 1017
Novartis v. Regents, IPR2023-01346
Page 1313 of 4460

sium as model compounds. In the present work, a preliminary report of which has been presented (Yuen et al., 1995), theophylline, which exists as an anhydrate and a monohydrate, is crystallized from methanol + water and IPA + water mixtures. The main objective here is to investigate whether a_w is a major factor determining the nature of the anhydrate and hydrate phases of theophylline which crystallize from these two organic solvent + water mixtures. The second objective is to study the influence of solvent composition on the solubility of the theophylline phases.

2. Experimental

2.1. Materials

Theophylline anhydrate was obtained from Sigma Chemical Co. (St. Louis, MO), dried for 24 h in an oven at 100°C and stored in a desiccator over phosphorus pentoxide at room temperature. Theophylline monohydrate was prepared by crystallization from distilled water, which was supersaturated by dissolving the anhydrate. The monohydrate was dried at room temperature and stored over a saturated aqueous solution of ammonium chloride (relative humidity 79.5%). Ammonium chloride was obtained from EM Science (Gibbstown, NJ). Methanol and 2-propanol (isopropyl alcohol, IPA) were obtained from Fisher Scientific (Fair Lawn, NJ).

2.2. Methods

2.2.1. Solubility studies

The solubilities of theophylline anhydrate and monohydrate were each determined in methanol + water and IPA + water mixtures of various water activities. Excess theophylline (1 g) was equilibrated for up to 5 days with 10 g solvent mixture (methanol + water or IPA + water, each containing a different mole fraction of water, corresponding to a defined a_w value) in a 20-ml vial at 25°C. Equilibration was attained by shaking the vials in a temperature-controlled water bath. Samples (1 ml) were withdrawn, filtered, suitably diluted with water and analyzed by UV spectrophotometry (Beckman UV-64) at 270 nm. Equilibration was judged to have occurred when three successive measurements differed by not more than 1%.

2.2.2. Powder X-ray diffraction

The powder X-ray diffraction patterns of the theophylline solid phases were determined using a Siemens D-500 powder X-ray diffractometer, with Cu Kα radiation at 30 mA and 45 kV with 2θ increasing at the rate of 3°/min. Counts were accumulated for 1 s at each step. The sample was packed into an aluminum holder and the instrument was operated between an initial and a final 2θ-angle of 5° and 35°, respectively, in increments of 0.05° 2θ.

2.2.3. Karl Fischer titrimetry

The amounts of water, expressed as % w/w and as the number of moles per mole of anhydrous theophylline, in the solid phases were determined using a Mitsubishi Moisturemeter (Model CA-05, Mitsubishi Chemical Industries Limited, Tokyo, Japan). The sample (6–8 mg) was accurately weighed and quickly transferred to the titration vessel before measuring the water content.

2.2.4. Relative humidity measurement

The relative humidity of the vapor phase above saturated aqueous solutions of theophylline was measured by a Rotronic-Hygroskop BT (Rotronic Instrument Corp., Huntington, NY). At equilibrium, the relative humidity, expressed as a decimal fraction, is equal to a_w both in the vapor phase and in the solution.

3. Results and discussion

Values of γ_w in methanol + water and IPA + water mixtures have been previous reported (Gölles, 1961; Udovenko and Mazanko, 1967) as stated above. Fig. 1 shows values of a_w in methanol + water and IPA + water mixtures calculated using Eq. 2 and plotted against x_w. These a_w values were fitted to polynomials of the fourth degree in x_w, and were then used to esti-

UM00012568
NOVARTIS EXHIBIT 1017
Novartis v. Regents, IPR2023-01346
Page 1314 of 4460

mate the water activity at any value of x_w in methanol + water mixtures (Eq. 4) or in IPA + water mixtures (Eq. 5).Methanol + water mixtures:

$$a_w = 0.0056 + 1.398x_w - 0.647x_w^2 + 0.153x_w^3 + 0.0845x_w^4 \ (R = 0.9996) \quad (4)$$

IPA + water mixtures:

$$a_w = 0.0215 + 2.828x_w - 1.837x_w^2 - 2.380x_w^3 + 2.379x_w^4 \ (R = 0.9985) \quad (5)$$

The diagonal straight line in Fig. 1 shows the Raoult's law plot from which methanol + water and IPA + water mixtures give positive deviations. The greater deviation in IPA + water mixtures may be attributed to the larger hydrophobic interaction in the solution resulting from the greater volume and surface area of the cavity created in water by the larger alkyl group of the co-solvent.

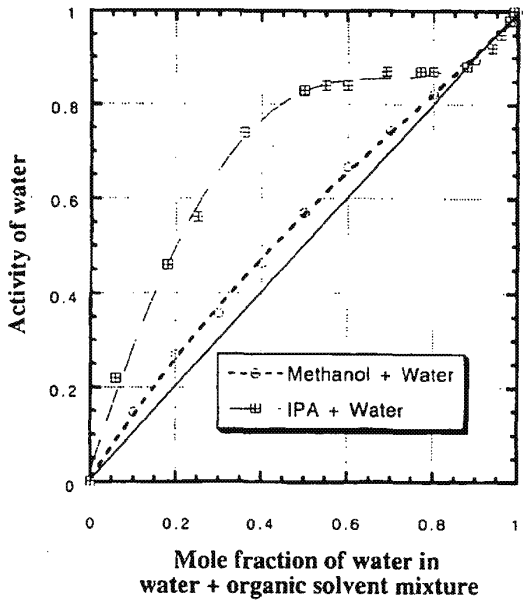


Fig. 1. Plot of the water activity versus the mole fraction of water in methanol + water and IPA + water mixtures at 25°C (data from Gölles, 1961; Udovenko and Mazanko, 1967). The diagonal straight line corresponds to ideal behavior according to Raoult's law.

A saturated solution of theophylline in water is in equilibrium with water vapor at the measured $a_w = 0.94$. Therefore, when the saturated solution ($a_w = 0.94$) is diluted infinitely with water ($a_w = 1.00$), a_w changes by only 6%. This relative small change in a_w appears to justify hypothesis (b) that the presence of theophylline, even at the solubility limit, has little effect on a_w in organic solvent + water mixtures.

Theophylline anhydrate or monohydrate was added to methanol + water or IPA + water mixtures of various compositions and equilibrated at 25°C for 5 days to determine the solubility. After equilibration, the excess solid was characterized by powder X-ray diffractometry. The water content of each phase was determined by Karl Fischer titrimetry. Theophylline anhydrate, theophylline monohydrate and mixtures of the above two forms in different proportions were obtained in the excess solid phase throughout the study. The powder X-ray diffraction patterns of the theophylline forms are shown in Fig. 2. Both the anhydrate and monohydrate forms are crystalline, as is evident from the presence of a number of diffraction peaks. The additivity of both the anhydrate and the monohydrate patterns in separate experiments was shown for mixtures of theophylline anhydrate and the monohydrate.

Theophylline anhydrate in contact with methanol + water mixtures for 5 days converted to the monohydrate at $a_w \geq 0.252$ and remained unchanged at $a_w < 0.227$ (Fig. 3, circles). In contact with IPA + water mixtures for 5 days, theophylline anhydrate completely converted to the monohydrate at $a_w \geq 0.749$ (Fig. 4, open circles). However, in contact with IPA + water mixtures for 5 days at $0.258 \leq a_w \leq 0.625$ (Fig. 4, full circles) the anhydrate was only partially converted to the monohydrate, since the X-ray patterns corresponded to mixtures of the anhydrate and the monohydrate, showing that equilibrium had still not been achieved. The water content of the excess solid phase increased with increasing a_w between 0.258 and 0.625, corresponding to increasing phase conversion of the anhydrate to the monohydrate (Fig. 4, full circles) and indicating that the higher the water activity, the greater the thermodynamic driving force and the greater the

UM00012569
NOVARTIS EXHIBIT 1017
Novartis v. Regents, IPR2023-01346
Page 1315 of 4460

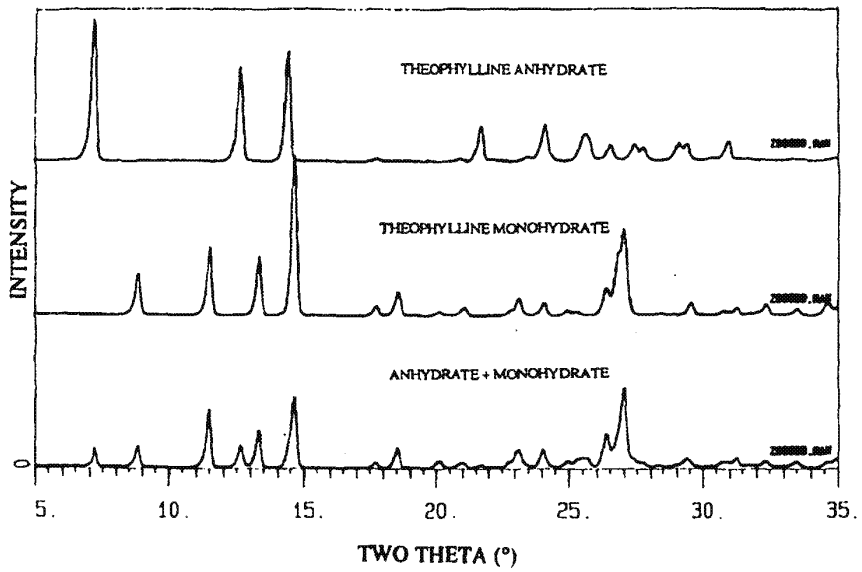


Fig. 2. Powder X-ray diffraction patterns of the two forms of theophylline investigated and of a mixture of the two forms.

rate of conversion. Since, at $0.258 \leq a_w \leq 0.625$, equilibrium was not achieved within 5 days (Fig. 4, full circles), the solid phases in contact with IPA + water mixtures within the range of $0.258 \leq a_w \leq 0.625$, were examined after 30 days by powder X-ray diffractometry and the water contents by Karl Fischer titrimetry. Within 30 days the phase conversion of the anhydrate to the monohydrate was complete (Fig. 5, circles).

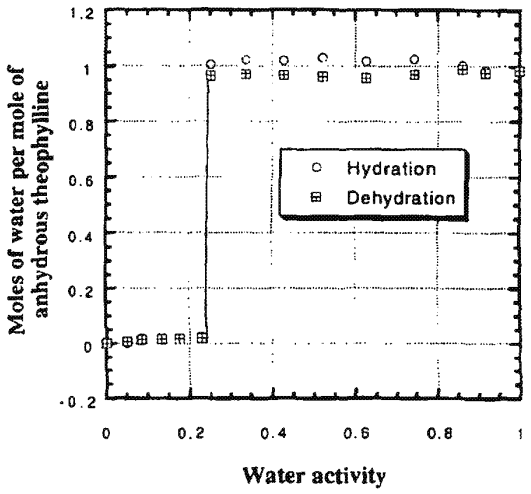


Fig. 3. Phase diagram after equilibration for 5 days showing the dependence of theophylline hydrate stoichiometry on water activity in methanol + water mixtures during theophylline hydration and dehydration processes at 25°C. Circles represent the fate of the anhydrate initially added. Squares represent the fate of the monohydrate initially added.

Theophylline monohydrate in contact with methanol + water mixtures changed to the anhydrate at $a_w \leq 0.227$ but remained as the monohydrate at $a_w \geq 0.252$ (Fig. 3, squares). After being in contact with IPA + water mixtures for 5 days, the monohydrate partially dehydrated to the anhydrate at $a_w \leq 0.541$ (Fig. 4, full squares). After being in contact with IPA + water mixtures for 30 days (Fig. 5, squares), the partially dehydrated monohydrate (Fig. 4, full squares) completely changed to the anhydrate at $a_w \leq 0.171$ (Fig. 5, squares), while at $0.229 \leq a_w \leq 0.541$, the partially dehydrated monohydrate (Fig. 4, full squares) converted back to the monohydrate (Fig. 5, squares). These results suggest that theophylline changes form reversibly in response to a_w in the crystallization medium (Figs. 3 and 5), although equilibration in IPA + water mixtures takes between 5 and 30 days to achieve.

UM00012570
NOVARTIS EXHIBIT 1017
Novartis v. Regents, IPR2023-01346
Page 1316 of 4460

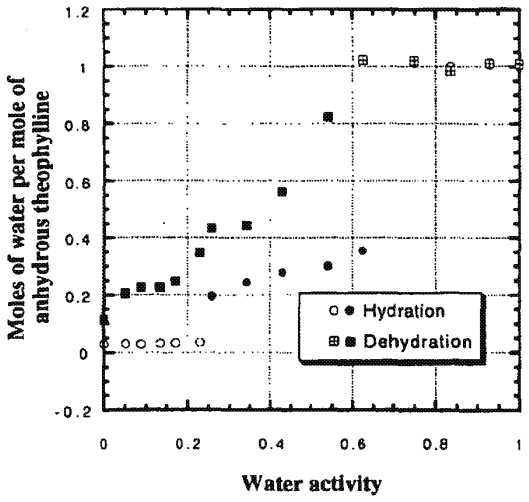


Fig. 4. Phase diagram after 5 days showing the dependence of theophylline hydrate stoichiometry on water activity in IPA + water mixtures during theophylline hydration and dehydration processes at 25°C (equilibrium not reached). Circles represent the fate of the anhydrate initially added. Squares represent the fate of the monohydrate initially added. Open circles and open squares represent a single phase, anhydrate or monohydrate, shown by powder X-ray diffraction. Full circles and full squares represent a mixture of the anhydrate and monohydrate shown by powder X-ray diffraction.

The water content of theophylline monohydrate, when added to an organic solvent + water mixture, contributes to x_w to a small extent and prevents the attainment of $a_w = 0$. The intrinsic water content in theophylline monohydrate could influence the water activity to a small but varying extent. This result may explain the discrepancy in water activity at which the monohydrate changes to the anhydrate ($a_w = 0.227$ in methanol + water mixture as compared with $a_w = 0.171$ in IPA + water mixture).

The phase transformation of theophylline anhydrate to the monohydrate is found to occur by a solvent-mediated process in which the anhydrate dissolves and creates the necessary supersaturation for the nucleation and growth of monohydrate crystals (De Smidt et al., 1986; Rodriguez-Hornedo et al., 1992). The kinetics of the transformation, anhydrate to monohydrate, for theophylline in water + organic solvent mixtures should take into consideration both the dissolution of the anhydrate phase and the nucleation and growth of the monohydrate phase. For theophylline in methanol + water mixtures, the equilibria were achieved within 5 days (Fig. 3), but in IPA + water mixtures the equilibria were not attained within 5 days (Fig. 4) but required 30 days (Fig. 5). Additional experiments, such as monitoring the concentration-time profiles during transformation, would be needed to explain why the kinetics of the phase transformation of theophylline anhydrate to the monohydrate is slower in IPA + water mixtures than in methanol + water mixtures.

In contact with IPA + water or methanol + water mixtures, the monohydrate was always present at equilibrium at $a_w > 0.25$. However, at $a_w < 0.25$ in either solvent mixture, the anhydrate form was the only solid phase obtained, no matter which solid form was initially added to the methanol + water or IPA + water mixtures. This observation indicates that equilibrium had been achieved with the more stable form. These results demonstrate the validity of hypothesis (a) that water activity is the major factor determining the nature of the theophylline phase, anhydrate or

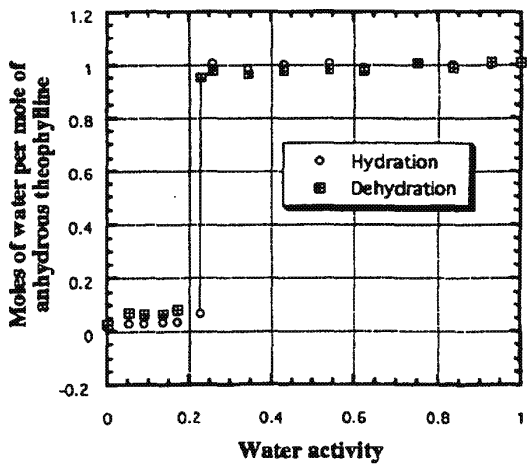


Fig. 5. Phase diagram after equilibration for 30 days showing the dependence of theophylline hydrate stoichiometry on water activity in IPA + water mixtures during theophylline hydration and dehydration processes at 25°C. Circles represent the fate of the anhydrate initially added. Squares represent the fate of the monohydrate initially added.

UM00012571
NOVARTIS EXHIBIT 1017
Novartis v. Regents, IPR2023-01346
Page 1317 of 4460

monohydrate, which crystallizes from methanol + water or IPA + water mixtures. At equilibrium, the a_w, at which theophylline anhydrate $\rightleftharpoons$ theophylline monohydrate, is found to be approximately 0.25. The stoichiometric number, m, in Eqs. 1 and 2 is unity. Substituting these values into Eq. 2 leads to $K_h = 4.0$. For the phase equilibrium between nedocromil sodium trihydrate and the heptahemihydrate, $a_w = 0.80$, $m = 4.5$ and $K_h = 2.7$ (Khankari and Grant, 1993). Similarly, for the equilibrium between ampicillin anhydrate and the trihydrate, $a_w = 0.34$, $m = 3$ and $K_h = 25.9$ (Zhu and Grant, 1994). Comparison of the respective K_h values enables the relative tendencies for the transition from the anhydrate to the hydrate or from the lower hydrate to the higher hydrate to be obtained for any pharmaceutical compound. Furthermore, these equilibrium constants apply in all liquid mixtures of water + organic solvents that are capable of providing these a_w values.

At $a_w = 0.25$, corresponding to $x_w = 0.2$ in methanol + water mixture and $x_w = 0.08$ in IPA + water mixture (Fig. 1), theophylline anhydrate is in equilibrium with theophylline monohydrate. Apparently, the phase transformation of theophylline anhydrate to the monohydrate occurs at a lower concentration of water in IPA + water mixture than in methanol + water mixture, yet the equilibrium water activity is essentially the same. This observation emphasizes the fact that the water activity in the crystallization medium is more important than water concentration in determining the nature of the phase (anhydrate or hydrate) that crystallizes.

Otsuka et al. (1990) studied the hydration behavior of two forms of theophylline anhydrate, Type I and Type II, at 35°C. Their Type I was obtained by recrystallization from distilled water at 95°C, whereas their Type II was obtained by dehydration of theophylline monohydrate of 100°C for 24 h, a more drastic treatment. Their reported powder X-ray diffraction patterns suggest that the crystal structures of Type I and Type II are identical with that of theophylline anhydrate. The observed difference in diffraction intensities with that of theophylline anhydrate. The observed difference in diffraction intensities may

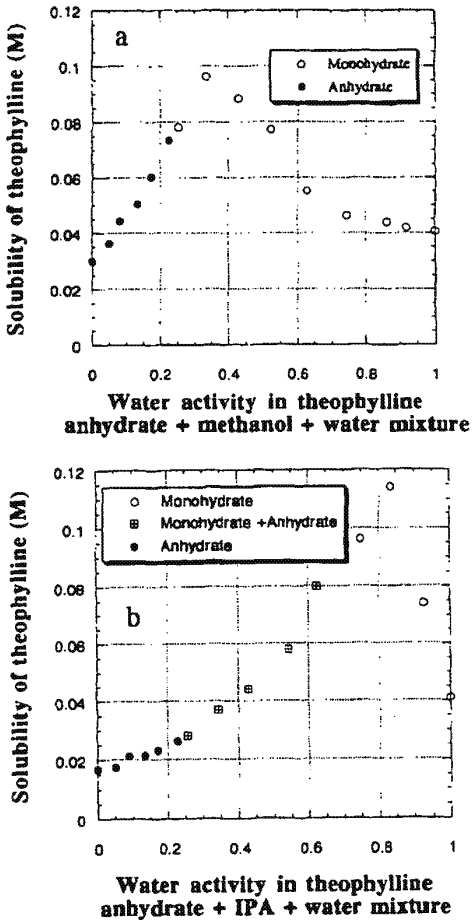


Fig. 6. Solubility profiles of theophylline anhydrate (initially added) as a function of water activity in (a) methanol + water mixtures and (b) IPA + water mixtures at 25°C. The legend designation of each data point refers to the solid phase obtained after 5 days. Full circles represent the formation of the anhydrate at equilibrium, open circles represent the formation of the monohydrate at equilibrium, and squares represents a mixture of both phases, not necessarily in equilibrium within 5 days.

be attributed to a preferred orientation effect due to differences in crystal habit. The reported powder X-ray diffraction pattern of Type I corresponds closely to that of the anhydrate employed in the present work (Fig. 2, top).

At 35°C in the presence of water vapor at various a_w values (which are equivalent to relative humidities, RH, expressed as decimal fractions),

UM00012572
NOVARTIS EXHIBIT 1017
Novartis v. Regents, IPR2023-01346
Page 1318 of 4460

Otsuka et al. (1990) found that the Type I anhydrate remains as the anhydrate at RH $\leq$ 0.82 but transforms to the monohydrate at RH $\geq$ 0.88. On the other hand, the Type II anhydrate remains as the anhydrate at RH $\leq$ 0.66 but transforms to the monohydrate at RH $\geq$ 0.75. The lower a_w (=0.25) for the solution phase transformation in the presence of organic solvent + water mixtures in the present work is mainly attributed to the attainment of true equilibrium, but not so in the vapor phase hydrations reported by Otsuka et al. (1990). However, a secondary factor may be the lower temperature employed in the present work. The different a_w (RH) values reported by Otsuka et al. (1990) may arise from the slower kinetics of hydration of the two other types of anhydrate. The fact that Type II, whose crystals contain cracks, is more readily hydrated than Type I, which gives more intense diffraction peaks, clearly points to kinetic factors in determining the observed hydrations of Otsuka et al. (1990).

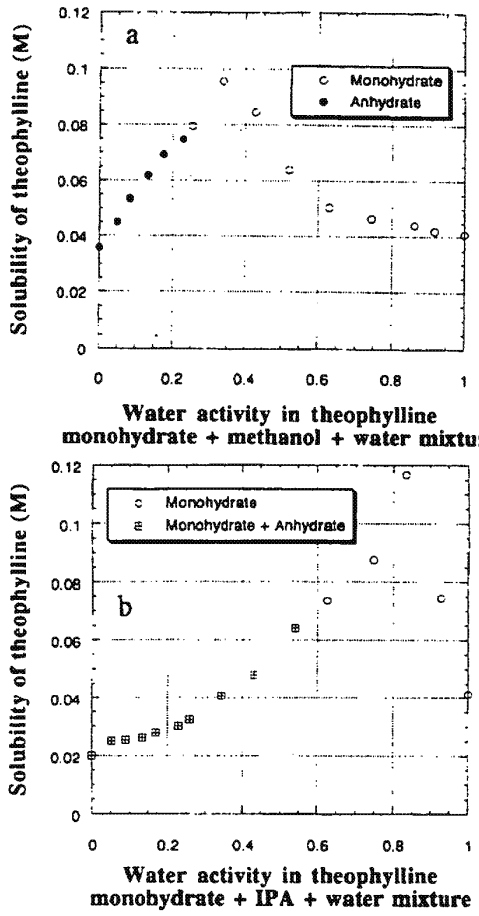


Fig. 7. Solubility profiles of theophylline monohydrate (initially added) as a function of water activity in (a) methanol + water mixtures and (b) IPA + water mixtures at 25°C. The legend designation of each data point refers to the solid phase obtained after 5 days. Full circles represent the formation of the anhydrate at equilibrium, open circles represent the formation of the monohydrate at equilibrium, and squares represents a mixture of both phases, not necessarily in equilibrium within 5 days.

The solubility of theophylline anhydrate in methanol + water mixtures, when plotted against a_w in these mixtures, increased to a maximum (0.0962 M at $a_w = 0.338$) and then decreased (Fig. 6a). IPA + water mixtures gave a similar pattern with a slightly higher maximum solubility (0.114 M at $a_w = 0.832$) (Fig. 6b). The solubility profiles of theophylline monohydrate in methanol + water and IPA + water mixtures (Fig. 7a,b) are similar to those of the anhydrate in the above two binary mixtures (Fig. 6a,b) and the a_w values at the maxima are identical. The ratio of the peak solubility of theophylline anhydrate to that of the monohydrate in both methanol + water and IPA + water mixtures is close to 1, indicating only a small difference between the thermodynamic activities of theophylline anhydrate and monohydrate at the above a_w values. These maxima have a complex thermodynamic origin, since they are a consequence of the influence of both enthalpy and entropy terms on the partial molar free energy of the solute (Gould et al., 1984; Grant and Higuchi, 1990).

These solubility maxima may be treated semi-empirically by regular solution theory (Gould et al., 1984) and by the extended solubility parameter approach (Martin et al., 1981). The original Hildebrand equation predicts that the solubility of a compound, for which the solubility parameter lies between the solubility parameters of the two solvents of a binary mixture, will exhibit a peak at which the solubility parameter of the mixed solvent, δ_1, equals that of the solute, δ_2. In a mixed solvent system, regular solution theory indicates that the solubility parameter, δ_1, should be represented by Eq. 6:

UM00012573
NOVARTIS EXHIBIT 1017
Novartis v. Regents, IPR2023-01346
Page 1319 of 4460

$$\delta_1 = \phi_a\delta_a + \phi_b\delta_b \quad (6)$$

where ϕ_a and ϕ_b are the volume fractions and δ_a and δ_b are the respective solubility parameters of the individual solvents (Snyder, 1980) in the binary liquid mixture. From the solubility parameter of each mixed solvent system at the composition giving the maximum solubility, the solubility parameter of theophylline, δ_2, was calculated to be 15.7 $cal^{1/2}cm^{-3/2}$ in methanol (δ_a = 14.5 $cal^{1/2}cm^{-3/2}$) + water (δ_b = 23.4 $cal^{1/2}cm^{-3/2}$) mixtures and 15.2 $cal^{1/2}cm^{-3/2}$ in IPA (δ_a = 12 $cal^{1/2}cm^{-3/2}$) + water (δ_b = 23.4 $cal^{1/2}cm^{-3/2}$) mixtures. These calculated solubility parameters, δ_2, for theophylline are appreciably larger than the value of 14 $cal^{1/2}cm^{-3/2}$ reported by Martin et al. (1981). The above calculations of the solubility parameter of theophylline employed the classical solubility parameter of water, δ_b = 23.4 $cal^{1/2}cm^{-3/2}$ (Hildebrand and Scott, 1962). This value accounts quite well for the solubility of water in paraffinic solvents (Black et al., 1948) at 25°C, partly because the solutions are so dilute that the solute-solvent interactions are dominated by London dispersion forces (Grant and Higuchi, 1990). However, Davis et al. (1972) have suggested that δ_b = 15.65 $cal^{1/2}cm^{-3/2}$ for water may better account for the solubility behavior of hydrocarbons and of the methylene group of other organic compounds, such as alkanols, in water at 25°C. Using δ_b = 15.65 $cal^{1/2}cm^{-3/2}$ for water, the solubility parameter of theophylline, δ_2, is calculated to be 14.7 $cal^{1/2}cm^{-3/2}$ in methanol + water mixtures and 13.0 $cal^{1/2}cm^{-3/2}$ in IPA + water mixtures. The differences between these calculated solubility parameters for theophylline and that derived by Martin et al. (1981) may be accounted for by differences in the relative emphasis of the hydrogen bonding and polar interaction in the ternary solutions, since regular solution theory in its simplest form is derived under the assumption that only London dispersion forces are the significant intermolecular interactions. These differences illustrate the difficulty of deriving reliable solubility parameters for polar solutes (Grant and Higuchi, 1990).

Pfeiffer et al. (1970) in their study of the pseudopolymorphism of cephaloglycine and cephalexin crystallized in several organic solvent + water mixtures observed a break in the solubility profile at that solvent composition at which one hydrate changes to another. Bogardus (1983) reported that the maximum in the solubility of cholesterol in water + glyceryl 1-monooctanoate mixtures coincided with the anhydrate-hydrate crystalline phase change of cholesterol. However, in the present study, the maximum solubility of theophylline occurred at a_w = 0.338, while phase transformation at equilibrium occurred at a_w = 0.25 in methanol + water mixtures. Similarly, in IPA + water mixtures, the maximum solubility of theophylline occurred at a_w = 0.832, but phase transformation occurred at a_w = 0.25. These discrepancies suggest that the maximum solubility and the change of crystal form of theophylline have different origins in these two binary solvent mixtures. The solubility maxima may reflect the sensitivity of the strong hydrogen bonding interactions in solution to a_w in each binary solvent system, methanol + water or IPA + water.

4. Conclusions

The first hypothesis (a) that "when a drug, which can form a hydrate, is crystallized from mixtures of organic solvent + water, the water activity, a_w, in the mixtures is the major factor determining the nature of the anhydrate or hydrate phase that crystallizes" is essentially correct for theophylline in water + methanol or water + IPA mixtures. The anhydrate is in equilibrium with the monohydrate at a_w = 0.25 in each of these solvent mixtures. Saturation of water with theophylline monohydrate reduces a_w by only 6%, confirming the second hypothesis (b) that "the dissolved drug in the aqueous solvent mixtures influences a_w to a much smaller extent than does the organic solvent".

The solubilities of theophylline anhydrate and monohydrate have maximum values (0.0962 M at a_w = 0.338) in methanol + water and (0.114 M at a_w = 0.832) in IPA + water mixtures. These a_w values do not correlate with a_w = 0.25 for the theophylline anhydrate-monohydrate equilibrium in either binary solvent mixture, emphasizing their different origins.

UM00012574
NOVARTIS EXHIBIT 1017
Novartis v. Regents, IPR2023-01346
Page 1320 of 4460

Acknowledgements

We thank the Pharmaceutical Research and Manufacturers of America Foundation, Inc. for an Undergraduate Research Fellowship in Pharmaceutics for Ceaminia Yuen.

References

Bacarella, A.L., Finch, A. and Grunwald, E., Vapor pressure and activities in the system dioxane-water. Second virial coefficients in the gaseous system nitrogen-dioxane-water. *J. Phys. Chem.*, 60 (1956) 573–576.

Black, C., Joris, G.G. and Taylor, H.S., The solubility of water in hydrocarbons. *J. Chem. Phys.*, 16 (1948) 537–543.

Bogardus, J.B., Unusual cholesterol solubility in water/glyceryl-1-monooctanoate solutions. *J. Pharm. Sci.*, 72 (1983) 837–838.

Chirikova, Z.P., Galata, L.A., Kotova, Z.N. and Kofman, L.S., Liquid-vapor equilibrium in the system acetonitrile-water. *Russian J. Phys. Chem.*, 40 (1966) 493–496.

Davis, S.S., Higuchi, T. and Rytting, J.H., Determination of thermodynamics of the methylene group in solutions of drug molecules. *J. Pharm. Pharmacol.*, 24 (Suppl.), (1972) 30P–46P.

De Smidt, J.G., Fokkens, J.G., Grijseels, H. and Crommelin, D.J.A., Dissolution of theophylline monohydrate and anhydrous theophylline in buffer solutions. *J. Pharm. Sci.*, 75 (1986) 497–501.

Gölles, F., Examination and calculation of thermodynamic data from experimental measurements. I. The numerical integration of the vapor-pressure curves of the system methanol-water. *Monatsh. Chem.*, 92 (1961) 981–991.

Gölles, F., Examination and calculation of thermodynamic data from experimental data. II. The numerical integration of the vapor-pressure curves of the system ethanol-water. *Monatsh. Chem.*, 93 (1962) 191–220.

Gould, P.L., Goodman, M., Hanson, P.A., Investigation of the solubility relationships of polar, semi-polar and non-polar drugs in mixed co-solvent systems. *Int. J. Pharm.*, 19 (1984) 149–159.

Grant, D.J.W. and Higuchi, T., *Solubility Behavior of Organic Compounds*, John Wiley and Sons, New York, NY, 1990, pp. 38–39; 52–57; 395–396.

Haleblian, J., Characterization of habits and crystalline modification of solids and their pharmaceutical applications. *J. Pharm. Sci.*, 64 (1975) 1269–1288.

Hildebrand, J.H. and Scott, R.L., *Regular Solutions*, Prentice-Hall, Englewood Cliffs, NJ, 1962.

Khankari, R.K. and Grant, D.J.W., Pharmaceutical hydrates. *Thermochim. Acta.*, 248 (1995) 61–79.

Khankari, R.K. and Grant, D.J.W., Prediction of nedocromil sodium hydrate phases in isopropanol + water mixtures from the relative humidity phase diagram. *Pharm. Res.*, 10 (1993), No.10, S-153 (PT 6106).

Martin, A, Paruta, A.N. and Adjei, A., Extended Hildebrand solubility approach: methylxanthines in mixed solvents. *J. Pharm. Sci.*, 70 (1981) 1115–1120.

Otsuka, M., Kaneniwa, N., Kawakami, K. and Umezama, O., Effect of surface characteristics of theophylline anhydrate powder on hydroscopic stability. *J. Pharm. Pharmacol.*, 42 (1990) 606–610.

Pfeiffer, R.R., Yan, K.S. and Tucker, M.A., Crystal pseudopolymorphism of cephaloglycin and cephalexin. *J. Pharm. Sci.*, 59 (1970) 1809–1814.

Rodriguez-Hornedo, N., Lechuga-Ballesteros, D. and Wu, H., Phase transition and heterogeneous/epitaxial nucleation of hydrated and anhydrous theophylline crystals. *Int. J. Pharm.*, 85 (1992) 149–162.

Shefter, E. and Higuchi, T., Dissolution behavior of crystalline solvated and non-solvated forms of some pharmaceuticals. *J. Pharm. Sci.*, 52 (1963) 781–791.

Snyder, L., Solutions to solution problems. 2. *Chemtech*, 10 (1980) 188–193.

Sokolova, E.P. and Morachevskii, A.G., Thermodynamic properties of the acetone-water system. *Vestn. Leningrad. Univ.*, 22(16), *Fiz. Khim.*, 3 (1967) 110–115.

Udovenko, V.V. and Mazanko, T.F., Liquid-vapour equilibrium in the propan-2-ol-water and propan-2-ol-benzene system. *Rus. J. Phys. Chem.*, 41(1967) 863–866.

Zhu, H and Grant, D.J.W., Influence of water activity on the anhydrate and hydrate phases of ampicillin crystallizing from water + methanol mixture. 26th Pharmaceutics Graduate Student Research Meeting, Omaha, Nebraska, June 16–18, 1994.

Yuen, C., Zhu, H. and Grant, D.J.W., Crystallization of drugs from organic solvent + water mixtures I: Theophylline. PhRMA Awardee Meeting, Washington, D.C. February 9, 1995.

UM00012575
NOVARTIS EXHIBIT 1017
Novartis v. Regents, IPR2023-01346
Page 1321 of 4460

SUPRAMOLECULAR CHEMISTRY, Vol. 9, pp. 127–135
Reprints available directly from the publisher
Photocopying permitted by license only

© 1998 OPA (Overseas Publishers Association) N.V.
Published by license under
the Harwood Academic Publishers imprint,
part of The Gordon and Breach Publishing Group.
Printed in India.

Aromatic Dicarboxylic Acids as Building Blocks of Extended Hydrogen-bonded Architectures

CHRISTER B. AAKERÖY[a], DEIRDRE P. HUGHES[b], JAMES M. McCABE[b] and MARK NIEUWENHUYZEN[b]

[a] *Department of Chemistry, Kansas State University, Manhattan, KS, 66506, USA;*
[b] *School of Chemistry, The Queen's University of Belfast, Belfast BT5 9AG, Northern Ireland*

(Received in final form 11 June 1997)

An examination of the crystal structures of four compounds, 5-amino *iso*-phthalic acid hemihydrate (monoclinic, $P2_1/n$, $a = 8.142(2)$, $b = 17.444(3)$, $c = 11.140(2)$ Å, $\beta = 94.19(3)°$, $D_c = 1.601\ g\,cm^{-3}$, $Z = 8$, $R_w^2 = 0.106$ for 1401 unique reflections), piperazinium (2+) 5-amino *iso*-phthalate (monoclinic, $P2_1/c$, $a = 11.820(2)$, $b = 9.516(2)$, $c = 12.618(3)$ Å, $\beta = 116.70(3)°$, $D_c = 1.400\ g\,cm^{-3}$, $Z = 4$, $R_w^2 = 0.104$ for 2222 unique reflections), 2-chloro-benzylammonium 2-carboxylate-6-carboxylic pyridine (monoclinic, $P2_1/c$, $a = 22.391(2)$, $b = 9.322(3)$, $c = 13.274(2)$ Å, $\beta = 92.567(11)$, $D_c = 1.482\ g\,cm^{-3}$, $Z = 8$, $R_w^2 = 0.113$ for 3610 unique reflections), and 3-fluoro-benzylammonium 2-carboxylate-6-carboxylic pyridine hydrate (monoclinic, $P2_1/c$, $a = 9.862(2)$, $b = 13.246(3)$, $c = 21.153(4)$ Å, $\beta = 98.00(3)$, $D_c = 1.463\ g\,cm^{-3}$, $Z = 8$, $R_w^2 = 0.154$ for 2552 unique reflections), has identified a robust hydrogen-bonded, ribbon-like motif, generated by the geometric fit and hydrogen-bond complementarity of the $[-COO]^-$ and the $[-COOH]$ functionalities. This preferred interaction between neighbouring anions results in infinite 1-D anionic architectures that are held together by short and near-linear O—H···O hydrogen bonds. In 1 and 2, the amino functionality acts as a crosslink (through N—H···O interactions) between adjacent sheets, thereby generating extended 2-D architectures. 5-Amino *iso*-phthalic acid exists as a zwitterion in the solid state, an observation which was also indicated by vibrational spectroscopic data. The crystal packing in both 3 and 4 consists of 2-D domains of anions and cations, stacked in an ..AABBAABB.. manner where the anionic sheets are constructed around the carboxylic-carboxylate supramolecular connector.

Keywords: Crystal engineering, hydrogen bonding, carboxylic acids

INTRODUCTION

Crystal engineering is concerned with the structural manifestations of intermolecular forces and the way in which such forces can be utilized for controlling the assembly of molecular building blocks into predictable architectures. Despite the inherent difficulties with using weak forces as primary synthetic tools, considerable progress has been made during the last decade. Cocrystals of melamines and barbiturates have been used to create a variety of structural motifs [1], and aromatic spacers have provided reliable backbones for well-organized, extended structures [2,3]. The selectivity and directionality of the hydrogen bond has been instrumental in the preparation of distinctive and predictable

UM00012576
NOVARTIS EXHIBIT 1017
Novartis v. Regents, IPR2023-01346
Page 1322 of 4460

structural aggregates [4], notably in molecular solids [5], and the use of hydrogen bonding as a steering force is now emerging as the most important strategy in crystal engineering [6–8]. Despite such progress, much more work is needed in order to identify robust supramolecular connectors that can be used in the programmed assembly of extended networks and new functional solids.

Although most efforts in crystal engineering have focused on molecular solids, an increasing number of strategies for the assembly of predictable ionic architectures have appeared recently [9]. We have previously demonstrated that substituted aliphatic dicarboxylic acids [9a,b] and monoamides [9c] of dicarboxylic acids can be used as versatile building blocks of low-dimensional architectures in organic salts. In this paper we report on the crystal structures of four compounds that are built around aromatic dicarboxylic acids, where the dominating hydrogen-bond interaction takes place between carboxylic and carboxylate moieties in a head-to-tail fashion; 5-amino *iso*-phthalic acid hemihydrate **1**, piperazinium (2+) 5-amino *iso*-phthalate **2**, 2-chloro-benzylammonium 2-carboxylate-6-carboxylic pyridine **3** and 3-fluoro-benzylammonium 2-carboxylate-6-carboxylic pyridine hydrate **4**. In the case of **1** and **2**, we wanted to combine the [$COO^- \cdots COOH$] supramolecular interaction with the hydrogen-bond donating ability of an amino group positioned almost perpendicular to the expected chain. This creates as an opportunity for crosslinking of neighbouring chains which could result in a 2-D structure. We were also interested in comparing the structural influence of the amino moiety in *iso*-phthalic acid, with the influence of the —CH moiety in the corresponding position in 2,6-dicarboxylic acid pyridine. The only previously reported structure related to this work is that of 2,6-dicarboxylic acid pyridine hydrate [10].

EXPERIMENTAL SECTION

Preparation of 5-Amino *iso*-Phthalic Acid Hemihydrate

A commercial sample (Aldrich) of 5-amino *iso*-phthalic acid was showly recrystallized at ambient temperatures from an aqueous solution to produce irregular, colourless crystals: mp. > 300° (dec.) Calc. (found) for $C_8H_8NO_{4.5}$; C, 50.53 (50.3); H, 8.08 (8.2); N, 7.76 (7.6)%.

Preparation of Piperazinium (2+) 5-Amino *iso*-Phthalate

An aqueous solution of 5-amino *iso*-phthalic acid (0.20 g; 1.10 mmol) was prepared by dissolving the acid in water (75 cm^3) and bringing the mixture to boil. Piperazine (0.095 g; 1.10 mmol) was dissolved in distilled water (15 cm^3) and added to the warm acidic solution. The volume was reduced by boiling to approximately 20 cm^3 and the remaining solvent was allowed to evaporate at ambient temperatures. This produced large, colourless crystals which were collected by filtration, washed with a small amount of cold ethanol and allowed to dry in air: mp. 275–277°C. Calc. (found) for $C_{12}H_{17}N_3O_4$; C, 53.93 (53.5); H, 6.37 (6.3); N, 15.73 (15.6)%.

Preparation of 2-Chloro-Benzylammonium 2-Carboxylate-6-Carboxylic Acid Pyridine

2-Chlorobenzylamine (0.18 ml, 1.5 mmol) was added to an aqueous solution of 2,6-dicarboxylic acid pyridine (0.25 g, 1.5 mmol). The mixture was gently heated for a few minutes, and then left at ambient temperature. After a few days colourless needle-like crystals were produced; mp. 209–210°C. Calc. (found) for: $C_{14}H_{13}N_2O_4Cl$, C, 54.46 (54.2); H, 4.21 (4.4); N, 9.08 (9.4)%.

UM00012577
NOVARTIS EXHIBIT 1017
Novartis v. Regents, IPR2023-01346
Page 1323 of 4460

Preparation of 3-Fluoro-Benzylammonium 2-Carboxylate-6-Carboxylic Acid Pyridine Hydrate

2,6-Dicarboxylic acid pyridine (0.25 g, 1.5 mmol) was dissolved in methanol, and added to 3-fluorobenzylamine (0.19 ml, 1.5 mmol). The mixture was gently heated for a few minutes and then left at ambient temperature. After a few days, a pale yellow crystalline solid appeared. The product was filtered off and recrystallized twice from methanol to produce pale yellow rod-like crystals; mp. 206–207°C. Calc. (found) for $C_{14}H_{15}N_2O_5F$; C, 54.19 (54.5); H, 4.84 (4.8); N, 9.03 (9.5)%.

Crystallography and Vibrational Spectroscopy

Crystal data were collected using a Siemens P4 four-circle diffractometer with graphite monochromated Mo-K_α radiation at ca. 150 K in a dinitrogen stream. Crystal stabilities were monitored by measuring standard reflections every 100 reflections, and there were no significant variations ($< \pm 1\%$). Cell parameters were obtained from 35 accurately centred reflections in the 2-θ range 10°–25°. ω scans were employed for data collection and Lorentz and polarization corrections were applied.

The structures were solved by direct methods and for compounds **1–3** the non-hydrogen atoms were refined with anisotropic thermal parameters. Hydrogen-atom positions were located from difference Fourier maps and a riding model with fixed thermal parameters (U_{iso}=1.2U_{eq} for the atom to which they are bonded), was used for subsequent refinements. For compound **4** the carbon atoms were refined isotropically and all other non-hydrogen atoms were refine anisotropically. Hydrogen atoms were added at idealised positions for the carbon atoms and those attached to the nitrogen and oxygen atoms were located from difference a Fourier map. A riding model with fixed thermal parameters (U_{iso}=1.2U_{eq} for the atom to which they are bonded), was used for subsequent refinements. For compound **1–4** the function minimised was $\Sigma[(\sigma^2|F_0| - |F_c|^2)]$ with reflection weights $\omega^{-1}=[\sigma^2|F_0|^2+(g_1P)^2+(g_2P)]$ where $P=[\max|F_0|^2+|F_c|^2]/3$. The SHELXTL PC and SHELXL-93 packages were used for data reduction and structure solution and refinement [11]. Additional material available from the Cambridge Crystallographic Data Centre comprises atomic coordinates, thermal parameters and relevant tables of observed and calculated structure factor amplitudes.

Data for structure determinations of **1–4** are listed in Table I. Geometry, labeling schemes (thermal ellipsoids (50%) for **1–3**) are shown in Figures 1a–d.

The infrared spectrum (KBr disk) of **1** was obtained on a Perkin 1430 spectrophotometer.

RESULTS AND DISCUSSION

The IR spectrum of **1** contains several bands that indicate that 5-amino *iso*-phthalic acid hemihydrate exists as a zwitterion, and not as a neutral molecule, in the solid state. Bands at 1402 cm^{-1} (s) and 1554 cm^{-1} (m), can be assigned to the symmetric and asymmetric Ar-COO^- stretches respectively. There are no distinctive bands in the 3400–3500 cm^{-1} region, where the symmetric and asymmetric R-NH_2 stretches would be expected to appear. Instead, there is a broad absorption at 2615 cm^{-1} and a well-defined band at 1591 cm^{-1} that can be assigned to $[-NH_3]^+$ stretching and bending modes, respectively.

The crystal structure determination of 5-amino *iso*-phthalic acid, **1**, conformed that the compound exists as a zwitterion, as indicated by the spectroscopic data. All protons were located, and the two C—O bond lengths, r[C(8)–C(81) 1.258(2) Å; C(8)–C(82) 1.261(2) Å] demonstrate that this is indeed a carboxylate moiety.

UM00012578
NOVARTIS EXHIBIT 1017
Novartis v. Regents, IPR2023-01346
Page 1324 of 4460

TABLE I Data Collection and Refinement for 1 and 2

Crystal data	1	2
Empirical formula	$C_8H_8NO_{4.5}$	$C_{12}H_{17}N_3O_4$
MW	190.15	267.29
Crystal size (mm)	0.4 × 0.30 × 0.10	0.6 × 0.43 × 0.51
Crystal system	monoclinic	monoclinic
Space group	$P2_1/n$	$P2_1/c$
a (Å)	8.142 (2)	11.820 (2)
b (Å)	17.444 (3)	9.516 (2)
c (Å)	11.140 (2)	12.618 (3)
α (deg)	90	90
β (deg)	94.19 (3)	116.70 (3)
γ (deg)	90	90
Volume (Å^3)	1578.0 (6)	1267.9 (5)
Z	8	4
D_{calc} (g cm^{-3})	1.601	1.400
$F(000)$	792	568
μ(Mo-K$_\alpha$) (mm^{-1})	0.133	0.106
Temp (K)	153	293
ω scans; θ range (deg)	2.34–25.00	2.80–24.98
Range h	−1 to 9	0 to 14
Range k	−18 to 20	0 to 11
Range l	−13 to 16	−15 to 13
Reflns collected	1558	2337
Unique reflns	1401	2222
Data : parameter ratio	11.39	12.92
Refinement	full-matrix least squares	full-matrix least-squares
R/R_w^2 (obs data)	0.038/0.099	0.038/0.096
R/R_w^2 (all data)	0.054/0.106	0.051/0.104
$\Delta\rho_{max/min}$ (e Å^{-3})	0.244/−0.222	0.205/−0.283
S	1.065	1.091

Data Collection and Refinement for 3 and 4

Crystal data	3	4
Empirical formula	$C_{14}H_{13}N_2O_4Cl$	$C_{14}H_{14}N_2O_{4.5}F$
MW	308.71	301.27
Crystal size (mm)	0.30 × 0.20 × 0.10	0.42 × 0.22 × 0.30
Crystal system	monoclinic	monoclinic
Space group	$P2_1/c$	$P2_1/c$
a (Å)	22.391 (2)	9.862 (2)
b (Å)	9.322 (3)	13.246 (3)
c (Å)	13.274 (2)	21.153 (4)
α (deg)	90	90
β (deg)	92.567 (11)	98.00 (3)
γ (deg)	90	90
Volume (Å^3)	2767.9 (7)	2736.5 (9)
Z	8	8
D_{calc} (g cm^{-3})	1.482	1.463
$F(000)$	1280	1256
μ(Mo-K$_\alpha$) (mm^{-1})	0.294	0.119
Temp (K)	153	173
ω scans; θ range (deg)	1.82–22.50	2.09–20.00
Range h	−24 to 24	0 to 9
Range k	−1 to 10	−12 to 12
Range l	−1 to 14	−20 to 20
Reflns collected	4756	2744
Unique reflns	3610	2552
Data : parameter ratio	9.53	10.08
Refinement	full-matrix least squares	full-matrix least-squares
R/R_w^2 (obs data)	0.048/0.099	0.079/0.110
R/R_w^2 (all data)	0.080/0.113	0.207/0.154
$\Delta\rho_{max/min}$ (e Å^{-3})	0.244/−0.283	0.291/−0.297
S	1.037	1.01

UM00012579
NOVARTIS EXHIBIT 1017
Novartis v. Regents, IPR2023-01346
Page 1325 of 4460

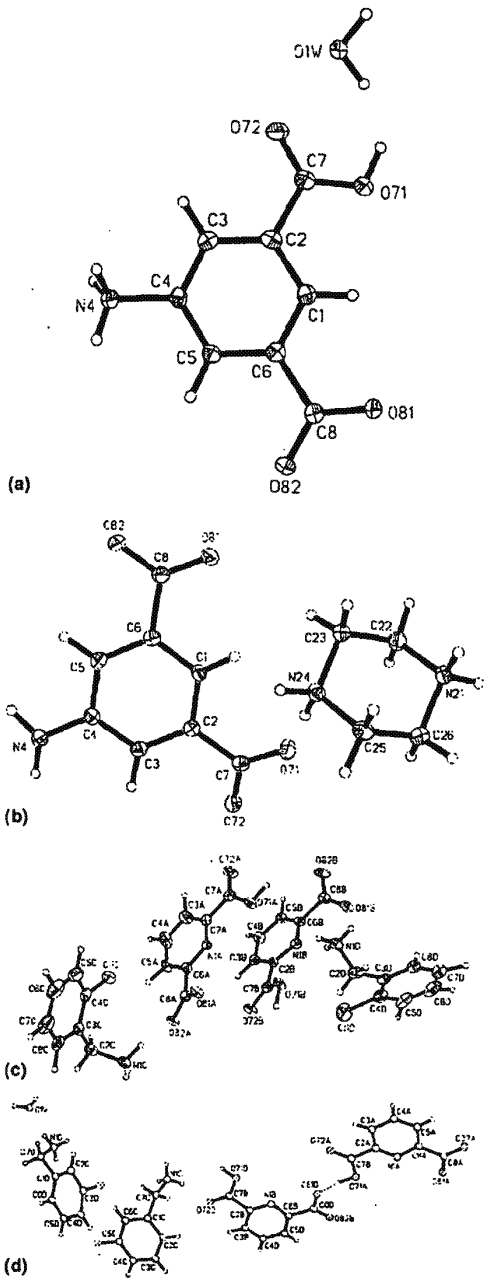


FIGURE 1 Geometry and labeling schemes for **1**–**4** (thermal ellipsoids at 50% for **1**–**3**).

Neighbouring zwitterions are linked by two symmetry related hydrogen bonds, *r*[N(4)–H(41)···O(82) 2.897(2) Å] to form dimeric units, Figure 2, Table II. At the same time, there is a short hydrogen-bond interaction *r*[O(71)–H(710)···O(81) 2.537(2) Å] between ions related by the screw axis parallel to *b*. This interaction, in combination with a C—H···O hydrogen bond (albeit long), gives rise to an infinite sheet of zwitterions, Figure 3. The water molecule is positioned between layers and is connected to neighbouring layers *via* two O—H···O hydrogen bonds, Figure 4. There is half a water molecule per zwitterion.

The structure determination of piperazinium(2+) 5-amino *iso*-phthalate(2–) shows that the amine has removed both acidic protons from the acid. Two symmetry related hydrogen bonds, *r*[N(4)–H(42)···O(72) 3.020(2) Å] link adjacent anions into a dimeric unit, Figure 5, Table III, which is identical to the one observed in the structure of **1**. This motif persists even in the presence of a divalent cation and even though the electronic structure of the acid has changed considerably. The geometric compatibility and the mutual complementarities of the $[-NH_3]^+$ group or $[-NH_2]$ group with the carboxylate functionality in **1** and **2** respectively, are adding considerable stability to the two structures. The robustness of this interaction means that we may consider this dimeric unit to be a new supramolecular synthon [12]. Through a combination of complimentary N—H···O and C—H···O interactions, the anions assemble in

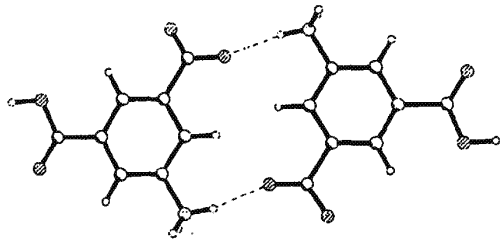


FIGURE 2 The dimeric motif of neighbouring zwitterions in **1**.

UM00012580
NOVARTIS EXHIBIT 1017
Novartis v. Regents, IPR2023-01346
Page 1326 of 4460

TABLE II Geometry of the hydrogen bonds in 1

D—H···A	r(H···A)/Å	r(D···A)/Å	∠(D—H···A)/°
N(4)—H(41)···O(82)^{i}	2.046(2)	2.897(2)	155.42(6)
N(4)—H(42)···O(82)^{ii}	1.816(2)	2.757(2)	166.58(6)
N(4)—H(43)···O(1W)^{iii}	1.849(2)	2.783(2)	169.07(6)
O(71)—H(710)···O(81)^{iv}	1.546(2)	2.537(2)	177.21(7)
O(1W)—H(1W)···O(81)^{v}	1.773(2)	2.735(2)	174.04(5)
C(3)—H(3)···O(72)	2.933(2)	3.880(2)	157.36(5)

Symmetry code: ^{i} −x, −y, 1−z; ^{ii} x, −y, −(1/2)+z; ^{iii} 1−x, −y, −z; ^{iv} (1/2)+x, (1/2)−y, −(1/2)+z; ^{v} (1/2)−x, (1/2)−y, −z.

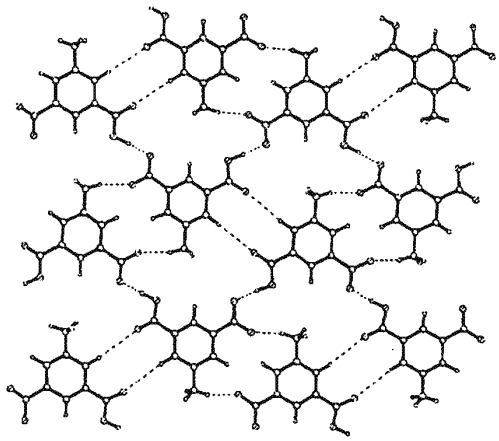


FIGURE 3 Infinite layer in 1.

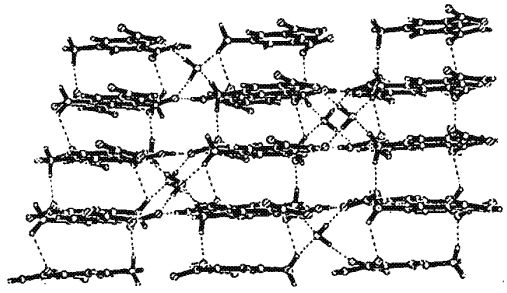


FIGURE 4 Edge-on view of layers of zwitterions bridged by water molecules in 1.

layered manner, although this 2-D motif is very buckled, Figure 6. Each nitrogen atom on the cation is involved in two hydrogen bonds to carboxylate moieties on different anions, Table III, and the cation is providing a bridge between anionic motifs in the same way as the water molecule acts as a 'glue' between layers in **1**.

The structure of **3** has two ion-pairs in the asymmetric unit. The unique anions form infinite chains, parallel with *c*, through short head-to-tail interactions, *r*[O(71B)···O(81B) 2.494(5) and O(71A)···O(81A) 2.505(5) Å] Table IV. Adjacent chains are crosslinked *via* C—H···O interactions which results in infinite 2-D layers. Each layer only contains one type of anion leading to two unique anionic sheets, Figures 7a, b. The anionic layers are arranged in bilayers interconnected *via* three C—H···O interactions. The cations are attached to only one side of each anionic layer *via* three N—H···O hydrogen bonds. The overall packing can be described as alternating bilayers, ..AABBAABB..,

TABLE III Geometry of the hydrogen bonds in 2

D—H···A	r(H···A)/Å	r(D···A)/Å	∠(D—H···A)/°
N(24)—H(242)···O(82)^{i}	1.824(2)	2.728(2)	164.50(6)
N(24)—H(241)···O(71)	1.832(2)	2.690(2)	171.25(6)
N(21)—H(212)···O(72)^{iii}	1.766(2)	2.726(2)	158.77(6)
N(21)—H(211)···O(82)^{iv}	1.858(2)	2.770(2)	126.36(8)
N(4)—H(42)···O(72)^{v}	2.159(2)	3.020(2)	101.79(6)
N(4)—H(41)···O(81)^{vi}	2.040(2)	2.990(2)	117.79(7)
C(5)—H(5)···O(81)^{ii}	2.574(2)	3.378(2)	138.22(5)

Symmetry code: ^{i}2−x, −y, 1−z; ^{ii} x, (1/2)−y, −(1/2)+z; ^{iii} 3−x, −y, 2−z; ^{iv} 2−x, −(1/2)+y, 1(1/2)−z; ^{v} 3−x, −y, 1−z; ^{vi} x, (1/2)−y, −(1/2)+z.

UM00012581
NOVARTIS EXHIBIT 1017
Novartis v. Regents, IPR2023-01346
Page 1327 of 4460

TABLE IV Geometry of the hydrogen bonds in 3

D—H···A	r(H···A)/Å	r(D···A)/Å	∠(D—H···A)/°
N(1D)—H(11D)···O(72B)^{i}	2.019(5)	2.840(4)	152.20(11)
N(1D)—H(12D)···O(82A)^{i}	1.985(4)	2.860(4)	144.80(11)
N(1C)—H(11C)···O(82B)^{v}	2.028(4)	2.822(4)	169.91(11)
N(1C)—H(12C)···O(82A)	1.947(4)	2.853(4)	157.69(11)
O(71A)—H(71A)···O(81A)^{i}	1.522(3)	2.505(5)	159.84(13)
O(71B)—H(71B)···O(81B)^{iii}	1.305(3)	2.494(5)	170.33(16)
C(4A)—H(4A)···O(72A)^{ii}	2.700(5)	3.432(5)	127.13(11)
C(5A)—H(5A)···O(72A)^{ii}	2.756(5)	3.460(5)	122.50(9)
C(3B)—H(3B)···O(82B)^{ii}	2.705(5)	3.439(5)	125.36(10)
C(4B)—H(4B)···O(82A)^{iv}	2.433(5)	3.350(5)	149.29(10)
C(6A)—H(6C)···O(72A)^{vi}	2.494(5)	3.355(5)	139.86(14)
C(7D)—H(7D)···O(81B)^{vii}	2.582(5)	3.462(5)	132.00(12)
N(1D)—H(13D)···N(1B)^{v}	2.146(4)	2.961(4)	160.87(11)
N(1C)—H(13C)···N(1A)^{iii}	2.138(4)	2.990(4)	163.87(11)

Symmetry code: ^{i} x, $(1/2)-y$, $(1/2)-z$; ^{ii} x, $1(1/2)-y$, $z+(1/2)$; ^{iii} x, $(1/2)-y$, $z+(1/2)$; ^{iv} x, $1(1/2)-y$, $(1/2)-z$; ^{v} x, y, $1+z$; ^{vi} $1-x$, $(1/2)-y$, $(1/2)-z$; ^{vii} $-x$, $(1/2)-y$, $(1/2)-z$;

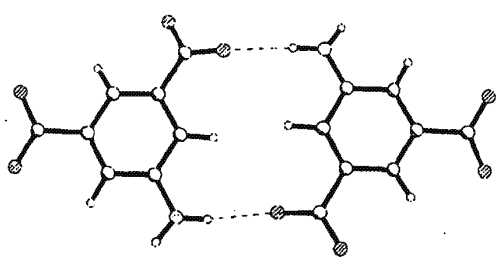


FIGURE 5 The dimeric motif of neighbouring anions in 2.

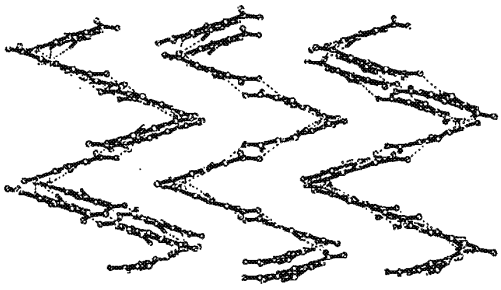


FIGURE 6 Edge-on view of buckled anionic sheets in 2.

Figure 8 and there are no significant Cl···Cl contacts in this structure.

The structure of 4 also contains two unique ion-pairs and the anionic 2-D sheets resulting from anion-anion contacts in 4 have the

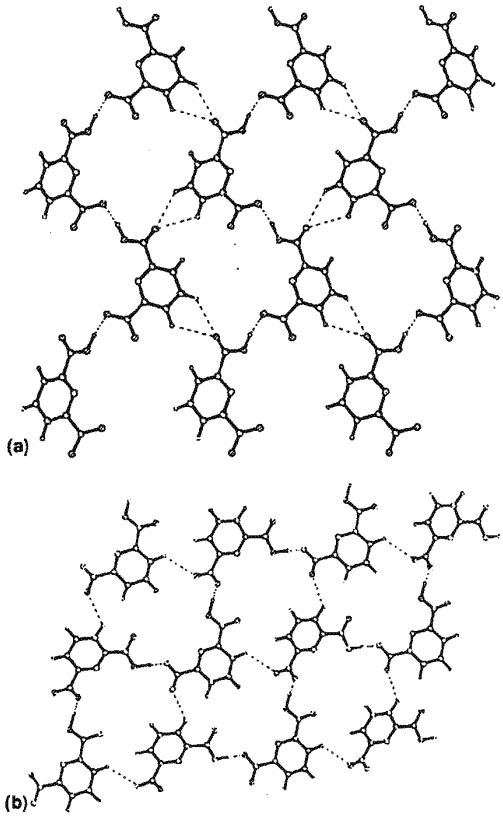


FIGURE 7 The two unique anionic sheets in 3.

UM00012582
NOVARTIS EXHIBIT 1017
Novartis v. Regents, IPR2023-01346
Page 1328 of 4460

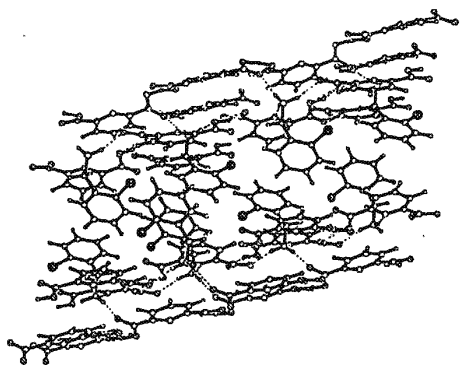


FIGURE 8 Side-ways view of the packing in 3 with alternating bilayers of cations and anions.

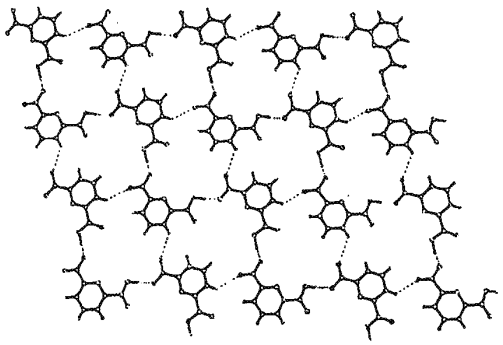


FIGURE 9 The two anions in 4 generate infinite sheets through O—H···O and C—H···O interactions.

same general apperance as the anionic networks in 3, with O···O hydrogen-bond distances of *r*[O(71B)···O(81A) 2.512(9) and O(71A)···O(81B) 2.526(10) Å], Table V. In addition, the two independent anions are present within the same 2-D network, Figure 9. Anionic sheets are arranged in bilayers which are interconnected by two O···O hydrogen bonds involving the water molecule. Again, the overall packing is of the ..AABBAABB.. type, Figure 10, and there are no significant F···F contacts between neighbouring cations.

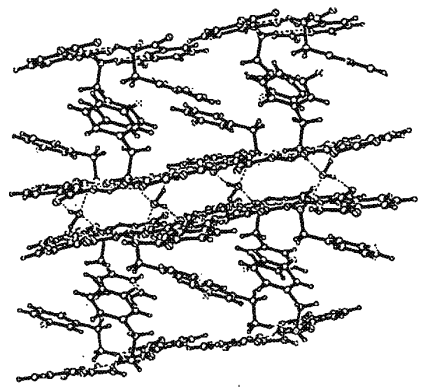


FIGURE 10 Edge-on view of the packing of alternating bilayers of cations and anions in the crystal structure of 4.

Both 5-amino *iso*-phthalic acid and 2,6-dicarboxylic acid pyridine are able to act as building blocks (both in the form of zwitterion, mono-anion and dianion) of reliable extended hydrogen-bonded anionic architectures even in the presence of different counterions and solvent molecules. Consequently, they represent additions to the collection of molecules that may be employed in the supramolecular synthesis of robust and transferable structural scaffolding for new materials. The strength of the carboxylic-carboxylate interaction is emphasised by the fact that replacing $[-NH_3]^+$ or $[-NH_2]$ (in **1** and **2**, respectively) with —CH (on the anion **3** and **4**) has little impact upon the assembly of the extended anionic motifs.

It is also worth pointing out that the overall shape (albeit with very different hydrogen-bonding possibilities) of 5-amino *iso*-phthalic acid is, in some ways, similar to that of trimesic acid which has been used extensively in the design and construction of predictable structures [13]. We intend to further examine how, and to what extent, competition and balance between functional groups on substituted aromatic dicarboxylic acids lead to predictable extended anionic assemblies.

UM00012583
NOVARTIS EXHIBIT 1017
Novartis v. Regents, IPR2023-01346
Page 1329 of 4460

TABLE V Geometry of the hydrogen bonds in 4

D—H···A	r(H···A)/Å	r(D···A)/Å	∠(D—H···A)/°
N(1C)—H(1C3)···O(1W)^{ix}	1.968(14)	2.820(9)	160.10(27)
N(1C)—H(1C1)···O(72B)	1.958(12)	2.819(10)	163.25(28)
N(1C)—H(1C2)···O(81A)^{i}	2.336(10)	2.811(10)	114.62(25)
N(1C)—H(1C2)···O(71A)^{i}	2.584(10)	2.891(9)	100.17(21)
C(4A)—H(4A)···O(1W)^{vi}	2.711(11)	3.419(11)	133.46(23)
N(1D)—H(1D2)···O(1W)	1.915(13)	2.796(9)	167.89(28)
N(1D)—H(1D3)···O(81B)^{i}	2.282(10)	3.988(10)	118.47(26)
N(1D)—H(1D3)···O(71B)^{i}	2.636(9)	2.801(10)	96.28(21)
O(71B)—H(71B)···O(81A)^{i}	1.488(9)	2.512(9)	174.12(36)
O(71A)—H(71A)···O(81B)	1.439(10)	2.526(10)	158.58(35)
O(1W)—H(10W)···O(82B)^{iv}	2.034(9)	2.644(9)	149.13(26)
O(1W)—H(20W)···O(82A)^{v}	1.771(9)	2.711(9)	144.22(31)
C(3A)—H(3A)···O(82B)^{ii}	2.585(12)	3.263(12)	130.09(28)
C(3B)—H(3B)···O(82A)^{iii}	2.706(13)	3.311(13)	123.41(28)
C(3C)—H(3C)···F(1C)^{vii}	2.537(14)	3.275(14)	136.56(30)
C(6D)—H(6D)···F(1D)^{vii}	2.714(13)	3.357(13)	127.01(29)
C(7D)—H(7D)···F(1D)^{vii}	2.614(12)	3.506(12)	153.04(26)
N(1D)—H(1D3)···N(1B)^{i}	2.074(17)	2.946(11)	166.10(25)
N(1C)—H(1C2)···N(1A)^{i}	2.101(11)	2.933(11)	155.29(76)

Symmetry code: $^{i}x, 1-y, z$; $^{ii}x-1, y, z$; $^{iii}1+x, y-1, z$; $^{iv}-x, -y, -z$; $^{v}x, y-2, z$; $^{vi}-1-x, -y, -z$; $^{vii}-1-x, (1/2)+y, (1/2)-z$; $^{viii}-x, -(1/2)+y, (1/2)-z$; $^{ix}-x, -1-y, -z$.

Acknowledgments

Financial support from NSF-EPSCoR (OSR-9550487), Kansas State University, NIDevR and The Queen's University of Belfast.

References

[1] Zerkowski, J. A. and Whitesides, G. M. (1994). *J. Am. Chem. Soc.*, **116**, 4298.

[2] Simard, M., Su, D. and Wuest, J. D. (1991). *J. Am. Chem. Soc.*, **113**, 4696.

[3] Garcia-Tellado, F., Geib, S. J., Goswami, S. and Hamilton, A. D. (1991). *J. Am. Chem. Soc.*, **113**, 9265.

[4] (a) Seto, C. T. and Whitesides, G. M. (1991). *J. Am. Chem. Soc.*, **113**, 9025. (b) Zhao, X., Chang, Y.-L., Fowler, F. W. and Lauher, J. W. (1990). *J. Am. Chem. Soc.*, **112**, 6627. (c) Weber, E., Finge, S. and Csöregh, I. (1991). *J. Org. Chem.*, **56**, 7281. (d) Lehn, J.-M., Mascal, M., DeCian, A. and Fischer, J. (1992). *J. Chem. Soc., Perkin Trans.*, **2**, 461. (e) Subramanian, S. and Zaworotko, M. J. (1992). *Can. J. Chem.*, **71**, 433. (f) Brunet, P., Simard, M. and Wuest, J. D. (1997). *J. Am. Chem. Soc.*, **119**, 2737. (g) Felix, O., Hosseini, M. W., DeCian, A. and Fischer, J. (1997). *Angew. Chem. Int. Ed. Engl.*, **36**, 102.

[5] (a) Seto, C. T. and Whitesides, G. M. (1991). *J. Am. Chem. Soc.*, **113**, 9025. (b) Zhao, X., Chang, Y.-L., Fowler, F. W. and Lauher, J. W. (1990). *J. Am. Chem. Soc.*, **112**, 6627. (c) Subramanian, S. and Zaworotko, M. J. (1992). *Can. J. Chem.*, **71**, 433.

[6] Russel, V. A. and Ward, M. D. (1996). *Chem. Mater.*, **8**, 1654.

[7] Aakeröy, C. B. and Sedden, K. R. (1993). *Chem. Soc. Rev.*, **22**, 397.

[8] Subramanian, S. and Zaworotko, M. (1994). *Coord. Chem. Rev.*, **137**, 357.

[9] (a) Aakeröy, C. B. and Nieuwenhuyzen, M. (1994). *J. Am. Chem. Soc.*, **116**, 10983. (b) Aakeröy, C. B. and Nieuwenhuyzen, M. (1996). *J. Mol. Struct.*, **374**, 223. (c) Aakeröy, C. B., Hughes, D. P. and Nieuwenhuyzen, M. (1996). *J. Am. Chem. Soc.*, **118**, 10134. (d) Russel, V. A. and Ward, M. D. (1996). *Chem. Mater.*, **8**, 1654. (e) Zyss, J., Pecaut, J., Levy, J. P. and Masse, R. (1993). *Acta Cryst.*, **B49**, 334.

[10] Takusagawa, F., Hirotsu, K. and Shimada, A. (1973). *Bull. Chem. Soc. Jpn.*, **A46**, 2020.

[11] Sheldrick, G. M., SHELXL-93, University of Göttingen.

[12] Desiraju, G. R., *Angew. Chem. Int. Ed. Engl.*, **34**, 2311.

[13] Melendez, R. E., Sharma, C. V. K., Zaworotko, M. J., Bauer, C. and Rogers, R. D. (1996). *Angew. Chem. Int. Ed. Engl.*, **35**, 2213.

UM00012584
NOVARTIS EXHIBIT 1017
Novartis v. Regents, IPR2023-01346
Page 1330 of 4460

This Page is Inserted by IFW Indexing and Scanning Operations and is not part of the Official Record

BEST AVAILABLE IMAGES

Defective images within this document are accurate representations of the original documents submitted by the applicant.

Defects in the images include but are not limited to the items checked:

- ☐ BLACK BORDERS
- ☐ IMAGE CUT OFF AT TOP, BOTTOM OR SIDES
- ☐ FADED TEXT OR DRAWING
- ☐ BLURRED OR ILLEGIBLE TEXT OR DRAWING
- ☐ SKEWED/SLANTED IMAGES
- ☐ COLOR OR BLACK AND WHITE PHOTOGRAPHS
- ☐ GRAY SCALE DOCUMENTS
- ☐ LINES OR MARKS ON ORIGINAL DOCUMENT
- ☐ REFERENCE(S) OR EXHIBIT(S) SUBMITTED ARE POOR QUALITY
- ☐ OTHER: _____

IMAGES ARE BEST AVAILABLE COPY.

As rescanning these documents will not correct the image problems checked, please do not report these problems to the IFW Image Problem Mailbox.

DALTON
FULL PAPER

Assembly of 2-D inorganic/organic lamellar structures through a combination of copper(I) coordination polymers and self-complementary hydrogen bonds †

Christer B. Aakeröy,* Alicia M. Beatty and Keith R. Lorimer

Department of Chemistry, Kansas State University, Manhattan, KS 66506, USA. E-mail: aakeroy@ksu.edu

Received 25th April 2000, Accepted 31st May 2000
First published as an Advance Article on the web 10th October 2000

A strategy for the deliberate assembly of lamellar inorganic/organic hybrid materials based on a combination of 1-D coordination polymers and intermolecular hydrogen bonds has been explored. Copper(I) halide coordination polymers provide infinite linear building blocks that are linked into 2-D layers by attaching a pyridine-based ligand to each metal ion. The ligand, which carries a self-complementary hydrogen-bond moiety, provides a selective non-covalent tool for connecting neighboring coordination polymers into a 2-D network. The strategy is illustrated by the crystal structures of $[CuCl(6\text{-Me-3-HO}_2CC_5H_3N)]_n$ and $[CuI(6\text{-Me-3-HO}_2CC_5H_3N)]_n$, both of which display the desired lamellar motifs.

Introduction

The reasons for incorporating metal ions into supramolecular networks are numerous, for example they give access to physical properties that are less common in organic solids *e.g.* magnetic properties, conductivity, and catalytic activity, and metal complexes with hydrogen-bonding capabilities may also be used as chemotherapeutic compounds.[1] Metal ions also display a range of coordination geometries allowing for greater flexibility in constructing materials with specific dimensions and topologies.[2] Supramolecular inorganic/organic hybrid materials have so far been constructed through two principal design philosophies.[3] First, transition-metal complexes can be assembled into coordination polymers using coordinate covalent bonds.[4] This is often achieved by employing bifunctional ligands such as 4,4′-bipyridine as linkers between adjacent metal ions.[5–7] Other examples of coordination polymers include Cu(SCN),[8] and Cu(CN)-based nets,[9] chiral silver assemblies,[10,11] interpenetrating diamondoid structures,[12] and supramolecular macrocycles.[13]

Second, weaker intermolecular forces (notably hydrogen bonding) have been used in deliberate strategies for connecting metal complexes into a wide variety of extended networks.[14–18] These results have shown that hydrogen bonds working in concert are capable of 'maneuvering' large complex ions into desirable motifs, even in the presence of competing cation–anion, solvent–metal ion, and solvent–solvent interactions.

Even though both methods have enjoyed considerable success, there have been few *systematic* attempts at using a combination of these approaches to build lamellar or 3-D hybrid materials.[19] Many coordination polymers containing hydrogen bonds (often involving solvent molecules) have been reported but those interactions are rarely part of a deliberate and predictable strategy for connecting 1-D or 2-D coordination polymers into structures of higher dimensionality. For example, it is doubtful that many practical assembly strategies can be based around versatile (and ultimately unpredictable) hydrogen-bond 'agents' such as water molecules or spherical anions; the multitude of potential hydrogen-bond geometries and interactions of these species limit the potential usefulness of such an approach.

Strategy and relevance

In crystal engineering there has been much interest in developing materials that resemble traditional inorganic zeolites[20,21] and, since selectivity is a particularly important aspect of inclusion chemistry, pore-size control is an important target. The modular approach generally employed in crystal engineering may be a particularly attractive avenue towards new porous materials since network structures can be modified by the geometric and topological characteristics of the individual building blocks. Furthermore, previous work on open-network materials has shown that the void space can occupy as much as 60–70% of the total volume and may be capable of selective guest binding or catalysis.[22]

A common problem in the design of porous inorganic/organic systems arises because most coordination polymers carry an overall positive charge, which means that anions have to be present to balance the charge. Regardless of how these anions are incorporated in the structure, *e.g.* coordinating, non-coordinating, bridging, *etc.*, they will occupy space that may hamper the construction of open channels or void space. Copper(I) halides, however, can form many neutral 1-D polymeric networks, Fig. 1, that can provide starting points for the construction of open framework inorganic–organic structures.

We recently demonstrated how the two common assembly methods for hybrid materials (the design of 1-D coordination polymers; hydrogen-bond based intermolecular synthesis) can be married into one supramolecular synthetic tool.[23] The strategy involves covalently attaching a substituted pyridine ligand to a 1-D copper(I) halide polymer whereupon self-complementary hydrogen-bond moieties on each ligand bridge neighboring coordination polymers *via* directional intermolecular hydrogen bonds. By using 1-D coordination polymers instead of discrete complexes as building blocks, the resulting network is partly 'locked' into place, which facilitates

† Based on the presentation given at Dalton Discussion No. 3, 9–11th September 2000, University of Bologna, Italy.

Electronic supplementary information (ESI) available: rotatable 3-D crystal structure diagram in CHIME format. See http://www.rsc.org/suppdata/dt/b0/b003306p/

DOI: 10.1039/b003306p

This journal is © The Royal Society of Chemistry 2000

UM00012586
NOVARTIS EXHIBIT 1017
Novartis v. Regents, IPR2023-01346
Page 1332 of 4460

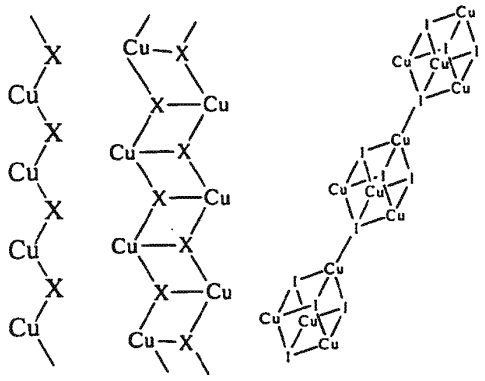


Fig. 1 Examples of coordination polymers formed by copper(I) halides.

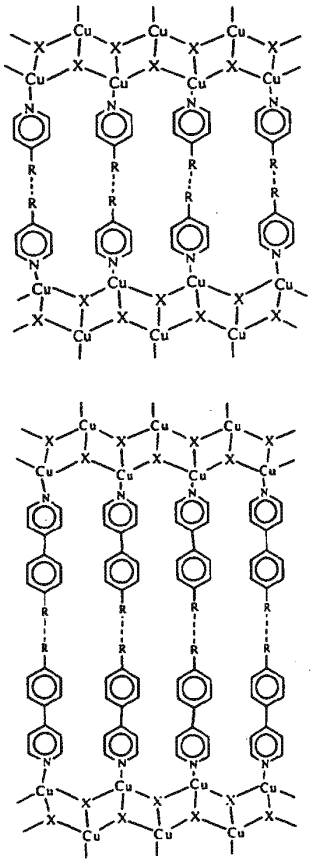


Fig. 2 Coordination polymers held together by predictable and directional hydrogen bonds (R = self-complementary hydrogen-bond moiety). The distance between adjacent chains is controlled by the ligand.

structural prediction and control. Furthermore, ligand size and shape influence the dimensionality and spatial characteristics of the extended network, thus providing a tool for fine-tuning the resulting structure, Fig. 2. In order to explore the use of this approach in the design of new lamellar structures, we report the syntheses and crystal structures of $[CuCl(6\text{-Me-3-HO}_2CC_5H_3N)]_\infty$, **1**, and $[CuI(6\text{-Me-3-HO}_2CC_5H_3N)]_\infty$, **2**.

Experimental

All starting materials were purchased from Aldrich and used as received. Melting points were determined on a Fisher–Johns melting point apparatus and are uncorrected.

Preparations

$[CuCl(6\text{-Me-3-HO}_2CC_5H_3N)]_\infty$, 1. 6-Methylnicotinic acid (0.04 g; 0.29 mmol) and copper(II) chloride dihydrate (0.05 g, 0.29 mmol) were dissolved with heating in ethanol (15 ml). An excess of ascorbic acid was added and heated until it had dissolved. The flask was then stoppered. Yellow rectangular plates crystallized after 24 h, mp >194 °C (decomp.). Yield = 43%.

$[CuI(6\text{-Me-3-HO}_2CC_5H_3N)]_\infty$, 2. Acetonitrile was carefully layered over a solution of 6-methylnicotinic acid in THF. A saturated solution of CuI was then added dropwise to the acetonitrile layer. The layered solutions were allowed to stand in ambient air. Slow diffusion produced fine, yellow needles of compound **2** after 24 h, mp >245 °C (decomp.). Yield = 70%.

X-Ray crystallography

Crystalline samples of compounds **1** and **2** were placed in inert oil, mounted on a glass pin, and transferred to the cold gas stream of the diffractometer. Crystal data were collected and integrated using a Bruker SMART 1000 system with graphite monochromated Mo-Kα ($\lambda = 0.71073$ Å) radiation at 173 K. The structures were solved using heavy-atom methods using SHELXS 97 and refined using SHELXL 97.[24] Non-hydrogen atoms were found by successive full matrix least squares refinement on F^2 and refined with anisotropic thermal parameters. Hydrogen atoms for **1** were located on the difference map and then refined using a riding model with fixed thermal parameters [$U_{ij} = 1.2\ U_{ij}$(eq.) for the atom to which they are bonded] for subsequent refinements. The hydrogen atoms for **2** were placed at calculated positions.

Crystal data for compound 1. $C_7H_7ClCuNO_2$, $M = 236.13$, monoclinic, space group $P2_1/c$, $a = 3.811(2)$, $b = 15.819(7)$, $c = 13.311$ Å, $\beta = 96.045(7)°$, $U = 797.9(6)$ Å^3, $Z = 4$, $T = 173(2)$ K, μ(Mo-Kα) = 3.022 mm^{-1}, $wR2 = 0.1873$ (1796 unique reflections, 1115 observed), $R = 0.0783$ [$I > 2\sigma(I)$].

Crystal data for compound 2. $C_7H_7CuINO_2$, $M = 327.58$, monoclinic, space group $P2_1/c$, $a = 4.096(1)$, $b = 13.656(5)$, $c = 16.114(5)$ Å, $\beta = 92.225(6)°$, $U = 900.7(5)$ Å^3, $Z = 4$, $T = 173(2)$ K, μ(Mo-Kα) = 5.809 mm^{-1}, $wR2 = 0.1613$ (1756 unique reflections, 1382 observed), $R = 0.0614$ [$I > 2\sigma(I)$].

CCDC reference number 186/2014.

See http://www.rsc.org/suppdata/dt/b0/b003306p/ for crystallographic files in .cif format.

Results

The crystal structure of $[CuCl(6\text{-Me-3-HO}_2CC_5H_3N)]_\infty$, **1**, contains a very simple asymmetric unit, Fig. 3(a), but the resulting extended structure is a robust lamellar solid. First, each tetrahedral copper(I) ion is coordinated to three μ_3-Cl ligands which generates a polymeric CuCl 1-D 'staircase'. The 6-methylnicotinic acid ligands are attached to the fourth coordination site of the copper ions through the pyridine nitrogen atom, [Cu(1)–N(1), 2.012(6) Å] and protrude outwards from the polymeric CuCl chain. Adjacent ligands are then hydrogen bonded to each other through acid–acid head-to-head interactions [O(7)···O(8), 2.631(7) Å] forming dimeric motifs. The ligand-based dimers thus act as bridges between CuCl 'staircases' and serve to propagate the 1-D polymeric chains into infinite 2-D layers, Fig. 4. The resulting sheets are non-

UM00012587
NOVARTIS EXHIBIT 1017
Novartis v. Regents, IPR2023-01346
Page 1333 of 4460

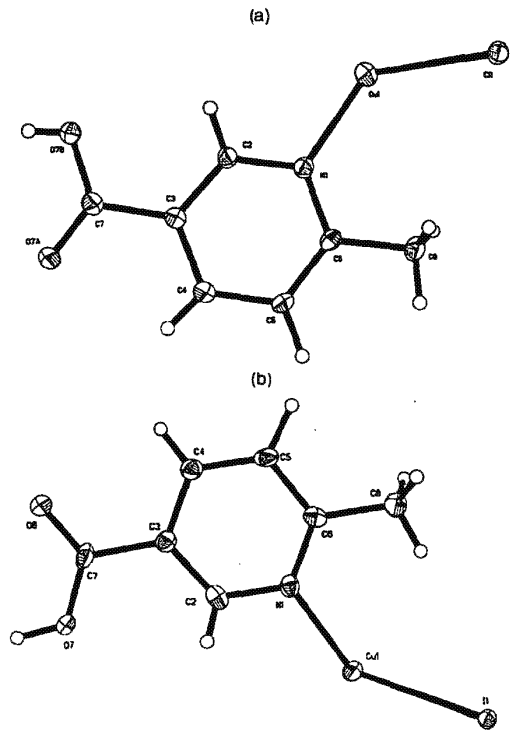


Fig. 3 Thermal ellipsoid plot (30%) and labeling schemes for compounds **1** (a) and **2** (b).

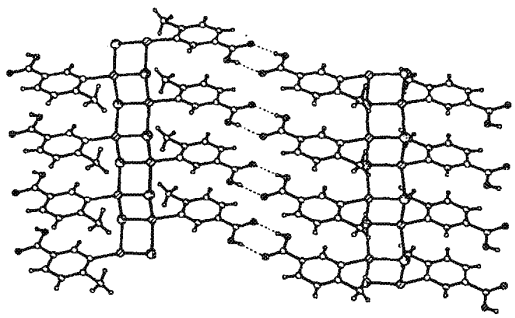


Fig. 4 Infinite 2-D sheet of $[CuCl(6\text{-Me-3-}HO_2CC_5H_3N)]_\infty$, **1**. Adjacent ligands bridge polymeric CuCl staircases *via* self-complementary O–H···O hydrogen bonds.

interpenetrating, slightly buckled, and stack on top of each other. The are no remarkable short contacts or noteworthy aryl–aryl interactions between adjacent sheets.

The crystal structure of $[CuI(6\text{-Me-3-}HO_2CC_5H_3N)]_\infty$, **2**, is very similar to that of **1** with an analogous asymmetric unit, Fig. 3(b). Each copper(I) ion is coordinated to three bridging iodide ligands which leads to 1-D polymeric chains arranged parallel to each other. A fourth coordination site of the metal ion is occupied by 6-methylnicotinic acid [Cu(1)–N(1), 2.06(1) Å] and all ligands protrude outwards from the 1-D CuI chain. As in **1**, the ligands form dimeric motifs through two O–H···O hydrogen bonds [O(7)···O(8), 2.64(1) Å], which subsequently bridge 1-D coordination polymers into 2-D inorganic/organic layers, Fig. 5. The buckled layers are non-interpenetrating and arranged on top of each other to yield a lamellar structure.

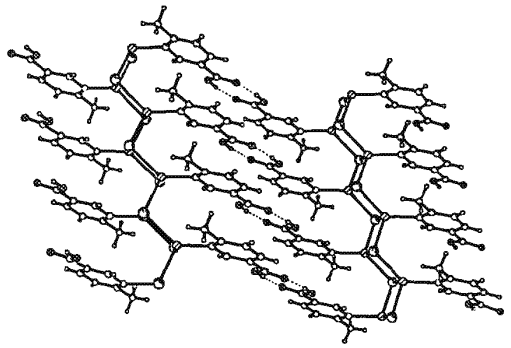


Fig. 5 Infinite 2-D sheet of $[CuI(6\text{-Me-3-}HO_2CC_5H_3N)]_\infty$, **2**. Adjacent ligands bridge polymeric CuI staircases *via* self-complementary O–H···O hydrogen bonds.

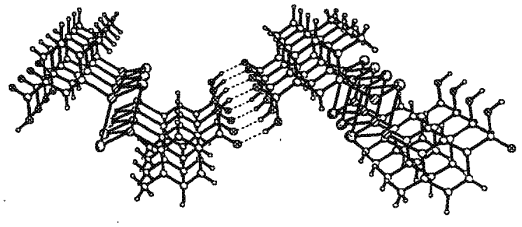


Fig. 6 Sideways view of an undulating layer in compound **2**. The layer is buckled due to the position of the hydrogen-bond moiety with respect to the pyridine nitrogen atom.

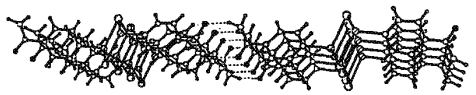


Fig. 7 Sideways view of a planar layer in $[CuI(4\text{-}H_2NCOC_5H_4N)]_\infty$.[23] The layer has a flat appearance due to the linearity of the bridging ligands.

Discussion

The structures of compounds **1** and **2** are almost identical to those of $[CuI(NC_5H_4CHNOH\text{-}3)]_\infty$, **3**,[24] $[CuI(4\text{-}H_2NCOC_5H_4N)]_\infty$, **4**,[24] and $[CuCl(4\text{-}HO_2CC_5H_4N)]_\infty$, **5**,[25] where infinite 1-D coordination polymers are interconnected into 2-D layers through a combination of coordinate–covalent bonds and intermolecular hydrogen bonds. In each case, the short axis of the unit cell corresponds to the separation of copper ions along the staircase (3.8 Å for **1**, 3.7 Å for **5**, and 4.1 Å for **2**–**4**). In all five structures the 1-D CuX polymers are aligned parallel with each other, but the separation between them is governed by the length of the ancillary ligands and by the position of the hydrogen-bonding moiety. This family of structures is also similar to Cu^IX architectures where copper–halide staircases are interconnected through covalent bonds by bridging bidentate ligands *e.g.* pyrazine[26] and pyrimidine.[27] The precise shape of the 2-D layers in all of these cases is determined by the ligand design (angle between coordination sites) or substituent position on the intermolecular connector. Pyridine derivatives with hydrogen-bond functionalities in the *ortho* position, as well as covalent bridging ligands with an angle between N-donors, create more undulating layers, Fig. 6. On the other hand, more 'linear' ligands and *para*-substituted hydrogen-bond connectors display planar sheets, Fig. 7.

The strategy presented here for the assembly of 2-D inorganic/organic structures has shown considerable versatility and reliability: (i) three different self-complementary hydrogen-bond functionalities (oxime, amide, and carboxylic acid) have

UM00012588
NOVARTIS EXHIBIT 1017
Novartis v. Regents, IPR2023-01346
Page 1334 of 4460

been successfully employed as directional non-covalent bridges; (ii) the layers can 'tolerate' or accommodate certain ligand modifications by changing from planar to undulating structures; and (iii) the structures are insensitive to small variations in intra-chain metal–metal separations and differences in the size of the bridging halide ligand. The structural consistency in these compounds is a result of using infinite 1-D chains as building blocks. Since the coordination polymers have a well defined geometry, they are structurally reliable and therefore reduce the task of predicting and controlling the resulting structure to a much simpler problem.

By extending this combined coordination polymer/hydrogen-bond design strategy, it is possible to envisage using a 'pre-formed' 2-D coordination polymer in combination with suitable organic hydrogen-bonding linkers to obtain custom-built porous solids with tunable pore sizes for a variety of host–guest applications. Further development and applications of this design principle are currently underway in our laboratories.

Acknowledgements

We acknowledge an FDA Award from Kansas State University (for C. B. A.) and financial support from the National Science Foundation.

References

1 Y. M. Qian, A. Vogt, A. Vasudevan, S. M. Sebti and A. D. Hamilton, *Bioorg. Med. Chem.*, 1998, **6**, 293.
2 B. F. Abrahams, S. R. Batten, H. Hamit, B. F. Hoskins and R. Robson, *Angew. Chem., Int. Ed. Engl.*, 1996, **35**, 1690; Crystal engineering: From molecules and crystals to materials, A NATO Advanced Study Institute and a Euroconference, eds. D. Braga, F. Grepioni and A. G. Orpen, Erice, 1999, p. 58.
3 C. B. Aakeröy, *Acta Crystallogr., Sect. B*, 1997, **53**, 569.
4 Z. Wang, R.-G. Xioing, B. M. Foxman, S. R. Wilson and W. Lin, *Inorg. Chem.*, 1999, **38**, 1523; G. K. H. Shimizu, G. D. Enright, C. I. Ratcliffe, J. A. Ripmeester and D. D. M. Wayner, *Angew. Chem., Int. Ed.*, 1998, **37**, 1407; K. Biradha, C. Seward and M. J. Zaworotko, *Angew. Chem., Int. Ed.*, 1999, **38**, 492; K. A. Hirsch, S. R. Wilson and J. S. Moore, *Chem. Commun.*, 1998, 13; S. W. Keller, *Angew. Chem., Int. Ed. Engl.*, 1997, **36**, 247; L. Carlucci, G. Ciani, P. Macchi and D. M. Proserpio, *Chem. Commun.*, 1998, 1837.
5 S. B. Copp, S. Subramanian and M. J. Zaworotko, *J. Am. Chem. Soc.*, 1992, **114**, 8719; S. Subramanian and M. J. Zaworotko, *Angew. Chem., Int. Ed. Engl.*, 1995, **34**, 2127; M. J. Zaworotko, *Chem. Soc. Rev.*, 1994, **23**, 283.
6 O. M. Yaghi and H. Li, *J. Am. Chem. Soc.*, 1996, **118**, 295; *Angew. Chem., Int. Ed. Engl.*, 1995, **34**, 207; M. Fujita, Y.-J. Kwon, S. Osamu, K. Yamaguchi and K. Ogura, *J. Am. Chem. Soc.*, 1995, **117**, 7287.
7 M. Fujita, Y.-J. Kwon, S. Washizu and K. Ogura, *J. Am. Chem. Soc.*, 1994, **116**, 1151.
8 Q.-M. Wang, G.-C. Guo and T. C. W. Mak, *Chem. Commun.*, 1999, 1849; A. J. Blake, N. R. Brooks, N. R. Champness, M. Crew, L. R. Hanton, P. Hubberstey, S. Parsons and M. Schröder, *J. Chem. Soc., Dalton Trans.*, 1999, 2813.
9 O. Teichert and W. S. Sheldrick, *Z. Anorg. Allg. Chem.*, 1999, **625**, 1860.
10 T. M. Garrett, U. Koert, J.-M. Lehn, A. Rigault, D. Meyer and J. Fischer, *J. Chem. Soc., Chem. Commun.*, 1990, 557.
11 A. J. Blake, N. R. Champness, P. A. Cooke and J. E. B. Nicolson, *Chem. Commun.*, 2000, 665.
12 A. J. Blake, N. R. Champness, S. S. M. Chung, W.-S. Li and M. Schroder, *Chem. Commun.*, 1997, 1005; K. A. Hirsch, D. Venkataraman, S. R. Wilson, J. S. Moore and S. Lee, *J. Chem. Soc., Chem. Commun.*, 1995, 2199.
13 C. M. Drain, K. C. Russell and J.-M. Lehn, *Chem. Commun.*, 1996, 337.
14 C. B. Aakeröy, A. M. Beatty and D. S. Leinen, *Angew. Chem., Int. Ed.*, 1999, **38**, 1815.
15 C. B. Aakeröy, A. M. Beatty and D. S. Leinen, *J. Am. Chem. Soc.*, 1998, **120**, 7383.
16 C. B. Aakeröy and A. M. Beatty, *Chem. Commun.*, 1998, 1067.
17 A. S. Batsanov, P. Hubberstey, C. E. Russel and P. H. Walton, *J. Chem. Soc., Dalton Trans.*, 1997, 2667; C.-W. Chan, D. M. P. Mingos and D. J. Williams, *J. Chem. Soc., Dalton Trans.*, 1995, 2469; J. C. M. Rivas and L. Brammer, *New J. Chem.*, 1998, **22**, 1315.
18 A. D. Burrows, D. M. P. Mingos, A. J. P. White and D. Williams, *Chem. Commun.*, 1996, 97.
19 M. Munakata, L. P. Wu, M. Yamamoto, T. Kuroda-Sowa and M. Maekawa, *J. Am. Chem. Soc.*, 1996, **118**, 3117.
20 T. Iwamoto, S. Nishikiori, T. Kitazawa and H. Yuge, *J. Chem. Soc., Dalton Trans.*, 1997, 4127.
21 O. M. Yaghi, H. Li, H. C. Davis, C. D. Richardson and T. L. Groy, *Acc. Chem. Res.*, 1998, **31**, 474.
22 P. Brunet, M. Simard and J. D. Wuest, *J. Am. Chem. Soc.*, 1997, **119**, 2737.
23 C. B. Aakeröy, A. M. Beatty, D. S. Leinen and K. R. Lorimer, *Chem. Commun.*, 2000, 935.
24 G. M. Sheldrick, SHELXS 97 and SHELXL 97, University of Göttingen, 1997.
25 M. A. S. Goher and T. C. W. Mak, *Inorg. Chim. Acta*, 1985, **101**, L27.
26 S. Kawata, S. Kitagawa, H. Kumagai, S. Iwabuchi and M. Katad, *Inorg. Chim. Acta*, 1998, **267**, 143.
27 A. J. Blake, N. R. Brooks, N. R. Champness, P. A. Cooke, M. Crew, A. M. Deveson, L. R. Hanton, P. Hubberstey, D. Fenske and M. Schröder, *Cryst. Eng.*, 1999, **2**, 181.

UM00012589
NOVARTIS EXHIBIT 1017
Novartis v. Regents, IPR2023-01346
Page 1335 of 4460

Pergamon

Crystal Engineering, Vol. 1, Nos. 3/4, pp. 225–241, 1998
Copyright © 1999 Elsevier Science Ltd
Printed in the USA. All rights reserved
0025-5408/98 $19.00 + .00

PII S0025-5408(98)00197-4

BUILDING ORGANIC ASSEMBLIES WITH 2-PYRIDONE AND DICARBOXYLIC ACIDS: RELATING MOLECULAR CONFORMATION AND SYNTHON STABILITY TO CRYSTAL STRUCTURE

C.B. Aakeröy*, A.M. Beatty, and Min Zou
Department of Chemistry, Kansas State University, Manhattan, Kansas, 66506, USA

(Refereed)
(Received August 17, 1998; Accepted September 7, 1998)

ABSTRACT

The syntheses and crystal structures of five cocrystals; 2-pyridone oxalic acid (2/1), 2-pyridone succinic acid (2/1), 2-pyridone adipic acid (2/1) dihydrate, 2-pyridone suberic acid (2/1), and 2-pyridone sebacic acid (2/1), are reported. The competition between two similar self-complementary hydrogen-bonded synthons (carboxylic acid and 2-pyridone) are examined systematically in this series of cocrystals. In each case, the crystal structure contains planar dimers of 2-pyridone which are bridged by a dicarboxylic acid *via* a combination of C–H · · · O and O–H · · · O hydrogen bonds to generate infinite 1-D ribbons. The orientation of these ribbons is determined by changes in molecular shape and conformational flexibility of the dicarboxylic acid. © *1999 Elsevier Science Ltd*

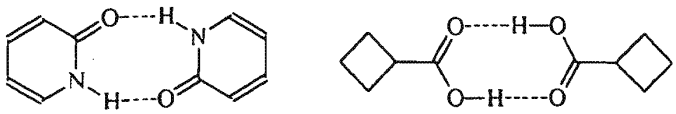
KEYWORDS: 2-pyridone, dicarboxylic acid, hydrogen bonding, crystal structure

INTRODUCTION

The field of crystal engineering is largely defined by intermolecular interactions and consequently we need to acquire a detailed and comprehensive understanding of the balance between, and the structural effects of, various intermolecular forces [1]. The strength and directionality of the hydrogen bond have made it the most prominent "tool" for intermolecular synthesis, but the outcome of competitions between different hydrogen-bond donors and acceptors in a crystalline solid is often unpredictable. Two goals in the development of design

*To whom correspondence should be addressed.

UM00012590
NOVARTIS EXHIBIT 1017
Novartis v. Regents, IPR2023-01346
Page 1336 of 4460



A B

SCHEME 1

(A) Hydrogen-bonded dimer formed by two 2-pyridone moieties. (B) Head-to-head dimer of two carboxylic acid moieties.

strategies for supramolecular synthesis are "specificity" and "transferability," and many functional groups have been explored in attempts to identify reliable connectors for the construction of predictable architectures. In this context, an intriguing analogy between covalent and supramolecular synthesis has been formulated with the introduction of the term 'intermolecular synthon'; a robust, transferable connector that can be used for linking molecules (not molecular fragments as in covalent synthesis) into predictable aggregates [2]. An elegant way of probing the relative strength of competing hydrogen bonds was pioneered by Etter and co-workers using cocrystallization techniques [3], and they were able to obtain invaluable information about preferred packing patterns and relative hydrogen-bond strengths of various donors/acceptors through structural studies series of related cocrystals.

Many of the best-known intermolecular connectors rely on the complementarity of two hydrogen-bonding moieties. Examples of such connectors include carboxylic acid/2-amino-pyridine [4], carboxylic acid/urea [5], amides/acids [6], and hydroxy/amino [7]. The robustness and reliability of the self-complementary 2-pyridone moiety, Scheme 1A, has also been utilized for crystal engineering: Wuest and co-workers have constructed several low-dimensional [8] and diamondoid [9] assemblies based upon intermolecular hydrogen bonds between neighboring 2-pyridone moieties.

Although 2-pyridone moieties are known to form rigid dimers in the solid state, the crystal structure of 2-pyridone itself [10] actually displays a catemer motif, indicating that it is possible to obtain alternative intermolecular arrangements of comparable energy with this moiety. The most well-known hydrogen bond motif, however, is arguably the carboxylic acid head-to-head dimer [11], Scheme 1B, which has been utilized extensively in crystal engineering both in the organic and the inorganic/organic solid state [1], despite the fact that carboxylic acids do engage in a variety of intermolecular hydrogen bonds and this synthon is not as reliable as initially thought [12].

One of the key challenges in crystal engineering is being able to predict the structural outcome of a combination of two self-complementary moieties that also can interact with each other. The carboxylic acid and 2-pyridone groups represent two such moieties; both are self-complementary, but they also have the potential to form heteromeric dimers. In order to examine the competition between these hydrogen-bond sites, we have determined the crystal structures of five cocrystals: 2-pyridone oxalic acid (2/1) **1**, 2-pyridone succininc acid (2/1) **2**, 2-pyridone adipic acid (2/1) dihydrate **3**, 2-pyridone suberic acid (2/1) **4**, and 2-pyridone sebacic acid (2/1) **5**. This series of compounds, which includes all even-numbered dicarboxylic acids in the range of two to ten carbon atoms, also allows us to investigate possible changes in crystal packing as a function of small but well-defined modifications to the molecular geometry. This also facilitates an examination of how increases in size and conformational flexibility are manifested in the resulting crystal structures.

UM00012591
NOVARTIS EXHIBIT 1017
Novartis v. Regents, IPR2023-01346
Page 1337 of 4460

TABLE 1
Data Collection and Refinement for **1** to **5**

Crystal data	**1**	**2**	**3**	**4**	**5**
Empirical formula	$C_6H_6NO_3$	$C_7H_8NO_3$	$C_8H_{12}NO_4$	$C_9H_{12}NO_3$	$C_{20}H_{28}N_2O_6$
CCDC deposit no.	CCDC-1294/57	CCDC-1294/58	CCDC-1294/59	CCDC-1294/60	CCDC-1294/61
MW	140.12	154.14	186.19	182.20	392.44
Crystal size (mm)	0.4 × 0.3 × 0.3	0.8 × 0.4 × 0.3	0.3 × 0.3 × 0.2	0.7 × 0.4 × 0.3	0.5 × 0.3 × 0.1
Crystal system	Triclinic	Monoclinic	Triclinic	Monoclinic	Triclinic
Space group	P-1	$P2_1/n$	P-1	I2/a	P-1
a (Å)	3.7694 (4)	8.461 (1)	5.1851 (9)	18.247 (2)	5.1823 (4)
b (Å)	9.1728 (8)	5.2036 (6)	7.441 (2)	5.3696 (4)	13.422 (2)
c (Å)	9.906 (1)	16.321 (1)	12.768 (2)	19.254 (3)	14.870 (2)
α (deg)	109.607 (7)	90	78.52 (2)	90	78.603 (9)
β (deg)	98.83 (1)	99.122 (9)	85.809 (11)	90.679 (5)	89.708 (8)
γ (deg)	97.666 (8)	90	70.78 (2)	90	86.919 (6)
Volume (Å^3)	312.47 (6)	709.5 (1)	455.9 (2)	1886.4 (4)	1012.5 (2)
Z	2	4	2	8	2
D_{calc} (g cm^{-3})	1.489	1.443	1.356	1.283	1.287
F (000)	146	324	198	776	420
μ, Mo-K_α (mm^{-1})	0.122	0.114	0.109	0.097	0.095
Temp (K)	173 (2)	173 (2)	173 (2)	173 (2)	173 (2)
R/R^2_w (obs. data)	0.0379/0.1009	0.0348/0.0918	0.0596/0.1706	0.0372/0.0947	0.0519/0.1175
R/R^2_w (all data)	0.0505/0.1075	0.0369/0.0939	0.0625/0.1773	0.0448/0.1007	0.0874/0.1348

EXPERIMENTAL

Preparation of 2-Pyridone Oxalic Acid (2/1). 2-Pyridone (0.21 g, 2.22 mmol) and oxalic acid (0.20 g, 2.22 mmol) were dissolved together in hot methanol (50 mL). A colorless, needle-like precipitate was collected by filtration and slowly recrystallized from water to produce rectangular prism-shaped crystals after 3 weeks (m.p. 156–158°C).

Preparation of 2-Pyridone Succinic Acid (2/1). 2-Pyridone (0.16 g, 1.69 mmol) was dissolved in hot water (50 mL) together with succinic acid (0.2 g, 1.69 mmol). Trigonal pyramidal, colorless crystals were formed after 3 weeks upon evaporation of the solvent (m.p. 167–170°C).

Preparation of 2-Pyridone Adipic Acid (2/1) Dihydrate. 2-Pyridone (0.13 g, 1.37 mmol) and adipic acid (0.20 g, 1.37 mmol) were dissolved together in hot water-ethanol (1:1) mixture (50 mL). The solution was filtered, producing irregular, colorless crystals which were recrystallized from THF to produce rectangular prism-like crystals after 2 weeks (m.p. 75–79°C).

Preparation of 2-Pyridone Suberic Acid (2/1). 2-Pyridone (0.11 g, 1.15 mmol) was dissolved in hot water (25 mL) and added to a solution of suberic acid (0.2 g, 1.15 mmol) in

UM00012592
NOVARTIS EXHIBIT 1017
Novartis v. Regents, IPR2023-01346
Page 1338 of 4460

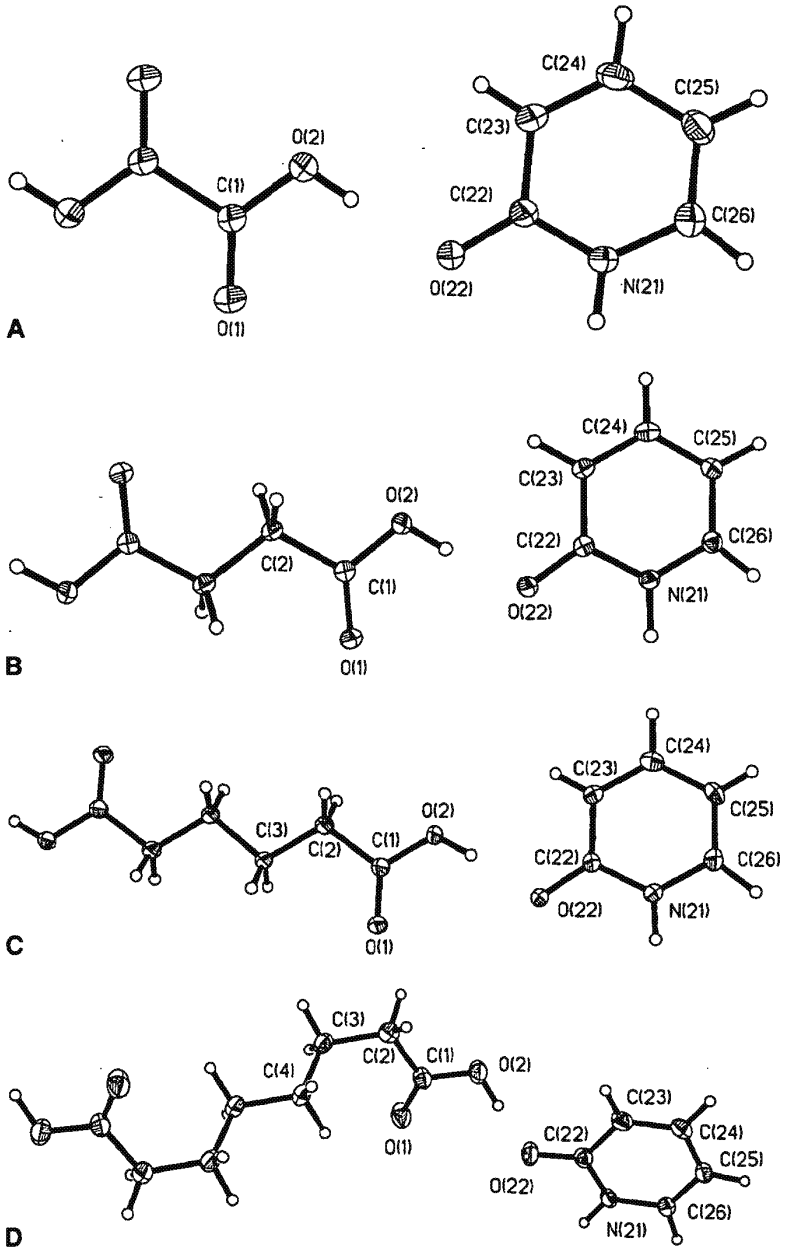
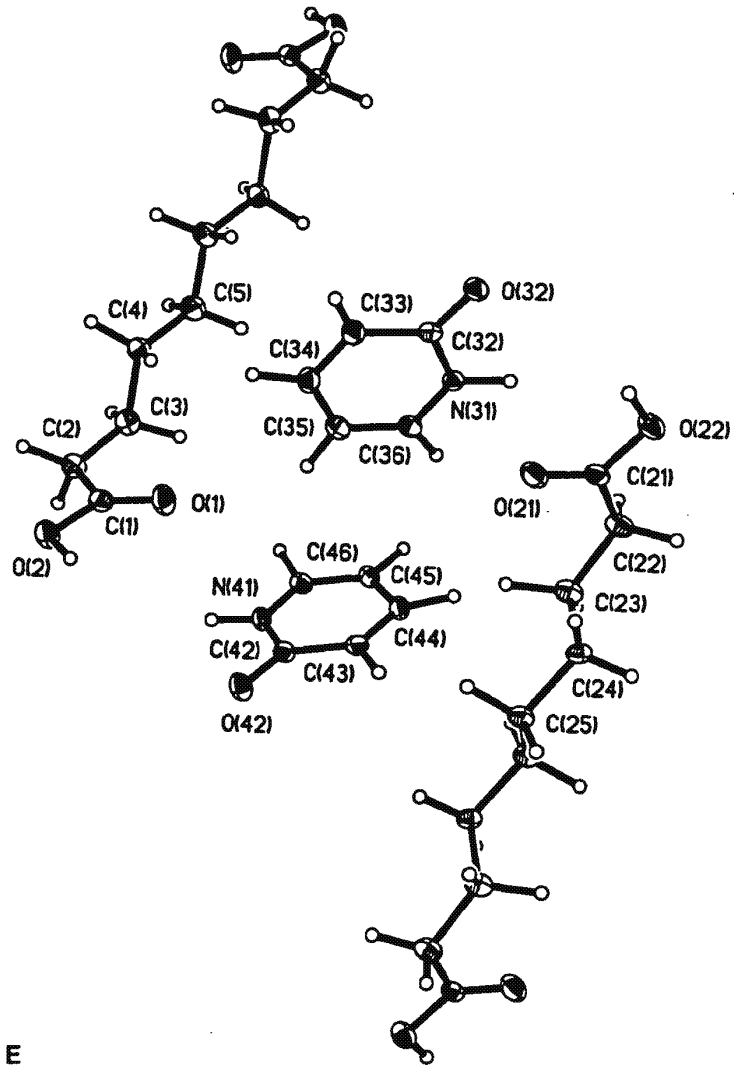


FIG. 1

(A) Molecular structure and labeling scheme (asymmetric unit) for **1** (30% thermal ellipsoids).
(B) Molecular structure and labeling scheme (asymmetric unit) for **2** (30% thermal ellipsoids).
(C) Molecular structure and labeling scheme (asymmetric unit) for **3** (30% thermal ellipsoids).
(D) Molecular structure and labeling scheme (asymmetric unit) for **4** (30% thermal ellipsoids).
(E) Molecular structure and labeling scheme (asymmetric unit) for **5** (30% thermal ellipsoids).

UM00012593
NOVARTIS EXHIBIT 1017
Novartis v. Regents, IPR2023-01346
Page 1339 of 4460



E

FIG. 1
(Continued)

hot ethanol (25 mL). Platelike, colorless crystals were collected by filtration and recrystallized in THF to produce hexagonal, colorless crystals after 2 weeks (m.p. 80–82°C).

Preparation of 2-Pyridone Sebacic Acid (2/1). 2-Pyridone (0.094 g, 0.99 mmol) was dissolved in hot water (25 mL) and added to a solution of sebacic acid (0.2 g, 0.99 mmol) in hot ethanol (25 mL). Platelike, colorless microcrystals were collected by filtration and recrystallized from THF to produce hexagonal, colorless crystals after 2 weeks (m.p. 98–100°C).

UM00012594
NOVARTIS EXHIBIT 1017
Novartis v. Regents, IPR2023-01346
Page 1340 of 4460

TABLE 2
Geometry of the Hydrogen Bonds for **1**

D–H · · · A	*r*(H · · · A)/Å	*r*(D · · · A)/Å	∠(D–H · · · A)/°
N21–H21 · · · O22^{i}	1.912 (2)	2.801 (2)	167.66 (5)
02–H2A · · · 022	1.735 (2)	2.582 (2)	170.83 (6)
C24–H24 · · · O2^{ii}	2.568 (2)	3.493 (2)	172.29 (5)
C25–H25 · · · O1^{iii}	2.677 (2)	3.363 (2)	127.89 (4)
C26–H26 · · · O1^{i}	2.576 (2)	3.440 (2)	145.32 (4)

Symmetry codes: i) −x, 2 − y, 2 − z; ii) 1 − x, 1 − y, 2 − z; iii) 1 + x, 1 − y, 2 − z.

X-Ray Crystallography. Crystal data were collected using a Siemens P4 four-circle diffractometer with graphite monochromated Mo-Kα radiation. Hydrogen-atom positions were located from difference Fourier maps (except for the hydrogen atoms on the water molecule in **3**, which were not located), and a riding model with fixed thermal parameters [u_{ij} = $1.2U_{ij}$(eq) for the atom to which they are bonded] was used for subsequent refinements. The weighting function applied was $w^{-1} = [\sigma^2(F_o^2) + (g_1P)^2 + (g_2P)]$ where $P = [F_o^2 + 2F_c^2]/3$. The SHELXTL PC and SHELXL-93 packages were used for data reduction and structure solution and refinement [13]. Table 1 contains crystallographic details and Figure 1a–e displays labeling schemes and thermal ellipsoids for **1** to **5**.

RESULTS

In all five cases, the reaction of 2-pyridone with a solution of a dicarboxylic acid resulted in a cocrystal, with two pyridone molecules for each molecule of dicarboxylic acid (in the case of **3**, two water molecules were also incorporated in the lattice). Furthermore, in each case, the dicarboxylic acid was located on an inversion center, leading to an asymmetric unit consisting of one pyridone molecule for one half of a dicarboxylic acid.

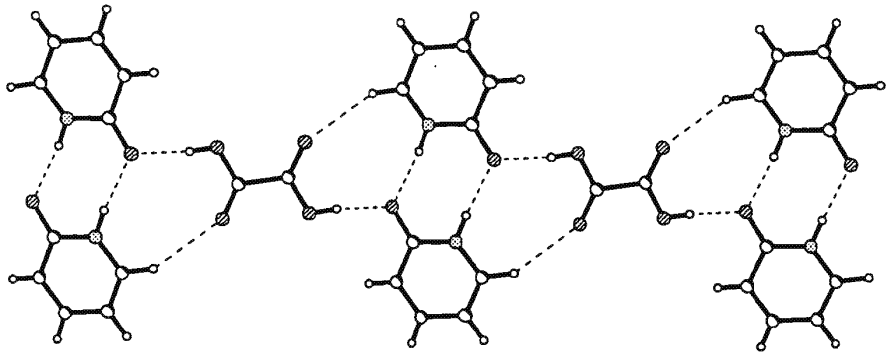


FIG. 2
Hydrogen-bonded ribbon in **1** with alternating pyridone dimers and oxalic acid molecules.

UM00012595
NOVARTIS EXHIBIT 1017
Novartis v. Regents, IPR2023-01346
Page 1341 of 4460

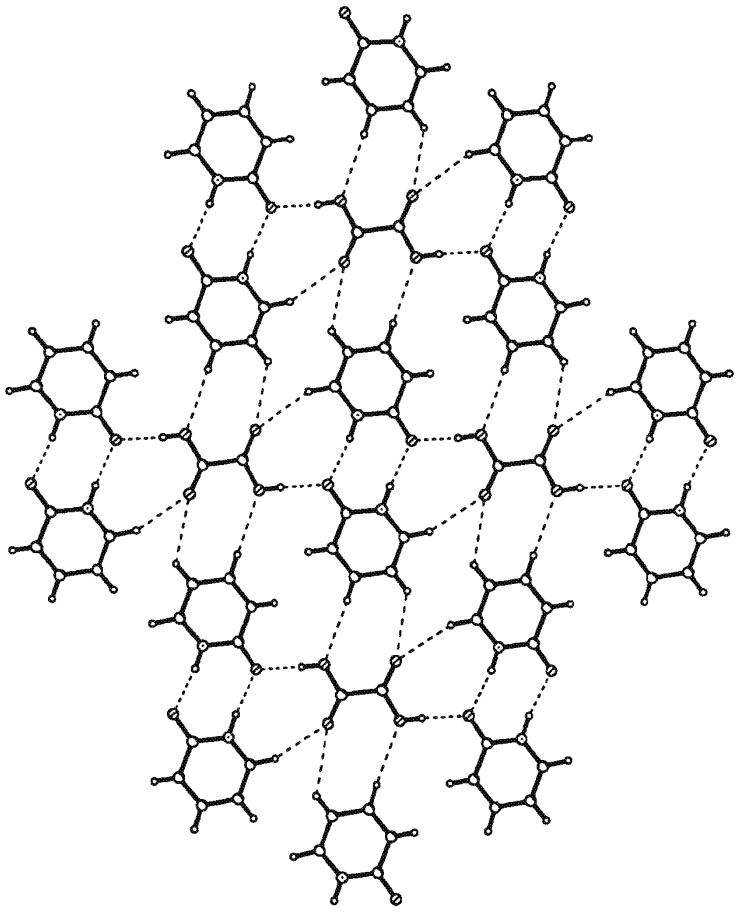


FIG. 3
An infinite layer in **1**, held together by N–H · · · O, O–H · · · O, and C–H · · · O hydrogen bonds.

As expected, the pyridone tautomer was present in all structures (instead of the pyridol form) as evidenced by the exocyclic C–O bond distance (1.265–1.275 Å), which is considerably shorter than the C–O(H) bond distances noted in 6-chloro-2-hydroxypyridine (1.35 Å) [14] and 3-hydroxypyridine (1.32 Å) [15]. Further support of the pyridone tautomer was provided by the location of the hydrogen atom on the amide nitrogen from a difference map in all cases **1** to **5**.

In **1**, the two carboxylic acid moieties are coplanar with each other resulting in an overall planar conformation of oxalic acid. The 2-pyridone molecules form dimers *via* two symmetry-related N–H · · · O hydrogen bonds (Table 2). Neighboring dimers are then connected by a molecule of oxalic acid through a short O–H · · · O and a C–H · · · O hydrogen bond (Fig. 2). These interactions lead to infinite chains of dimer · · · acid · · · dimer · · · acid groups. Adjacent chains are further organized into infinite layers stabilized by two C–H · · · O hydrogen bonds. Since the pyridone dimers and oxalic acid molecules within chains are not

UM00012596
NOVARTIS EXHIBIT 1017
Novartis v. Regents, IPR2023-01346
Page 1342 of 4460

TABLE 3
Geometry of the Hydrogen Bonds for **2**

D–H · · · A	*r*(H · · · A)/Å	*r*(D · · · A)/Å	∠(D–H · · · A)/°
$N21^{i}$–$H21^{i}$ · · · O22	1.754 (2)	2.787 (2)	171.61 (6)
O2–H2A · · · O22	1.658 (2)	2.594 (2)	171.07 (6)
$C24^{ii}$–$H24^{ii}$ · · · O2	2.462 (2)	3.331 (2)	146.37 (5)
$C24^{iii}$–$H24^{iii}$ · · · O1	2.659 (2)	3.330 (2)	125.34 (5)
$C26^{i}$–$H26^{i}$ · · · O1	2.346 (2)	3.311 (2)	160.40 (5)

Symmetry codes: i) 1 − x, −y, 1 − z; ii) ½ + x, ½ − y, ½ + z; iii) 1½ − x, ½ + y, ½ − z.

coplanar, the result is a slightly buckled infinite layer (Fig. 3). There are no hydrogen bonds between layers and the orientation and distance between neighboring aromatic rings indicate an absence of any influential π-π interactions in **1**.

In **2**, the molecular conformation of succinic acid is antiperiplanar with a 180° torsion angle of the carbon backbone. Similar to **1**, the carboxylic moiety is coplanar with the carbon backbone, ∠[O(1)–C(1)–C(2)–C(2A)] 3.6°, leading to a planar conformation of succinic acid. The 2-pyridone molecules assemble into dimers *via* symmetry-related N–H · · · O hydrogen bonds (Table 3). As in **1**, the acid molecules link adjacent pyridone dimers together into infinite chains through two hydrogen bonds, O–H · · · O and C–H · · · O (Fig. 4). Pyridone dimers and succinic acid molecules within chains are in the same plane, resulting in a flat one-dimensional ribbon. These ribbons are not arranged in layers, as in **1**; instead adjacent ribbons are oriented nearly perpendicular to each other (*ca.* 82°) leading to an

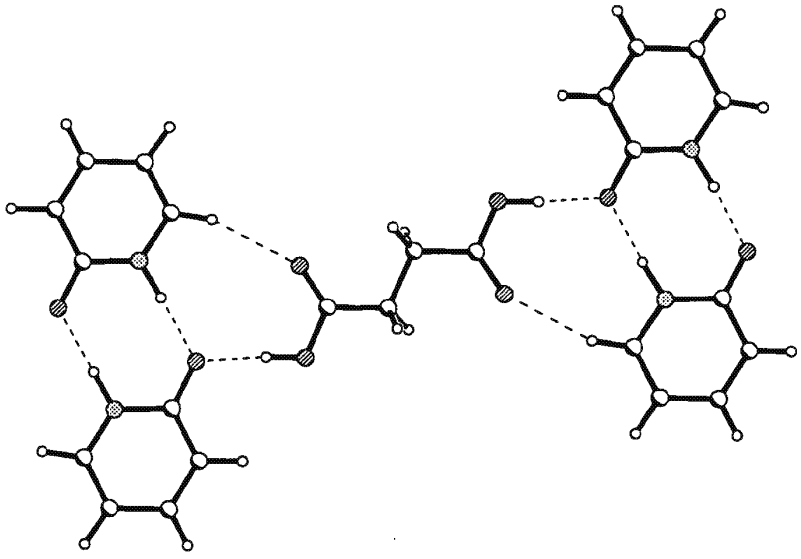


FIG. 4
2-pyridone dimers held together by a succinic acid molecule in **2**.

UM00012597
NOVARTIS EXHIBIT 1017
Novartis v. Regents, IPR2023-01346
Page 1343 of 4460

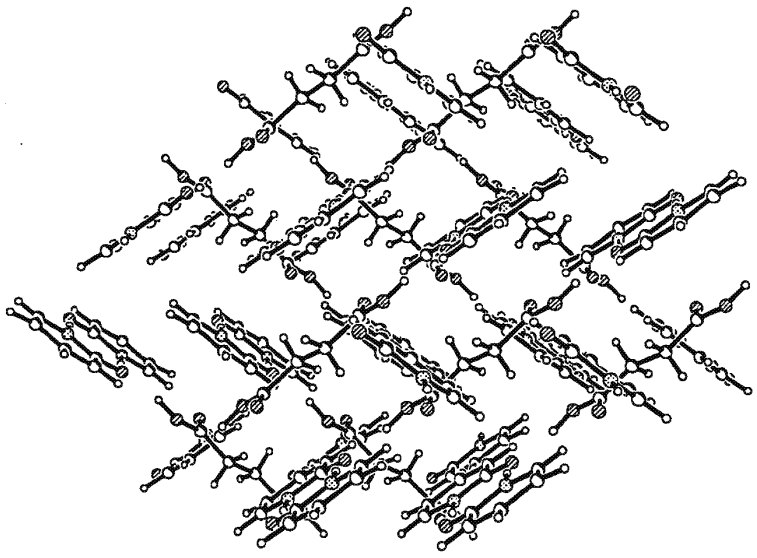


FIG. 5
The criss-cross assembly of ribbons in **2**.

interwoven, criss-cross assembly (Fig. 5). Furthermore, neighboring ribbons are linked through one C–H · · · O hydrogen bond.

The crystal structure of **3** is the only lattice which incorporates solvent molecules but this does not affect the primary intermolecular intercations. Adipic acid resides in an antiperiplanar conformation with a torsion angle of the carbon backbone close to 180°. The near-planar carboxylic moiety is slightly twisted out of the plane of the carbon back bone, with a torsion angle, ∠[O(1)–C(1)–C(2)–C(3)], of 10.7°. The crystal structure of **3** displays 2-D hydrogen-bonded layers of pyridones and acids very similar to the assemblies present in **1**. Dimers of symmetry related 2-pyridone molecules are formed *via* an N–H · · · O hydrogen bond (Table 4), and then linked by adipic acid molecules through two hydrogen bonds, O–H · · · O and C–H · · · O, into infinite ribbons (Fig. 6). Adjacent 1-D motifs are connected by C–H · · · O hydrogen bonds (Fig. 7), but they are also crosslinked by a water molecule, thereby generating an infinite layer. The interplanar orientation of aromatic rings with respect to each other do not suggest any attractive π-π interactions between sheets.

TABLE 4
Geometry of the Hydrogen Bonds for **3**

D–H · · · A	r(H · · · A)/Å	r(D · · · A)/Å	∠(D–H · · · A)/°
N21–H21 · · · O22^{i}	1.851 (3)	2.770 (3)	166.89 (9)
O2–H2A · · · O22	1.660 (3)	2.557 (3)	173.8 (1)
C24–H24 · · · O2^{ii}	2.545 (3)	3.534 (3)	168.66 (8)
C26–H26 · · · O1^{i}	2.490 (3)	3.475 (3)	154.74 (8)

Symmetry codes: i) 1 − x, −y, −z; ii) −1 − x, 1 − y, −z.

UM00012598
NOVARTIS EXHIBIT 1017
Novartis v. Regents, IPR2023-01346
Page 1344 of 4460

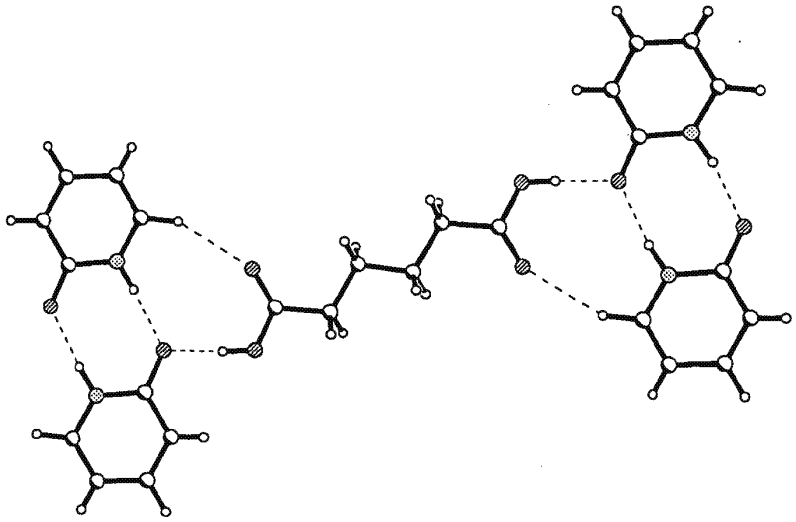


FIG. 6
2-pyridone dimers held together by an adipic acid molecule in **3**.

The increased conformational flexibility with increasing chain length is manifested in the crystal structures of **4** and **5**. In contrast to the previous acids, suberic and sebacic acid both exhibit nonplanar conformations. The carbon backbone of suberic acid is twisted with a torsion angle, ∠C(1)–C(2)–C(3)–C(4)), of −70.7°. Pyridone dimers are formed through symmetry related N–H · · · O hydrogen bonds (Fig. 8). A buckled ribbon is the result of alternating pyridone-acid molecules held together by two hydrogen bonds: O–H · · · O and C–H · · · O (Fig. 9). The overall crystal structure of **4** is very similar to **2**, with adjacent ribbons arranged in a criss-cross pattern (the angle between carbon backbones is *ca.* 45°), leading to an interwoven 3-D structure without any hydrogen-bond interactions between ribbons (Table 5).

The most unusual structural behavior in this series is displayed by **5**, which contains two unique pyridone molecules and two unique halves of sebacic acid. The two acid molecules display very different conformations. In one case, the carbon backbone from C(2) to C(2A) is antiperiplanar with a torsion angle close to 180°, while the torsion angle defined by C(1)–C(2) and C(1A)–C(2A) is 78.9°. This is very similar to the conformation observed in the crystal structure of sebacic acid [16]. The second acid molecule, however, is significantly different from the antiperiplanar conformation (Fig. 1e). Each of the two unique pyridone molecules form dimers *via* symmetry related N–H · · · O hydrogen bonds (Table 6). The combination of these dimers with the two acid molecules leads to two unique 1-D ribbons constructed by alternating 2-pyridone dimers and sebacic acids held together by O–H · · · O hydrogen bonds (Fig. 10). These 1-D assemblies are oriented at an angle with respect to each other (*ca.* 27°) resulting in an interwoven criss-cross pattern which is very similar to the structures of **2** and **4** (Fig. 11). There are no hydrogen bonds between adjacent chains.

UM00012599
NOVARTIS EXHIBIT 1017
Novartis v. Regents, IPR2023-01346
Page 1345 of 4460

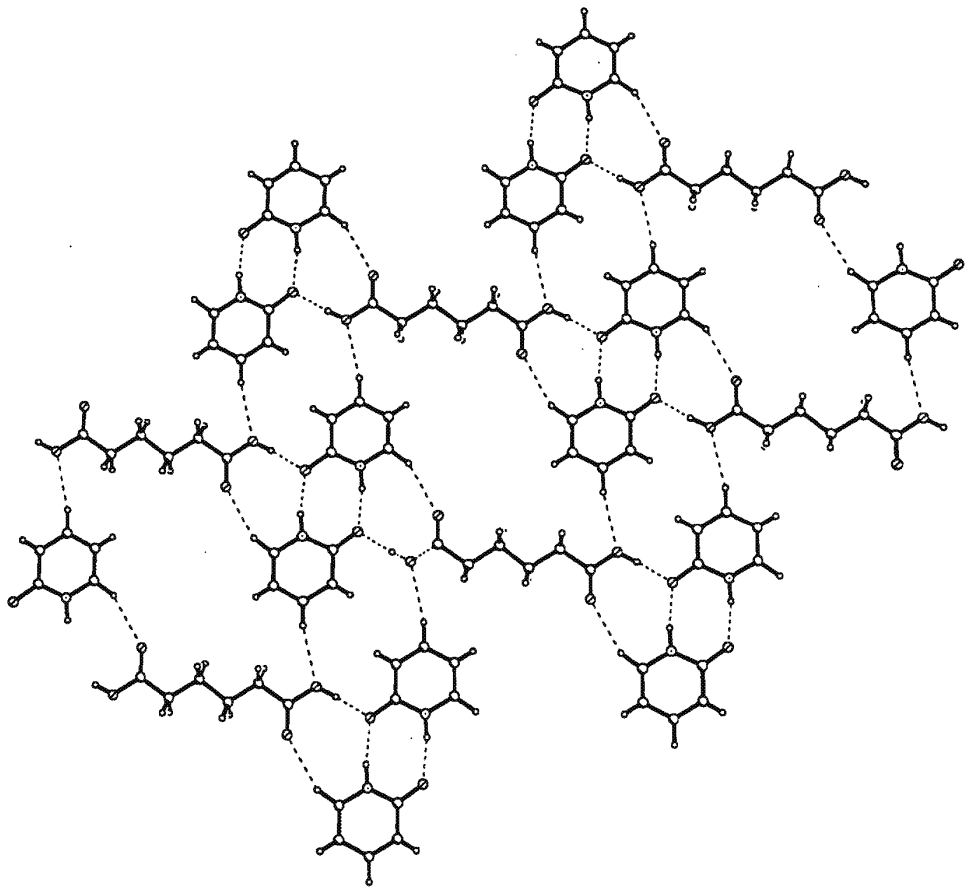


FIG. 7
An infinite layer in **3**, held together by N–H · · · O, O–H · · · O, and C–H · · · O hydrogen bonds. Water molecules removed for clarity.

DISCUSSION

In each crystal structure, **1** to **5**, the primary intermolecular assembly consists of dimers of 2-pyridone linked together by the dicarboxylic acid into infinite ribbons. The carbonyl oxygen of 2-pyridone is an effective hydrogen-bond acceptor and participates in two strong hydrogen-bond interactions, N–H · · · O and O–H · · · O, both of which lie in the plane containing the two lone pairs of the amide oxygen atom. Within this plane, the H · · · O=C angles of these two hydrogen bond interactions are very close to 120° in all the five cases, which shows that the directional preference of X–H · · · O (X=N, O) contacts are directed toward the location of the two lone pairs. This geometric preference has been noted many times, and is in accordance with the earlier study by Murray-Rust and Glusker of X–H · · · O (X=N, O) interactions involving carbonyl oxygen atoms [17].

The molecular conformations of the acids examined in this series become more complicated with increasing chain length culminating in the crystal structure containing sebacic acid

UM00012600
NOVARTIS EXHIBIT 1017
Novartis v. Regents, IPR2023-01346
Page 1346 of 4460

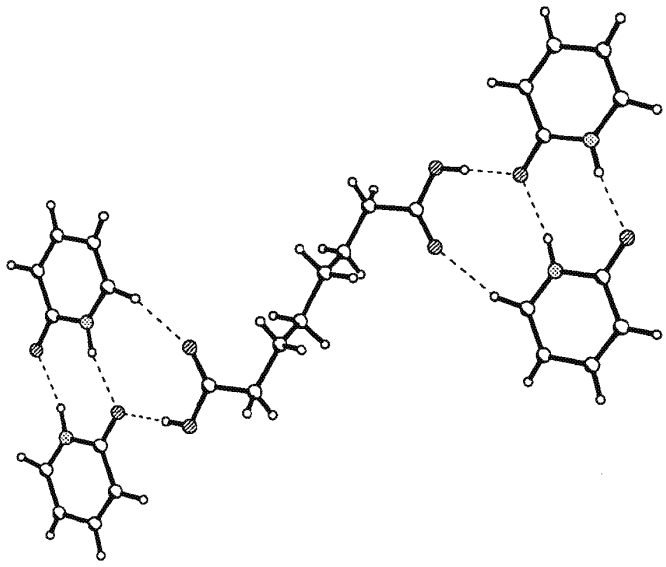


FIG. 8
2-pyridone dimers held together by a suberic acid molecule in **4**.

(ten carbon atoms in the aliphatic backbone), where two crystallographically independent carboxylic acids with significantly different geometries are present. On the other hand, the shorter acids, succinic acid and adipic acid, are planar with a regular antiperiplanar conformation. Somewhat surprisingly, all acids were positioned such that an inversion center was located on the C–C bond in the middle of the molecule.

The self-complementarity of the 2-pyridone moiety has resulted in the formation of very stable dimers. These dimers are seemingly undisturbed by the presence of both the carboxylic acid moiety and a water molecule, both of which are able to form strong intermolecular hydrogen bonds. In this series there are no examples of "classic" head-to-head carboxylic acid dimers, and the acids instead interact with the remaining hydrogen-bond sites on the pyridone dimer; a C–H donor, and a C=O acceptor. It seems unlikely that one of these structures would contain homomeric acid-acid and pyridone-pyridone dimers simultaneously, since the driving force for cocrystal formation, i.e., some preferential interactions between different components, would then be absent. In such cases, the two starting materials are more likely to precipitate out of solution by themselves. If the two moieties are present on the same molecule, however, it is quite possible to have homomeric interactions in preference to heteromeric interactions. A search of the CSD [18] uncovered only one crystal structure of a relevant compound containing both a carboxylic acid and a 2-pyridone moiety, 2,2-dimethyl-4-(2-oxo-1*H*-6-pyridyl)-3-butynoic acid [19]. This structure contains dimers held together by two pyridone-acid interactions (Scheme 2a). However, the formation of molecular dimers connected by two homomeric interactions is precluded due to the positioning of the pyridone moiety, so this option is not available (although it is possible to envisage chains of molecules (Scheme 2b)).

We have carried out preliminary semiempirical calculations [20] on some of the different dimers that can occur in our systems, and these results indicate that (i) a

UM00012601
NOVARTIS EXHIBIT 1017
Novartis v. Regents, IPR2023-01346
Page 1347 of 4460

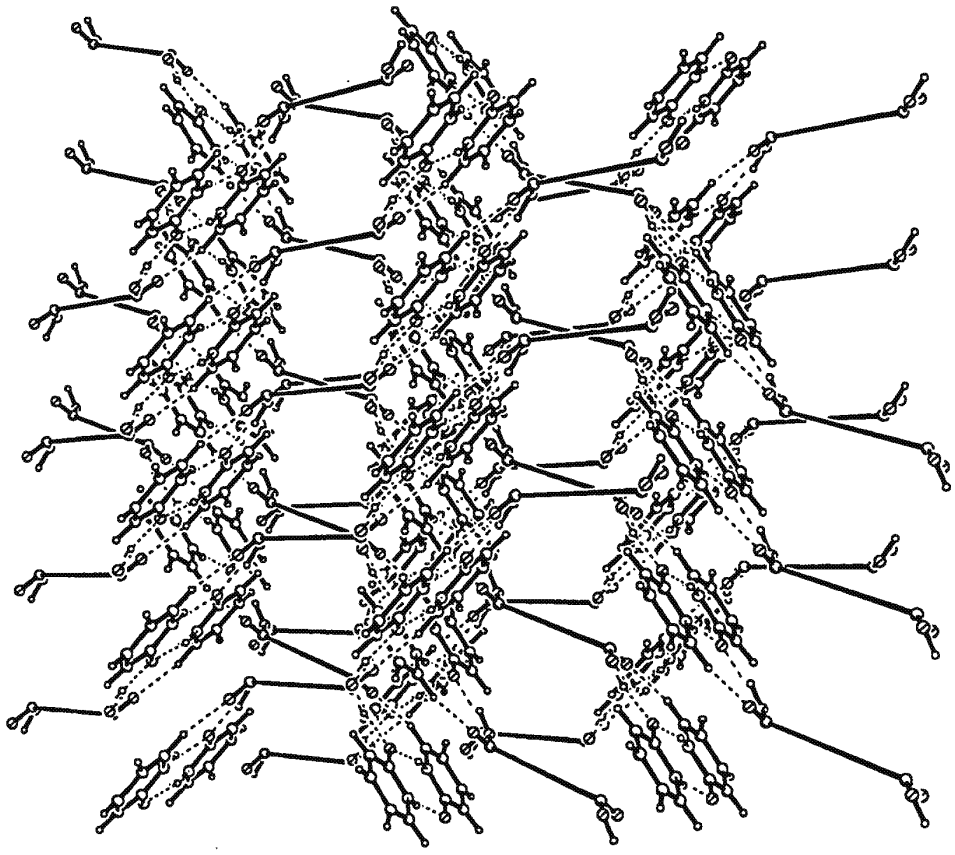


FIG. 9
The criss-cross orientation of infinite ribbons in **4**. The acid and the pyridone molecules have been simplified for sake of clarity.

homomeric 2-pyridone dimer is stabilized by 44.0 kJ/dimer, (ii) a homomeric oxalic acid dimer is stabilized by 26.3 kJ/dimer, and (iii) a heteromeric N–H · · · O/O–H · · · O dimer is stabilized by 34.1 kJ/dimer. A geometry optimization of the core tetramer observed in **1**, (Scheme 3), gives a stabilization of 87.02 kJ/tetramer, which is larger than some other

TABLE 5
Geometry of the Hydrogen Bonds for **4**

D–H · · · A	r(H · · · A)/Å	r(D · · · A)/Å	∠(D–H · · · A)/°
N21–H21 · · · O22^{i}	1.888 (2)	2.779 (2)	165.84 (6)
O2–H2A · · · O22	1.663 (2)	2.612 (2)	165.87 (8)
C25^{ii}–H25^{ii} · · · O1	2.686 (2)	3.469 (2)	137.49 (6)
C26^{i}–H26^{i} · · · O1	2.196 (2)	3.191 (3)	156.52 (6)

Symmetry codes: i) −x, −1 − y, −z; ii) x, −½ − y, ½ + z.

UM00012602
NOVARTIS EXHIBIT 1017
Novartis v. Regents, IPR2023-01346
Page 1348 of 4460

TABLE 6
Geometry of the Hydrogen Bonds for **5**

D–H · · · A	*r*(H · · · A)/Å	*r*(D · · · A)/Å	∠(D–H · · · A)/°
N31^{i}–H31^{i} · · · O32	1.701 (3)	2.797 (3)	173.1 (1)
N41^{ii}–H41^{ii} · · · O42	1.759 (3)	2.762 (3)	171.7 (1)
O2^{iii}–H2A^{iii} · · · O42	1.615 (3)	2.620 (3)	164.6 (1)
O22^{iv}–H22A^{iv} · · · O32	1.614 (3)	2.634 (3)	164.1 (1)
C36^{v}–H36^{v} · · · O21	2.286 (4)	3.259 (4)	153.2 (1)
C44^{v}–H44^{v} · · · O21	2.418 (4)	3.266 (4)	133.9 (1)
C46^{v}–H46^{v} · · · O1	2.296 (4)	3.303 (4)	146.3 (1)

Symmetry codes: i) −x, 2 − y, −z; ii) 1 − x, 1 − y, 1 − z; iii) −x, 1 − y, 1 − z; iv) −1 − x, 2 − y, −z; v) x − 1, y, z.

possible combinations; two homomeric interactions give 70.3 kJ/tetramer, and two heteromeric interactions give 68.1 kJ/tetramer. Even though these calculations are relatively simplistic and obviously neglect interactions with molecules other than the ones explicitly included, they emphasize that there is no energy penalty by positioning oxalic acid and 2-pyridone together as in **1**.

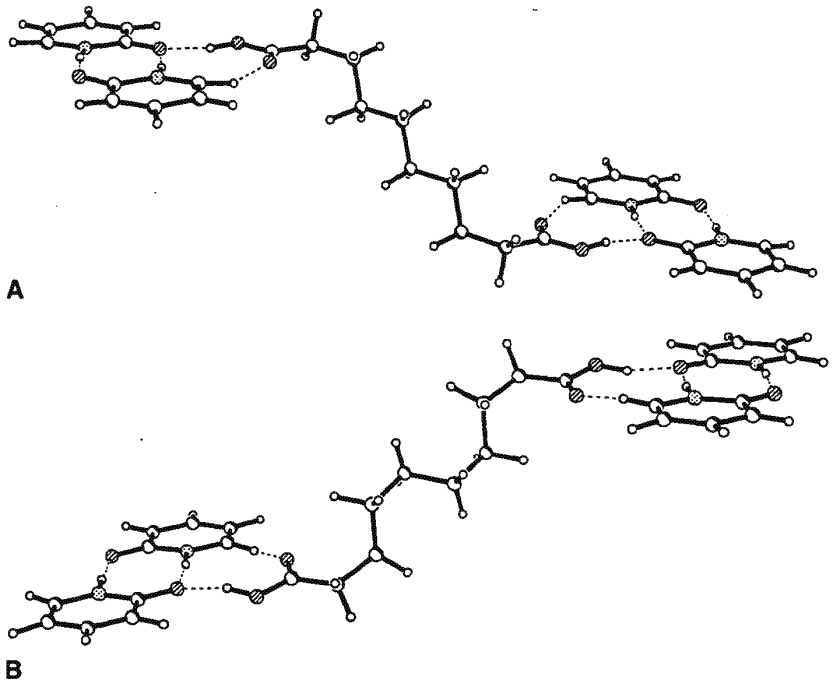


FIG. 10
Two sets of independent ribbons of 2-pyridone dimers held together by a sebacic acid molecule in **5**.

UM00012603
NOVARTIS EXHIBIT 1017
Novartis v. Regents, IPR2023-01346
Page 1349 of 4460

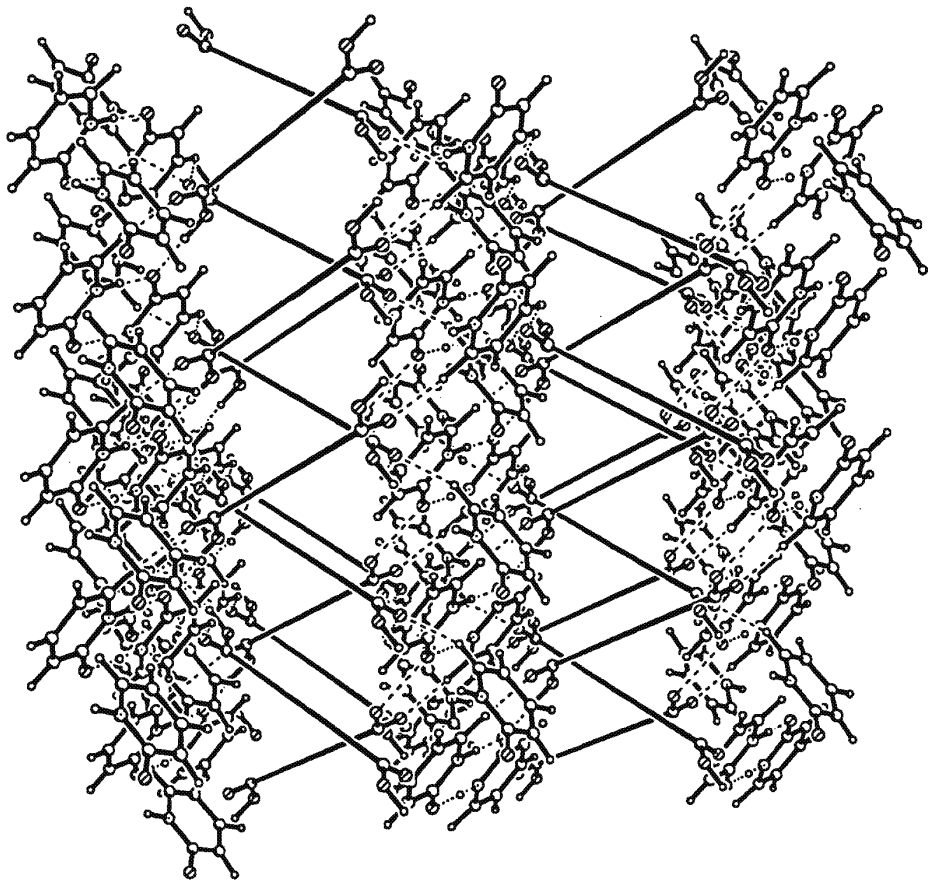
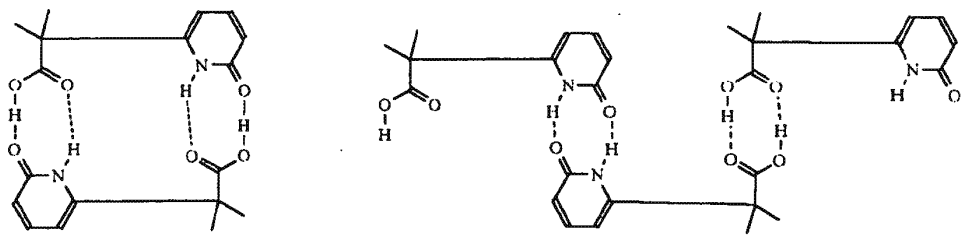


FIG. 11

The criss-cross assembly of infinite hydrogen-bonded ribbons in **5**. The acid molecules have been simplified for sake of clarity.

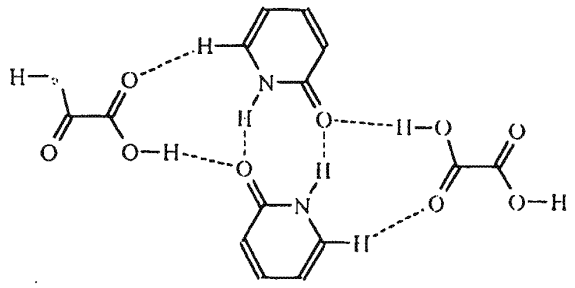


A **B**

SCHEME 2

(A) Schematic representation of the molecular dimers 2,2-dimethyl-4-(2-oxo-1*H*-6-pyridyl)-3-butynoic acid (see ref. [19]). (B) Hypothetical alternative motif of 2,2-dimethyl-4-(2-oxo-1*H*-6-pyridyl)-3-butynoic acid.

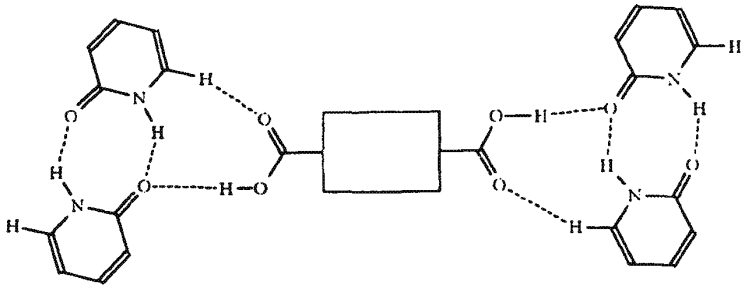
UM00012604
NOVARTIS EXHIBIT 1017
Novartis v. Regents, IPR2023-01346
Page 1350 of 4460



SCHEME 3
The central tetrameter in **1**.

Although there are considerable differences in the size and conformational flexibility of the acids that have been examined in this series of cocrystals, the primary intermolecular interactions in **1** to **5** (O–H · · · O, N–H · · · O, C–H · · · O) cooperate to generate the same "supermolecule" in all five cases (Scheme 4).

These building blocks are then propagated into infinite ribbons regardless of the nature of the dicarboxylic acid. The subsequent spatial orientation of these robust ribbons leads essentially to two distinct types of structures. Either the ribbons generate layers, as in **1** and **3**, or they are twisted with respect to each other, leading to an interwoven network of infinite ribbons. Even though the tilt angle between adjacent ribbons on **2**, **4**, and **5** varies considerably (a range of 27–88°), the three structures are very similar. The fact that the primary intermolecular interactions generate a building block which is propagated into 1-D architectures has significantly reduced the possible variations in packing arrangement that could occur in these cocrystals. This idea represents one of the corner stones in many crystal engineering strategies. If we employ infinite 1-D or 2-D building blocks instead of discrete molecules or complexes in the construction of new crystalline materials, we are limited to a much smaller number of possible structures due to the fact that the positional and orientational freedom of individual molecules and ions have been severely curtailed. Therefore, if molecules can be "locked" into infinite assemblies in a predictable manner, typically using robust and specific intermolecular interactions, the task of predicting and controlling crystal structure becomes somewhat easier. Nevertheless, it is important to remember that even though we can construct hydrogen-bonded 1-D and 2-D motifs, the detailed crystal structure



SCHEME 4
The "supermolecule" present in all five cocrystals, **1** to **5**.

UM00012605
NOVARTIS EXHIBIT 1017
Novartis v. Regents, IPR2023-01346
Page 1351 of 4460

is a consequence of all intermolecular forces, not just the primary intermolecular interactions. In the case of 2-pyridone/dicarboxylic acid cocrystals, we intend to further examine how different substituents on 2-pyridone may effect the final crystal structure through "secondary" intermolecular interactions; e.g., π-π, hydrophobic-hydrophilic, dispersion and halogen–halogen interactions.

ACKNOWLEDGEMENTS

We acknowledge financial support from NSF-EPSCoR (OSR-9550487), DuPont, and Kansas State University.

NOTES AND REFERENCES

1. C.B. Aakeröy, *Acta Crystallogr., Sect., B* **53**, 569 (1997); S. Subramanian and M. Zaworotko, *Coord. Chem. Rev.* **137**, 357 (1994); G.R. Desiraju, *Crystal Engineering: The Design of Organic Solids*, Elsevier, Amsterdam, 1989.
2. G.R. Desiraju, *Angew. Chem. Int. Ed. Engl.* **34**, 2311 (1995).
3. M.C. Etter and P.W. Baures, *J. Am. Chem. Soc.* **110**, 639 (1988); M.C. Etter, Z. Urbanczyk-Lipkowska, M. Zia-Ebrahimi, and P.W. Panunto, *J. Am. Chem. Soc.* **110**, 8415 (1990); M.C. Etter and S. Reutzel *J. Am. Chem. Soc.* **113**, 2586 (1991).
4. F. Garcia-Tellado, S.J. Geib, S. Goswami and A.D. Hamilton, *J. Am. Chem. Soc.* **113**, 9265 (1991); E. Fan, C. Vincent, S.J. Geib and A.D. Hamilton, *Chem. Mater.* **6**, 1113 (1994).
5. S. Coe, J.J. Kane, T.L. Nguyen, L.M. Toledo, E. Wininger, F.F. Fowler, and J.W. Lauher, *J. Am. Chem. Soc.* **119**, 119 (1986).
6. G.T.R. Palmore and M.T. McBride, *Chem. Commun.* **145** (1998).
7. O. Ermer and A. Eling, *J. Chem. Soc. Perkin Trans.* **2**, 925 (1994).
8. Y. Ducharme and J.D. Wuest, *J. Org. Chem.* **53**, 5787 (1988).
9. M. Simard, D. Su, and J.D. Wuest, *J. Am. Chem. Soc.* **113**, 4696 (1991).
10. B.R. Penfold, *Acta Crystallogr.* **6**, 591 (1953).
11. L. Leiserowitz, *Acta Crystallogr.* **B32**, 775 (1976).
12. J. Bernstein and R.E. Davis, private communication.
13. G.M. Sheldrick, SHELXL-93, University of Göttingen.
14. Å. Kvick and I. Olovsson, *Ark. Kemi.* **30**, 71 (1969).
15. U. Ohms, H. Guth, and W. Treutmann, *Z. Kristallogr.* **99**, 159 (1982).
16. J.D. Morrison and J.M. Robertson, *J. Chem. Soc.* 993 (1949).
17. P. Murray-Rust and J.P. Glusker, *J. Am. Chem. Soc.* **106**, 1018 (1984).
18. F.H. Allen and O. Kennard O. *Chemical Design and Automation News* **8**, 3137 (1993).
19. P.L. Walsh, E. Maverick, J. Chiefari, and D.A. Lightner, *J. Am. Chem. Soc.* **119**, 3802 (1997).
20. Enthalpies of formation were calculated using the AM1 methodology within the MOPAC suite of programs.

UM00012606
NOVARTIS EXHIBIT 1017
Novartis v. Regents, IPR2023-01346
Page 1352 of 4460

Structural Chemistry, Vol. 10, No. 3, 1999

Charge-Assisted Hydrogen Bonds and Halogen-Halogen Interactions in Organic Salts: Benzylammonium Benzoates and Pentafluorobenzoates

Christer B. Aakeröy,[1] Alicia M. Beatty,[1] and Keith R. Lorimer[1]

Received September 5, 1998; accepted January 5, 1999

The enhanced influence of charge-assisted hydrogen bonds upon the resulting crystal structure in the presence of competing noncovalent interactions has been examined using single-crystal X-ray diffraction. The crystal structures of six organic salts are presented: 4-chlorobenzylammonium 2,4-dichlorobenzoate, 3-chlorobenzylammonium 2,4-dichlorobenzoate, 4-methylbenzylammonium pentafluorobenzoate, 4-chlorobenzylammonium pentafluorobenzoate, 3-methylbenzylammonium benzoate, and 4-chlorobenzylammonium benzoate monohydrate. All structures are dominated by charge-assisted $-NH_3^+\cdots{}^-OOC-$ hydrogen bonds that generate either one-dimensional ribbons or two-dimensional sheets. The structural influence of weaker intermolecular interactions is limited as there are very few short, halogen-halogen, π-π, or C—H···X distances in this series of compounds.

KEY WORDS: Hydrogen bonding; intermolecular interactions; crystal engineering; benzylammonium; benzoate.

INTRODUCTION

Predictable assembly of specific molecular and ionic building blocks into robust infinite architectures can only be achieved through an extensive understanding of the directional influence of intermolecular forces [1]. Since these noncovalent forces typically differ considerably in strength from their covalent counterparts, intermolecular synthesis and crystal engineering are not straightforward processes. To improve our understanding of the balance between different intermolecular forces with a view to providing more efficient crystal engineering tools, several structural and theoretical studies have been examined, for example, hydrogen-bond and various π-π interactions [2–4]. One of the more controversial topics of study in this context has been the importance (or otherwise) of short halogen-halogen contacts [1]. The occurrence of unexpectedly short halogen···halogen distances in several crystal structures has been interpreted as evidence for the attractive nature of such contacts [5], but these geometric data have also been explained as a function of inherently anisotropic atoms [6].

A recent structural database study of F···F distances in organic solids led to the conclusion that such interactions are unlikely to play an important role in the overall crystal packing [7]. However, the situation is less clear regarding larger, more polarizable halogen substituents, especially if they are attached to an aromatic backbone [8]. It is also unclear how these halogen···halogen contacts will compete against other intermolecular interactions, notably hydrogen bonds [2]. The focus of this paper is an examination of the competition between π-π, halogen-halogen, and charge-assisted hydrogen-bond interactions.

As the hydrogen bond is primarily electrostatic in nature, it can be expected that the importance of such interactions increases if the participating hydrogen-bond donors and acceptors are positioned on oppositely

[1] Department of Chemistry, Kansas State University, Manhattan, Kansas, 66506.

1040-0400/99/0600-0229$16.00/0 © 1999 Plenum Publishing Corporation

UM00012607
NOVARTIS EXHIBIT 1017
Novartis v. Regents, IPR2023-01346
Page 1353 of 4460

charged ions [9]. In this study, the supply of the anionic "anchoring" units has been provided by a series of substituted benzoic acids, and the cationic counter ion has been furnished by a series of substituted primary benzylamines. Such a combination of building blocks locates the best conventional hydrogen-bond donors on the cation, $R—NH_3^+$, and the strongest acceptors on the anion, COO^-, thereby limiting the possibilities of strong cation-cation or anion-anion interactions. Thus, the assembly process has been constrained to some extent, thereby making it easier to identify the specific influence of the weaker intermolecular interactions upon the resulting crystal structure.

In order to contribute more information to the ongoing discussion about the relative importance of intermolecular forces and crystal packing, we report the crystal structures of six new compounds: 4-chlorobenzylammonium 2,4-dichlorobenzoate **1**, 3-chlorobenzylammonium 2,4-dichlorobenzoate **2**, 4-methylbenzylammonium pentafluorobenzoate **3**, 4-chlorobenzylammonium pentafluorobenzoate **4**, 3-methylbenzylammonium benzoate **5**, and 4-chlorobenzylammonium benzoate monohydrate **6**.

EXPERIMENTAL

X-ray Crystallography

Crystallographic data for **1–3** and **5–6** were collected using a Siemens P4 four-circle diffractometer with graphite monochromated Mo-Kα radiation. Crystal stabilities were monitored by measuring 3 standard reflections after every 97 reflections, with no significant decay observed. Cell parameters were obtained from accurately centered reflections in the 2θ range 10–25°. Data were collected using a θ-2θ scanning technique, and Lorentz and polarization corrections were applied. Crystallographic data for **4** were collected on a Siemens CCD area detector-equipped diffractometer with Mo-Kα radiation.

The structures were solved by direct methods, with remaining nonhydrogen atoms found by successive full matrix least squares refinement on F^2. All nonhydrogen atoms were refined with anisotropic thermal parameters and hydrogen-atom positions were located from difference Fourier maps (except for **3**, where hydrogen atom positions on C28 and C48 were calculated). A riding model with fixed thermal parameters [u_{ij} = 1.2 U_{ij}(eq) for the atom to which the hydrogen atoms are bonded] was used for subsequent refinements. The SHELXTL PC and SHELXL-93 packages were used for data reduction and structure solution and refinement [10]. Table I contains crystallographic details and Fig. 1 displays labeling schemes and thermal ellipsoids for **1–6**.

Synthesis of 4-chlorobenzylammonium 2,4-dichlorobenzoate 1

A solution of 2,4-dichlorobenzoic acid (0.1 g, 0.52 mmol) in ethanol (30 mL) was added to 4-chlorobenzylamine (0.07 g, 0.52 mmol). The mixture was heated with stirring until both components were dissolved. Thin, white needles were collected after a week by slow evaporation of the solvent, mp 141–143°C.

Synthesis of 3-chlorobenzylammonium 2,4-dichlorobenzoate 2

An ethanolic solution of 2,4-dichlorobenzoic acid (0.1 g, 0.52 mmol), was added to 3-chlorobenzylamine (0.07 g, 0.52 mmol). The mixture was heated with stirring until a clear solution was formed. After a week, thin, white needles were collected by filtration, mp 122–124°C.

Synthesis of 4-methylbenzylammonium pentafluorobenzoate 3

Pentafluorobenzoic acid (0.1 g, 0.47 mmol) was dissolved in ethanol (10 mL) and added to 4-methylbenzylamine (0.06 g, 0.47 mmol). The solvent was allowed to evaporate slowly at ambient temperature and large, irregularly shaped crystals were collected by filtration after 1 week, mp 158–160°C.

Synthesis of 4-chlorobenzylammonium pentafluorobenzoate 4

A solution of pentafluorobenzoic acid (0.1 g, 0.47 mmol) in ethanol (10 mL) was added to 4-chlorobenzylamine (0.07 g, 0.47 mmol). A straw-colored solution formed and was allowed to slowly evaporate at ambient temperature. After several days, large, white, plate-like crystals were collected by filtration, washed with ethanol, and dried in air, mp 166–168°C.

UM00012608
NOVARTIS EXHIBIT 1017
Novartis v. Regents, IPR2023-01346
Page 1354 of 4460

Table I. Data Collection and Refinement for 1–6

Crystal data	1	2	3	4	5	6
Empirical formula	$C_{14}H_{12}No_2Cl_3$	$C_{14}H_{12}NO_2Cl_3$	$C_{15}H_{12}NO_2F_5$	$C_{14}H_9NO_2ClF_5$	$C_{15}H_{17}NO_2$	$C_{14}H_{16}NO_3Cl$
MW	332.60	332.60	333.26	353.67	243.30	281.73
Crystal size (mm)	0.1 × 0.6 × 0.3	0.5 × 0.7 × 0.5	0.4 × 0.8 × 0.5	0.5 × 0.4 × 0.3	0.7 × 0.6 × 0.4	0.4 × 0.8 × 0.6
Crystal system	monoclinic	monoclinic	monoclinic	monoclinic	monoclinic	monoclinic
Space group	$P2_1/c$	$P2_1/c$	$P2_1/c$	$C2/c$	$P2_1/c$	$P\bar{1}$
a (Å)	14.939(2)	16.726(2)	18.415(3)	24.469(5)	13.336(2)	5.9718(5)
b (Å)	8.163(1)	6.240(1)	12.173(1)	13.106(3)	6.540(1)	7.1602(8)
c (Å)	11.561(1)	15.547(1)	13.332(1)	9.409(2)	15.259(1)	16.620(1)
α (deg)	90	90	90	90	90	99.304(9)
β (deg)	92.60(1)	110.60(1)	91.63(1)	95.00(3)	91.04(1)	92.118(8)
γ (deg)	90	90	90	90	90	90.722(8)
Volume (Å^3)	1408.4(3)	1518.9(3)	2987.4(6)	3006(1)	1330.6(3)	700.7(1)
Z	4	4	4	8	4	2
D_{calc} (g cm^{-3})	1.569	1.454	1.482	1.563	1.214	1.335
F(000)	680	680	1360	1424	520	296
μ(Mo-K$_\alpha$) (mm^{-1})	0.650	0.602	0.140	0.316	0.080	0.276
Temp (K)	173	173	173	173	173	173
$\theta - 2\theta$ scans; θ range (deg)	1.36 to 22.51	1.30–23.87	1.11–22.50	1.67–25.00	1.53–22.50	1.24–22.50
Range h	−16 to 16	−18 to 18	−19 to 19	−32 to 30	−1 to 14	−6 to 1
Range k	0 to 8	−6 to 1	−13 to 1	−17 to 17	−7 to 1	−7 to 7
Range l	−12 to 0	−1 to 16	−14 to 1	−12 to 6	−16 to 16	−17 to 17
Reflns collected	1956	2729	4802	7778	2407	2461
Unique reflns	1843	1978	3891	2654	1729	1828
Observed reflns ($I > 2\sigma I$)	1636	1828	3142	1796	1504	1737
Data:parameter (obs. data)	9.04	10.10	7.48	8.59	9.23	10.04
Refinement	full-matrix lsq. on F^2	full-matrix lsq. on F^2	full-matrix lsq. on F^2	full-matrix lsq. on F^2	full-matrix lsq. on F^2	full-matrix lsq. on F^2
R/R_w^2 (obs data)	0.0306/0.0967	0.0344/0.0959	0.0457/0.1249	0.0555/0.1380	0.0445/0.1310	0.0338/0.0839
R/R_w^2 (all data)	0.0363/0.1085	0.0375/0.0983	0.0591/0.1380	0.0850/0.1593	0.0511/0.1375	0.0353/0.0856
$\Delta\rho_{max/min}$ (e Å^{-3})	0.243/−0.265	0.233/−0.318	0.264/−0.232	0.407/−0.355	0.289/−0.237	0.220/−0.378
S	1.157	1.245	1.105	1.051	1.145	1.081
Weighting function (w^{-1} = $[\sigma^2(F_0^2) + (g_1P)^2 + (g_2P)]$ where $P = [F_0^2 + 2F_c^2]/3$	g_1 = 00587 g_2 = 0.8168	g_1 = 0.0267 g_2 = 2.4877	g_1 = 0.0674 g_2 = 1.6854	g_1 = 0.1008 g_2 = 0.0000	g_1 = 0.0788 g_2 = 0.4952	g_1 = 0.0365 g_2 = 0.5586

Synthesis of 3-methylbenzylammonium benzoate 5

Benzoic acid (0.1 g, 0.8 mmol) in ethanol (10 mL) was added to 3-methylbenzylamine (0.1 g, 0.8 mmol) and the solution was allowed to evaporate slowly. After several days, white, plate-like crystals were collected by filtration and dried in air, mp 145–147°C.

Synthesis of 4-chlorobenzylammonium benzoate monohydrate 6

Benzoic acid (0.1 g, 0.8 mmol) in water (10 mL) was added to 4-chlorobenzylamine (0.11 g, 0.8 mmol) in ethanol (5 mL) and heated with stirring. The solution was allowed to evaporate slowly. After several days, translucent, needle-like crystals were collected by filtration, mp 158–160°C.

RESULTS

The crystal structure of **1** contains infinite one-dimensional stacks of alternating, parallel anions and cations hydrogen-bonded through N—H···O interactions between both acceptors of the carboxylate anion and two donors of each benzylammonium cation (Table II). Adjacent stacks cross-link through the remaining donor site of the $-NH_3^+$ moiety of the cation to form infinite two-dimensional sheets (Fig. 2). Within these sheets, there are two distinctive ring-like motifs: $R_4^2(8)$ and $R_8^8(24)$ [11]. The aromatic components of both the ions arrange themselves in a herringbone motif.

All hydrogen-bonding functionalities in **1** are oriented toward the center of each sheet and, as a consequence, the *para*-chloro substituents of the anions

UM00012609
NOVARTIS EXHIBIT 1017
Novartis v. Regents, IPR2023-01346
Page 1355 of 4460

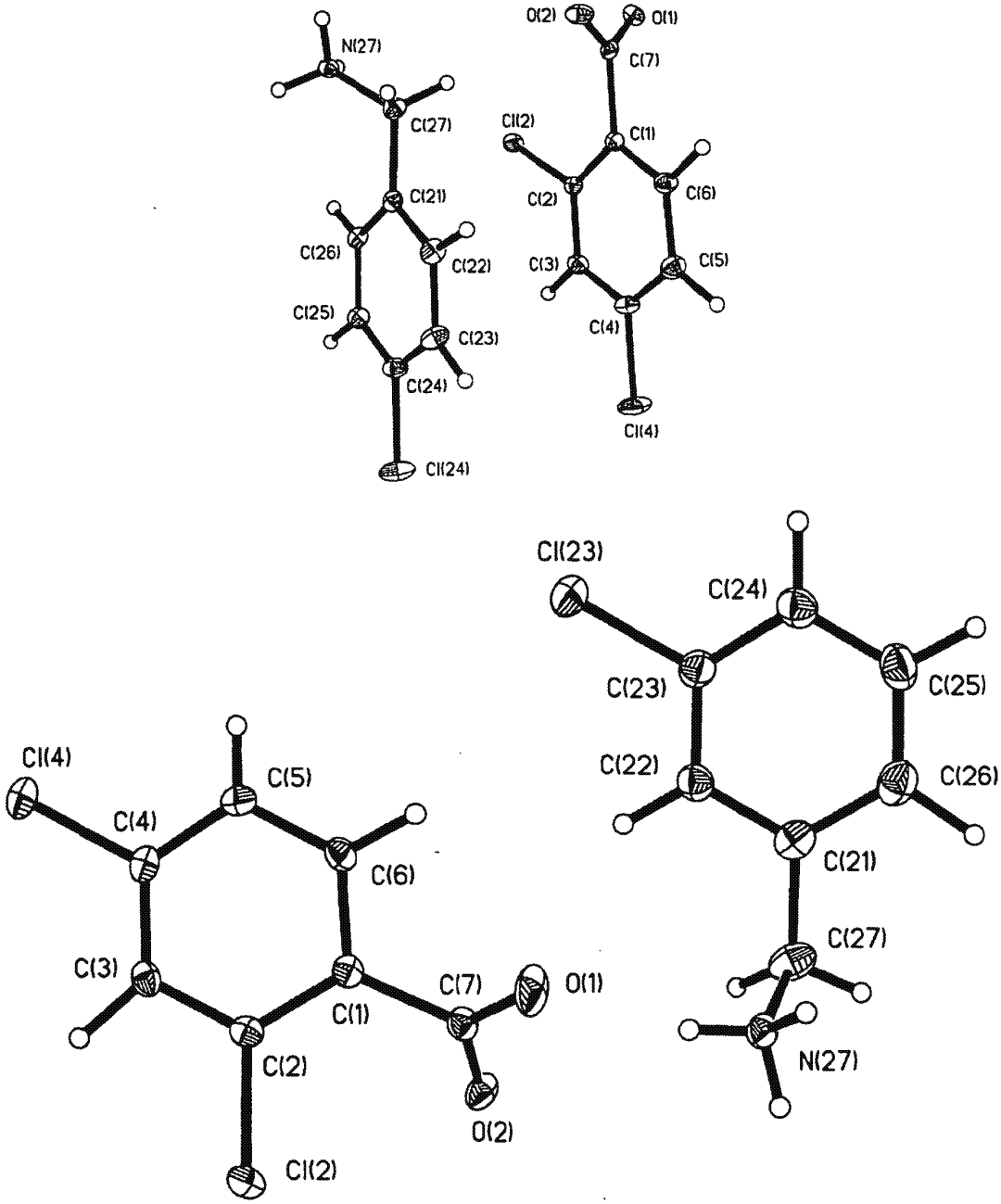


Fig. 1. Molecular geometry and numbering schemes for 1–6. Thermal ellipsoids at 30% probability.

UM00012610
NOVARTIS EXHIBIT 1017
Novartis v. Regents, IPR2023-01346
Page 1356 of 4460

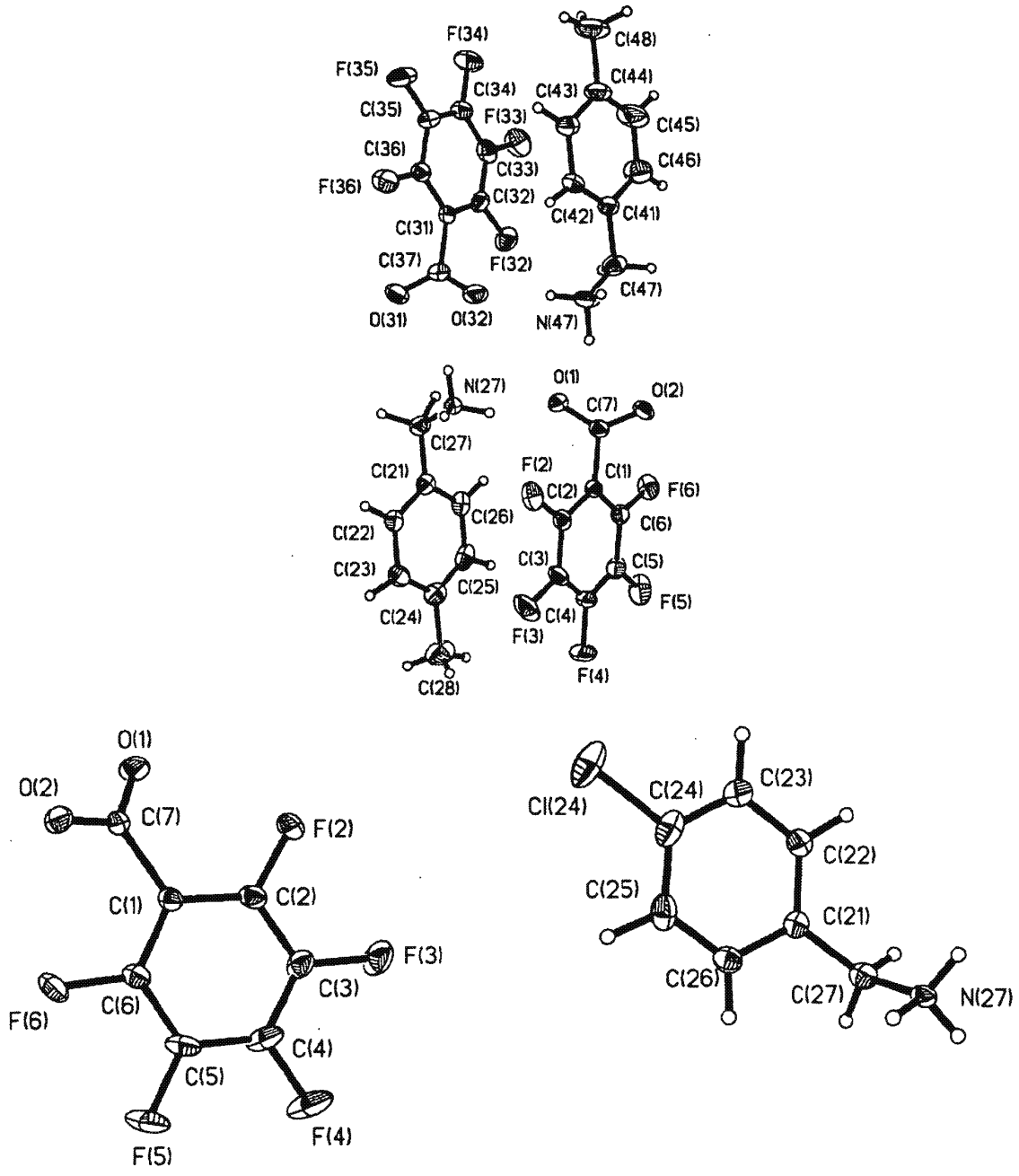


Fig. 1. Continued.

UM00012611
NOVARTIS EXHIBIT 1017
Novartis v. Regents, IPR2023-01346
Page 1357 of 4460

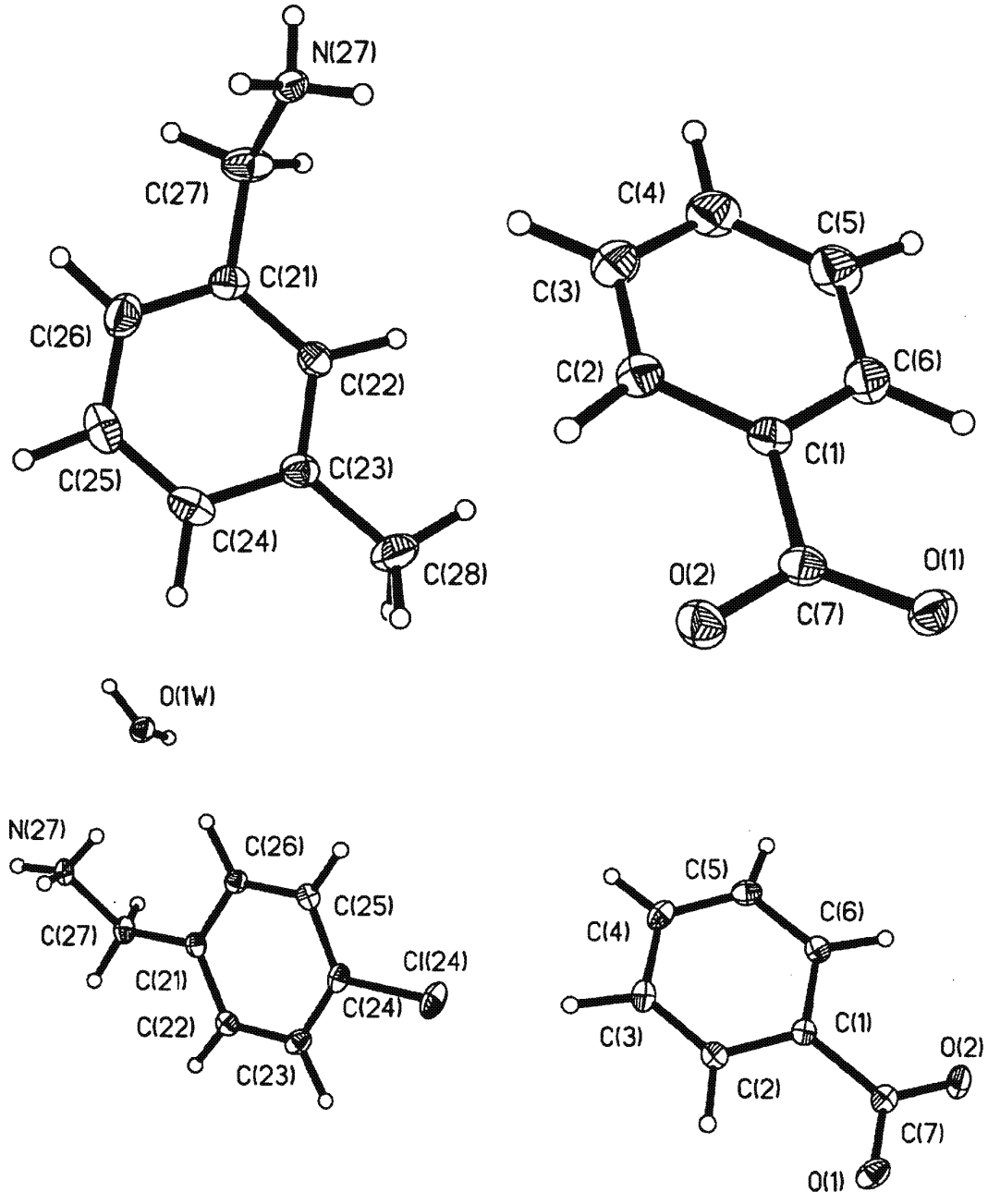


Fig. 1. Continued.

UM00012612
NOVARTIS EXHIBIT 1017
Novartis v. Regents, IPR2023-01346
Page 1358 of 4460

Table II. Geometry of the Hydrogen Bonds in 1

D—H···A	r(H···A)/Å	r(D···A)/Å	∢(D—H···A) (°)
N(27)—H(27C)···O(1)′	1.904(3)	2.795(3)	168.79(8)
N(27)—H(27D)···O(1)″	1.880(3)	2.802(3)	167.55(8)
N(27)—H(27E)···O(2)‴	1.941(3)	2.743(3)	159.81(8)

Symmetry code: (′)$x, y-1, z$; (″) $-x+1, -y, -z+1$; (‴) $-x+1, y-\frac{1}{2}, -z+1\frac{1}{2}$

and the cations point outward to the "surface" of each infinite sheet (Fig. 3). There are no hydrogen bonds between neighboring layers, but relatively short Cl···Cl distances of 3.351(1) Å are present between the 4-chloro substituents of a cation and an anion in adjacent layers, with ∠C(24)—Cl(24)···Cl(4), 157.2(1)°, and ∠C(4)—Cl(4)···Cl 160.9(1)°.

By changing the position of the chloro substituent on the benzylammonium cation from *para* (as in **1**) to *meta* (as in **2**), a slightly different packing arrangement results even though both **1** and **2** have the same anion. The structure of **2** consists of cations and anions linked by N—H···O hydrogen bonds into a 10-membered ring, $R_4^3(10)$, forming tetrameric units (Table III). Adjacent tetramers are linked together via hydrogen bonds through the remaining donor and acceptor sites. This combination of hydrogen bonds generates an infinite one-dimensional ladder (Fig. 4). The only short halogen-halogen contact in **2** takes place between the 3-Cl substituents on cations from neighboring ribbons: C(23)—Cl(23)···Cl(23), 3.352(2) Å, ∠169.0(1)°. The core of the ribbon in **2** consists of all the hydrogen-bonding functionalities, which means that the *para*- and *ortho*-chloro substituents all face outward into the space between ribbons. The arrangement of the aromatic moieties in **1** and **2** is very similar (Figs. 3 and 4).

The structure determination of **3** (which does not

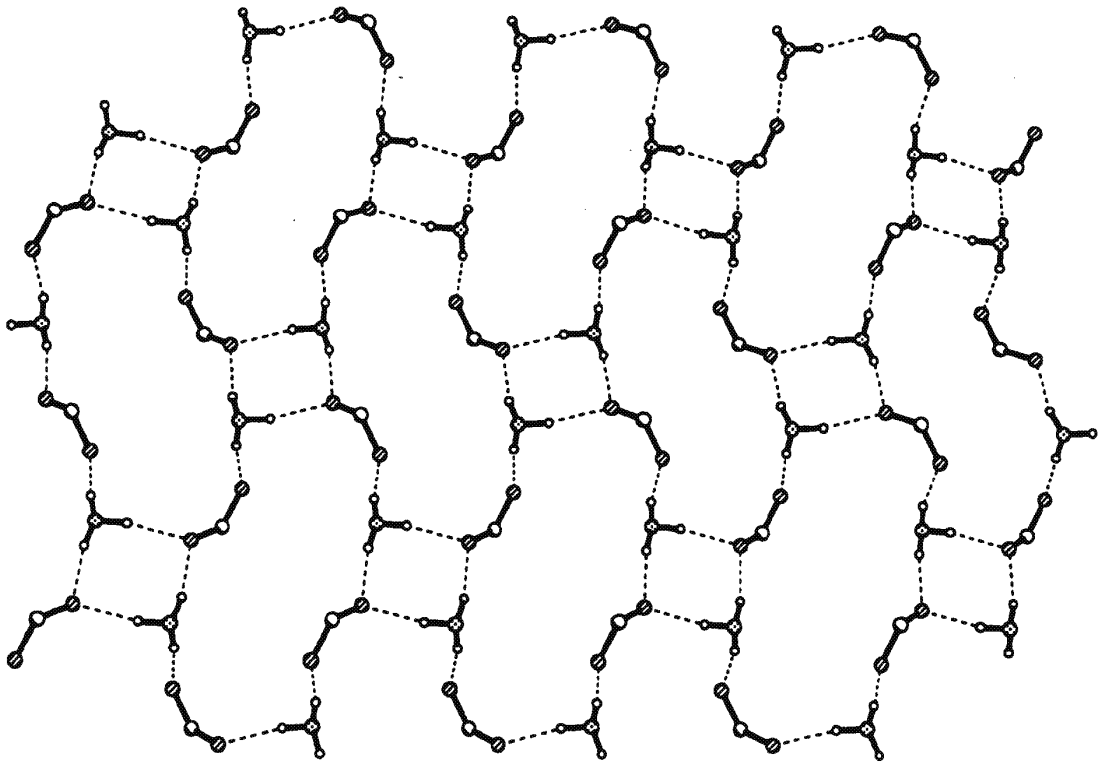


Fig. 2. Face-on view of the infinite two-dimensional sheet of anions and cations in **1**. Aromatic rings removed for clarity.

UM00012613
NOVARTIS EXHIBIT 1017
Novartis v. Regents, IPR2023-01346
Page 1359 of 4460

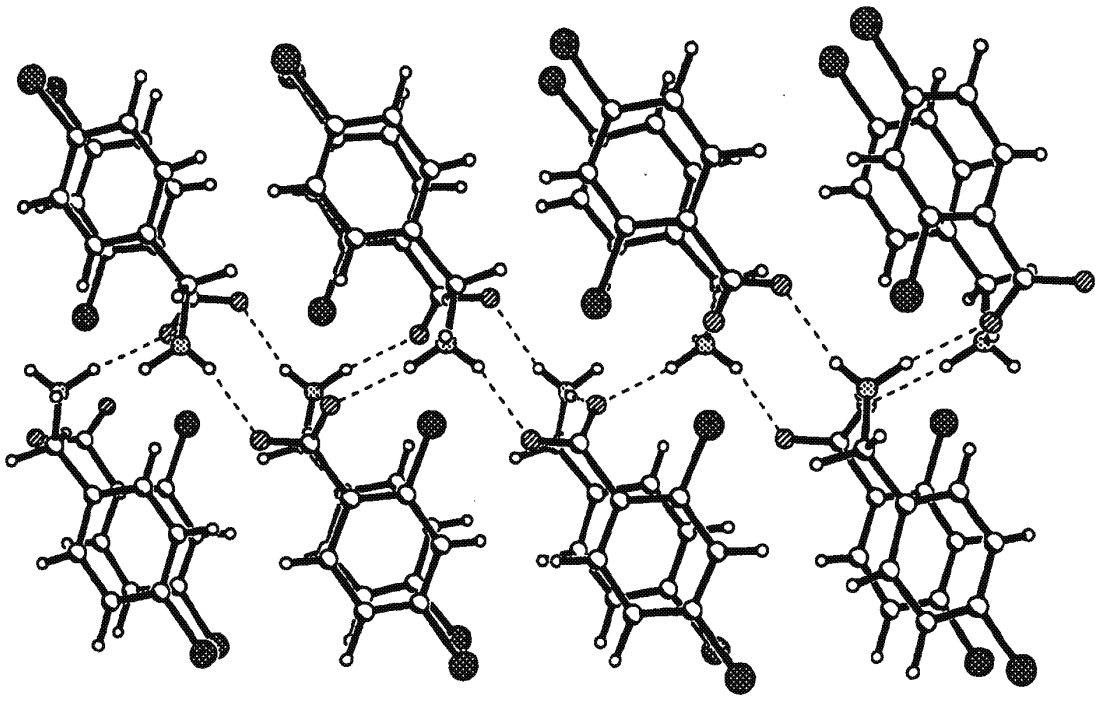


Fig. 3. Edge-on view of two-dimensional layers in 1.

Table III. Geometry of the Hydrogen Bonds in 2

D—H···A	r(H···A)/Å	r(D···A)/Å	<(D—H···A) (°)
N(27)—H(27C)···O(1)′	1.877(3)	2.732(3)	167.9(1)
N(27)—H(27D)···O(1)	1.889(3)	2.746(3)	166.9(1)
N(27)—H(27E)···O(2)″	1.823(3)	2.734(3)	174.2(1)

Symmetry code: (′) $x, y+1, z$; (″) $-x+1, y+\frac{1}{2}, -z+1\frac{1}{2}$

contain any chloro substituents) revealed the presence of two crystallographically independent ion pairs. Again the charge-assisted N—H···O hydrogen bonds between anions and cations (Table IV) operate in concert to generate an infinite low-dimensional motif; in this case, a two-dimensional layer (Fig. 5). The hydrogen-bond connectivity is complicated by the presence of two unique ion pairs in this structure, which leads to three rings within the infinite two-dimensional sheet: $R_4^2(8)$, $R_8^8(24)$, and $R_{12}^{10}(32)$. The topology is also more buckled than the corresponding two-dimensional layer in **1**. Nevertheless, as in **1**, the dominating hydrogen-bonding sites are confined to the core of each sheet, with the aromatic moieties protruding out from either side of the layer. The shortest F···F distances in the crystal structure of **3** are 2.96 and 2.88 Å.

The change in cation substitution from **3** to **4** (replacing a *para*-methyl with a *para*-chloro) provides the basis for a specific comparison of the structural influence of $-CH_3$ vs. —Cl. The two substituents are sterically similar but electronically very different. The main feature, a hydrogen-bonded two-dimensional sheet generated by $-NH_3^+\cdots{}^-OOC-$ interactions, is maintained in both structures (Table V). The infinite sheet in **4** is parallel with *b-c* (Fig. 6), and the hydrogen-bonding connectivity within the layer is identical to that observed for the two-dimensional layer in **1**: $R_4^2(8)$ and $R_8^8(24)$. There are no unusual intermolecular distances between neighboring layers, indicating a lack of specific and directional aryl-aryl or Cl···Cl attractions. An unusual aspect of this structure is the presence of narrow open channels parallel to *c* (Fig. 7). The diameter of each channel is approximately 3 Å. The interior of each microchannel is lined with chlorine and hydrogen atoms

UM00012614
NOVARTIS EXHIBIT 1017
Novartis v. Regents, IPR2023-01346
Page 1360 of 4460

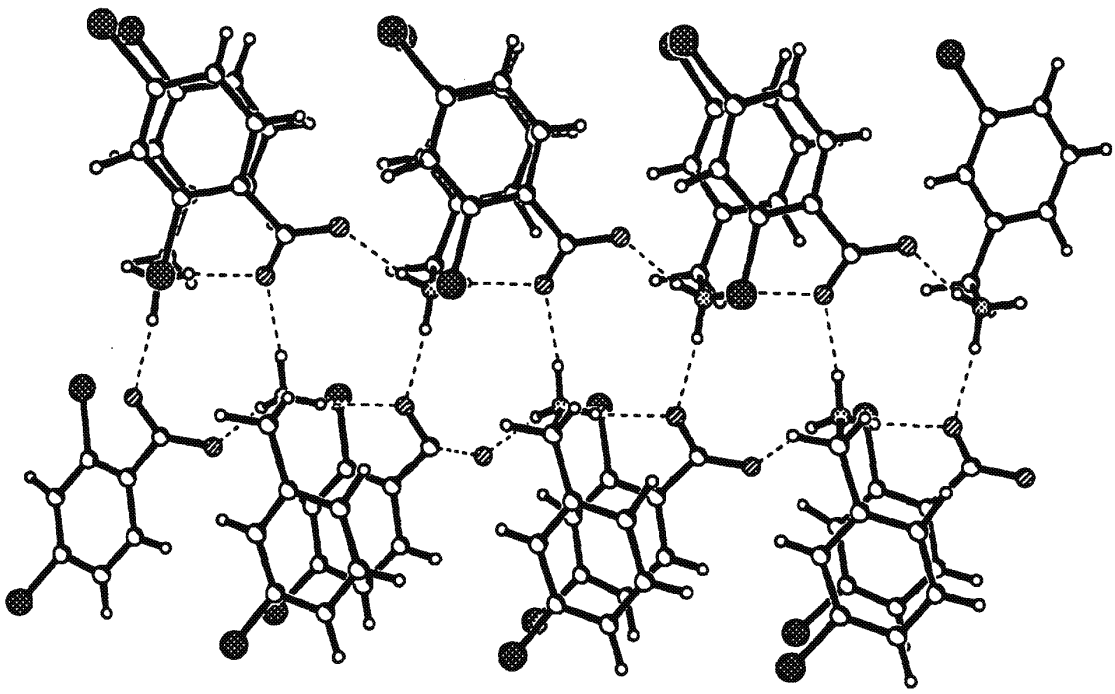


Fig. 4. A one-dimensional hydrogen-bonded ladder in 2.

Table IV. Geometry of the Hydrogen Bonds in 3

D—H···A	r(H···A)/Å	r(D···A) Å	<(D—H···A) (°)
N(27)—H(27C)···O(32)	2.023(3)	2.853(3)	151.70(9)
N(27)—H(27D)···O(2)′	1.869(3)	2.789(3)	164.25(9)
N(27)—H(27E)···O(1)	1.829(3)	2.762(3)	161.93(9)
N(47)—H(47C)···O(32)	1.896(4)	2.800(4)	174.4(1)
N(47)—H(47D)···O(1)	1.909(3)	2.864(3)	150.8(1)
N(47)—H(47E)···O(31)″	1.831(3)	2.756(3)	163.4(1)

Symmetry code: (′) $-x+1, y-\frac{1}{2}, -z+\frac{1}{2}$; (″) $x, -y+\frac{1}{2}, z-\frac{1}{2}$.

and no guest molecules reside in the channels. Despite the presence of these voids, the density of this material, 1.56 g cm^{-3}, is not unusual in any sense and the structure is, in fact, more dense than **3**, 1.48 g cm^{-3}.

The crystal structure of **5** consists of tetrameric units connected through a 10-membered ring, $R_4^3(10)$, generated by N—H···O hydrogen bonds between two anions and two cations (Table VI). A total of four hydrogen bond donors and three acceptors make up the ring, leaving two donors free to hydrogen bond to neighboring tetramers through a bifurcated hydrogen bond, thus creating one-dimensional ribbons (Fig. 8). The connectivity within this ribbon is identical to that displayed by the one-dimensional hydrogen-bonded ribbon in **2**. The aromatic units of each cation and anion point outward from the center of each chain, leading to a hydrophobic environment between adjacent chains. There are no notable π-π interactions (face-face or face-edge) in the hydrophobic region, and the overall assembly of ribbons is similar to that observed in **2**, despite the fact that the 3-Cl (on the cation in **2**) and 2,4-dichloro substituents (on the anion in **2**) have been replaced with protons in **5**.

Although water was present during the syntheses of several of these compounds, only one compound, **6**, incorporated water into its lattice. The incorporation of water in this structure does not provide much disruption to the primary intermolecular assembly: Adjacent hydrogen-bonded $NH_3^+\cdots{}^-OOC$ ribbons (Table VII) are connected via water molecules into infinite layers (Fig. 9). Two distinct hydrogen-bond patterns exist within these layers: $R_6^4(12)$ and $R_4^4(12)$. If the water molecules are removed from the structures, only discrete tetramers, composed of two cations and two anions hydrogen-

UM00012615
NOVARTIS EXHIBIT 1017
Novartis v. Regents, IPR2023-01346
Page 1361 of 4460

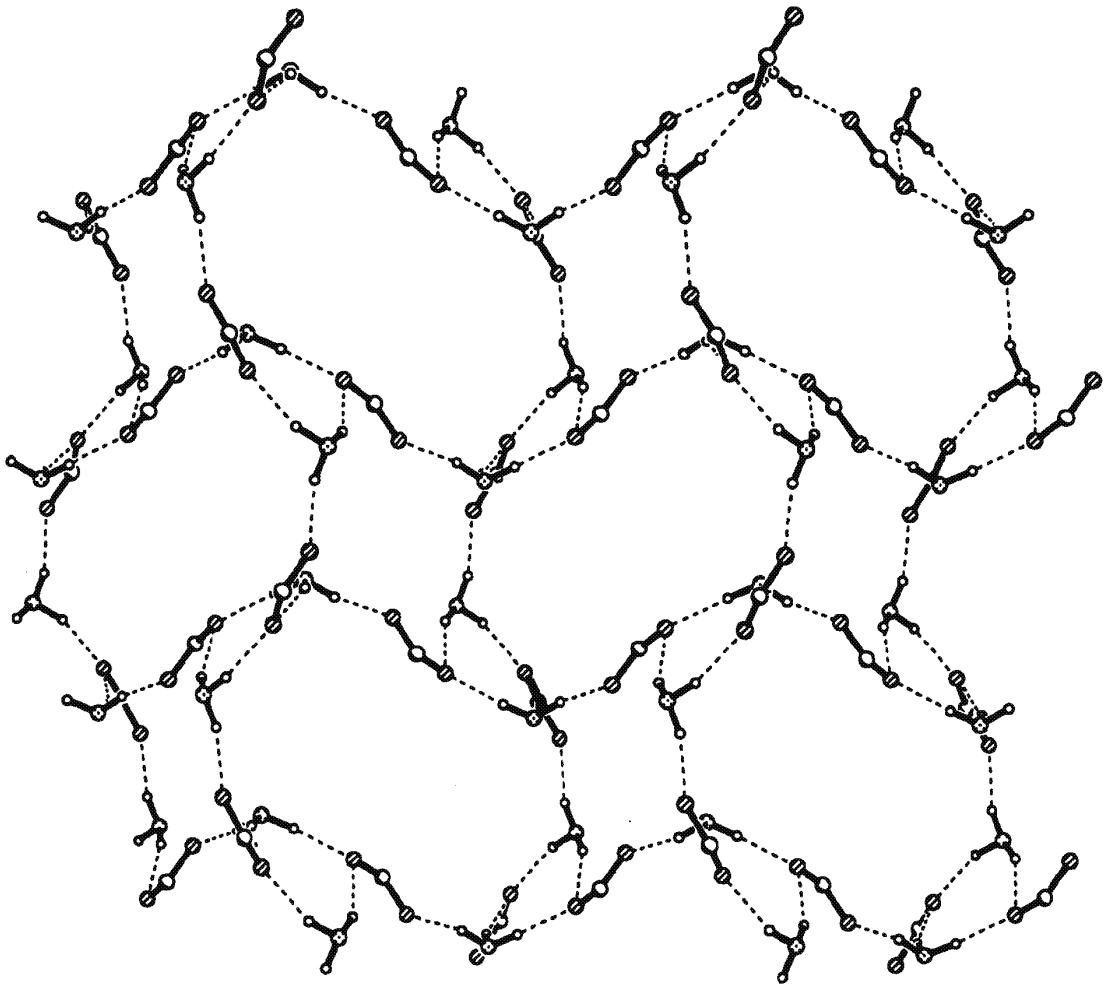


Fig. 5. Face-on view of the infinite two-dimensional sheet of anions and cations in 3. Aromatic rings removed for clarity.

Table V. Geometry of the Hydrogen Bonds in 4

D—H···A	r(H···A) Å	r(D···A) Å	<(D—H···A) (°)
N(27)—H(27D)···O(7)′	1.854(3)	2.750(3)	173.14(9)
N(27)—H(27E)···O(7)″	1.945(3)	2.760(3)	161.29(9)
N(27)—H(27C)···O(7)‴	1.905(3)	2.792(3)	168.47(9)

Symmetry code: (′) $x-\frac{1}{2}, -y+\frac{1}{2}, z-\frac{1}{2}$; (″) $x-\frac{1}{2}, y-\frac{1}{2}, z-1$; (‴) $-x, -y+1, -z$

bonded in a 12-membered ring pattern, remain. The water molecules therefore act as bridges in two different directions, linking individual tetrameric units together to form the resulting two-dimensional motifs. As was the case with all the structures containing two-dimensional anionic-cation sheets, the aromatic moieties in **6** are confined to the "outside" of the layer. Even so, there are no particularly short Cl···Cl or π-π intermolecular interactions in this crystal structure.

DISCUSSION

The molecular geometries of the participating anions in **1–6** do not display any unexpected features.

UM00012616
NOVARTIS EXHIBIT 1017
Novartis v. Regents, IPR2023-01346
Page 1362 of 4460

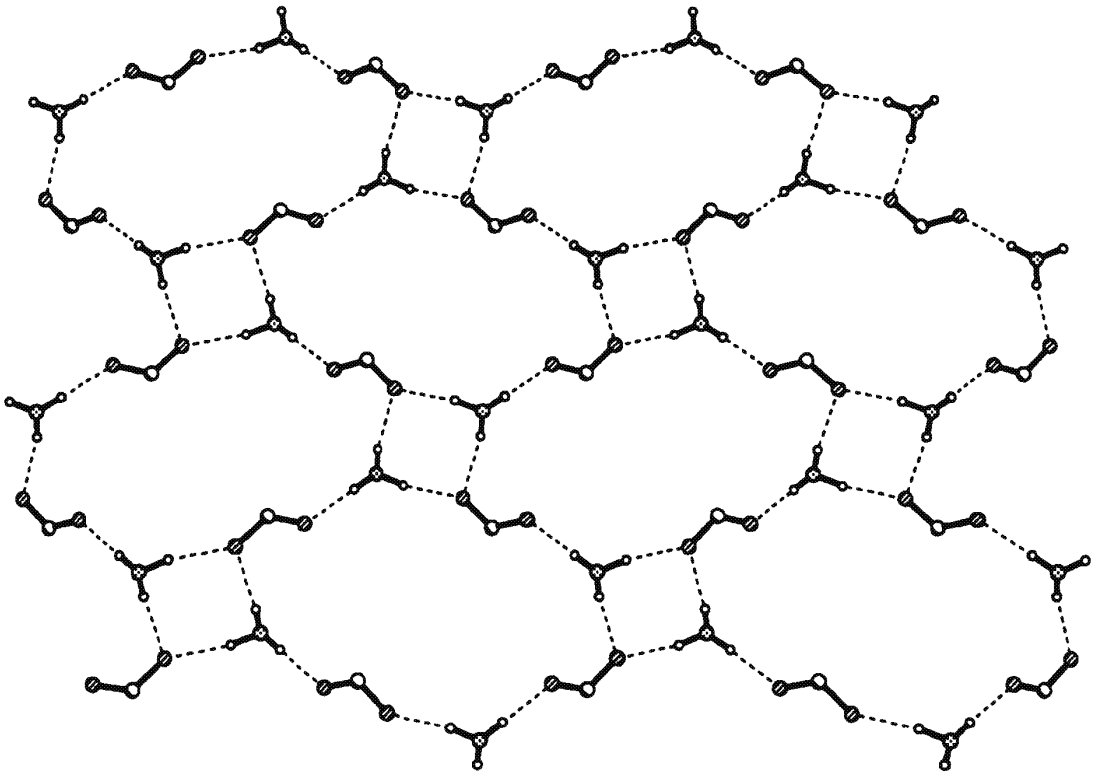


Fig. 6. Face-on view of the infinite two-dimensional sheet of anions and cations in **4**. Aromatic rings removed for clarity.

The major conformational variable of the cation, the position of the $-CH_2NH_3^+$ moiety with respect to the ring, is well-behaved; in six cases the C—C—C—N torsion angle is close to 90°, and in two cases this angle is close to 30°. A search of the Cambridge Structural Database [12] resulted in 32 examples of benzylammonium cations; 19 examples have torsion angles close to 90° and 13 have angles close to 30°. The rotation of the near-planar carboxylate moiety with respect to the ring varies from 40° to 72° for anions in **1–4**, which can be rationalized in terms of interactions (repulsion) between the substituents in the 2 and 6 positions on the aromatic ring of the anion, and the oxygen atoms of the carboxylate moieties. In contrast, the carboxylate moieties are nearly coplanar with the aromatic rings in **5** and **6** (7° and 11°, respectively), where there are no substituents *ortho* to the carboxylic group.

Although compounds **1–6** vary considerably in the types of substituents and substituent positioning, only a few basic structural features appear in their crystal structures. Without exception, all six structures are dominated by charge-assisted N—H···O hydrogen bonds between benzylammonium cations and carboxylate anions, resulting in infinite low-dimensional architectures. The majority of the structures (**1**, **3**, **4**, and **6**) contain two-dimensional hydrogen-bonded sheets while the remaining two compounds (**2** and **5**) exhibit one-dimensional hydrogen-bonded ribbons. The reason for the differentiation between one-dimensional and two-dimensional motifs in this set of structures is not clear. However, it is noteworthy that **2** and **5** are the only compounds with a substituent in the 3 position on the cationic ring, whereas the remaining salts contain 4-substituted cations. However, as the anions in those two compounds are very different, it is difficult to rationalize the appearance of one-dimensional ribbons solely based upon substitution position in the cations of **2** and **5**.

The presence of strong, charge-assisted hydrogen-

UM00012617
NOVARTIS EXHIBIT 1017
Novartis v. Regents, IPR2023-01346
Page 1363 of 4460

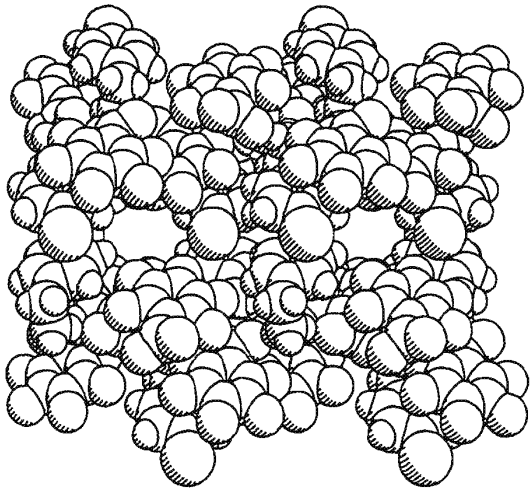


Fig. 7. Space filling view down the small open channels along c in 4.

Table VI. Geometry of the Hydrogen Bonds in 5

D—H···A	r(H···A) (Å)	r(D···A) (Å)	<(D—H···A) (°)
N(27)—H(27C)···O(1)′	1.817(2)	2.773(2)	177.11(7)
N(27)—H(27D)···O(2)″	1.885(2)	2.738(2)	167.67(7)
N(27)—H(27E)···O(3)‴	1.929(2)	2.761(2)	157.65(7)

Symmetry code: (′) $-x+1, y+\frac{1}{2}, -z+\frac{1}{2}$; (″) $-x+1, y-\frac{1}{2}, -z+\frac{1}{2}$; (‴) $x-1, y, z$

bond interactions between cations and anions means that the $-NH_3^+$ and the $-COO^-$ moieties are confined to well-defined regions in space, and they provide the central backbone of the one-dimensional ribbons (**2** and **5**) and two-dimensional sheets (**1**, **3**, **4**, and **6**), respectively. A consequence of this spatial aggregation of NH_3^+/COO^- moieties is that the aromatic moieties of the cations and

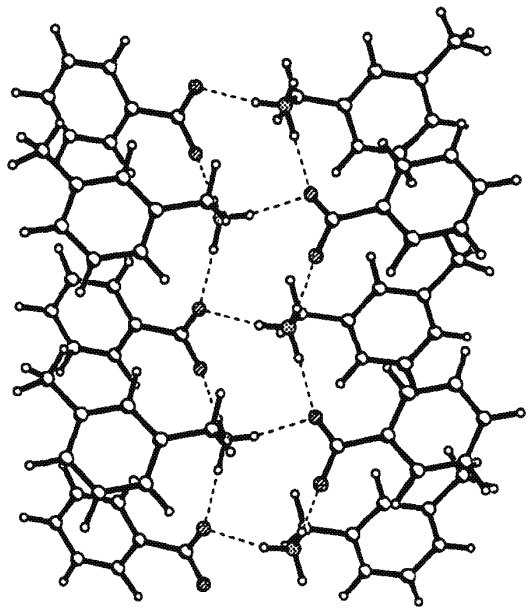


Fig. 8. A one-dimensional hydrogen-bonded ladder in 5.

the anions are always facing "outward" from the one-dimensional or two-dimensional "core," leading to specific hydrophobic regions throughout each structure.

Despite the fact that the aromatic components are directed by the NH_3^+/COO^- moieties into a confined space and are therefore in close proximity to each other, there are no intermolecular aryl-aryl distances (neither face-face nor face-edge contacts) that attest to the presence of significantly directional or stabilizing π-π interactions. Thus, although such interactions contribute to the overall lattice energy and stability of the crystals, they are unlikely to play a major role in the assembly of these materials.

As the halogen substituents in **1–6** do not partici-

Table VII. Geometry of the Hydrogen Bonds in 6

D—H···A	r(H···A) Å	r(D···A)/Å	<(D—H···A) (°)
N(27)—H(27C)···O(2)′	1.781(2)	2.741(2)	164.12(7)
N(27)—H(27D)···O(1)″	1.872(2)	2.790(2)	175.49(7)
N(27)—H(27E)···O(1W)	2.084(2)	2.769(2)	140.56(6)
O(1W)—H(1W)···O(1)‴	1.818(2)	2.719(2)	170.52(6)
O(1W)—H(2W)···O(2)⁗	1.877(2)	2.809(2)	177.89(6)

Symmetry code: (′) $x+1, y, z+1$; (″) $-x+1, -y+1, -z$; (‴) $x, y, z+1$; (⁗) $-x, -y, -z$

UM00012618
NOVARTIS EXHIBIT 1017
Novartis v. Regents, IPR2023-01346
Page 1364 of 4460

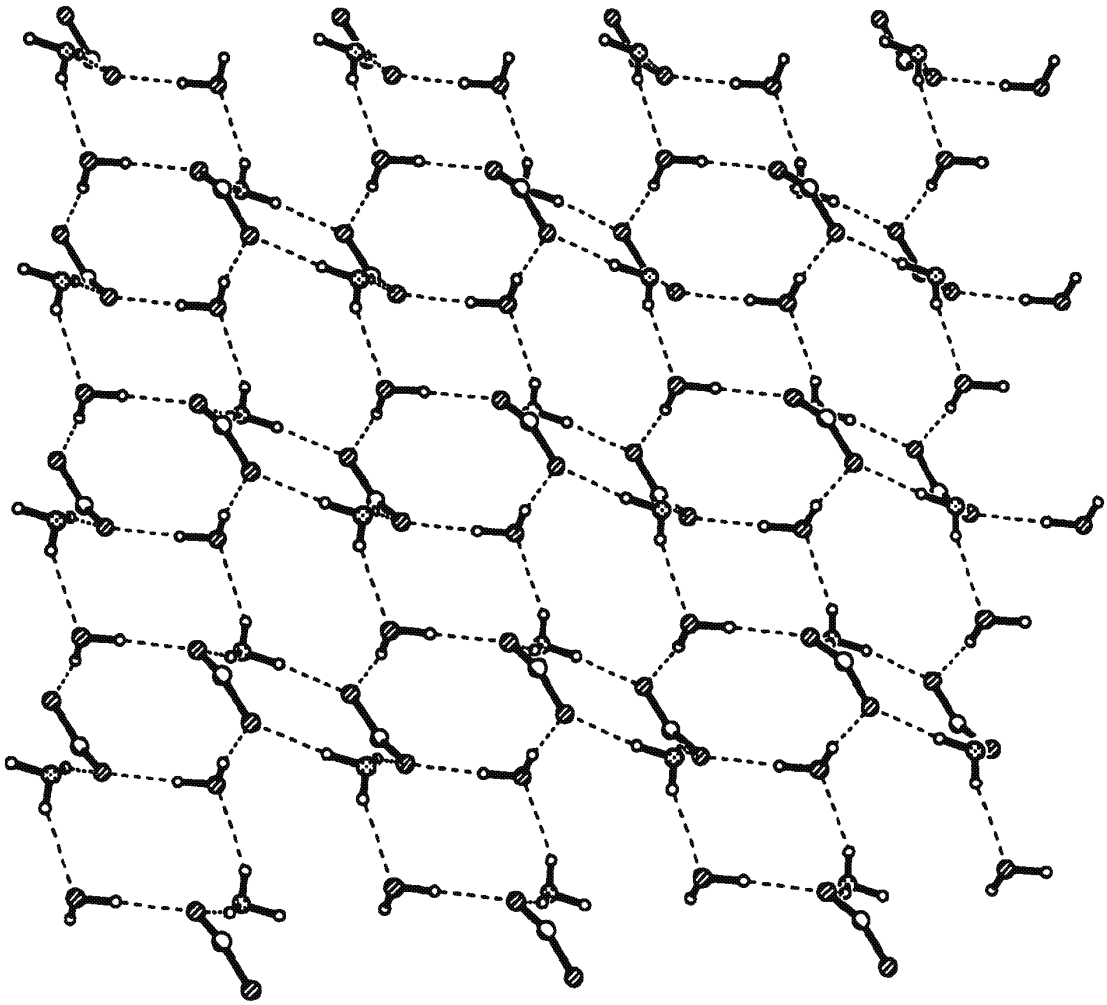


Fig. 9. Face-on view of anions, cations, and water molecules in 6, connected by hydrogen bonds into an infinite two-dimensional layer. Aromatic rings removed for clarity.

pate in any recurring patterns and motifs generated by short halogen-halogen distances, the structural influence of halogen-halogen contacts in this series of structures is relatively limited. In the case of 3 and 4, where there is an abundance of fluorine substituents, there are no F···F contacts below the combined van der Waals radii. This is in agreement with earlier work stating that F···F interactions are unlikely to have much control over the intermolecular assembly in the organic solid state [7]. The only remarkable Cl···Cl contacts appear in 1 and 2 (both are 3.35 Å). Even though these distances are shorter than the combined van der Waals radii for two chlorine atoms, it is hard to see that these two Cl···Cl geometries are indispensable to the supramolecular assembly process of each structure; in 1 the substituents are located on oppositely charged ions, whereas in 2 the chlorine atoms involved in the short contact are located on the cations. Furthermore, the C—Cl···Cl angles are very different

UM00012619
NOVARTIS EXHIBIT 1017
Novartis v. Regents, IPR2023-01346
Page 1365 of 4460

in the two compounds. It is reasonable to assume that, if they were significant, the interaction type would be the same in the two compounds, and there would be other occurrences of short Cl···Cl in these structures.

Based upon the systematic crystallographic investigation of **1–6**, it seems that the charge-assisted hydrogen bonds present in these structures constitute the primary intermolecular interactions that dominate the assembly of these ammonium and carboxylate ions into three-dimensional crystalline materials. The hydrogen-bond layers in **1** and **4** are identical, and the hydrogen-bonded ribbons in **2** and **5** are also identical. Nevertheless, as both one-dimensional and two-dimensional motifs are present, the precise and final structure is influenced by a combination of weaker and less well-defined intermolecular interactions.

The results presented herein can form the basis for a crystal engineering strategy that utilizes hydrogen bonds between carboxylate and quarternary ammonium cations as a way of "anchoring" aromatic units together in a relatively consistent manner. This can be done since intermolecular charge-assisted hydrogen bonds between ions are responsible for the assembly of the low-dimensional cation-anion architectures observed in **1–6**. Other noncovalent forces play a subordinate role until the primary motifs have been constructed. The next challenge will be to influence and control the subsequent orientation of these cation-anion aggregates through a combination of weaker intermolecular forces, for example, C—H···X, π-π, and halogen-halogen interactions.

ACKNOWLEDGMENTS

We are grateful to Robin Rogers and Lil Rogers, University of Alabama, Tuscaloosa, for collecting the crystallographic data for **4**. We acknowledge the financial support from Kansas State University, NSF-EPSCoR (OSR-9550487), and DuPont.

REFERENCES

1. (a) Desiraju, G. R. *Crystal Engineering: The Design of Organic Solids*; Elsevier: Amsterdam, 1989. (b) Desiraju, G. R. *Angew. Chem. Int. Ed. Engl.* **1995**, *34*, 2311.
2. Gavezzotti, A. *Acc. Chem. Res.* **1994**, *27*, 309.
3. (a) Aakeröy, C. B. *Acta Crystallogr. Sect. B.*, **1997**, *53*, 569. (b) Zaworotko, M. J. *Nature* **1997**, *386*, 220.
4. Braga, D.; Grepioni, F.; Desiraju, G. R. *Chem. Rev.* **1998**, *98*, 1375.
5. Pedireddi, V. R.; Reddy, D. S.; Goud, B. S.; Craig, D. C.; Rae, A. D.; Desiraju, G. R. *J. Chem. Soc. Perkin Trans. 2*, **1994**, 2353–2360.
6. (a) Price, S. L.; Stone, A. J.; Lucas, J.; Rowland, R. S.; Thornley, A. *J. Am. Chem. Soc.* **1994**, *116*, 4910. (b) Lommerse, J. P. M.; Stone, A. J.; Taylor, R.; Allen, F. A. *J. Am. Chem. Soc.* **1996**, *118*, 3108.
7. Dunitz, J. D.; Taylor, R. *Chemistry—A European J.* **1997**, *3*, 89.
8. Nyburg, S. C.; Wong-Ng, W. *Proc. R. Soc. London Ser. A* **1971**, *367*, 29.
9. Braga, D.; Angeloni, A.; Grepioni, F. *J. Chem. Soc., Dalton Trans.* **1998**, 1961.
10. Sheldrick, G. M. SHELXL-93, University of Göttingen.
11. (a) Bernstein, J.; Davis, R. E.; Shimoni, L.; Chang, N.-L. *Angew. Chem. Int. Ed. Engl.* **1995**, *34*, 1555. (b) Etter, M. C.; MacDonald, J. C.; Bernstein, J. *Acta Crystallogr. Sect. B* **1990**, *46*, 256.
12. Allen, F. H.; Kennard, O. *Chem. Design Automation News* **1993**, *8*, 1 and 31–37.

UM00012620
NOVARTIS EXHIBIT 1017
Novartis v. Regents, IPR2023-01346
Page 1366 of 4460

The C–H···Cl hydrogen bond: does it exist?

Christer B. Aakeröy,[a] Timothy A. Evans[b], Kenneth R. Seddon[b] and István Pálinkó[c]

[a] *Department of Chemistry, Kansas State University, Manhattan, KS 66506-3701, USA*
[b] *School of Chemistry, The Queen's University of Belfast, Belfast, Northern Ireland, UK BT9 5AG*
[c] *Department of Organic Chemistry, József Attila University, Dóm tér 8, Szeged H-6720, Hungary*

Received 5th November 1998, Accepted 30th November 1998

The extensive occurrence of C–H···Cl hydrogen bonds has been established through a systematic statistical analysis of the Cambridge Crystallographic Database; chloride anions are shown to be better hydrogen-bond accepor systems than neutral chloride-containing molecules, and a similar situation pertains for the other halides. As a result of this study, we propose that the conceptual van der Waals cut-off criterion be dropped for establishing the presence of weak intermolecular and intramolecular interactions, and be replaced by a distance/angle criterion determined by the empirical approach outlined here.

The existence of C–H···X hydrogen bonding has been a matter of controversy ever since it was first proposed by Glasstone[1] in 1937. Donohue's categoric rejection[2] of such interactions has been methodically eroded through several systematic examinations of existing crystallographic information,[3,4] and C–H···X hydrogen bonds have been shown to be of great importance in molecular recognition processes,[5] the reactivity and structure of biomolecular species,[6] the stability of inclusion complexes,[7] crystal engineering,[8] molecular conformation[9] and ionic liquids.[10] However, elements of the chemical and biochemical community ignore, or are unaware of, such interactions, or, more dangerously, dismiss them as insignificant, as exemplified in the recent paper by Kool and coworkers.[11,12]

It is common practice to attempt to identify C–H···X interactions on the basis of absolute geometrical cutoffs for the H···X distance ($d_{H\cdots X}$) and the C–H···X angle ($\alpha_{CH\cdots X}$). While this is apparently a logical procedure, we had reason to doubt the distance cutoff parameter normally used, the sum of the van der Waals radii, as a meaningful selection criterion. Hydrogen bonding is mainly electrostatic in origin, an attractive force which does not decrease greatly with increasing distance,[13] and is thus still expected to be significant well beyond the van der Waals separation. Indeed, as we will demonstrate, to use van der Waals cutoffs as a means of identifying C–H···X hydrogen bonds is a sure way to miss most of them. The additional consideration of an angle dependence with a cutoff of $\alpha_{CH\cdots X} > 90°$ is much more satisfactory: the C–H bond must not point away from the acceptor atom.

Several authors have studied the C–H···O interaction in great detail, and this is now widely accepted.[14–16] Other C–H···X interactions, however, have been infrequently proposed and rarely verified. Having identified several C–H···Cl^- hydrogen bonds during a re-examination of pyridinium chloride,[17] we proposed[18] that C–H···Cl hydrogen bonds might be present in a wide range of compounds containing heterocyclic aromatic systems. Desiraju believes that the C–H···Cl interaction is still questionable,[15] others (including Steiner[19] and Zefirov[20]) recognise its existence. We demonstrate here that the phenomenon is universal, and not restricted to any specific category of compounds.

The Cambridge Structural Database (CSD)[21] affords the opportunity to investigate intermolecular hydrogen-bonding statistically. Currently containing over 160 000 entries, investigations of weak attractive hydrogen-bond interactions will normally result in a data set which is large enough to permit conclusions. Firstly, in order to examine a case where there should be no intermolecular attractive interactions, the QUEST[21] program was used to locate all intermolecular H_2C–H···H–CH_2 contacts for all non-aromatic, non-organometallic systems in the H···H range 1.0–6.0 Å. No restrictions were placed upon the H_2C–H···H angle for the search, in contrast to the recent excellent study by Steiner and Desiraju.[22] The H···H and C···H distances and the C–H···H angle were recorded for all contacts with an H···H distance within the specified range, and with a crystallographic *R*-factor of 0.08 or smaller. Using a program, QUESTPLUS, specifically designed[23] to process the extremely large data sets obtained from the CSD, observations with a C–H···H angle $< 90°$ were eliminated. In order to statistically correct the data for the fact that the solid angle C–H···H is smaller for linear than for bent angles, the correction introduced by Kroon and Kanters[24] was applied during the sorting procedure.

Fig. 1 shows that while C–H···H–C contacts do occur at or near the sum of the van der Waals radii (2.4 Å as determined by Pauling and Bondi[25]) there is no significant angular dependance displayed [Fig. 1(c)], as would be expected in the case of a specific interaction. Moreover, there is no marked maximum in the distance dependance [Fig. 1(a) and (b)].

Further searches of the CSD were performed for the following contacts, using identical parameterisation and limits (*e.g.* H···Cl range 1.0–6.0 Å): O–H···Cl, C–H···Cl^-, C–H···Cl^0 (no ions present), C–H···Cl^0–C (no ions present) and C–H···Cl^0–E (E is any element other than carbon; no ions present). The data were processed as above.

Fig. 2 displays a very distinct angular and distance dependancy for the traditional hydrogen-bonding case of the O–H···Cl intermolecular interaction, with the vast majority of contacts clustered across a small range at short distances, well within the sum of the van der Waals radii (3.0 Å[25]), and at high angles, as would be expected for such a strong hydrogen-bonding interacion.

Fig. 3 and 4 show the distribution of C–H···Cl^- contacts and C–H···Cl^0 (for the neutral chlorine atom, where no ionic species are present) respectively. For the C–H···Cl^- case, there is a marked distance dependancy, displaying a maximum between 2.7 and 3.0 Å. Whilst this maximum is within the sum of the van der Waals radii of H and Cl (3.0 Å[25a], 2.95 Å[25b]), many of the contacts lie outside this cutoff, with a well defined angular dependance [Fig. 3(a) and 3(c)]. The data in this range show a propensity towards shorter distances with more linear contacts, as would be expected with an attractive hydrogen-bonding type interaction, as in the O–H···Cl case

UM00012621
NOVARTIS EXHIBIT 1017
Novartis v. Regents, IPR2023-01346
Page 1367 of 4460

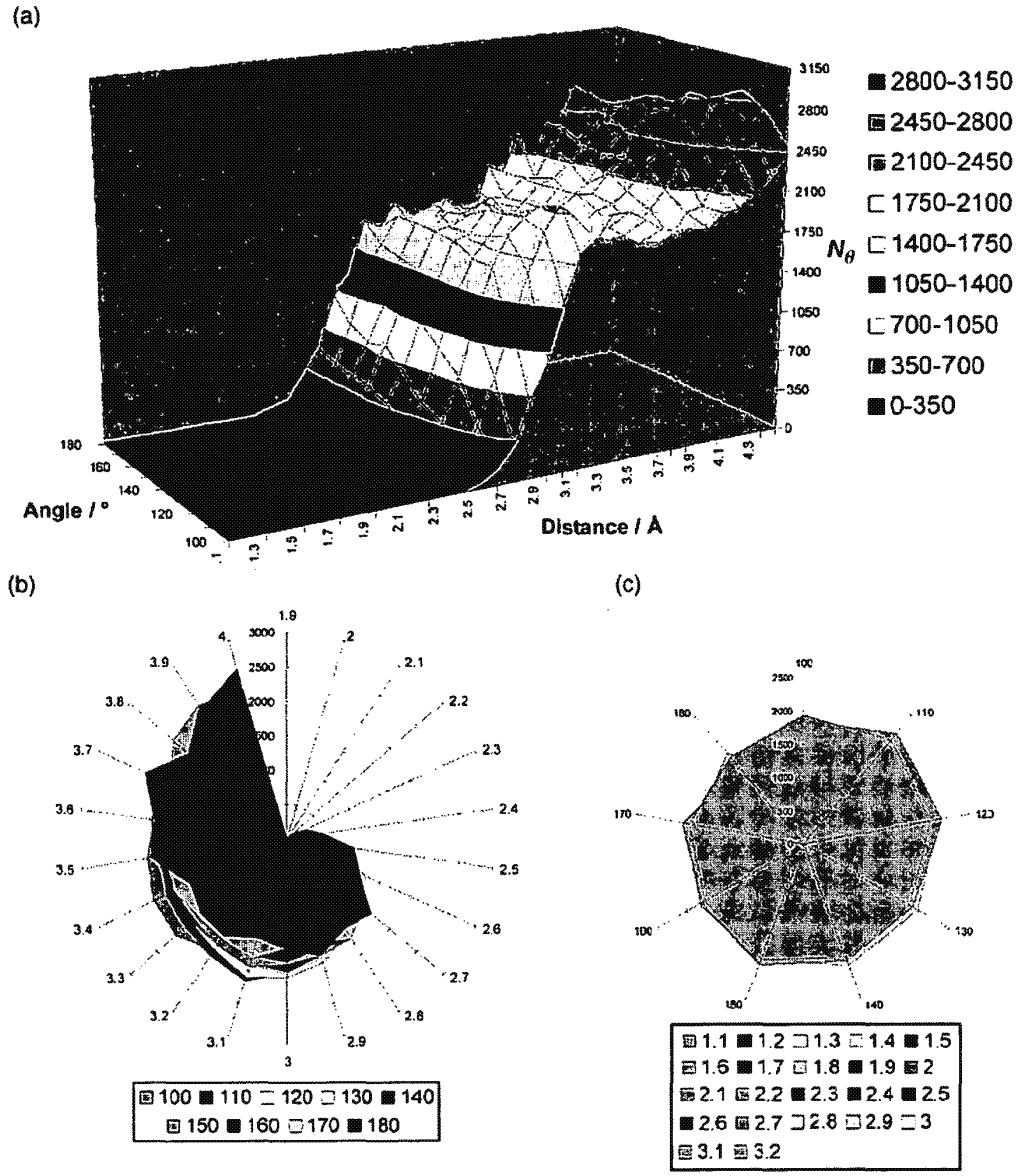


Fig. 1 (a) Three-dimensional representation of the geometrically corrected number of hits (N_θ) as a function of C–H···H angle and H···H distance. (b) Radar representation of the number of C–H···H–C contacts as a function of distance. (c) Radar representation of the number of C–H···H–C contacts as a function of angle.

(or indeed O–H···O),[26] although much less pronounced (C–H being a much weaker hydrogen bond donor). This establishes the C–H···Cl^- interaction to be an attractive, hydrogen-bonding interaction, commonly displayed at distances greater then the conventional van der Waal's limit.

For the case of C–H···Cl^0, where no ionic species are present, the maximum is now between 2.9 and 3.1 Å and the majority of the contacts lie beyond the sum of the van der Waals radii. This maximum peak is less well defined than for the C–H···Cl^- case, as the hydrogen bonds, while demonstrably real, are weaker. More careful investigation of the C–H···Cl^0 case (no ions), shows that when Cl^0–C is the acceptor group (Fig. 5) the maximum now moves outside the sum of the van der Waals radii, and its distribution is broader yet again. This suggests ever weaker hydrogen bonding. This is mirrored in a recent paper,[27] in which C–Cl functions are shown to be poor, but real, hydrogen bond acceptors for O–H and N–H hydrogen bond donors.

Fig. 6 demonstrates that when chlorine is bonded to atoms other than carbon (mostly metals), the maximum is found to

UM00012622
NOVARTIS EXHIBIT 1017
Novartis v. Regents, IPR2023-01346
Page 1368 of 4460

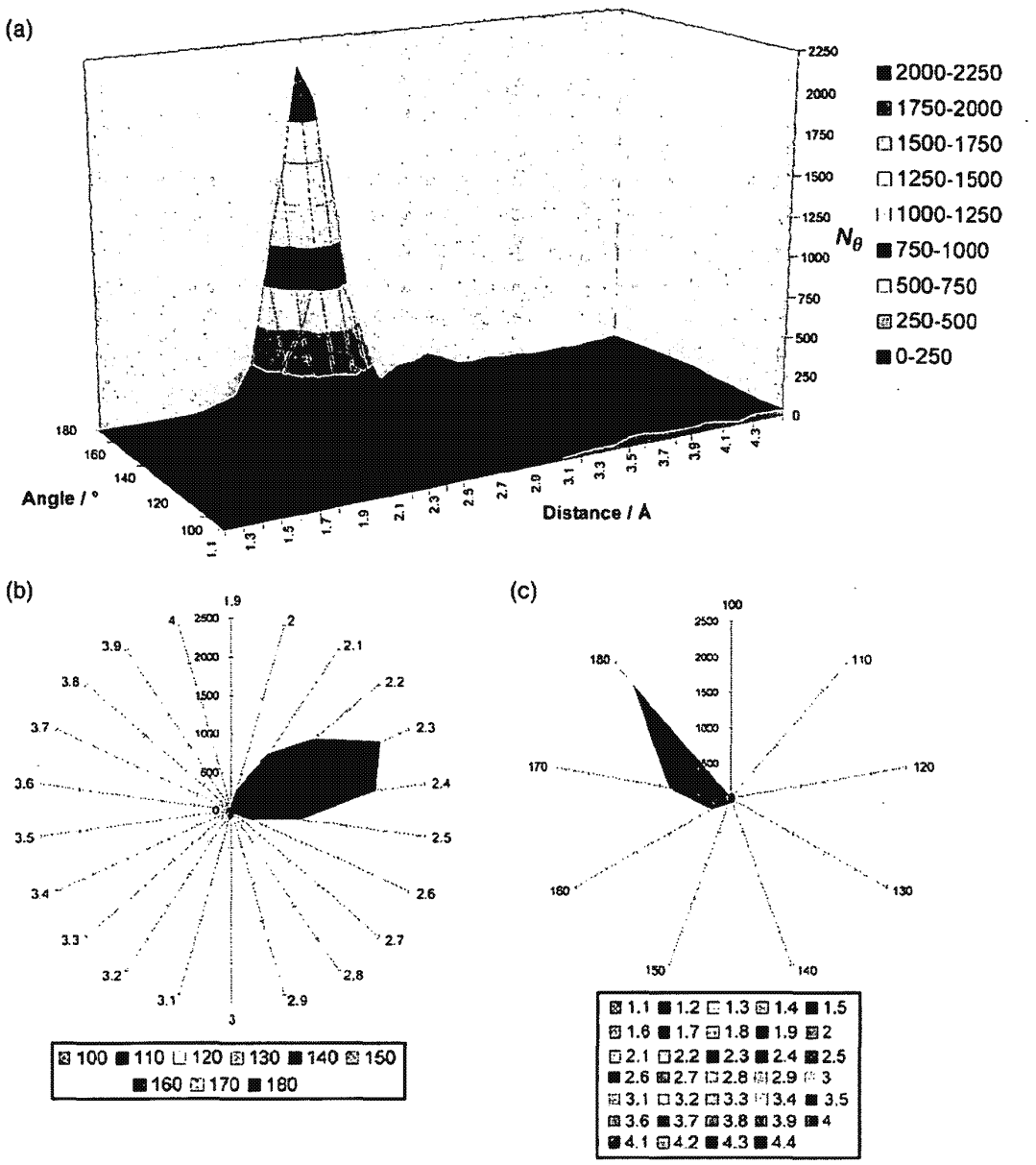


Fig. 2 (a) Three-dimensional representation of the geometrically corrected number of hits (N_θ) as a function of O–H···Cl angle and H···Cl distance. (b) Radar representation of the number of O–H···Cl contacts as a function of distance. (c) Radar representation of the number of O–H···Cl contacts as a function of angle.

be at 3.0 Å, with the shape of the distribution more closely mirroring the C–H···Cl^- case (see Fig. 3). So, for all possible cases, chlorine is behaving as a C–H hydrogen bond acceptor, but with the strength of interaction depending on the charge density on the chlorine. We find that C–H hydrogen bonds to fluorine, bromine and iodine show similar patterns of bonding to the chlorine case.

We have represented the results of the searches in three complementary graphical formats. The first, Figures (a), is a three-dimensional representation of the data, which gives an immediate visual representation of the distribution of contacts in distance and angular space. Thus a flat angular response with a continuously rising number of hits as an irregular function of distance, *viz.* Fig. 1(a), represents an isotropic distribution of contacts. In other words, this is the non-specific interaction situation, with no identifiable hydrogen bonding. A sharp peak, *viz.* Fig. 2(a), represents a classically strong, directional hydrogen bond. Fig. 3(a)–6(a) show weaker hydrogen bonds, and the sharpness of the peak and the rate of fall off from the maximum with distance, are clear indicators of

UM00012623
NOVARTIS EXHIBIT 1017
Novartis v. Regents, IPR2023-01346
Page 1369 of 4460

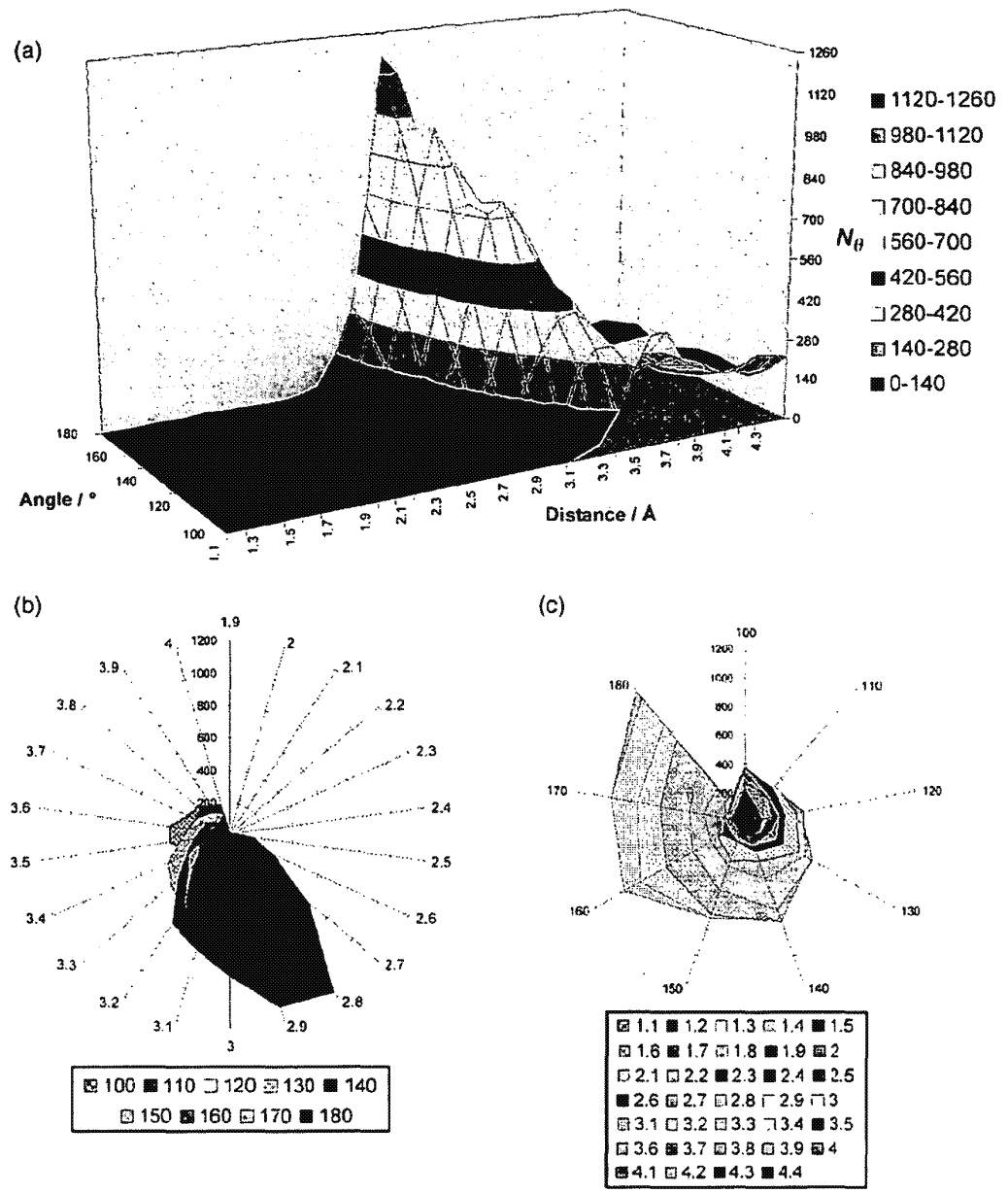


Fig. 3 (a) Three-dimensional representation of the geometrically corrected number of hits (N_θ) as a function of C–H···Cl⁻ angle and H···Cl⁻ distance. (b) Radar representation of the number of C–H···Cl⁻ contacts as a function of distance. (c) Radar representation of the number of C–H···Cl⁻ contacts as a function of angle.

the strength of that interaction. Thus, this representation gives both an immediate recognition of the presence and a measure of the strength of a directional interaction. Although pedagogically useful, however, this representation is rather poor for extracting numerical information. The other two representations are radar plots: Figures (b) plot the number of contacts on a distance grid, colour-coded for angle; Figures (c) plot the number of contacts on an angular grid, colour-coded for distance. Thus, the 'sea-shell' in Fig. 1(b), with contacts increasing with increasing distance, represents the non-interacting case, whereas the peaks in Fig. 2(b)–6(b) represent clearly defined interactions: the sharper the peak, the stronger the interaction. The maximum of the peak represents the most common distance encountered empirically, and the onset of the peak represents the shortest contact. In contrast, the circle in Fig. 1(c) represents an isotropic situation (the antithesis of hydrogen bonding), whereas the 'sea-shells' in Fig. 2(c)–6(c), all with maxima at 180°, represent the anisotropy of the inter-

UM00012624
NOVARTIS EXHIBIT 1017
Novartis v. Regents, IPR2023-01346
Page 1370 of 4460

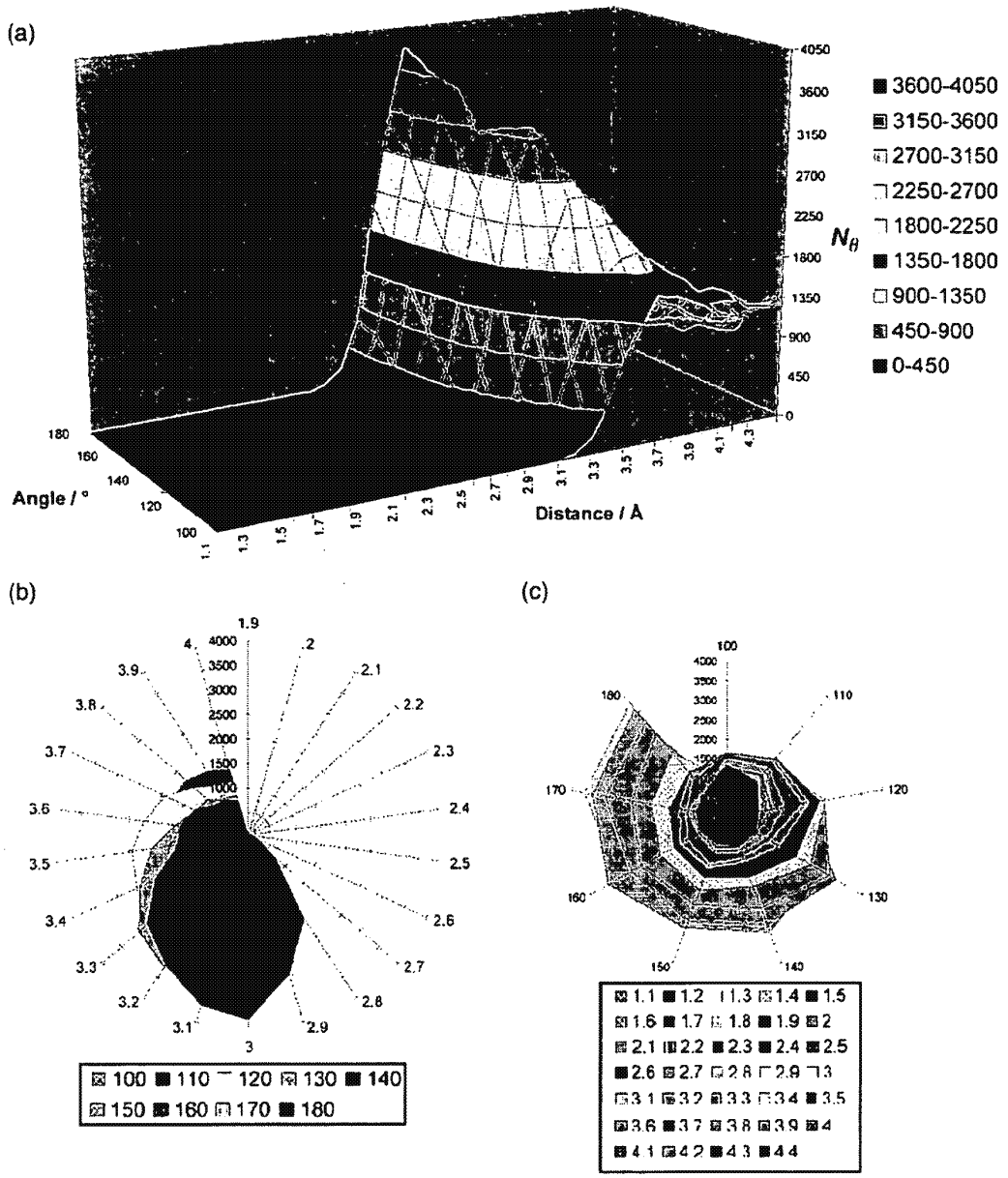


Fig. 4 (a) Three-dimensional representation of the geometrically corrected number of hits (N_θ) as a function of C–H···Cl^0 angle and H···Cl^0 distance. (b) Radar representation of the number of C–H···Cl^0 contacts as a function of distance. (c) Radar representation of the number of C–H···Cl^0 contacts as a function of angle.

action. Again, the sharper the peak, the stronger the interaction. Thus, a combination of all three representations gives a very clear view of the interaction; it transforms the arbitrary traditional arguments based on van der Waals radii (a very shaky theoretical concept) to one based on experimental evidence. It also establishes a clearly quantifiable grey scale, allowing a gradual definable transition from strong angularly dependent interactions to classical dispersion forces. Moreover, the same methodology has been applied to more traditional hydrogen-bonding situations, and to X···X interactions (*cf.* Desiraju's seminal reports),[8,28] with great success.[29]

The investigation described in this paper demonstrates that the C–H···Cl hydrogen bond is a much more common phenomenon than previously thought. Many computer simulation studies do not treat C–H adequately to account properly for C–H···X hydrogen bonds, which can play a significant role, and we believe that the importance of such interactions to crystal engineering has been vastly underestimated. In addi-

UM00012625
NOVARTIS EXHIBIT 1017
Novartis v. Regents, IPR2023-01346
Page 1371 of 4460

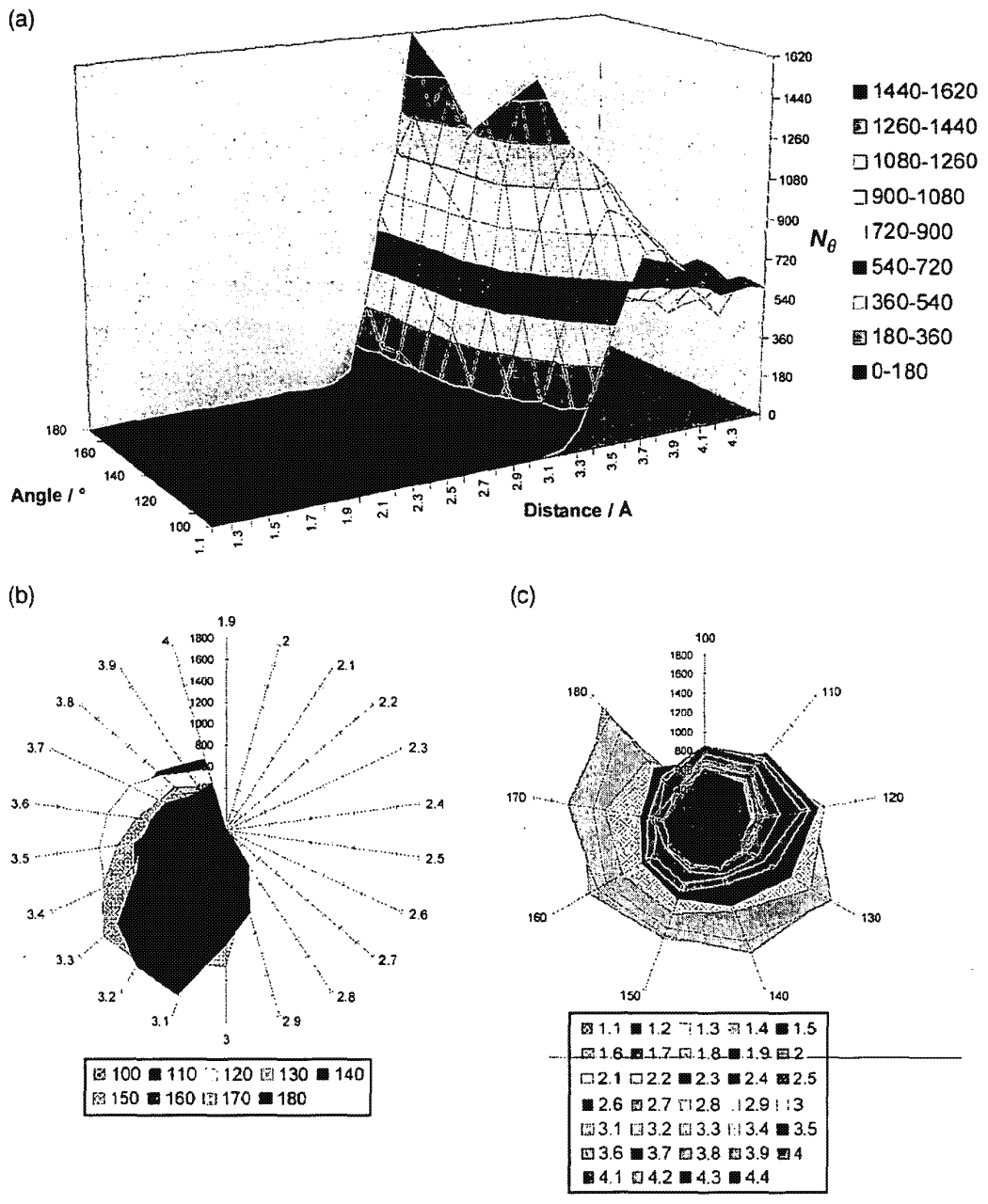


Fig. 5 (a) Three-dimensional representation of the geometrically corrected number of hits (N_θ) as a function of C–H···Cl^0 angle and H···Cl^0 distance. (b) Radar representation of the number of C–H···Cl^0–C contacts as a function of distance. (c) Radar representation of the number of C–H···Cl^0–C contacts as a function of angle.

tion, it is shown that use of the sum of the van der Waals radii to validate intermolecular hydrogen-bonding interactions is a very poor criterion; an approach similar to the method used here is much more satisfactory. Indeed, we would propose that the conceptual van der Waals cut-off criterion be dropped for establishing the presence of intermolecular and intramolecular hydrogen-bonding interactions, and replaced by a distance/angle criterion determined by the empirical approach outlined here.

Acknowledgements

We wish to acknowledge support from the EPSRC in the form of a ROPA award, the EPSRC and Royal Academy of Engineering for the award of a Clean Technology Fellowship (to K.R.S.), the National Science Foundation of Hungary (F4297/1992) and the Commission of the European Communities East-West Mobility Scheme for Scientists (to I.P.; grant 12009).

UM00012626
NOVARTIS EXHIBIT 1017
Novartis v. Regents, IPR2023-01346
Page 1372 of 4460

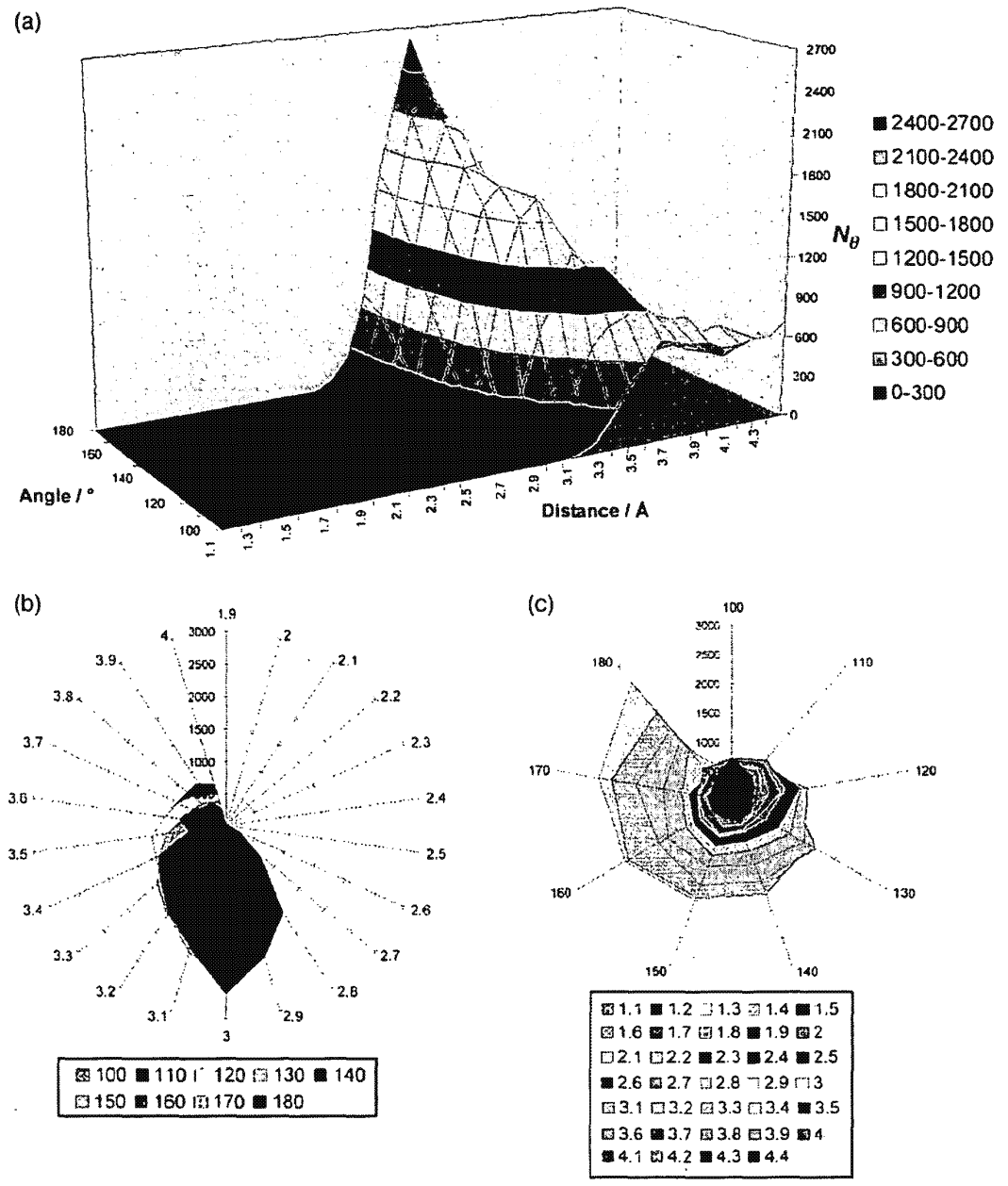


Fig. 6 (a) Three-dimensional representation of the geometrically corrected number of hits (N_θ) as a function of C–H···Cl^0 angle and H···Cl^0 distance. (b) Radar representation of the number of C–H···Cl^0–E contacts as a function of distance. (c) Radar representation of the number of C–H···Cl^0–E contacts as a function of angle.

Notes and references

1 S. Glasstone, *Trans. Faraday Soc.*, 1937, **33**, 200.
2 J. Donohue, in *Structural Chemistry and Molecular Biology*, ed. A. Rich and N. Davidson, W. H. Freeman, San Francisco, CA, 1968.
3 R. Taylor and O. Kennard, *J. Am. Chem. Soc.*, 1982, **104**, 5063.
4 D. Braga, F. Grepioni, K. Biradha, V. R. Pedireddi and G. R. Desiraju, *J. Am. Chem. Soc.*, 1995, **117**, 3156.
5 L. J. W. Shimon, M. Vaida, L. Addadi, M. Lahav and L. Leiserowitz, *J. Am. Chem. Soc.*, 1990, **112**, 6215; E. M. D. Keegstra, A. L. Spek, J. W. Zwikker and L. W. Jenneskens, *J. Chem. Soc., Chem. Commun.*, 1994, 1633; G. R. Desiraju, *Angew. Chem., Int. Ed. Engl.*, 1995, **34**, 2311.
6 G. A. Jeffrey and W. A. Saenger, in *Hydrogen Bonding in Biological Structures*, Springer-Verlag, Berlin, 1991; Z. S. Derewenda, U. Derewenda and P. M. Kobos, *J. Mol. Biol.*, 1994, **241**, 83; Z. S. Derewenda, L. Lee and U. Derewenda, *J. Mol. Biol.*, 1995, **252**, 248.
7 T. Steiner and W. Saenger, *J. Chem. Soc., Chem. Commun.*, 1995, 2087; D. Braga, F. Grepioni, J. J. Byrne and A. Wolf, *J. Chem. Soc., Chem. Commun.*, 1995, 125.
8 J. A. R. P. Sarma and G. R. Desiraju, *Acc. Chem. Res.*, 1986, **19**, 222.

UM00012627
NOVARTIS EXHIBIT 1017
Novartis v. Regents, IPR2023-01346
Page 1373 of 4460

9 G. Müller, M. Lutz and S. Harder, *Acta Crystallogr., Sect. B*, 1996, **52**, 1014.
10 A. K. Abdul-Sada, A. M. Greenway, P. B. Hitchcock, T. J. Mohammed, K. R. Seddon and J. A. Zora, *J. Chem. Soc., Chem. Commun*, 1986, 1753; A. G. Avent, P. A. Chaloner, M. P. Day, K. R. Seddon and T. Welton, *J. Chem. Soc., Dalton Trans.*, 1994, **23**, 3405.
11 S. Moran, R. X.-F. Ren, S. Rumney IV and E. T. Kool, *J. Am. Chem. Soc.*, 1997, **119**, 2056.
12 T. A. Evans and K. R. Seddon, *Chem. Commun.*, 1997, 2023
13 H. Umeyama and K. Morokuma, *J. Am. Chem. Soc.*, 1977, **99**, 1316.
14 G. R. Desiraju, *Acc. Chem. Res.*, 1991, **24**, 290; T. Steiner and W. Saenger, *J. Am. Chem. Soc.*, 1992, **114**, 10146; T. Steiner and W. Saenger, *J. Am. Chem. Soc.*, 1993, **115**, 4540; T. Steiner, *Chem. Commun.*, 1997, 727.
15 G. R. Desiraju, *Angew. Chem., Int. Ed. Engl.*, 1995, **34**, 2311.
16 J. J. Novoa, B. Tarron, M.-H. Whangbo and J. M. Williams, *J. Chem. Phys.*, 1991, **95**, 5179; T. van Mourik and F. B. van Duijneveldt, *J. Mol. Struct. (THEOCHEM)*, 1995, **341**, 63.
17 K. Hensen, P. Pullmann and J. W. Bats, *Z. Anorg. Allg. Chem.*, 1988, **556**, 62; D Mootz and J. Hocken, *Z. Naturforsch, Teil B*, 1989, **44**, 1239.
18 C. B. Aakeröy and K. R. Seddon, *Z. Naturforsch., Teil B*, 1993, **48**, 1023.
19 T. Steiner, *Acta Crystallogr., Sect. B*, 1998, **54**, 456.
20 Y. V. Zefirov, *Crystallogr. Rep.*, 1998, **43**, 283.
21 Cambridge Structural Database version 5.14 (October 1997); F. H. Allen and O. Kennard, *Chem. Des. Automat. News*, 1993, **8**, 3137.
22 T. Steiner and G. R. Desiraju, *Chem. Commun.*, 1998, 891.
23 T. A. Evans, QUESTPLUS, The Queen's University of Belfast, 1994–1998.
24 J. Kroon and J. A. Kanters, *Nature (London)*, 1974, **248**, 667.
25 (*a*) L. Pauling, *The Nature of the Chemical Bond*, Cornell University Press, USA, 1947; (*b*) A. Bondi, *J. Phys. Chem.*, 1964, **68**, 441.
26 H. F. J. Savage and J. L. Finney, *Nature (London)*, 1986, **322**, 717.
27 G. Aullón, D. Bellamy, L. Brammer, E. A. Bruton and G. Orpen, *Chem. Commun.*, 1998, 653.
28 G. R. Desiraju, *Crystal Engineering, The Design of Organic Solids*, Elsevier, Amsterdam, 1989.
29 T. A. Evans and K. R. Seddon, unpublished work.

Letter 8/09309A

UM00012628
NOVARTIS EXHIBIT 1017
Novartis v. Regents, IPR2023-01346
Page 1374 of 4460

CRYSTAL ENGINEERING OF IONIC SOLIDS

Polymorphism, Crystallography, Inter-Ring Interactions and C—H Hydrogen Bonding

CHRISTER B. AAKERÖY, TIMOTHY A. EVANS AND KENNETH R. SEDDON
School of Chemistry, The Queen's University of Belfast,
Stranmillis Road, BELFAST, BT9 5AG, Northern Ireland
WWW: http://www.ch.qub.ac.uk/krs/krs.html; e-mail: k.seddon@qub.ac.uk

ABSTRACT. This paper considers aspects of crystal engineering which are relevant to the design of salts as functional solids, with specific reference to the design of novel non-centrosymmetric materials for second harmonic generation. In addition, some aspects of polymorphism, current practice in the field of single-crystal X-ray diffraction, inter-ring interactions, and C—H hydrogen bonding in the salts of heterocyclic cations are discussed.

1. Introduction

In 1988, the editor of *Nature*, John Maddox, wrote:

> ***"One of the continuing scandals in the physical sciences is that it remains impossible to predict the structure of even the simplest crystalline solids from a knowledge of their chemical composition"***

This was true then, and is still largely true today, but this simple and accurate summary of the state of ignorance of the chemical community underlines the need for, and in essence defines, the field of crystal engineering [1,2]. This is a field in its formative years; it is at the interface between a number of crucial, but fundamentally different, areas, and has all the challenge and excitement expected of interdisciplinary research. We present, then, our thoughts on the crystal engineer's tool kit, and consider its effectiveness for granting topological control [3,4] over crystalline form, and hence control over such crucial physical phenomena as melting point, optical properties, thermal stability, solubility, colour, conductivity, crystal habit, and mechanical strength. This is an area of fundamental and pivotal interest to industry and academia, but it does not yet attract the full attention that it deserves.

The purpose of this paper is not to present a philosophy of crystal engineering - space does not permit this, and an up-to-date account of some recent developments can be found elsewhere [5]. Instead, the intention is to highlight, using examples taken from our

J. Michl (ed.), Modular Chemistry, 153–162.
© 1997 *Kluwer Academic Publishers. Printed in the Netherlands.*

UM00012629
NOVARTIS EXHIBIT 1017
Novartis v. Regents, IPR2023-01346
Page 1375 of 4460

own work, in particular, some of the applications of this new field, and indicate some of the possibilities which open up when chemists turns their attention from the intramolecular bond (with which they are familiar) to the world of intermolecular and interionic interactions and supramolecular chemistry [6], where the rule book remains to be written.

2. The Design of Novel Materials for Second Harmonic Generation

2.1 PRACTICAL CONSIDERATIONS

Recent years have seen considerable interest in nonlinear optical materials, including those capable of second harmonic generation (SHG)[¶] [7]. Such materials, and the basis of their properties, have attracted both academic and commercial investigators, and their applications include:

- Controlling the flow of optical data
- Advanced telecommunications
- Optical computing
- Improving densities in optical storage media
- Weapons guidance systems
- Laser defence systems

The existence of the phenomenon of SHG is determined by the crystal symmetry of the medium: SHG can only occur in a non-centrosymmetric medium [8]. However, this is only an on-off switch: the efficiency (*i.e.* intensity) of the SHG effect is governed, *inter alia*, by the second-order coefficient of the polarizability of the medium, $\chi^{(2)}$, which (for molecular solids) is related to second-order coefficient of the polarizability of the molecule, β. Thus, provided the crystal is non-centrosymmetric (*i.e.* if $\chi^{(2)} \neq 0$), then the larger the value of the molecular coefficient, β, the more intense the emitted SHG radiation, and hence the more effective the material, provided that the molecules are organized within the crystal structure in such a way that the dipoles reinforce, rather than oppose, each other. Large values of β are related to the dipole moment of the molecule (or, to be more precise, to the difference in dipole moment between the ground state and the first excited electronic state), and hence efficient molecular SHG materials frequently usually have large ground state dipole moments. It is received wisdom in this field that molecules with a large dipole

---

[¶] Second harmonic generation is the phenomenon of doubling the frequency of laser light, induced by passage of light through a non-centrosymmetric medium. Thus invisible infrared radiation of wavelength 1064 nm will be frequency-doubled to green 532 nm light.

UM00012630
NOVARTIS EXHIBIT 1017
Novartis v. Regents, IPR2023-01346
Page 1376 of 4460

moment tend to crystallize in centrosymmetric space groups,[¶] and therefore that attempts to create high-β materials are bedevilled by a tendency of these materials to be inactive in their normal crystalline form, because $\chi^{(2)}$ is zero. Irrespective of whether this folklore is correct or not [9], it is evident that merely preparing molecules with high β values does not guarantee that they will form SHG active crystals. Moreover, molecules with a high β value usually possess a small HOMO-LUMO gap, and hence are COLOURED. Indeed, large β values usually imply that the crystals are intensely coloured, and hence that they will absorb any visible light generated by the frequency doubling of infrared radiation. It follows that these materials are, for applications where the required radiation is visible, about as much use as a glass hammer! Despite these empirical observations, the open literature upon the synthesis of novel materials for SHG is dominated by papers for which the *raison d'être* is the synthesis of high β-value molecules, to the exclusion of all other practical considerations. In any practical device in a fully integrated optoelectronic circuit, the construction temperature is likely to approach 320 °C [10], and the properties of any useful materials **MUST** include:

- Thermal stability
- Involatility
- Optical clarity
- Lack of colour
- Mechanical strength
- Suitable crystal habit

and last, and **DEFINITELY** least:

- Large β values

Although for more specific uses (especially non-integrated applications), one or more of these restrictions may ne relaxed, the cynosure of designing new materials for SHG must be to prepare optically clear, colourless, thermally robust, mechanically strong, non-centrosymmetric crystals, with the value of $\chi^{(2)}$ (and hence β) being relatively unimportant, as long as it is not zero. Indeed, the current commercially important materials, potassium dihydrogen phosphate and lithium niobate(V), have risibly small values of $\chi^{(2)}$ compared with the least efficient of the organic materials available, and yet these are the industrial materials of choice.

[¶] In a recent paper, Whitesell [9] has shown, statistically, using the structures in the Cambridge Structural Database, that there is an equal probability that molecules with large dipole moments will crystallize in polar (centrosymmetric) or non-polar (non-cetrosymmetric) space groups.

UM00012631
NOVARTIS EXHIBIT 1017
Novartis v. Regents, IPR2023-01346
Page 1377 of 4460

The question thus remains - why are so few synthetic papers concerned with designing materials with the **NECESSARY** properties for incorporating into practical devices? The answer is simple - because it is a much more difficult and diffuse problem to design materials which match the needs of industry than it is to maximize β. Nevertheless, crystal engineering, as will be demonstrated below, does offer solutions to these hitherto difficult problems. It is perhaps not as enticing to design colourless materials with high lattice energies as it is to be able to claim a molecule with the world's largest β value, but it is significantly more important.

2.2 THE CRYSTAL ENGINEER'S TOOL KIT

Before dealing with the problems raised in Section 2.1, it perhaps worth examining the tools available in the crystal engineer's tool kit. These include:

1 SYNTHETIC VECTORS

- Hydrogen bonding
- Inter-ring interactions (the misleadingly named π–π stacking)
- Covalent bonds
- Coulombic forces

2 COMPUTATIONAL CHEMISTRY

3 VISUALIZATION TOOLS

4 CAMBRIDGE STRUCTURAL DATABASE

These are, perhaps, worth examining in a little more detail.

2.2.1 *Synthetic Vectors*

Synthetic vectors are to the crystal engineer what covalent bonds are to the molecular chemist. They are the intermolecular or interionic cohesive forces which hold the crystalline structure together. These can include many varied forces, encompassing hydrogen bonds (see Section 5) [1], inter-ring interactions (see Section 4), conventional covalent σ-bonds,[1] Coulombic forces and dipole-dipole interactions. The goal of the crystal engineer is to apply these synthetic vectors to the problems of the control of functional crystal structures with the same degree of success as the synthetic chemist designs and prepares funtionalized molecules. This goal lies a long time in the future, but the last decade (as so well illustrated by other papers in this book) has provided real and significant insights, and if we do not yet have rules, at least we now understand some of the guidelines.

---

[1] See the articles by Mike Zaworotko and by Jeffrey Moore, elsewhere in this volume.

UM00012632
NOVARTIS EXHIBIT 1017
Novartis v. Regents, IPR2023-01346
Page 1378 of 4460

2.2.2 *Computational Chemistry*

Just as computational chemistry is growing in importance in conventional chemical synthesis (especially drug design), then it has achieved a parallel, if not more significant, *rôle* in crystal engineering. The Cerius, CAChe and Spartan packages offer the ability to perform molecular mechanics, semi-empirical (especially AM1 and PM3), *ab initio* Hartree-Fock, and *ab initio* density functional calculations. Moreover, the results of these calculations can be visualized in three-dimensions - not only the structure of the molecules, ions or crystals, but also the molecular orbitals of the system (including the HOMO and the LUMO) and the total electron density and the charge and spin distribution.[¶] In addition, *inter alia*, lattice energy calculations are available, as are lattice optimization and crystal morphology packages. The use of computational techniques is central to the crystal engineer, and to ignore them would be as short-sighted as for the synthetic chemist to ignore NMR spectroscopy and X-ray crystallography!

2.2.3 *Visualization Tools*

Structural visualization is a rather different use of computer techniques than computational chemistry (although the uninitiated tyro, in our personal experience, regards the only worthwhile aim of computational chemistry to be the production of high quality graphics for publication!) - it enables the graduate and postdoctoral student not only to gain a quite remarkable insight into three-dimensional architecture and structure, in spatial terms, but also to enable structure-determining interactions to be identified and appreciated.

2.2.4 *Cambridge Structural Database*

The Cambridge Structural Database[§] offers a unique resource to the crystal engineer. Now available on CD-ROM, at trivial cost to academic institutions, it enables all organic and many inorganic (as long as they contain carbon) structures which are known to be rapidly scanned for structural or functional features, and to be imported in to, say, Cerius for visualization and detailed examination. Apart from the incalculable value of this resource for reevaluating known structures (see, for example, Section 5), it enables structures to be readily compared, using Etter's topological analysis [3,4], and many hypotheses to be tested using extant data, without the need for new structural determinations {*e.g.* [11]}.

2.3 CRYSTAL ENGINEERING AND SHG-ACTIVE MATERIALS

We have reported elsewhere on the development of several series of novel SHG-active salts with a wide range of desirable chemical and physical properties [12-15], using the strong and directional hydrogen-bonding between ions [16] as the principal synthetic vector, and

---

¶ See the article by Olivier Kahn, elsewhere in this volume.

§ Details available from:
Dr. Olga Kennard, Cambridge Structural Database, Cambridge Crystallographic Data Centre, CAMBRIDGE CB2 1EW, U.K.

UM00012633
NOVARTIS EXHIBIT 1017
Novartis v. Regents, IPR2023-01346
Page 1379 of 4460

it is not the purpose of a NATO ARW presentation to dwell on published material. However, it is worth, perhaps, expanding upon the crystal engineering principles which underpin this work, as they have a greater generality than the specific published targets. As early as 1989 [12], we proposed that it would be possible to use salts, in preference to neutral molecules, to enhance the thermal stability and eliminate the vapour pressure of novel materials for SHG applications. Of greater significance, however, we also proposed that it should be possible to use salts to "factorize" the properties of a material, so that the anion and the cation would have different, discrete functions. For example, in our own work on dihydrogen phosphates [12], hydrogen tartrates [13,14], hydrogen malates [17] and hydroxybenzoates [15], the anion is used to determine the crystal architecture, and impart thermal and structural stability, whilst the cation is used to "carry" the SHG activity.[¶] In addition to the intellectual satisfaction of separating function and associating it with identifiable and discrete chemical units, the preparation of simple salts of this type is **MUCH** easier than the covalent synthesis of new materials in which it would be necessary to combine all the functions in one molecule. The use of salts, then, represents not just practical and synthetic convenience, but also represents significant economic, and hence commercial, advantage.

3. Polymorphism

3.1 INTRODUCTION

Polymorphism is a unique feature of the solid state, being a form of isomerism that is not conventionally considered by synthetic chemists. A recent court case in the USA has focussed attention on polymorphism, in a way that only multi-billion dollar litigation can! The true extent of polymorphism among crystalline materials is very difficult to assess (*vide infra*). However, as it has been more often encountered in areas of research where structure is of paramount importance, we are in strong agreement with McCrone [18] who stated (in 1965):

> ***"[...] every compound has different polymorphic forms and that, in general, the number of forms known for a given compound is proportional to the time and money spent in research on that compound."***

It is generally accepted that differences in lattice energies between different polymorphs are in the region 5-20 kJ mol^{-1}, and, especially for ionic compounds, these differences are

---

[¶] In a spectacular and elegant independent demonstration of this principle, reported elsewhere in this volume, Olivier Kahn has factorized the properties of a salt such that it contains ferromagnetic anionic layers, and luminescent cationic layers: cooling the material below its Curie temperature results in a magneto-optical modification of its emission spectrum.

UM00012634
NOVARTIS EXHIBIT 1017
Novartis v. Regents, IPR2023-01346
Page 1380 of 4460

small compared to the total lattice energies of such materials. Thus, different methods of recrystallization are often sufficient to induce the formation of a new structural form (polymorph). However, as will be discussed in the following Section, the whole subject of crystal engineering in general, and polymorphism in particular, has been afflicted by the routine and normal practice of X-ray crystallographers (which is rather sad to have to report in 1995, which marks the centenary of the discovery of X-rays by Röntgen).

3.2 ARE CRYSTALLOGRAPHERS **BAD** SCIENTISTS?

The normal practice in determining a crystal or molecular structure is for the X-ray crystallographer to select one, or more, "perfect" crystals from the batch provided by the synthetic chemist. The process of selecting a single perfect crystal, and claiming (implicitly) it to be "characteristic" of the bulk material, is thus **scientifically indefensible**, as the selected single crystal is, **BY DEFINITION**, atypical of the bulk material from which it was removed. Thus the determined structure can only be ascribed to the single crystal for which it was determined, and **NOT** to the whole synthetic batch of material prepared. It may, or may not, represent the same compound as the bulk material. It may, for example, be a recrystallized minor impurity, or represent a different solvate, or a polymorph of the bulk material.

The above situation would not be so lamentable if there was not an easy remedy - but there is! It merely requires that the powder XRD pattern of the BULK sample should always be recorded, and compared with the simulated powder pattern from the single crystal data. This would provide absolute evidence as to whether or not the determined structure is that of the bulk material, and the whole procedure would take less than an hour. It is difficult to imagine another field of scientific endeavour where such appallingly lax procedures should be adopted as the norm, and be almost universally adopted, when such a simple remedy is available. It is quite incredible that the practice still persists, and we wish to suggest that it should, under normal circumstances, be an absolute prerequisite for publication in reputable journals that evidence be provided that the single crystal and the bulk material are crystallographically identical. The question of structural purity is, in many areas of chemistry, as important as that of chemical purity.

4. Inter-Ring Interactions

In Section 2.2.1, inter-ring interactions (frequently given the misleading term "π-π" interactions) were cited as synthetic vectors, alongside hydrogen bonds, which could lead to structural control in the solid state. The structural manifestation of inter-ring interactions is ring stacking, and this is an extremely common phenomenon found in the crystal structures of materials containing aromatic rings, particularly when these are functionalized. An important question which remains to be answered is: how strong are these interactions compared to, say, hydrogen bonds, and are they powerful enough to grant structural

UM00012635
NOVARTIS EXHIBIT 1017
Novartis v. Regents, IPR2023-01346
Page 1381 of 4460

control? In previously unpublished work [19], we have been able do demonstrate computationally, using a simple electrostatic model based upon the Coulombic forces between localized computed atomic charges, that the inter-ring interactions are of the order of 20-30 kJ mol^{-1}, the same order of magnitude as a weak hydrogen bond. It is thus entirely reasonable to consider these interactions as synthetic vectors.

5. C—H Hydrogen Bonds Involving Heterocyclic Cations

Although there is now an increasing awareness of the existence of C—H···X (X = F, Cl, Br or I) hydrogen bonds in neutral organic molecules [20,21], there have been surprisingly few studies of C—H···X^- interactions in organic salts. We have demonstrated the existence of extensive hydrogen bonding between aromatic C—H groups and halide ions, C—H···X, within a series of imidazolium salts [22-24], and in two polymorphs of pyridinium chloride [11]. At the time, we concluded [11]:

> ***"The existence of aromatic C—H···X hydrogen bonds in ionic compounds containing charged heterocyclic systems is very likely to be a regularly occurring phenomenon which needs to be further analyzed in a systematic and stringent fashion in order to rationalize the structural behaviour displayed by such ions."***

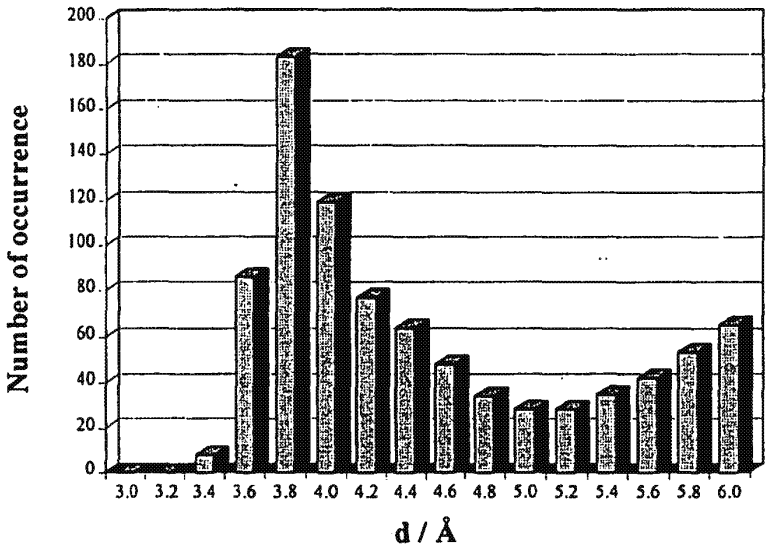


Figure 1: *The distribution of C-H...Cl contact distances between heterocyclic cations and chloride-containing anions, using data from the CSD*

UM00012636
NOVARTIS EXHIBIT 1017
Novartis v. Regents, IPR2023-01346
Page 1382 of 4460

By writing special code to supplement the normal search and display procedures which are supplied with the Cambridge Structural Database (CSD), we have now performed this further analysis, and demonstrated that C—H···X^- interactions in organic salts of charged heterocyclic systems are extremely common, but are precluded by adjacent bulky substituents (*e.g.* -CMe_3 or -$SiMe_3$) [25]. Figure 1 illustrates the distribution of C—H···X^- bond lengths for all well-defined structures in the CSD containing heterocyclic cations and chloride-containing anions. We have similar data for oxygen-, nitrogen-, sulfur-, fluoride-, bromide- and iodide-containing anions, and all show a strong propensity towards hydrogen-bonding. The tetramethylammonium cation also shows significant C—H···X hydrogen bonds, too. Thus, it is our contention that, although weak, C—H···X hydrogen bonds are present in many crystals, and that their presence has been largely unsuspected. As, say, the pyridinium cation is capable of forming hydrogen bonds with **ALL** its ring protons, then the summed effect of C—H···X hydrogen bonding is significant, despite each bond being individually weak. We cannot, as yet, associate an energy with these bonds, and this will be the subject of future research.

Acknowledgements

We are indebted to the BP Venture Research Unit, Unilever, and the Queen's University of Belfast for their generous funding of this project, to the EPSRC and Royal Academy of Engineering for the award of a Clean Technology Fellowship (to K.R.S.), and to Prof. J. Michl for his invitation allowing one of us (K.R.S.) to participate in this NATO ARW.

References

1. Aakeröy, C.B. and Seddon, K.R. (1993) The hydrogen bond and crystal engineering, *Chem. Soc. Rev.* **22**, 397-407.
2. Desiraju, G.R. (1989) *Crystal Engineering: The Design of Organic Solids*, Elsevier, Amsterdam.
3. Etter, M.C. (1990) Encoding and decoding hydrogen-bond patterns of organic compounds, *Acc. Chem. Res.* **23**, 120-126.
4. Etter, M.C., Macdonald, J.C. and Bernstein, J. (1990) Graph-set analysis of hydrogen-bond patterns in organic crystals, *Acta Crystallogr., Sect. B* **46**, 256-262.
5. Desiraju, G.R. (ed.) (1996) *The Crystal as a Supramolecular Entity*, Wiley, Chichester.
6. Lehn, J.-M. (1995) *Supramolecular Chemistry: Concepts and Perspectives*, VCH, Weinheim.
7. Chemla, D.S. and Zyss, J. (eds.) (1987) *Nonlinear Optical Properties of Organic Molecules and Crystals*, Vols. 1 and 2, Academic Press, New York.
8. Marder, S.R., Sohn, J.E. and Stucky, G.D. (eds.) (1991) *Materials for Nonlinear Optics, ACS Symp. Ser. 455*, 455, American Chemical Society, Washington D.C.
9. Whitesell, J.K., Davis, R.E., Saunders, L.L., Wilson, R.J. and Feagins, J.P. (1993) Do molecular dipole interactions influence solid-state organization?, *J. Phys. D* **26**, B56-B59.

UM00012637
NOVARTIS EXHIBIT 1017
Novartis v. Regents, IPR2023-01346
Page 1383 of 4460

10. Lytel, R., Lipscombe, G.F., Binkley, E.S., J.T., K. and Ticknor, A.J. (1991) Electrooptic polymer wave-guide devices - status and applications, in S.R. Marder, J.E. Sohn and G.D. Stucky (eds.), *Materials for Nonlinear Optics, ACS Symp. Ser. 455*, American Chemical Society, Washington D.C., pp. 103-112.
11. Aakeröy, C.B. and Seddon, K.R. (1993) The crystal-structures of pyridinium chloride revisited - evidence for extensive C-H...Cl hydrogen-bond interactions, *Z. Naturforsch., Teil B* **48**, 1023-1025.
12. Aakeröy, C.B., Hitchcock, P.B., Moyle, B.D. and Seddon, K.R. (1989) A novel class of salts for second harmonic generation, *J. Chem. Soc., Chem. Commun.*, 1856-1859.
13. Aakeröy, C.B., Hitchcock, P.B. and Seddon, K.R. (1992) Organic salts of L-tartaric acid - materials for second harmonic generation with a crystal-structure governed by an anionic hydrogen-bonded network, *J. Chem. Soc., Chem. Commun.*, 553-555.
14. Aakeröy, C.B. and Hitchcock, P.B. (1993) Hydrogen-bonded layers of hydrogentartrate anions - building-blocks for crystal engineering, *J. Mater. Chem.* **3**, 1129-1135.
15. Aakeröy, C.B., Bahra, G.S., Hitchcock, P.B., Patell, Y. and Seddon, K.R. (1993) Crystal engineering - hydrogen-bonded salts of hydroxybenzoic acids for second harmonic generation, *J. Chem. Soc., Chem. Commun.*, 152-156.
16. Aakeröy, C.B., Seddon, K.R. and Leslie, M. (1992) Hydrogen-bonding contributions to the lattice energy of salts for second harmonic generation, *Struct. Chem.* **3**, 63-65.
17. Aakeröy, C.B. and Nieuwenhuyzen, M. (1994) Hydrogen-bonded layers of hydrogen malate anions - a framework for crystal engineering, *J. Am. Chem. Soc.* **116**, 10983-10991.
18. McCrone, W.C. (1965) Polymorphism, in D. Fox, M.M. Labes and A. Weissberger (eds.), *Physics and Chemistry of the Organic Solid State*, Interscience, New York, pp. 725-767.
19. Aakeröy, C.B. and Seddon, K.R. (1992) unpublished results.
20. Desiraju, G.R. and Parthasarathy, R. (1989) The nature of halogen ... halogen interactions. Are short halogen contacts due to specific attractive forces or due to close packing of nonspherical atoms?, *J. Am. Chem. Soc.* **111**, 8725-8726.
21. Jeffrey, G.A. and Saenger, W. (1991) *Hydrogen Bonding in Biological Structures*, Springer-Verlag, Berlin.
22. Abdul-Sada, A.K., Greenway, A.M., Hitchcock, P.B., Mohammed, T.J., Seddon, K.R. and Zora, J.A. (1986) Upon the structure of room-temperature halogenoaluminate ionic liquids, *J. Chem. Soc., Chem. Commun.*, 1753-1754.
23. Abdul-Sada, A.K., Al-Juaid, S., Greenway, A.M., Hitchcock, P.B., Howells, M.J., Seddon, K.R. and Welton, T. (1990) Upon the hydrogen-bonding ability of the H(4) and H(5) protons of the imidazolium cation, *Struct. Chem.* 1, 391-394.
24. Avent, A.G., Chaloner, P.A., Day, M.P., Seddon, K.R. and Welton, T. (1994) Evidence for hydrogen-bonding in solutions of 1-ethyl-3-methylimidazolium halides, and its implications for room-temperature halogenoaluminate(III) ionic liquids, *J. Chem. Soc., Dalton Trans.*, 3405-3413.
25. Aakeröy, C.B., Evans, T., Pálinkó, I. and Seddon, K.R. (1993-1995) unpublished results.

UM00012638
NOVARTIS EXHIBIT 1017
Novartis v. Regents, IPR2023-01346
Page 1384 of 4460

This Page is Inserted by IFW Indexing and Scanning Operations and is not part of the Official Record

BEST AVAILABLE IMAGES

Defective images within this document are accurate representations of the original documents submitted by the applicant.

Defects in the images include but are not limited to the items checked:

- ☐ BLACK BORDERS
- ☐ IMAGE CUT OFF AT TOP, BOTTOM OR SIDES
- ☐ FADED TEXT OR DRAWING
- ☐ BLURRED OR ILLEGIBLE TEXT OR DRAWING
- ☐ SKEWED/SLANTED IMAGES
- ☐ COLOR OR BLACK AND WHITE PHOTOGRAPHS
- ☐ GRAY SCALE DOCUMENTS
- ☐ LINES OR MARKS ON ORIGINAL DOCUMENT
- ☐ REFERENCE(S) OR EXHIBIT(S) SUBMITTED ARE POOR QUALITY
- ☐ OTHER: _____

IMAGES ARE BEST AVAILABLE COPY.
As rescanning these documents will not correct the image problems checked, please do not report these problems to the IFW Image Problem Mailbox.

TOPICAL REVIEW

Acta Cryst. (1997). B53, 569–586

Crystal Engineering: Strategies and Architectures

CHRISTER B. AAKERÖY

Department of Chemistry, Kansas State University, Manhattan, KS 66506, USA. E-mail: aakery@pop.ksu.edu

(Received 15 March 1997; accepted 6 June 1997)

Abstract

The area broadly described as crystal engineering is currently expanding at a brisk pace. Imaginative schemes for supramolecular synthesis, and correlations between molecular structure, crystal packing and physical properties are presented in the literature with increasing regularity. In practice, crystal engineering can be many different things; synthesis, statistical analysis of structural data, *ab initio* calculations *etc.* Consequently, we have been provided with a new playing field where chemists from traditionally unconnected parts of the spectrum have exchanged ideas, defined goals and made creative contributions to further progress not only in crystal engineering, but also in other disciplines of chemistry. Crystal engineering is delineated by the nature and structural consequences of intermolecular forces, and the way in which such interactions are utilized for controlling the assembly of molecular building blocks into infinite architectures. Although it is important to acknowledge that a crystal structure is the result of a subtle balance between a multitude of non-covalent forces, this article will focus on design strategies based upon the hydrogen bond and will present a range of approaches that have relied on the directionality and selectivity of such interactions in the synthesis of predictable one-, two- and three-dimensional motifs.

Dr Christer B. Aakeröy, although a Norwegian citizen, was educated in Sweden where he obtained an M.Sc. at Uppsala University in 1986. He then embarked on further studies at the University of Sussex, England, where he acquired a D.Phil. in Chemistry in 1990. He was subsequently awarded a Scholarship from the Royal Swedish Academy of Sciences that enabled him to spend 8 months as a Research Fellow at the University of Minnesota in the laboratory of the late Professor M. C. Etter. From 1993 to 1996 he held a Lectureship in Chemistry at the Queen's University of Belfast, Northern Ireland. In September 1996 he accepted a position as Assistant Professor in Supramolecular Chemistry at Kansas State University, Manhattan, Kansas, where he continues to develop his research in crystal engineering, intermolecular interactions, molecular modelling and polymorphism.

1. Concept and background

Since the early days of structural and solid-state chemistry, many chemists have (sometimes unbeknown to themselves!) been working in the field of crystal engineering. Although the phrase itself did not appear until 1971 when it was introduced by Schmidt (1971), we only need to visit a recent definition by Desiraju (1989) to realise that structural chemistry and X-ray crystallography were involved with crystal engineering long before the concept itself had been explicitly verbalized:

> ...crystal engineering....the understanding of intermolecular interactions in the context of crystal packing and in the utilization of such understanding in the design of new solids with desirable physical and chemical properties.

It is also becoming clear that this particular topic must hold considerable and widespread appeal and fascination because, all of a sudden, it seems as if everyone is doing crystal engineering! Manuscripts dealing specifically with 'designer-architectures' and with strategies for controlling and predicting structures are published on a regular basis, and several review articles (Lehn, 1988, 1990; Aakeröy & Seddon, 1993; Braga & Grepioni, 1996; Russel & Ward, 1996; Subramanian & Zaworotko, 1994; Desiraju, 1995*a*; Rebek, 1996) and books (Desiraju, 1989, 1995*b*; Vögtle, 1991; Lehn, 1995) have provided valuable overviews of the exciting and inspiring research efforts that have been presented during the last decade.

Before examining recent developments, it is useful to remind ourselves of the origins of the term 'crystal engineering'. During a study of photochemical dimerization reactions of cinnamic acid derivatives, Schmidt and co-workers established that the spatial relationship between neighbouring molecules played a dramatic role in determining reactivity (Cohen & Schmidt, 1964). These topochemical reactions were controlled by the structure of the material, *i.e.* the spatial arrangement of molecules in the solid. The ability to selectively change or optimize such reactions would therefore only come

© 1997 International Union of Crystallography
Printed in Great Britain – all rights reserved

UM00012640
NOVARTIS EXHIBIT 1017
Novartis v. Regents, IPR2023-01346
Page 1386 of 4460

about with control over the structure. Unfortunately, it turns out to be very difficult to foresee structural changes as a function of changes in molecular substitution patterns or in molecular geometry. Molecular shape does not necessarily manifest itself in a predictable manner in the crystalline lattice either in terms of space group, unit-cell dimensions or packing patterns. Since each crystal structure is the result of a delicate balance between a range of intermolecular forces, many of which are weak and non-directional, even a small change in the molecular structure, or isomerism, may lead to dramatic and unpredictable changes in the extended crystal structure. Hence, an improved understanding of the strength, directional behaviour, structural influence, in short, the very essence of non-covalent forces, becomes the underlying focus for initial research into crystal engineering.

Since intermolecular interactions govern molecular recognition at every level, every crystal structure is eventually the result of recognition processes which lead to thermodynamically favourable (albeit sometimes temporary) 3-D (three-dimensional) assemblies of molecules or ions. Bearing in mind that a crystalline material can, in theory, be assembled in an almost infinite number of ways (even within the constraints of crystal symmetry), these recognition mechanisms are extraordinarily selective, since most crystallites in every bulk sample display the same structural arrangement. This situation was recognized by Dunitz (1991) who succinctly described the crystal as the '*supramolecule per excellence*'. Indeed, each crystal represents the culmination of highly specific, reliable and reproducible molecular recognition. Consequently, each crystal structure contains important information about the way in which intermolecular forces compete and collaborate and eventually create an energetically balanced system. Therefore, it seems a shame to resort to rather crude phrases like 'packing forces' (which appear far too often in the literature) when attempting to rationalize and describe new structures. Instead, if we try to take a little bit more care in the analysis of structures, packing motifs and differences in molecular conformation, our crystals may release their inherent information to us in a more digestible and understandable format.

Nowacki (1942) examined space-group preference of *ca* 3000 structures and noticed that almost every other organic compound could be found in one of three space groups, $P2_1/c$, $P2_1$ and $P2_12_12_1$. He related this skewed distribution to the presence of specific symmetry elements within these space groups which, in turn, optimized electrostatic interactions between neighbouring molecules. At the same time, Kitaigorodsky (1961, 1973) began to study crystal systematics and the vast body of his work has arguably made him one of the key figures in developing a better understanding of crystal packing and structure analysis of organic compounds. His principles of close packing provided much needed organization of a rapidly growing pool of structural information and they neatly summarize the structural consequences of the balance between non-covalent forces within a crystalline lattice. Kitaigorodsky pioneered the notion that molecules strive to pack with maximum density (thus minimizing the free, 'empty', volume). In the course of this work, Kitaigorodsky also asked decisive questions about *e.g.* lattice dynamics, static crystals, imperfect crystals and phase transformations, and his contributions also gave inspiration and momentum to the development of molecular mechanics and force-field calculations.

Other notable contributions to the interpretation of observed intermolecular bond distances include Sutor's (1962, 1963) contention that attractive C—H···O hydrogen-bond interactions could play a role in determining extended crystal structures. This notion was initially met with considerable skepticism (Donohue, 1968), but was later completely vindicated using neutron diffraction data (Taylor & Kennard, 1982). Hassel & Romming (1967) made incisive observations about distances and preferential geometries for oxygen···halogen interactions in acyl halides. The question of how we can rationalize and interpret these, and other, unexpectedly short intermolecular distances is still hotly debated and both experimental and theoretical data have been furnished in order to shed more light on these arguments.

Systematic analyses of structural data continue to provide invaluable information about packing preferences, space-group bias and conformational partiality, and these studies have become even more powerful thanks to ongoing improvements and developments of the Cambridge Structural Database (Allen, Kennard & Taylor, 1983). Today, it makes perfect sense to expect that every structural paper is accompanied by a comparative study of related structures (if available), in order to place the characteristics of a new crystal structure in the proper context. In this way, unusual intra- or intermolecular features can be detected readily and the 'unexpected' can often stimulate new ideas or reinterpretations of 'well known' behaviour.

Consequently, crystal engineering is not just about finding quick routes to new materials with improved thermal stabilities, shorter response times or larger non-linear optical coefficients. Equally important, and equally valid, is the task of searching for a better understanding of how fundamental laws of physics manifest themselves in ordered, three-dimensional, crystalline materials.

2. Strategies

2.1. *Looking for that molecular 'glue'*

Synthetic chemistry, organic as well as inorganic, is today at a highly advanced stage and the nature of the covalent bond, the primary tool in intramolecular synthesis, is well established. Supramolecular synthesis,

UM00012641
NOVARTIS EXHIBIT 1017
Novartis v. Regents, IPR2023-01346
Page 1387 of 4460

on the other hand, does not have the benefit of a lengthy history. Many non-covalent forces present in a solid are still ill-defined, poorly understood and difficult both to calculate and to measure. Quite often then we have to learn something about these forces in an indirect manner through an examination of crystal packing. Such observations may allow us to gain more insight into the relative strengths, selectivities and directionalities of hydrogen bonds, hydrophobic–hydrophilic interactions, halogen–halogen contacts, dispersive forces and the whole gamut of interactions often lumped together under the heading 'van der Waals forces'.

The hydrogen bond, primarily electrostatic in nature, has arguably been quoted most often as the architect in design strategies in crystal engineering. However, it can be misleading to analyse the overall structure of a material only in terms of hydrogen-bond geometries and donor/acceptor ratios. Competition, cooperation and balance between different intermolecular forces must all be considered, which makes this such a challenging field.

The presence and influence of hydrogen bonds in molecular and ionic solids have been catalogued in detail, and correlations between bond lengths and angles, and geometric variations as a function of donor/acceptor strengths have been presented for series of functional groups (Taylor & Kennard, 1983, 1984; Taylor, Kennard & Versichel, 1983; Jeffrey & Saenger, 1991). For some time, a hydrogen bond, D—H···A, was only considered possible (or important) if it involved a highly electronegative acceptor atom (A = O, N, F) in combination with a —NHR or —OH donor moiety. However, convincing evidence has been presented which indicates that attractive hydrogen-bond interactions can involve a wide variety of acceptors (A = S, Se, Cl, Br, I, π) and donor moieties (—CH, —SH). Olovsson and co-workers examined structures of simple organic and inorganic compounds over several decades (Kvick & Olovsson, 1968) and they were among the first to introduce the notion of a C—H···Cl interaction in 2-pyridone 6-chloro-2-hydroxypyridine (1/1) (Almlöf, Kvick & Olovsson, 1971). In a recent overview of some more exotic (but probably very common) hydrogen-bond interactions, Brammer, Zhao, Ladipo & Braddock-Wilking (1995) suggested some guidelines for characterizing three-centre, four-electron X—H···M interactions. For example, the bridging hydrogen is reasonably acidic and the metal involved is electron rich, typically with filled d orbitals. Furthermore, the X—H···M angle is usually close to linear and 18-electron complexes are also able to form these interactions. The X—H···M interaction can be identified experimentally through a shift in the ^{1}H NMR signal of the bridging H atom. There have also been many descriptions of three-centre, two-electron, agostic interactions X—H···M (where X = B, C, Si, P, S, Ge, Sn), which may be thought of as hydrogen bonds. These compounds are sometimes referred to as σ-bond complexes (Crabtree, 1993).

In addition, several theoretical examinations of more 'unusual' hydrogen-bond interactions have been presented. In a comparison of A···HF complexes (where A = S, O), it was found that a sulfur base is weaker and prone to adopt a more angular approach to the HF donor (Platts, Howard & Bracke, 1996). The observed geometries can be rationalized on the grounds of multipoles. The S···H bond, which is stabilized primarily by charge(H)–quadrupole (S) interactions, favours an angle of 90° (S···H—F), whereas the O···H monopole–monopole prefers a linear geometry.

Other intermolecular forces that have been proposed and debated include unexpectedly short halogen···halogen contacts, which may be interpreted as attractive in nature (Pedireddi, Reddy, Goud, Craig, Rae & Desiraju, 1994) or simply as a function of inherently anisotropic atoms (Price, Stone, Lucas, Rowland & Thornley, 1994). Recently, I···O_2N—R contacts (Desiraju, Pedireddi, Sarma & Zacharias, 1993) and cyano···halogen interactions (Reddy, Panneerselvam, Pilati & Desiraju, 1993; Desiraju & Harlow, 1989) have all been identified as influencing spatial orientation of substituted aromatic solids.

Even though electrostatic interactions are less pronounced in molecular solids, asymmetric molecules have non-spherical charge distributions which amplify the Coulombic component of the overall lattice energy of the solid. Higher-order moments, *e.g.* dipoles, quadrupoles *etc.*, also contribute *via* pairwise multipole interactions (which are highly directional), although these interaction energies decay rapidly with distance. Finally, since molecules and ions are fixed with respect to each other in a crystalline solid, some modification of charge distribution will take place on each molecule due to the influence of the charge on the nearest neighbours. The resulting attractions that may occur, inductive effects, are also short-range and directional, and are strongly dependent upon the polarizability of the molecule.

Any strategy for effective supramolecular synthesis requires some means for connecting neighbouring molecules into predictable arrangements. Consequently, we need to identify non-covalent connectors that are selective enough to be reliable and strong enough to be transferable between different systems. In short, we need to know how specific functional groups or moieties are going to interact given a choice of potential 'partners'. Much of the necessary ground work was carried out by groups at the Weizmann Institute and the thorough and systematic approach to the analyses of packing preference of classes of organic molecules presented by Leiserowitz and co-workers set important standards for how structural information should be classified and interpreted. The results obtained for carboxylic acids (Leiserowitz, 1976), substituted amides (Leiserowitz & Tuval, 1978) and other functional molecules have inspired many strategies in contemporary supramolecular synthesis.

UM00012642
NOVARTIS EXHIBIT 1017
Novartis v. Regents, IPR2023-01346
Page 1388 of 4460

2.2. *Cocrystals*

Some features of the solid state sometimes hinder our investigations of the influence of intermolecular forces upon the conformational and structural behaviour of molecular building blocks. In solution, interactions between a molecule and its surroundings can be investigated simply by varying the solvent. *Via* such systems we can study specific solvent–solute interactions, competitions and recognition processes in a systematic fashion. However, the solid phase of a particular compound is often uniquely defined (although polymorphism does expand the range of available solid phases to some extent) and, therefore, we are forced to rationalize the influence of non-covalent interactions on the packing and geometry of a specific molecule based upon one single-crystal structure determination, which is clearly not an ideal situation. One route towards a larger sample is *via* structural studies of closely related molecules, but the effects of intermolecular forces are often very subtle and even a slight chemical modification can have a profound impact upon structure, which makes it difficult to trace specific structural consequences to specific chemical moieties. Another route to developing a large number of potential test cases is provided by cocrystallization techniques. A cocrystal can be defined as a crystalline material that consists of different molecular (and electrically neutral) species held together by non-covalent forces.

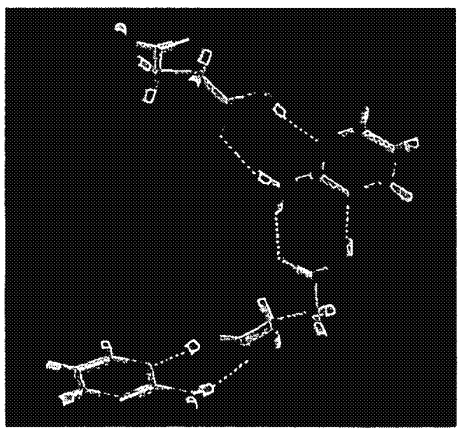


Fig. 1. The complementarity of hydrogen bonds in the cocrystal of 2-aminopyrimidine–succinic acid (1/2) (Etter & Adsmond, 1990).

Cocrystals are not necessarily easy to prepare since such a heteromeric system will only form if the non-covalent forces between two (or more) molecules are stronger than those between the molecules in the corresponding homomeric crystals. In general, it seems to be thermodynamically favourable to assemble similar molecules (pure *A* or pure *B*) in a 3-D solid compared with the corresponding process of packing dissimilar molecules into the same solid (*AB*). Cocrystals can be prepared either *via* evaporation of a heteromeric solution or by grinding the two components together (Etter & Adsmond, 1990; Pedireddi, Jones, Chorlton & Docherty, 1996). In the first case, the two components must have similar solubilities (otherwise the least soluble component will precipitate out exclusively), but this in itself is not a guarantee for success. It may be helpful to use molecules which can adopt alternative packing patterns whilst still satisfying the demands of the hydrogen-bond donors/acceptors that are present on the two (or more) components. Another important consideration when attempting to prepare cocrystals is to choose a compound which is already known to be polymorphic. Clearly, if a molecular compound exists in several polymorphs, it has demonstrated a structural flexibility and it is not as energetically locked into a single packing mode. Consequently, the chances of bringing such a molecule into a different packing arrangement in coexistence with another molecule is greatly enhanced (Aakeröy & Nieuwenhuyzen, 1997).

The use of cocrystals for studying packing patterns, hydrogen-bond motifs and intermolecular forces was

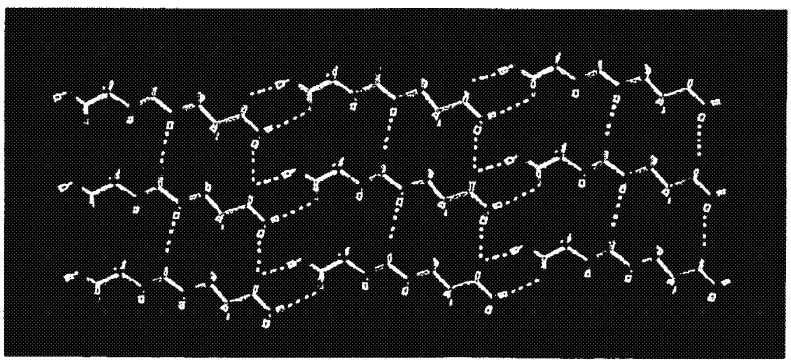


Fig. 2. A 2-D sheet in the crystal structure of *N*-(carboxymethyl)-*N*-(2-carboxyethyl)urea (Chang, West, Fowler & Lauher, 1993).

UM00012643
NOVARTIS EXHIBIT 1017
Novartis v. Regents, IPR2023-01346
Page 1389 of 4460

brought to the forefront by Etter and co-workers (Etter & Baures, 1988; Etter, 1991; Etter & Adsmond, 1990). One high-impact manuscript describes the use of 2-aminopyrimidine as a means of probing hydrogen-bond preferences of carboxylic acids (Fig. 1). The affinity between carboxylic acids and the 2-aminopyrimidine moiety has since been employed in several design strategies. Structural studies of cocrystals have also served to underline how the competition and balance between intermolecular forces can be examined in an unbiased way (Ung, Bishop, Craig, Dance & Scudder, 1994; Smith, Gentner, Lynch, Byriel & Kennard, 1995).

Another lasting contribution by Etter and co-workers has been the construction of a language, based upon graph theory, for describing and analysing hydrogen-bond networks in three-dimensional solids (Etter, MacDonald & Bernstein, 1990; Bernstein, Davis, Shimoni & Chang, 1995). According to this methodology, any hydrogen-bond interaction can be classified into one of four groups; discrete dimers, chains, rings or intramolecular hydrogen bonds. A specific motif is then described in terms of the number of donors and acceptors that participate and the degree of the motif is determined by the number of unique hydrogen bonds that are present. With the aid of graph sets, it is possible to analyse even complex structures in a systematic and consistent manner, and this methodology (nomenclature) has been applied to hundreds of hydrogen-bonded structures over the last 5 years.

3. Form

3.1. *Molecular solids*

Molecular solids have been the most popular targets for crystal engineering, both in terms of structural analysis of existing data, as well as in the synthesis and characterization of new compounds. The relevant molecular building blocks have been 'glued' together with a variety of intermolecular forces and conventional hydrogen bonding is by no means the only interaction that will provide the desired structural outcome. Nevertheless, mutually complementary hydrogen-bonding sites have been employed in many elegant routes to low-dimensional motifs. Fowler, Lauher and co-workers (Zhao, Chang, Fowler & Lauher, 1990; Chang, West, Fowler & Lauher, 1993) utilized carboxylic, amide and urea functionalities in the preparation of anisotropic 2-D motifs (Fig. 2). The design strategies for these compounds are uncomplicated (thus appealing!) and make good use of the expected packing patterns for each individual functionality.

A combination of interactions can also be employed in a directed manner, as demonstrated in the 2-D layers of substituted alkoxy-1,4-benzoquinones (Keegstra, van der Mieden, Zwikker, Jenneskens, Schouten, Kooijman, Veldman & Spek, 1996). Neighbouring molecules are connected *via* C—H···O=C interactions and aligned through the hydrophobic ordering of alkoxy chains.

Studies of packing motifs in acyclic sugar amphiphiles (which may be used as simple structural models for biological membranes) identified commonly occurring homodromic rings generated by O—H···O hydrogen bonds (André, Luger, Fuhrhop & Rosengarten, 1993).

A monumental article by Ermer & Eling (1994) describes the hydrogen-bond complementarity of hydroxy (two acceptors–one donor) and amino (one acceptor–two donors) groups, and proceeds to illustrate how alcohols and primary amines can be combined in 1:1 cocrystals whilst forming predictable structural motifs, Fig. 3.

Hamilton and co-workers have shown that substituted bis(amidopyridines) can generate 2-D hydrogen-bonded layers (Garcia-Tellado, Geib, Goswami & Hamilton, 1991) and self-assembly of hydrogen-bonded helices is also possible with dicarboxylic acids and derivatives of bis-(2-amino-6-methylpyridine) (Geib, Vicent, Fan & Hamilton, 1993), Fig. 4. Stoddart and co-workers have built interwoven supramolecular cages (Ashton, Collins, Fyfe, Glink, Menzer, Stoddart & Williams, 1997), assembled through hydrogen bonds and π—π stacking.

Both Lehn (Lehn, Mascal, DeCian & Fischer, 1990), Fig. 5, and Whitesides (Zerkowski, MacDonald & Whitesides, 1994; Zerkowski, MacDonald, Seto, Wierda & Whitesides, 1994), Fig. 6, have employed combinations of triaminopyrimidine derivatives and barbituric acid in the design of molecular 'tapes' held together by selective hydrogen-bond interactions. Substituted 2-benzimidazolones have also been used in the preparation of infinite aggregates (Schwiebert, Chin,

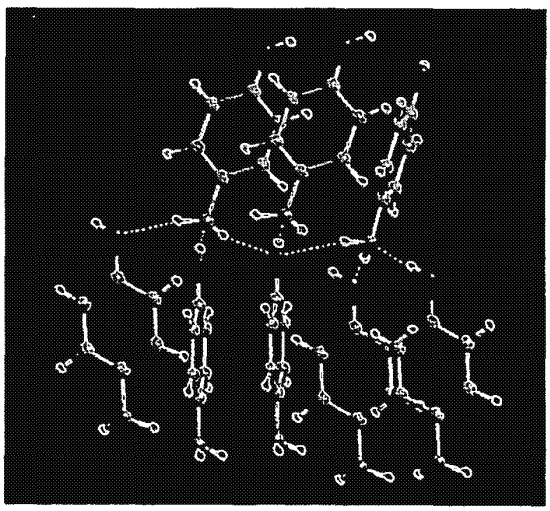


Fig. 3. The complementary of $—NH_2$ and —OH moieties create tetrahedral coordination centres in 4-aminophenol (Ermer & Eling, 1994).

UM00012644
NOVARTIS EXHIBIT 1017
Novartis v. Regents, IPR2023-01346
Page 1390 of 4460

MacDonald & Whitesides, 1996). Many other connectors have been used in the assembly of low-dimensional motifs, *e.g.* 2-pyridones (Ducharme & Wuest, 1988), C—H···O/O—H···N pairwise interactions (Pedereddi, Jones, Chorlton & Docherty, 1996) and urea/quinone (Ge, Lilienthal & Smith, 1996), and the examples given here represent but a small portion of existing approaches to the design of molecular solids.

The preponderance of strategies for supramolecular synthesis prompted Desiraju (1995*a*,*b*) to introduce the term 'supramolecular synthons', defined as

> ...structural units within supermolecules which can be formed and/or assembled by known or conceivable synthetic operations involving intermolecular interactions.

Knowledge about supramolecular synthons is clearly as important to crystal engineering as is an understanding of reaction mechanisms and reagents in conventional covalent synthesis.

Although much progress has been made in the synthesis of specific structural features in molecular solids, detailed control over the assembly of low-dimensional motifs (chains, ladders *etc.*) remains an elusive goal and further work is required in order to increase the choice of reliable supramolecular synthons.

3.2. *Ionic organic compounds*

When looking for materials with specific physical properties, there are sometimes good reasons for moving from molecular to ionic solids. Typically, solubilities are different, and thermal and mechanical properties may also differ significantly, and depending upon the potential application, ionic compounds can provide advantages over molecular analogues. There may also be strategic reasons for working with materials containing two components, a cation and an anion. The design of a single molecule, capable of controlling the assembly selectively and specifically in three dimensions simultaneously, may require ingenious and complex synthetic programmes. However, in an ionic material, one of the ions can be used for creating a 2-D architecture and the final step, the link to 3-D, can be provided by a suitable counterion.

In recent years, several examples of engineering of ionic organic and organic–inorganic compounds with specific packing motifs have appeared. Most of these rely on hydrogen bonding as the active intermolecular tool and, furthermore, the majority of such structures are built around anionic aggregates. Since the hydrogen bond is primarily electrostatic in nature, the strength of such interactions involving charged species is enhanced and, as a result, the hydrogen bond becomes a powerful tool for linking ions together in a predictable manner.

Russel, Etter & Ward (1994*a*,*b*) utilized the complementarity of hydrogen-bond sites on guanidinium cations and substituted sulfonate anions in the preparation of materials containing infinite hydrogen-bonded sheets, Fig. 7. The precise topology of these motifs can be modified through appropriate substitution of the anion.

In our group we have developed predictable hydrogen-bonded architectures generated by anionic species. We have adopted a strategy of taking one step (one degree of freedom) at a time, thereby simplifying the synthetic component. The CSD is as always an invaluable starting point when looking for inspiration and existing information shows that carboxylic acids tend to form discrete dimers (zero-dimensional elements) in the solid state.

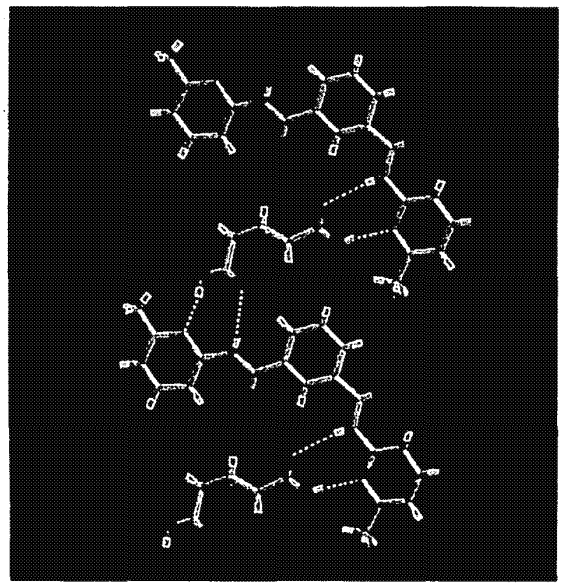


Fig. 4. An infinite spiral in 1,3-bis((6-methylpyrid-2-yl)amino)carbonyl)–benzene glutaric acid (1/1) (Geib, Vicent, Fan & Hamilton, 1993).

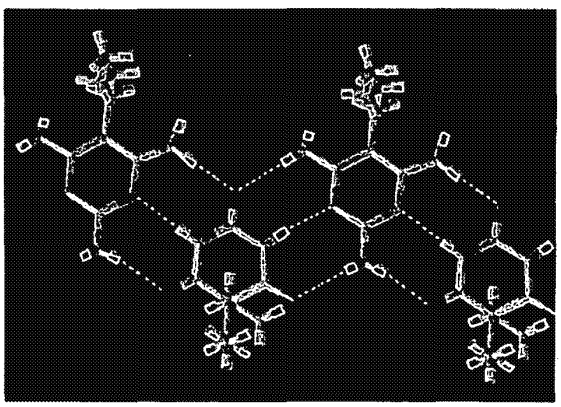


Fig. 5. An infinite hydrogen-bonded ribbon in 5-*tert*-butyl-2,4,6-triaminopyrimidine diethylbarbituric acid (Lehn, Mascal, DeCian & Fischer, 1990).

UM00012645
NOVARTIS EXHIBIT 1017
Novartis v. Regents, IPR2023-01346
Page 1391 of 4460

Similarly, dicarboxylic acids are known to form infinite hydrogen-bonded chains (1-D elements) *via* $R_2^2(8)$ motifs, almost irrespective of the overall geometry of the molecule. Moving from molecular to ionic motifs simply requires deprotonation of the acid which creates an asymmetric anion with a carboxylate 'tail' (with strong hydrogen-bond acceptors) and a carboxylic 'head', acting as a powerful hydrogen-bond donor. Typically, mono-anions of dicarboxylic acids have a propensity to form infinite chains through a very short and near-linear O—H···O hydrogen bond between the 'head' and 'tail' of adjacent anions. Two O—H···O interactions between neutral species are thereby replaced with one O—H···O interaction between anions, but the overall structural outcome is unchanged; a 1-D motif. An additional bonus is given by the fact that this chain is inherently polar, which may have useful implications for the physical properties of the resulting material. The next step involves combining 1-D elements into 2-D features in a reliable manner. In these anions there are several hydrogen-bond acceptors available, so by introducing a donor group on the anion, preferably positioned so that it can provide a link between neighbouring chains, it should be possible to create infinite anionic layers. With

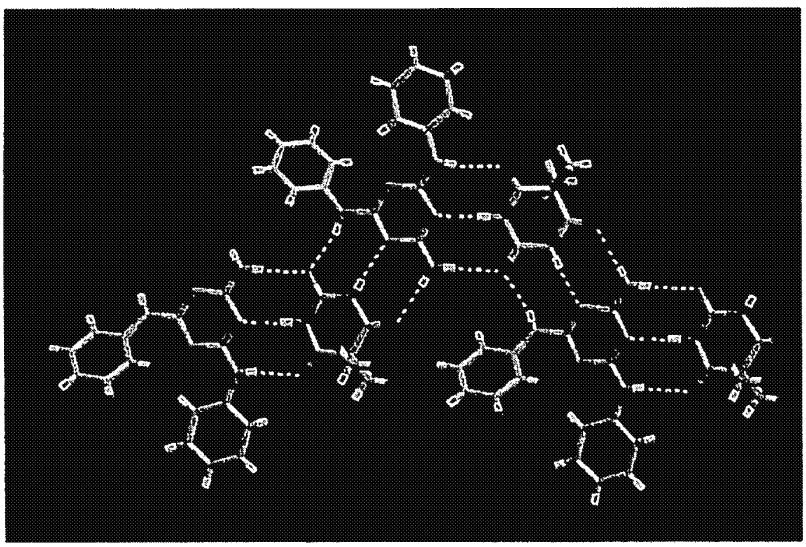


Fig. 6. A hydrogen-bonded tape in 5,5-dimethylbarbituric acid *N,N'*-diphenylmelamine (Zerkowski, MacDonald & Whitesides, 1994).

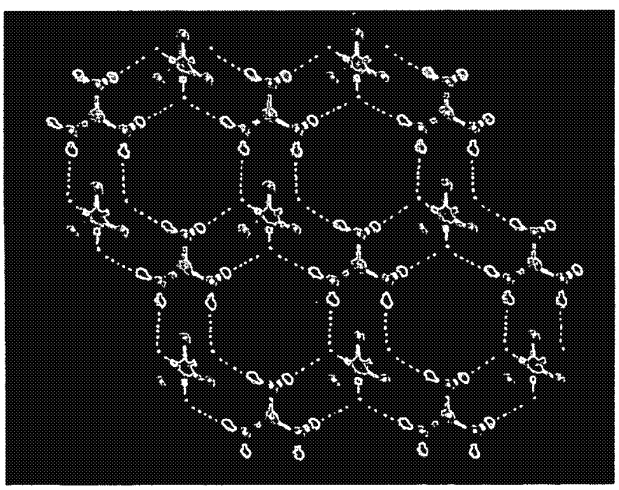


Fig. 7. An infinite hydrogen-bonded sheet in guanidinium trifluoromethanesulfonate (Russel, Etter & Ward, 1994*a*).

UM00012646
NOVARTIS EXHIBIT 1017
Novartis v. Regents, IPR2023-01346
Page 1392 of 4460

this task in mind, we characterized a number of structures of hydrogen tartrate (Aakeröy, Hitchcock & Seddon, 1992; Aakeröy & Hitchcock, 1993) and hydrogen malate salts (Aakeröy & Nieuwenhuyzen, 1994, 1996). These data, in combination with existing information from the CSD, show that the expected anionic chains are almost invariably formed. Secondly, the additional —OH groups (two in the case of tartaric acid, one in the case of malic acid) generate robust O—H···O hydrogen bonds between neighbouring chains, which give rise to the desired 2-D anionic network, Fig. 8. Although the 2-D arrangement of anions is reliable, two different network 'types' are possible. If adjacent chains are aligned in a parallel fashion (giving rise to a highly polar structure), the layer tends to be planar, or near-planar. If, on the other hand, neighbouring chains are aligned in an antiparallel fashion, the anionic layer is normally buckled, Fig. 9. Obviously, the existence of flat *vs* buckled anionic layers, as well as the degree of distortion away from a planar geometry, is governed by the structural influence of the cation.

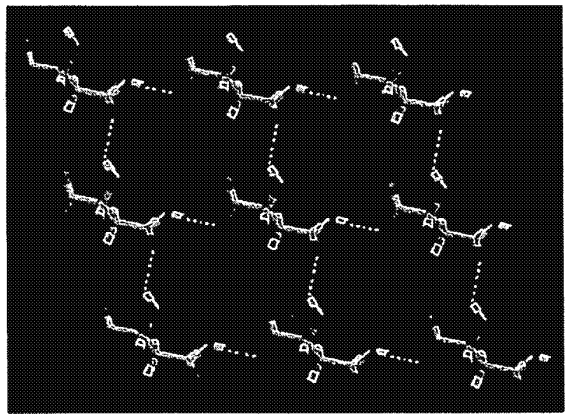


Fig. 8. A layer of anions in 3-chlorobenzylammonium hydrogen-L-malate. The horizontal chains are aligned in a parallel manner (Aakeröy & Nieuwenhuyzen, 1996).

At this stage we have established that hydroxydicarboxylic acids (exemplified by tartaric and malic acid) may be used as reliable building blocks of infinite 2-D motifs. The advantage of employing ions as building blocks now becomes apparent since the final step in our design strategy, moving from 2-D to 3-D, can be achieved through a suitable choice of cation. The cation can act as a bridge which actively associates with neighbouring anionic layers through directional intermolecular interactions. Examples of structures where the cation forms a bridge between anionic layers are imidazolium hydrogen-L-tartrate, Fig. 10, and 3-hydroxy-6-methylpyridinium hydrogen-L-malate, Fig. 11. In the first case the links are generated by two N—H···O interactions and in the second case through one N—H···O and one O—H···O hydrogen bond. These particular cations were chosen since they contain hydrogen-bond donors at opposite ends of a rigid spacer which were expected to generate crosslinks between neighbouring anionic layers. Alternatively, if the cations only have one hydrogen-bond donor (or several donors in close proximity) they would be expected to attach themselves to one side of the layer and simply act as spacers, as a means of varying the interplanar distance between the infinite anionic layers, Fig. 12.

The use of similar building blocks in crystal engineering (notably in the design of non-linear optical materials) has received widespread attention and many groups are making important contributions to our

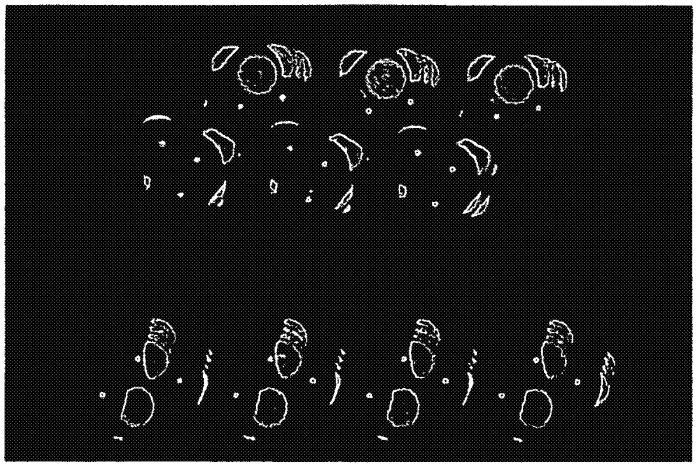


Fig. 9. Edge-on view of the two 'types' of anionic layers in hydrogen malate and hydrogen tartrate structures. Above, a buckled layer (antiparallel chains) and below, a flat layer (parallel chains) (Aakeröy & Nieuwenhuyzen, unpublished results).

UM00012647
NOVARTIS EXHIBIT 1017
Novartis v. Regents, IPR2023-01346
Page 1393 of 4460

understanding of exercising precise control over interplanar distances, layer topology and other structural features that eventually determine the physical properties of these materials (Zyss, Pecaut, Levy & Masse, 1993; Watanabe, Noritake, Hirose, Okada & Kurauchi, 1993; Kadirvelraj, Umarji, Robinson, Bhattacharaya & Guru Row, 1996; Bhattacharaya, Dastidar & Guru Row, 1994; Lefur, Bagieu-Beucher, Masse, Nicoud & Levy, 1996).

Although these structures contain several predictable structural features, they do not represent materials over which we can claim complete control. For example, we do not yet know how a cation can induce parallel or antiparallel alignment of anionic chains. Furthermore, we cannot control the orientation of one anionic layer with respect to another and this is clearly of great importance since parallel sheets would give rise to highly polar and strongly anisotropic materials.

An important aspect of crystal engineering pertains to the uncovering of practical guidelines for estimating the structural outcome when combining different functional groups. In order to achieve this, it is helpful to study a simple system that can give rise to a small number of well defined structural motifs. With this in mind, we synthesized and characterized several organic salts based upon the oxamate anion, $[H_2NCOCOO]^-$ (Aakeröy, Hughes & Nieuwenhuyzen, 1996). This particular anion was selected since it possesses complementary hydrogen-bond donors and acceptors that can lead to three dimeric motifs. *Ab initio* calculations showed very small energetic differences between these 'postulated' patterns, indicating that oxamate anions can aggregate in at least three different ways which, in turn, can give rise to distinctive anionic extended motifs. In fact, all three dimeric features have appeared in crystalline oxamates. Furthermore, the anions invariably give rise to either 1-D motifs, Fig. 13, or infinite 2-D layers, Fig. 14. As discussed previously, the detailed arrangement of anions and cations is determined by specific cation–anion interactions. By grouping cations together depending upon what type of anionic motif they are associated with, we can identify some common geometric characteristics which lead us to propose simple guidelines for predicting oxamate structures. Primary ammonium ions with three hydrogen-bond donors positioned in close proximity to each other (the $[—NH_3]^+$ moiety) will form hydrogen bonds to at least two different anions and, in doing so, bring anions close together (*via* N—H···O interactions), which in turn forces the anions into a layered arrangement. On the other hand, secondary or tertiary ammonium ions can only bring together a smaller number of anions which may be insufficient to cause the formation of an infinite 2-D sheet. In these cases, *e.g.* imidazolium oxamate, the anions instead create 1-D motifs. In addition, cation size may also be important, since a small cation will inevitably bring neighbouring anions within close proximity of each other and this will also encourage anionic layer formation. This is exemplified by the crystal structure of potassium oxamate hydrate (Aakeröy, Hughes & Nieuwenhuyzen, 1996). Conversely, a bulky cation will expand the size of the lattice and will therefore increase the distance between anions, which should result in the formation of 1-D anionic motifs.

The hydrogen bond is arguably of sufficient strength to link neighbouring ions together into infinite architectures, even in the presence of different cations and in competition with other non-covalent interactions, and it is likely that there will be many more forays into the design of desired structural functionalities in organic salts.

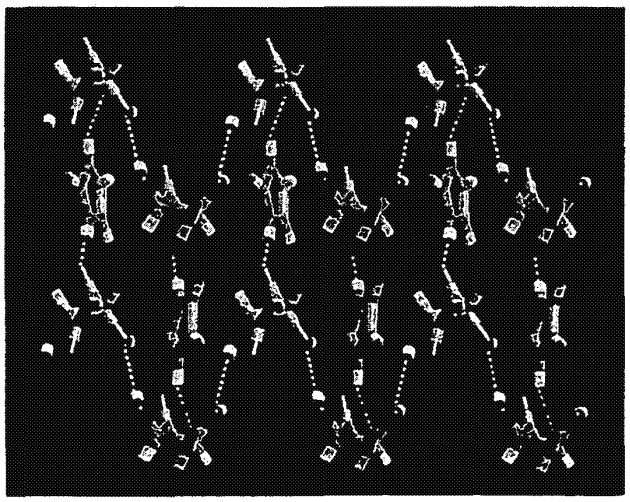


Fig. 10. Edge-on view of buckled anionic layers held together by cations in imidazolium hydrogen-L-tartrate (Aakeröy & Hitchcock, 1993).

UM00012648
NOVARTIS EXHIBIT 1017
Novartis v. Regents, IPR2023-01346
Page 1394 of 4460

3.3. *Metal complexes*

Many approaches to the programmed design of metal-containing compounds with predictable dimensions have recently been presented. For example, Robson and Hoskins outlined the possibilities of creating infinite 2-D and 3-D metal-containing frameworks based around metal-4,4′-bipyridine derivatives (Robson, Abrahams, Batten, Gable, Hoskins & Liu, 1992). Interpenetration of such 2-D sheets can give rise to 3-D solids with channels and cavities of specific dimensions. Zaworotko and co-workers have employed similar building blocks in the design of porous 'coordination-polymers' with diamondoid structures (Copp, Subramanian & Zaworotko, 1992; Subramanian & Zaworotko, 1995; Robinson & Zaworotko, 1995; Zaworotko, 1994), Fig. 15.

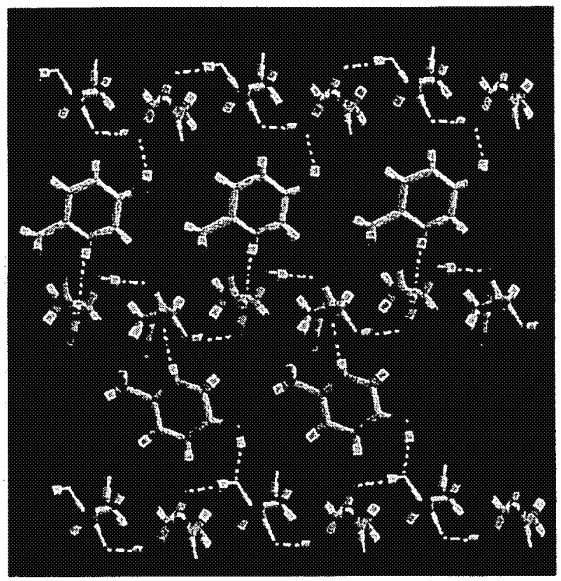


Fig. 11. Edge-on view of sheets of cations and anions held together by hydrogen bonds in 3-hydroxy-6-methylpyridinium hydrogen-L-malate (Aakeröy & Nieuwenhuyzen, 1994).

Lehn and co-workers have generated some extraordinary structures covering silver(I) helicates (Garrett, Koert, Lehn, Rigault, Meyer & Fischer, 1990), circular double helicates (Hasenknopf, Lehn, Kneisel, Baum & Fenske, 1996), supramolecular macrocycles (Drain, Russel & Lehn, 1996) and zinc(II) porphyrins assembled into cages (Drain, Fischer, Nolen & Lehn, 1993). Many of these motifs are built with a combination of well established coordination chemistry (coordination number, geometry *etc.*) and site-specific and self-complementary hydrogen-bonds. Mingos and co-workers (Burrows, Mingos, White & Williams, 1996; Chowdhry, Mingos, White & Williams, 1996) have utilized intermolecular connectors, *e.g.* thiourea//carboxylate, diaminopyridine///uracil *etc.*, as a way of linking neighbouring metal complexes into extended 'tapes' and sheets, Fig. 16. On the one hand, the presence of a metal complex provides access to properties which cannot be obtained with molecular solids alone, but at the same time, the organic connectors provide the basis for new pre-organized structural arrangements. This strategy can be applied to both organometallic and coordination compounds.

The hydrogen-bonding capability of polycarboxylic acids has been used extensively in the design of preordered cationic metal complexes. For example, terephthalic acid was used by Kimura, Ikeda, Shionoya & Shiro (1995) as a link between substituted zinc(II)

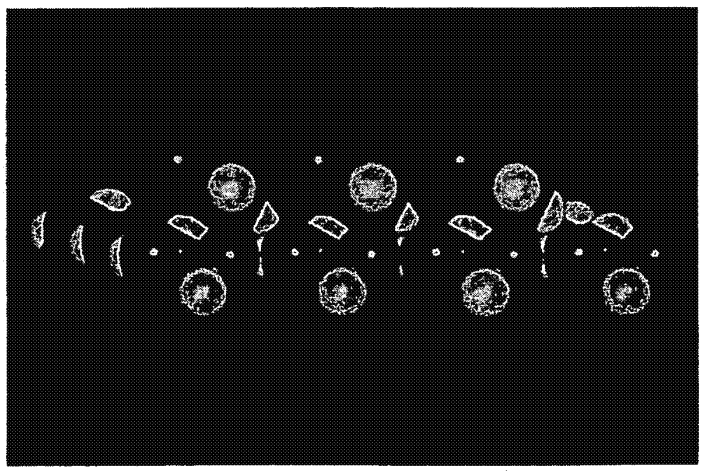


Fig. 12. Cations, acting as spacers, attached to one side of the flat anionic layer in 4-chlorobenzylammonium hydrogen-L-malate (Aakeröy & Nieuwenhuyzen, 1996).

UM00012649
NOVARTIS EXHIBIT 1017
Novartis v. Regents, IPR2023-01346
Page 1395 of 4460

complexes of cyclene. Both ends of the dianion coordinate to a zinc ion in a neighbouring complex. James, Verspui, Spek & van Koten (1995) employed CCH···Cl—Pt hydrogen bonds to create infinite chains in an organoplatinum compound. Munakata and co-workers prepared hydrogen-bonded copper(I) complexes with large channels occupied by cations, using the well known dimeric 2-pyridone synthon (Munakata, Wu, Yamamoto, Kuroda-Sowa & Maekawa, 1996).

Dance and co-workers have made extensive use of the 'phenyl factor' (interactions between adjacent aromatic groups) in inorganic supramolecular chemistry.

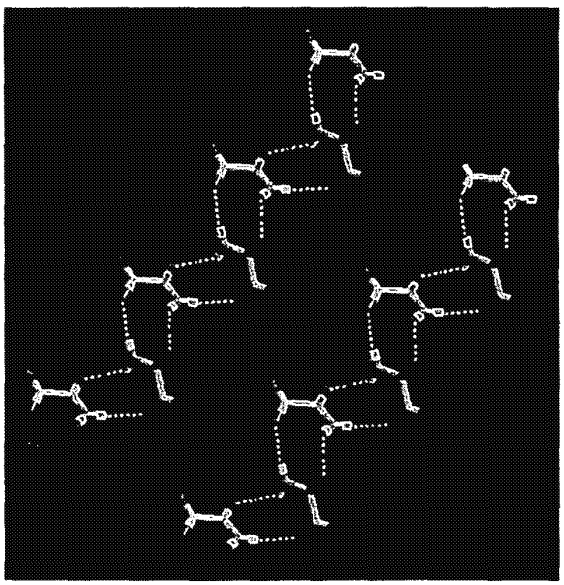


Fig. 13. Adjacent ribbons of anions in piperidinium oxamate (Aakeröy, Hughes & Nieuwenhuyzen, 1996).

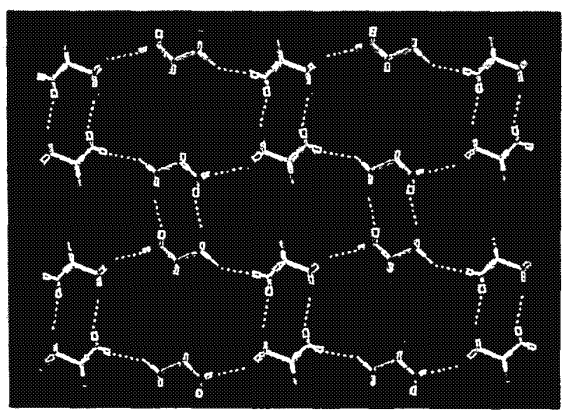


Fig. 14. The infinite layer of anions in 4-chlorobenzylammonium oxamate (Aakeröy, Hughes & Nieuwenhuyzen, 1996).

Calculations of the non-bonded Ph—Ph interaction energies in a series of $[M(SPh)_4]$ derivatives show that such interactions make a significant contribution to the overall lattice energy of the solid and thus can play a vital part in the assembly and orientation of these complexes (Dance, 1995). This has been illustrated by the commonly occurring 'sextuple embrace' involving three phenyl rings on neighbouring $[Ph_4P]^+$ cations (Banda, Cusick, Scudder, Craig & Dance, 1989). Aryl rings are positioned such that one or two H atoms are pointing towards the π-cloud of an adjacent ring resulting in an edge-to-face interaction. Alternatively, H atoms are positioned over C atoms in the adjacent π-system, leading to offset face-to-face interactions. There are several hundred examples of this motif in crystals containing $[Ph_4P]^+$ cations, which clearly shows the anisotropic, directional and, thus, supramolecular behaviour of this building block.

Braga, Grepioni and co-workers have been at the forefront of developing an organometallic 'branch' of crystal engineering through a combination of synthesis, database analysis and packing-energy calculations (Braga & Grepioni, 1996). Based upon structural data for hexanuclear carbonyl cluster anions, they were able to demonstrate that the relative size of the component ions is a determining factor in the assembly process of the solid (Braga, Grepioni, Milne & Parisini, 1993). Very significantly (but often overlooked) they also showed that the formal charge associated with each ion was very effectively distributed over the ions, thus making cation–cation or anion–anion interactions perfectly acceptable. Braga and co-workers also encapsulated a paramagnetic chromium species within an organic, anionic framework with the aid of CH···O interactions (Braga, Grepioni, Byrne & Wolf, 1995).

There is no reason why this particular branch of crystal engineering will not expand at an exponential rate. Organometallic chemistry has for a long time been preoccupied with molecular structure, but if a fraction of this attention is devoted to intermolecular interactions in organometallic compounds, we will uncover a wealth of information in the next few years. It will also be interesting to examine to what extent the introduction of additional interactions, *e.g.* metal–ligand, Lewis acid–base, will facilitate, or hamper, structure predictions.

3.4. *Polymorphism*

You are working with a seemingly flawless design strategy, every synthon stays intact, the synthesis is straightforward and the product crystallizes into beautiful well shaped crystals. All you need to do is to solve the structure and your approach is instantly validated. Surely, nothing can go wrong at this stage? Well, this may depend upon how far you are prepared to look.

Possible complications may be introduced by the obdurate riddles furnished by polymorphism. Not only

UM00012650
NOVARTIS EXHIBIT 1017
Novartis v. Regents, IPR2023-01346
Page 1396 of 4460

must we uncover how to control the delicate balance between a multitude of weak interactions, but once the material appears it may make a mockery of our design and rationalizations by appearing in several guizes!

Although polymorphism is a well known phenomenon (be it pervasive or not), it is still difficult to define accurately. Suggested criteria for assessing polymorphs include statistically different unit-cell dimensions, differences in crystal packing or distinctly different physical properties. In addition, several sub-classes have been discussed, ranging from pseudo-polymorphs *via* conformational polymorphs (Bernstein & Hagler, 1978) to disappearing polymorphs (Dunitz & Bernstein, 1995)! Although in some cases these discussions spill over into either faith or semantics, there is no doubt that the question of structural purity is, from a materials perspective, of equal importance to chemical purity. Furthermore, this is not just an esoteric academic topic, which was clearly illustrated in a recent high-profile court case involving one of the best selling drugs world-wide (Leadbeater, 1991). With several billion dollars at stake (which does tend to make people pay attention), we can expect much more interest in this field over the next few years, not just from the pharmaceutical industry.

If we define polymorphism provisionally as different crystalline forms of the same chemical compound (with identical composition!) leading to measurable differences in physical properties, what means do we have for identifying such systems? X-ray crystallography (single-crystal and powder) is often the method of choice, but hot-stage microscopy, spectroscopy or thermochemistry are commonly used for recognizing and characterizing polymorphic forms. As a matter of routine, differences in solubility and crystal morphology should also be noted and reported for different polymorphs since these properties can be of great practical importance, *e.g.* for bioavailability and filterability, respectively. An excellent review by Threlfall (1995) provides an extensive overview of various experimental techniques for studying polymorphs of organic compounds.

The frequency of occurrence of polymorphism is another question which remains largely unanswered and although it is arguably true to say that the more time we spend looking for polymorphs, the more often we will come across the phenomenon, we also need to know where to look. For example, aromatic hydrocarbons rarely exhibit polymorphism which, *prima facia*, may seem counter-intuitive since such compounds are held together by relatively weak forces that are often considered to display much less pronounced directionality and structural specificity. However, this serves to illustrate that weaker non-covalent interactions, *e.g.* C—H$\cdots\pi$ or $\pi\cdots\pi$, working in concert, can display exceptional selectivity.

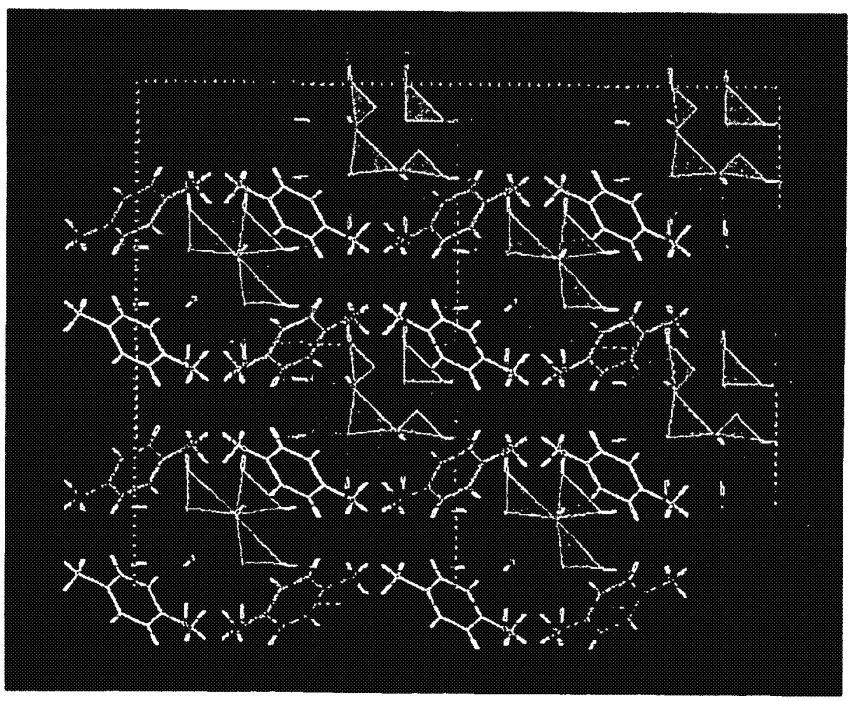


Fig. 15. An example of a diamond structure based upon tetrakis($(\mu_3$-hydroxo)tricarbonylmanganese) 4-xylene clathrate (Copp, Holman, Sangster, Subramanian & Zaworotko, 1995).

UM00012651
NOVARTIS EXHIBIT 1017
Novartis v. Regents, IPR2023-01346
Page 1397 of 4460

In some polymorphic systems, the dominating synthon (strongest intermolecular interaction) stays intact, but the relative orientation of one motif with respect to another is changed. However, there are also examples of systems where the expected synthon is rejected in favour of an alternative arrangement. For example, one polymorph of 3-hydroxybenzoic acid (3HBA) does contain the commonly occurring hydrogen-bonded dimeric motif, whereas in the second polymorph (3HBA′), the dimer is abandoned in favour of a new motif, Figs. 17(*a*) and 17(*b*) (Gridunova, Furmanova, Struchov, Ezhkova, Grigorieva & Chayanov, 1982). This structural pair illustrates that the same compound can exist in both centroymmetric (3HBA) and non-centrosymmetric structures (3HBA′).

Polymorphism brings, at first glance, added complications to crystal engineering and structural chemistry. On the other hand, polymorphic systems provide excellent opportunities to study specific chemical entities in different crystalline environments (Bernstein & Hagler, 1979). By comparing differences in experimentally determined thermodynamic quantities and trends displayed by calculated lattice energies for a series of polymorphs, energy differences between observed molecular conformations can be estimated. Subsequent analyses of the results may highlight the influence of different functional groups on the overall crystalline arrangement of each material and this represents a case where experiment and theory are combined into a powerful probe of intermolecular interactions.

Finally, from a crystal engineering or solid-state chemistry perspective, structural purity is as important as chemical purity. Unfortunately, it is rather rare that a single-crystal X-ray diffraction study is accompanied by a powder diffraction experiment in order to establish that the chosen crystal is, indeed, representative of the bulk material. A single crystal is, after all, just that, one crystal. Furthermore, crystals with the same morphology may have different structures and crystals with different morphology may have the same structure! The structural homogeneity of a crystalline material can be assessed very easily and rapidly: (i) simulate the X-ray powder pattern from the existing single-crystal data, (ii) record the X-ray powder pattern on the bulk sample and (iii) if there is a good match between the simulated and experimental patterns, we can be much more confident that the crystal structure that has been obtained is typical for the bulk material. Of course, this does not preclude the possibility of finding other polymorphic forms if the compound is prepared under different conditions or in a different location (!), but at least we have carried out a more comprehensive analysis of our material. If it is worth spending time on design and crystal engineering, it is probably worth finding out if the material is structurally pure!

4. Function and future

What types of properties do we seek in our new 'designer' materials and what level of predictability can we realistically expect in the near future? The field itself does hold much promise, but what if we are unable to deliver real crystalline materials that are cheaper than current materials or that can perform certain tasks more efficiently, more selectively or with greater speed than existing candidates? Will the whole area be reduced to

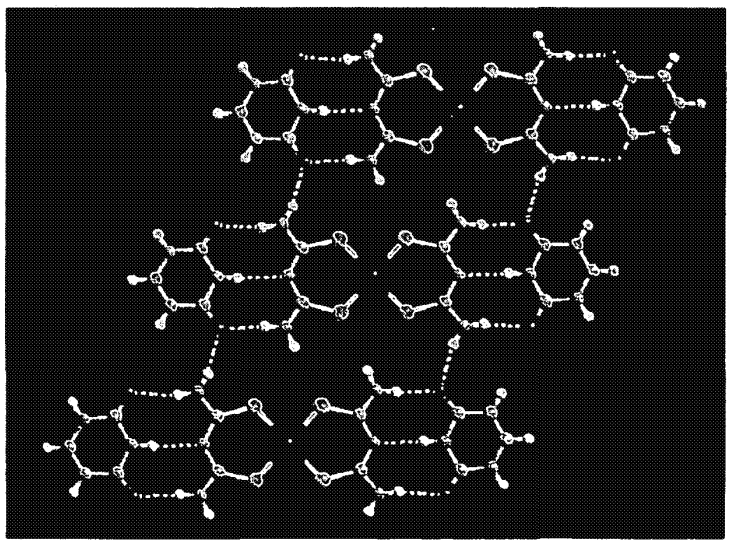


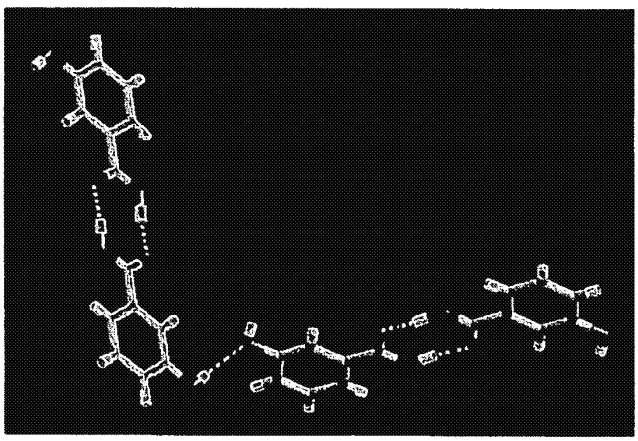
Fig. 16. An infinite Ribbon of nickel complexes, propaged *via* hydrogen bonds in bis(dithiobiuret-*S*,*S*′)nickel(II) diuracil dihydrate. Water molecules removed for clarity (Houlton, Mingos & Williams, 1994).

UM00012652
NOVARTIS EXHIBIT 1017
Novartis v. Regents, IPR2023-01346
Page 1398 of 4460

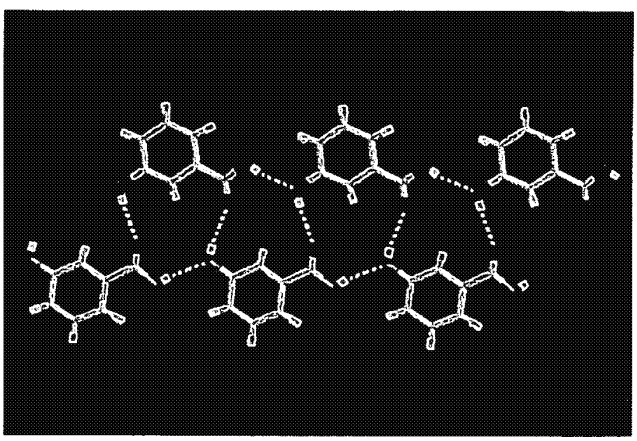
the design and synthesis of compounds with 'aesthetically pleasing' packing motifs with no regard to functionality and properties?

An outsider could be of the opinion that crystal engineering is only about making yet more 'pretty structures', but it is important to realise that supramolecular synthesis is still very much in its infancy. It is necessary to collect structural information, to search the CSD for recurring packing motifs and to test the reliability and robustness of simple non-covalent interactions. Furthermore, none of this has to be performed on complicated synthetically challenging compounds. On the contrary, a simple system (amenable to small geometric or chemical variations) is likely to furnish more easily extractable information about competition and balance between intermolecular forces. We have certainly become more aware of the importance of looking at the 'chemistry beyond the molecule' (Lehn, 1990) and this will allow us both to identify new synthons and to learn more about exotic weaker intermolecular interactions. However, eventually, we will need to supply materials for applications and practical devices.

Broadly speaking, control over molecular orientation, packing patterns and lattice dimensions would provide us with the ability to improve or fine-tune any physical property determined by structure. On one hand, successful crystal engineering would allow us to understand such 'basic' physical properties as solubility and thermal stability. For example, the observation that *para* isomers almost invariably have higher melting points than *meta* isomers (Gavezzotti, 1995) is still in need of a rational explanation. Other important functions such as second-order optical effects and piezoelectric behaviour are determined by space group, centrosymmetric (off)–noncentrosymmetric (on) and the relative alignment and



(*a*)



(*b*)

Fig. 17. (*a*) Hydrogen-bonded dimers, linked by O—H···O hydrogen bonds in the centrosymmetric polymorph of 3-hydroxybenzoic acid (Gridunova, Furmanova, Struchov, Ezhkova, Grigorieva & Chayanov, 1982). (*b*) Crystal packing in the non-centrosymmetric polymorph of 3-hydroxybenzoic acid (Gridunova, Furmanova, Struchov, Ezhkova, Grigorieva & Chayanov, 1982).

UM00012653
NOVARTIS EXHIBIT 1017
Novartis v. Regents, IPR2023-01346
Page 1399 of 4460

orientation of individual molecules/ions within the solid. Clearly, with control of the spatial arrangement of molecules and ions, we would be in a strong position to make better functional materials.

In the case of non-linear optical materials, the earliest studies were carried out primarily on inorganic materials such as potassium dihydrogenphosphate (KDP) and lithium niobate(V). Although KDP is commonly used for second harmonic generation (SHG) in commercial laser systems, it is not an ideal material since its non-linear response is relatively low. Subsequently, much attention was diverted to the design of organic molecules that, individually, would exhibit enormous non-linear effects. Unfortunately, much less attention was paid to intermolecular interactions and crystal properties and, as a consequence, many carefully designed molecules only became short-lived entries on the most current top-ten list of molecular SHG activity. Today, after a decade of intense interest in supramolecular synthesis, it may be worthwhile to revisit some of those classes of molecules. Our understanding of the structural effects of intermolecular forces and of the way in which we may influence the balance between them has improved considerably and the tools of crystal engineering may bring new enthusiasm to the design of improved SHG-active materials. Furthermore (and against the backdrop of polymorphism), should we throw away our carefully synthesized molecular solid, designed for SHG, simply because, at the first attempt, it crystallizes in a symmetric space group? Probably not.

The ability to control lattice dimensions immediately brings attention to correlations between the shape and size of the molecular scaffolding and the subsequent properties of that material. Even with a chemically 'unreactive' architecture, we can design functional solids. Porous materials (3-D materials) with variable cavity sizes, infinite channels or with specific interplanar separations (for 2-D structures) can be useful in applications concerned with 'separation techniques', 'selectivity', 'inclusion' or 'intercalation', all of which have considerable commercial potential. Do zeolites and clays represent the final summits of sophistication in 3-D and 2-D materials, respectively? There is no obvious reason to believe that they do and consequently there should be room for improvements in terms of both physical properties and chemical reactivity. Although ultimately we want control over the assembly of 3-D solids, there is much to be said for attempting to make low-dimensional solids. A single-crystal containing well defined 2-D molecular motifs is inherently highly anisotropic and will display physical properties that are strongly dependent upon the direction of the incident input or stimulus. The response to an external electromagnetic signal can therefore be modulated, or even cancelled, simply by rotating the crystal with respect to the incident 'probe'. If we can make precise alterations to the interplanar separations in such materials (whilst leaving the fundamental chemistry intact), we have a way of directly correlating lattice dimensions with physical properties. In principle, there is little difference between the attempted assembly of 1-D, 2-D or 3-D motifs. Clearly, the ability to prepare low-dimensional supramolecular assemblies is as important as 3-D crystal engineering, since the practical relevance of many materials is directly derived from their structural anisotropy.

There are other areas where supramolecular synthesis may provide a fresh approach to solving long-standing problems. Colours of organic compounds are commonly thought to be a function of molecular electronic structure alone, but there are examples of organic solids where the colour is determined by crystal packing. This phenomenon, crystallochromy (Klebe, Graser, Hädicke & Berndt, 1989), has been observed in *e.g.* phthalocyanines (Wagner, Loutfy & Hsiao, 1982). A theoretical study of some perylenes (Kazmaier & Hoffmann, 1994) also showed that the bandwidth of the valence and conduction bands is a direct function of the stack angle and, thus, the degree of overlap between adjacent molecules within the stack. The observed colour differences of many perylene pigments must be a function of crystal packing as they have very similar absorption spectra in solution (Klebe, Graser, Hädicke & Berndt, 1989). With this in mind, supramolecular design of new photoconducting materials for xerographic applications is another field with considerable potential.

We may also revisit topochemistry where Schmidt carried out his first experiments in 'crystal engineering'. The fact that crystalline solids are, by definition, ordered solids means that we can utilize these media as a way of imparting stereochemical control over the reaction. For example, in solution, disubstituted penta-1,4-diene-3-ones may undergo photochemically induced isomerization reactions which lead to mixtures of *cis–trans* products. However, in the solid state, where each molecule is locked in place, typically only one product is obtained (Green & Schmidt, 1970). Not only does the solid state impart positional restrictions on molecules, but inherently flexible molecules will also be confined, which may provide control over the stereochemistry of the product.

Another area which may fall into the realm of crystal engineering is the 'responsibility' for providing better insight into the way in which intermolecular recognition processes govern spatial orientation, space-group partiality *etc.* Sometimes it may also be necessary to re-evaluate or re-interpret existing information. Until quite recently it was commonly thought that molecules with large dipole moments align in an antiparallel fashion. Since such a packing arrangement will lead to an overall cancellation of individual contributions to the overall polarity of the solid, this notion may well have had a rather detrimental effect upon synthetic efforts and the search for polar solids. However, Whitesell and co-

UM00012654
NOVARTIS EXHIBIT 1017
Novartis v. Regents, IPR2023-01346
Page 1400 of 4460

workers (Whitesell, Davis, Saunders, Wilson & Feagins, 1991) have demonstrated that there is no correlation between a high dipole moment and a propensity for centrosymmetric space groups, especially if directional intermolecular forces, *e.g.* hydrogen bonds, are present. This is an important statement which could affect existing approaches to the design of new polar solids. These issues will be addressed by scientists concerned with the utilization and understanding of intermolecular forces.

Computational chemistry and molecular simulation will continue to add to our understanding of how to predict unknown structures, polymorphs and physical properties of 'hypothetical' materials. An in-depth overview of computational chemistry in the context of crystal engineering is beyond the scope of this article. Several authors have outlined many of the possibilities and challenges of theoretical supramolecular chemistry (Gavezzotti, 1990; Gavezzotti & Filippini, 1995, 1996; Holden, Du & Ammon, 1993; Hagler & Bernstein, 1978). Gavezzotti (1994) asked the crucial question in a recent review, 'Are crystal structures predictable', and the current answer would have to be 'Sometimes'. Such a reply is unlikely to set the academic world ablaze with excitement, but it is nevertheless a realistic viewpoint (although the answer may also depend upon your definition of the term 'crystal structure'). Despite the complexities of these problems, progress has been made both with dynamic and static methods. Perlstein (1992, 1994) has used a Monte Carlo cooling method in combination with empirical potentials for calculating intermolecular energies. The 3-D structure is built up from substructures (*e.g.* stacks and layers) which are in local energy minima. Karfunkel & Gdanitz (1992) employed simulated annealing to generate collections of low-energy structures by searching the lattice energy hypersurface. Gavezzotti (1991) has calculated interaction energies of clusters of rigid molecules using force-field methods and the clusters are then translated in space or coupled together to give the 3-D crystal structure. Price & Wibley (1997) showed that the observed crystal structures of several heterocycles corresponded to calculated minima in the lattice energy. Particular attention was paid to the electrostatic contributions which were calculated from an *ab-initio*-based distributed multipole model of the charge density.

Considerable advancement has been made in the *a priori* prediction of crystal structures and further progress would be greatly facilitated if existing databases continue to be developed with new search algorithms and statistical tools. More importantly, if the CSD also contained information about enthalpies of fusion, enthalpies of melting, solubilities and thermal stabilities, we would have an immensely powerful research tool that would contain essential data for further statistical and quantum mechanical studies. Obviously, this information is not available for more than a small fraction of all structures in the CSD, but it would still represent a crucial step in the right direction.

Finally, leaving the commercial applications perspective aside, we should also remind ourselves that one of the most important targets for crystal engineering is to provide improved understanding of the very essence and consequences of non-covalent forces. We need to know more about their relative strengths and preferred geometries, we need to pinpoint their physical origin and we need to establish appropriate criteria for recognizing these interactions.

I would like to express my sincere gratitude to past and present members of my research group, and a special thank you to Gautam Desiraju and Joel Bernstein who have been immensely generous with time, advice and plenty of inspiration. Financial support from NSF-EPSCOR (OSR-9550487).

References

Aakeröy, C. B. & Hitchcock, P. B. (1993). *J. Mater. Chem.* **3**, 1129–1135.
Aakeröy, C. B., Hitchcock, P. B. & Seddon, K. R. (1992). *J. Chem. Soc. Chem. Commun.* pp. 553–555.
Aakeröy, C. B., Hughes, D. P. & Nieuwenhuyzen, M. (1996). *J. Am. Chem. Soc.* **118**, 10134–10140.
Aakeröy, C. B. & Nieuwenhuyzen, M. (1994). *J. Am. Chem. Soc.* **116**, 10983–10991.
Aakeröy, C. B. & Nieuwenhuyzen, M. (1996). *J. Mol. Struct.* **374**, 223–239.
Aakeröy, C. B. & Nieuwenhuyzen, M. (1997). In preparation.
Aakeröy, C. B. & Seddon, K. R. (1993). *Chem. Soc. Rev.* **22**, 397–407.
Allen, F. H., Kennard, O. & Taylor, R. (1983). *Acc. Chem. Res.* **16**, 146–153.
Almlöf, J., Kvick, Å. & Olovsson, I. (1971). *Acta Cryst.* B**27**, 1201–1208.
André, C., Luger, P., Fuhrhop, J.-H. & Rosengarten, B. (1993). *Acta Cryst.* B**49**, 375–382.
Ashton, P. R., Collins, A. N., Fyfe, M. C. T., Glink, P. T., Menzer, S., Stoddart, J. F. & Williams, D. J. (1997). *Angew. Chem. Int. Ed. Engl.* **36**, 59–62.
Banda, R. M. H., Cusick, J., Scudder, M. L., Craig, D. C. & Dance, I. G. (1989). *Polyhedron*, **8**, 1995–1998.
Bernstein, J., Davis, R. E., Shimoni, L. & Chang, N.-L. (1995). *Angew. Chem. Int. Ed. Engl.* **34**, 1555–1573.
Bernstein, J. & Hagler, A. T. (1978). *J. Am. Chem. Soc.* **100**, 673–681.
Bernstein, J. & Hagler, A. T. (1979). *Mol. Cryst. Liq. Cryst.* **50**, 223–234.
Bhattacharaya, S., Dastidar, P. & Guru Row, T. N. (1994). *Chem. Mater.* **6**, 531–537.
Braga, D. & Grepioni, F. (1996). *Chem. Commun.* pp. 571–578.
Braga, D., Grepioni, F., Byrne, J. J. & Wolf, A. (1995). *J. Chem. Soc. Chem. Commun.* pp. 1023–1024.
Braga, D., Grepioni, F., Milne, P. & Parisini, E. (1993). *J. Am. Chem. Soc.* **115**, 5115–5122.
Brammer, L., Zhao, D., Ladipo, F. T. & Braddock-Wilking, J. (1995). *Acta Cryst.* B**51**, 632–640.
Burrows, A. D., Mingos, D. M. P., White, A. J. P. & Williams, D. J. (1996). *Chem. Commun.* pp. 97–99.
Chang, Y.-L., West, M.-A., Fowler, F. W. & Lauher, J. W. (1993). *J. Am. Chem. Soc.* **115**, 5991–6000.

UM00012655
NOVARTIS EXHIBIT 1017
Novartis v. Regents, IPR2023-01346
Page 1401 of 4460

Chowdhry, M. M., Mingos, D. M. P., White, A. J. P. & Williams, D. J. (1996). *Chem. Commun.* pp. 899–900.
Cohen, M. D. & Schmidt, G. M. J. (1964). *J. Chem. Soc.* pp. 1996–2000.
Copp, S. B., Holman, K. T., Sangster, J. O. S., Subramanian, S. & Zaworotko, M. J. (1995). *J. Chem. Soc. Dalton Trans.* pp. 2233–2243.
Copp, S. B., Subramanian, S. & Zaworotko, M. J. (1992). *J. Am. Chem. Soc.* **114**, 8719–8720.
Crabtree, R. H. (1993). *Angew. Chem. Int. Ed. Engl.* **32**, 789–805.
Dance, I. (1995). *Perspectives in Supramolecular Chemistry. Vol. 2. The Crystal as a Supramolecular Entity*, ch. 5. Chichester: Wiley.
Desiraju, G. R. (1989). *Crystal Engineering: The Design of Organic Solids*. Amsterdam: Elsevier.
Desiraju, G. R. (1995*a*). *Angew. Chem. Int. Ed. Engl.* **34**, 2311–2327.
Desiraju, G. R. (1995*b*). Editor. *Perspectives in Supramolecular Chemistry, Vol. 2, The Crystal as a Supramolecular Entity*. Chichester: Wiley.
Desiraju, G. R. & Harlow, R. L. (1989). *J. Am. Chem. Soc.* **111**, 6757–6764.
Desiraju, G. R., Pedireddi, V. R., Sarma, J. A. R. P. & Zacharias, D. E. (1993). *Acta Chim. Hung.* **130**, 451–465.
Donohue, J. (1968). *Structural Chemistry and Molecular Biology*, pp. 443–465. San Francisco: W.H. Freeman.
Drain, C. M., Fischer, R., Nolen, E. G. & Lehn, J.-M. (1993). *J. Chem. Soc. Chem. Commun.* pp. 243–245.
Drain, C. M., Russell, K. C. & Lehn, J.-M. (1996). *Chem. Commun.* pp. 337–338.
Ducharme, Y. & Wuest, J. D. (1988). *J. Org. Chem.* **53**, 5789–5791.
Dunitz, J. D. (1991). *Pure Appl. Chem.* **63**, 177–185.
Dunitz, J. D. & Bernstein, J. (1995). *Acc. Chem. Res.* **28**, 193–200.
Ermer, O. & Eling, A. (1994). *J. Chem. Soc. Perkin Trans. 2*, pp. 925–944.
Etter, M. C. (1991). *J. Phys. Chem.* **95**, 4601–4610.
Etter, M. C. & Adsmond, D. A. (1990). *J. Chem. Soc. Chem. Commun.* pp. 589–591.
Etter, M. C. & Baures, P. W. (1988). *J. Am. Chem. Soc.* **110**, 639–640.
Etter, M. C., MacDonald, J. C. & Bernstein, J. (1990). *Acta Cryst.* B**46**, 256–262.
Garcia-Tellado, F., Geib, S. J., Goswami, S. & Hamilton, A. D. (1991). *J. Am. Chem. Soc.* **113**, 9265–9269.
Garrett, T. M., Koert, U., Lehn, J.-M., Rigault, A., Meyer, D. & Fischer, J. (1990). *J. Chem. Soc. Chem. Commun.* pp. 557–558.
Gavezzotti, A. (1990). *Acta Cryst.* B**46**, 275–283.
Gavezzotti, A. (1991). *J. Am. Chem. Soc.* **113**, 4622–4629.
Gavezzotti, A. (1994). *Acc. Chem. Res.* **27**, 309–314.
Gavezzotti, A. (1995). *J. Chem. Soc. Perkin Trans. 2*, pp. 1399–1404.
Gavezzotti, A. & Filippini, G. (1995). *J. Am. Chem. Soc.* **117**, 12299–12305.
Gavezzotti, A. & Filippini, G. (1996). *J. Am. Chem. Soc.* **118**, 7153–7157.
Ge, Y., Lilienthal, R. R. & Smith, D. K. (1996). *J. Am. Chem. Soc.* **118**, 3976–3977.
Geib, S. J., Vicent, C., Fan, E. & Hamilton, A. D. (1993). *Angew. Chem. Int. Ed. Engl.* **32**, 119–120.
Green, B. S. & Schmidt, G. M. J. (1970). *Tetrahedron Lett.* pp. 4249–4252.
Gridunova, G. V., Furmanova, N. G., Struchov, Y. T., Ezhkova, Z. I. Grigorieva, L. P. & Chayanov B. A. (1982). *Kristallografiya*, **27**, 267–272.
Hagler, A. T. & Bernstein, J. (1978). *J. Am. Chem. Soc.* **100**, 6349–6354.
Hasenknopf, B., Lehn, J.-M., Kneisel, B. O., Baum, G. & Fenske, D. (1996). *Angew. Chem. Int. Ed. Engl.* **35**, 1838–1840.
Hassel, O. & Romming, C. (1967). *Acta Chem. Scand.* **21**, 2659.
Holden, J. R., Du, Z. & Ammon, H. L. (1993). *J. Comput. Chem.* **14**, 422–437.
Houlton, A., Mingos, D. M. P. & Williams, D. J. (1994). *Transit. Met. Chem.* **19**, 653–656.
James, S. L., Verspui, G., Spek, A. L. & van Koten, G. (1995). *Chem. Commun.* pp. 1309–1310.
Jeffrey, G. A. & Saenger, W. (1991). *Hydrogen Bonding in Biological Structures*. Berlin: Springer.
Kadirvelraj, R., Umarji, A. M., Robinson, W. T., Bhattacharaya, S. & Guru Row, T. N. (1996). *Chem. Mater.* **8**, 2313–2323.
Karfunkel, H. R. & Gdanitz, R. J. (1992). *J. Comput. Chem.* **13**, 1171–1183.
Kazmaier, P. M. & Hoffmann, R. (1994). *J. Am. Chem. Soc.* **116**, 9684–9691.
Keegstra, E. M. D., van der Mieden, V., Zwikker, J. W., Jenneskens, L. W., Schouten, A., Kooijman, H., Veldman, N. & Spek, A. L. (1996). *Chem. Mater.* **8**, 1092–1105.
Kimura, E., Ikeda, T., Shionoya, M. & Shiro, M. (1995). *Angew. Chem. Int. Ed. Engl.* **34**, 663–664.
Kitaigorodsky, A. I. (1961). *Organic Chemical Crystallography*. New York: Consultants Bureau.
Kitaigorodsky, A. I. (1973). *Molecular Crystals and Molecules*. New York: Academic Press.
Klebe, G., Graser, F., Hädicke, F. & Berndt, J. (1989). *Acta Cryst.* B**45**, 69–77.
Kvick, Å. & Olovsson, I. (1968). *Ark. Kem.* **30**, 71–80.
Leadbeater, C. (1991). *Financial Times*, April 9.
Lefur, Y., Bagieu-Beucher, M., Masse, R., Nicoud, J. F. & Levy, J. P. (1996). *Chem. Mater.* **8**, 68–75.
Lehn, J.-M. (1988). *Angew. Chem. Int. Ed. Engl.* **29**, 90–112.
Lehn, J.-M. (1990). *Angew. Chem. Int. Ed. Engl.* **29**, 1304–1319.
Lehn, J.-M. (1995). *Supramolecular Chemistry*. Weinheim: VCH.
Lehn, J.-M., Mascal, M., DeCian, A. & Fischer, J. (1990). *J. Chem. Soc. Chem. Commun.* pp. 479–480.
Leiserowitz, L. (1976). *Acta Cryst.* B**32**, 775–802.
Leiserowitz, L. & Tuval, M. (1978). *Acta Cryst.* B**34**, 1230–1247.
Munakata, M., Wu, L. P., Yamamoto, M., Kuroda-Sowa, T. & Maekawa, M. (1996). *J. Am. Chem. Soc.* **118**, 3117–3124.
Nowacki, W. (1942). *Helv. Chem. Acta*, **25**, 863–878.
Pedireddi, V. R., Jones, W., Chorlton, A. P. & Docherty, R. (1996). *Chem. Commun.* pp. 997–998.
Pedireddi, V. R., Reddy, D. S., Goud, B. S., Craig, D. C., Rae, A. D. & Desiraju, G. R. (1994). *J. Chem. Soc. Perkin Trans. 2*, pp. 2353–2360.
Perlstein, J. (1992). *J. Am. Chem. Soc.* **114**, 1955–1963.
Perlstein, J. (1994). *J. Am. Chem. Soc.* **116**, 11420–11432.
Platts, J. A., Howard, S. T. & Bracke, B. R. F. (1996). *J. Am. Chem. Soc.* **118**, 2726–2733.
Price, S. L., Stone, A. J., Lucas, J., Rowland, R. S. & Thornley, A. (1994). *J. Am. Chem. Soc.* **116**, 4910–4918.
Price, S. L. & Wibley, K. S. (1997). *J. Phys. Chem. A*, **101**, 2198–2206.
Rebek, J. Jr (1996). *Acta Chem. Scand.* **50**, 707–716.
Reddy, D. S., Panneerselvam, K., Pilati, T. & Desiraju, G. R. (1993). *J. Chem. Soc. Chem. Commun.* pp. 661–662.
Robinson, F. & Zaworotko, M. J. (1995). *J. Chem. Soc. Chem. Commun.* pp. 2413–2414.

UM00012656
NOVARTIS EXHIBIT 1017
Novartis v. Regents, IPR2023-01346
Page 1402 of 4460

Robson, R., Abrahams, B. F., Batten, S. R., Gable, R. W., Hoskins, B. F. & Liu, J. (1992). *Supramolecular Architectures*, pp. 256–273. Am. Chem. Soc. Publication, Washington, DC.
Russel, V. A., Etter, M. C. & Ward, M. D. (1994*a*). *J. Am. Chem. Soc.* **116**, 1941–1952.
Russel, V. A., Etter, M. C. & Ward, M. D. (1994*b*). *Chem. Mater.* **6**, 1206–1217.
Russel, V. A. & Ward, M. D. (1996). *Chem. Mater.* **8**, 1654–1666.
Schmidt, G. M. J. (1971). *Pure Appl. Chem.* **27**, 647–678.
Schwiebert, K. E., Chin. D. N., MacDonald, J. C. & Whitesides, G. M. (1996). *J. Am. Chem. Soc.* **118**, 4018–4029.
Smith, G., Gentner, J. M., Lynch, D. E., Byriel, K. A. & Kennard, C. H. L. (1995). *Aust. J. Chem.* **48**, 1151–1166.
Subramanian, S. & Zaworotko, M. (1994). *Coord. Chem. Rev.* **137**, 357–401.
Subramanian, S. & Zaworotko, M. J. (1995). *Angew. Chem. Int. Ed. Engl.* **34**, 2127–2129.
Sutor, D. J. (1962). *Nature (London)*, **195**, 68–69.
Sutor, D. J. (1963). *J. Chem. Soc.* pp. 1105–1110.
Taylor, R. & Kennard, O. (1982). *J. Am. Chem. Soc.* **104**, 5063–5070.
Taylor, R. & Kennard, O. (1983). *Acta Cryst.* B**39**, 133–138.
Taylor, R. & Kennard, O. (1984). *Acc. Chem. Res.* **17**, 320–326.
Taylor, R., Kennard, O. & Versichel, W. (1983). *J. Am. Chem. Soc.* **105**, 5761–5766.
Threlfall, T. L. (1995). *Analyst*, **120**, 2435–2460.
Ung, A. T., Bishop, R., Craig, D. C., Dance, I. G. & Scudder, M. S. (1994). *Chem. Mater.* **6**, 1269–1281.
Vögtle, F. (1991). *Supramolecular Chemistry: An Introduction*. Chichester: Wiley.
Wagner, H. J., Loutfy, R. O. & Hsiao, C.-K. (1982). *J. Mater. Sci.* **17**, 2781–2791.
Watanabe, O., Noritake, T., Hirose, Y., Okada, A. & Kurauchi, T. (1993). *J. Mater. Chem.* **3**, 1053–1057.
Whitesell, J. K., Davis, R. E., Saunders, L. L., Wilson, R. J. & Feagins, J. P. (1991). *J. Am. Chem. Soc.* **113**, 3267–3270.
Zaworotko, M. J. (1994). *Chem. Soc. Rev.* **23**, 283–288.
Zerkowski, J. A., MacDonald, J. C., Seto, C. T., Wierda, D. A. & Whitesides, G. M. (1994). **116**, *J. Am. Chem. Soc.* pp. 9025–9026.
Zerkowski, J. A., MacDonald, J. C. & Whitesides, G. M. (1994). *Chem. Mater.* **6**, 1250–1257.
Zhao, X., Chang, Y.-L., Fowler, F. W. & Lauher, J. W. (1990). *J. Am. Chem. Soc.* **112**, 6627–6634.
Zyss, J., Pecaut, J., Levy, J. P. & Masse, R. (1993). *Acta Cryst.* B**49**, 334–342.

UM00012657
NOVARTIS EXHIBIT 1017
Novartis v. Regents, IPR2023-01346
Page 1403 of 4460

This Page is Inserted by IFW Indexing and Scanning Operations and is not part of the Official Record

BEST AVAILABLE IMAGES

Defective images within this document are accurate representations of the original documents submitted by the applicant.

Defects in the images include but are not limited to the items checked:

- ☐ BLACK BORDERS
- ☐ IMAGE CUT OFF AT TOP, BOTTOM OR SIDES
- ☐ FADED TEXT OR DRAWING
- ☐ BLURRED OR ILLEGIBLE TEXT OR DRAWING
- ☐ SKEWED/SLANTED IMAGES
- ☐ COLOR OR BLACK AND WHITE PHOTOGRAPHS
- ☐ GRAY SCALE DOCUMENTS
- ☐ LINES OR MARKS ON ORIGINAL DOCUMENT
- ☐ REFERENCE(S) OR EXHIBIT(S) SUBMITTED ARE POOR QUALITY
- ☐ OTHER: _____

IMAGES ARE BEST AVAILABLE COPY.
As rescanning these documents will not correct the image problems checked, please do not report these problems to the IFW Image Problem Mailbox.

CRYSTAL ENGINEERING USING INTERMOLECULAR HYDROGEN-BONDED CONNECTORS AND CLASSIC COORDINATION CHEMISTRY

Christer B. Aakeröy*, Alicia M. Beatty, Brian A. Helfrich, and Destin S. Leinen

Department of Chemistry, Kansas State University, Manhattan, Kansas 66506

Crystal engineering is governed by the structural consequences of intermolecular forces, and by the way in which such interactions are utilized for controlling the assembly of molecules into predictable structural motifs. A vital part of crystal engineering is thus dedicated to identifying robust intermolecular synthons that can be used as reliable connectors between molecules. In an effort to design new transition-metal containing materials, we have combined geometric features from coordination chemistry (notably of linear silver(I) complexes) with intermolecular connectors developed in organic crystal engineering. The aim is to examine how the structural balance in such materials is influenced by competition and/or cooperation between intermolecular hydrogen-bonded synthons and the spatial requirements of transition-metal complexes. In this paper we report the crystal structures of di(3-acetyloximepyridine)silver(I) tetrafluoroborate and di(nicotinamide)silver(I) nitrate, two compounds that are dominated in the solid state by low-dimensional cationic motifs generated by complementary oxime-oxime and amide-amide hydrogen-bond interactions, respectively.

1. BACKGROUND

The construction of extended solid-state architectures in crystal engineering is delineated by the nature and directionality of intermolecular forces [1], and any strategy for effective supramolecular synthesis requires some means for connecting neighboring molecules into predictable arrangements. Consequently, we need to identify non-covalent connectors that are selective enough to be directional and strong enough to be transferable between different systems. Despite the inherent difficulties with using relatively weak forces as primary synthetic tools, considerable progress has been made during the last decade, notably in the preparation of organic molecular solids. The selectivity and directionality of the hydrogen bond have been instrumental in the preparation of distinctive and predictable structural aggregates, and the use of hydrogen bonding as a steering force is now emerging as the most important strategy in crystal engineering [2,3], Figure 1.

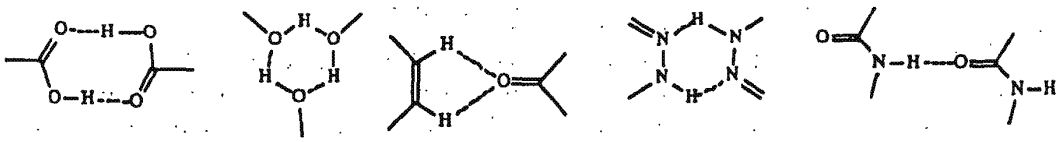


Figure 1. Some strategies for linking molecules together with hydrogen bonds.

While the assembly of organic molecular solids has received much attention, much less work has been done with transition-metal complexes. Nevertheless, this field has considerable potential,

©1999 American Crystallographic Association

97

UM00012659
NOVARTIS EXHIBIT 1017
Novartis v. Regents, IPR2023-01346
Page 1405 of 4460

as the presence of transition-metal ions within a molecular scaffolding provides improved access to conductors, magnetic materials and catalysts. Metal ions have been incorporated into networks using coordinate-covalent bonds (coordination polymers) [4], or (to a lesser extent) using intermolecular interactions [5,6]. The advantages of combining crystal engineering with coordination chemistry was elegantly illustrated by Robson and Hoskins in the design of 2-D and 3-D metal-containing frameworks based around metal-4,4'-bipyridine derivatives [7]. Several groups have since employed similar building blocks in the design of extended architectures where neighboring transition-metal complexes are covalently connected into 'coordination-polymers' [8,9].

Mingos and co-workers have successfully utilized hydrogen bonding between thiourea/carboxylate, diaminopyridine/uracil, *etc.* for linking neighboring metal-complexes into extended 'tapes' and 'sheets' [10,11]. Other examples of non-covalent linking of complex ions include the use of the well-known dimeric 2-pyridone synthon for the construction of hydrogen-bonded copper(I) complexes with large channels occupied by cations [12]. Much weaker hydrogen bonds, CH···Cl-Pt interactions, were employed for creating infinite chains in an organoplatinum compound [13]. Recent database surveys have also shown that M-H···O hydrogen bonds are prevalent in organometallic compounds [14]. These studies indicate that supramolecular synthesis can provide the basis for new pre-organized structural arrangements ,where organometallic and coordination compounds can be made to assemble into specific structural motifs directed by intermolecular interactions working in concert.

2. RATIONALE

Our strategy for the assembly of transition-metal complexes within low-dimensional molecular networks is based upon the following general approach: we will use the coordinating ability of transition-metal ions by allowing them to act as templates for the 'local' assembly of ligands. These ligands will then interact with each other to create rigid hydrogen-bonded networks, providing control over the supramolecular assembly and orientation of neighboring coordination centers. Suitable hydrogen-bond functionalities that can interact in a complementary fashion include carboxylic acids, amides, oximes, *etc.* In this paper we describe the crystal structures of two compounds assembled using this approach, di(3-acetyloximepyridine)silver(I) tetrafluoroborate, **1**, and di(nicotinamide)silver(I) nitrate, **2**. The structural information provides a basis for a discussion about the structural competition and balance between the steric demands of the metal-ligand interaction and the influence of a range of intermolecular forces, notably hydrogen-bonds.

2.1 Choice of Metal

As we intend to move from low-dimensional assemblies (chains, ribbons and sheets) to structures of increased complexity (3-D porous materials) in a step-by-step manner, silver(I) becomes a natural starting point for designing 1-D motifs due to its propensity for linear coordination. If suitably substituted ligands are coordinated to a silver(I) ion in a linear fashion, the geometry of these silver 'rods' can be propagated throughout the lattice into infinite low-dimensional networks using complementary ligand-ligand hydrogen-bond interactions.

2.2 Choice of Intermolecular Connectors: Amides and Oximes

In order to identify functional moieties that can act as intermolecular linking-groups, it is necessary to examine the preferential packing modes of a series of related molecular solids. For example, the packing modes of primary amides are well-known and such compounds will typically form head-to-head dimers (often extended to 1-D ribbons) [15]. A combination of silver(I) and amide-containing ligands could therefore give rise to infinite chains if the ligands are able to coordinate to the metal ion *via* an alternative donor site. This would leave the amide groups free to interact with each other, thereby generating the desired extended motif.

UM00012660
NOVARTIS EXHIBIT 1017
Novartis v. Regents, IPR2023-01346
Page 1406 of 4460

Our second choice of connector has been unexplored in the context of crystal engineering until recently [16]. The oxime moiety (-C(R)=NOH) is a functional group that has the potential for the assembly of low-dimensional networks through complementary hydrogen bonds involving a dimeric $R_2^2(6)$ motif [17], Figure 2.

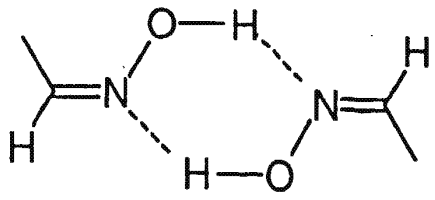


Figure 2. The head-to-head hydrogen-bonding interactions between adjacent oxime moieties.

Although the oxime functionality is not new to synthetic organic chemists, it remains unexplored as an intermolecular connector. This synthon is particularly appealing since it is electronically and sterically 'tunable'; the *R* group can be modified to include a wide range of electron donors/acceptors or bulky substituents, and these functional groups are accessible through well-known synthetic methods [18]. If the oxime functionality is attached to a moiety that can act as coordinating site for a metal ion, we have access to a bridge between coordination complexes and supramolecular assembly. Thus we have used pyridine as the basic building block, (the pyridine nitrogen atom readily coordinates to the metal center) with the amide and oxime substituents *meta* to the ring nitrogen atom.

3. EXPERIMENTAL

3.1 Synthesis

Compound **1** was obtained by adding a solution of 3-acetyloximepyridine (0.14 g) in a minimum amount of ethanol to a solution of silver(I) tetrafluoroborate (0.10 g) in ethanol (50 mL). Slow evaporation of the solvent yielded colorless, prismatic crystals (m.p. 164-167°C).

Compound **2** was obtained by adding a solution of nicotinamide (0.15 g) in water (10 mL) to a solution of silver(I) nitrate (0.10 g) in 1:1 water/ethanol (20 mL). The solution was allowed to evaporate at room temperature, yielding colorless, irregular crystals (m.p. 210°C).

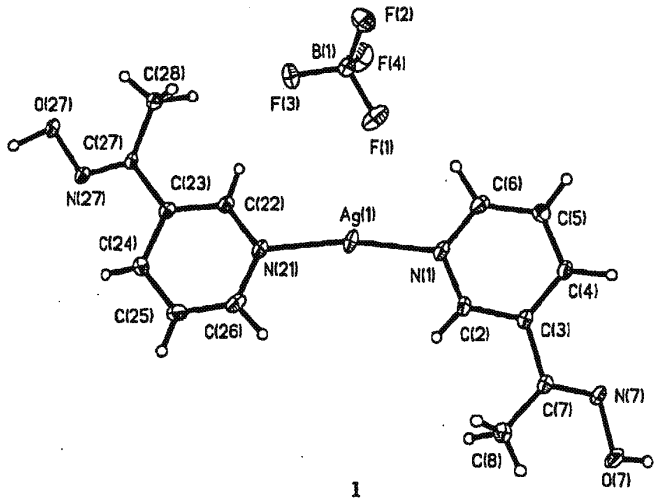
4. X-RAY CRYSTALLOGRAPHY

Crystal data were collected using a Siemens P4 four-circle diffractometer with graphite monochromated Mo-Kα radiation. Crystal stabilities were monitored by measuring 3 standard reflections after every 97 reflections, with no significant decay observed. Cell parameters were obtained from 35 accurately centered reflections in the two-theta range 10 - 25. Data were collected using a θ-2θ scanning technique, and Lorentz and polarization corrections were applied. The structures were solved by the Patterson method, with non-hydrogen atoms found by successive full matrix least squares refinement on F^2 and refined with anisotropic thermal parameters. Hydrogen-atom positions were located from difference Fourier maps and a riding model with fixed thermal parameters [$u_{ij} = 1.2U_{ij}(eq)$ for the atom to which they are bonded], was used for subsequent refinements. The weighting function applied was $w^{-1} = [\sigma^2(F_o^2) + (g_1P)^2 + (g_2P)]$ where $P = [F_o^2 + 2F_c^2]/3$. (Compound 1: $g_1 = 0.0262$, $g_2 = 0.6513$; Compound 2: $g_1 = 0.0192$, $g_2 = 0.3809$). The SHELXTL PC and SHELXL-93 packages were used for data reduction and structure solution and refinement [19].

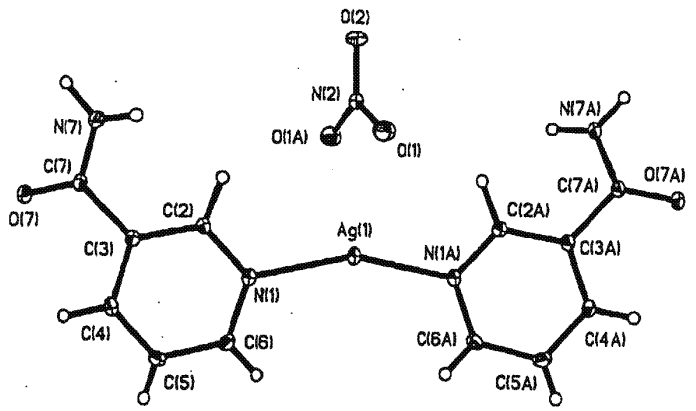
UM00012661
NOVARTIS EXHIBIT 1017
Novartis v. Regents, IPR2023-01346
Page 1407 of 4460

5. RESULTS

Numbering schemes, molecular geometries and thermal ellipsoids of **1** and **2** are presented in Figure 3.



1



2

Figure 3. Thermal ellipsoid plots of **1** and **2**. Ellipsoids are shown at 30% probability

The crystal structure of di(3-acetyloximepyridine)silver(I) tetrafluoroborate, **1**, [20] contains cations comprised of two 3-acetyloximepyridine ligands coordinated through the pyridine nitrogen atoms to a silver(I) ion, [N_{py}-Ag-N_{py} 171.7(1)°]. The oxime moieties are *trans* with respect to each other, and cations are linked by complementary O-H···N hydrogen bonds between oxime moieties on neighboring ligands, generating infinite 1-D chains [21]. Adjacent chains are linked by two C-H···O hydrogen bonds, resulting in 2-D cationic sheets, Figure 4. The $[BF_4]^-$ counter-ions occupy the resulting 'holes' between the cationic sheet, and are held in position by several C-H···F hydrogen bonds. The result is the anisotropic, lamellar structure shown in Figure 5.

The structure determination of **2** [22] reveals that two ligands are coordinated to the silver(I) ion with their amide functionalities oriented in a *cis*-arrangement. As expected, the coordination to the silver ion is through the ring nitrogen atoms. Neighboring amide moieties are hydrogen-bonded *via* two symmetry-related N···O hydrogen bonds [23] forming a "head-to-head" $R_2^2(8)$ motif. This interaction propagates the inherent 1-D geometry of the cationic complex into undulating infinite chains. The 'wavelength' of this 1-D motif is ca. 27 Å. Adjacent chains are then oriented in phase with each other,

UM00012662
NOVARTIS EXHIBIT 1017
Novartis v. Regents, IPR2023-01346
Page 1408 of 4460

creating infinite 2-D layers, Figure 6, with an interplanar distance of ca. 3.2 Å. The anion is positioned between chains and is hydrogen-bonded to the remaining donor site on the amide moiety in the adjacent layers. There is also a short nitrate-silver contact, O···Ag (2.639(2) Å), which is apparently responsible for the significant distortion away from a linear N-Ag-N geometry, ∠158.08(9)°. Finally, the remaining oxygen atom on the anion is hydrogen bonded to the aromatic ring, C-H(6)···O, 2.404(2) Å, ∠168.61(6)°.

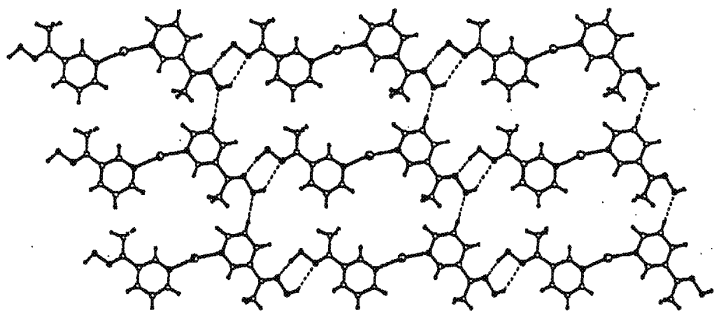


Figure 4. Cationic sheet in **1** formed through O-H···N and C-H···O hydrogen bonds.

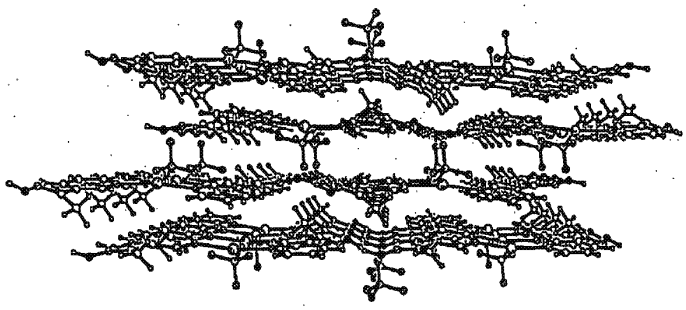


Figure 5. Lamellar structure of **1**. Tetrafluoroborate anions are located between cationic sheets.

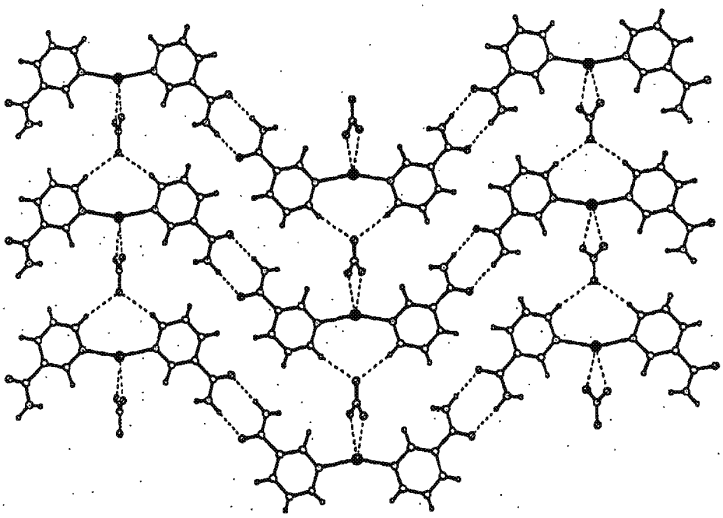


Figure 6. Sheet motif in **2**. Nitrate-cation interactions link chains formed *via* amide-amide hydrogen bonds.

UM00012663
NOVARTIS EXHIBIT 1017
Novartis v. Regents, IPR2023-01346
Page 1409 of 4460

6. DISCUSSION

The structure of **1** is nearly identical to the analogous $[ClO_4]^-$, $[PF_6]^-$, and $[AsF_6]^-$ salts [16], despite the fact that the tetrafluoroborate anion is considerably smaller than *e.g.*, $[AsF_6]^-$. The oxime-oxime hydrogen bonds remain the dominating intermolecular interactions, and thus there are no drastic changes in the supramolecular architectures. This suggests that the hydrogen bonds that generate the cationic sheets are robust but not too rigid, allowing the sheets to flex to accommodate a change in counter-ion size.

The assemblies are connected by O-H···N and C-H···O hydrogen bonds, thus creating low-dimensional networks such as chains (1-D motifs) and sheets (2-D motifs). The similarities between **1** and the recently reported oxime-pyridine silver(I) complexes [16], provide further evidence for the usefulness of the oxime moiety as a supramolecular connector and to the oxime-oxime interaction as a robust intermolecular synthon.

The structure of **2** also contains the desired low-dimensional assembly of cationic complexes. Such architectures have also been reported previously [6,24], although in this case the counterion is a nitrate anion, which has several strong hydrogen bond acceptors. Despite this, the amide-amide link persists and propagates the linear coordination geometry around silver(I) into infinite 1-D motifs.

The structures of **1** and **2** demonstrate that the silver ion provides the desired linear AgL_2 building unit, and neighboring ligands assemble these complexes into either 1-D or 2-D supramolecular architectures *via* intermolecular hydrogen bonds. Although the precise geometry of the hydrogen-bond networks change in this series, amide-amide and oxime-oxime interactions persist in the presence of anions with widely differing geometries and coordinating abilities. This provides further evidence that directional hydrogen bonds can be used in the assembly of transition-metal complexes, even in competition with the inherent steric demands of the metal-ligand geometry and potentially disruptive anion-anion or anion-cation interactions. Consequently, we can expect that many principles of crystal engineering that have been developed and tested in organic solid-state chemistry will assume further relevance in supramolecular aspects of coordination chemistry.

7. ACKNOWLEDGMENTS

We acknowledge financial support from Kansas State University, DuPont and NSF-EPSCoR (OSR-9550487).

8. REFERENCES

[1] (a) J.-M. Lehn, *Angew. Chem. Int. Ed. Engl.* **29** (1990), 1304. (b) C.B. Aakeröy, *Acta Crystallogr., Sect.* **B53** (1997), 569.

[2] (a) C.T. Seto and G.M. Whitesides, *J. Am. Chem. Soc.* **113** (1991), 712. (b) X. Zhao, Y.-L. Chang, F.W. Fowler and J.W. Lauher, *J. Am. Chem. Soc.* **112** (1990), 6627. (c) J.-M. Lehn, M. Mascal, A. DeCian and J. Fischer, *J. Chem. Soc., Perkin Trans. 2* (1992), 461. (d) O. Felix, M.W. Hosseini, A. DeCian and J. Fischer, *Angew. Chem. Int. Ed. Engl.* **36** (1997), 102. (e) J.C. MacDonald and G.M. Whitesides, *Chem. Rev.* **94** (1994), 22383. (f) L.M. Toledo, J.W. Lauher and F.W. Fowler, *J. Am. Chem. Soc.* **112** (1990), 6627.

[3] (a) V.A. Russel and M.D. Ward, *Chem. Mater.* **8** (1996), 1654. (b) C.B. Aakeröy and K.R. Seddon, *Chem. Soc. Rev.* **22** (1993), 397. (c) S. Subramanian and M.J. Zaworotko, *Coord. Chem. Rev.* **137** (1994), 357.

[4] (a) B.F. Abrahams, S.R. Batten, H. Hamit, B.F. Hoskins and R. Robson, *Angew. Chem. Int. Ed. Engl.* **35** (1996), 1690. (b) C. Janiak, *Angew. Chem. Int. Ed. Engl.* **36** (1997), 1431.

[5] L. Carlucci, G. Ciani, D.M. Proserpio and A. Sironi, *J. Chem. Soc. Dalton Trans.* (1991), 1801.

UM00012664
NOVARTIS EXHIBIT 1017
Novartis v. Regents, IPR2023-01346
Page 1410 of 4460

[6] C.B. Aakeröy and A.M. Beatty, *Chem. Commun.* (1998), 1067.

[7] R. Robson, B.F. Abrahams, S.R. Batten, R.W. Gable, B.F. Hoskins and J. Liu, *Supramolecular Architectures* (ACS Publication, Washington, DC, 1992) pp. 256.

[8] (a) S.B. Copp, S. Subramanian and M.J. Zaworotko, *J. Am. Chem. Soc.* **114** (1992), 8719. (b) S. Subramanian and M.J. Zaworotko, *Angew. Chem. Int. Ed. Engl.* **34** (1995), 2127. (c) M.J. Zaworotko, *Chem. Soc. Rev.* **23** (1994), 283.

[9] (a) O.M. Yaghi and H. Li *J. Am. Chem. Soc.* **118** (1996), 295. (b) O.M. Yaghi and G. Li, *Angew. Chem. Int. Ed. Engl.* **34** (1995), 207. (c) M. Fujita, Y.-J. Kwon, S. Washizu and K. Ogura, *J. Am. Chem. Soc.* **116** (1994), 1151. (d) M. Fujita, Y.-J. Kwon, S. Osamu, K. Yamaguchi and K. Ogura, *J. Am. Chem. Soc.* **117** (1995), 287.

[10] A.D. Burrows, D.M.P. Mingos, A.J.P. White and D.J. Williams, *Chem. Commun.* (1996), 97.

[11] M.M. Chowdhry, D.M.P Mingos, A.J.P White and D.J. Williams, *Chem. Commun.*, (1996), 899.

[12] M. Munakata, L.P. Wu, M. Yamamoto, T. Kuroda-Sowa and M. Maekawa, *J. Am. Chem. Soc.* **118** (1996), 3117.

[13] S.L. James, G. Verspui, A.L. Spek and G. van Koten, *Chem. Commun.* (1997), 1309.

[14] D. Braga, F. Grepioni, E. Tedesco, K. Biradha and G.R. Desiraju, *Organometallics* **15** (1996), 2692.

[15] L. Leiserowitz and G.M.J. Schmidt, *J. Chem. Soc. (A).* (1969), 2372.

[16] C.B. Aakeröy, A.M. Beatty and D.S. Leinen, *J. Am. Chem. Soc.* **20** (1998), 7383.

[17] For information about graph-set notation, see J. Bernstein, R.E. Davis, L. Shimoni and N.-L Chang, *Angew. Chem. Int. Ed. Engl.* **34** (1995), 1555; M.C. Etter, J.C. MacDonald and J. Bernstein, *Acta Crystallogr. Sect. B,* **46** (1990), 256.

[18] (a) G.A. Pearse, Jr. and M. Ericsson, *Chromatogr.* 177 (1979) 174. (b) E. Bernasek, *J. Org. Chem.* (1957), 1263.

[19] G.M. Sheldrick, *SHELXL-93*, University of Göttingen, Germany.

[20] Crystal data for (1): $C_{14}H_{16}AgF_4N_4O_2B$ M_r = 466.99 g mol^{-1}, colorless, irregular prism (0.6 x 0.2 x 0.2 mm), triclinic, space group P$\bar{1}$, a = 7.635(1), b = 8.240(2), c = 13.889(2) Å, α = 75.43(1), β = 111.300(8), γ = 82.62(1)°, U = 838.6(3) Å^3, Z = 2, ρ_{calcd} = 1.849 g cm^{-1}, $\mu(Mo_{K\alpha})$ = 1.261 mm^{-1}. Of 3107 reflections collected, 2927 were independent; T = 173 K; Final R value 0.0229, wR = 0.0536, for 2695 data with I>2σ(I) and 235 parameters; largest diff. peak and hole 0.383 and -0.317 e Å^{-3}.

[21] Intermolecular OH···N_{oxime} hydrogen bonds for (1): O7-N27, 3.239(3) Å, ∠O7-H7···N27, 127.15(6)°; O27···N27, 2.731(3) Å, ∠O27-H27···N27, 170.43(9)°; cation-anion CH···F hydrogen bond distances for 1: C2···F2, 3.152(3) Å, ∠C2-H2···F2, 159.11(8)°; C6···F1, 3.237(3) Å, ∠C6-H6···F1, 151.42(9)°; C22···F3, 3.330(3) Å, ∠C22-H22···F3, 169.83(7)°; C26···F2, 3.432(3) Å, ∠C26-H26···F2, 151.28(8)°.

[22] Crystal data for (2): $C_{12}H_{12}AgN_5O_5$ M_r = 514.14 g mol^{-1}, colorless, irregular prism (0.4 x 0.4 x 0.2 mm), monoclinic, space group P2/c, a = 11.644(1), b = 8.0006(8), c = 7.9943(9) Å, β = 109.121(8)°, U=703.6(1) Å^3, Z = 4, ρ_{calcd} = 1.955 g cm^{-1}, $\mu(Mo_{K\alpha})$ = 1.468 mm^{-1}. Of 2245 reflections collected, 1630 were independent; T = 173 K; Final R value 0.0200, wR = 0.0451, for 1513 data with I>2σ(I) and 106 parameters; largest diff. peak and hole 0.373 and -0.431 e Å^{-3}.

[23] Intermolecular N-H···O_{amide} hydrogen bonds for 2: N7···O7, 2.961(2)Å, ∠N7-H7A···O7, 167.37(7)°. Amide-anion N-H···O hydrogen bond distance for 2: N7···O1, 2.933(2) Å, ∠N7-H7B···O1, 158.31(6)°.

[24] C.B. Aakeröy and A.M. Beatty, *Crystal Engineering* **1** (1998), 39.

UM00012665
NOVARTIS EXHIBIT 1017
Novartis v. Regents, IPR2023-01346
Page 1411 of 4460

This Page is Inserted by IFW Indexing and Scanning Operations and is not part of the Official Record

BEST AVAILABLE IMAGES

Defective images within this document are accurate representations of the original documents submitted by the applicant.

Defects in the images include but are not limited to the items checked:

- ☐ BLACK BORDERS
- ☐ IMAGE CUT OFF AT TOP, BOTTOM OR SIDES
- ☐ FADED TEXT OR DRAWING
- ☐ BLURRED OR ILLEGIBLE TEXT OR DRAWING
- ☐ SKEWED/SLANTED IMAGES
- ☐ COLOR OR BLACK AND WHITE PHOTOGRAPHS
- ☐ GRAY SCALE DOCUMENTS
- ☐ LINES OR MARKS ON ORIGINAL DOCUMENT
- ☐ REFERENCE(S) OR EXHIBIT(S) SUBMITTED ARE POOR QUALITY
- ☐ OTHER: _____

IMAGES ARE BEST AVAILABLE COPY.
As rescanning these documents will not correct the image problems checked, please do not report these problems to the IFW Image Problem Mailbox.

SUPRAMOLECULAR CHEMISTRY, Vol. 7, pp. 153–156
Reprints available directly from the publisher
Photocopying permitted by license only

© 1996 OPA (Overseas Publishers Association)
Amsterdam B.V. Published in The Netherlands under license by
Gordon and Breach Science Publishers SA
Printed in Malaysia

The crystal structure of the molecular cocrystal *L*-malic acid *L*-tartaric acid (1/1)

CHRISTER B. AAKERÖY, TREVOR I. COOKE and MARK NIEUWENHUYZEN

School of Chemistry, The Queen's University of Belfast, BT9 5AG Belfast, Northern Ireland.

(Received September 25, 1995)

The synthesis and X-ray single crystal structure determination of the molecular cocrystal *L*-malic acid *L*-tartaric acid (1/1) 1, the first example of a dimeric cocrystal incorporating two aliphatic carboxylic acids, are reported. $[C_4H_6O_5][C_4H_6O_6]$, triclinic, $P1$, a = 4.835(1), b = 6.488(1), c = 9.227(1) Å, α = 73.83(1), β = 88.32(1), γ = 77.32°, V = 271.06(8) Å^3, Z = 1, D_{calc} = 1.741 Mg m^{-3}, T = 123(2) K, μ(Mo-K$_\alpha$) = 0.169 mm^{-1}. A total of 1238 reflections were measured and 1181 unique reflections were used in the refinement. The final parameters for observed data were R = 0.030, R^2_w = 0.085 and R = 0.033, R^2_w = 0.134 for all data. The competition between complimentary hydrogen-bond sites of the two acids, which results in the unexpected heteromeric complex, is discussed, and the observed packing arrangements, and the structural consequences arising from the presence of the extended hydrogen-bond networks, are examined in detail.

INTRODUCTION

L-tartaric acid and *L*-malic acid are two naturally occurring, chiral, dicarboxylic acids which have been closely linked to a range of important scientific discoveries during the last 150 years. From Pasteur's separation of crystalline enantiomers,[1] *via* chiral synthesis[2] and solid-state physics (ferroelectricity and nonlinear optics),[3] to recent efforts in crystal engineering,[4] the structure and properties of tartaric acid have provided considerable material for multidisciplinary research. Malic acid, an important contributor to several areas of biochemistry (*e.g.* the citric acid cycle and carbohydrate research), has also been employed as a building block of predictable anionic hydrogen-bonded motifs in crystal engineering.[5] The endurance of the broad academic interest in these compounds is illustrated by the fact that, in the last four years, 336 and 296 papers have been abstracted under the keywords tartaric acid and malic acid, respectively. Much of this attention has its origin in the structures and hydrogen-bonding abilities of the two acids, both in solution and in the solid state.

The different 'versions' of tartaric acid, (the racemate, the two pure enantiomers and the *meso* compound), have previously been subjected to crystallographic examinations (X-ray and neutron) and the crystallographic literature also contains numerous examples of inorganic and organic salts of both the monovalent and the divalent anion.[6] Although malic acid is, chemically, very similar, it has traditionally been very difficult to grow reasonably sized crystals of either malic acid itself, or of salts thereof.[7] Despite these differences in crystal-growing ability, extant organic salts of hydrogentartrates and hydrogenmalates display considerable structural similarities. In most such salts, the anions create infinite, 2-D, layers, held together by two, or more, O-H ··· O interactions. Neighbouring anions are invariably linked in a head-to-tail fashion into infinite chains *via* a short O-H ··· O hydrogen bond.[5,8] The consistency of these anionic networks (even in the presence of very different cations), has provided a basis for reliable 'scaffolding' for several new nonlinear optical materials.

The close resemblance between the structural behaviour of the two acids, both as molecular solids and in ionic compounds, in addition to their similar chemical properties, *e.g.* solubilities, pK_a-values, inspired our efforts to combine both molecules within the same framework in a molecular cocrystal.

RESULTS AND DISCUSSION

During our attempts at preparing a cocrystal of malic acid and tartaric acid, a range of experimental conditions (ratios and solvents) were used, but in most cases the product was simply a physical mixture of the two acids (as determined by X-ray powder diffraction). However, by mixing equimolar solutions (ethanol-water; 1:1) of the two acids, followed by slow evaporation of the

UM00012667
NOVARTIS EXHIBIT 1017
Novartis v. Regents, IPR2023-01346
Page 1413 of 4460

solvent, colourless rhombohedral crystals (mp. 161–162°C) were obtained. The powder X-ray diffraction pattern did not correspond to that of either of the starting materials, and the elemental analysis confirmed the presence of both acids. The crystal structure of this material was then determined using X-ray diffraction.

The single-crystal study showed that the rhombohedral crystals were indeed the desired compound, *L*-malic acid *L*-tartaric acid (1/1). Fractional atomic coordinates are listed in Table 1, and relevant bond distances and bond angles are presented in Table 2. The triclinic structure is held together by a complex network comprising seven unique hydrogen bonds, Table 3. There are no unexpected intramolecular geometric features; both acids display *trans* configurations of the C-C-C-C backbone (177.8° [malic acid], 177.2° [tartaric acid]), Fig. 1. There are, furthermore, no dramatic deviations from coplanarity between the carbonyl groups and the α-hydroxy group (9.4 to −15.93°). The most important intermolecular interactions are the four O ··· O hydrogen bonds which generate the two dimeric head-to-head motifs, $R_2^2(8)$,[9] between neighbouring malic acid and tartaric acid molecules, Fig. 2. These interactions result in infinite, straight, chains composed of alternating malic acid and tartaric acid entities. The geometries of these four hydrogen bonds (r[O ··· O] < 2.69 Å, ∠ (DH···A) > 165°) provide evidence for the relative strength of these selective hydrogen bonds. As expected, neighbouring chains are crosslinked *via* an O···O interaction between hydroxy groups of adjacent tartaric acid molecules, to form a 2-D, flat, layer, Fig. 2. Neighbouring layers are, in turn, crosslinked *via* two hydrogen bonds, Fig. 3, resulting in a compact 3-D structure (D_{calc} = 1.74 g cm^{-3}). There are no hydrogen-bond interactions between adjacent malic acid molecules, but tartaric acid molecules are linked through one hydrogen bond involving the 'surplus' hydroxy moiety. In comparison, the crystal structure of *L*-tartaric acid[10] itself displays a complex 3-D network but without the commonly occurring (among carboxylic acids) head-to-head motif. The structure of *L*-malic acid[11] (hydrogen atoms were not located) displays a 3-D network incorporating the hydrogen-bonded head-to-head motif, with an overall packing which is very similar to that observed in **1**.

The appearance of a cocrystal is rarely the result of a straightforward mixture of two, or more, components. In order to obtain a heteromeric cocrystal, the interactions between the two components, must be stronger than the attractive forces that exist between the homomeric as-

Table 1 Atomic coordinates [× 10^4] and equivalent isotropic displacement parameters [Å^2 × 10^3] for L. U(eq) is defined as one third of the trace of the orthogonalized U_{ij} tensor

Atom	*x*	*y*	*z*	*U(eq)*
O(11A)	1289(5)	5650(4)	11177(2)	19(1)
O(12A)	3259(5)	3613(4)	13421(2)	14(1)
C(1A)	3280(8)	4141(5)	12032(4)	12(1)
C(2A)	5621(9)	3145(6)	11164(4)	17(1)
C(3A)	4380(8)	2257(5)	9991(4)	15(1)
O(3A)	2707(6)	762(4)	10631(3)	21(1)
C(4A)	6805(7)	1348(5)	9103(3)	12(1)
O(41A)	7885(5)	2906(3)	8198(2)	17(1)
O(42A)	7614(5)	−618(4)	9220(3)	15(1)
O(11B)	2107(5)	7701(4)	7885(3)	18(1)
O(12B)	2491(6)	11204(4)	6867(2)	14(1)
C(1B)	3254(8)	9246(5)	6997(3)	13(1)
C(2B)	5634(8)	8289(5)	6107(4)	12(1)
O(2B)	7094(5)	9914(4)	5316(3)	14(1)
C(3B)	4416(8)	7256(5)	5022(3)	12(1)
O(3B)	2333(5)	8768(3)	4006(2)	14(1)
C(4B)	6843(8)	6426(5)	4102(4)	13(1)
O(41B)	8814(5)	4882(4)	4955(2)	16(1)
O(42B)	6935(5)	7167(4)	2732(2)	15(1)
H(11A)	−171(5)	6200(4)	11820(2)	23
H(21A)	6436(9)	4456(6)	10623(4)	20
H(22A)	6961(9)	2035(6)	11823(4)	20
H(3A)	3162(8)	3471(5)	9218(4)	18
H(30A)	3971(6)	−362(4)	11414(3)	25
H(41A)	9348(5)	2275(3)	7824(2)	20
H(11B)	771(5)	8364(4)	8398(3)	21
H(2B)	6949(8)	7085(5)	7014(4)	15
H(20B)	5888(5)	10959(4)	4825(3)	17
H(3B)	3642(8)	6167(5)	5616(3)	15
H(30B)	818(5)	9053(3)	4591(2)	17
H(41B)	10438(5)	4350(4)	4401(2)	20

Table 2 Bond lengths [Å] and angles [°] for L

O(11A)-C(1A)	*1.307(4)*	*O(12A)-C(1A)*	*1.231(4)*
C(1A)-C(2A)	1.501(5)	C(2A)-C(3A)	1.549(4)
C(3A)-O(3A)	1.393(5)	C(3A)-C(4A)	1.518(4)
C(4A)-O(42A)	1.224(4)	C(4A)-O(41A)	1.314(4)
O(11B)-C(1B)	1.320(4)	O(12B)-C(1B)	1.215(4)
C(1B)-C(2B)	1.517(5)	C(2B)-O(2B)	1.418(5)
C(2B)-C(3B)	1.542(4)	C(3B)-O(3B)	1.402(4)
C(3B)-C(4B)	1.519(4)	C(4B)-O(42B)	1.225(4)
C(4B)-O(41B)	1.310(4)		

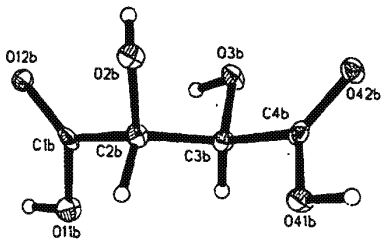
O(12A)-C(1A)-O(11A)	123.0(3)	O(12A)-C(1A)-C(2A)	123.2(3)
O(11A)-C(1A)-C(2A)	113.7(3)	C(1A)-C(2A)-C(3A)	110.2(3)
O(3A)-C(3A)-C(4A)	113.4(3)	O(3A)-C(3A)-C(2A)	113.1(3)
C(4A)-C(3A)-C(2A)	108.3(3)	O(42A)-C(4A)-O(41A)	124.7(3)
O(42A)-C(4A)-C(3A)	123.0(3)	O(41A)-C(4A)-C(3A)	112.3(3)
O(12B)-C(1B)-O(11B)	125.2(4)	O(12B)-C(1B)-C(2B)	123.2(3)
O(11B)-C(1B)-C(2B)	111.6(3)	O(2B)-C(2B)-C(1B)	111.0(3)
O(2B)-C(2B)-C(3B)	111.4(3)	C(1B)-C(2B)-C(3B)	109.4(3)
O(3B)-C(3B)-C(4B)	107.5(2)	O(3B)-C(3B)-C(2B)	113.0(2)
C(4B)-C(3B)-C(2B)	107.5(3)	O(42B)-C(4B)-O(41B)	125.0(4)
O(42B)-C(4B)-C(3B)	123.1(3)	O(41B)-C(4B)-C(3B)	111.9(3)

Table 3 Geometric parameters for the hydrogen bonds in 1[a]

D-H ... A	*r*(H ... A)/Å	*r*(D ... A)/Å	*(DH ... A)*/°
O(11A)-H ... O(42B)'	1.702(3)	2.676(3)	171.3(1)
O(3A)-H ... O(42B)"	2.027(3)	2.999(3)	170.2(1)
O(41A)-H ... O(12B)"'	1.836(4)	2.684(4)	173.8(1)
O(11B)-H ... O(42A)""	1.764(4)	2.641(4)	166.6(1)
O(2B)-H ... O(12A)""'	2.038(3)	2.856(3)	173.2(1)
O(3B)-H ... O(2B)""'	1.923(3)	2.815(3)	164.8(1)
O(41B)-H ... O(12A)"""	1.670(3)	2.644(3)	176.1(1)

[a]Symmetry elements: (') $x-1, y, z+1$; (") $x, y-1; z+1$; ("') $x+1, y-1, z$ (""") $x-1, y+1, z$; (""') $x, y+1, z-1$; (""") $x-1, y, z$; (""") $x+1, y, z-1$.

LIM00012668
NOVARTIS EXHIBIT 1017
Novartis v. Regents, IPR2023-01346
Page 1414 of 4460



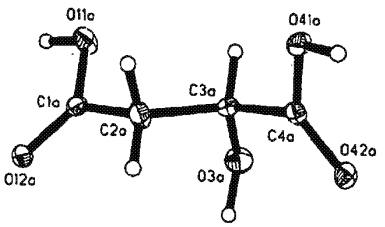


Figure 1 Geometry, labelling scheme and thermal ellipsoids (50%) for the cocrystal *L*-malic acid *L*-tartaric acid (1/1) **1**.

semblies. Also, if the reaction is carried out in solution, the solubilities of the starting materials must be very similar. A possible key to the successful preparation of *L*-malic acid *L*-tartaric acid, is the collection of short, and nearly linear, head-to-head dimeric interactions (O-H···O hydrogen bonds) that dominate the crystal structure of **1**. Furthermore, the number of unique intermolecular hydrogen bonds is seven in **1**, six in malic acid and four in tartaric acid. An illustration of the thermodynamic balance between the acids and the cocrystal, is provided by a series of lattice energy calculations. Using charge equilibrium charges[12] and the Universal force-field,[13] as implemented in the Crystal Packer module within Cerius[2], the lattice energies for malic acid, tartaric acid and **1**, are *ca.* 80, 125 and 160 kJ mol^{-1}, respectively. The value for malic acid is based upon estimated hydrogen-atom positions, and may therefore be somewhat unreliable, but there are nevertheless some significant differences between the three compounds, favouring the formation of **1**.

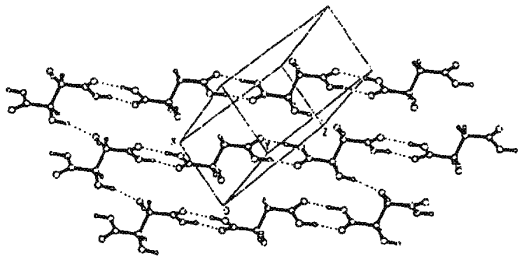


Figure 2 Face-on view of the hydrogen bonded layer in **1**, incorporating the dimeric, head-to-head, interactions between neighbouring malic acid and tartaric acid molecules, and the O···O crosslink between adjacent chains. (See color plate I.)

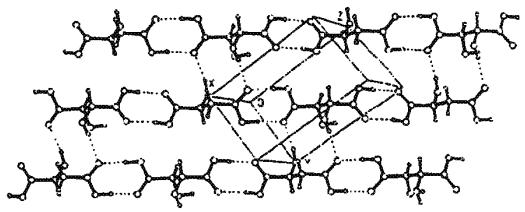


Figure 3 Edge-on view of the dominating structural planes in **1**, showing the two hydrogen-bonded interactions between adjacent layers. (See color plate II.)

Several important lines of work can be identified as a result of the synthesis and structure determination of **1**. First of all, the physical properties of the cocrystal *e.g.* optical and electrical, must be examined. Secondly, it may also be possible to incorporate both hydrogenmalate and hydrogentartartrate anions within the same ionic framework, either with divalent, or monovalent cations.[14] This also introduces the exciting possibility of combining several different stereochemical 'versions' of the two anions in order to induce subtle changes to the anionic scaffolding, a feature which is critical in crystal engineering.

EXPERIMENTAL SECTION

Data collection

$C_8H_{12}O_{11}$, Mw = 284.18, triclinic, $P1$, Z = 1, a = 4.835(1), b = 6.488(1), c = 9.227(1) Å, α = 73.83(1), β = 88.32(1), γ = 77.32°, V = 271.06(8) Å^3, Z = 1, $F(000)$ = 148, D_{calc} = 1.741 Mg m^{-3}, T = 123(2) K, μ(Mo-K$_\alpha$) = 0.169 mm^{-1}.

Data were collected using a Siemens P4 four-circle diffractometer with graphite monochromated Mo-K$_\alpha$ radiation. Crystal stability was monitored every 100 reflections and there were no significant variations (±1%). Cell parameters were obtained from 35 accurately centred reflections in the 2θ-range 10–28°. ω scans were employed for the data collection, and Lorentz and polarization corrections were applied. A total of 1238 reflections were measured for $2.3 < 2\theta < 25.0°$ and $-5 \leq h \leq 1$, $-7 \leq k \leq 7$, $-10 \leq l \leq 10$, and 1181 unique reflections with $|F^2| > 3\sigma(F^2)$ were used in the refinement where $\sigma(F^2) = \{\sigma(I) + (0.04I)^2\}^{1/2}/Lp$. The configuration for the cocrystal was determined by the fact that enantiomerically pure *L*-malic acid and *L*-tartaric acid were used as starting materials.

Structure determination

The structure was solved by direct methods and the non-hydrogen atoms were refined with anistropic ther-

UM00012669
NOVARTIS EXHIBIT 1017
Novartis v. Regents, IPR2023-01346
Page 1415 of 4460

mal parameters by full-matrix least-squares. Hydrogen atom positions were located from difference Fourier maps. A riding model with fixed thermal parameters (U_{ij} = $1.2U_{eq}$) was used for subsequent refinement. The function minimized was $\Sigma[\omega(|F_0|^2 - |F_c|^2)]$ with reflection weights $\omega^{-1} = [\sigma^2|F_0|^2 + (g_1P)^2 + (g_2P)]$ where $P = [\max |F_0|^2 + 2|F_c|^2]/3$. Final parameters for observed data were $R = 0.0303$, $R^2_w = 0.0855$ and $R = 0.0337$, $R^2_w = 0.1344$ for all data. $S = 1.125$, 172 variables, $(\Delta\rho)\max,\min = 0.299, -0.249$ e Å^{-3} on a final difference map. The XSCANS, SHELXTL PC and SHELXL-93 packages were used for data reduction and structure solution and refinement.

ACKNOWLEDGEMENT

We thank the NIDevR for financial assistance.

REFERENCES

1 Pasteur, L. *Ann. Chim. Phys.* **1848**, **24**, 442.
2 Marshall, J.A.; Luke, G.P. *Syn. Lett.* **1992**, **12**, 1007.
3 Fousek, J. *Ferroelectrics* **1991**, **113**, 3.
4 Aakeröy, C.B.; Hitchcock, P.B.; Seddon, K.R. *J. Chem. Soc., Chem. Commun.* **1992**, 553; Zyss, J.; Pecaut, J.; Levy, J.P.; Masse, R. *Acta Crystallogr., Sect. B* **1993**, **49**, 334; Dastidar, P.; Row, T.N.G.; Prasad, B.R.; Subramanian, C.K.; Bhattacharya, S. *J. Chem. Soc., Perkin Trans. 2* **1993**, **12**, 2419; Bhattacharya, S.; Dastidar, P.; Row, T.N.G. *Chem. Mat.* **1994**, **6**, 531; Watanabe, O.; Noritake, T.; Hirose, Y.; Okada, A.; Kurauchi, T. *J. Mater. Chem.* **1993**, **23**, 321.
5 Aakeröy, C.B.; Nieuwenhuyzen, M. *J. Am. Chem. Soc.* **1994**, **116**, 10983.
6 Cambridge Crystallographic Database (Version 5.07), Allen, F.H.; Kennard, O.; Taylor, R. *Acc. Chem. Res.* **1983**, **16**, 46.
7 van der Sluis, P.; Kroon, J. *Acta Crystallogr., Sect. C* **1985**, **41**, 956.
8 Aakeröy, C.B.; Hitchcock, P.B. *J. Mater. Chem.* **1993**, **3**, 1129.
9 Etter, M.C.; MacDonald, J.C.; Bernstein, J. *Acta Crystallogr., Sect. B* **1990**, **46**, 256.
10 Hope, H.; de la Camp, U. *Acta Crystallogr., Sect. A* **1972**, **28**, 201.
11 van der Sluis, P.; Kroon, J. *Acta Crystallogr., Sect. C* **1989**, **45**, 1406.
12 Rappe, A.K.; Goddard, W.A. III. *J. Phys. Chem.* **1991**, **95**, 3358.
13 Rappe, A.K.; Casewit, C.J.; Colwell, K.S.; Goddard, W.A. III.; Skiff, W.M. *J. Am. Chem. Soc.* **1992**, **114**, 10024.
14 Aakeröy, C.B.; Nieuwenhuyzen, M., unpublished results.

UM00012670
NOVARTIS EXHIBIT 1017
Novartis v. Regents, IPR2023-01346
Page 1416 of 4460

This Page is Inserted by IFW Indexing and Scanning Operations and is not part of the Official Record

BEST AVAILABLE IMAGES

Defective images within this document are accurate representations of the original documents submitted by the applicant.

Defects in the images include but are not limited to the items checked:

- ☐ BLACK BORDERS
- ☐ IMAGE CUT OFF AT TOP, BOTTOM OR SIDES
- ☐ FADED TEXT OR DRAWING
- ☐ BLURRED OR ILLEGIBLE TEXT OR DRAWING
- ☐ SKEWED/SLANTED IMAGES
- ☐ COLOR OR BLACK AND WHITE PHOTOGRAPHS
- ☐ GRAY SCALE DOCUMENTS
- ☐ LINES OR MARKS ON ORIGINAL DOCUMENT
- ☐ REFERENCE(S) OR EXHIBIT(S) SUBMITTED ARE POOR QUALITY
- ☐ OTHER: _____

IMAGES ARE BEST AVAILABLE COPY.
As rescanning these documents will not correct the image problems checked, please do not report these problems to the IFW Image Problem Mailbox.

Deliberate combination of coordination polymers and hydrogen bonds in a supramolecular design strategy for inorganic/organic hybrid networks

Christer B. Aakeröy, Alicia M. Beatty, Destin S. Leinen and Keith R. Lorimer

Department of Chemistry, Kansas State University, Manhattan, KS, USA. E-mail: aakeroy@ksu.edu

Received (in Columbia, MO, USA) 1st February 2000, Accepted 20th April 2000

Two crystal structures containing infinite CuI chains connected into 2-D layers by non-covalent interactions demonstrate how coordinate covalent bonds and hydrogen bonds can be combined in the design of new inorganic/organic hybrid materials.

Crystal engineering of inorganic/organic hybrid materials is typically based on a modular approach, where discrete building blocks are linked into larger networks.[1] The construction of these metal-containing networks has, so far, been achieved using two different design philosophies: adjacent transition-metal complexes are linked either through (i) coordinate covalent bonds[2] or (ii) weaker intermolecular forces (*e.g.* hydrogen bonds, aryl–aryl interactions, *etc.*).[3] Both methods have enjoyed considerable success, but there have been few *planned* attempts at using a combination of these approaches to build lamellar or 3-D architectures. Here we present two crystal structures based on copper(I) iodide and an auxiliary hydrogen-bonding ligand that demonstrate how the two philosophies can be forged into a supramolecular tool that has not yet been employed in a systematic manner.

One of the main challenges in crystal engineering is to control the assembly and solid state structures in three dimensions. This task is complicated by the fact that ionic/molecular building blocks are capable of adopting a vast number of orientations in the crystal, thus making predictions of the resulting structure very difficult. Coordination polymers, however, are typically very robust and the topology of such networks can often be predicted with the aid of well known principles of coordination chemistry.[4] Thus, by using an infinite coordination polymer with known topology instead of a discrete complex as a synthetic module, the resulting assembly process will have fewer degrees of freedom, which facilitates intermolecular synthesis. Why then use anything but coordination polymers in the design of hybrid materials? Weaker intermolecular forces can impart properties to solids that sometimes offer advantages over 'pure' coordination polymers. Materials held together by hydrogen bonds tend to be more readily soluble, which is desirable for reasons ranging from ease of synthetic modification and manipulation to crystal growth and structural characterization.[5] In addition, unlike the more rigid frameworks of coordination polymers, a network generated through hydrogen bonds[6] can 'flex' to accommodate changes in its environment, and may therefore lend itself to host–guest applications that are less accessible in a rigid framework.[7]

Copper(I) complexes with monodentate ligands, $(CuXL)_\infty$ (where L is a pyridine derivative and X is a halide), are known to form robust halogen-bridged 1-D step, stair or chain structures,[8] and several 2-D coordination polymers based on 'pre-formed' 1-D copper(I) iodide chains and cross-linking bidentate ligands have recently been reported.[9–11]

In order to change network strength and flexibility without making significant changes to the *topology* of the structure, we have replaced the bidentate bridging ligand (*e.g.* pyrazine or 4,4′-bipyridine) with a supramolecular linker capable of simultaneous metal coordination and self-complementary hydrogen bonding. To this end, we report the syntheses† and crystal structures‡ of $[CuI(3\text{-pyridinealdoxime})]_\infty$ **1** and $[CuI(\text{isonicotinamide})]_\infty$ **2**.

The crystal structure of **1** contains 3-pyridinealdoxime ligands coordinated to a polymeric 'staircase' of CuI. Each tetrahedral Cu(I) ion is coordinated to three μ_3-I ligands to generate an infinite 1-D motif. The 3-pyridinealdoxime ligand is attached to each Cu(I) ion through the pyridine nitrogen atom [Cu(1)–N(1) 2.059(3) Å], to complete the coordination sphere. The oxime ligands are staggered ($N_{py}\cdots N_{py}$ internuclear distance *ca.* 4.1 Å) along the polymeric CuI chain and protrude outward. Adjacent oxime moieties are connected *via* O–H···N hydrogen bonds [O(7)···N(7), 2.841(3) Å], in a catemer-like fashion, to propagate the 1-D polymeric chains into an infinite 2-D sheet (Fig. 1). The sheets are non-interpenetrating resulting in a lamellar structure. There are no short contacts or noteworthy aryl–aryl interactions between adjacent chains, or between neighboring sheets.

The crystal structure of **2** is very similar to **1** and also contains infinite polymeric Cu(I) chains. The isonicotinamide ligand occupies the fourth coordination site of the Cu(I) center by coordination through the pyridine nitrogen atom [Cu(1)–N(1) 2.02(2) Å].

Adjacent isonicotinamide molecules form two self-complementary N–H···O hydrogen bonds [N(8)···O(9) 2.87(3) Å] to yield a head-to-head amide–amide dimer. Through this intermolecular interaction, the carboxamide functionalities act as linear, bridging linkers between CuI 'staircases' to generate two-dimensional infinite sheets almost identical to those displayed by **1**, Fig. 2.

The structures of **1** and **2** are very similar to copper(I) iodide architectures where copper–halide staircases are interconnected through covalent bonds by bridging bidentate ligands.[10] In general, these staircases are normally aligned parallel to each other along the short axis of the unit cell. The length of this axis (which also corresponds to the Cu···Cu separation within a staircase) is *ca.* 4.1–4.4 Å for CuI,[9,10] 3.95–3.98 Å for CuBr, and 3.75–3.78 Å for CuCl containing motifs. The precise orientation and separation of neighbouring ribbons is determined by the specific geometry of the ligand(s). Variations in

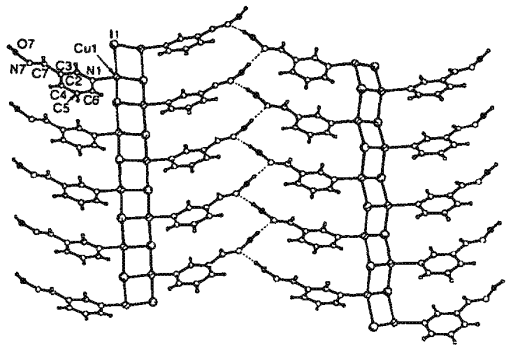


Fig. 1 Infinite 2-D sheets of $[CuI(3\text{-pyridinealdoxime})]_\infty$ **1**. Adjacent oxime moieties bridge polymeric 'staircases' of CuI *via* catemeric hydrogen bonds.

DOI: 10.1039/b001001o

This journal is © The Royal Society of Chemistry 2000

UM00012672
NOVARTIS EXHIBIT 1017
Novartis v. Regents, IPR2023-01346
Page 1418 of 4460

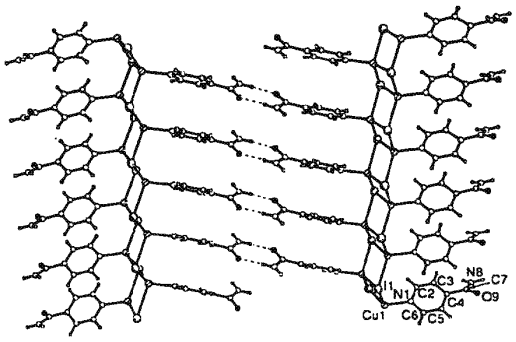


Fig. 2 Infinite 2-D sheets of [CuI(isonicotinamide)]$_\infty$ **2**. Head-to-head amide–amide interactions between isonicotinamide ligands cross-link CuI 'staircases'.

the size and substituent position(s) of the ligand also lead to modifications of the resulting layer (*e.g.* planar *vs.* undulating).

Although the chemical properties of the hydrogen-bonding moieties on the two pyridine-based ligands in **1** and **2** are different, their structural influence is very similar: network topologies and unit cell dimensions are nearly identical.[12] This, of course, is a benefit of using 1-D polymeric chains as building blocks; they are structurally reliable and therefore reduce the task of prediction and control to a much simpler problem. By extending this combined coordination polymer/hydrogen-bond design strategy, one can envisage using a 'pre-formed' 2-D coordination polymer in combination with suitable organic hydrogen-bonding linkers to obtain custom-built porous solids for host–guest applications, *e.g.* separation and catalysis. Further development and applications of this design principle are currently underway in our laboratories.

We acknowledge financial support from Kansas State University and DuPont.

Notes and references

† All starting materials were purchased from Aldrich and used as received. Melting points were determined on a Fisher–Johns melting point apparatus and are uncorrected. In both cases, yields were *ca.* 70–75%.

[CuI(3-pyridinealdoxime)]$_\infty$, **1**: 3-pyridinealdoxime (0.10 g, 0.82 mmol) in the minimum amount of diethyl ether was layered on top of CuI (0.16 g, 0.84 mmol) in acetonitrile. The layered solution was covered and allowed to stand in ambient air. After 1–2 days, yellow rods of **1** were obtained. Mp > 210 °C (decomp.).

[CuI(isonicotinamide)]$_\infty$, **2**: acetonitrile was carefully layered over a solution of isonicotinamide in THF. A saturated solution of CuI in acetonitrile was then added dropwise to the acetonitrile layer. The layered solution was allowed to stand in ambient air. Slow diffusion produced yellow rods of **2** in 1–2 days. Mp > 270 °C (decomp.).

‡ *X-Ray crystallography*: crystalline samples of **1** and **2** were placed in inert oil, mounted on a glass pin, and transferred to the cold gas stream of the diffractometer. Crystal data were collected and integrated using a Bruker SMART 1000 system with graphite monochromated Mo-Kα (λ = 0.71073 Å) radiation at 173 K. The structures were solved using heavy-atom methods using SHELXS-97 and refined using SHELXL-97 (G. M. Sheldrick, University of Göttingen). Non-hydrogen atoms were found by successive full matrix least squares refinement on F^2 and refined with anisotropic thermal parameters. Hydrogen atoms for **1** were located on the difference map, and those for **2** were placed at calculated positions. All hydrogen atoms were then refined using a riding model with fixed thermal parameters [U_{ij} = 1.2 U_{ij}(eq) for the atom to which they are bonded] for subsequent refinements.

Crystal data: for **1**: $C_6H_6N_2OCuI$, M = 312.57, monoclinic, space group $P2_1/c$, a = 13.544(1), b = 4.1098(4), c = 15.094(1) Å, β = 105.583(2)°, U = 809.3(1) Å^3, Z = 4, D_c = 2.565 g cm^{-3}, T = 173(2) K, μ(Mo-Kα) = 6.452 mm^{-1}, wR_2 = 0.0665 (1859 reflections collected, 1752 unique), R = 0.0253 [$I > 2\sigma(I)$].

For **2**: $C_6H_6N_2OCuI$, M = 312.57, monoclinic, space group $P2_1/c$, a = 13.459(2), b = 4.0960(6), c = 16.649(3) Å, β = 109.617(3)°, U = 864.6(2) Å^3, Z = 4, D_c = 2.401 g cm^{-3}, T = 173(2) K, μ(Mo-Kα) = 6.040 mm^{-1}, wR_2 = 0.3177 (1997 reflections collected, 1768 unique), R = 0.0868 [$I > 2\sigma(I)$].

CCDC 182/1617. See http://www.rsc.org/suppdata/cc/b0/b001001o/ for crystallographic files in .cif format.

1 B. F. Abrahams, S. R. Batten, H. Hamit, B. F. Hoskins and R. Robson, *Angew. Chem., Int. Ed. Engl.*, 1996, **35**, 1690; *Crystal engineering: From molecules and crystals to materials*, A NATO Advanced Study Institute and a Euroconference, ed. D. Braga, F. Grepioni and A. G. Orpen, Erice, Italy, 1999, p. 58.

2 Z. Wang, R.-G. Xioing, B. M. Foxman, S. R. Wilson and W. Lin, *Inorg. Chem.*, 1999, **38**, 1523; G. K. H. Shimizu, G. D. Enright, C. I. Ratcliffe, J. A. Ripmeester and D. D. M. Wayner, *Angew. Chem., Int. Ed.*, 1998, **37**, 1407; K. Biradha, C. Seward and M. J. Zaworotko, *Angew. Chem., Int. Ed.*, 1999, **38**, 492; K. A. Hirsch, S. R. Wilson and J. S. Moore, *Chem. Commun.*, 1998, 13; S. W. Keller, *Angew. Chem., Int. Ed. Engl.*, 1997, **36**, 247.

3 C. B. Aakeröy, A. M. Beatty and D. S. Leinen, *Angew. Chem., Int. Ed.*, 1999, **38**, 1815; C. B. Aakeröy, A. M. Beatty and D. S. Leinen, *J. Am. Chem. Soc.*, 1998, **120**, 7383; C. B. Aakeröy and A. M. Beatty, *Chem. Commun.*, 1998, 1067; A. S. Batasanov, P. Hubberstey, C. E. Russel and P. H. Walton, *J. Chem. Soc., Dalton Trans.*, 1997, 2667; C.-W. Chan, D. M. P. Mingos and D. J. Williams, *J. Chem. Soc., Dalton Trans.*, 1995, 2469; M. Munkata, L. P. Wu, M. Yamamoto, T. Kuroda-Sowa and M. Maekawa, *J. Am. Chem. Soc.*, 1996, **118**, 3117; J. C. M. Rivas and L. Brammer, *New J. Chem.*, 1998, **22**, 1315; M. Scudder and I. Dance, *J. Chem. Soc., Dalton Trans.*, 1998, 3167.

4 O. M. Yaghi and H. Li, *J. Am. Chem. Soc.*, 1996, **118**, 295; M. Fujita, Y.-J. Kwon, S. Osamu, K. Yamaguchi and K. Ogura, *J. Am. Chem. Soc.*, 1995, **117**, 7287; C. Janiak, *Angew. Chem., Int. Ed. Engl.*, 1997, **36**, 1431.

5 M. M. Chowdhry, D. M. P. Mingos, A. J. P. White and D. J. Williams, *Chem. Commun.*, 1996, 899; Z.-N. Chen, H.-X. Zhang, K. B. Yu, K. C. Zheng, H. Cai and B.-S. Kang, *J. Chem. Soc., Dalton Trans.*, 1998, 1133; L. Carlucci, G. Ciani, D. M. Proserpio and A. Sironi, *J. Chem. Soc., Dalton Trans.*, 1997, 1801; C. B. Aakeröy and A. M. Beatty, *Cryst. Eng.*, 1998, **1**, 39.

6 V. A. Russell and M. D. Ward, *Chem. Mater.*, 1996, **8**, 1654; C. B. Aakeröy, *Acta Crystallogr., Sect. B*, 1997, **53**, 569; S. Subramanian and M. Zaworotko, *Coord. Chem. Rev.*, 1994, **137**, 357.

7 P. Brunet, M. Simard and J. D. Wuest, *J. Am. Chem. Soc.*, 1997, **119**, 2737.

8 Cu(I)X complexes are also capable of forming cube-like clusters and other discrete species, see: F. A. Cotton and G. Wilkinson, *Advanced Inorganic Chemistry*, Wiley, New York, 5th edn., 1998.

9 S. Kawata, S. Kitagawa, H. Kumagai, S. Iwabuchi and M. Katada, *Inorg. Chim. Acta*, 1998, **267**, 143.

10 A. J. Blake, N. R. Brooks, N. R. Champness, P. A. Cooke, M. Crew, A. M. Deveson, L. R. Hanton, P. Hubberstey, D. Fenske and M. Schröder, *Cryst. Eng.*, 1999, **2**(2/3), 181.

11 B. Rossenbeck and W. S. Sheldrick, *Z. Naturforsch., Teil B*, 1999, **54**, 1510.

12 The same type of lamellar structure with Cu(I)X ribbons connected into sheets is also present in [Cu(I)Cl(isonicotinic acid)]$_\infty$; M. A. S. Goher and T. C. W. Mak, *Inorg. Chim. Acta*, 1985, **101**, L27.

UM00012673
NOVARTIS EXHIBIT 1017
Novartis v. Regents, IPR2023-01346
Page 1419 of 4460

Journal of Chemical Crystallography, Vol. 28, No. 2, 1998

Di-hydroxy malonic acid as a building block of hydrogen-bonded 3-dimensional architectures

Christer B. Aakeröy,[1]* Mark Nieuwenhuyzen,[2] and Paul Robinson[2]

Received July 7, 1997

An examination of the crystal structures of di-hydroxy malonic acid **1** ($P2_1/na$ = 5.384(2), b = 6.268(2), c = 14.354(8) Å, β = 103.57(3)°) and *N*-ethylbenzylammonium di-hydroxy hydrogenmalonate **2** ($P2_12_12_1$ a = 13.373(2), b = 15.342(4), c = 18.741(4) Å,) has highlighted the influence of directional O-H···O interactions in the assembly of hydroxy-substituted dicarboxylic acids. The complementarity of carboxylic and hydroxy groups in **1** creates a very dense 3-D structure (D_c = 1.919 g cm^{-3}) through four O−H···O hydrogen bonds. In **2**, the anions form infinite, spiraling chains created by head-to-tail O−H···O hydrogen bonds. Neighbouring chains are crosslinked into a complex 3-D anionic network with channels parallel to a and b. The cations are positioned within these channels and held in place *via* two N−H···O interactions.

KEY WORDS: Di-hydroxymalonic acid; hydrogen bonding; crystal engineering; supramolecular chemistry.

Introduction

Interest in the controlled assembly of molecules and ions into specific and desirable architectures is gathering considerable momentum, and most strategies for supramolecular synthesis and crystal engineering have relied upon the strength and directionality of the hydrogen bond.[1-5] Crystal engineering has primarily been employed in the design of molecular solids,[6] but considerable efforts are now being made in the programed assembly of ionic organic[7,8] and organometallic compounds.[9]

We have for some time been interested in the selectivity and strength of O−H···O hydrogen-bond interactions involving substituted dicarboxylic acids and anions thereof, and the way in which such species can be used as building blocks for extended, robust architectures for functional materials.[10] We now report the crystal structure of di-hydroxy malonic acid **1**, and also the first example of a crystal structure containing the di-hydroxy hydrogenmalonate anion; *N*-ethylbenzylammonium di-hydroxy hydrogen malonate **2**.

[1] Department of Chemistry, Kansas State University, Manhattan, Kansas, 66506.
[2] School of Chemistry, The Queen's University of Belfast, Belfast, BT9 5AG, Northern Ireland.
* To whom correspondence should be addressed.

Experimental

Preparation of di-hydroxy malonic acid

A commercial sample (Aldrich) of di-hydroxymalonic acid monohydrate was recrystallized from water at ambient temperature. Translucent, colourless, irregular crystals appeared after approximately three months. Calc. (found) for $C_3H_4O_6$: C, 26.47 (26.3); H, 2.94 (2.9)%, mp. 116–118°C.

Preparation Of N-ethylbenzylammonium di-hydroxy hydrogen malonate

A solution of di-hydroxymalonic acid monohydrate (0.40 g; 2.94 mmol) in water (2 cm^3) was added

1074-1542/98/0200-0111$15.00/0 © 1998 Plenum Publishing Corporation

UM00012674
NOVARTIS EXHIBIT 1017
Novartis v. Regents, IPR2023-01346
Page 1420 of 4460

Table 1. Data collection and refinement for 1 and 2

Crystal data	1	2
Empirical formula	$C_3H_4O_6$	$C_{36}H_{51}N_3O_{18}$
MW	136.06	813.80
Crystal size (mm)	0.66×0.18×0.16	0.64×0.34×0.18
Crystal system	Monoclinic	Orthorhombic
Space group	$P2_1/n$	$P2_12_12_1$
a(Å)	5.384(2)	13.373(4)
b(Å)	6.268(2)	15.342(4)
c(Å)	14.354(8)	18.741(4)
α(deg)	90	90
β(deg)	103.57(3)	90
γ(deg)	90	90
Volume (Å^3)	470.9(3)	3845(2)
Z	4	4
D_{calc} (g cm^{-3})	1.919	1.406
F(000)	280	1728
μ(Mo-K_α) (mm^{-1})	0.197	0.113
Temp (K)	293(2)	293(2)
ω scans; τ range (deg)	2.92–25.00	2.82–25.00
Range h	−6 to 10	0 to 15
Range k	0 to 7	−1 to 18
Range l	−16 to 17	−1 to 22
Reflns collected	930	4331
Unique reflns	833	4234
Data:parameter ratio	10.03	8.24
Refinement	Full-matrix least squares	Full-matrix least-squares
R/R_w^2 (obs data)	0.0453/0.1043	0.0466/0.1130
R/R_w^2 (all data)	0.0544/0.1361	0.0800/0.1390
$\Delta\rho_{max/min}$ (e Å^{-3})	0.451/−0.267	0.219/−0.241
S	1.214	0.890

to *N*-ethylbenzylamine (0.40 g; 2.94 mmol) in ethanol (5 cm^3). The solution was covered and left at 5°C overnight. Large colourless crystal were collected by filtration, washed with acetone and left to dry in air. Calc.(found) for $C_{36}H_{51}N_3O_{18}$: C, 52.94(53.3); H, 6.25(6.3); N, 5.15(5.2)%, m.p. 68–70°C.

Crystallography

Crystal data were collected using a Siemens P4 four-circle diffractometer with graphite monochromated Mo-K_α radiation at *ca.* 293 K. Crystal stability was monitored by measuring standard reflections every 100 reflections, and there were no significant variations (< ± 1%). Cell parameters were obtained from 35 accurately centred reflections in the 2-θ range 10°–25°. ω scans were employed for data collection and Lorentz and polarization corrections were applied.

The structures were solved by direct methods and the nonhydrogen atoms were refined with anisotropic thermal parameters. Hydrogen-atom positions were located from difference Fourier maps and a riding model with fixed thermal parameters (U_{iso} = 1.2U_{eq} for the atom to which they are bonded), was used for subsequent refinements. The function minimized was $\Sigma[(\sigma^2|F_o|-|F_c|^2)]$ with reflection weights $\omega^{-1} = [\sigma^2|F_o|^2 + (g_1P)^2 + (g_2P)]$ where $P = [\max|F_o|^2 + |F_c|^2]/3$. The SHELXTL PC and SHELXL-93 packages were used for data reduction and structure solution and refinement.[11] Data for the structure determinations of **1** and **2** are listed in Table 1, and final fractional atomic coordinates and displacement coefficients are given in Tables 2 and 3.

Results and discussion

The molecular geometry and labeling scheme of di-hydroxymalonic acid is shown in Fig. 1. The crystal structure of **1** is, as expected, dominated by O−H···O hydrogen-bond interactions (Table 4). Typically, dicarboxylic acids are prone to form infinite chains *via* two head-to-head dimeric motifs involving pairwise O−H···O hydrogen bonds. In **1**, however, one carboxylic acid moiety is hydrogen bonded to the two hydroxy groups,

Table 2. Atomic coordinates [×10^4] and equivalent isotropic displacement parameters (Å^2 × 10^3] for 1

	x	y	z	U(eq)
O(11)	5257(3)	−667(3)	6034(1)	14(1)
O(12)	6333(3)	1354(3)	7372(1)	14(1)
C(1)	4775(5)	547(4)	6714(2)	11(1)
C(2)	1886(5)	891(4)	6591(2)	12(1)
O(21)	1502(3)	1443(3)	7494(1)	12(1)
O(22)	421(3)	−874(3)	6202(1)	12(1)
C(3)	1062(5)	2758(5)	5873(2)	12(1)
O(31)	−1358(4)	3152(3)	5745(1)	18(1)
O(32)	2599(4)	3671(3)	5513(1)	17(1)
H(11)	6967(3)	−807(3)	6215(1)	17
H(21)	−367(3)	1360(3)	7400(1)	14
H(22)	1022(3)	−1997(3)	6599(1)	14
H(31)	−2016(4)	3974(3)	5380(1)	22

UM00012675
NOVARTIS EXHIBIT 1017
Novartis v. Regents, IPR2023-01346
Page 1421 of 4460

Table 3. Atomic coordinates [x 10^4] and equivalent isotropic displacement parameters ($Å^2$ x 10^3] for 2

	x	y	z	U(eq)
C(1C)	3333(3)	3885(3)	4192(2)	16(1)
C(1B)	−4399(3)	7226(3)	3573(2)	18(1)
C(1A)	−740(3)	5716(3)	4840(2)	16(1)
C(2C)	4146(3)	3193(3)	4217(2)	18(1)
C(2B)	−4550(3)	6620(3)	4201(2)	19(1)
C(2A)	−1(3)	5154(3)	5261(2)	17(1)
C(3C)	4068(3)	2568(3)	3583(2)	18(1)
C(3B)	−3734(3)	5933(3)	4246(2)	18(1)
C(3A)	517(3)	4425(3)	4839(2)	19(1)
C(4C)	11132(3)	3985(3)	7149(3)	33(1)
C(4B)	2306(4)	2406(3)	6074(2)	35(1)
C(4A)	−3065(4)	8411(3)	6334(2)	41(1)
C(5C)	10705(3)	4833(3)	7406(2)	27(1)
C(5B)	2319(3)	1696(3)	5519(2)	28(1)
C(5A)	−2653(3)	8024(3)	5664(2)	27(1)
N(6C)	9585(2)	4831(2)	7331(2)	21(1)
N(6A)	−2441(3)	8714(2)	5127(2)	20(1)
N(6B)	1809(3)	2007(2)	4857(2)	24(1)
C(7C)	9129(3)	5684(3)	7534(2)	28(1)
C(7B)	1725(3)	1326(3)	4294(2)	28(1)
C(7A)	−2015(3)	8353(3)	4460(2)	26(1)
C(8C)	8041(3)	5717(3)	7334(2)	23(1)
C(8B)	1342(3)	1674(3)	3601(2)	23(1)
C(8A)	−1810(3)	9021(3)	3903(2)	22(1)
C(9C)	7770(4)	5967(3)	6651(2)	28(1)
C(9B)	484(3)	2174(3)	3571(3)	33(1)
C(9A)	−2073(4)	8867(4)	3204(2)	35(1)
C(10C)	6779(4)	5995(3)	6465(3)	35(1)
C(10B)	116(4)	2451(3)	2926(3)	39(1)
C(10A)	−1815(4)	9452(5)	2677(3)	53(2)
O(11C)	3578(2)	4654(2)	4182(2)	22(1)
O(11B)	−4111(2)	6863(2)	3002(1)	21(1)
O(11A)	−672(2)	6501(2)	4852(2)	31(1)
C(11C)	6061(4)	5797(3)	6958(3)	37(1)
C(11B)	577(4)	2209(3)	2297(3)	36(1)
C(11A)	−1315(4)	10206(5)	2852(3)	57(2)
O(12C)	2453(2)	3587(2)	4187(2)	20(1)
O(12B)	−4581(2)	8009(2)	3637(2)	26(1)
O(12A)	−1423(2)	5271(2)	4527(2)	22(1)
C(12C)	6317(4)	5545(3)	7632(3)	32(1)
C(12B)	1435(4)	1714(3)	2331(3)	36(1)
C(12A)	−1091(4)	10373(3)	3550(3)	48(2)
C(13C)	7314(4)	5504(3)	7818(2)	28(1)
C(13B)	1813(4)	1462(3)	2979(3)	32(1)
C(13A)	−1319(4)	9786(3)	4068(3)	37(1)
O(21C)	5101(2)	3546(2)	4195(2)	24(1)
O(21B)	−5489(2)	6228(2)	4079(2)	25(1)
O(21A)	777(2)	5647(2)	5539(1)	21(1)
O(22C)	4005(2)	2740(2)	4848(1)	24(1)
O(22B)	−4543(2)	7054(2)	4851(1)	23(1)
O(22A)	−564(2)	4778(2)	5809(1)	23(1)
O(31C)	4013(2)	2946(2)	2974(1)	22(1)
O(31B)	−2858(2)	6216(2)	4297(2)	24(1)
O(31A)	1168(2)	4705(2)	4393(2)	22(1)
O(32C)	4067(2)	1781(2)	3677(2)	26(1)

Table 3. Continued

	x	y	z	U(eq)
O(32B)	−23988(2)	5153(2)	4217(2)	28(1)
O(32A)	311(2)	3671(2)	4957(2)	23(1)
H(4C1)	11848(4)	4002(7)	7184(14)	50
H(4C2)	10943(18)	3893(9)	6660(5)	50
H(4C3)	10879(17)	3517(4)	7437(10)	50
H(41B)	2664(19)	2214(8)	6489(7)	53
H(42B)	1627(4)	2537(14)	6201(12)	53
H(43B)	2620(20)	2919(7)	5885(6)	53
H(41A)	−23190(23)	7956(4)	6674(7)	62
H(42A)	−23679(13)	8710(18)	6229(4)	62
H(43A)	−22591(11)	8817(16)	6529(10)	62
H(51C)	10985(3)	5309(3)	7131(2)	32
H(52C)	10884(3)	4921(3)	7903(2)	32
H(51B)	3004(3)	1537(3)	5410(2)	33
H(52B)	1979(3)	1184(3)	5701(2)	33
H(51A)	−22041(3)	7711(3)	5772(2)	32
H(52A)	−23130(3)	7612(3)	5469(2)	32
H(61C)	9366(2)	4386(2)	7618(2)	25
H(62C)	9563(2)	4786(2)	6858(2)	25
H(61A)	−22010(3)	9172(2)	5388(2)	25
H(62A)	−23057(3)	8990(2)	5033(2)	25
H(61B)	1177(3)	2186(2)	5026(2)	28
H(62B)	2228(3)	2410(2)	4719(2)	28
H(71C)	9483(3)	6152(3)	7294(2)	34
H(72C)	9198(3)	5771(3)	8044(2)	34
H(71B)	1279(3)	870(3)	4459(2)	33
H(72B)	2378(3)	1067(3)	4216(2)	33
H(71A)	−22477(3)	7926(3)	4268(2)	31
H(72A)	−21396(3)	8053(3)	4573(2)	31
H(9C)	8259(4)	6116(3)	6320(2)	33
H(9B)	154(3)	2323(3)	3990(3)	40
H(9A)	−22428(4)	8366(4)	3087(2)	42
H(10C)	6596(4)	6149(3)	6003(3)	42
H(10B)	−2448(4)	2805(3)	2913(3)	47
H(10A)	−21979(4)	9337(5)	2204(3)	64
H(110)	−23993(2)	7414(2)	2538(1)	25
H(11C)	5389(4)	5835(3)	6832(3)	45
H(11B)	314(4)	2378(3)	1859(3)	43
H(11A)	−21132(4)	10599(5)	2498(3)	68
H(120)	−22044(2)	5616(2)	4346(2)	26
H(12C)	5825(4)	5402(3)	7962(3)	38
H(12B)	1759(4)	1550(3)	1913(3)	43
H(12A)	−2778(4)	10893(3)	3672(3)	58
H(13C)	7494(4)	5330(3)	8276(2)	34
H(13B)	2402(4)	1141(3)	2994(3)	38
H(13A)	−21143(4)	9901(3)	4539(3)	44
H(21C)	5016(2)	4216(2)	4170(2)	28
H(21B))	−25401(2)	5623(2)	4158(2)	30
H(21A)	432(2)	6178(2)	5749(1)	25
H(22C)	4172(2)	2228(2)	4835(1)	29
H(22B)	−24849(2)	7614(2)	4776(1)	28
H(22A)	−2490(2)	4187(2)	5819(1)	27
H(31A)	1828(2)	4221(2)	4244(2)	27

UM00012676
NOVARTIS EXHIBIT 1017
Novartis v. Regents, IPR2023-01346
Page 1422 of 4460

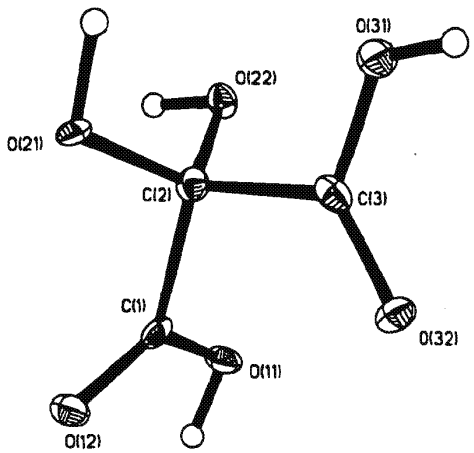


Fig. 1. Molecular geometry, thermal ellipsoids (50%) and labeling scheme for 1.

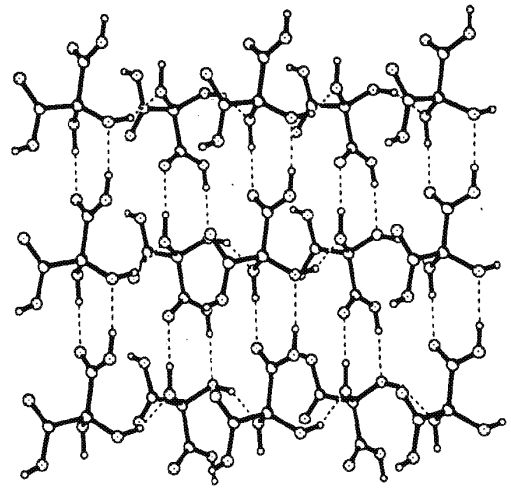


Fig. 2. O-H···O hydrogen bonds generate an infinite sheet in 1.

O(11)−H(11)···O(22) and O(12)···H(21)−O(21), resulting in an infinite chain, parallel with *a* (Fig. 2). Neighbouring chains are linked through two symmetry related O−H···O interactions within the only head-to-head motif creating a 2-D sheet. Adjacent sheets are finally brought together *via* an O−H···O hydrogen bond, which results in a very compact 3-D structure (Fig. 3). The calculated density for this material is 1.919 g cm^{-3}, which is unusually high for an organic molecular solid.

The structure determination of **2** showed that the product had crystallized with three "ion-pairs" in the asymmetric unit, which upon closer examination turned out to be three cations, one dianion, one monoanion, and a neutral molecule of di-hydroxy malonic acid. Molecular geometries, thermal ellipsoids (50%) and labeling schemes are shown in Figs. 4a,b. All the hydrogen atoms were located, and this information, in combination with an examination of the relevant C−O bond lengths of the carboxylic functionalities confirm that this crystal structure does contain a neutral molecule *r*(C−O; 1.208(6), 1.280(5), 1.211(6), 1.281(6) Å), a monoanion *r*(C−O; 1.220(6), 1.262(5), 1.207(6), 1.281(6) Å), and a dianion *r*(C−O; 1.226(6), 1.267(6), 1.236(6), 1.255(6) Å). Consequently, this compound is more appropriately named *tris-n*-ethylbenzylammonium di-hydroxymalonate di-hydroxyhydrogen malonate dihydroxy malonic acid. There are existing precedents for this type of behavior, most recently in a structure of trimesic acid, where all three types of deprotonated anions where present simultaneously.[12]

Table 4. Hydrogen bond geometries for 1[a]

D−H···*A*	*r*(H···*A*)/Å	*r*(*D*···*A*)/Å	···(*D*−H···*A*)°
O(31)−H(31)···O(32)^{i}	1.931(3)	2.665(3)	162.12(8)
O(21)−H(21)···O(12)^{ii}	1.768(3)	2.748(3)	173.00(8)
O(22)−H(22)···O(21)^{iii}	1.901(3)	2.760(3)	155.50(8)
O(11)−H(11)···O(22)^{iv}	1.865(3)	2.737(3)	162.58(8)

[a] Symmetry codes: (i) −*x*, 1 − *y*, 1 − *z*; (ii) *x* − 1, *y*, *z*; (iii) 1/2 − *x*, − 1/2 + *y*, 11/2 − *z*; (iv) 1 +*x*, *y*, *z*.

In **2**, the three forms of di-hydroxy malonic acid (labeled A, B, and C), combine to form an extended 3-D motif. These asymmetric units are first of all connected, head-to-tail (···-A-B-C-···), into infinite spiraling chains, parallel with *b* (Fig. 4a). The three O···O hydrogen bonds within this spiral are all very short, 2.445(4), 2.474(5), and 2.458(4) Å, respectively (Table 5). From each chain, there are nine unique hydrogen bonds to neighboring chains which gives rise to a complex 3-D anionic network.. There are infinite channels running through the material, parallel with *a* (Fig. 5), and parallel with *b*, Fig. 6. The three unique cations are positioned within the channels and, as expected, each cation is locked into a channel *via* two N−H···O interactions.

UM00012677
NOVARTIS EXHIBIT 1017
Novartis v. Regents, IPR2023-01346
Page 1423 of 4460

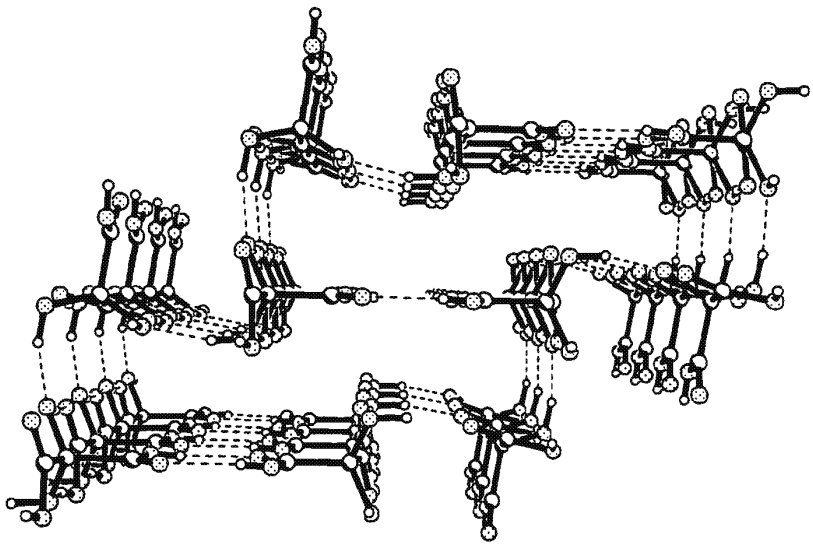


Fig. 3. A compact, 3-D arrangement of molecular building blocks in 1.

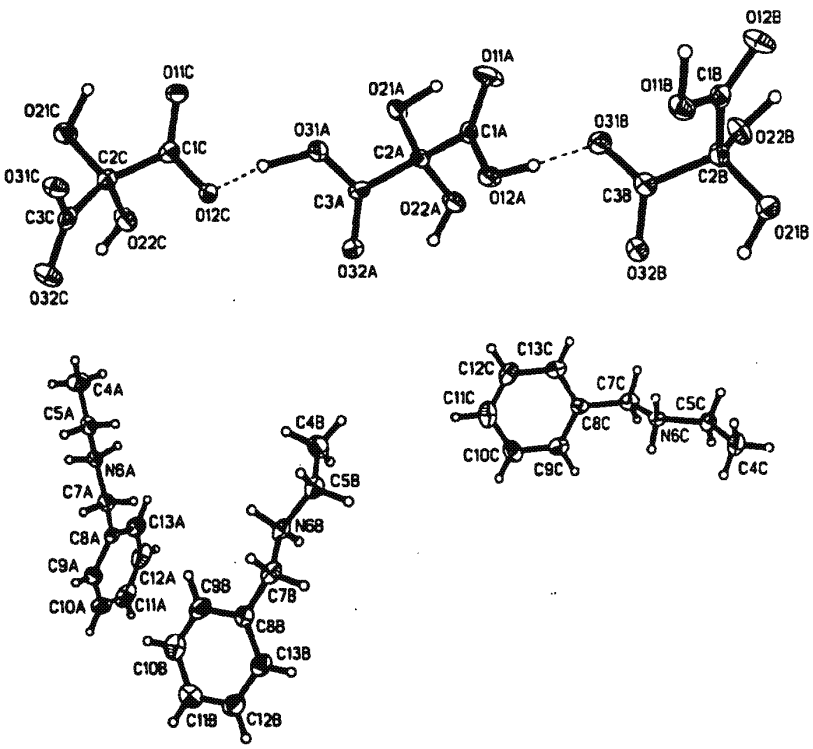


Fig. 4. (a) Molecular geometry, thermal ellipsoids (50%) and labeling scheme for three forms of di-hydroxy malonic acid present in the crystal structure of 2. (b) Molecular geometry, thermal ellipsoids (50%) and labeling scheme for the three unique cations in the crystal structure of 2.

UM00012678
NOVARTIS EXHIBIT 1017
Novartis v. Regents, IPR2023-01346
Page 1424 of 4460

Table 5. Hydrogen bond geometries for 2[a]

$D-H\cdots A$	$r(H\cdots A)$/Å	$r(D\cdots A)$/Å	$\angle(D\text{-}H\cdots A)$°
N(6A)−H(61A)···O(11C)^{iii}	2.124(4)	3.131(4)	164.65(12)
N(6A)−H(61A)···O(21B)^{iv}	2.348(4)	3.005(4)	120.41(11)
N(6A)−H(61B)···O(21A)^{iii}	1.972(4)	2.864(4)	156.83(13)
N(6B)−H(61B)···O(21C)^{ii}	2.337(4)	3.016(4)	128.50(11)
N(6B)−H(62B)···O(12C)	2.086(4)	2.863(4)	147.91(12)
N(6C)−H(61C)···O(11B)^{viii}	2.075(4)	2.956(4)	160.61(12)
N(6C)−H(62C)···O(22A)^{vi}	1.972(4)	2.860(4)	174.93(13)
O(31A)−H(31A)···O(12C)	1.287(4)	2.458(4)	167.33(17)
O(12A)−H(120)···O(31B)	1.429(4)	2.444(4)	162.86(16)
O(22C)−H(22C)···O(32A)^{i}	2.091(4)	2.805(4)	145.84(11)
O(22A)−H(22A)···O(32C)^{ii}	1.857(4)	2.625(4)	140.42(12)
O(22B)−H(22B)···O(11A)^{iii}	1.882(4)	2.739(4)	147.07(13)
O(21A)−H(21A)···O(12B)^{iv}	1.698(4)	2.621(4)	148.99(13)
O(21B)−H(21B)···O(11C)^{v}	2.020(4)	2.725(4)	129.84(11)
O(21C)−H(21C)···O(32B)^{vi}	1.962(4)	2.752(4)	130.69(11)
O(11B)−H(110)···O(31C)^{vii}	1.259(4)	2.474(4)	170.54(18)

[a] Symmetry codes: (i) 1/2 + x, 1/2 − y, 1 − z; (ii) −1/2 + x, 1/2 − y, 1 − z; (iii) −1/2 + x, 1 1/2 − y, 1 − z; (iv) 1/2 + x, 1 1/2 − y, 1 − z; (v) −1 + x, y, z; (vi) 1 + x, y, z; (vii) −x, 1/2 + y, 1/2 − z; (viii) 1/2−x, 1 − y, 1/2 + z.

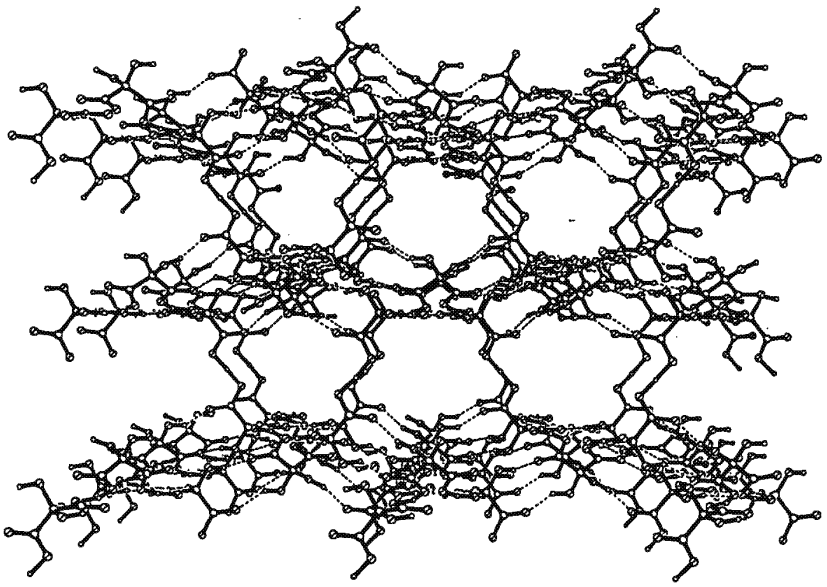


Fig. 5. Infinite channels, parallel with a, in the anionic network of 2.

The complementarity of O···O hydrogen bonds in these hydroxy-substituted carboxylic acids has produced a highly structured, rigid anionic network in 2. We intend to further establish (i) how reliable this anionic network structure is and (ii) if there is any degree of selectivity or preference in terms of cation incorporation into this scaffolding.

Acknowledgment

Financial support from NSF-EPSCOR (OSR-9550487) and NIDevR (Northern Ireland) is gratefully accepted.

Supplementary Material. Crystallographic data (excluding-structure factors) for the structures reported in this paper have been

UM00012679
NOVARTIS EXHIBIT 1017
Novartis v. Regents, IPR2023-01346
Page 1425 of 4460

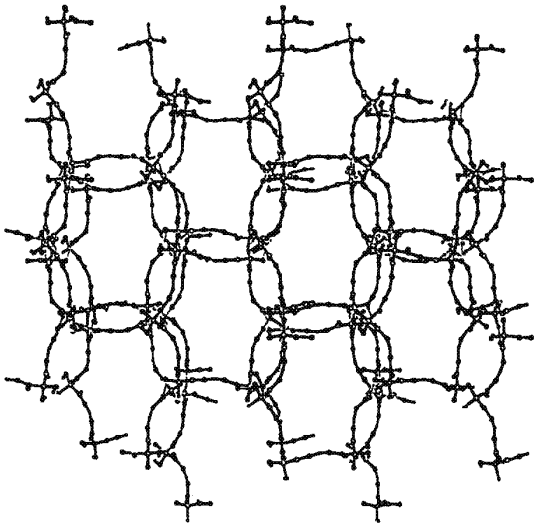


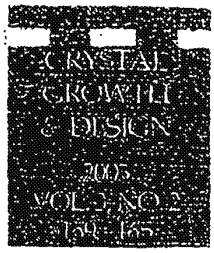
Fig. 6. Infinite channels, parallel with *b*, in the anionic network of **2**.

deposited with the Cambridge Crystallographic Data Centre as supplementary publication No. CCDC-1003/5284 (for **1**) and CCDC-1003/5285 (for **2**). Copies of available material can be obtained, free of charge, on application to the CCDC, 12 Union Road, Cambridge CB2 1EZ, UK, (fax: +44-(0) 1223-336033 or e-mail: deposit@ccdc.cam.ac.uk.)

References

1. Aakeröy, C. B. *Acta Crystallogr. Sect. B.* **1997**, *53*, 569.
2a. Desiraju, G. R. *Angew. Chem. Int. Ed. Engl.* **1995**, *34*, 2311.
b. Desiraju, G. R. (Ed.) *Perspectives in Supramolecular Chemistry. Vol. 2. The Crystal as a Supramolecular Entity;* Wiley: Chichester, 1995.
3. Lehn, J.-M. *Supramolecular Chemistry;* VCH: Weinheim, 1995.
4. Subramanian, S.; Zaworotko, M. *Coord. Chem. Rev.* **1994**, *437*, 357.
5. Vögtle, F. *Supramolecular Chemistry: An Introduction;* Wiley: Chichester, 1991.
6a. Zerkowski, J. A.; MacDonald, J. C.; Whitesides, G. M. *Chem. Mater.* **1994**, *6*, 1250.
b. Zhao, X.; Chang, Y.-L.; Fowler, F. W.; Lauher, J. W. *J. Am. Chem. Soc.* **1990**, *112*, 6627.
7. Aakeröy, C. B.; Hughes, D. P.; Nieuwenhuyzen, M. *J. Am. Chem. Soc.* **1996**, *118*, 10134.
8. Russel, V. A.; Ward, M. D. *Chem. Mater.* **1996**, *8*, 1654.
9a. Braga, D.; Grepioni, F. *Chem. Commun.* **1996**, 571.
b. Burrows, A. D.; Mingos, D. M. P.; White, A. J. P.; Williams, D. J. *Chem. Commun.* **1996**, 97.
10a. Aakeröy, C. B.; Nieuwenhuyzen, M. *J. Am. Chem. Soc.* **1994**, *116*, 10983.
b. Aakeröy, C. B.; Nieuwenhuyzen, M. *J. Mol. Struct.* **1996**, *374*, 223.
11. Sheldrick, G. M. *SHELXL-93;* University of Göttingen: Germany.
12. Melendez, R. E.; Sharma, C. V. K.; Zaworotko, M. J.; Baure, C.; Rogers, R. D. *Angew. Chem. Int. Ed. Engl.* **1996**, *35*, 2213.

UM00012680
NOVARTIS EXHIBIT 1017
Novartis v. Regents, IPR2023-01346
Page 1426 of 4460



Do Polymorphic Compounds Make Good Cocrystallizing Agents? A Structural Case Study that Demonstrates the Importance of Synthon Flexibility

Christer B. Aakeröy,*,† Alicia M. Beatty,‡ Brian A. Helfrich,† and Mark Nieuwenhuyzen§

Department of Chemistry, Kansas State University, Manhattan, Kansas 66506, Department of Chemistry and Biochemistry, University of Notre Dame, Notre Dame, Indiana 46556 and School of Chemistry, The Queen's University of Belfast, Belfast BT9 5AG, Northern Ireland

Received October 2, 2002; Revised Manuscript Received December 31, 2002

Ⓦ This paper contains enhanced objects available on the Internet at http://pubs.acs.org/crystal.

ABSTRACT: The ability of four polymorphic compounds, *isonicotinamide* (**1**), 2-amino-3-nitropyridine (**2**), 4-chlorobenzamide (**3**), and maleic hydrazide (**4**), to form molecular cocrystals has been examined in a systematic structural study. Compounds **1**−**3** participate in a wide variety of binary and ternary (in the case of **1**) cocrystals with aromatic or aliphatic compounds substituted with a multitude of functional groups. However, despite considerable efforts, it has not been possible to form any cocrystals with **4**. The reason for this may be due to the fact that even though there are three known polymorphs of **4**, they all contain the same hydrogen-bonding synthons. In contrast, the polymorphs of **1**−**3** display considerable synthon flexibility, e.g., different hydrogen bond interactions are present in polymorphs of the same compound. Because **1**−**3** can form robust synthons in a variety of ways, whereas **4** always engages in the same primary hydrogen bond interactions, it may explain why the former compounds are readily able to accommodate other molecules within the same lattice whereas there are no known cocrystals of **4**.

Introduction

The ability to change key physical properties, e.g., solubility, crystal morphology, mechanical stability, etc., of a specialty chemical while retaining its essential biophysical or molecular activity is of enormous commercial and fundamental interest. Classic examples of how this can be achieved are regularly demonstrated through the conversion of a pharmacologically active molecule into its chloride or nitrate salt.[1] Alternatively, many drugs are manufactured and processed as solvates, normally as a hydrate. Despite the fact that these two avenues can lead to materials that eventually become commercially viable, potentially useful drugs may never reach this point because they fail to meet one or more of the stringent standards required from the point of view of processing, storage, or bioavailability. Recent developments in solid state organic chemistry and crystal engineering[2] may furnish an alternative approach that can offer better control (and tunability) of fundamental physical properties of speciality chemicals.

If a crystalline material that contains both a pharmaceutically relevant molecule and a structure-directing (but biologically/environmentally passive) component can be rationally assembled through intermolecular synthesis, then the inherent activity of the drug molecule remains intact while the physical properties of the bulk material are modified. The efficient preparation of such cocrystals hinges on an a priori ability to identify reliable and versatile cocrystallizing agents (CAs) without having to resort to endless crystallization experiments.[3]

A good CA should be able to form intermolecular interactions with the target molecule that are more favorable than the homomeric interactions that exist between target···target or between CA···CA.[4] The CA must also have the ability to "tolerate" the presence of a different molecular building block within the same crystalline lattice, which makes it seem reasonable to search for CAs among polymorphic compounds.[5] Polymorphism means that a compound is found in more than one crystalline manifestation, which,[6] in turn, indicates that such compounds display a degree of structural flexibility. In other words, the multidimensional potential energy surface that describes the thermodynamics governing the molecular recognition processes that eventually leads to crystal growth is likely to be rather shallow with many accessible local energy minima.

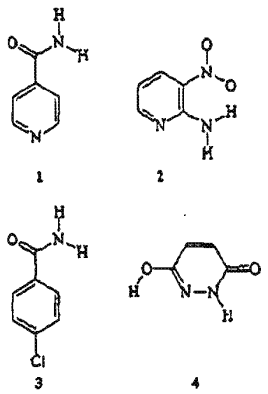
The hypothesis that polymorphic compounds are more likely to form cocrystals than are compounds that never display polymorphism is, at this stage, little more than a notion based upon empirical observations. However, from a practical perspective, it would be extremely useful to have access to reliable guidelines for how we might focus and target a search for reliable CAs for a specific family of compounds. Furthermore, if we encounter cases that do not follow our initial hypothesis, it would be equally important to be able to rationalize the results in the context of intermolecular forces and molecular recognition. To address some of these challenges, we herein report our results from a structural study on three polymorphic compounds, *isonicotinamide* (**1**), 2-amino-5-nitropyrimidine (**2**), 4-chlorobenzamide (**3**), and maleic hydrazide (**4**) and several cocrystals thereof. The reason for selecting these four compounds (apart from the fact that they are all polymorphic) is that they are all potentially capable of engaging in

† Kansas State University.
‡ University of Notre Dame.
§ The Queen's University of Belfast.

10.1021/cg025593z CCC: $25.00 © 2003 American Chemical Society
Published on Web 01/28/2003

NOVARTIS EXHIBIT 1017
Novartis v. Regents, IPR2023-01346

Scheme 1. Four Polymorphic Molecules Capable of Forming a Variety of Hydrogen-Bonded Synthons[a]



[a] *iso*Nicotinamide, **1**; 2-amino-3-nitropyridine, **2**; 4-chlorobenzamide, **3**; and maleic hydrazide, **4**.

several well-defined and robust intermolecular hydrogen bond motifs (Scheme 1).[7,8]

Experimental Section

Crystal Growth and Polymorphism of 1. Upon recrystallization of **1** from nitrobenzene or nitromethane, colorless, rodlike crystals, **1a**, were formed. When **1** was recrystallized from a wide variety of other solvents, e.g., ethanol, water, tetrahydrofuran (THF), dioxane, etc., colorless platelike crystals, **1b**, were obtained. No other crystalline forms have been obtained either by slow evaporation or by liquid/vapor diffusion methods. Sublimation under reduced pressure yields crystals with a structure corresponding to that of **1a**.

Crystal Growth and Polymorphism of 2. Compound **2** is known to exist in three different polymorphic forms. Form I **2a** appears as yellow needles.[9] Form II **2b** can be obtained by recrystallization from ethanol at ambient temperature (yellow, diamond-like crystals).[10] Form III **2c** was obtained when **2** was recrystallized from ethanol at ambient conditions in the presence of fumaric acid (yellow, thick plates).[10] No other polymorphs have been reported to date.

Crystal Growth and Polymorphism of 4. Compound **4** is known to exist in three different crystalline forms: **4a** (form I) is triclinic,[11] **4b** (form II) is monoclinic,[12] and **4c** (form III), another monclinic structure, can be obtained by slowly cooling a solution of **4** in acetic acid.[13]

Cocrystals of 1.[14] **(a) 2-Hexenoic Acid/1 (1:1), 11.** Compound **1** (0.050 g; 0.41 mmol) dissolved in ethanol (3 mL) was mixed with 2-hexenoic acid (0.047 g; 0.41 mmol) dissolved in ethanol (3 mL) in a small test tube. After 48 h of slow evaporation at room temperature, colorless, needlelike crystals formed on the side of the test tube (mp 110−112 °C).

(b) 4-Nitrobenzoic Acid/1 (1:1), 12. Compound **1** (0.050 g; 0.41 mmol) dissolved in ethanol (5 mL) was mixed with 4-nitrobenzoic acid (0.068 g; 0.41 mmol) dissolved in ethanol (5 mL) in a small test tube. After 48 h of slow evaporation at room temperature, rectangular, colorless crystals formed on the side of the test tube (mp 181−183 °C).

(c) 3,5-Dinitrobenzoic Acid/1/4-Methylbenzoic Acid (1:1:1), 13. Equimolar quantities of **1** (0.050 g; 0.41 mmol), 3,5-dinitrobenzoic acid (0.086 g; 0.41 mmol), and 4-methylbenzoic acid (0.056 g; 0.41 mmol) were dissolved separately in ethanol (3 mL) and mixed together in a small test tube. After 48 h of slow evaporation at room temperature, pale yellow, irregular prisms were formed on the side of the test tube (mp 141−143°C).

Cocrystal of 2. (a) 2-Amino-5-nitropyrimidine/2 (1:1), 21. 2-Amino-5-nitropyrimidine (0.250 g; 1.68 mmol) and **2** (0.254 g; 1.81 mmol) were dissolved together in hot ethanol (50 mL). Slow evaporation at ambient conditions yielded yellow, needlelike crystals that consistantly grew in clumps from one point (mp 178−181 °C).

Cocrystals of 3. (a) 3,5-Dinitrobenzoic Acid/3 (1:1), 31. Compound **3** (0.064 g, 0.41 mmol) and 3,5-dinitrobenzoic acid (0.086 g; 0.41 mmol) were dissolved together in hot methanol (8 mL). Slow evaporation at ambient conditions yielded colorless, platelike crystals (mp 164−166 °C).

(b) 3-Dimethylaminobenzoic Acid/3 (1:1), 32. Compound **3** (0.064 g, 0.41 mmol) and 3-dimethylaminobenzoic acid (0.068 g, 0.41 mmol) were dissolved together in hot ethanol (8 mL). Slow evaporation at ambient conditions yielded pale yellow, irregular prism crystals (mp 118−121 °C).

(c) Fumaric Acid/3 (1:1), 33. Compound **3** (0.065 g, 0.42 mmol) and fumaric acid (0.024 g, 0.21 mmol) were dissolved together in hot ethanol (8 mL). Slow evaporation at ambient conditions yielded colorless, block crystals (mp 174−178 °C). Crystals of individual components could also be found and were confirmed by single-crystal X-ray diffraction.

Cocrystals of 4. Despite numerous attempts (about 25 different compounds) at forming cocrystals with **4** and a variety of aromatic (including heterocyclic) or aliphatic compounds with different functional groups, e.g., carboxylic acids, amides, oximes, etc., we were only ever able to isolate unreacted starting materials. Crystal growth experiments involved slow evaporation and liquid/vapor diffusion using a range of solvents, e.g., MeOH, EtOH, MeCN, etc. Essentially, **4** was put through the same cycle of experiments as were **1**−**3**.

Single-Crystal X-ray Diffraction. Single crystals were placed in paratone, mounted on a glass pin, and transferred into the cold stream of the diffractometer. Crystal data for **11**−**13** were collected and integrated using a Bruker SMART 1000 system with graphite monochromated Mo Kα (λ = 0.71073 Å) radiation at 173 K. Crystal data for **21** were collected at 301 K and for **31**−**33** at 203 K. Crystal data for **1a,b** were collected using a Siemens P4 four circle diffractometer with graphite monochromated Mo Kα radiation at ca. 150 K in a dinitrogen stream. Crystal stability was monitored by measuring standard reflections every 100 reflections, and there were no significant variations (<±1%). ψ-Scans were employed for data collection, and Lorentz and polarization corrections were applied. Each of the structures was solved by direct methods, using SHELXS-97 and refined using SHELXL-97. Nonhydrogen atoms were found by successive least-squares refinement on F^2 and refined with anisotropic parameters. All hydrogen atoms, except for those on the methyl group in **13**, were located on the difference map. A riding model with fixed thermal parameters ($[u_{iso} = 1.2U_{eq}]$) for the atom that the hydrogen atoms are riding) was applied, except for **32**, where the methyl hydrogen atoms were calculated. Crystallographic data for **1a,b**, **11**−**13**, **21**, and **31**−**33** can be found in Table 1.

Results

Crystal Structure of 1 (Form I). Form I of **1** is monoclinic with one molecule in the asymmetric unit. The molecular geometry does not display any unexpected behavior, and the amide moiety is slightly twisted out of the plane of the aromatic ring (30.5°) (Figure 1).

The amide moieties in **1a** generate a slight variation on the extended ribbonlike motif, which occurs frequently in primary amides. There is a self-complementary N−H···O head-to-head synthon between adjacent molecules, and neighboring dimers are connected into an infinite assembly through symmetry-related N−H···O hydrogen bonds aligned perpendicular to the long axis of the dimers (Figure 2).

UM00012682
NOVARTIS EXHIBIT 1017
Novartis v. Regents, IPR2023-01346
Page 1428 of 4460

Table 1. Crystallographic Data for 1a,b, 11–13, 21, and 31–33

compd	1a	1b	11	12	13
formula	$C_6H_6N_2O$	$C_6H_6N_2O$	$C_{12}H_{12}N_2O_2$	$C_{12}H_{11}N_3O_5$	$C_{21}H_{18}N_4O_3$
FW	122.13	122.13	216.27	289.25	470.39
temp (K)	173(2)	173(2)	173(2)	173(2)	173(2)
cryst syst	monoclinic	monoclinic	monoclinic	monoclinic	triclinic
space group, Z	$P2_1/c$, 4	$P2_1/c$, 4	$I2/a$, 8	$I2/a$, 8	$P\bar{1}$, 2
a (Å)	10.176(1)	15.735(3)	20.445(4)	20.512(4)	7.763(1)
b (Å)	5.7319(6)	7.998(2)	5.2309(9)	5.1675(8)	8.722(1)
c (Å)	23.003(4)	9.885	23.008(4)	23.694(5)	15.743(2)
α (deg)					93.483(2)
β (deg)	98.042(3)	105.59(2)	96.981(3)	90.66(3)	98.981(3)
γ (deg)					93.913(7)
V (Å)	579.5(1)	1196.2(5)	2442.3(7)	2511.3(0)	1047.6(2)
density (g/cm^3)	1.400	1.354	1.285	1.530	1.491
$M_{(MoK\alpha)}$ (mm^{-1})	0.100	0.096	0.093	0.120	0.119
θ range	2.92–27.49	1.34–22.48	1.72–28.04	2.51–26.19	2.81–28.9
range h	−13 to 13	−16 to 16	−26 to 26	−26 to 26	−9 to 10
range k	0 to 7	−8 to 0	−6 to 6	−6 to 5	−11 to 11
range l	−13 to 0	0 to 10	−30 to 30	−30 to 31	−19 to 20
refl collected	1413	1680	8158	8293	7248
ind refl (R_{int})	1334 (0.0164)	1565 (0.0151)	2808 (0.1235)	2759 (0.0544)	2622 (0.0548)
data/restraints/params	1334/0/82	1565/0/163	2808/0/154	2759/0/190	4662/0/307
R/R_w[a] (obs datn)	0.0395/0.0985	0.0487/0.1185	0.0736/0.1794	0.0432/0.1097	0.0483/0.1052
R/R_w[a] (all data)	0.0494/0.1050	0.0528/0.1258	0.1129/0.1969	0.0678/0.1200	0.0839/0.1209
$\Delta\rho_{max/min}$ (e Å^{-3})	0.229/−0.218	0.179/−0.280	0.229/−0.388	0.315/−0.232	0.314/−0.199

compd	21	31	32	33
formula	$C_9H_9N_7O_4$	$C_{14}H_{13}ClN_3O_7$	$C_{16}H_{17}ClN_2O_3$	$C_{18}H_{16}Cl_2N_2O_6$
FW	279.23	367.70	320.77	427.23
temp (K)	301(2)	203(2)	203(2)	203(2)
cryst syst	monoclinic	triclinic	triclinic	triclinic
space group, Z	$P2(1)/n$, 4	$P\bar{1}$, 2	$P\bar{1}$, 2	$P\bar{1}$, 2
a (Å)	11.786(3)	7.246(1)	7.173(1)	9.2674(8)
b (Å)	5.161(1)	8.626(1)	8.369(2)	10.1386(9)
c (Å)	19.975(5)	13.281(2)	12.997(3)	10.481(1)
α (deg)		92.565(3)	88.638(4	86.428(6)
β (deg)	95.275(5)	101.875(3)	80.875(4)	72.174(6)
γ (deg)		109.472(3)	77.463(4)	89.506(7)
V (Å)	1210.0(5)	760.0(2)	752.0(3)	935.6(2)
density (g/cm^3)	1.533	1.607	1.417	1.517
$M_{(MoK\alpha)}$ (mm^{-1})	0.124	0.298	0.268	0.356
θ range	1.93–28.36	2.52–28.14	1.59–28.28	2.05–28.25
range h	−15 to 14	−9 to 9	−9 to 9	−12 to 12
range k	−6 to 6	−11 to 11	−11 to 10	−13 to 13
range l	−26 to 26	−16 to 17	−15 to 16	−13 to 13
refl collected	10 429	5265	5256	6971
ind refl (R_{int})	2767 (0.1056)	3375 (0.0368)	3371 (0.0309)	4128 (0.0291)
data/restraints/params	2767/0/182	3375/0/227	3371/0/200	4128/0/254
R/R_w[a] (obs data)	0.0555/0.1433	0.0452/0.1021	0.0545/0.1277	0.0388/0.1003
R/R_w[a] (all data)	0.1112/0.1690	0.0724/0.1141	0.1014/0.1513	0.0546/0.1082
$\Delta\rho_{max/min}$ (e Å^{-3})	0.221/−0.304	0.301/−0.283	0.287/−0.320	0.361/−0.289

Somewhat surprisingly, there are no prominent hydrogen bond interactions involving the pyridine nitrogen atom (Table 2). Although adjacent molecules are positioned tail-to-tail, the rings are not coplanar and the symmetry-related C···N distances are over 3.47 Å (Figure 3).

Crystal Structure of 1 (Form II). Form II of 1 is also monoclinic but with two molecules in the asymmetric unit. As in 1a, there are no remarkable intramolecular features in either molecule, and the amide moiety is twisted out of the plane in each molecule (by 25.4 and 24.0°, respectively) (Figure 4).

In 1b, the dimeric head-to-head motif has been abandoned in favor of an N−H(amide)···N(pyridine),

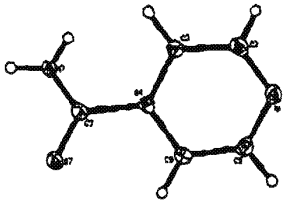


Figure 1. Thermal ellipsoids (30%) and numbering scheme in 1a.

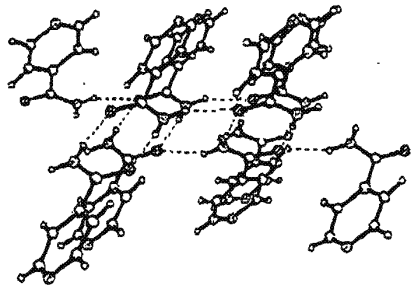


Figure 2. Dominating hydrogen bond interactions in 1a. ⓦ A 3D rotatable image of 1a in PDB format is available.

UM00012680
NOVARTIS EXHIBIT 1017
Novartis v. Regents, IPR2023-01346
Page 1429 of 4460

Table 2. Hydrogen Bond Geometries[a]

Hydrogen Bonds for 1a (Å and °)

D−H···A	d(D−H)	d(H···A)	d(D···A)	<(DHA)
N(7)−H(72)···O(7)#1	0.89	2.09	2.9354(14)	157.9
N(7)−H(71)···O(7)#2	0.86	2.08	2.9366(16)	173.5
C(2)−H(2)···N(1)#3	0.88	2.63	3.4275(19)	151.1
C(6)−H(6)···N(1)#4	0.98	2.72	3.4790(19)	135.0

Hydrogen Bonds for 1b (Å and °)

D−H···A	d(D−H)	d(H···A)	d(D···A)	<(DHA)
N(7)−H(71)···N(1)#1	0.97	2.02	2.982(3)	171.4
N(7)−H(72)···O(7)#2	0.93	2.01	2.934(2)	170.4
N(17)−H(171)···N(11)#1	0.96	2.02	2.974(3)	168.7
N(17)−H(172)···O(17)#3	0.96	1.99	2.947(2)	174.0

Hydrogen Bonds for 11 (Å and °)

D−H···A	d(H···A)	d(D···A)	<(DHA)
N(7)−H(72)···O(17)#1	2.09	2.952(2)	163.4
N(7)−H(71)···O(7)#2	2.02	2.8720(19)	169.3
O(18)−H(18)···N(1)	1.67	2.5768(19)	178.2

Hydrogen Bonds for 12 (Å and °)

D−H···A	d(H···A)	d(D···A)	<(DHA)
N(7)−H(71)···O(7)#1	1.94	2.880(2)	168.0
N(7)−H(72)···O(10)#2	2.02	2.919(3)	160.9
O(11)−H(11)···N(1)	1.66	2.655(3)	169.2

Hydrogen Bonds for 13 (Å and °)

D−H···A	d(H···A)	d(D···A)	<(DHA)
N(7)−H(71)···O(27)	1.93	2.886(2)	176.0
N(7)−H(72)···O(17)#1	2.09	2.995(2)	167.9
O(18)−H(18)···N(1)	1.69	2.5479(19)	159.8
O(28)−H(28)···O(7)	1.67	2.6423(18)	168.4

Hydrogen Bonds for 21 (Å and °)

D−H···A	d(D−H)	d(H···A)	d(D···A)	<(DHA)
N(2)−H(21)···N(11)	0.88	2.21	3.074(3)	169.8
N(2)−H(22)···O(2)#1	0.82	2.32	2.970(3)	136.3
N(12)−H(121)···N(1)	0.97	1.99	2.958(3)	178.9
N(12)−H(122)···N(13)#2	0.92	2.14	3.057(3)	173.3
N(2)−H(22)···O(2)	0.82	2.11	2.677(3)	126.7

Hydrogen Bonds for 31 (Å and °)

D−H···A	d(D−H)	d(H···A)	d(D···A)	<(DHA)
N(7)−H(72)···O(14)#1	0.95	2.81	2.890(2)	118.8
N(7)−H(71)···O(18)	0.97	2.01	2.967(2)	167.0
O(17)−H(17)···O(7)	1.05	1.50	2.531(2)	169.8

Hydrogen Bonds for 32 (Å and °)

D−H···A	d(D−H)	d(H···A)	d(D···A)	<(DHA)
N(7)−H(71)···O(18)	0.99	1.98	2.937(3)	164.6
N(7)−H(72)···O(18)#1	0.87	2.22	3.045(3)	156.4
O(17)−H(17)···O(7)	0.91	1.68	2.586(3)	172.9

Hydrogen Bonds for 33 (Å and °)

D−H···A	d(D−H)	d(H···A)	d(D···A)	<(DHA)
N(7)−H(71)···O(32)	0.88	2.10	2.957(2)	164.8
N(7)−H(72)···O(22)	0.81	2.12	2.930(2)	172.9
N(17)−H(171)···O(22)	0.89	2.08	2.942(2)	164.4
N(17)−H(172)···O(32)#1	0.81	2.23	3.027(2)	168.2
O(21)−H(21)···O(17)	0.85	1.71	2.565(2)	172.7
O(31)−H(31)···O(7)	0.80	1.73	2.518(2)	168.5

[a] Symmetry transformations used to generate equivalent atoms. 1a: #1, x, $-y + 1/2$, $z - 1/2$; #2, $-x$, $-y + 1$, $-z$; #3, $-x + 1$, $y + 1/2$, $-z - 1/2$; #4, $-x + 1$, $-y - 1$, $-z$. 1b: #1, x, $y - 1$, z; #2, x, $-y + 1/2$, $z - 1/2$; #3, x, $-y - 1/2$, $z - 1/2$. 11: #1, $-x - 1/2$, $y + 1$, $-z + 1$; #2, $-x$, $-y + 1$, $-z + 1$. 12: #1, $-x$, $-y + 1$, $-z$; #2, $-x - 1/2$, $y - 1$, $-z$. 13: #1, x, $y - 1$, z. 21: #1, $-x + 1$, $-y$, $-z$; #2, $-x$, $-y + 2$, $-z$. 31: #1, $-x + 1$, $-y + 4$, $-z + 1$. 32: #1, $-x - 2$, $-y$, $-z + 1$. 33: #1, $x + 1$, y, z.

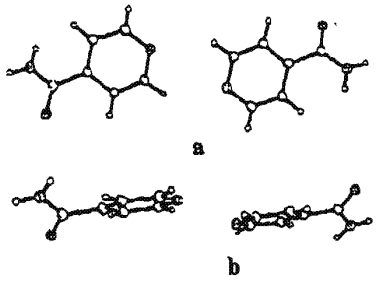


Figure 3. (a) Face-on view of the orientation of adjacent molecules in 1a. Although the relative positions of the molecules indicate the existence of complementary C−H···N hydrogen bonds, the edge-on view (b) makes this less likely as the rings are not coplanar.

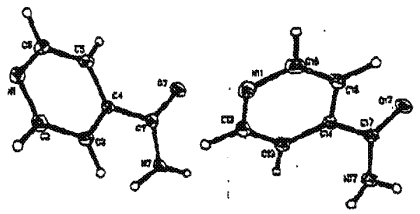


Figure 4. Thermal ellipsoids (30%) and numbering scheme in 1b.

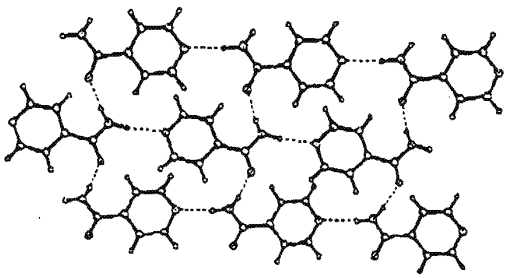


Figure 5. One of the two unique infinite 2D assemblies ribbons in 1b (both networks have identical connectivity).

⊛ A 3D rotatable image of 1b in PDB format is available.

head-to-tail, interaction and a catemeric N−H···O hydrogen bond; the direction of the catemer is almost perpendicular with respect to the chain generated by the amide···pyridine interaction (each asymmetric molecule gives rise to an independent assembly but with identical hydrogen bond connectivity) (Figure 5). We have not observed any phase changes between polymorphs even after an extended period of time (several years).

Crystal Structure of 2-Hexenedioic Acid/1 (1:1), 11. The crystal structure of 11 contains one molecule of the carboxylic acid and one molecule of 1. These two building blocks are connected into a tetrameric supermolecule constructed from a dimeric, head-to-head amide···amide interaction plus two symmetry equivalent acid···pyridine interactions (Figure 6). The anti amide hydrogen atom forms a hydrogen bond with the

UM00012684
NOVARTIS EXHIBIT 1017
Novartis v. Regents, IPR2023-01346
Page 1430 of 4460

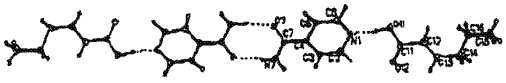


Figure 6. Thermal ellipsoids (30%) and numbering scheme in **11**.

Ⓦ A 3D rotatable image in PDB format is available.

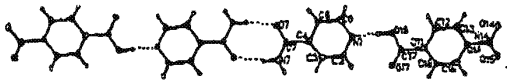


Figure 7. Thermal ellipsoids (30%) and numbering scheme in **12**.

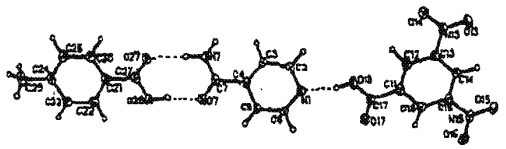


Figure 8. Thermal ellipsoids (30%), numbering scheme, and the complete ternary supermolecule in **13**.

Ⓦ A 3D rotatable image in PDB format is available.

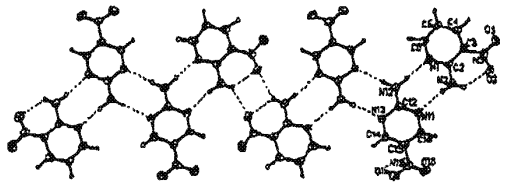


Figure 9. Extended hydrogen-bonded 1D network in **21**.

Ⓦ A 3D rotatable image in PDB format is available.

carbonyl group of an adjacent carboxylic acid. There are no other notable hydrogen bonds in **11** (Table 2).

Crystal Structure of 4-Nitrobenzoic Acid/1 (1:1), 12. The crystal structure of **12** contains one molecule of the carboxylic acid and one molecule of **1**. As is the case in **11**, the two components are connected into a tetrameric supermolecule constructed from a dimeric, head-to-head amide···amide interaction plus a pair of symmetry equivalent acid···pyridine interactions (Figure 7). The anti amide hydrogen atom forms a hydrogen bond with the carbonyl group of an adjacent carboxylic acid. There are no other notable hydrogen bonds in **12**.

Crystal Structure of 3,5-Dinitrobenzoic Acid/1/ 4-Methylbenzoic Acid (1:1:1), 13. The crystal structure of **13** is a 1:1:1 ternary cocrystal that contains a three component supermolecule with the expected connectivity. The stronger acid ($pK_a = 2.8$)[15] interacts with the pyridine nitrogen atom, and the weaker acid ($pK_a = 4.4$)[15] competes successfully for the amide moiety and forms a heteromeric hydrogen-bonded motif (Figure 8). This motif is consistent with that reported for several other ternary cocrystals of **1** and two carboxylic acids of different strength.[16]

Crystal Structure of 2/2-Amino-5-nitropyrimidine (1:1), 21. The asymmetric unit of **21** contains one molecule of each component. Near linear, symmetry-related, N–H···N hydrogen bond interactions connect

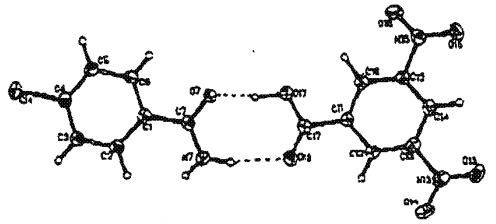


Figure 10. Thermal ellipsoids (30%) and numbering scheme in **31**.

Ⓦ A 3D rotatable image in PDB format is available.

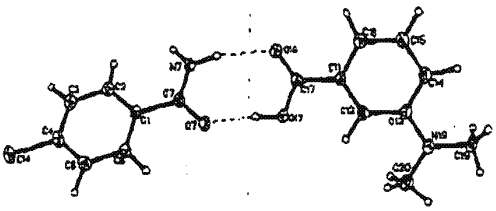


Figure 11. Thermal ellipsoids (30%) and numbering scheme in **32**.

Ⓦ A 3D rotatable image in PDB format is available.

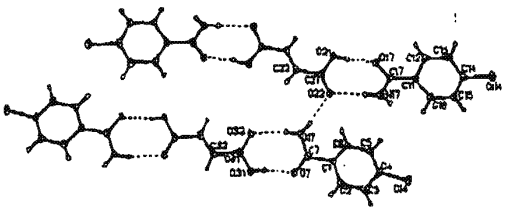


Figure 12. Thermal ellipsoids (30%) and numbering scheme in **33**.

Ⓦ A 3D rotatable image in PDB format is available.

neighboring molecules into tetrameric (A···B···B···A) assemblies. Adjacent tetramers are linked into infinite chains via symmetry-related N–H···O hydrogen bonds (Figure 9).

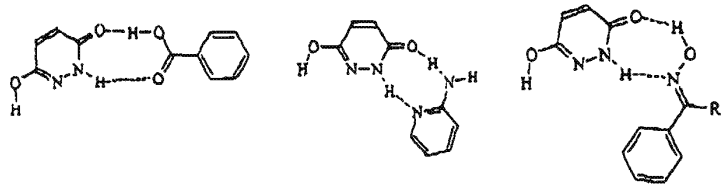
Crystal Structure of 3,5-Dinitrobenzoic Acid/3 (1:1), 31. The asymmetric unit of **31** consists of one molecule of each component connected by an acid/amide heterodimer (Figure 10). The anti amide hydrogen atom forms a hydrogen bond with a nitro moiety from an adjacent acid molecule. The binary supermolecules form extended stacks with adjacent heterodimer oriented in an antiparallel fashion.

Crystal Structure of 3-Dimethylaminobenzoic Acid/3 (1:1), 32. The asymmetric unit of **32** consists of one molecule of each component connected by an acid/amide heterodimer (Figure 11). The anti amide hydrogen atom forms a hydrogen bond with the carbonyl of an adjacent acid molecule. The acid and amide molecules stack separately as AAAA and BBBB, such that each individual molecular dipole is canceled by the dipole of the molecule above or below it.

Crystal Structure of Fumaric Acid/3 (1:2), 33. The asymmetric unit of **33** consists of two molecules of the

UM00012685
NOVARTIS EXHIBIT 1017
Novartis v. Regents, IPR2023-01346
Page 1431 of 4460

Scheme 2. Three Examples of Known Synthons that Could Facilitate the Formation of Cocrystals Involving 4



amide and two inequivalent halves of the acid forming two different acid/amide heterodimers (Figure 12). The anti amide hydrogen atoms form a hydrogen bond with a carbonyl of an adjacent acid molecule. The three component (A···B···A) heterodimer stacks in an alternating pattern of ABAABA.

Discussion

We have shown that cocrystals can readily be formed from both **2**, **1**, and **3** with a variety of aliphatic and aromatic carboxylic acids. This is in agreement with the suggestion that polymorphs make good CAs (provided that solubility differences are not too large). However, we have been completely unsuccessful in forming any kind of cocrystals with **4**, despite the fact that it exists by itself in three different crystalline forms. We have tried a range of crystallization techniques as well as an extensive series of molecular compounds that in principle, can form effective complementary hydrogen bond interactions with a 2-pyridone moiety (e.g., carboxylic acids, 2-aminopyridines, 2-aminopyrimidines, oximes, etc.) (Scheme 2).

The failure to produce any cocrystals with **4** obviously casts doubts on the notion that polymorphic compounds make good CAs unless there is a significant structural difference in the polymorphic behavior of **1**–**4**. We decided to take a closer look at all the polymorphs **1a,b**, **2a**–**c**, **3a**–**c**, and **4a**–**c** in an attempt to uncover possible reasons for the unwillingness of **4** to participate in molecular cocrystals. Previous work on polymorphs containing extensive hydrogen-bonded networks has demonstrated that even very complex intermolecular interactions and subtle structural differences are readily identified and categorized through a systematic use of graph-set notation.[17] Consequently, a graph-set analysis was applied to the hydrogen bond patterns displayed by **1a,b**, **2a**–**c**, and **3a**–**c**. The two polymorphs of *isonicotinamide*, **1a** and **1b**, display very different intermolecular connectivities. In **1a**, there is a "classic" amide···amide head-to-head interaction as well as the commonly occurring N–H···O link between adjacent dimers resulting in a $C(4)R_2^2(8)$ notation for the primary hydrogen bonds in this polymorph. However, the primary intermolecular forces in **1b** are significantly different as there is a catemeric amide···amide hydrogen bond, C(4), as well as an amide···pyridine interaction, C(7). A similar classification of the three polymorphs of **2** reveals that the expected intramolecular amine···nitro hydrogen bond is present in all three forms. In addition, **2b** and **2c** have identical intermolecular connectivities and the primary hydrogen bond motifs are thus described with the same graph-set notion, $R_2^2(12)R_2^2(8)S(6)$. In **2a**, however, there are infinite hydrogen-bonded ribbons that are described by the following notation, $R_2^2(10)R_2^2(8)S(6)$. The structures of **3a** and **3c** reveal the amide moieties forming the classic amide one-dimensional catemer, $C(4)$ $R_2^2(8)R_1^2(8)$. The difference between the two structures lies in the arrangement of aromatic rings with respect to one another. While the graph-set notation for **3b** is similar to **3a** and **3c**, the larger hydrogen-bonded ring creates a two-dimensional network, $C(4)$ $R_2^2(8)R_6^4(16)$. In contrast, all three polymorphs of **4** contain the same hydrogen-bonded ladders held together by identical synthons; $S(7)R_4^2(14)R_2^2(8)$ (Figure 13).

The fact that these three different polymorphs all contain the same extended networks was also noted in the original paper, "Three Forms of MH(4) Provide a Unique Example of Polymorphic Structures Built of Similar Hydrogen-Bonded Aggregates. The Same Hydrogen-Bonded Supramolecular Aggregates Organize into Different Lattices of Different Symmetries...".[12]

A detailed structural examination of **1**–**4** has enabled the identification of significant differences, in terms of molecular recognition patterns, between the different polymorphs that in turn, may provide practical guidelines for distinguishing between (or ranking) candidates that are potentially suitable as CAs. Cocrystals are not necessarily easy to prepare since such heteromeric systems are only likely to appear if the noncovalent forces between different molecules are more favorable than those that exist between molecules in the corre-

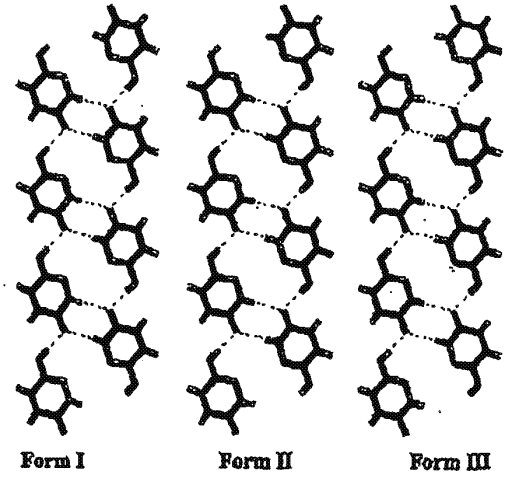


Figure 13. Primary hydrogen bond motifs in the three known polymorphs of **4** display the same connectivity.

UM00012686
NOVARTIS EXHIBIT 1017
Novartis v. Regents, IPR2023-01346
Page 1432 of 4460

sponding homomeric crystals. An important consideration when attempting to prepare cocrystals is to choose a CA that is already known to be polymorphic. Clearly, if a molecular compound exists in several polymorphs, it has demonstrated a structural flexibility and it is not as energetically locked into a single type of crystalline lattice or packing mode. However, as the current study shows, structural flexibility alone is not always enough. It may be equally important to select molecules that can adopt alternative packing patterns as well as display synthon flexibility, an ability to participate in several different robust and well-defined intermolecular interactions that can satisfy the demands of multiple hydrogen bond donors/acceptors on a variety of molecules.

Acknowledgment. We are grateful for financial support from NSF (CHE-0078996).

Note Added After ASAP Posting

An earlier version of this paper posted ASAP on January 28, 2003 contained an incorrect name (2-amino-3-nitropyridine/2) in two paragraphs describing compound 21 in Experimental Section and Results. The corrected name (2-amino-5-nitropyrimidine/2) appears in this version posted February 7, 2003. Links to web-enhanced object files were added March 5, 2003.

Supporting Information Available: X-ray crystallographic files (CIF). This material is available and free of charge via the Internet at http://pubs.acs.org.

References

(1) *Solid State Chemistry of Drugs*; Byrn, S. E., Pfeiffer, R. R., Stowell, J. G., Eds.; SSCI Inc.: West Lafayette, 1999.
(2) Aakeröy, C. B. *Acta Crystallogr. Sect. B* **1997**.
(3) A few examples of successful cocrystallization experiments. (b) Sarma, J. A. R. P.; Desiraju, G. R. *J. Chem. Soc., Perkin Trans. 2* **1985**, 1906. (c) Huang, C.; Leiserowitz, L.; Schmidt, G. M. *J. Chem. Soc., Perkin Trans. 2* **1973**, 503. (d) Tamura, C.; Sakurai, N.; Sato, S. *Bull. Chem. Soc. Jpn.* **1971**, *44*, 1473. (e) Pan, F.; Wong, M. S.; Gramlich, V.; Bosshard, C.; Gunter, P. *Chem. Commun.* **1996**, 2. (f) LeFur, Y.; Bagieu-Beucher, M.; Masse, R.; Nicoud, J. F.; Levy, J. P. *Chem. Mater.* **1996**, *8*, 8. (g) Zerkowski, J. A.; MacDonald, J. C.; Whitesides, G. M. *Chem. Mater.* **1997**, *9*, 9. (h) Liao, R.-F.; Lauher, J. W.; Fowler, F. W. *Tetrahedron* **1996**, *52*, 3153. (i) Shan, N.; Bond, A. D.; Jones, W. *Cryst. Eng.* **2002**, *5*, 9. (j) Pedireddi, V. R.; Jones, W.; Chorlton, A. P.; Docherty, R. *Chem. Commun.* **1996**, 997. (k) Vishweshwar, P.; Nangia, A.; Lynch, V. M. *J. Org. Chem.* **2002**, *67*, 556.
(4) Aakeröy, C. B.; Beatty, A. B.; Helfrich, B. H. *J. Am. Chem. Soc.* **2002**, *124*, 14425−14432.
(5) There are, of course, other aspects that need to be considered (e.g., solubility differences between drug and CA (if the cocrystals are to be prepared via solution-based methods)) before embarking upon a series of cocrystallizations.
(6) Bernstein, J. *Polymorphism in Molecular Crystals*; Oxford University Press: New York, 2002.
(7) After the initial submission of this manuscript, one reviewer pointed out that **3** (a compound that was not originally part of the study) is also known to be polymorphic (with different hydrogen bond motifs); yet, there are no reported cocrystals or solvates. Because we suggest in this paper that a polymorphic compound displaying synthon flexibility should be a good CA, it seemed that **3** would provide a perfect, independently selected, "test case" for our hypothesis, and it was subsequently included in our study.
(8) Forms I and III of **3**: (a) Taniguch, T.; Nakata, K.; Takaki, Y.; Sakurai, K. *Acta Crystallogr. Sect. B* **1978**, *34*, 2574. Form II: (b) Hayashi, T.; Nakata, K.; Takaki, Y.; Sakurai, K. *Bull. Chem. Soc. Jpn.* **1980**, *53*, 801.
(9) Destro, R.; Filati, T.; Simonetta, M. *Acta Crystallogr. Sect. B* **1975**, *31*, 2383.
(10) Aakeröy, C. B.; Beatty, A. M.; Nieuwenhuyzen, M.; Zou, M. *J. Mater. Chem.* **1998**, *8*, 1385.
(11) Cradwick, P. D. *Nature* **1975**, *253*, 774.
(12) Katrusiak, A. *Acta Crystallogr. Sect. C* **1993**, *49*, 36.
(13) Katrusiak, A. *Acta Crystallogr. Sect. B* **2001**, *57*, 697.
(14) The three cocrystals **11**−**13** can also be obtained by manually grinding equimolar mixtures of the relevant components together. The experimental XRD patterns for all solids obtained from grinding match well with the simulated X-ray powder patterns based upon experimental single-crystal data obtained from the corresponding cocrystals prepared from solution.
(15) Kortüm, G., Vogel, W., Andrussov, K. *Dissociation Constants of Organic Acids in Aqueous Solution*; Butterworth: London, 1961.
(16) Aakeröy, C. B.; Beatty, A. M.; Helfrich, B. A. *Angew. Chem., Int. Ed.* **2001**, *40*, 3240.
(17) Etter, M. C.; MacDonald, J. C.; Bernstein, J. *Acta Crystallogr. Sect. B* **1990**, *46*, 256.

CG025592Z

UM00012687
NOVARTIS EXHIBIT 1017
Novartis v. Regents, IPR2023-01346
Page 1433 of 4460

This Page is Inserted by IFW Indexing and Scanning Operations and is not part of the Official Record

BEST AVAILABLE IMAGES

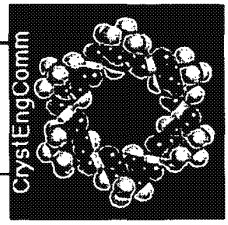
Defective images within this document are accurate representations of the original documents submitted by the applicant.

Defects in the images include but are not limited to the items checked:

- ☐ BLACK BORDERS
- ☐ IMAGE CUT OFF AT TOP, BOTTOM OR SIDES
- ☐ FADED TEXT OR DRAWING
- ☐ BLURRED OR ILLEGIBLE TEXT OR DRAWING
- ☐ SKEWED/SLANTED IMAGES
- ☐ COLOR OR BLACK AND WHITE PHOTOGRAPHS
- ☐ GRAY SCALE DOCUMENTS
- ☐ LINES OR MARKS ON ORIGINAL DOCUMENT
- ☐ REFERENCE(S) OR EXHIBIT(S) SUBMITTED ARE POOR QUALITY
- ☐ OTHER: _____

IMAGES ARE BEST AVAILABLE COPY.
As rescanning these documents will not correct the image problems checked, please do not report these problems to the IFW Image Problem Mailbox.

Heteromeric intermolecular interactions as synthetic tools for the formation of binary co-crystals



Paper

Christer B. Aakeröy, John Desper and Brian A. Helfrich

Department of Chemistry, Kansas State University, Manhattan, KS 66506, USA.
E-mail: aakeroy@ksu.edu; Fax: 1 785 532 6666; Tel: 1 785 532 6665

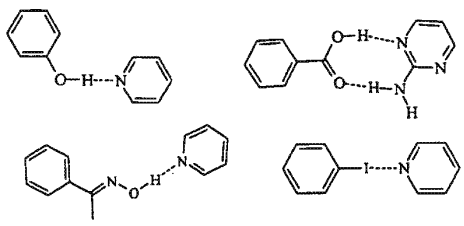
Received 24th November 2003, Accepted 8th January 2004
First published as an Advance Article on the web 21st January 2004

The crystal structure of 4-nitrobenzamide pyrazinecarboxamide (1 : 1) contains two homomeric amide···amide dimers, which is in sharp contrast with the structural motifs displayed by the vast majority of binary co-crystals (illustrated here with five new examples), where the driving force for the supramolecular assembly is one or more strong heteromeric intermolecular interactions.

Introduction

Recent years have witnessed many systematic and elegant studies that demonstrate how molecular assemblies of increasing complexity can be constructed with the aid of complementary intermolecular interactions, *e.g.* hydrogen bonds, halogen···halogen, π–π interactions, *etc.*[1] Typically, these assemblies consist of homomeric architectures,[2] which is fully consistent with the fact that recrystallisation as a means of purification takes full advantage of the general "selfishness" of molecules resulting in an exclusion of unwanted impurities from a crystalline lattice.

With this in mind, it is not surprising that most supramolecular synthetic strategies employed in the deliberate design of binary co-crystals[3] are based upon suitable combinations of chemical entities (or functional groups) located on different molecules that would prefer to interact with each other rather than with themselves.[4] For example, hydrogen bonds often form in a hierarchical fashion (best-donor to best-acceptor, second best-donor to second best-acceptor, *etc.*),[5] and by positioning the best hydrogen-bond donor and the best hydrogen-bond acceptor on different molecular building blocks, the chances of producing a new binary co-crystal are greatly enhanced.[6] Approaches such as this are also predicated upon the idea that a small number of specific intermolecular interactions can provide a significant part of the stabilization energy of molecular crystals.[7] In this way, a large number of binary co-crystals have been synthesised using reliable supramolecular protocols (Scheme 1).[8]



Scheme 1 Generic examples of binary co-crystals constructed from heteromeric intermolecular interactions.

The physical validity of a best-donor/best-acceptor approach to supramolecular chemistry based on hydrogen-bond interactions can, at least qualitatively, be rationalised in terms of a desire of the system to maximise electrostatic attractions. When this idea is extended to more complex systems with several pairs of potentially complementary interactions, it is possible to develop modular supramolecular synthetic approaches that rely on a hierarchy of intermolecular interactions.[9]

Herein we present five examples of binary co-crystals that were prepared based upon the supramolecular synthetic principles outlined above. All five co-crystals display the expected intermolecular connectivity including a specific and strong heteromeric interaction between the two reagents; 3,5-dinitrobenzoic acid methyl red[10] (1 : 1), **1**; 3-nitrobenzoic acid isonicotinamide (1 : 1), **2**; 4-fluorobenzoic acid isonicotinamide (1 : 1), **3**; 4-(N,N-dimethylamino)benzoic acid 3,5-dinitrobenzamide (1 : 1), **4**; 3-(N,N'-dimethylamino)benzoic acid 4-nitrobenzoic acid (1 : 1), **5**. In addition, we present a rare example of a binary co-crystal where the dominating intermolecular motifs are rather more unexpected and highly unpredictable, 4-nitrobenzamide pyrazinecarboxamide (1 : 1), **6**.†

X-ray crystallography

Crystalline samples of **1**–**6** were placed in inert oil, mounted on a glass pin, and transferred to the cold gas stream of the diffractometer. X-ray data were collected on a Bruker SMART 1000 four-circle CCD diffractometer using a fine-focus Mo-Kα tube (λ = 0.71073 Å). Data were collected using SMART.[11] Initial cell constants were found by small and widely separated "matrix" runs. Preliminary Laué symmetry was determined from axial images. Generally, an entire hemisphere of reciprocal space was collected regardless of Laué symmetry. Scan speed and scan width were chosen based on scattering power and peak rocking curves.

Unit cell constants and orientation matrix were improved by least-squares refinement of reflections from the entire dataset. Integration was performed with SAINT[12] using this improved unit cell as a starting point. Precise unit cell constants were calculated in SAINT from the final merged dataset. Lorenz and polarization corrections were applied, but data were generally not corrected for absorption. Laué symmetry, space group, and unit cell contents were found with XPREP.

Data were reduced with SHELXTL.[13] The structures were solved in all cases by direct methods. All CH hydrogen atoms were assigned to idealized positions and were allowed to ride.

† Generic synthetic approach stoichiometric amounts (1 : 1 molar equivalents) of the two reagents were dissolved separately in warm ethanol. The solutions were then added together and allowed to cool to room temperature. Crystals formed upon slow evaporation (anywhere from hours to days) of the solvent.

DOI: 10.1039/b315181f

This journal is © The Royal Society of Chemistry 2004

UM00012689
NOVARTIS EXHIBIT 1017
Novartis v. Regents, IPR2023-01346
Page 1435 of 4460

Positional parameters for all NH and OH hydrogen atoms were allowed to refine. Methyl hydrogen atoms were assigned an isotropic thermal parameter $u = 1.5\ U_{ij}$(eq) of the carbon to which they are bound; all other hydrogen atoms were assigned $u = 1.2\ U_{ij}$(eq) of the atom to which they are bound. Table 1 provides crystallographic details for 1–6 and Table 2 provides information about hydrogen-bond geometries. Fig. 1a–f shows labelling schemes and thermal ellipsoids (50%) for all six compounds.

Results and discussion

The structure determination of 1 shows that the compound contains one equivalent of each component without any remarkable intramolecular bond lengths or bond angles. The carboxylic acid moiety in methyl red is engaged in an expected intramolecular O–H···N hydrogen bond, similar to the contact observed in the structures of methyl red[14] and ethyl red, respectively.[15] The two different molecules in this co-crystal are interconnected primarily *via* a short (O···O 2.68 Å) and near-linear O–H···O (175°) hydrogen bond from 3,5-dintrobenzoic acid to one of the carboxylic acid oxygen atoms on methyl red, Fig. 2.

Neighbouring methyl red molecules are stacked in an antiparallel fashion at a distance of *ca.* 3.4 Å indicative of attractive π···π interactions. In addition, there are two relatively short heteromeric C–H···O contacts involving the carbonyl oxygen atom on 3,5-dinitrobenzoic acid (2.68 and

Table 1 Crystallographic data for 1–6

Compound	1	2	3
Systematic name	2-[4-(Dimethylamino)phenylazo]benzoic acid, 3,5-dinitrobenzoic acid	3-Nitrobenzoic acid, isonicotinamide	Isonicotinamide, 4-fluorobenzoic acid
Formula moiety	$(C_{15}H_{15}N_3O_2)(C_7H_4N_2O_6)$	$(C_7H_5NO_4)(C_6H_6N_2O)$	$(C_6H_6N_2O)(C_7H_5FO_2)$
Empirical formula	$C_{22}H_{19}N_5O_8$	$C_{13}H_{11}N_3O_5$	$C_{13}H_{11}FN_2O_3$
Molecular weight	481.42	289.25	262.24
Color, habit	Red plate	Colorless plate	Colorless prism
Melting point/°C	148–150 (dec)	160–162	153–155
Crystal system	Triclinic	Triclinic	Monoclinic
Space group, Z	P-1, 2	P-1, 2	$C2/c$, 8
a/Å	7.0051(5)	5.9827(4)	22.725(13)
b/Å	8.6187(7)	9.1713(8)	5.231(3)
c/Å	18.5866(15)	12.1893(8)	20.785(12)
α/°	101.186(2)	84.149(5)	90
β/°	97.114(2)	77.407(6)	95.402(11)
γ/°	101.401(2)	74.927(5)	90
Volume/Å^3	1063.66(14)	629.54(8)	2460(2)
Density/g cm^{-3}	1.503	1.526	1.416
Temperature/K	203(2)	203(2)	203(2)
X-ray wavelength/Å	0.71073	0.71073	0.71073
μ/mm^{-1}	0.117	0.12	0.112
Θ_{min}/°	2.27	1.71	1.8
Θ_{max}/°	28.21	28.27	26.55
Reflections collected	8137	4649	8008
Independent reflections	4765	2786	2520
Observed reflections	2692	1306	1070
Threshold expression	$>2\sigma(I)$	$>2\sigma(I)$	$>2\sigma(I)$
R_1 (observed)	0.0471	0.0464	0.0604
wR_2 (all)	0.1278	0.1036	0.1624

Compound	4	5	6
Systematic name	3,5-Dinitrobenzamide, 4-(dimethylamino)benzoic acid	4-Nitrobenzoic acid, 3-(dimethylamino)benzoic acid	Pyrazinecarboxamide, 4-nitrobenzamide
Formula moiety	$(C_7H_5N_3O_5)(C_9H_{11}NO_2)$	$(C_7H_5NO_4)(C_9H_{11}NO_2)$	$(C_5H_5N_3O)(C_7H_6N_2O_3)$
Empirical formula	$C_{16}H_{16}N_4O_7$	$C_{16}H_{16}N_2O_6$	$C_{12}H_{11}N_5O_4$
Molecular weight	376.33	332.31	289.26
Color, habit	red prism	orange-red plate	colorless prism
Melting point/°C	198–200	163–165	148–150
Crystal system	Triclinic	Triclinic	Triclinic
Space group, Z	P-1, 2	P-1, 2	P-1, 4
a/Å	8.0266(14)	7.1538(13)	7.6155(7)
b/Å	8.5974(16)	7.9978(15)	7.6980(9)
c/Å	12.514(2)	14.315(3)	21.587(2)
α/°	84.563(3)	91.111(3)	95.590(8)
β/°	89.934(4)	91.483(4)	94.719(7)
γ/°	75.345(3)	111.582(3)	90.268(8)
Volume/Å^3	831.5(3)	761.0(2)	1255.1(2)
Density/g cm^{-3})	1.503	1.45	1.531
Temperature/K	153(2)	153(2)	203(2)
X-ray wavelength/Å	0.71073	0.71073	0.71073
μ/mm^{-1}	0.12	0.113	0.119
Θ_{min}/°	1.64	1.42	1.9
Θ_{max}/°	28.24	26.37	28.27
Reflections collected	5780	4919	9111
Independent reflections	3682	3060	5621
Observed reflections	1658	1669	1659
Threshold expression	$>2\sigma$ (I)	$>2\sigma$ (I)	$>2\sigma$ (I)
R_1 (observed)	0.0519	0.0412	0.0569
wR_2 (all)	0.1297	0.115	0.1514

UM00012690
NOVARTIS EXHIBIT 1017
Novartis v. Regents, IPR2023-01346
Page 1436 of 4460

Table 2 Hydrogen-bond geometries for 1–6

	D-H	H···A	D···A	<(DHA)	Generator for A
1					
O28–H28···O7	0.81(2)	1.82(2)	2.6069(19)	163(2)	
O8–H8···N9	1.01(2)	1.58(2)	2.5353(19)	156(2)	
C13–H13···O25	0.94	2.45	3.184(2)	134.6	$-1+x, -1+y, -1+z$
2					
O27–H27···N11	1.11(2)	1.48(2)	2.584(2)	173.9(18)	
N17–H17A···O17	0.99(2)	1.91(2)	2.907(2)	178.4(19)	$3-x, -y, 2-z$
N17–H17B···O28	0.84(2)	2.21(2)	3.040(2)	169(2)	$1-x, 1-y, 2-z$
C12–H12···O29	0.94	2.43	3.356(3)	168.0	$2-x, 2-y, 1-z$
C24–H24···O30	0.94	2.47	3.248(3)	140.1	$-x, 3-y, 1-z$
3					
O17–H17···N1	1.04(3)	1.57(3)	2.608(3)	173(3)	
N7–H72···O18	0.93(3)	2.04(3)	2.964(3)	170(2)	$1-x, -1+y, 0.5-z$
C3–H3···O18	0.94	2.46	3.378(4)	165.3	$1-x, -1+y, 0.5-z$
N7–H71···O7	0.91(2)	2.00(3)	2.901(3)	177(2)	$1-x, -1-y, 1-z$
4					
N7–H71···O20	0.99(2)	1.95(3)	2.924(3)	167(2)	
N7–H72···O4	0.87(3)	2.19(3)	3.063(3)	177(2)	$1-x, -1+y, 0.5-z$
O19–H19···O7	1.01(3)	1.61(3)	2.618(2)	173(2)	
5					
O10–H10···O19	0.99(2)	1.60(2)	2.5941(18)	179.5(16)	
O20–H20···O9	0.95(2)	1.68(2)	2.6288(18)	174.9(19)	
C18–H18C···O7	0.98	2.44	3.340(2)	151.9	$x, 1+y, -1+z$
6					
N17–H171···O27	1.05(4)	1.88(4)	2.927(4)	175(3)	
N17–H172···O27	0.82(4)	2.27(4)	3.018(4)	152(4)	$1-x, -y, 1-z$
N27–H271···O17	1.14(3)	1.69(3)	2.828(4)	177(3)	
N27–H272···O37	0.86(3)	2.24(3)	3.056(4)	159(3)	
N37–H371···O47	1.01(4)	1.85(4)	2.856(4)	179(3)	
N47–H471···O37	1.06(3)	1.83(3)	2.876(4)	169(3)	
N47–H472···N31	0.88(3)	2.49(3)	3.153(4)	132(3)	$x, -1+y, z$
C13–H13···N34	0.94	2.50	3.328(5)	147.0	$-x, 1-y, 1-z$
N37–H372···N41	0.99(3)	2.52(3)	3.198(4)	126(3)	$x, 1+y, z$

2.69 Å, respectively). The main driving force for the assembly of this binary co-crystal is arguably the collection of heteromeric hydrogen bonds that take place between the two different building blocks, primarily the heteromeric O–H···O hydrogen bond.

The crystal structure of **2** shows that the two building blocks are connected into tetrameric supermolecules constructed from hydrogen bonds from the carboxylic acid (best donor) to the pyridine nitrogen atom (best acceptor), Fig. 3.

This allows neighbouring amide moieties to form a classic self-complementary N–H···O/O···H–N dimer. Neighbouring tetrameric supermolecules are connected laterally through an N–H···O hydrogen bond involving the anti-amide proton resulting in a layered structure. There are no remarkable π···π distances in this co-crystal. Again, the main driving force for the assembly of this binary co-crystal is undoubtedly the frequently occurring carboxylic acid···pyridine hydrogen bond.[4] Both R–COOH···py and R–OH···py hydrogen bonds have been previously used very effectively in the directed assembly of a large number of co-crystals, and these interactions represent some of the most reliable heteromeric hydrogen-bond interactions known.[16]

The crystal structure of **3** contains the expected tetrameric supermolecules with the same primary connectivity pattern as was observed in the supermolecules in **2**, Fig. 4. Adjacent supermolecules are also bridged *via* an N–H···O hydrogen bond involving the anti-amide proton, however, they are oriented almost perpendicular with respect to each other resulting in a more complex 3-D assembly compared to that observed in the crystal structure of **2**. The orthogonal nature of the assembly of supermolecules reduces opportunities for π···π stacking.

The intermolecular coupling of an aromatic monocarboxylic acid and isonicotinamide into a binary co-crystal follows directly from a hierarchical supramolecular strategy and demonstrates again that intermolecular reactions between pyridine-based molecules and carboxylic acids proceed in a high supramolecular yield.[4] By positioning the best hydrogen-bond donor and the best hydrogen-bond acceptor to different building blocks, the synthetic procedure is essentially programmed to provide a co-crystal.

Another example of a binary co-crystal prepared *via* heteromeric dimer formation is shown in the crystal structure of **4**. The carboxamide and the carboxylic acid moieties located on two different molecules preferentially interact in a heteromeric fashion instead of self-complementary acid···acid and amide···amide hydrogen-bonded dimers, Fig. 5.

The co-crystal of **5** contains two different carboxylic acids and the primary motif in this structure is a heteromeric dimeric feature, Fig. 6. As expected, the two inequivalent O–H···O hydrogen bonds within the dimer are short and near linear, providing an intermolecular driving force for the assembly of this binary structure. It is interesting to note that the O···O distance involving the most acidic proton is somewhat shorter than the O–H···O interaction involving the less acidic proton, 2.59 and 2.63 Å, respectively. This indicates that the relative strength of the hydrogen-bond donor is more important than the relative strength of the hydrogen-bond acceptor.[17]

Finally, the supramolecular reaction between 4-nitrobenzamide and pyrazinecarboxamide produced a crystalline solid with a melting point that was significantly different from that of either component, Table 3. In addition, ^{1}H NMR indicated that the product contained the two components in a 1 : 1 stoichiometry. At this stage there was no reason to suspect that this co-crystal would yield any unexpected motifs. However, the crystal structure determination of **6** did indeed reveal some very unusual and unpredictable intermolecular interactions, Fig. 7.

Instead of having the primary intermolecular interactions between different molecules, each building block is engaged in a self-complementary, homomeric, amide···amide dimer. In fact, the different building blocks seem almost oblivious to one another and although there is a relatively short C–H···N

UM00012691
NOVARTIS EXHIBIT 1017
Novartis v. Regents, IPR2023-01346
Page 1437 of 4460

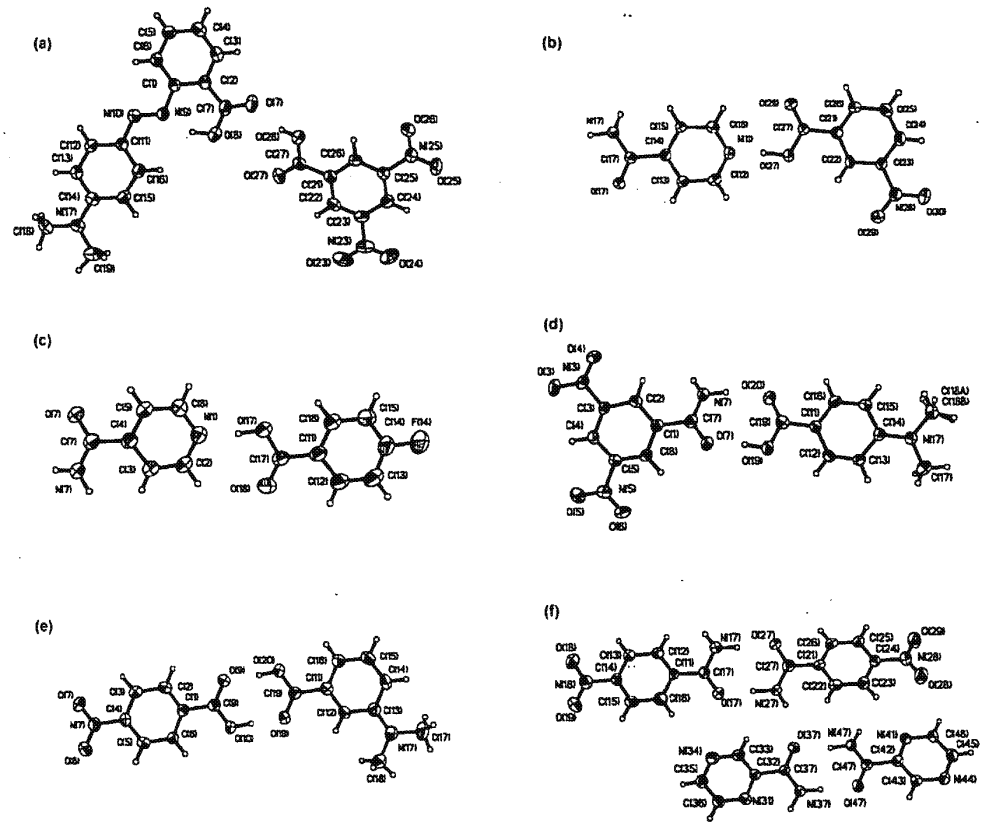


Fig. 1 (a) Molecular geometry of 1. (b) Molecular geometry of 2. (c) Molecular geometry of 3. (d) Molecular geometry of 4. (e) Molecular geometry of 5. (f) Molecular geometry of 6.

contact between homodimers, this type of interaction would have been equally possible (for steric reasons) if the co-crystal had been constructed from heteromeric dimers.

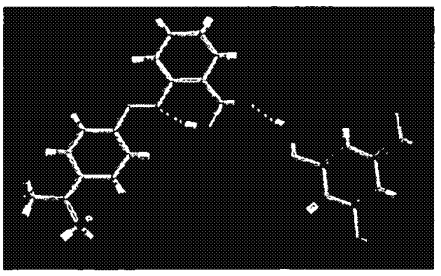


Fig. 2 The heteromeric O–H···O interaction between the two components in 1. Click here for a 3D view of Fig. 2.

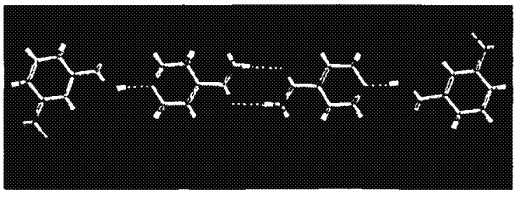


Fig. 3 A tetrameric supermolecule in 2 held together by a heteromeric acid···pyridine interaction and a self-complementary amide···amide dimeric interaction. Click here for a 3D view of Fig. 3.

This structure exists even though the intermolecular interactions fail to obey an important guideline for the supramolecular assembly of binary co-crystals; there are no preferential intermolecular interactions between the two molecules and the two components are located in ribbon-like motifs running parallel along the *y* axis, Fig. 8.

Furthermore, the crystal structure of 4-nitrobenzamide[18]

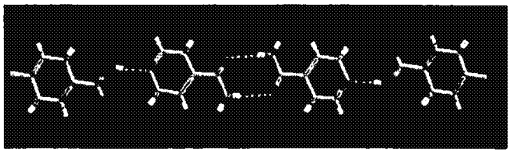


Fig. 4 A tetrameric supermolecule in 3 held together by a heteromeric acid···pyridine interaction and a self-complementary amide···amide dimeric interaction. Click here for a 3D view of Fig. 4.

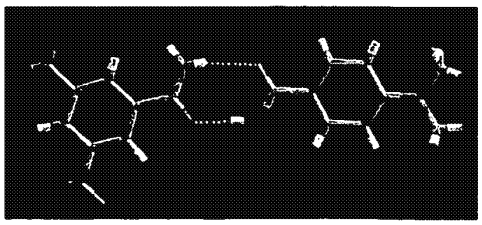


Fig. 5 The heteromeric acid···amide dimeric interaction driving the formation of a binary co-crystal in 4. Click here for a 3D view of Fig. 5.

UM00012692
NOVARTIS EXHIBIT 1017
Novartis v. Regents, IPR2023-01346
Page 1438 of 4460

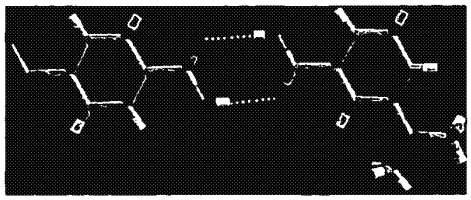


Fig. 6 The heteromeric acid···acid dimeric interaction driving the formation of a binary co-crystal in 5. Click here for a 3D view of Fig. 6.

Table 3 Melting points for 1–6 and for their individual constituents

Compound (A:B)	Mp A/°C	Mp B/°C	Mp A:B/°C
3,5-Dinitrobenzoic acid methyl red	205–207	179–182	148–150(d)
3-Nitrobenzoic acid isonicotinamide	140–142	155–157	160–162
4-Fluorobenzoic acid isonicotinamide	184–187	155–157	153–155
4-(N,N-dimethylamino)benzoic acid 3,5-dinitrobenzamide	241–243	183–185	198–200
3-(N,N'-dimethylamino) benzoic acid 4-nitrobenzoic acid	148–150	239–245	163–165
4-Nitrobenzamide pyrazinecarboxamide	199–201	189–191	148–150

contains the same dimeric interaction as is observed between adjacent 4-nitrobenzamide molecules in **6**. There are also significant similarities between the intermolecular interactions in the crystal structure of pyrazinecarboxamide and the way in which neighbouring pyrazinecarboxamide molecules interact in the crystal structure of **6**, Fig. 9. From these observations one would readily conclude that the individual components are relatively unrestricted in how they assemble within the co-crystal, which makes the crystal structure of **6** even more difficult to rationalise. What is the driving force for the formation of this particular co-crystal?

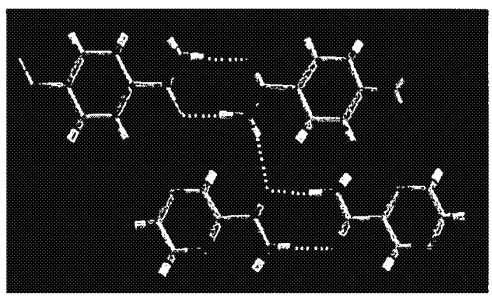


Fig. 7 Two homomeric dimers in the binary co-crystal of **6**. Click here for a 3D view of Fig. 7.

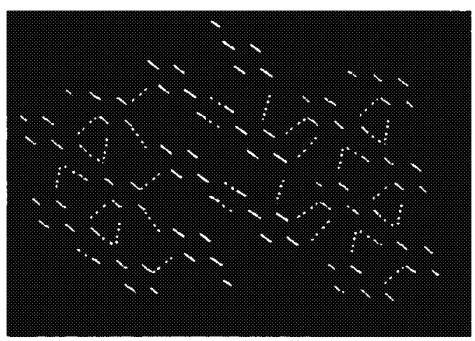


Fig. 8 Hydrogen-bonded ribbons of pyrazinecarboxamide (red) and 4-nitrobenzamide (green) in the binary co-crystal of **6**. Click here for a 3D view of Fig. 8.

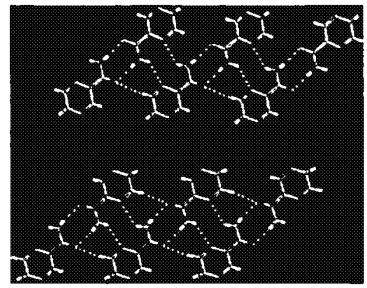


Fig. 9 Top: infinite ribbons in the crystal structure of pyrazinecarboxamide. Bottom: infinite ribbon of pyrazinecarboxamide in the co-crystal of **6**.

Conclusions

We have not been able to identify any strong or weak intermolecular interactions present in **6**, which could not have been generated just as readily if the co-crystal had been composed of heterodimers instead. This absence of pronounced heteromeric interactions in binary molecular solids is very rare indeed; one such example is in the crystal structure of 3,5-dinitrobenzoic acid 4-(N,N'-dimethylamino)benzoic acid (1 : 1). This structure represented the only case, in a series of ten acid···acid co-crystals, where two homomeric dimers were formed in preference to one heteromeric dimer.[19] The proposed explanation for the existence of homomeric dimers was based upon a lack of opportunities for C–H···O interactions and favourable π···π interactions. Unfortunately, a similar explanation can not be called upon in order to explain the lack of heterodimers in **6**, as pyrazinecarboxamide forms the same number of weaker C–H···O hydrogen bonds by itself as it does when it is part of the solid in **6**. Furthermore, the presence of homomeric motifs in **6** also runs contrary to earlier structural studies that have shown how heterodimers in acid···acid co-crystals,[20] motifs gain increased stability due to the variation in hydrogen-bond donating/accepting ability of the two different carboxylic acid moieties.[21]

The overriding conclusion from this structural study (amply supported by directly relevant crystallographic data available from the CSD) is very clear. In order to convince two different discrete chemical species to co-exist in a molecular co-crystal there needs to be some specific molecular-recognition based reason for their solid-state union. Although individual structures that defy rationalisation will appear from time to time, there is no doubt that the important 'big picture' reveals structural trends, patterns of behaviour, and reproducible motifs that, when combined, can be developed into a library of high-yielding supramolecular reactions.

CCDC reference numbers 224989–224994. See http://www.rsc.org/suppdata/ce/b3/b315181f for crystallographic data in CIF format.

Acknowledgements

Financial support from NSF (CHE-0316479) and Kansas State University is gratefully acknowledged.

References

1 C. B. Aakeröy, *Acta Crystallogr., Sect. B*, 1997, 53, 569; C. B. Aakeröy and A. M. Beatty, *Aust. J. Chem.*, 2001, 54, 409; *Crystal engineering: From molecules and crystals to materials*, A

UM00012693
NOVARTIS EXHIBIT 1017
Novartis v. Regents, IPR2023-01346
Page 1439 of 4460

NATO Advanced Study Institute and a Euroconference, ed. D. Braga, F. Grepioni and A. G. Orpen, Erice, Italy, 1999, 538; CrystEngComm Discussion 1; Innovation in Crystal Engineering (http://www.rsc.org/is/journals/current/crystengcomm/discussion.htm); G. R. Desiraju, *Angew. Chem., Int. Ed. Engl.*, 1995, **34**, 2311.
2 J. D. Dunitz, in *Perspectives in Supramolecular Chemistry: The Crystal as a Supramolecular Entity*, ed. G. R. Desiraju, Wiley, 1995.
3 We favor the term "co-crystal" in preference to "molecular complex" see J. D. Dunitz, *CrystEngComm*, 2003, **5**, 506; G. R. Desiraju, *CrystEngComm*, 2003, **5**, 466.
4 C. B. Aakeröy, A. M. Beatty and B. A. Helfrich, *J. Am. Chem. Soc.*, 2002, **124**, 14425.
5 M. C. Etter, *J. Phys. Chem.*, 1991, **95**, 4601.
6 M. C. Etter, *Acc. Chem. Res.*, 1990, **23**, 120.
7 P. Dauber and A. T. Hagler, *Acc. Chem. Res.*, 1980, **13**, 105–112.
8 J. A. R. P. Sarma and G. R. Desiraju, *J. Chem. Soc., Perkin Trans. 2*, 1985, 1905; C. Huang, L. Leiserowitz and G. M. Schmidt, *J. Chem. Soc., Perkin Trans. 2*, 1973, 503; F. Pan, W. S. Wong, V. Gramlich, C. Bosshard and P. Gunter, *Chem. Commun.*, 1996, **2**; J. A. Zerkowski, J. C. MacDonald and G. M. Whitesides, *Chem. Mater.*, 1997, **9**, 9; R.-F. Liao, J. W. Lauher and F. W. Fowler, *Tetrahedron*, 1996, **52**, 3153; N. Shan, A. D. Bond and W. Jones, *Cryst. Eng.*, 2002, **5**, 9; V. R. Pedireddi, W. Jones, A. P. Chorlton and R. Docherty, *Chem. Commun.*, 1996, 997; P. Vishweshwar, A. Nangia and V. M. Lynch, *J. Org. Chem.*, 2002, **67**, 556; C. B. Aakeröy, A. M. Beatty, M. Nieuwenhuyzen and M. Zou, *Tetrahedron*, 2000, **56**, 6693; C. B. Aakeröy, A. M. Beatty and M. Zou, *Cryst. Eng.*, 1998, **3**(4), 225; R. D. Bailey Walsh, M. W. Bradner, S. Fleischman, L. A. Morales, B. Moulton, N. Rodriguez-Hornedo and M. J. Zaworotko, *Chem. Commun.*, 2003, 186; L. R. MacGillivray, J. L. Reid and J. A. Ripmeester, *J. Am. Chem. Soc.*, 2000, **122**, 7817.
9 C. B. Aakeröy, A. M. Beatty and B. A. Helfrich, *Angew. Chem. Int. Ed.*, 2001, **40**, 3240.
10 2-(4'-(dimethylamino)phenylazo)benzoic acid.
11 SMART v5.060, © 1997–1999, Bruker Analytical X-ray Systems, Madison, WI.
12 SAINT v6.02, © 1997–1999, Bruker Analytical X-ray Systems, Madison, WI.
13 SHELXTL v5.10, © 1997, Bruker Analytical X-ray Systems, Madison, WI.
14 D. Moreiras, J. Solans, X. Solans, C. Miravitlles, G. Germain and J. P. Declerq, *Cryst. Struct. Commun.*, 1980, **9**, 921.
15 S. Lovell, Dept. Biochemistry, Univ. Wisconsin, USA, Private communication, 2000.
16 G. S. Papaefstathiou and L. R. MacGillivray, *Org. Lett.*, 2001, **3**, 3835; T. L. Nguyen, F. W. Fowler and J. W. Lauher, *J. Am. Chem. Soc.*, 2001, **123**, 11057; L. R. MacGillivray, J. L. Reid and J. A. Ripmeester, *J. Am. Chem. Soc.*, 2000, **122**, 7817; B. R. Bhogala and A. Nangia, *Cryst. Growth Des.*, 2003, **3**, 547; U. Kumar, T. Kato and J. M. J. Frechet, *J. Am. Chem. Soc.*, 1992, **114**, 6630; G. T. R. Palmore, T.-J. M. Luo, M. T. McBride-Wieser, E. A. Picciotto and C. M. Reynoso-Paz, *Chem. Mater.*, 1999, **11**, 3315.
17 This can be rationalized by noting that the differences of the charge/size ratio for the acidic protons in different carboxylic acids are going to be larger than the corresponding changes in 'basicity' for the carbonyl oxygen atom on different acids.
18 F. di Rienzo, A. Domenicano and E. Foresti Serantoni, *Acta Crystallogr., Sect. B*, 1977, **33**, 3854.
19 C. V. K. Sharma, K. Panneerselvam, T. Pilati and G. R. Desiraju, *J. Chem. Soc., Perkin Trans. 2*, 1993, 2209.
20 L. R. Hanton, C. A. Hunter and D. H. Purvis, *J. Chem. Soc., Chem. Commun.*, 1992, 1134; M. C. Etter, *Acc. Chem. Res.*, 1990, **23**, 120.
21 M. C. Etter and G. M. Frankenbach, *Chem. Mater.*, 1989, **1**, 10.

UM00012694
NOVARTIS EXHIBIT 1017
Novartis v. Regents, IPR2023-01346
Page 1440 of 4460

This Page is Inserted by IFW Indexing and Scanning Operations and is not part of the Official Record

BEST AVAILABLE IMAGES

Defective images within this document are accurate representations of the original documents submitted by the applicant.

Defects in the images include but are not limited to the items checked:

- ☐ BLACK BORDERS
- ☐ IMAGE CUT OFF AT TOP, BOTTOM OR SIDES
- ☐ FADED TEXT OR DRAWING
- ☐ BLURRED OR ILLEGIBLE TEXT OR DRAWING
- ☐ SKEWED/SLANTED IMAGES
- ☐ COLOR OR BLACK AND WHITE PHOTOGRAPHS
- ☐ GRAY SCALE DOCUMENTS
- ☐ LINES OR MARKS ON ORIGINAL DOCUMENT
- ☐ REFERENCE(S) OR EXHIBIT(S) SUBMITTED ARE POOR QUALITY
- ☐ OTHER: _____

IMAGES ARE BEST AVAILABLE COPY.
As rescanning these documents will not correct the image problems checked, please do not report these problems to the IFW Image Problem Mailbox.

J|A|C|S
ARTICLES
Published on Web 11/09/2002

A High-Yielding Supramolecular Reaction

Christer B. Aakeröy,*,† Alicia M. Beatty,‡ and Brian A. Helfrich†

Contribution from the Department of Chemistry, Kansas State University, Manhattan, Kansas and the Department of Chemistry and Biochemistry, University of Notre Dame, Notre Dame, Indiana

Received July 24, 2002

Abstract: The X-ray crystal structure determinations of twelve cocrystals involving *iso*-nicotinamide and a variety of carboxylic acids have revealed a very consistent pattern of hydrogen-bond preferences. The combination of a monocarboxylic acid, an amide, and a pyridine moiety leads, in every case, to discrete "supermolecules" (consisting of two molecules of *iso*-nicotinamide and two molecules of the relevant carboxylic acid) with well-defined and robust connectivity. The two dominant (regularly occurring) supramolecular synthons in these crystal structures are (1) the heteromeric carboxylic acid···pyridine hydrogen bond and (2) a self-complementary amide···amide hydrogen-bond interaction, both of which prevail in the presence of widely differing chemical functionalities. In four of these cocrystals, a dicarboxylic acid is employed, which alters the structural outcome from discrete entities to infinite assemblies (or to a hexameric complex in a "U-shaped" dicarboxylic acid), which is fully expected since the two primary supramolecular synthons remain intact. This structural study shows that *iso*-nicotinamide is a supramolecular reagent that can produce well-defined supermolecules (containing carboxylic acids) in very high yields.

Introduction

Intermolecular forces are responsible for the extraordinarily specific way in which molecules can interact to form a highly ordered crystalline material.[1] Once positioned within a lattice, the communication between these molecules is also governed by intermolecular interactions and this ensemble of interactions ultimately defines the physical properties and reactivity of any given solid. It should be no surprise then that an improved understanding of noncovalent interactions[2] is an important interdisciplinary research goal.[3] The ability to utilize molecular recognition processes in the construction of supermolecules or extended architectures is particularly important in supramolecular synthesis and crystal engineering, where molecules or ions, not atoms, act as building blocks of new materials, and noncovalent forces are employed as synthetic tools.

Much of the fundamental work in current crystal engineering is geared toward developing reliable supramolecular reactions, where the success and efficiency of a reaction can be judged by the frequency of occurrence of desired intermolecular interactions and connectivities. The probability that a certain motif will appear in a crystalline lattice is, in many ways, a measure of the yield of a supramolecular reaction. Just as a covalent synthetic chemist searches for ways in which a specific reaction can be promoted or prevented, a supramolecular chemist tries to identify the experimental regime where a supramolecular synthon prevails despite competition from other noncovalent forces.

While it is important to acknowledge that every intermolecular force will have some influence on the outcome of a crystallization process, it is self-evident that some noncovalent forces are more significant than others.[4] To further develop reliable supramolecular reactions based on robust supramolecular synthons,[5] it is therefore essential to determine (whenever possible) the relative influence of, and balance between, competing intermolecular interactions.[6-8] In this context, Etter formulated an empirical guideline regarding the hierarchy of hydrogen-bond interactions,[9] "the best hydrogen-bond donor and the best hydrogen-bond acceptor will preferentially form hydrogen bonds to one another"—a consequence of this statement is that the second-best donor will form a hydrogen bond to the second-best acceptor, and so forth. If this idea is coupled with the fact that a few intermolecular interactions can provide a significant part of the lattice energy of a molecular solid,[10] it is reasonable to surmise that directed assembly of multicomponent networks of predictable connectivity may be accomplished with just a few well-chosen supramolecular synthons. In recent years, efforts have been made to identify robust supramolecular synthons, and the reliability of homomeric self-

* Address correspondence to this author. E-mail: aakeroy@ksu.edu.
† Kansas State University.
‡ University of Notre Dame.

(1) Desiraju, G. R. *Crystal Engineering: The Design of Organic Solids*; Elsevier: Amsterdam, 1989.
(2) Steiner, T. *Angew. Chem., Int. Ed.* **2002**, *41*, 48.
(3) Aakeröy, C. B. *Acta Crystallogr.* **1997**, *B53*, 569. Zaworotko, M. J. *Chem. Commun.* **2001**, 1. Nangia, A.; Desiraju, G. R. *Top. Curr. Chem.* **1998**, *198*, 57. Nangia, A.; Desiraju, G. R. *Acta Crystallogr.* **1998**, *A54*, 934.
(4) Lehn, J.-M. *Supramolecular chemistry: concepts and perspectives*; VCH: Weinheim, 1995.
(5) Desiraju, G. R. *Angew. Chem., Int. Ed. Engl.* **1995**, *34*, 2311.
(6) Aakeröy, C. B.; Beatty, A. M.; Helfrich, B. A.; *Angew. Chem., Int. Ed.* **2001**, *40*, 3240.
(7) Lynch, D. E.; McClenaghan, I. *Acta Crystallogr.* **2001**. *C57*, 830.
(8) Nguyen, T. L.; Fowler, F. W.; Lauher, J. W. *J. Am. Chem. Soc.* **2001**, *123*, 11057.
(9) Etter, M. C. *Acc. Chem. Res.* **1990**, *23*, 120.
(10) Dauber, P.; Hagler, A. T. *Acc. Chem. Res.* **1980**, *13*, 105.

10.1021/ja027845q CCC: $22.00 © 2002 American Chemical Society

UM00012696
NOVARTIS EXHIBIT 1017
Novartis v. Regents, IPR2023-01346
Page 1442 of 4460

complementary pair-wise hydrogen bonds, for example, carboxylic acid···carboxylic acid, amide···amide, oxime···oxime, and 2-pyridone···2-pyridone, have been established through extensive structural[11] or database studies.[12] Some heteromeric pair-wise interactions are particularly robust, for example, carboxylic acid···pyridine,[13,14] hydroxy···pyridine,[15] and hydroxy···amine,[16] and these heteromeric interactions have allowed for the assembly of a range of binary cocrystals.[17] However, to add more versatility and refinement to crystal engineering, it is necessary to further explore the possibility of "ranking" different supramolecular synthons. Crystal engineering and noncovalent synthesis based on such a dominance hierarchy of intermolecular interactions would set the stage for highly modular design principles that would enable the directed assembly of multicomponent heteromeric structures in high supramolecular yields.

Herein, we describe a systematic crystallographic study of the competition between three prevalent hydrogen-bonding moieties; carboxylic acid, primary amide, and pyridine. The main reason for choosing these particular moieties is that they are ubiquitous in biochemistry as well as in materials science, and versatile supramolecular synthesis requires assembly strategies that take advantage of (and tolerate) the interplay between common chemical functional groups. The objectives of this particular study are to establish the presence of preferential hydrogen-bond interactions and to determine how a supramolecular reaction is likely to proceed in the presence of all three components. Despite the preponderance of carboxylic acids, amides, and pyridine-based molecules, only a handful of crystal structures that contain all three fragments simultaneously have been reported.[18] The paucity of suitable crystal structures containing all three moieties means that we are not able to establish reliable patterns of behavior based on existing crystallographic data. Hence, the necessary structural data have been obtained through the syntheses and single-crystal structure determinations of cocrystals of *iso*-nicotinamide with a wide range of aromatic and aliphatic carboxylic acids.

Table 1. Compound Names and Melting Points for **1**−**12**

compound	melting point
cinnamic acid: *iso*-nicotinamide (**1**)	146−148 °C
3-hydroxybenzoic acid: *iso*-nicotinamide (**2**)	144−146 °C
3-*N*,*N*-dimethylaminobenzoic acid: *iso*-nicotinamide (**3**)	138−140 °C
3,5-bis(trifluoromethyl)benzoic acid: *iso*-nicotinamide (**4**)	160−163 °C
d,*l*-mandelic acid: *iso*-nicotinamide (**5**)	168−170 °C
chloroacetic acid: *iso*-nicotinamide (**6**)	95−98 °C
fumaric acid monoethyl ester: *iso*-nicotinamide (**7**)	92−95 °C
12-bromododecanoic acid: *iso*-nicotinamide (**8**)	88−90 °C
fumaric acid: 2 *iso*-nicotinamide (**9**)	145−148 °C
succinic acid: 2 *iso*-nicotinamide (**10**)	134−136 °C
4-ketopimelic: 2 *iso*-nicotinamide (**11**)	111−114 °C
thiodiglycolic: 2 *iso*-nicotinamide (**12**)	138−140 °C

Experimental Section

Synthesis. Stoichiometric amounts (one *iso*-nicotinamide per monocarboxylic acid, two *iso*-nicotinamides per dicarboxylic acid) of the two compounds were dissolved in warm ethanol. The solutions were then cooled to room temperature and crystals formed upon slow evaporation (anywhere from hours to days) of the solvent. Melting points for **1**−**12** are given in Table 1.

X-ray Crystallography. Crystalline samples of **1**−**12** were placed in inert oil, mounted on a glass pin, and transferred to the cold gas stream of the diffractometer. Crystal data were collected and integrated using a Bruker SMART 1000 system, with graphite monochromated Mo−Kα (λ = 0.71073 Å) radiation. The structures were solved by direct methods using SHELXS-97 and refined using SHELXL-97.[19] Non-hydrogen atoms were found by successive full matrix least-squares refinement on F^2 and refined with anisotropic thermal parameters. Hydrogen atom positions were located from difference Fourier maps and a riding model with fixed thermal parameters [$u_{ij} = 1.2U_{ij}$(eq) for the atom to which they are bonded] was used for subsequent refinements. Table 2 provides crystallographic details for **1**−**12**, and the molecular geometries and numbering scheme are shown in Figure 1a−l.

Results

Thermal analyses and X-ray powder diffraction[20] of **1**−**12** revealed that only one new phase was present in each experiment, and single-crystal X-ray diffraction demonstrated that all twelve structures were composed of molecular cocrystals of *iso*-nicotinamide and the relevant acid. The ratio of *iso*-nicotinamide to acid was 1:1 when monocarboxylic acids were employed (**1**−**8**) and 2:1 when dicarboxylic acids were used (**9**−**12**). The structural data, supported by IR spectroscopy, confirmed that no proton transfer had taken place in any of these structures.[21]

(11) Leiserowitz, L. *Acta Crystallogr.* **1976**, *B32*, 775. Leiserowitz, L.; Tuval, M. *Acta Crystallogr.* **1978**, *B34*, 1230. Dunitz, J. D. *Pure Appl. Chem.* **1991**, *63*, 177.

(12) Allen, F. H.; Motherwell, W. D. S.; Raithby, P. R.; Shields, G. P.; Taylor, R. *New J. Chem.* **1999**, *1*, 25.

(13) Some examples of crystal structures containing intermolecular carboxylic acid···pyridine hydrogen bonds: Kane, J. J.; Liao, R.-F.; Lauher, J. W.; Fowler, F. W. *J. Am. Chem. Soc.* **1995**, *117*, 12003. Grunert, M.; Howie, R. A.; Kaeding, A.; Imrie, C. T. *J. Mater. Chem.* **1997**, *7*, 211. Vishweshwar, P.; Nangia, A.; Lynch, V. M. *J. Org. Chem.* **2002**, *67*, 556. Palmore, G. T. R.; Luo, T.-J. M.; McBride-Wieser, M. T.; Picciotto, E. A.; Reynoso-Paz, C. M. *Chem. Mater.* **1999**, *11*, 3315. Aakeröy, C. B.; Beatty, A. M.; Tremayne, M.; Rowe, D. M. *Cryst. Growth Des.* **2001**, *1*, 377. Sharma, C. V. K.; Zaworotko, M. J. *Chem. Commun.* **1996**, 2655. Pedireddi, V. R.; Chatterjee, S.; Ranganathan, A. *Tetrahedron* **1998**, *54*, 9457. Amai, M.; Endo, T.; Nagase, H.; Ueda, H.; Nakagaki, M. *Acta Crystallogr.* **1998**, *C54*, 1367.

(14) A search of the CSD (V. 5.23) for structures containing both carboxylic acids and 2,6-unsubstituted pyridine (excluding *N*-alkylpyridines and pyridine-*N*-oxides) resulted in over fifty hits; the overwhelming majority of these structures contain a complementary acid···pyridine hydrogen bond (see Supporting Information).

(15) Huang, K.-S.; Britton, D.; Etter, M. C.; Byrn, S. R. *J. Mater. Chem.* **1997**, *7*, 713. MacGillivray, L. R.; Reid, J. L.; Ripmeester, J. A. *J. Am. Chem. Soc.* **2000**, *122*, 7817.

(16) Ermer, O.; Eling, A. *J. Chem. Soc., Perkin Trans. 2* **1994**, 925.

(17) A few examples of binary cocrystals based on principles of molecular recognition are Sarma, J. A. R. P.; Desiraju, G. R. *J. Chem. Soc., Perkin Trans., 2* **1985**, 1905. Huang, C.; Leiserowitz, L.; Schmidt, G. M. *J. Chem. Soc., Perkin Trans. 2* **1973**, 503. Tamura, C.; Sakurai, N.; Sato, S. *Bull. Chem. Soc. Jpn.* **1971**, *44*, 1473. Pan, F.; Wong, M. S.; Gramlich, V.; Bosshard, C.; Gunter, P. *Chem. Commun.* **1996**, 2. LeFur, Y.; Bagieu-Beucher, M.; Masse, R.; Nicoud, J. F.; Levy, J. P. *Chem. Mater.* **1996**, *8*, 8. Zerkowski, J. A.; MacDonald, J. C.; Whitesides, G. M. *Chem. Mater.* **1997**, *9*, 9. Liao, R.-F.; Lauher, J. W.; Fowler, F. W. *Tetrahedron* **1996**, *52*, 3153. Shan, N.; Bond, A. D.; Jones, W. *Cryst. Eng.* **2002**, *5*, 9. Pedireddi, V. R.; Jones, W.; Chorlton, A. P.; Docherty, R. *Chem. Commun.* **1996**, 997.

(18) Throughout this manuscript we will deal only with molecular species where there have been no proton transfer from acid to pyridine.

(19) Sheldrick, G. M. University of Göttingen,

(20) In all cases, there was a satisfactory match between the experimental powder X-ray diffraction pattern and the simulated pattern on the basis of the single-crystal data. Furthermore, it was not possible to detect any significant amounts of un-reacted *iso*-nicotinamide or carboxylic acid. These observations were supported by DSC measurements, which did not indicate any appreciable amounts of starting materials. A combination of these data suggests that an estimate of crystal yields of **1**−**12** of no less than 90% would be conservative (see Supporting Information for representative examples of DSC and XRD data).

(21) Chloroacetic acid is the strongest carboxylic acid employed in this study (pK_a = 2.7, Kartrum, G.; Vogel, W.; Andrussov, K. *Constants of Organic Acids in Aqueous Solution*; Butterworth: London, 1961), and proton transfer did not take place between *iso*-nicotinamide and any of the twelve acids presented in this study. It is, of course, possible to protonate *iso*-nicotinamide with stronger organic acids (e.g., maleic acid) or with mineral acids but it has not yet been possible to establish the precise conditions for when a salt will be formed in preference to a molecular cocrystal.

UM00012697
NOVARTIS EXHIBIT 1017
Novartis v. Regents, IPR2023-01346
Page 1443 of 4460

Table 2. Data Collection, Structure Solution, and Refinement Parameters for **1**–**12**

compound	**1**	**2**	**3**	**4**
formula	$C_{30}H_{28}N_4O_6$	$C_{13}H_{12}N_2O_4$	$C_{15}H_{17}N_3O_3$	$C_{15}H_{10}F_6N_2O_3$
MW	270.28	260.25	287.32	380.25
color, habit	colorless, plates	colorless, prisms	colorless, plates	colorless, blocks
crystal system	triclinic	monoclinic	monoclinic	triclinic
space group, *Z*	*P*-1, 2	*C*2/*c*, 8	*C*2/*c*, 8	*P*-1, 2
a (Å)	8.4779(8)	22.419(3)	27.360(8)	7.349(3)
b (Å)	10.703(1)	5.1408(6)	5.311(2)	8.748(3)
c (Å)	15184(1)	20.867(3)	20.180(6)	12.555(5)
α (deg)	75.560(2)			81.605(7)
β (deg)	81.882(2)	97.717(2)	101.541(6)	82.488(6)
γ (deg)	82.980(2)			78.004(6)
V (Å^3)	1315.5(2)	2383.1(5)	2872.(1)	776.7(5)
density (g/cm^3)	1.365	1.451	1.329	1.626
temperature (K)	173(2)	173(2)	203(2)	203(2)
X-ray wavelength	0.71073	0.71073	0.71073	0.71073
$M_{(MoK\alpha)}$ (mm^{-1})	0.097	0.110	0.095	0.161
θ range (deg)	1.97–28.28	1.83–28.22	1.52–22.27	1.65–24.01
reflections collected	8842	8091	6222	4161
independent reflections (R_{int})	5641 (0.0176)	2768 (0.0595)	1830 (0.0427)	2438 (0.0349)
R(F), R_w(F)	0.0440, 0.0614	0.0418, 0.0667	0.0556, 0.0999	0.0685, 0.1249

compound	**5**	**6**	**7**	**8**
formula	$C_{19}H_{22}N_4O_7$	$C_8H_9C_lN_2O_3$	$C_{12}H_{14}N_2O_5$	$C_{18}H_{29}BrN_2O_3$
MW	418.41	216.62	266.25	401.34
color, habit	colorless, plates	colorless, plates	colorless, needles	colorless, blocks
crystal system	triclinic	monoclinic	monoclinic	triclinic
space group, *Z*	*P*-1, 2	*C*2/*c*, 8	*P*2$_1$/*n*	*P*-1, 2
a (Å)	6.667(1)	21.031(3)	3.8803(6)	6.783(1)
b (Å)	8.433(2)	5.1179(7)	7.822(1)	8.363(1)
c (Å)	17.964(4)	19.845(3)	42.606(7)	17.949(3)
α (deg)	78.697(4)			98.148(3)
β (deg)	82.533(4)	117.344(2)	91.238(4)	91.846(3)
γ (deg)	88.018(4)			107.580(3)
V (Å^3)	981.9(4)	1897.3(5)	1293.0(4)	957.8(3)
density (g/cm^3)	1.415	1.517	1.368	1.392
temperature (K)	173(2)	203(2)	203(2)	203(2)
X-ray wavelength	0.71073	0.71073	0.71073	0.71073
$M_{(MoK\alpha)}$ (mm^{-1})	0.110	0.385	0.108	2.164
θ range (deg)	1.17–28.34	2.18–28.28	0.96–28.27	1.15–26.39
reflections collected	6729	6279	8273	6219
independent reflections (R_{int})	4355 (0.0180)	2203 (0.0141)	2974 (0.0515)	3910 (0.0218)
R(F), R_w(F)	0.0469, 0.0755	0.0350, 0.0440	0.0449, 0.0908	0.0370, 0.0695

compound	**9**	**10**	**11**	**12**
formula	$C_8H_8N_2O_3$	$C_8H_9N_2O_3$	$C_{14}H_{14}N_2O_4$	$C_{16}H_{18}N_4O_6S$
MW	180.16	181.17	274.27	394.40
color, habit	colorless, rods	colorless, rods	colorless, plates	colorless, prisms
crystal system	triclinic	triclinic	monoclinic	monoclinic
space grooup, *Z*	*P*-1, 2	*P*-1, 2	*P*2(1)/*c*, 4	*P*2(1)/*c*, 4
a (Å)	6.8062(9)	6.8317(7)	5.2275(8)	8.912(2)
b (Å)	7.0018(6)	7.0624(6)	27.857(5)	13.628(3)
c (Å)	8.9692(5)	9.0970(9)	9.245(2)	15.266(3)
α (deg)	80.745(6)	80.495(7)		
β (deg)	78.314(6)	77.573(6)	99.678(3)	105.301(4)
γ (deg)	73.474(9)	72.777(8)		
V (Å^3)	398.85(7)	406.98(7)	1327.2(4)	1788.4(6)
density (g/cm^3)	1.500	1.478	1.373	1.465
temperature (K)	203(2)	203(2)	173(2)	203(2)
X-ray wavelength	0.71073	0.71073	0.71073	0.71073
$M_{(MoK\alpha)}$ (mm^{-1})	0.117	0.115	0.102	0.224
θ range (deg)	2.33–25.00	2.31–24.99	1.46–28.22	2.04–24.78
reflections collected	1780	1818	9180	9802
independent reflections (R_{int})	1394 (0.0073)	1427 (0.0273)	3044 (0.0588)	3057 (0.0491)
R(F), R_w(F)	0.0325, 0.0860	0.0397, 0.0535	0.0527, 0.1065	0.0448, 0.0931

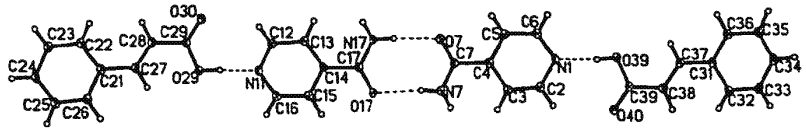
Since the primary intermolecular interactions were the same throughout **1**–**12**, the descriptive part of the twelve crystal structures will be relatively limited.[22]

All eight structures that involve monocarboxylic acids, **1**–**8**, contain a "supermolecule"[23] constructed from two molecules of the carboxylic acid and two molecules of *iso*-nicotinamide, Figure 1a–h. This tetrameric supermolecule is held together by two robust supramolecular synthons, a carboxylic acid···pyridine interaction, and a self-complementary amide···amide pair-wise hydrogen bond (in each case the carboxylic acid adopts a syn conformation). An N···H–O hydrogen bond between a

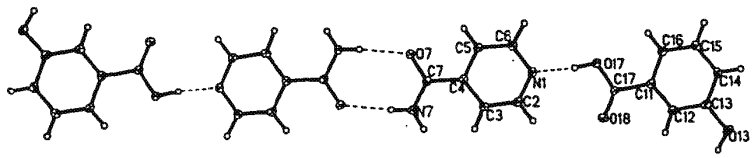
(22) Furthermore, since the aim of this study is the intermolecular interactions, specific details of the intramolecular geometries (which were all within expected values) will not be discussed. For information about hydrogen-bond geometries, see Supporting Information.

(23) The term supermolecule used here indicates a discrete 0-dimensional species composed of molecular building blocks, assembled via directional noncovalent forces. Thus, ternary systems formed by ionic interactions (salts) or by incorporation of solvent molecules within a lattice (e.g., clathrates, heterosolvates, or inclusion compounds) are distinctly different from the supermolecules that we discuss in this paper.

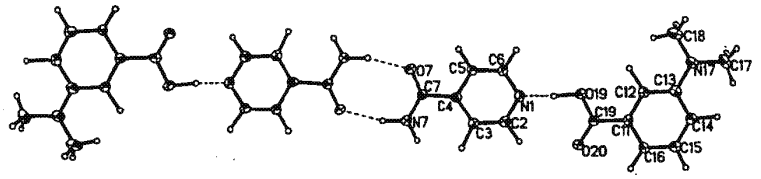
UM00012698
NOVARTIS EXHIBIT 1017
Novartis v. Regents, IPR2023-01346
Page 1444 of 4460



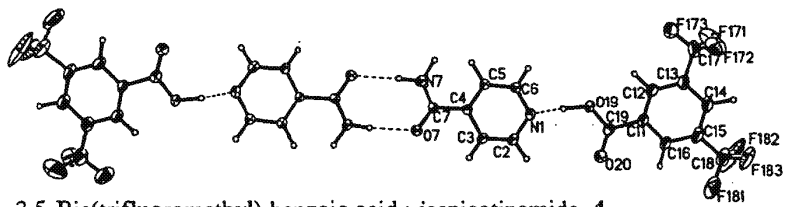
a. Cinnamic acid : isonicotinamide, **1**



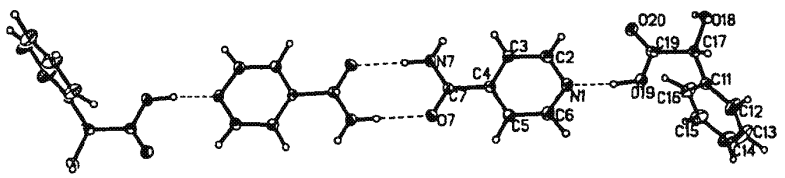
b. 3-Hydroxybenzoic acid : *iso*nicotinamide, **2**



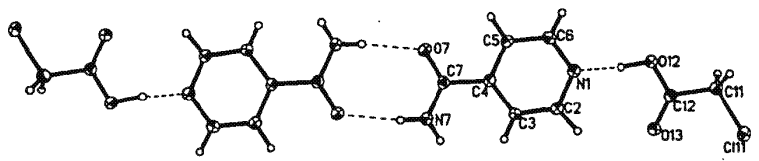
c. 3-N,N-dimethylaminobenzoic acid : *iso*nicotinamide, **3**



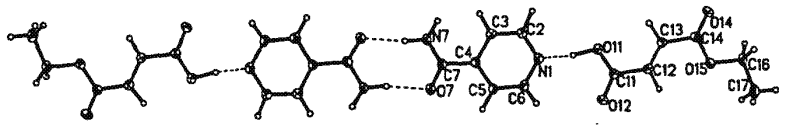
d. 3,5-Bis(trifluoromethyl)-benzoic acid : *iso*nicotinamide, **4**



e. *d,l*- Mandelic acid : *iso*nicotinamide, **5**

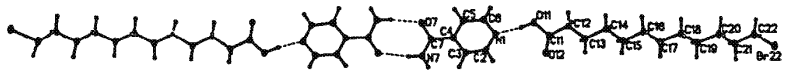


f. Chloroacetic acid : *iso*nicotinamide, **6**

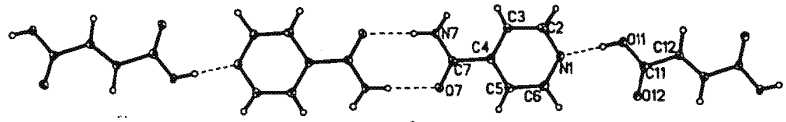


g. Fumaric acid monoethyl ester: *iso*nicotinamide, **7**

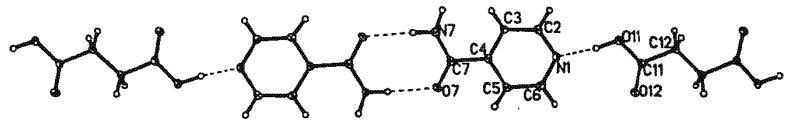
UM00012699
NOVARTIS EXHIBIT 1017
Novartis v. Regents, IPR2023-01346
Page 1445 of 4460



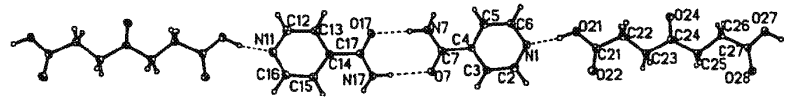
h. 12-Bromododecanoic acid : *iso*nicotinamide, **8**



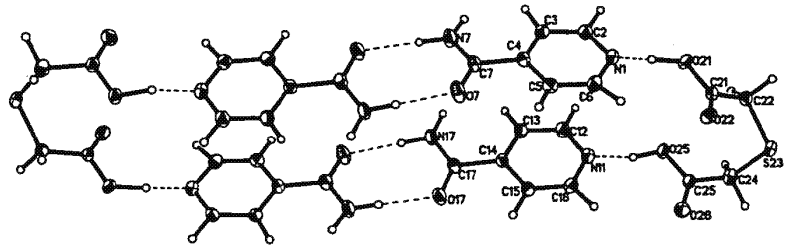
i. Fumaric acid : 2 *iso*nicotinamide, **9**



j. Succinic acid : 2 *iso*nicotinamide, **10**



k. 4-Ketopimelic acid : 2 *iso*nicotinamide, **11**



l. Thiodiglycolic acid : 2 *iso*nicotinamide, **12**

Figure 1. a–l. Molecular geometries, labeling schemes, and primary hydrogen-bond interactions in **1**–**12**.

2,6-unsubstituted pyridine molecule and a carboxylic acid is sometimes accompanied by a stabilizing C–H···O hydrogen bond.[24] However, this interaction does not seem to play an important role in **1**–**12**; neighboring pyridine···carboxylic acid moieties within "supermolecules" in this set of structures frequently deviate from a coplanar arrangement. Furthermore, the C–H...O distances display dramatic variations (H···O, 2.56–3.59 Å; C···O 3.27–3.96 Å), which indicate that the formation (and importance) of the O–H···N hydrogen bond is not necessarily the result of a pair-wise C–H···O/N···H–O supramolecular synthon.

The resulting supermolecules in **1**–**8** exist in two different conformations; a flexibility that is due to the possibility of "rotation" around the two O–H···N hydrogen bonds, Figure 1a–h. Given an overall near-planar geometry of the supermolecules, the carbonyl moieties of the carboxylic acids and the amides (four in total) can be organized in a trans-trans-trans manner (I), Scheme 1a (observed in **1**–**3**, **5**–**6**, **8**, and **11**), or they can be arranged in a cis-trans-cis configuration (II), Scheme 1b (observed in **4**, **7**, **9**–**10**, **12**).

(24) Steiner, T.; Desiraju, G. R. *The Weak Hydrogen Bond in Structural Chemistry and Biology*; Oxford University Press: New York, 1999.

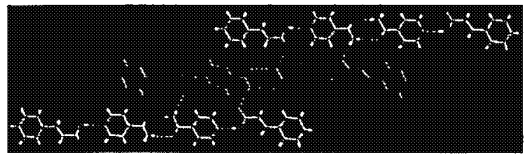


Figure 2. An example of a one-dimensional ribbon in the crystal structure of **1**; the C=O moieties are arranged in trans-trans-trans manner (conformation "I") within each tetrameric supermolecule. One supermolecule highlighted in red.

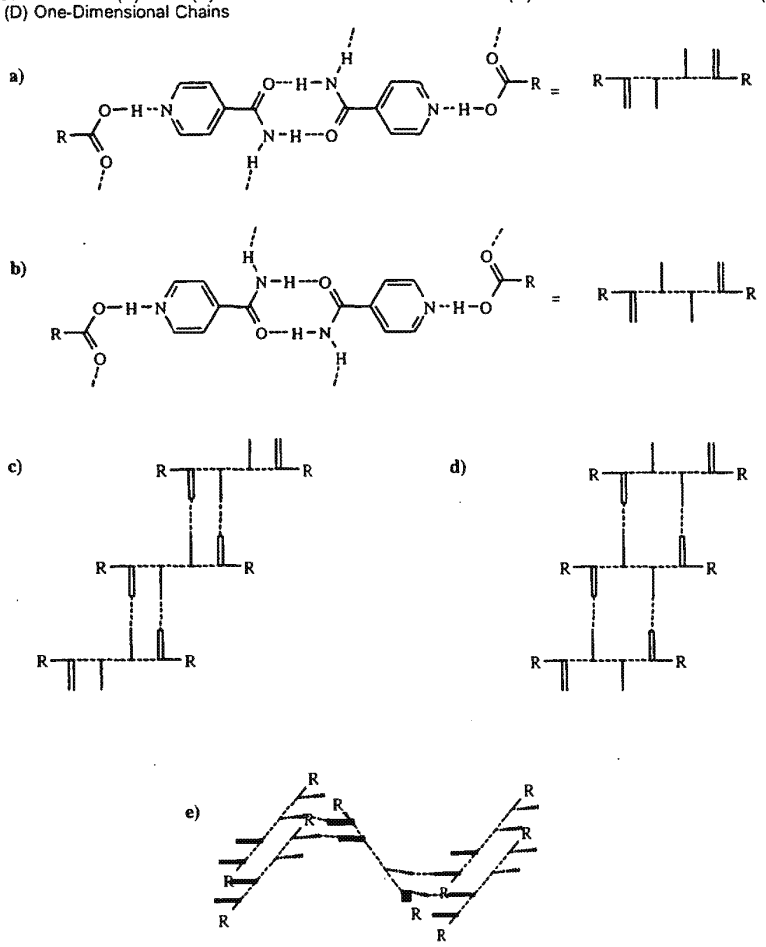
These conformational differences dictate (or are the result of) the way in which these supermolecules are positioned with respect to each other resulting in supramolecular isomerism.[25] For example, neighboring supermolecules with the (I)-conformation are interconnected via the *anti*-amide proton and a carbonyl oxygen atom resulting in infinite 1-D ribbons, Figure 2, or in a cross-linked 2-D network, Figure 3.

Supermolecules with the alternative conformation (II) also form infinite ribbons through N–H···O hydrogen bonds, but the horizontal displacement of supermolecules in adjacent ribbons is now slightly smaller, Figure 4.

(25) Moulton, B.; Zaworotko, M. J. *Chem. Rev.* **2001**, *101*, 1629.

UM00012700
NOVARTIS EXHIBIT 1017
Novartis v. Regents, IPR2023-01346
Page 1446 of 4460

Scheme 1. The Two Conformations (A) I and (B) II Present in **1**–**8**. I Results in Either (C) One-Dimensional Chains or (E) Two-Dimensional Networks. II Leads to (D) One-Dimensional Chains



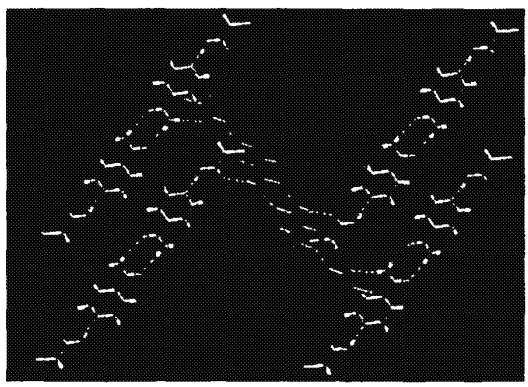


Figure 3. An example of a cross-linked network as observed in the crystal structure of **6** (conformation "I"). One supermolecule highlighted in red.

In the reactions between dicarboxylic acids and *iso*-nicotinamide, the results are again molecular cocrystals but this time in a ratio of two molecules of *iso*-nicotinamide for every dicarboxylic acid, Figure 1i–l. All four of these structures,

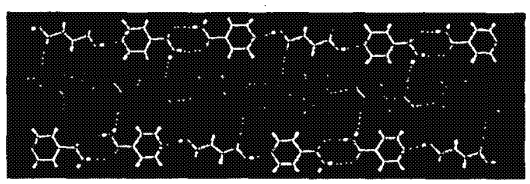


Figure 4. An example of a two-dimensional sheet as found in the crystal structure of **7**. The C=O moieties are positioned in a cis-trans-cis manner, conformation "II". Part of one infinite chain highlighted in red.

9–**12**, contain the same primary supramolecular synthons as were observed in **1**–**8**; each dicarboxylic acid forms two expected acid···pyridine hydrogen bonds, and neighboring *iso*-nicotinamide molecules are connected via homomeric self-complementary amide···amide interactions. The fact that the three dicarboxylic acids in **9**–**11** are ditopic means that the resulting dominating supramolecular motifs in these structures are infinite 1-D chains instead of discrete 0-dimensional entities. In **12**, which does contain a dicarboxylic acid, the primary structural motif is a hexameric supermolecule, which is a result of the observed "U-conformation" of thiodiglycolic acid—the

UM00012701
NOVARTIS EXHIBIT 1017
Novartis v. Regents, IPR2023-01346
Page 1447 of 4460

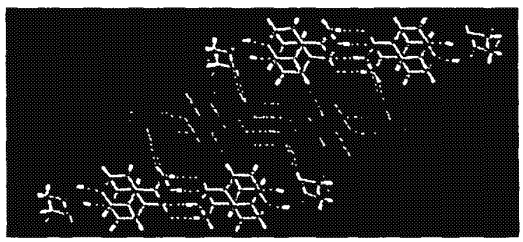


Figure 5. A one-dimensional ribbon composed of hexameric supermolecules (one of the supermolecules highlighted in red) observed in **12**.

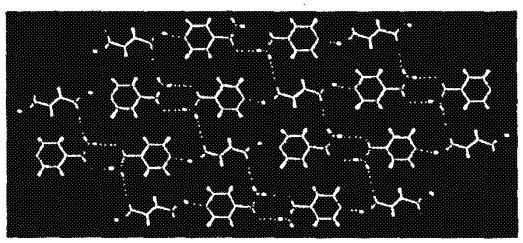
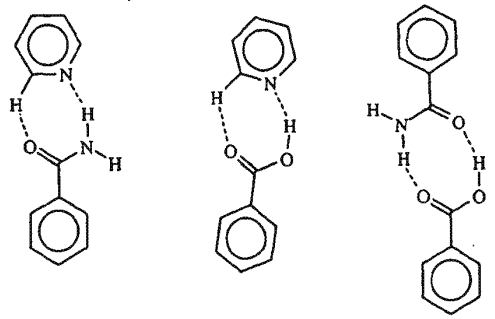


Figure 6. The two-dimensional sheet observed in the crystal structure of **9**; C=O moieties in conformation "II".

Scheme 2. Three Heteromeric Interactions Involving Pyridine, Carboxylic Acid, and Primary Carboxamide (All of Which Are Found in the CSD)



six components are held together by two amide···amide and four acid···pyridine interactions, Figure 11. Neighboring supermolecules are connected into infinite ribbons, Figure 5.

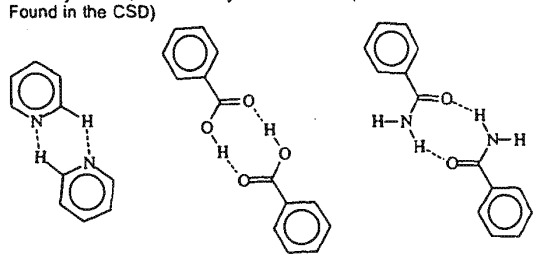
As was the case with the supermolecules in **1**−**8**, two different conformations of the infinite chains can be envisaged (with respect to the relative orientations of the C=O bonds) and one example of how the infinite chains are interconnected into 2-D sheets through N−H···O hydrogen bonds is shown in Figure 6.

Discussion

In theory, an attempted cocrystallization of a carboxylic acid, an amide, and a pyridine-based molecule could result in a plethora of intermolecular interactions and products, in particular since these three moieties are known to form a variety of different heteromeric, Scheme 2, and homomeric, Scheme 3, supramolecular synthons.

However, the supramolecular reaction between *iso*-nicotinamide and a variety of aromatic/aliphatic mono- and dicarboxylic acids does, in fact, proceed in high yield. We have obtained twelve molecular cocrystals containing discrete supermolecules

Scheme 3. Three Homomeric Interactions Involving Pyridine, Carboxylic Acid, and Primary Carboxamide (All of Which Are Found in the CSD)



(**1**−**8**, **12**) or infinite architectures (**9**−**11**) that are all constructed from exactly the same primary supramolecular synthons (a) an acid···pyridine interaction and (b) a self-complementary amide···amide pair of hydrogen bonds.

Reaction conditions have not been varied significantly (in each case the reagents were introduced in a consistent manner; one equivalent of *iso*-nicotinamide per carboxylic acid moiety), but the chemical, geometric, and structural nature of the different acids employed in this study cover a significant range. As a consequence, the resulting supermolecules vary widely in shape, size, and functionalization. The tetrameric supermolecule containing chloroacetic acid (a very short aliphatic carboxylic acid) is 24 Å long (from Cl to Cl) whereas the 12-bromododecanoic analogue, **8**, is 50 Å long (from Br to Br). Likewise, the supermolecules in **2**, **4**, and **7** (which are all about the same length, 35 Å), contain −OH, $-CF_3$, and $-OC(=O)CH_3$ substituents, respectively. Furthermore, this supramolecular reaction can be carried out with aliphatic (seven structures) as well as with aromatic (five structures) carboxylic acids. Since these materials contain very different supermolecules, it is not surprising that physical properties vary significantly. For example, an examination of the melting points of **1**−**12** shows that three compounds, **6**−**8**, are much lower melting than the remaining members in this study. A possible reason for this may be the fact that since these three cocrystals contain aliphatic monocarboxylic acids, they are unable to participate in stabilizing π···π interactions and they also cannot form infinite architectures held together by strong hydrogen bonds. The remaining cocrystals, which all melt at temperatures above 110 °C, contain either (a) dicarboxylic acids that generate 1-D extended structures or (b) aromatic carboxylic acids.

Just as different molecules crystallize with a variety of 3-D assembly patterns and crystallographic parameters, the supermolecules in **1**−**12** adopt several different crystal structures. In other words, *iso*-nicotinamide can be viewed as a supramolecular reagent capable of acting upon carboxylic acids in the construction of predictable extended assemblies with well-defined connectivity. The versatility of this reaction is further illustrated by the fact that this reagent is capable of producing either discrete or infinite assemblies.

It is inevitable that certain carboxylic acids in combination with *iso*-nicotinamide will provide exceptions, supramolecular byproducts, compared to the structures observed in this study. However, this does not detract from the importance of *iso*-nicotinamide as a useful supramolecular reagent. Comparisons with organic chemistry are inevitable—very few covalent reactions lead to quantitative yields and most standard organic

UM00012702
NOVARTIS EXHIBIT 1017
Novartis v. Regents, IPR2023-01346
Page 1448 of 4460

substitution or coupling reactions are subject to specific reaction conditions (e.g., absence of certain functional groups). To develop more sophisticated supramolecular chemistry, it is therefore necessary to identify a wide range of supramolecular reagents, each of them with the ability to direct the assembly of families of compounds into predictable networks or supermolecules.

In conclusion, we have shown that a hierarchical view of intermolecular interactions based on structural trends, probabilities, and patterns of behavior can support a modular approach to noncovalent assembly thus providing reliable and transferable guidelines for pragmatic supramolecular synthesis.

Acknowledgment. We are grateful for financial support from NSF (CHE-0078996) and Kansas State University.

Supporting Information Available: X-ray crystallographic files (CIF) and representative DSC and powder X-ray diffraction data (experimental and simulated). This material is available and free of charge via the Internet at http://pubs.acs.org.

JA027845Q

UM00012703
NOVARTIS EXHIBIT 1017
Novartis v. Regents, IPR2023-01346
Page 1449 of 4460

The Hydrogen Bond and Crystal Engineering†

Christer B. Aakeröy and Kenneth R. Seddon
Department of Chemistry, David Keir Building, The Queen's University of Belfast, Belfast BT9 5AG, Northern Ireland

1 Introduction

The purpose of this review is to present a philosophy of crystal engineering. The chemist is comfortable and familiar with intramolecular bonding; our advanced knowledge of synthetic chemistry (which could almost be considered as the *raison d'être* of the chemist) is constructed around our understanding of the essential principles of covalent bonding. Less well-known and acceptable are the concepts of intermolecular bonds between molecules and/or ions (even the field of supramolecular chemistry has only just established itself),[1,2] and our understanding of the factors which control crystal habit and morphology is rudimentary. The chemist, in designing molecules, rarely turns his attention to the crystalline form which that molecule will adopt in the solid state. The crystal form is usually a matter of serendipity; the ubiquitous occurrence of polymorphism (see Section 4.4) is either ignored or treated as a problem beyond control.

We present here our thoughts on the field of 'crystal engineering', which has been advanced in recent years by the elegant synthetic work and shrewd topological analysis of Margaret Etter.[3] This is a field in its infancy; it is at the interface between a number of demanding disciplines, and has all the challenge and excitement expected of interdisciplinary research. We present the hydrogen bond as a synthetic 'vector' for granting topological control over crystalline form, and hence control over such crucial physical phenomena as optical properties, thermal stability, solubility, colour, conductivity, crystal habit, and mechanical strength. The significance of this area to industry and academia cannot be overstated.

2 The Hydrogen Bond

The object of this section is not to define in detail what a hydrogen bond is, nor to exhaustively record experimental techniques for studying it, but to raise healthy questions in the mind of the reader. The field of hydrogen bonding tends to be clouded by preconception and prejudice about the nature, strength, occurrence, and importance of the hydrogen bond. It is hoped that, by the end of this review, the reader will not dismiss it as a weak bond of relatively marginal importance to material chemists.

2.1 What is a Hydrogen Atom?

This is not a rhetorical question, and nor are we the first to raise it. The following is quoted verbatim from a recent paper by Cotton and Luck:[4]

> 'There is a kind of conventional wisdom that neutron diffraction finds hydrogen atoms better than *X*-ray diffraction does. But is this even a meaningful statement, let alone a true one? It can be argued that it is not meaningful and thus incapable of being true. The simple facts are that neutrons and *X*-rays see two different parts of the hydrogen atom and that these parts do not coincide. It is then a Solomonic question whether either technique is justifiably considered to 'see' the hydrogen atom. The neutron experiment sees, with considerable accuracy (*ca.* ± 0.001 Å), the location of the hydrogen atom's *nucleus, the proton*. In a very favourable case [. . .], the *X*-ray experiment sees, with less accuracy (*ca.* ± 0.02 Å), the hydrogen atom's *electron cloud*. Which of these is '*the* hydrogen atom'? Both the nucleus and the electron density of an atom are essential parts, and it is therefore impossible to assert rationally that the position of either the one or the other is 'the' position of the atom.'

Only Cotton has the standing, insight, and gall to ask questions like this in a manuscript primarily concerned with the crystal and molecular structure of (diethylbis(1-pyrazolyl)borato)allyldicarbonylmolybdenum(II)! It is a pity that this manuscript, principally of interest to organometallic chemists, may not attract the universal readership that it deserves. The question raised is of fundamental importance, and should be considered carefully and seriously by all chemists, especially those with a

† This review is dedicated to the memory of Professor Margaret C. Etter, whose contributions to the field of crystal engineering have been of inestimable value; her vital enthusiasm and inspired insights will be sadly missed.

Christer Björn Aakeröy, although of Norwegian extraction, was educated in Sweden where he obtained an M.Sc. at Uppsala University in 1986. His participation in the Sussex–Uppsala exchange programme resulted in further studies at the University of Sussex where he acquired a D.Phil. in 1990. He remained as a Research Fellow and was then awarded a Scholarship from the Royal Swedish Academy of Science. This enabled him to spend nine months as a Research Fellow at the University of Minnesota where he worked in the laboratory of the late Professor Etter. He has recently accepted a Lectureship in Inorganic Chemistry at the Queen's University of Belfast.



Professor K. R. Seddon was appointed to the Chair of Inorganic Chemistry at the Queen's University of Belfast earlier this year; he was previously Reader in Experimental Chemistry at the University of Sussex. His principal research interests include chemistry in ionic liquids, novel materials for non-linear optics, crystal engineering, coordination chemistry (especially of the metal halides), and the application of chemical techniques to the identification of dyes and mordants in ancient papers and textiles. He is co-author of a book 'The Chemistry of Phosgene and Related Carbonyl Halides' which will be published in 1994.



UM00012704
NOVARTIS EXHIBIT 1017
Novartis v. Regents, IPR2023-01346
Page 1450 of 4460

central interest in hydrogen bonding. If there is not universal agreement about the absolute positon of a hydrogen atom in a molecule or lattice, how can serious qualitative and quantitative studies of its bonding be made? In other words, if we are not sure what we mean by a hydrogen atom, how can we enter detailed discussions and calculations on hydrogen bonding?

2.2 What is a Hydrogen Bond?

Again, this is not a rhetorical question: currently, a definitive answer does not exist. Ideas of what constitutes a hydrogen bond are in a constant state of flux. The following quotes, arranged chronologically, may illustrate the nature of the problem of producing even a simple definition:

Latimer and Rodebush (1920)[5]

'Water [...] shows tendencies both to add and give up hydrogen, which are nearly balanced. Then [...] a free pair of electrons on another water molecule might be able to exert sufficient force on a hydrogen held by a pair of electrons on another water molecule to bind the two molecules together. [...]. Indeed the liquid may be made up of large aggregates of molecules, continually breaking up and reforming under the influence of thermal agitation. [...]. Such an explanation amounts to saying that the hydrogen nucleus held between two octets constitutes a weak 'bond'.'

Pauling (1940)[6]

'It has been recognized in recent years that under certain conditions an atom of hydrogen is attracted by rather strong forces to two atoms, instead of only one, so that it may be considered to be acting as a bond between them. This is called the *hydrogen bond*. It is now recognized that [...] the hydrogen bond is largely ionic in character, and is formed only between the most electronegative atoms. [...]. Although the hydrogen bond is not a strong bond (its bond energy [...] being only about 5 kcal/mole†), it has great significance in determining the properties of substances.'

Pimentel and McClellan (1960)[7]

'A hydrogen bond exists between a functional group A–H and an atom or a group of atoms B in the same or a different molecule when:

(a) there is evidence of bond formation (association or chelation),

(b) there is evidence that this new bond linking A–H and B specifically involves the hydrogen atom already bonded to A.'

Zeegers-Huyskens and Huyskens (1991)[8]

'Specific interactions are short-range site-bounded cohesion forces that considerably weaken a given chemical bond of one of the partners. Hydrogen bonding constitutes a particular case of specific interactions where the weakened chemical bond involves a hydrogen atom and a more electronegative one (in general O, N, S, halogens).'

Attempts at simpler explanations seem doomed to failure. The following quotation could form the basis of a critical finals examination question:

Atkins (1989)[9]

'A hydrogen bond is a link formed by a hydrogen atom lying between two strongly electronegative atoms.'

This has the seductive appeal of appearing correct at first sight, but being in error in almost every detail and at every level of understanding.

The problems of defining the hydrogen bond are manifest. All too frequently, current descriptions of hydrogen bonds include phrases which refer to them as 'involving hydrogen bonded to an electronegative atom', 'thermodynamically weak', or 'essentially ionic in nature'. As can be seen, these hark back to Pauling,[6] a definition that was insightful and visionary when proposed, but now should be viewed with the hindsight of fifty years of chemical progress: although many hydrogen bonds do fall within Pauling's definition, it is now too restrictive, and precludes many examples of intermolecular bonding now universally accepted as hydrogen bonding (*e.g.* C–H···O). Many definitions are empirical, usually boiling down to 'a hydrogen bond exists where there is evidence that it exists'. Theoretical descriptions of the hydrogen bond are rapidly improving, but are extraordinarily sensitive to details of the basis set, and to electron-correlation effects: there is not yet general agreement as to whether, in weak hydrogen bonds, D–H···A, there is any significant electron density in the H···A bond (*i.e.* is a hydrogen bond essentially electrostatic in nature, or is there a significant covalent contribution). This review is not the correct place to extend this controversy, fascinating though it is. A detailed, multidisciplinary study of this area is greatly needed – an updated and expanded version of the seminal volumes edited by Schuster *et al.*[10] is long overdue.

Perhaps the last words in this Section should go to Samuel Butler:

'A definition is the enclosing a wilderness of idea within a wall of words.'

Notebooks (1912)

We will thus not attempt a formal definition here, but draw from the descriptions above as appropriate, recognizing that the value of the hydrogen-bond concept lies in the wilderness of idea, and not within the wall of words.

2.3 Occurrence of Hydrogen Bonds

Hydrogen bonds occur between atoms, molecules, or ions (positive or negative) in the gas, liquid, solid, or supercritical phases. Hydrogen bonds may be simple (involving only one donor and one acceptor), bifurcated (three-centre), or trifurcated (four-centre) (see Figure 1). Some hydrogen bond donors and acceptors are given in Table 1. However, there are now examples of aliphatic methylene protons acting as hydrogen bond donors,[4] and transition metals,[4] alkenes,[11] alkynes,[11] and aromatic π-clouds[12] acting as hydrogen bond acceptors. Moreover, it could be convincingly argued that even the hydrogen atom is not essential to a hydrogen bond, and that lithium could be described, in the wilderness of idea, as 'hydrogen bonds'.[13]

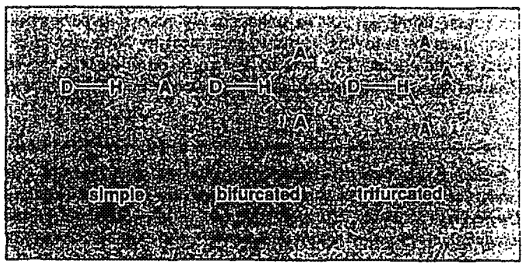


Figure 1 Common hydrogen bond arrangements: note that the simple bond is rarely linear.

2.4 Characterization and Effects of Hydrogen Bonding

Let us consider the simple, and most common, arrangement for a hydrogen bond (see Figure 1). In this description, where r(D–H) is shorter than r(H···A), the element D is referred to as a hydrogen bond donor, and the element A as a hydrogen bond acceptor. Most hydrogen-bond acceptors (see Table 1) have one feature in common: they formally possess a lone-pair of electrons in conventional formalisms. Some unusual acceptors, such as transition metals, alkenes, and aromatic π-clouds, all have centres of high electron density (an occupied d_{z^2} orbital, or the π-molecular orbitals). Similarly, the elements, D, of the hydrogen

† 5 cal mol^{-1} = 20.92 kJ mol^{-1}.

UM00012705
NOVARTIS EXHIBIT 1017
Novartis v. Regents, IPR2023-01346
Page 1451 of 4460

Table 1 Some hydrogen bond donors and acceptors

Donors	Acceptors
C–H	C=C, C≡C, arenes
N–H	N
P–H	P
O–H	O
S–H	S
F–H	F
Cl–H	Cl
Br–H	Br
I–H	I

bond donors (or, to be more precise, the functional groups or moieties of which D is a part) have the effect of removing electron density from the hydrogen atom, leaving it with a significant partial positive charge. Note, however, that this has little to do with our outmoded ideas of electronegativity (a concept that is perhaps best left for heated tutorial debates about the validity of imprecise definitions, and about the use of terms such as 'atoms within molecules'), and a lot more to do with the overall electronic structure of the molecule of which D–H forms a part. Thus, methane does not readily form strong directional hydrogen bonds (although methane activation WILL occur *via* a mechanism involving initial hydrogen bond formation, when a viable system is discovered), whereas *all* the C–H ring protons of the imidazolium cation form three-dimensional, structure-determining hydrogen-bonded networks.[14]

Clearly, then, a hydrogen bond cannot be defined in terms of the elements which might partake in it. Nevertheless, certain elements and functional groups exhibit a higher propensity than others to form hydrogen bonds, and it is these (which were, of course, the earliest recognized and most easily detected) which formed the basis of the Pauling definition (see Section 2.2).

So, how is a hydrogen bond detected? Its nett effect, in the system D–H···A is to weaken the D–H bond (compared with D–H in an isolated system), and this is the basis of the Zeegers-Huyskens and Huyskens definition (see Section 2.2).[8] Thus, a wide ranging collection of spectroscopic, structural, and thermodynamic techniques can be used to study the nature of hydrogen bonding, the most common being IR and NMR spectroscopy, and single-crystal *X*-ray diffraction (see Section 3). The use of these techniques, and many others, has been extensively reviewed elsewhere.[7,8,10]

2.5 Strength of the Hydrogen Bond

The thermodynamic strength of a hydrogen bond is, as might be expected, extremely variable.[7,8,10] For neutral molecules, it normally lies in the range of 10—65 kJ mol^{-1}, being greater than that found for van der Waals interactions (< 8 kJ mol^{-1}), but weaker than conventional covalent bonds. However, when one component of the hydrogen bond is ionic, the range of bond strengths rises to 40—190 kJ mol^{-1}. In order to place the strength of a hydrogen bond in perspective, a summary of some typical σ-bond strengths is presented in Figure 2, along with some of the stronger characterized hydrogen bonds (between an ion and a neutral molecule).[8,15] It is clear that a strong hydrogen bond is energetically on a par with a weak covalent bond.

3 Hydrogen Bonding in Crystals

3.1 Philosophy

In many areas of chemistry, an *X*-ray single-crystal structure determination of a novel compound represents the solution to a particular problem, or the end of a specific project: the cynosure is usually the identity of the molecule itself, or some particular feature within its molecular structure. An alternative view, however, would be to treat the structural information as the beginning of a new venture, leading to questions of far reaching

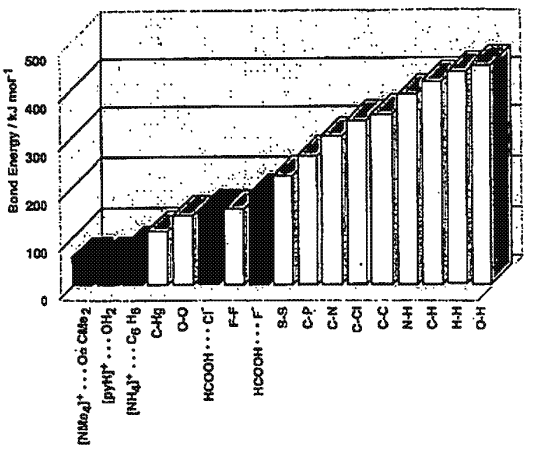


Figure 2 Bond energies for a range of common σ-bonds compared with a number of the stronger hydrogen bonds.

and fundamental importance regarding the interrelationships between molecules and ions in the solid state.

Since the crystal structure represents a situation where all the bonding and non-bonding forces are poised at an energetic minimum (not necessarily a global minimum!), it contains all the information regarding the importance of, and balance between, intermolecular forces. If this information could be extracted and deconvoluted, then prospects of designing materials with specific properties would be vastly enhanced. Consequently, it is of great importance to improve our understanding of the forces that determine the structures of crystalline materials, and single-crystal data provide a natural starting point.

3.2 Hydrogen-bond Geometry in Crystals

The existence of hydrogen bonds in solids is often detected and determined purely by applying geometric criteria.[7,16] These criteria, when based solely upon estimated van der Waals radii, are somewhat controversial,[17] and there have been several suggestions as to which radii are 'correct'.[6,18,19] Depending upon which set is chosen, certain interactions may, or may not, be regarded as 'legimate' hydrogen bonds. This is clearly not an ideal situation, but there are no better ways to discriminate between very weak hydrogen bonds and close contacts generated by lattice forces, especially since this question is difficult to answer unambiguously with current experimental techniques.

Nevertheless, several important publications containing tabulated data and statistical analyses of the known geometries of a wide range of hydrogen-bonded materials are available.[10,16] These studies, in combination with the information available in the Cambridge Structural Database,† constitute a vital base from which our understanding of solid-state hydrogen bonds can be developed.

Many surveys have correlated geometries of hydrogen bonds in the solid state with the nature and environment of the donor and acceptor groups, and some important trends have been identified.[7,10,11,16] It has been demonstrated that longer, weaker hydrogen bonds are more likely to deviate from a linear arrangement. Furthermore, it is more common for N–H···O bonds to deviate from linear arrangements than it is for O–H···O bonds, even when their bond distances are similar. In addition, the covalent D–H bond is also found to be influenced by the H···A

† Details available from: Dr. Olga Kennard, Cambridge Structural Database, Cambridge Crystallographic Data Centre, CAMBRIDGE CB2 1EW, U.K.

UM00012706
NOVARTIS EXHIBIT 1017
Novartis v. Regents, IPR2023-01346
Page 1452 of 4460

distance: a shorter H···A bond will lead to a longer D–H bond, as shown in Figure 3.

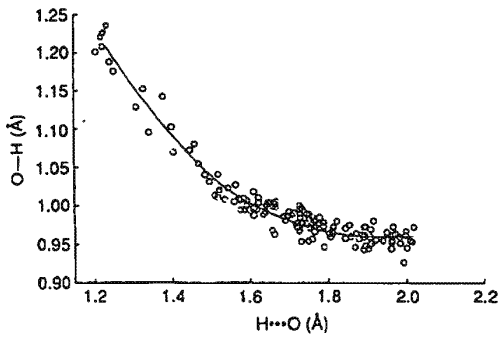


Figure 3 O–H distance as a function of H···O distance in a O–H···O system.
(Reproduced with permission from reference 10.)

In recent years, the importance, and frequency, of relatively weak interactions have been widely recognized, *e.g.* it has become clear that C–H···X hydrogen bonds (where X = F, O, N, Cl, Br, or I)[14,16,20] may be of significant importance to the organization of the solid-state. Situations where C–H groups are found to participate in C–H···X hydrogen bonds, are particularly common when they are found adjacent to a nitrogen atom (aliphatic or aromatic) and, hence, such hydrogen bonds may be very important in amino acid and nucleoside chemistry.

3.3 The Influence of Hydrogen Bonding on the Lattice Energy of Crystals

3.3.1 Introduction

Before the hydrogen bond can be 'employed' as a regiospecific, structure-controlling agent (*i.e.* as a synthetic vector), the energetic contribution made by hydrogen bonding to the lattice energy of a crystalline ionic material must be evaluated. Unless the hydrogen bond is seen to make a significant energetic contribution, the underlying assumptions about its usefulness in crystal engineering will be invalidated.

The lattice energy, U, of an ionic crystalline material, MX, is often defined as the energy change associated with the process described by equation 1.

$$MX(s) \rightarrow M^+(g) + X^-(g) \qquad (1)$$

The lattice energy of a solid is generally assumed to receive contributions from four main components: electrostatic, E_C; repulsive, E_r; dispersive, E_d; and zero-point energy, E_0, (equation 2).

$$U = -E_C + E_r - E_d + E_0 \qquad (2)$$

The main dilemma with lattice energy calculations (see Section 3.3.3) results from the problems associated with the evaluation of the repulsive and the dispersive contributions. Such calculations are normally based upon extensive empirical parameterizations and, consequently, accurate lattice energy calculations require substantial effort.

3.3.2 Experimental Lattice Energies

Direct measurements of lattice energies are not feasible, but it is possible to relate the lattice energy of an ionic compound to various measurable thermodynamic quantities using a Born–Haber cycle, such as that illustrated for a Group 1 halide in Figure 4, where ΔH_{VM} and ΔH_{DX} are the enthalpies of vaporization and dissociation for the respective elements M and X, ΔH_{IE}

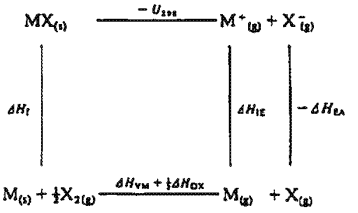


Figure 4 A typical Born–Haber cycle for a Group 1 halide.

is the ionization energy, $-\Delta H_{EA}$ is the electron affinity, ΔH_f is the enthalpy of formation of the crystalline salt, and U_{298} is the lattice energy of MX at 25 °C and 1 atm. The lattice energy at 0 K, U_0, is obtained by combining U_{298} with the appropriate heat capacity correction. Contributions arising from the heat capacities, C_v, of the species involved are normally small enough to be ignored.

It is worth noting that values for lattice energies obtained from a Born–Haber cycle are often referred to as 'experimental' data, U_{exp}, even though these data have only been deduced from the experimental values for the various steps involved in the cycle. The accuracy of 'experimental' lattice energies is therefore determined by the reliability of the available data for the enthalpies of ionization, vaporization, *etc.* Consequently, 'experimentally' determined lattice energies are not necessarily accurate and, in many cases, a situation exists where only simulations/calculations can give an indication of the lattice energy of a material.

3.3.3 Lattice Energy Calculations

Recent years have seen considerable interest in nonlinear optical materials, notably those capable of second harmonic generation (SHG).[21] Such materials, and the basis of their properties, have attracted both academic and commercial investigators.

The structural investigation of a series of SHG-active dihydrogenphosphate salts of organic cations[22] prompted our own interest in the role played by hydrogen bonding in the crystal structures of such salts, specifically concerning the energetic contribution made by hydrogen bonding to their lattice energies. Further, from the discussion in Section 3.3.2, it should be clear that accurate lattice energy calculations require much time and effort, and there would appear to be little point in developing separate potential models for all pair-wise interactions within these materials, *if* appropriate simplifications would yield an approximate value. Furthermore, since it is also impossible to assign an accurate value to the energy associated with each hydrogen bond in the solid state, the quality of the comparison will always be limited by estimates of hydrogen bond strengths. Hence, to a first approximation, it was assumed that in these ionic materials, the electrostatic forces would dominate, and the dispersive and repulsive forces would be of equal magnitude and, hence, would cancel each other. This approximation simplifies the lattice energy calculation significantly, as it has now been reduced to an Ewald summation of point charges. In the Ewald method, each point charge is replaced by a Gaussian charge distribution at the appropriate lattice site, resulting in a smoothly varying charge distribution, which leads to a quickly converging series. As the charge of an ion is a periodic function throughout the lattice, the Coulombic potential can be evaluated using a Fourier transformation of the charge.

A justification for the approximations adopted in this approach was provided by calculating the lattice energy, U_{cal}, for two salts with experimentally determined lattice energies, $[NH_4]_2[SnCl_6]$ and $[NH_4]_2[ReCl_6]$: the results are presented in Table 2, and justify the approximation that the dispersive and repulsive forces cancel. This approach has also been validated by extensive work carried out by Lubkowski *et al.* on a range of halide salts of mononitrogen bases.[23]

UM00012707
NOVARTIS EXHIBIT 1017
Novartis v. Regents, IPR2023-01346
Page 1453 of 4460

Table 2 Lattice energies (kJ mol^{-1}) and atomic charges for $[NH_4]_2[MCl_6]$[a]

M	z_{Cl}[b]	z_H[c]	U_{cal}	U_{exp}	ΔU[d]
Sn	−0.66	0.35	1329	1334	+0.4%
Re	−0.56	0.35	1397	1390	−0.5%

[a] Energy terms are defined in the main text. [b] z_{Cl} = atomic charge on chloride (H. D. B. Jenkins and K. F. Pratt, *Adv. Inorg. Chem. Radiochem.*, 1979, 22, 1). [c] z_H = atomic charge on hydrogen (A. Pullman and A. M. Armbruster, *Int. J. Quant. Chem. Symp.*, 1974, 8S, 69). [d] $\Delta U = 100(U_{exp} - U_{cal})/U_{exp}$.

3.3.4 *Lattice Energies of Organic Dihydrogenphosphates*

As the organic salts of dihydrogenphosphate consist of structurally complex ions without either a symmetrical, or a centralized, charge distribution, it was necessary to perform *ab initio* calculations on the participating ions in order to obtain the desired information; charges obtained with the STO-3G basis set were used in these lattice energy calculations.[24]

Following the method outlined in Section 3.3.3, the lattice energies of a series of organic dihydrogenphosphate salts were calculated and compared with the strength of the hydrogen bonds present in each structure (Table 3).[24]

Table 3 Minimum calculated hydrogen bond contributions (kJ mol^{-1}) to the total lattice energy of four dihydrogenphosphate salts, $[AH][H_2PO_4]$

A	U_{Cal}[a]	E_{HB}[b]	U_{tot}[c]	δ_{HB}[d]
Piperidine	500	130	630	21%
3-hydroxypyridine	545	135	680	20%
3-hydroxy-6-methylpyridine	410	135	545	25%
4-hydroxypyridine	515	135	650	21%

[a] Calculated lattice energy. [b] Hydrogen bond energy. [c] Total lattice energy, $U_{cal} + E_{HB}$. [d] $100(E_{HB}/U_{tot})$.

Based upon extensive experimental and theoretical data,[25] each O−H···O interaction was assigned an energy content of 35 kJ mol^{-1}, and each N−H···O interaction was assigned a value of 30 kJ mol^{-1} (both values are significantly lower – by a factor of two – than those found experimentally and theoretically for ionic hydrogen bonds of this type). By adding these values for each structure to give a total hydrogen bond energy, E_{HB}, depending upon the number of hydrogen bonds, and comparing this with the total lattice energy, an estimate of the minimum contribution made by hydrogen bonding is obtained (Table 3).

It should be pointed out that some of the hydrogen bond energy (*i.e.* the electrostatic part) has, in reality, already been included in the calculated lattice energy, U_{cal}. Hence, an incorrect value (*i.e.* too large) for the total lattice energy U_{tot} will be the result if U_{cal} and E_{HB} are simply added together. As no attempt has been made to estimate the relative magnitude of the electrostatic part of the hydrogen bond energy, it is not possible to obtain an accurate value for the contribution made by hydrogen bonding to the total lattice energy. However, the minimum level of contribution can be estimated.

The results displayed in Table 3 show that hydrogen bonding provides a notable energetic contribution, 20—25%, to the total lattice energy of dihydrogenphosphates of organic cations. It is also likely that the true values are significantly higher than that, given the significant underestimation of E_{HB}, and the overestimation of U_{tot}. Consequently, hydrogen bonding *can* act as a regiospecific, controlling and directing, structural tool in the crystal engineering of ionic and molecular solids.

3.4 Effects of Hydrogen Bonding on Charge Density

The fundamental nature of chemical bonding and molecular structure is determined by the electron density distribution in the system. Information regarding this feature can be made available through quantum mechanical calculations, but it can also be observed experimentally using high-intensity *X*-ray diffraction measurements.[26] By combining such experiments with neutron diffraction data, it is possible to gain added insight into the redistribution of electron density that occurs upon bond formation, including hydrogen bonding.[27] Such X-N maps, based upon structure factor amplitudes and thermal parameters from neutron data, can furnish information about the deviation of electron density around the nuclei from spherical symmetry.

Electron-density distribution studies of hydrogen-bonded complexes can be divided into two groups, (a) those involving weak or moderately strong hydrogen bonds, and (b) those containing strong hydrogen bonds. This division is made because of the presence of some distinctly different features within the two groups.

The observable changes in electron distribution that take place in materials with weak, or moderately strong, hydrogen bonds are close to the limit of current experimental techniques, but many studies have obtained a good agreement between X-N maps and theoretical deformation maps, both showing the general features of such hydrogen bonded systems. These features are, commonly, a build up of electron density in the D−H bond, and in a space close to the acceptor atom in the H···A interaction, which is accompanied by a decrease in the electron density closer to the hydrogen atom in the D−H···A bond,[28] see Figure 5.

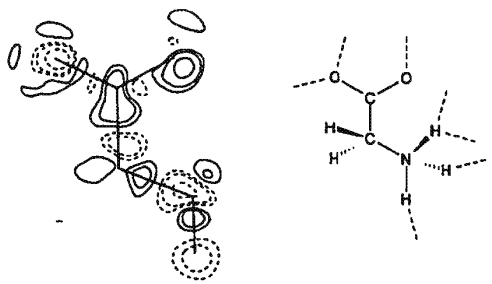


Figure 5 The difference density map for glycine, between a molecule in the crystal field and a free molecule. A schematic (right) shows the hydrogen-bond pattern.
(Reproduced with permission from reference 28.)

However, the same features can be obtained, qualitatively, by superimposing deformation maps of the isolated, unperturbed molecules in the system. Consequently, a weak or moderately strong hydrogen bond can be represented by a simple electrostatic model, since contributions from charge transfer and exchange repulsion effects are significantly smaller and tend to cancel each other. The accuracy of this description is also supported by the fact that the strength of these hydrogen bonds (the total hydrogen bond energy) correlates well with the electrostatic energy of the interaction. Detailed theoretical calculations have indicated, though, that some electron migration does take place as a second-order effect.[26b]

The situation regarding strong hydrogen bonds [most studies have been performed on systems with short O−H···O bonds, with r(O···O) in the range of 0.24—0.25 nm], however, is more complex. Normally, the charge distribution is more symmetrically arranged around the centre of the hydrogen bond and there is less charge build up both in the O−H bond and in the H···O region, see Figure 6.[29] It also becomes much more difficult to separate contributions from various components, *e.g.* polarization *vs.* charge-transfer effects, as well as trying to partition the electron distribution arising from the different molecules/ions in the complex.

Another question regarding electron distribution and hydrogen bonding, which has attracted much attention, concerns the role played by the lone-pair as a hydrogen-bond acceptor. Both

UM00012708
NOVARTIS EXHIBIT 1017
Novartis v. Regents, IPR2023-01346
Page 1454 of 4460

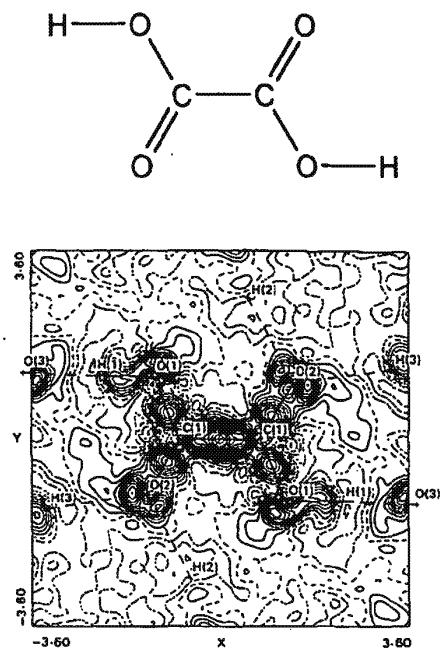


Figure 6 The experimental deformation density for α-$C_2O_4H_2.2H_2O$ in the plane of the oxalic acid molecule (schematic top). (Reproduced with permission from reference 29.)

theoretical and experimental studies have been carried out in order to clarify the stereoelectronic effect caused by lone-pair regions around acceptor atoms in hydrogen-bond interactions, and the main issue has been whether, or not, it is possible always to view a lone-pair as the distinct acceptor of a hydrogen bond.

Theoretical studies of the electron density around C=O groups normally reveal a double maximum of electron density corresponding to the lone-pair regions, although it should be pointed out that because of the very nature of these deformation-density calculations, only the difference between the molecular electron density and the superpositioning of spherical densities is evaluated, not an absolute location of excess electron density due to a specific orbital.

Attempted correlations of solid-state bond angles and lone-pair directionality have not been completely conclusive.[10,15] An extensive study of neutron-diffraction data of C=O···H angles found an accumulation of data around 120°, albeit with several large variations. Other studies have also highlighted the importance of correlating such data with steric factors, which may otherwise bias the existing data. On the whole, however, double bonded oxygen atoms in certain groups, −C(O)OH and $-C(O)O^-$, appear to favour a hydrogen bond approach at an angle of 120°.

In contrast, theoretical investigations of the water molecule and hydroxy groups normally only reveal one broad electron-density maximum, and a study of a large number of crystalline ROH compounds[30] found a tendency for the acceptor atom to occupy a position in the plane of the lone-pairs, although there was no accumulation of acceptor atoms in the tetrahedral direction within the plane.

Overall, there is no absolute correlation between lone-pair regions and acceptor angles and, hence, it would seem somewhat simplistic to view the 'classical' lone-pairs as specific receivers of hydrogen bonds. Instead, it is probably more fruitful, albeit more complex, to investigate both steric factors and the whole electrostatic potential energy surface, in order to elucidate the preferred approach for a hydrogen-bond donor.

4 Crystal Engineering

4.1 *Rationale*

Within the fields of supramolecular chemistry, molecular recognition, and crystal engineering, it has been recognized that hydrogen bonding is an indispensable tool for designing molecular aggregates.[1,31]

It is our firm belief that an improved understanding of hydrogen bonding in general, and hydrogen bonds in ionic solids in particular, can strengthen our awareness of the tools with which we may be able to 'persuade' molecules and ions to form specific aggregate structural units. Since the properties of a solid are critically dependent upon its structure, it is feasible to design materials with desired characteristics by incorporating specific properties into the subunits. There are clearly numerous diverse areas where such an approach could be very fruitful, *e.g.* studies of biomolecular substrate binding and recognition, reactivity and catalysis, development of improved detergents, the petrochemical industry, and the synthesis of novel nonlinear optical and ferroelectric materials.

4.2 Pattern Recognition

Probably the most well known, and most easily identifiable, hydrogen-bonded aggregate is a monocarboxylic acid dimer (Figure 7). Several groups have carried out extensive studies of solid-state structures of a wide range of related molecular and ionic solids, and these studies have led to the realization that hydrogen-bond aggregation is not random: patterns do exist. Certain functional groups, and ions, display a clear pattern preference, and this insight will have important consequences for the development of crystal engineering. If certain molecular building blocks tend to crystallize in specific, energetically favourable, arrangements, then molecules containing these blocks can be encouraged to form aggregates with specific structural features.

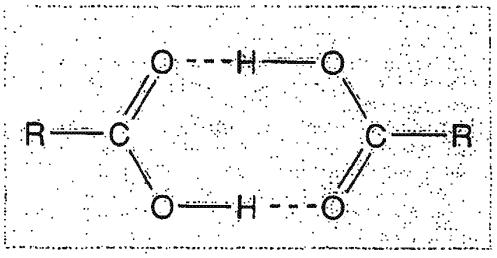


Figure 7 The common hydrogen-bonded dimeric form of a carboxylic acid.

Lehn and co-workers have studied, *inter alia*, macromolecular recognition involving cryptands and other macrocyclics, interactions between phosphates and carboxylates with polyammonium macrocyclics, the formation of helical metal complexes of bipyridine strands, and supramolecular liquid crystalline polymers.[1] Other groups have investigated molecular tweezers, organometallics, and small organic molecules as subunits of extended structures.[32] Although all of these studies fall into the broad categories of molecular recognition or crystal engineering, the discussion in the remainder of this review will be focused upon relatively small organic/inorganic systems in the absence of preorganized, custom-designed cavities. Such systems are more amenable to an examination and evaluation of hydrogen-bond selectivity, preference, and topology, without an *a priori* directional bias.

The most extensive studies of organic hydrogen-bonded solid-state structures have been carried out by Etter and co-workers.[33] Their work has identified the pattern preference displayed by a range of functional groups and molecular types, *e.g.* amides, diaryl ureas, imides, nitroanilines, and 2-aminopyrimidines. A

UM00012709
NOVARTIS EXHIBIT 1017
Novartis v. Regents, IPR2023-01346
Page 1455 of 4460

detailed description of some of these patterns will be found in Section 4.3.2. As a result of this work, a method for describing hydrogen-bond patterns has been developed, in addition to several general rules (guide-lines) regarding expected hydrogen-bond organization in organic solid-state structures.[3]

Ionic compounds, both inorganic–organic salts and pure organic salts, have also been studied recently. A series of organic salts with the dihydrogenphosphate anion, $[H_2PO_4]^-$, displayed certain specific, reoccurring, arrangements of the anionic network; the anions were lined together by short, strong hydrogen bonds into specific chains (Figure 8), sheets, or three-dimensional infinite arrangements.[22] It is likely that the character of the cation, and the nature of its hydrogen-bond interactions with the anionic matrix, will discriminate between the three possible structures. Similarly, a structural study of organic salts of hydrogen-L-tartrates[34] showed that the anionic network was remarkably consistent, regardless of the nature of the cation. The strongly hydrogen-bonded sheet of anions created a matrix, see Figure 9, which dominated the structure and only allowed limited flexibility regarding the positioning and packing of the cations.[34]

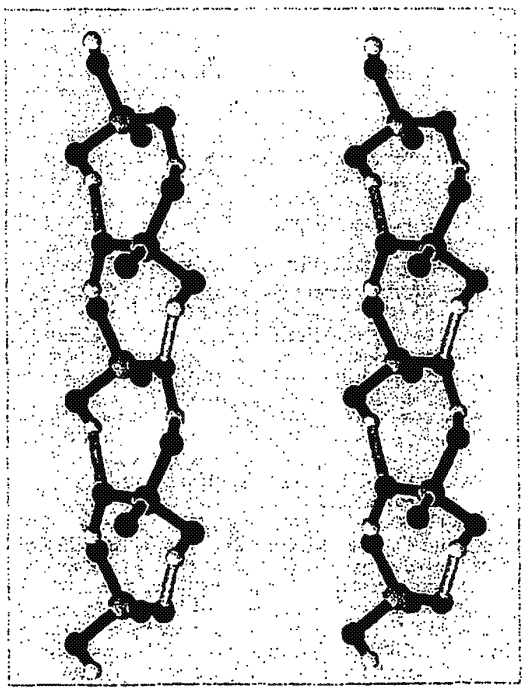
The presence of rigid, frequently occurring, hydrogen-bonded aggregate structures in both molecular and ionic compounds, creates a necessary platform for intermolecular synthesis. By identifying, classifying, and rationalizing such networks, it may be possible to utilize them as active design tools in the crystal engineering of novel materials with specific structural features.

4.3 Encoding Hydrogen-bonded Networks

4.3.1 Pattern Designation

Once it has been established, *via* crystallographic data, that there are several different hydrogen bonds within a material, how can this information be translated into a form, or code, which allows for the classification and recognition of hydrogen-bond interactions as aggregate structures? Furthermore, how can this information be communicated in a precise fashion? Clearly, in order to achieve this objective, it is essential to find a way of describing even complex hydrogen-bond patterns in a simple, yet comprehensive, language.

Figure 8 Chains of dihydrogenphosphate anions within the crystal structure of the piperidinium dihydrogenphosphate.[22] Covalent bonds, red; hydrogen bonds, yellow and green.



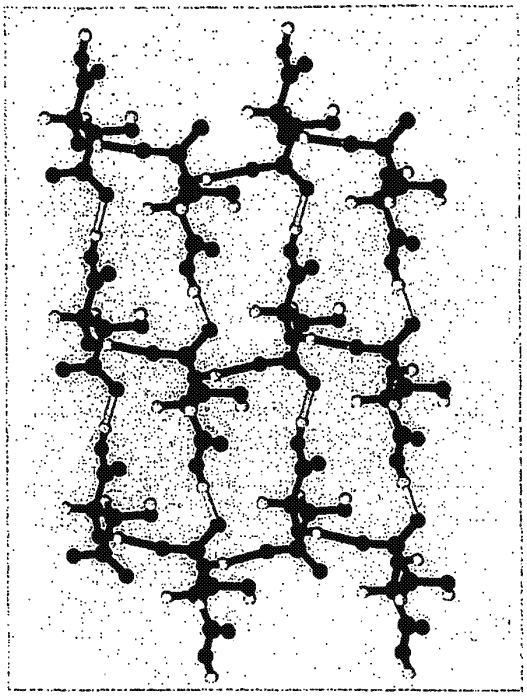


Figure 9 A two-dimensional sheet of hydrogen-L-tartrate anions, as found in piperazinium(2+) bis-hydrogen-L-tartrate.[34] Covalent bonds, red; hydrogen bonds, yellow and green.

The most successful method for encoding hydrogen-bond patterns of organic solids has been developed by Margaret Etter and co-workers,[3] who have demonstrated that, by analysing hydrogen-bond interactions in organic molecular solids in a systematic and consistent fashion, it is possible to establish the pattern-preference displayed by many functional groups. The methodology, loosely based upon graph-theory, adopts a topological approach to analysing hydrogen-bond patterns, but instead of viewing molecules as points and hydrogen bonds as lines, chemical structure and functionality have been retained.

A graph set is specified using the pattern designator (G), its degree (n) and the number of donors (d) and acceptors (a):

$$G_d^a(n)$$

G, the descriptor referring to the pattern of hydrogen bonding, can be either S (for intramolecular bonds), C (for infinite chains), R (for intermolecular rings), or D (for non-cyclic dimers and other finite structures), and the parameter n refers to the number of atoms in a ring, or the repeat unit of a chain. Graph sets are assigned initially to motifs (hydrogen-bond patterns constructed by only one type of hydrogen bond), and then to higher-level networks (combinations of the relevant motifs). Thus, if the compound contains four different hydrogen bond types, then the first-level graph set, N_1, is a sequential listing of these four motifs. Higher-level graph sets are assigned to networks generated by combinations of different hydrogen bond types (*e.g.* the second-level graph set is created by combinations of two hydrogen-bond types, the third-level set by combinations of three *etc.*).

UM00012710
NOVARTIS EXHIBIT 1017
Novartis v. Regents, IPR2023-01346
Page 1456 of 4460

4.3.2 Encoding in Practice

The method outlined in Section 4.3.1 will now be demonstrated with a series of examples, illustrated in Figure 10, which shows the four fundamental motifs that may be generated by a hydrogen bond; dimers (*D*), chains (*C*), intramolecular bonds (*S*), and rings (*R*).

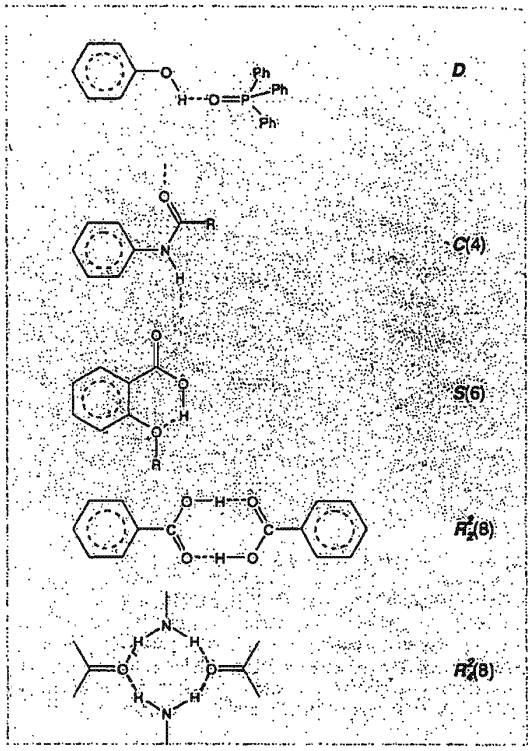


Figure 10 Some examples of assigning graph sets to simple hydrogen-bonded systems.[3]

Examples of higher-level graphs sets are presented in Figure 11, where several hydrogen bonds are combined to form specific patterns. The compounds depicted in Figure 11 each contain two unique hydrogen bonds and, therefore, their first-level graph sets, N_1, contain two motifs. The second-level graph sets, N_2, describe patterns that are created by combining the unique hydrogen bonds within each structure.

By applying this procedure in a systematic fashion, it is possible to characterize and recognize patterns that appear within crystals containing fundamentally different, as well as closely related, molecules. By correlating pattern preference with functional groups or molecular types, certain specific aggregate structures may be induced to form, and may be incorporated into a material by the introduction of a specific functionality.

This encoding technique has also been employed in the analysis of closely related hydrogen-bond networks in polymorphs,[35] where subtle differences in various hydrogen-bond arrangements can be very difficult to detect and describe. Furthermore, the realization that specific hydrogen-bonded aggregates occur very frequently should also influence the way in which we investigate and approach topics like protein recognition and nucleation processes, as the 'active' species involved in such interactions may be hydrogen-bonded aggregates, and *not* isolated molecules or ions.

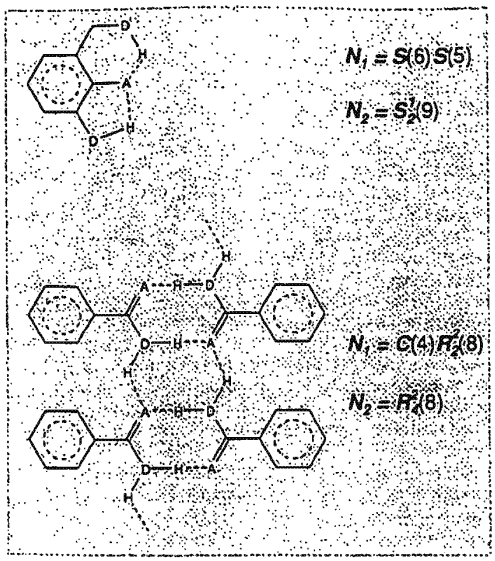


Figure 11 Some examples of assigning graph sets to more complex hydrogen-bonded systems.[3]

4.3.3 Hydrogen-bond Directed Co-crystallization

Etter and co-workers have employed co-crystallization techniques extensively, in order to identify competition in hydrogen-bond accepting/donating capability between different molecular types and functional groups.[3]

The co-crystals were prepared not only by traditional methods (involving evaporation of a solution containing two, or more, components), but also by grinding the starting materials together in the solid-state. A prerequisite for the formation of co-crystals is that the heteromeric species, the co-crystal, contains stronger hydrogen-bonds than either of the homomeric starting materials. In addition, formation of a co-crystal from solution is obviously hampered if there is a large solubility differences between the various starting materials. Figure 12 shows some common hydrogen-bond motifs that have been identified in co-crystals of diarylurea derivatives (top) with a wide range of hydrogen-bond acceptors (*e.g.* triphenylphosphine oxide).[3] Each pattern is identified with the relevant graph-set notation, described in Section 4.3.1.

4.4 Polymorphism

Polymorphism is a unique feature of the solid-state, but although this phenomenon has been known for more than a century, surprisingly little use has been made of it in solid-state studies. The true extent of polymorphism among crystalline materials is very difficult to gauge. However, as it has been more often encountered in areas of research where structure is of paramount importance, we are in strong agreement with McCrone[36] who stated (in 1965):

> '[...] every compound has different polymorphic forms [...] and the number of forms known for a given compound is proportional to the time spent in research on that compound.'

It is generally accepted that differences in lattice energies between different polymorphs are in the region of 5—20 kJ mol^{-1}, and, especially for ionic compounds, these differences are small compared to the total lattice energies of such materials. Consequently, it would be fair to assume that, for example, different methods of recrystallization would be sufficient to induce the formation of a new structural form. If this is true, then

UM00012711
NOVARTIS EXHIBIT 1017
Novartis v. Regents, IPR2023-01346
Page 1457 of 4460

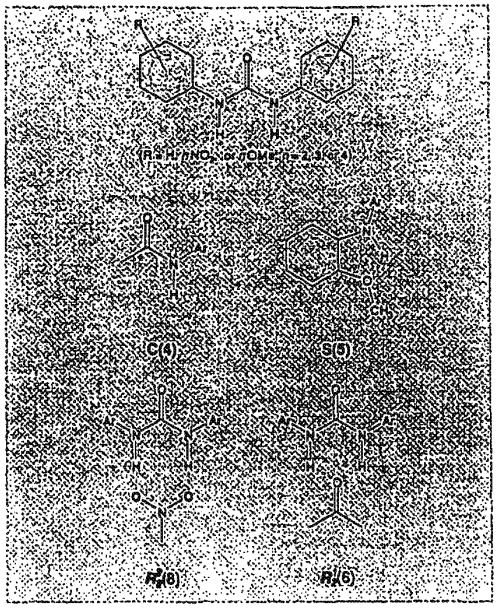


Figure 12 Some common hydrogen-bond patterns found in diaryl urea crystals and co-crystals.[33c]

the whole process of identifying and classifying a material, based upon a single-crystal study, may, on its own, be less than satisfactory. When selecting individual crystals for structure determination, it is not necessarily true that the chosen crystals are representative of the structure of the bulk material. In fact, normally, the 'best' crystal is chosen – by definition, that must be atypical of the majority of the material. It would therefore seem critical always to compare the structure of the single-crystal with that of the bulk material, obtainable from powder diffraction. By simulating a diffraction pattern from the single-crystal data, and comparing that with the powder pattern recorded experimentally on the bulk sample, it is very easy to make an assessment as to the structural purity of, and agreement between, single-crystal and bulk material. We strongly believe that this procedure should be carried out routinely, in parallel with single-crystal structure determinations. The question of structural purity is, in many areas of chemistry, as important as that of chemical purity.

Polymorphic systems provide excellent opportunities to study specific chemical entities in different crystalline environments. Hence, information about the interplay between ionic or molecular geometry, and intermolecular and crystalline forces, may be extracted from such studies, *e.g.* the lattice energies of the observed structures can be calculated and evaluated against DSC measurements, the energy differences between observed ionic conformations can be estimated, and an analysis of the results may be correlated to a partitioning of the lattice energies into its individual atomic contributions.

A careful investigation of closely related polymorphic salts facilitates a comparison between the relative differences displayed by measurable thermodynamic quantities (obtainable from DSC techniques), and trends displayed by theoretically determined lattice energies. In this case, experimental and theoretical chemistry are combined into a very powerful probe of intermolecular interactions. Such an approach will also highlight the relative effects and importance of different ionic, or molecular, subunits, on the overall crystalline arrangement of each material.

4.5 Design of Crystals with Specific Structural Features and Properties

Although we are still a long way away from being able to predict the precise structure of an unknown material, several imaginative efforts have been made at utilizing hydrogen bonding as a means of creating specific structural features.

Wuest and co-workers[37] have utilized the well known cyclic dimeric motif of lactams, *cf.* 2-pyridones, in combination with rigid spacers, in order to create new extended structural motifs (Figure 13). Ureylendicarboxylic acids have been employed by Fowler and co-workers[32c] as building blocks for several infinite two-dimensional hydrogen-bonded layer structures. Whitesides and co-workers[38] have synthesized co-crystals of melamin derivatives and barbituric acids which contain extended hydrogen-bonded 'tapes'.

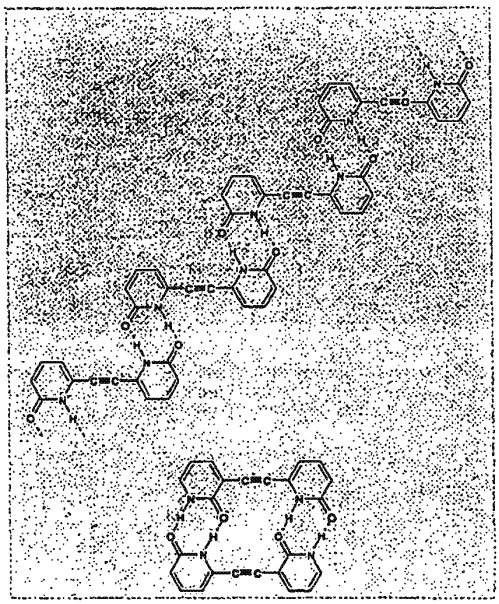


Figure 13 Novel structural motifs generated by isomeric derivatives of 2-pyridone.[37]

Our own work has focused on the preparation of salts with predictable structural features, and recent efforts include the use of infinite sheets of hydrogentartrate[34] anions as a means of imposing structural consistency within a series of non-linear optical salts (Figure 14 and Figure 15).

Furthermore, in an attempt to produce transparent, colourless, non-centrosymmetric crystals (a non-centrosymmetric medium is an absolute condition for certain non-linear optical effects) with a needle-like morphology (a condition required for the successful incorporation into thermally aligned polymer films),[39] 3- and 4-hydroxybenzoic acids were treated with a chiral amine, (*S*)-1-phenylethylamine, to produce crystals with the desired properties.[40] It was assumed that the anions would create infinite chains by a head-to-tail hydrogen bond, and that this aggregate structure would manifest itself macroscopically as needle-like crystals. Single-crystal studies of these two materials, both of which had a needle-like habit, revealed the presence of infinite chains of anions (Figure 16 and Figure 17), and, in the case of 1-phenylethylammonium 4-hydroxybenzoate, the direction of the infinite chain coincided with the long-axis of the needle.[40]

Further studies are also needed in order to identify correlations between microscopic structure and macroscopic appearance. Will the regions of strong hydrogen-bonds or the hydro-

UM00012712
NOVARTIS EXHIBIT 1017
Novartis v. Regents, IPR2023-01346
Page 1458 of 4460

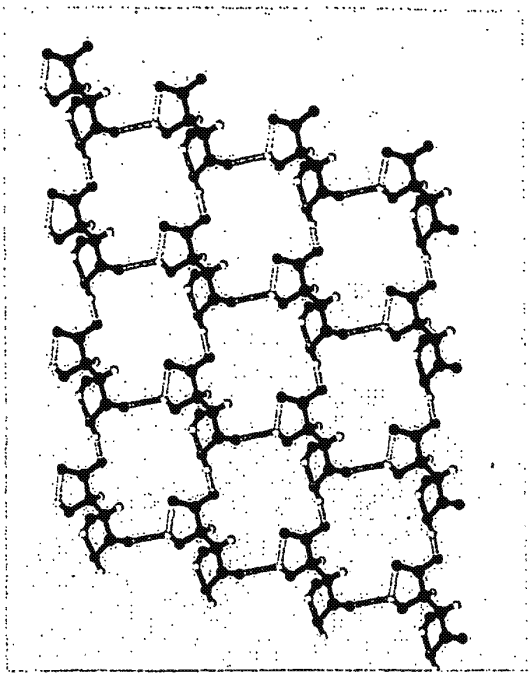


Figure 14 The two-dimensional sheet formed by the hydrogen-L-tartare anion in its (*S*)-1-phenylethylammonium salt.[34] Covalent bonds, red; hydrogen bonds, yellow, green, grey, and white.

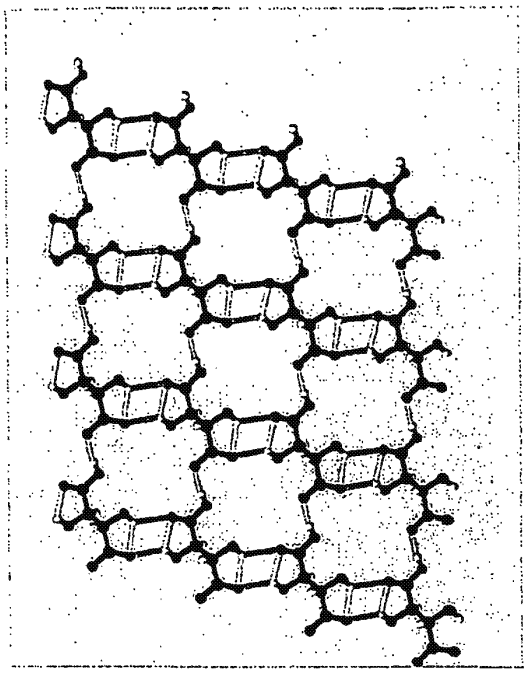


Figure 15 The two-dimensional sheet formed by the hydrogen-*meso*-tartrate anion in its (*S*)-1-phenylethylammonium salt.[34] Covalent bonds, red; hydrogen bonds, yellow, green, grey, and white.

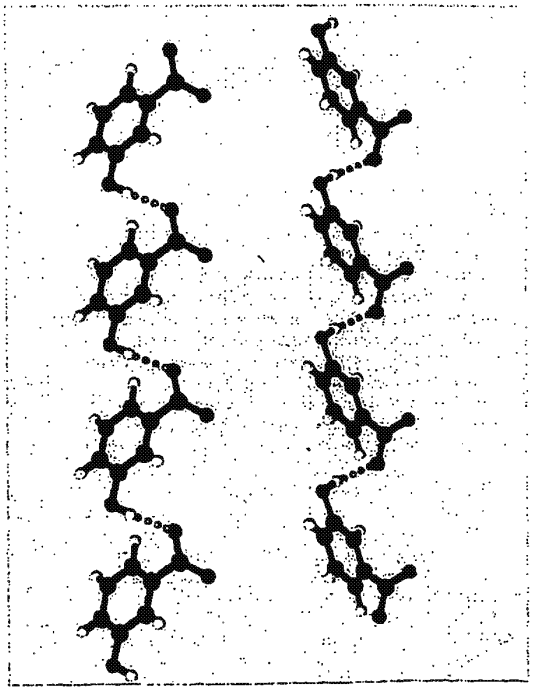


Figure 16 Infinite chains of anions, parallel to the *a* axis, in (*S*)-1-phenylethylammonium 3-hydroxybenzoate, viewed down *b*.[40] Hydrogen bonds indicated by dotted lines.

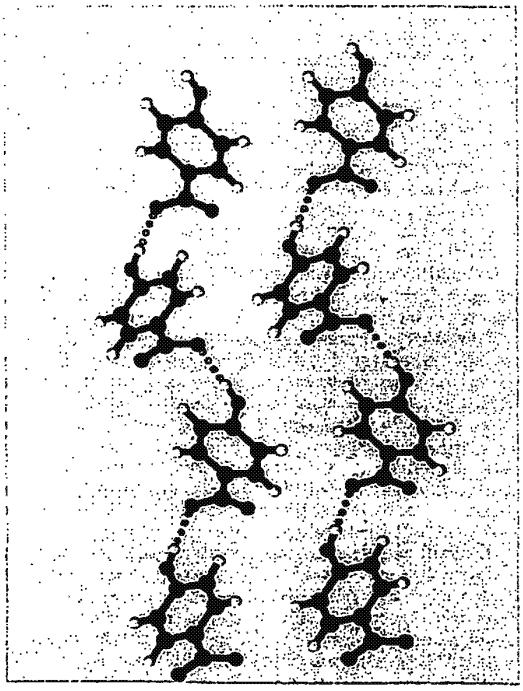


Figure 17 Infinite chains of anions, parallel to the *b* axis, in (*S*)-1-phenylethylammonium 4-hydroxybenzoate, viewed down *c*.[40] Hydrogen bonds indicated by dotted lines.

UM00012713
NOVARTIS EXHIBIT 1017
Novartis v. Regents, IPR2023-01346
Page 1459 of 4460

phobic regions crystallize more quickly upon precipitation from aqueous solvent? Answers to such questions are also likely to cast more light on the path towards successful crystal engineering.

5 The Future

The last five years have witnessed a significantly increased awareness of the importance of being able to understand and rationalize the effects of hydrogen bonding on the solid state. As a consequence, several groups, worldwide, have made very important and useful contributions to the field of crystal engineering by employing hydrogen bonds as active design elements in the synthesis of novel materials and extended aggregates. In the past few years, Zyss and co-workers have developed an independent parallel approach to the design of novel materials for non-linear optics, of combining organic cations (to carry the high optical polarizability) with hydrogen-bonding inorganic (or organic) anions (to provide thermal and structural stability), similar to that which we proposed in 1989.[22] The resulting crystalline salt, 2-amino-5-nitropyridinium dihydrogenphosphate, shows significant SHG-activity.[41]

Clearly, because of the potential impact that crystal engineering may have on a range of areas with significant commercial interests, we are likely to see substantial advances being made, both theoretical and practical, during the next few years. Control of crystalline structure is an ambitious, but achievable, target, and the next decade promises to be extremely exciting.

Acknowledgments. We would like to thank Dr. J. McDonald (Harvard University) for invaluable comments regarding the graph-sets, and the Royal Swedish Academy of Sciences for generous financial support (to CBA). We are indebted to Drs. D. Braben and D. Ray of Venture Research International for nurturing (financially and intellectually) our interest in this field, and to Drs. C. J. Adams, G. Armstrong, and J. Warr (Unilever Research Laboratory), and the SERC for actively supporting our current research.

6 References

1 J. M. Lehn, *Angew. Chem., Int. Ed. Engl.*, 27, 89, 1988; J. M. Lehn, *Angew. Chem., Int. Ed. Engl.*, 1990, 29, 130.
2 J. P. Mathias and J. F. Stoddart, *Chem. Soc. Rev.*, 1992, 21, 215.
3 M. C. Etter, *Acc. Chem. Res.*, 1990, 23, 120; M. C. Etter, J. C. MacDonald, and J. Bernstein, *Acta Crystallagr., Sect. B*, 1990, 46, 256.
4 F. A. Cotton and R. L. Luck, *Inorg. Chem.*, 1989, 28, 3210.
5 W. M. Latimer and W. H. Rodebush, *J. Am. Chem. Soc.*, 1920, 42, 1419.
6 L. Pauling, 'The Nature of the Chemical Bond and the Structure of Molecules and Crystals – An Introduction to Modern Structural Chemistry', 2nd Edn., Oxford University Press, London, 1940.
7 G. C. Pimentel and A. L. McClellan, 'The Hydrogen Bond', Freeman, San Francisco, 1960.
8 Th. Zeegers-Huyskens and P. Huyskens, in 'Intermolecular Forces – An Introduction to Modern Methods and Results', ed. P. L. Huyskens, W. A. P. Luck, and T. Zeegers-Huyskens, Springer-Verlag, Berlin, 1991, p.1.
9 P. W. Atkins, 'General Chemistry', Scientific American Books, New York, 1989.
10 'The Hydrogen Bond. Recent Developments in Theory and Experiments', ed. P. Schuster, G. Zundel, and C. Sandorfy, Vols. I–III, North Holland, Amsterdam, 1976.
11 M. A. Viswamitra, R. Radhakrishna, J. Bandekar, and G. R. Desiraju, *J. Am. Chem. Soc.*, 1993, 115, 4868.
12 H. S. Rzepa, M. L. Webb, A. M. Z. Slawin, and D. J. Williams, *J. Chem. Soc., Chem. Commun.*, 1991, 765; S. S. Al-Juaid, A. K. A. Al-Nasr, C. Eaborn, and P. B. Hitchcock, *J. Chem. Soc., Chem. Commun.*, 1991, 1482; S. S. Al-Juaid, A. K. A. Al-Nasr, C. Eaborn, and P. B. Hitchcock, *J. Organomet. Chem.*, 1992, 429, C9.
13 M. C. Etter and G. Ranawake, *J. Am. Chem. Soc.*, 1992, 114, 4430.
14 A. K. Abdul-Sada, A. M. Greenway, P. B. Hitchcock, T. J. Mohammed, K. R. Seddon, and J. A. Zora, *J. Chem. Soc., Chem. Commun.*, 1986, 1753; A. K. Abdul-Sada, S. Al-Juaid, A. M. Greenway, P. B. Hitchcock, M. J. Howells, K. R. Seddon, and T. Welton, *Struct. Chem.*, 1990, 1, 391; A. G. Avent, P. A. Chaloner, M. P. Day, K. R. Seddon, and T. Welton; in 'Proceedings of the Seventh International Symposium on Molten Salts', ed. C. L. Hussey, J. S. Wilkes, S. N. Flegas, and Y. Ito, The Electrochemical Society Inc., Pennington, New Jersey, PV 90-17, 1990, p.98.
15 R. Yamdagni and P. Kebarle, *J. Am. Chem. Soc.*, 1971, 93, 7139.
16 (*a*) R. Taylor and O. Kennard, *Acc. Chem. Res.*, 1984, 17, 320. (*b*) R. Taylor and O. Kennard, *J. Am. Chem. Soc.*, 1982, 104, 5063.
17 G. A. Jeffrey and W. Saenger, 'Hydrogen Bonding in Biological Structures', Springer-Verlag, Berlin, 1991.
18 A. Bondi, *J. Phys. Chem.*, 1964, 68, 441.
19 S. C. Nyburg and C. H. Faerman, *Acta Crystallogr., Sect. B*, 1985, 41, 360.
20 G. R. Desiraju, *Acc. Chem. Res.*, 1991, 24, 290.
21 'Nonlinear Optical Properties of Organic Molecules and Crystals', ed. D. S. Chemla and J. Zyss, Vols. 1 and 2, Academic Press, New York, 1987.
22 C. B. Aakeröy, P. B. Hitchcock, B. D. Moyle, and K. R. Seddon, *J. Chem. Soc., Chem. Commun.*, 1989, 1856.
23 J. Lubkowski and J. Blazejowski, *J. Phys. Chem.*, 1991, 95, 2311; J. Lubkowski, P. Dokurno, and J. Blazejowski, *Thermochim. Acta*, 1991, 176, 183.
24 C. B. Aakeröy, M. Leslie, and K. R. Seddon, *Struct. Chem.*, 1992, 3, 56.
25 (*a*) M. Meot-Ner (Mautner), in 'Molecular Structure and Energetics', Vol. 4, ed. J. F. Liebman and A. Greenberg, VCH Verlag, New York, 1987, p.72. (*b*) C. A. Deakyne, in 'Molecular Structure and Energetics', Vol. 4, ed. J. F. Liebman and A. Greenberg, VCH Verlag, New York, 1987, p.105.
26 (*a*) P. Coppens, *J. Chem. Educ.*, 1984, 61, 761. (*b*) 'Electron and Magnetization Densities in Molecules and Crystals', ed. P. Becker, Plenum, New York, 1980.
27 I. Olovsson, *Croat. Chem. Acta*, 1982, 55, 171.
28 J. Almlöf, Å. Kvick, and J. O. Thomas, *J. Chem. Phys.*, 1973, 59, 3901.
29 E. D. Stevens and P. Coppens, *Acta Crystallogr., Sect. B*, 1980, 36, 1864.
30 J. Kroon, J. A. Kanters, J. G. C. M. Van Duijneveldt-Van de Rijdt, F. B. Duijneveldt, and J. A. Vliegenhart, *J. Mol. Struct.*, 1975, 24, 1975.
31 G. R. Desiraju, 'Crystal Engineering: The Design of Organic Solids', Elsevier, Amsterdam, 1989.
32 (*a*) M. Haramata and C. L. Barnes, *J. Am. Chem. Soc.*, 1990, 112, 5655; (*b*) P. J. Fagan, M. D. Ward, and J. C. Calabrese, *J. Am. Chem. Soc.*, 1989, 111, 1698; (*c*) X. Zhao, Y.-L. Chang, F. W. Fowler, and J. W. Lauher, *J. Am. Chem. Soc.*, 1990, 112, 6627; (*d*) F. Garcia-Tellado, S. J. Geib, S. Goswami, and A. D. Hamilton, *J. Am. Chem. Soc.*, 1991, 113, 9265.
33 (*a*) S. M. Reutzel and M. C. Etter, *J. Phys. Org. Chem.*, 1992, 5, 44; (*b*) M. C. Etter and D. A. Adsmond, *J. Chem. Soc., Chem. Commun.*, 1990, 589; (*c*) M. C. Etter, Z. Urbanczyk-Lipkowska, M. Zia-Ebrahimi, and T. W. Panunto, *J. Am. Chem. Soc.*, 1990, 112, 8415; (*d*) M. C. Etter, *J. Phys. Chem.*, 1991, 95, 4601.
34 C. B. Aakeröy, P. B. Hitchcock, and K. R. Seddon, *J. Chem. Soc., Chem. Commun.*, 1992, 553.
35 J. Bernstein, *Acta Crystallogr., Sect. B*, 1991, 47, 1004.
36 W. C. McCrone, in 'Physics and Chemistry of the Organic Solid State', ed. D. Fox, M. M. Labes, and A. Weissberger, Vol. 2, Interscience, New York, 1965, p.725.
37 (*a*) Y. Ducharme and J. D. Wuest, *J. Org. Chem.*, 1988, 53, 5789; (*b*) M. Simard, D. Su, and J. D. Wuest, *J. Am. Chem. Soc.*, 1991, 113, 4696.
38 (*a*) J. H. Zerkowski, G. T. Seto, D. H. Wierda, and G. M. Whitesides, *J. Am. Chem. Soc.*, 1990, 112, 9025; (*b*) G. T. Seto and G. M. Whitesides, *J. Am. Chem. Soc.*, 1990, 112, 6409.
39 (*a*) C. B. Aakeröy, N. E. Azoz, P. D. Calvert, M. Kadim, A. J. McCaffery, and K. R. Seddon, *ACS Symp. Ser.*, 1991, 455, 516; C. B. Aakeröy, N. Azoz, M. Kadim, K. R. Seddon, and L. Trowbridge, *Adv. Mater.*, 1993, 5, 364.
40 C. B. Aakeröy, G. S. Bahra, P. B. Hitchcock, Y. Patell, and K. R. Seddon, *J. Chem. Soc., Chem. Commun.*, 1993, 152.
41 R. Masse and J. Zyss, *Mol. Eng.*, 1991, 1, 141; Z. Kotler, R. Hierle, D. Josse, J. Zyss, and R. Masse, *J. Opt. Soc. Am. B*, 1992, 9, 534.

UM00012714
NOVARTIS EXHIBIT 1017
Novartis v. Regents, IPR2023-01346
Page 1460 of 4460

This Page is Inserted by IFW Indexing and Scanning Operations and is not part of the Official Record

BEST AVAILABLE IMAGES

Defective images within this document are accurate representations of the original documents submitted by the applicant.

Defects in the images include but are not limited to the items checked:

- ☐ BLACK BORDERS
- ☐ IMAGE CUT OFF AT TOP, BOTTOM OR SIDES
- ☐ FADED TEXT OR DRAWING
- ☐ BLURRED OR ILLEGIBLE TEXT OR DRAWING
- ☐ SKEWED/SLANTED IMAGES
- ☐ COLOR OR BLACK AND WHITE PHOTOGRAPHS
- ☐ GRAY SCALE DOCUMENTS
- ☐ LINES OR MARKS ON ORIGINAL DOCUMENT
- ☐ REFERENCE(S) OR EXHIBIT(S) SUBMITTED ARE POOR QUALITY
- ☐ OTHER: _____

IMAGES ARE BEST AVAILABLE COPY.
As rescanning these documents will not correct the image problems checked, please do not report these problems to the IFW Image Problem Mailbox.

HYDROGEN-BOND ASSISTED ASSEMBLY OF ORGANIC AND ORGANIC-INORGANIC SOLIDS

C.B. AAKERÖY and D.S. LEINEN
Department of Chemistry, Kansas State University
Manhattan, Kansas 66506, USA.

Abstract

The ability to predict and control the assembly of molecular and ionic species into ordered networks has become an important target area in chemistry, biochemistry and materials science. In this context, the strength, selectivity and directionality of the hydrogen bond have been instrumental in the preparation of distinctive and predictable structural aggregates, and the use of hydrogen bonding as a steering force has emerged as the most important strategy in crystal engineering.

An improved insight into the structural consequences of intermolecular interactions is crucial when considering that most physical properties, *e.g.* melting point, solubility, mechanical strength, *etc.*, are a function of the relative orientation of molecules in a 3-D solid. At this stage, however, we do not have the necessary understanding of non-covalent forces and their influence over solid-state structures. This point is amply illustrated by the fact that many fundamental properties of solids can not be simulated or calculated with any great degree of confidence. Furthermore, we are still lacking sufficient information about crystallization processes, structural phase changes and other events where thermodynamic and kinetic factors are precariously balanced. Nevertheless, considerable efforts and progress have been made in recent years, and this Chapter provides an overview of some of the strategies, structures, successes and pitfalls (notably involving hydrogen bonding) that have been presented in the crystal engineering of organic and organic/inorganic materials.

1. Introduction

Crystal engineering, "*the understanding of intermolecular interactions in the context of crystal packing and in the utilisation of such understanding in the design of new solids with desirable physical and chemical properties.*"[1], is concerned with challenges and opportunities associated with supramolecular synthesis and molecular recognition [2,3,4,5]. Unfortunately, the ability to modify reactivity and properties of a crystalline solid through precise control over its structure presents a formidable task, since a small change in molecular structure may lead to dramatic changes in the crystal structure.

Covalent bonds are the primary design elements in organic chemistry and these bonds have been extensively studied to the point where even very complex biomolecules can be prepared through organic synthesis. The next step should take us beyond the molecule to organized polymolecular systems held together by non-covalent interactions; this is the field of "supramolecular chemistry" [2]. Intermolecular interactions form the basis of the highly specific recognition, reaction and regulation processes that occur in life, *e.g.* antigen-antibody association, gene expression, cellular recognition, *etc.* These processes display astoundingly high selectivity based upon efficient manipulation of the energetic and stereochemical features of non-covalent intermolecular forces. Any attempt to predict or design solid-state assembly must take these forces into account.

Despite recent advances in supramolecular synthesis, detailed control over the assembly of molecules into ordered solids remains an elusive goal, and we are rarely able to predict the structure of a simple crystalline material. Much more work is required to increase the choice of reliable building blocks of low-dimensional architectures and, more importantly, to allow us to rationalize and predict structural arrangements of

D. Braga et al. (eds.), Crystal Engineering: From Molecules and Crystals to Materials 89 -106.
© 1999 *Kluwer Academic Publishers. Printed in the Netherlands.*

UM00012716
NOVARTIS EXHIBIT 1017
Novartis v. Regents, IPR2023-01346
Page 1462 of 4460

molecules within new crystalline materials. An enhanced understanding of intermolecular forces may also enable us to better address crucial questions about polymorphism and crystal morphology.

As crystal engineering is still in its infancy, it *is* necessary to assemble structural information, to identify recurring packing motifs and to test the reliability of intermolecular interactions. At the same time, we are at a stage where supramolecular skills should be put into practice by advancing towards functional materials that are cheaper, faster or more efficient that current alternatives.

The term 'crystal engineering' was coined by Schmidt in 1971 as a result of a study of the interrelationship between crystal structure and solid-state reactivity [6]. It was shown that a photodimerizable derivative of cinnamic acid crystallized in three forms, α, β and γ. When irradiated in the solid state, the α and β forms reacted in a 2+2 manner to form cyclobutane dimers, whereas the γ form was photostable. It was further demonstrated that the distance and orientation of double bonds in adjacent molecules determined the solid-state reactivity; a reaction would only occur if the distance between reactive parallel double bonds was less than 4.2 Å. In the case of the γ form, with a separation of 4.9 Å, the distance was simply too large for a topochemical reaction to take place.

Subsequent studies of crystal packing and photoreactivity of anthracene derivatives brought about the notion of 'crystal engineering'. Further work on carboxylic acid derivatives [7] and quinones [8] strengthened the topochemical argument. At the time, Schmidt stated that further development of this concept would "be difficult, if not impossible, until we understand the intermolecular forces responsible for the stability of the crystal lattice" [6]. Nevertheless, many elegant examples of crystal engineering have been reported and a range of intermolecular interactions is being utilized to preferentially orient molecules into organic and inorganic-organic structures with the ultimate intent of preparing new functional solids.

2. Intermolecular forces

The unambiguous identification of a molecule or of some particular feature within the molecular structure represents the ultimate goal in many areas of chemistry. However, for a crystal engineer, this stage is only a starting point. Since the crystal structure represents a system where all covalent and non-covalent forces are poised at an energetic minimum [9], it contains all the information regarding the structural influence of, and balance between, intermolecular forces. If we could effectively decode this information, then the prospects of designing materials with specific properties would be greatly enhanced.

2.1 HYDROGEN BONDING

"Hydrogen-bonding is surely the most frequently encountered and hence most important interaction in crystals. The frequency with which the elements nitrogen and oxygen occur in organic compounds, coupled with the strength and directionality of the hydrogen-bond as compared to other intermolecular forces account for its significance."[1]. It is the most reliable directional force in supramolecular synthesis, and as such, can be considered as the "master key" for molecular recognition [2].

2.1.1 What is a hydrogen bond?

Hydrogen-bond interactions have been defined as "short-range site-bounded cohesion forces that considerably weaken a given chemical bond of one of the partners" [10]. A hydrogen bond represents a particular case where the weakened chemical bond involves a hydrogen atom and a region of increased electron density. This region is often provided by a more electronegative atom *e.g.* O, N, S, Cl, *etc.*, but hydrogen-bond acceptors may also include π-electrons in unsaturated organic molecules. Since the hydrogen bond causes a weakening of the covalent D-H bond, it can be identified and quantified using IR and NMR spectroscopy, and X-ray and neutron diffraction. Note that it is important to consider the particular prejudicial quality of the technique that is used to locate the hydrogen atom [11]; neutron and X-ray diffraction detect two non-coincidental areas of the hydrogen atom. As "the nucleus and the electron density of an atom are essential parts, it is therefore impossible to assert rationally that the position of either the one or the other is *the* position of the atom" [12]. Despite this apparent paradox, the hydrogen bond has been extensively studied both experimentally and theoretically primarily due to its importance in life itself.

UM00012717
NOVARTIS EXHIBIT 1017
Novartis v. Regents, IPR2023-01346
Page 1463 of 4460

2.1.2 *Hydrogen-bond strength and geometry*

The thermodynamic strength of a hydrogen bond depends crucially upon the atoms involved in the bond. For neutral molecules, typical values fall in the range of 10-65 kJmol^{-1}. This is greater than for van der Waals forces, but less than for conventional covalent bonds. However, if one of the species involved in the hydrogen bond is ionic (a charge-assisted hydrogen bond) the strength can increase to 80-120 kJmol^{-1}. This means that the strongest hydrogen bonds are energetically equal to some of the weaker covalent bonds [9]. The characteristic geometry of a hydrogen bond D-H····A-X is given by the lengths A····D and H····D, the angles AHD, (θ), and HAX, (Φ), and the planarity of the system, DHAX, Fig. 2.1, [13].

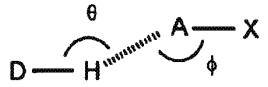


Figure 2.1 Schematic drawing illustrating important geometric parameters of a hydrogen bond.

The most commonly used criteria for identification of a hydrogen bond, are the interatomic distance, H····A, and the angle, θ. If the distance between two atoms is significantly shorter than the sum of their van der Waals radii, [14] and if θ is larger than 110°, then the presence of a hydrogen bond is usually evoked. Some typical values for hydrogen bond distances are 1.80-2.00 Å for an N-H····O bond, and 1.60-1.80 Å for an O-H····O bond [15]. If the hydrogen bond is bifurcated or trifurcated, a more relaxed distance criterion is often applied [16]. When a carbonyl oxygen atom is accepting two hydrogen bonds, the N-H bonds tend to lie close to a 'lone pair' on the oxygen atom (N-H····O=C < 120^0), whereas when one bond is formed, the N-H bond is positioned between the formal lone pairs. The directionality of hydrogen bonds and the preference for the N-H or O-H vector to point towards the 'lone pair' direction on the acceptor atom, has been found to depend upon the 'hybridization' of the acceptor atom [17]. This view is further supported by a study of the crystal structures of all ether, epoxide, ketone, and ester structures in the Cambridge Structural Database [18] with a O····X (X=O, N) distance of less than 3.00 Å; most hydrogen-bond donors lie along the lone pair direction, and this angular preference decreases when moving from epoxide to ketone to ether [1].

2.1.3 *Weak hydrogen bonds*

There is no doubt that hydrogen bonds involving O-H and N-H moieties influence crystal packing but in recent years, several studies have demonstrated that weaker hydrogen bonds, such as C-H····O, C-H····Cl, and C-H····π, can play an important role in determining the crystal structure [19]. The existence of C-H····X hydrogen bonds has been a matter of controversy ever since it was proposed by Glasstone in 1937 [20]. Physical consequences of these interactions were suggested by Pauling who attributed the higher boiling point of acetyl chloride (51^{0}C), compared to that of trifluoroacetyl chloride (<0^{0}C), to hydrogen bonding even though no conventional hydrogen-bonding groups were present [14b]. Even so, the ability of C-H moieties to act as hydrogen-bond donors remained a subject of contention for many years [21], until a survey of 113 organic structures, solved from neutron diffraction, provided conclusive evidence for the existence of C-H····O hydrogen bonding [22]. The study also indicated that the C-H····O bond is essentially electrostatic in nature, which was inferred by the fact that the hydrogen atoms point towards the lone pair of the oxygen atom. As this bond is electrostatic, its strength will decrease slowly with distance, and it can therefore be considered an attractive interaction at distances equal to, or larger than the van der Waals limit. The long range orienting nature of a C-H····O interaction underscores its important role in crystal engineering. Despite an accumulating body of evidence supporting the existence of weaker hydrogen bonds, the debate regarding the strength, directionality and relative abundance of such interactions has continued [23]. As a consequence, considerable theoretical and experimental efforts have been made to probe the structural consequences of 'weaker' hydrogen-bond interactions [24]. Typically, the directional preferences of these bonds are satisfied within the geometrical constraints of stronger hydrogen bonds, such as O-H····O and N-H····O interactions. However, the energy of weaker hydrogen bonds (4-8 kJmol^{-1}) is certainly large enough to allow these interactions to compete with van der Waals forces, especially if they are working in concert. Furthermore, C-H····X interactions can tilt the balance between several options of stronger bonded networks, thus acting as an important "steering force" in the solid-state assembly.

UM00012718
NOVARTIS EXHIBIT 1017
Novartis v. Regents, IPR2023-01346
Page 1464 of 4460

2.1.4 Halogen-halogen and other non-covalent hetero-atom interactions

Halogen substituents in molecular solids are capable of forming short contacts to other heteroatoms, such as nitrogen, oxygen and sulfur, and they may also participate in hydrogen bonds with N-H, O-H, and C-H moieties. The nature of short halogen-halogen atom distances is still not fully understood; short contacts may be the result of elliptically shaped atoms [25], or due to specific attractive forces [26]. Polarization does play a role since there is a distinction between symmetrical interactions, Cl····Cl and I····I, and unsymmetrical interactions, I····Cl and Br····F [1]. The directional interactions between halogen atoms and oxygen and/or nitrogen atoms are also induced by polarization. Such interactions have been successfully used in creating robust molecular tapes, Fig. 2.2 [27].

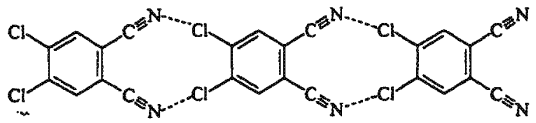


Figure 2.2 One-dimensional tape motif generated by C≡N····Cl interactions

Polarization effects are also important for sulfur atoms, which are known to engage in short intermolecular contacts. Such interactions have been employed to generate "supramolecular carpets" *via* the self-assembly of *bis*-4,4-dihydroxyphenol sulfone sustained by S····O interactions [28].

2.1.5 General rules for hydrogen bonding

After an extensive examination of preferential packing preferences and hydrogen-bond patterns in a vast number of organic crystals, Etter and co-workers put forward the following guidelines to facilitate deliberate design of hydrogen-bonded solids [29];

(i) All good proton donors and acceptors are used in hydrogen bonding.

(ii) Six-membered ring intramolecular hydrogen bonds form in preference to intermolecular hydrogen bonds.

(iii) The best proton donor and acceptor remaining after intramolecular hydrogen bond formation will form intermolecular hydrogen bonds.

These empirical 'rules' are the consequences of correlations between hydrogen-bond patterns and functional groups. The first rule was originally put forth by Donohue [30], and generally as the proton increases in acidity, its donor properties will improve. Good donors are generally found in carboxylic acids, amides, urea derivatives, anilines, imines and phenols, and good proton acceptors are typically acid and amide carbonyl groups, sulfoxides, phosphoryls, nitroxides, and amine nitrogen atoms. The second rule derives from competition studies, which showed that an intramolecular hydrogen bond was more difficult to break than a comparable intermolecular bond formed from similar donors. The third rule can be illustrated by 2-aminopyrimidine succinic acid cocrystals, where the best donors (the acidic protons) are paired with the best acceptors (the ring nitrogen atoms), Fig. 2.3 [31].

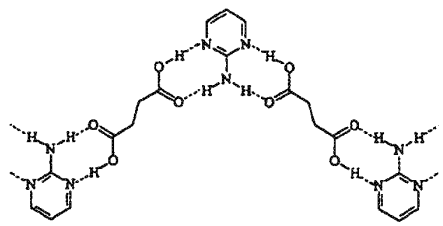
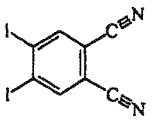


Figure 2.3 Hydrogen-bonding pattern of 2-aminopyrimidine and succinic acid.

UM00012719
NOVARTIS EXHIBIT 1017
Novartis v. Regents, IPR2023-01346
Page 1465 of 4460

ctions
ontacts to other heteroatoms, such as
ien bonds with N-H, O-H, and C-H
not fully understood; short contacts
: attractive forces [26]. Polarization
interactions, Cl···Cl and I···I, and
eractions between halogen atoms and
h interactions have been successfully



y C≡N···Cl interactions

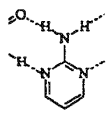
own to engage in short intermolecular
lecular carpets" *via* the self-assembly
].

nd hydrogen-bond patterns in a vast
wing guidelines to facilitate deliberate

onding.
reference to intermolecular hydrogen

lecular hydrogen bond formation will

:tween hydrogen-bond patterns and
ue [30], and generally as the proton
re generally found in carboxylic acids,
oton acceptors are typically acid and
ne nitrogen atoms. The second rule
r hydrogen bond was more difficult to
iors. The third rule can be illustrated
the acidic protons) are paired with the



rimidine and succinic acid.

2.1.6 *Graph sets: classification of hydrogen bonds*

Etter and coworkers proposed a systematic method based upon graph sets for describing hydrogen-bond patterns [32]. The process of assigning a graph set begins with the identification of the number of different types of hydrogen bonds present in the structure, and then by defining the bonds by the nature of its donors and acceptors, Fig. 2.4.

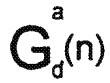


Figure 2.4 A generic graph-set descriptor.

A set of molecules hydrogen bonded in a repeat unit, a motif, is characterized by one of four designators, C (chain), R (ring), D (dimer), or S (self) which denotes an intramolecular hydrogen bond. The number of donors and acceptors used in each motif are assigned as subscripts and superscripts respectively, and the total number of atoms in the repeat unit is denoted in brackets. One of the advantages of using graph sets is that it brings the focus onto the hydrogen-bonded pattern, and not solely on the geometrical constraints of non-covalent interactions. Some examples of hydrogen-bonded motifs and their graph set assignments are given in Fig. 2.5.

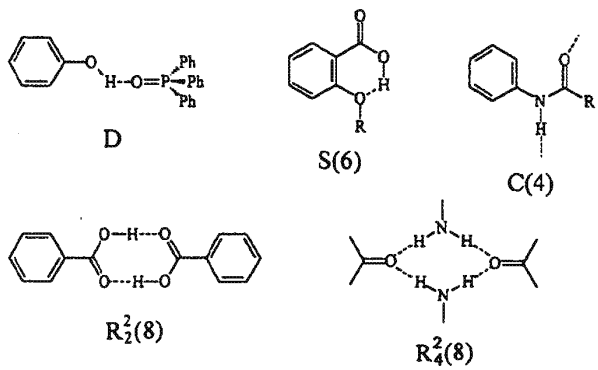


Figure 2.5 Graph set assignments for various hydrogen-bonded motifs.

3. Polymorphism

Polymorphism, a unique feature of the solid state, has been defined as "a solid crystalline phase of a given compound resulting from the possibility of at least two crystalline arrangements of the molecules of that compound in the solid state." [33]. The extent of polymorphism amongst crystalline materials is difficult to measure, and estimates range from 3% to 30% to virtually every compound [34]. Polymorphism arises because the subtle intermolecular forces that establish the stability in a crystal typically are weak and numerous, and since entropic factors are temperature dependent, the observed crystal structure is often only one of several minima in the free energy surface, not necessarily corresponding to the global minimum. The conflicting demands of entropy and enthalpy, and of different types of intermolecular interactions may yield many local minima in the energy surface. As the free energy difference between these minima starts to merge, it will increase the possibility of polymorphism. As a consequence, it is rare that polymorphs have widely different lattice energies; typically the difference is no greater that 2.5 kJ mol^{-1} at ambient conditions.

Polymorphism in flat rigid molecules can be described as "alternative ways of close packing within the framework of a constant heteroatom pattern," [1] as the directional requirements of heteroatom interactions

UM00012720
NOVARTIS EXHIBIT 1017
Novartis v. Regents, IPR2023-01346
Page 1466 of 4460

tend to be satisfied. This is demonstrated by the crystal structure of 1,4-dichlorobenzene [35] which can exist in a monoclinic or a triclinic form, both of which are composed of layers with optimal Cl···Cl interactions, but assembled in different ways. Polymorphism can also be found in compounds that have the same hydrogen-bonding pattern within the layers, but the layers will be stacked differently. This has been observed in the triclinic and tetragonal forms of 2,2-aziridine dicarboxamide [36].

Flexible molecules permit more variation in crystal packing than rigid molecules, since the torsional and conformational behavior of the molecular structure can induce a larger variety of non-covalent interactions between adjacent molecules. Conformational polymorphism occurs when the intermolecular interactions in each polymorph are similar, but each form will contain a specific molecular conformation that can be considered as characteristic of that particular polymorph. These conformations also may exist in solution. An example of this is seen in the chloro derivatives of *n*-benzylideneaniline [37], Fig. 3.1. In the triclinic form both torsion angles (α and β) are equal to 0^{o}, and in the orthorhombic form they are equal to 25^{0}.

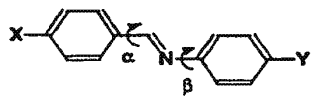


Figure 3.1 Schematic diagram of *n*-benzylideneaniline.

An examination of the lattice energies of the two structures showed that the planar triclinic form is marginally more stable, however, attempts to determine which atom type was contributing to the extra stabilization were inconclusive. The relatively small energy difference between the two forms is consistent with the expected energy difference found in polymorphs. Although polymorphism still poses many vexing questions, a few general observations can be made [1,13]. The frequency of occurrence of polymorphism is not equal in all categories of compounds, *i.e.*, rigid flat molecules are unlikely to have many polymorphic conformations at normal temperature and pressure. Furthermore, molecules with multipoint recognition are likely to yield a unique pattern of synthons, and thus decrease the likelihood of polymorphism. Polymorphism does not always adversely affect a particular application of the material, as the property-defining fragment may remain intact in all the polymorphs. Finally, polymorphism may be strongly solvent dependent in some cases, and the computer simulation of a crystal structure, with and without solvent molecules being incorporated, may give useful guidelines when crystallizing a particular polymorph.

We recently reported the crystal structures of three previously unknown polymorphs of 2-amino-5-nitropyrimidine [38]. All three forms were stable over several months at ambient temperature and pressure, and no changes in crystal morphology or macroscopic appearance could be detected as a function of time. Each structure is characterized by an extensive network of hydrogen-bond interactions (including C-H···N and C-H···O interactions), and short inter-layer distances. All three polymorphs were also obtained separately through a careful choice of solvent or *via* sublimation. Although this molecule itself is relatively simple with very limited flexibility (rotation of the amino or nitro groups with respect to the aromatic ring), our crystal structure modeling has shown that this structural system presents a considerable challenge to current models of structure prediction. The best such a prediction can do is to find the minima in the lattice energy (calculated using the assumed model potential), which are closest to the experimental structures, using a rigid molecular structure derived by theoretical calculations. The 2-amino-5-nitropyrimidine polymorphic system has shown the limitations of this crude static thermodynamic criterion as well as the assumed rigidity and intermolecular potential. It is clear that the conformational flexibility of 2-amino-5-nitropyrimidine does play an important role in providing alternative packing arrangements and this is a good example of a system where a small change in molecular geometry allows a qualitatively different and more favourable crystal packing. This observation also serves to underline the pitfalls and difficulties involved with structure predications. A small change in molecular structure may lead to dramatic changes in the crystal structure and we therefore need more refined potential models and more structural and thermodynamic data.

The appearance of polymorphs also raises an important point regarding the reliability of single-crystal X-ray diffraction. When an individual crystal is chosen, it is generally the 'best' in the sample, and therefore, by its very nature, atypical of the majority of the sample. It is thus important to compare the structure of the

UM00012721
NOVARTIS EXHIBIT 1017
Novartis v. Regents, IPR2023-01346
Page 1467 of 4460

'best' crystal with the bulk of the material and this can be done using powder diffraction. By simulating a powder diffraction pattern from the single crystal data and comparing this with the pattern recorded for the bulk sample, it can be easily determined if the chosen crystal is a true representative of the sample; that is, if the sample is structurally homogenous.

4. Strategies in crystal engineering: Organic solids

4.1 INTRODUCTION

Strategies for organic synthesis are based upon an understanding and utilization of the covalent bond. Supramolecular synthesis, on the other hand, is defined in terms of intermolecular connectivity and interactions. For the rational design of predictable assemblies, hydrogen bonding is the most commonly used supramolecular "glue", due to its strength and directionality. These non-covalent interactions can be refined by judicious placement of specific functional groups onto the molecular skeleton to generate "supramolecular synthons" [13]. Some common examples of supramolecular synthons are given in Fig. 4.1.

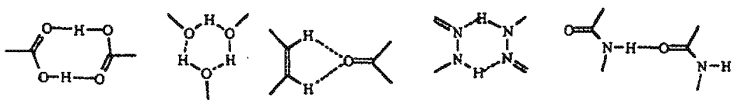


Figure 4.1 Examples of supramolecular synthons.

Supramolecular synthons are structural units within assemblies that can be generated by known or conceivable synthetic operations involving intermolecular interactions. One goal in crystal engineering is to recognize and design synthons that are robust enough to be exchanged from one network to another, thus leading to generality and predictability. This structural predictability can then be used in the construction of one, two, or three-dimensional patterns. In general, with careful molecular design, a 1-D array held together by strong intermolecular forces can be obtained relatively easily. The addition of functional groups or weaker intermolecular forces can then be used to bridge the 1-D networks into 2-D layers or sheets. Finally, these assemblies can be built up to yield a 3-D solid architecture by the same process, or by addition of new molecules/counterions that are capable of connecting the layers. This step-wise process can help to simplify the design process of a new solid, Fig. 4.2.

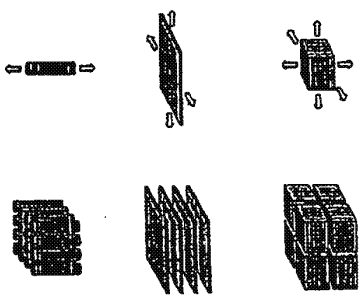
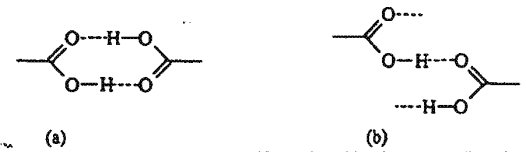


Figure 4.2 Step-wise construction of a 3-D lattice.

UM00012722
NOVARTIS EXHIBIT 1017
Novartis v. Regents, IPR2023-01346
Page 1468 of 4460

4.2 DESIGN OF ORGANIC MOLECULAR SOLIDS

Of the many supramolecular synthons that employ hydrogen bonds as the main intermolecular connectors, the carboxylic acid moiety is the most widely recognized. Leiserowitz [39] has shown that the carboxylic acid functionality is capable of forming two different hydrogen-bonding motifs, Fig. 4.3. They include the head-to-head interaction, which forms cyclic hydrogen-bonded dimers *via* two O-H····O hydrogen bonds, and the less common catemer interaction, in which each carboxyl group is linked to two adjacent carboxyl groups *via* one O-H····O hydrogen bond.



(a) (b)

Figure 4.3 The two hydrogen-bonding motifs displayed by the carboxylic acid functionality - (a) head-to-head motif, and (b) catemer motif.

The solid-state structures of various aromatic carboxylic acids illustrate the utility of the carboxylic acid moiety for assembling supramolecular architectures of varying dimensionality, Fig. 4.4. When only one carboxylic acid functionality is present per molecule (*i.e.* benzoic acid [40]), discrete dimers are formed in the solid-state. However, if two carboxylic acid functionalities are present per molecule (*i.e. iso*-phthalic acid [41] or terephthalic acid [42]), infinite 1-D chains are produced. And finally, if three carboxylic acid functionalities are present per molecule (*i.e.* trimesic acid [43]), the resulting supramolecular structure is an infinite 2-D sheet.

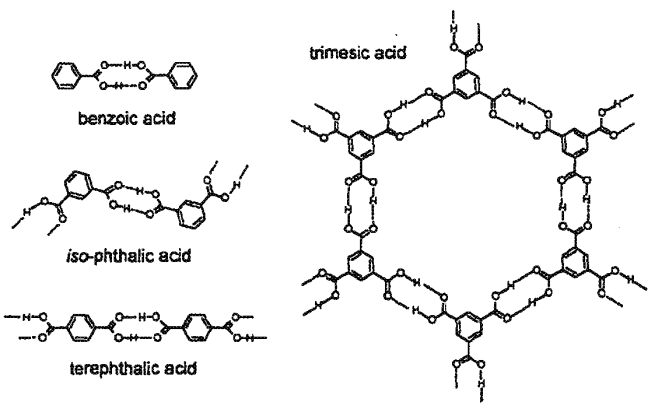


Figure 4.4 Solid-state structures of varying dimensionality assembled *via* the carboxylic acid head-to-head interaction.

Another prominent synthon widely used in supramolecular synthesis is the amide functionality. Much like the carboxylic acid cyclic dimer, unsubstituted amides primarily form head-to-head hydrogen-bonding interactions (although exceptions exist) [44]. This head-to-head interaction is composed of complementary N-H····O hydrogen bonds between adjacent amide functionalities, Fig. 4.5. However, unlike the carboxylic acid functionality, the second amide hydrogen will often form another hydrogen bond with the carbonyl oxygen of a neighboring amide. This 'extra' hydrogen bond adds to the overall dimensionality of the solid-state structure.

UM00012723
NOVARTIS EXHIBIT 1017
Novartis v. Regents, IPR2023-01346
Page 1469 of 4460

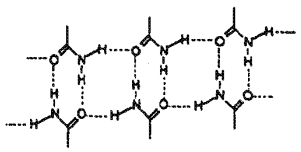


Figure 4.5 Common hydrogen-bonded ribbon in primary amides.

As previously mentioned, the amide functionality may be used to assemble supramolecular architectures in much the same way as the carboxylic acid moiety. This point is illustrated by the similarities of the solid-state structures of various aromatic carboxamides, Fig. 4.6, when compared to their carboxylic acid analogs, Fig. 4.4. When one amide functionality is present per molecule (*i.e.* benzamide [45]), cyclic dimers again are formed. In addition, these dimers are propagated into a 1-D tape through two complementary N-H···O hydrogen bonds between neighboring dimers. When two amide functionalities are present per molecule (i.e. terephthalamide [46]), infinite 1-D chains are produced. These 1-D infinite chains then are propagated into the corresponding 2-D sheets *via* a second N-H···O hydrogen bond involving the 'extra' amide proton and the carbonyl oxygen of a neighboring amide.

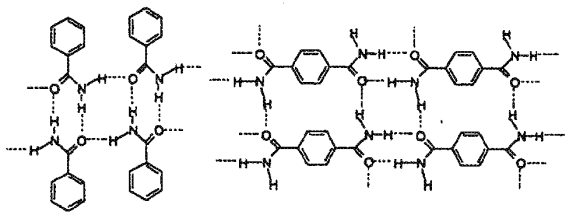


Figure 4.6 Solid-state architectures assembled *via* amide head-to-head interactions.

The oxime moiety represents another synthon capable of generating supramolecular architectures. Although this functionality is nothing new to organic chemists, it remains relatively unexplored as an intermolecular connector. In the absence of other strong hydrogen bond acceptors, the oxime functionality has been shown to form head-to-head cyclic dimers in the solid-state [47]. The cyclic dimer is held together by complementary O-H···N hydrogen bonds between adjacent molecules, Fig. 4.7.

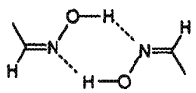


Figure 4.7 Head-to-head hydrogen-bonding interactions between adjacent oxime moieties.

4.3 DESIGN OF IONIC ORGANIC SOLIDS

In recent years, several examples of engineering of ionic organic and organic-inorganic compounds with specific packing motifs have appeared. Ward and co-workers have utilized the complementarity of hydrogen-bond sites on guanidinium cations and substituted sulfonate anions in the preparation of materials containing infinite hydrogen-bonded sheets [48]. The precise topology of these motifs can be modified through appropriate substitution of the anion. Anions of trimesic acid have also been used in the design of porous organic solids [49].

UM00012724
NOVARTIS EXHIBIT 1017
Novartis v. Regents, IPR2023-01346
Page 1470 of 4460

In our group, we have developed several predictable hydrogen-bonded architectures generated by anionic species. We have employed a variety of monoanions of dicarboxylic acids in the design of 2-D layers held together primarily by charge-assisted O-H····O hydrogen bonds between the 'head' and 'tail' of adjacent anions. In this way, we have synthesized and characterized a number of salts of tartaric acid [50], malic acid [51] and amino-*iso*phthalic acid [52]. First, these structures illustrate that the expected anionic chains are almost invariable formed. Second, the additional -OH groups (two in the case of tartaric acid, one in the case of malic acid) generate robust hydrogen-bonds between neighboring chains which gives rise to the desired 2-D anionic network, Fig. 4.8.

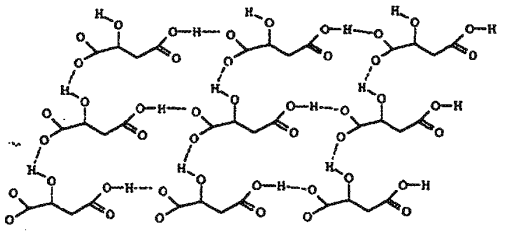


Figure 4.8 Schematic illustration of a 2-D sheet based upon hydrogenmalate anions

The final step in our design strategy, going from 2-D to 3-D, can now be achieved through a suitable choice of cation. The cations can act as bridges between neighboring anionic layers through directional intermolecular interactions. Examples of such structures are imidazolium hydrogen-*L*-tartrate [50b] and 3-hydroxy-6-methylpyridinium hydrogen-*L*-malate [51].

An important aspect of crystal engineering pertains to uncovering practical guidelines for estimating the structural outcome when combining different functional groups. In order to achieve this, it is helpful to study a simple system that can give rise to a small number of well-defined structural motifs. With this in mind we determined the structures of several organic salts based upon the oxamate anion, which contains complementary hydrogen-bond donors and acceptors. *Ab initio* calculations showed three dimeric motifs, Fig. 4.9, with very small energy differences and, in fact, all three features have appeared in crystalline oxamates [53].

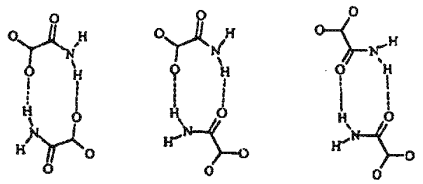
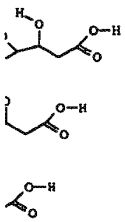


Figure 4.9 Three possible dimeric motif of oxamate anions.

In addition, the anions invariably give rise to either infinite 1-D motifs or 2-D layers and the subsequent detailed arrangement of anions and cations is determined by specific cation-anion interactions. Since certain cations lead to specific anionic motifs, we can propose simple guidelines for predicting oxamate structures. Primary ammonium ions, with three hydrogen-bond donors positioned in close proximity of each other, form hydrogen bonds to at least two different anions and, in doing so, bring anions close together (*via* N-H····O interactions), forcing the anions into a layered arrangement. Secondary or tertiary ammonium ions only bring together a smaller number of anions which is insufficient to cause the formation of an infinite 2-D sheet. In those cases, *e.g.* imidazolium oxamate, the anions instead create 1-D motifs. In addition, cation size may also be important since a small cation will inevitably bring neighboring anions within close proximity of each thereby encouraging anionic layer formation. This is exemplified by the crystal structure

UM00012725
NOVARTIS EXHIBIT 1017
Novartis v. Regents, IPR2023-01346
Page 1471 of 4460

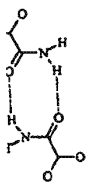
d architectures generated by anionic
cids in the design of 2-D layers held
een the 'head' and 'tail' of adjacent
r of salts of tartaric acid [50], malic
rate that the expected anionic chains
in the case of tartaric acid, one in the
ring chains which gives rise to the



ipon hydrogenmalate anions

now be achieved through a suitable
g anionic layers through directional
olium hydrogen-*L*-tartrate [50b] and

ractical guidelines for estimating the
order to achieve this, it is helpful to
fined structural motifs. With this in
n the oxamate anion, which contains
dations showed three dimeric motifs,
eatures have appeared in crystalline



oxamate anions.

ifs or 2-D layers and the subsequent
tion-anion interactions. Since certain
ies for predicting oxamate structures.
in close proximity of each other, form
g anions close together (*via* N-H····O
lary or tertiary ammonium ions only
nuse the formation of an infinite 2-D
reate 1-D motifs. In addition, cation
ing neighboring anions within close
is exemplified by the crystal structure

of potassium oxamate hydrate [53]. Conversely, a bulky cation will expand the size of the lattice thus increasing the distance between anions resulting in the formation of 1-D anionic motifs. The hydrogen bond is arguably sufficiently strong to link neighboring ions together into infinite architectures, even in the presence of different cations and in competition with other non-covalent interactions, and it is likely that there will be many more journeys into the design of desired structural functionalities in organic salts.

5. Strategies in crystal engineering: organic-inorganic hybrid materials

5.1 COORDINATION POLYMERS

The most common approach to supramolecular assembly of metal complexes has led to a wide variety of coordination polymers [54]. Several coordination polymers, 1-D, 2-D, and 3-D, have been prepared by coordinating bifunctional ligands such as 4, 4'-bipyridine or pyrazine to a transition metal ion. In these systems, the coordination environment (linear, square planar, trigonal, or octahedral) of the metal ion can dictate the dimensionality of the porous solid, as well as the influencing the nature of the cavity created.

Robson and co-workers have outlined the possibilities of creating infinite 2-D and 3-D metal-containing frameworks based around metal-4,4'-bipyridine derivatives [55]. Interpenetration of 2-D sheets can give rise to 3-D solids with channels and cavities of specific dimensions. Zaworotko and co-workers have employed similar building blocks in the design of porous 'coordination-polymers' with diamondoid structures [56]. Chen, *et. al.* [57], provide another notable example of this type of design strategy. Coordination of both 4,4'-bipyridine and pyrazine to copper(II) ions produces a 2-D rectangular network with small, rectangular channels, Fig. 5.1. Each copper(II) ion is coordinated by two 4,4'-bpy molecules, two pyrazine molecules, and two water molecules to give an octahedral coordination environment. The bpy molecules and the two pyrazine molecules are mutually *trans* and occupy the equatorial plane. Similar 2-D square networks with open channels have been constructed from Zn(II) ions and 4,4'-bpy [58] and from Cd(II) and 4,4'-bpy [59].

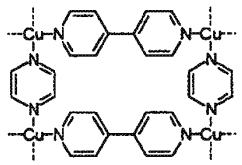


Figure 5.1 Schematic representation of the main structural feature in $\{[Cu(4,4'\text{-bpy})(pyz)(H_2O)_2][PF_6]_2\}_\infty$.

Rogers, *et. al.* [60], provide another example of a square supramolecular coordination complex. The fundamental difference between this structure and many others lies in how the 'squares' are assembled. In the previous example, the supramolecular squares are assembled by linear ligands connecting metal ions. The coordination geometry of the metal ion ensures that the ligands are orthogonal to each other, and in doing so, forms the 'corners' of the grid-like network. However, in these squares, the 'corners' of the squares are the *ligands* (pyrimidine) and the linear connectors are silver(I) ions, Fig. 5.2.

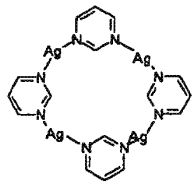


Figure 5.2 Schematic representation (a) and packing diagram of [Ag(pyrimidine)][NO_3].

UM00012726
NOVARTIS EXHIBIT 1017
Novartis v. Regents, IPR2023-01346
Page 1472 of 4460

5.2 INTERMOLECULAR ASSEMBLY OF ORGANIC/INORGANIC MATERIALS

Recently, efforts have been made to combine intermolecular hydrogen-bonding interactions of organic molecules with the strict geometrical constraints imposed by transition metal ions to produce inorganic/supramolecular hybrids [61]. In each of these examples, a coordination complex of a transition metal ion with a coordinating ligand assembles *via* hydrogen bonds into a supramolecular architecture. As described above for coordination polymers, 1-D, 2-D, and 3-D structures are possible from this type of design strategy.

Lehn and co-workers, have generated some extraordinary structures covering silver(I) helicates [62], circular double helicates [63], and supramolecular macrocycles [64]. Many of these motifs are built with a combination of well-established coordination chemistry (coordination number, geometry, *etc.*) and site-specific and self-complementary hydrogen-bonds. Mingos and co-workers [65] have utilized intermolecular connectors (*e.g.* thiourea//carboxylate, diaminopyridine///uracil), *etc.* as a way of linking neighboring metal-complexes into extended 'tapes' and sheets. Munakata *et al* prepared hydrogen bonded copper(I) complexes with large channels occupied by cations, using the well-known dimeric 2-pyridone synthon [66]. Braga, Grepioni and co-workers have been at the forefront of developing an organometallic 'branch' of crystal engineering through a combination of synthesis, database analysis, and packing-energy calculations [67] (and elsewhere in this volume).

Noncovalent assembly of coordination complexes can sometimes provide advantageous physical properties that are not always displayed by coordination polymers. Unlike coordination polymers, these types of assemblies tend to be more readily soluble. Increased solubility is desirable for reasons ranging from ease of synthetic modification and manipulation to crystal growth. The other advantage these types of systems have over coordination polymers is flexibility. Unlike the rigid frameworks of coordination polymers, assemblies generated through hydrogen-bonding interactions can 'flex' in order to accommodate changes in their environment since the hydrogen bonds holding the supramolecular array together are weaker than a covalent bond. Therefore, this type of system may lend itself to a variety of host-guest applications that would be inaccessible if the framework was rigid [68].

Aakeröy and co-workers have also demonstrated the utility of this type of design strategy for assembling low-dimensional architectures. The majority of this work is based upon coordination complexes of silver(I) salts with substituted pyridine rings [69]. The substituents on the pyridine rings are various moieties capable of solid-state self-assembly through hydrogen bonding *e.g.* carboxylic acids, carboxamides, and oximes [70]. The silver(I) complexes predominantly form infinite 1-D chains held together by the head-to-head hydrogen-bonding interactions, Fig. 5.3.

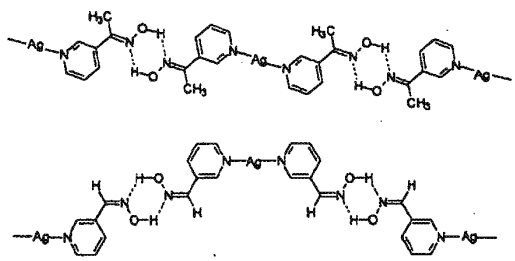


Figure 5.3 Schematic representation of infinite 1-D chains based on a linear silver(I) complex.

To increase the dimensionality of the assembly, other metal ions (*e.g.* nickel(II) and platinum(II)), can be used as the corner stone of the network. By complexing such metal ions with ligands capable of hydrogen bonding, new porous materials with a variety of guest molecules have been prepared [71]. Typically, the pyridine-based ligand coordinates to the metal ion, and an amide, oxime, or carboxylic moiety provides the cross link between adjacent metal-ion complexes, Fig. 5.4.

UM00012727
NOVARTIS EXHIBIT 1017
Novartis v. Regents, IPR2023-01346
Page 1473 of 4460

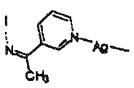
MATERIALS

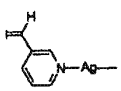
en-bonding interactions of organic
ransition metal ions to produce
oordination complex of a transition
a supramolecular architecture. As
ures are possible from this type of

s covering silver(I) helicates [62],
lany of these motifs are built with a
number, geometry, *etc.*) and site-
ers [65] have utilized intermolecular
a way of linking neighboring metal-
drogen bonded copper(I) complexes
c 2-pyridone synthon [66]. Braga,
n organometallic 'branch' of crystal
acking-energy calculations [67] (and

ide advantageous physical properties
ordination polymers, these types of
ible for reasons ranging from ease of
lvantage these types of systems have
of coordination polymers, assemblies
to accommodate changes in their
together are weaker than a covalent
ost-guest applications that would be

pe of design strategy for assembling
a coordination complexes of silver(I)
ne rings are various moieties capable
cids, carboxamides, and oximes [70].
ether by the head-to-head hydrogen-





ased on a linear silver(I) complex.

, nickel(II) and platinum(II)), can be
ons with ligands capable of hydrogen
e been prepared [71]. Typically, the
ne, or carboxylic moiety provides the

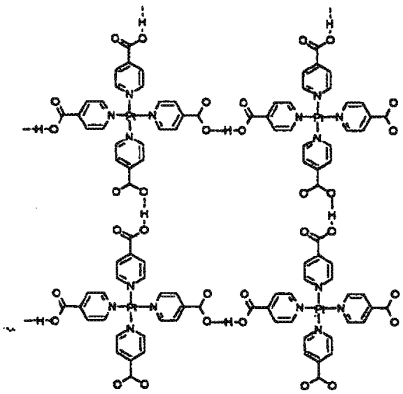


Figure 5.4 Supramolecular square grid based on platinum(II) complexes.

These types of structures demonstrate that metal complexes can be linked through hydrogen bonds to form porous structures with large cavities. The approach is quite versatile, as either octahedral or square planar metal centers can be used. In addition, a variety of ligands can link through hydrogen bonds to assemble porous 3-D networks that are thermally stable (melting points are typically > 300°C).

Crystal engineering, which is built upon an amalgamation of structural techniques, powerful theoretical models and general principles of synthetic methods, is a prime example of a truly interdisciplinary topic. As such, it is in a position to combine resources and expertise that can produce new materials for optical and electronic devices as well as more efficient catalysts, while, at the same time, addressing fundamental issues with broader implications, *e.g.* intermolecular forces and structure-property correlations. Indeed, a rational design of crystalline materials may create opportunities of considerable academic and commercial importance.

References

1. Desiraju, G.R. (1989) *Crystal Engineering: The Design of Organic Solids*, Elsevier, Amsterdam.

2. Lehn, J.-M. (1995) *Supramolecular Chemistry*, VCH, Weinheim.

3. Aakeröy, C.B. (1997) Crystal engineering: strategies and architectures, *Acta Crystallogr.* **B53**, 569- 586.

4. Desiraju, G.R. (ed.) (1995) *Perspectives in Supramolecular Chemistry, Vol. 2, The Crystal as a Supramolecular Entity*, Wiley, Chichester.

5. Lehn, J.-M. (1990) Perspectives in supramolecular chemistry – From molecular recognition towards molecular information-processing and self-organization, *Angew. Chem. Int. Ed. Engl.* **29**, 1304-1319.

6. Schmidt, G.M.J. (1971) Photodimerizations in the solid state, *Pure Appl. Chem.* **27**, 647-657.

7. Rabinovich, D. and Schmidt, G.M.J. (1967) Topochemistry. Part XIX. The crystal structure of monomethyl *trans, trans*-muconate, *J. Chem. Soc. (B)*, 286-289.

UM00012728
NOVARTIS EXHIBIT 1017
Novartis v. Regents, IPR2023-01346
Page 1474 of 4460

8. Rabinovich, D. and Schmidt, G.M.J. (1967) Topochemistry. Part XV. The solid-state photochemistry of *p*-quinones, *J. Chem. Soc. (B)*, 144-149.

9. Aakeröy, C.B. and Seddon, K.R. (1993) The Hydrogen Bond and Crystal Engineering, *Chem. Soc. Rev.* 397-407.

10. Huyskens, P.L. and Zeegers-Huyskens, T. (1991) *Intermolecular Forces: An Introduction to Modern Methods and Results*, Springer-Verlag.

11. Taylor, R. and Kennard, O. (1984) Hydrogen-bond geometry in organic crystals, *Acc. Chem. Res*, **17**, 320-326.

12. Cotton, F.A. and Luck, R.L. (1989) Strong interaction between an aliphatic carbon hydrogen-bond and a metal atom, *Inorg. Chem.* **28**, 3210-3213.

13. Desiraju, G.R. (1995) Supramolecular synthons in crystal engineering – A new organic synthesis, *Angew. Chem. Int. Ed. Engl.* **34**, 2311-2327.

14. (a) Bondi, A. (1964) Van der Waals volumes and radii, *J. Phys. Chem*, **68**, 441-449; (b) Pauling, L. (1940) *The Nature of the Chemical Bond and the Structure of Molecules and Crystals*, Oxford University Press; (c) Nyburg, S.C. and Faerman, C.H. (1985) A revision of van der Waals radii for molecular crystals – N, O, F, S, Cl, Se, Br, and I bonded to carbon, *Acta Crystallogr.* **B41**, 274-279.

15. (a) Jeffrey, G.A. and Saenger, W. (1991) *Hydrogen Bonding In Biological Structures*, Springer; (b) Speakman, J. (1975) *MTP Internationa Review of Science Vol 2*, Butterworths.

16. Allinger, N.L. (1976) Calculation of molecular structure and energy by force-field methods, *Adv. Phys. Org. Chem*, **13**, 1-82.

17. Murray-Rust, P. and Glusker, J.P. (1984) Directional hydrogen bonding to sp^2-hybridized and sp^3-hybridized oxygen atoms and its relevance to ligand macromolecule interactions, *J. Am. Chem. Soc.* **106**, 1018-1025.

18. Allen, F.H. and O. Kennard, (1993) Integrated 3d search facilities for the Cambridge Structural Database (CSD),*Chemical Design and Automation News*, *8*, 3137.

19. Subramanian, S. and Zaworotko, M.J. (1994) Exploitation of the hydrogen bond – Recent developments in the context of crystal engineering, *Coord. Chem. Rev.***137**, 357-401.

20. Glasstone, S. (1937) The structure of some molecular complexes in the liquid state, *Trans. Faraday Soc.* **33**, 200-214.

21. Donohue, J. (1968) *Structural Chemistry and Molecular Biology*, W.H.Freeman.

22. Taylor, R. and Kennard, O. (1982) Crystallographic evidence for the existence of CH····O, C-H····N, and C-H····Cl hydrogen bonds, *J. Am. Chem. Soc.* **104**, 5063-5070.

23. Cotton, F.A., Daniels, L.M., Jordan, G.T., and Murillo, C.A. (1997) The crystal packing of *bis*(2,2'-dipyridylamido)cobalt(II), $Co(dpa)_2$ is stabilized by C-H center dot center dot center dot N bonds: are there any real precedents? *Chem. Commun.* 1673-1674.

24. (a) Allen, F.H., Lommerse, J.P.M., Hoy, V.J., Howard, J.A.K., and Desiraju, G.R. (1996) The hydrogen-bond C-H donor and π-acceptor characteristics of three-membered rings, *Acta Crystallogr.*

UM00012729
NOVARTIS EXHIBIT 1017
Novartis v. Regents, IPR2023-01346
Page 1475 of 4460

B52, 734-735; (b) Reddy, D.S., Goud, B.S., Panneerselvan, K., and Desiraju, G.R. (1993) C-H····N mediated hexagonal network in the crystal structure of the 1/1 molecular complex 1,3,5- tricyanobenzene hexamethylbenzene, *J. Chem. Soc. Chem. Commun.* 663-665; (c) Desiraju, G.R. (1992) C-H····O hydrogen-bonding and the deliberate design of organic crystal structures, *Mol. Cryst. Liq. Cryst.* **211**, 63-74; (d) Desiraju, G.R. (1991) The C-H...O hydrogen bond in crystals – What is it? *Acc. Chem. Res.* **10**, 290-296; (e) Steiner, T. and Desiraju, G.R. (1998) Distinction between the weak hydrogen bond and the van der Waals interaction, *Chem. Commun.* 81-892; (f) Mascal, M. (1998) Statistical analysis of C-H····N hydrogen bonds in the solid state: there *are* real precedents, *Chem. Commun.* 303-304.

25. Lucas, J., Price, S.L., Rowland, R.S., Stone, A.J., and Thornley, A.E. (1994) The nature of –Cl-center-dot-center-dot-Cl- intermolecular interactions, *J. Am. Chem. Soc.* **116**, 4910-4918.

26. Desiraju, G.R. and Parthasarathy, R. (1989) The nature of halogen····halogen interactions – Are short halogen contacts due to specific attractive forces or due to close packing of nonspherical atoms? *J. Am. Chem. Soc.* **111**, 8725-8726.

27. Desiraju, G.R., Ovchinnikov, Y.E., Reddy, D.S., Shishkin, O.V., and Struchkov, Y.T. (1996) Supramolecular synthons in crystal engineering 3. Solid state architectures and synthon robustness in some 2,3-dicyano-5,6-dichloro-1,4-dialkoxybenzene, *J. Am.Chem. Soc.* **118**, 4085-4089.

28. Davies, C., Langler, R.F., Sharma, C.V.K. and Zaworotko, M.J. (1997) A supramolecular carpet formed *via* self-assembly of *bis*(4,4'-dihydroxyphenyl) sulfone, *Chem. Commun*, 567-568.

29. Etter, M.C. (1990) Encoding and decoding hydrogen-bond patterns of organic compounds, *Acc. Chem. Res.* **23**, 120-126.

30. Donohue, J. (1952) The hydrogen bond in organic crystals, *J. Phys. Chem.* **56**, 502-510.

31 Etter, M.C. and Adsmond, D.A. (1990) The use of cocrystallization as a method of studying hydrogen-bond preferences of 2-aminopyrimidine, *J. Chem. Soc. Chem. Commun.*, **8**, 589-591.

32. (a) Etter, M.C. (1985) Aggregate structures of carboxylic-acids and amides, *Israel. J. Chem*, **25**, 312-319; (b) Etter, M.C., Bernstein, J.B. and MacDonald, J.C. (1990) Graph-set analysis of hydrogen-bond patterns in organic crystals, *Acta Crystallogr*, **B46**, 256-262; (c) Bernstein, J., Davis, R.E., Shimoni, L., and Chang, N. (1995) Patterns in hydrogen bonding – functionality and graph-set analysis in crystals, *Angew. Chem. Int. Ed. Engl.* **34**, 1555-1573.

33. McCrone, W.C. (1965) *Physics and Chemistry of the Organic Solid State, Vol. B*, Weissberger.

34. Burger, A. (1982) Thermodynamic and other aspects of the polymorphism of drugs, *Pharm. Int.* **3**, 158-163.

35. Mnyukh, Y.V. (1963) The crystal structure of 1,4-dichlorobenzene, *J. Phys. Chem. Solids*, **24**, 631-638.

36. Bruckner, S. (1982) An unusual example of packing among molecular layers – The structures of two crystalline forms of 2,2-aziridinecarboxamide, $C_4H_7N_3O_2$, *Acta Crystallogr.* **B38**, 2405-2408.

37. Bernstein, J. and Hagler, A.T. (1978) Conformational polymorphism. The influence of crystal structure on molecular conformation, *J. Am. Chem. Soc.*, **100**, 673-681.

38. Aakeröy, C.B., Nieuwenhuyzen, M., Price, S.L. (1998) Three polymorphs of 2-amino-5-nitropyrimidine: Experimental structures and theoretical predictions, *J. Am. Chem. Soc.* **120**, 8986-8993.

UM00012730
NOVARTIS EXHIBIT 1017
Novartis v. Regents, IPR2023-01346
Page 1476 of 4460

39. Leiserowitz, L. (1976) Molecular packing modes. Carboxylic acids *Acta Crystallogr.*, ***B32***, 775-802

40. Bruno, G. and Randaccio, L. (1980) A refinement of the benzoic acid structure at room temperature, *Acta Crystallogr.* **B36**, 1711-1712.

41. Derissen, J.L. (1974) Isophthalic acid, Acta *Crystallogr.* **B30**, 2764-2765.

42. Bailey, M. and Brown, C.J. (1967) The crystal structure of terephthalic acid, *Acta Crystallogr.* **22**, 387-391.

43. Duchamp, D. J. and Marsh, R.E. (1969) The crystal structure of trimesic acid, *Acta Crystallogr.* **B25**, 5-19.

44. Leiserowitz, L. and Schmidt, G.M.J. (1969) Molecular packing modes. Part III. Primary amides, *J. Chem. Soc. (A)*, 2372-2382.

45. Penfold, B.R. and White, J.C.B. (1959) The crystal and molecular structure of benzamide, *Acta Crystallogr.* **12**, 130-135.

46. Cobbledick, R. E. and Small, R. W. H. (1972) The crystal structure of terephthalamide, *Acta Crystallogr.* **B28**, 2893-2896.

47. Jerslev, B. and Larsen, S. (1992) Crystallizations and crystal-structure at 122 K of anhydrous (*E*)-4-hydroxybenzaldehyde oxime, *Acta Chem. Scand.* **46**, 1195-1199.

48. (a) Russell, V.A., Evans, C.C., Li, W.J., and Ward, M.D. (1997) Nanoporous molecular sandwiches: Pillared two-dimensional hydrogen-bonded networks with adjustable porosity, *Science* **276** 575-579; (b) Russell, V.A. and Ward, M.D. (1996) Molecular crystals with dimensionally controlled hydrogen-bonded nanostructures, *Chem. Mater.* **8**, 1654-1666.

49. Melendez, R.E., Sharma, C.V.K., Zaworotko, M.J., Bauer, C., and Rogers, R. (1996) Toward the design of porous organic solids: modular honeycomb grids sustained by anions of trimesic acid, *Angew. Chem. Int. Ed Engl.* **35**, 2213-2215

50. (a) Aakeröy, C.B., Hitchcock, P.B., and Seddon, K.R. (1992) Organic salts of *L*-tartaric acid: Materials for second harmonic generation with a crystal structure giverned by an anionic hydrogen-bonded *J. Chem. Soc., Chem. Commun.*, 553-555; (b) Aakeröy, C.B. and Hitchcock, P.B. (1993) Hydrogen-bonded layers of hydrogentartrate anions: two-dimensional building blocks for crystal engineering, *J. Mater. Chem.* **3**, 1129-1135.

51. (a) Aakeröy, C.B. and Nieuwenhyzen, M. (1994) Hydrogen-bonded layers of hydrogenmalate anions: A framework for crystal engineering, *J. Am. Chem. Soc.* **116**, 10983-10991; (b) Aakeröy, C.B. and Nieuwenhyuzen, M. (1996) Hydrogen Bonding in crystal engineering: 2-D layers of hydrogen-*L*-malate anions, *J. Mol. Struct.*, **374**, 223-239.

52. Aakeröy, C.B., Hughes, D.P. McCabe, J.M., and Nieuwenhuyzen, M. (1998) Aromatic dicarboxylic acids as building blocks of extended hydrogen-bonded architectures, *Supramolecular Chemistry*, **9**, 127-135.

53. Aakeröy, C.B., Hughes, D.P., and Nieuwenhuyzen, M. (1996) The oxime functionality: A versatile synthon for supramolecular assembly of metal-containing hydrogen-bonded architectures, *J. Am Chem. Soc.* **120**, 7383-7384.

UM00012731

NOVARTIS EXHIBIT 1017
Novartis v. Regents, IPR2023-01346
Page 1477 of 4460

Acta Crystallogr., *B32*, 775-802

acid structure at room temperature,

2765.

phthalic acid, *Acta Crystallogr.* **22**,

imesic acid, *Acta Crystallogr.* **B25**,

nodes. Part III. Primary amides, *J.*

ular structure of benzamide, *Acta*

structure of terephthalamide, *Acta*

cture at 122 K of anhydrous (*E*)-4-

Nanoporous molecular sandwiches:
e porosity, *Science* **276** 575-579; (b)
dimensionally controlled hydrogen-

Rogers, R. (1996) Toward the
by anions of trimesic acid, *Angew.*

nic salts of *L*-tartaric acid: Materials
by an anionic hydrogen-bonded *J.*
Hitchcock, P.B. (1993) Hydrogen-
ng blocks for crystal engineering, *J.*

l layers of hydrogenmalate anions: A
983-10991; (b) Aakeröy, C.B. and
ng: 2-D layers of hydrogen-*L*-malate

M. (1998) Aromatic dicarboxylic acids
olecular Chemistry, **9**, 127-135.

996) The oxime functionality: A
g hydrogen-bonded architectures, *J.*

54. (a) Janiak, C. (1997) Functional organic analogues of zeolites based on metal-organic coordination frameworks, *Angew. Chem. Int. Ed. Engl.* **36**, 1431-1434; (b) Abrahams, B. F., Batten, S. R., Hamit, H., Hoskins, B. F., and Robson, R. (1996) A cubic (3,4) connected net with large cavities in solvated $[Cu_3(tpt)_4](ClO_4)_3$, *Angew. Chem. Int. Ed. Engl.* **35**, 1690-1692; (c) Kawata, S., Kitagawa, S., Kumagai, H., Iwabuchi, S., and Katada, M. (1997) The structural characterization of the novel ribbon sheet $[Cu_2Cl_2(pyz)]_n$ (pyz=pyrazine), *Inorg. Chim. Acta* **267**, 143-145.

55. Batten, S.R. and Robson, R. (1998) Interpenetrating nets: Ordered, periodic entanglement, *Angew. Chem. Int. Ed. Engl.* **37**, 1460-1494.

56. (a) Copp, S.B., Subramanian, S., and Zaworotko, M.J. (1993) Spontaneous strict self-assembly of distorted super-diamondoid networks that are capable of enclathrating acetonitrile, *J. Chem. Soc., Chem. Commun.* 1078-1079; (b) Robinson, F. and Zaworotko, M.J. (1995) Triple interpenetration in [Ag(4,4'-bipyridine)][NO_3], a cationic polymer with a 3-dimensional motif generated by self-assembly of t-shaped building blocks, *J. Chem. Soc., Chem. Commun.* 2413-2414; (c) Zaworotko, M.J. (1994) Crystal engineering of diamondoid networks, *Chem. Soc. Rev.* **23**, 283-288.

57. Tong, M.-L., Chen, X.-M., Yu, X.-L., and Mak, T. C. W. (1998) A novel two-dimensional rectangular network, *J. Chem. Soc. Dalton Trans.* 5-6.

58. Subramanian, S. and Zaworotko, M. J. (1995) Porous solids by design – $[Zn(4,4'bpy)_2(SiF_6)]_n$ center-dot-xDMF, a single framework octahedral coordination polymer with large square channels, *Angew. Chem. Int. Ed. Engl.* **34**, 2127-2129.

59. Fujita, M., Kwon, Y. J., Washizu, S., and Ogura, K. (1994) Preparation, clathration ability, and catalysis of a 2-dimensional square network material composed of cadmium(II) and 4,4'-bipyridine, *J. Am. Chem. Soc* **116**, 1151-1152.

60. Sharma, C.V.K., Griffin, S.T., and Rogers, R.D. (1998) Simple routes to supramolecular squares with ligand corners: 1:1 Ag(I):pyrimidine cationic tetranuclear assemblies, *J. Chem. Soc., Chem. Commun.* 215-216.

61. (a) Blake, A.J., Hill, S.J., Hubberstey, P. and Li, W.-S. (1997) Rectangular grid two-dimensional sheets of copper(II) bridged by both coordinated and hydrogen bonded 4,4'-bipyridine (4,4'-bipy) in [Cu(μ-4,4'- bipy)$(H_2O)_2$ $(FBF_3)_2$] center dot 4,4'-bipy, *J. Chem. Soc., Dalton Trans.* 6, 913-914; (b) Carlucci, L.,Ciani, G., Proserpio, D. M., and Sironi, A. (1997) Extended networks via hydrogen bond cross-linkages of [M(bipy)] ($M=Zn^{2+}$ or Fe^{2+}) linear co-ordination polymers, *J. Chem. Soc., Dalton Trans.* **11**, 1801-1803; (c) Chan, C.- W., Mingos, D.M.P., White, A.J.P., and Williams, D.J. (1996) A crystal engineering study of copper(II) complexes with 2,4-diamino-6-(4-pyridyl)-1,3,5-triazine and 2-amino-4-phenylamino-6-(4-pyridyl)-1,3,5-triazine, *Polyhedron*, **15**, 1753-1767.

62. Garrett, T.M., Koert, U., Lehn, J.-M., Rigault, A., Meyer, D., and Fischer, J. (1990) Self-assembly of silver(I) helicates, *J. Chem. Soc., Chem. Commun.* 557-558.

63. Hasenknopf, B., Lehn, J.-M., Kneisel, B.O., Baum, G., and Fenske, D. (1996) Self-assembly of a circular double helicate, *Angew. Chem. Int. Ed. Engl.* **35**, 1838-1840.

64. Drain, C.M., Russel, K.C., and Lehn, J.-M. (1996) Self-assembly of a multi-porphyrin supramolecular macrocycle by hydrogen bond molecular recognition, *Chem. Commun.*337-338.

65. (a) Burrows, A.D., Mingos, D.M.P., White, A.J.P., Williams, D.J. (1996) Molecular recognition of 2,6-diaminopyrimidine by platinum orotate complexes, *J. Chem. Soc. Dalton Trans.* 149-151; (b) Chowdhry, M.M., Mingos, D.M.P., White, A.J.P., and Williams, D.J. (1996) Novel supramolecular self-assembly of

UM00012732
NOVARTIS EXHIBIT 1017
Novartis v. Regents, IPR2023-01346
Page 1478 of 4460

a transition-metal organo network based on simultaneous coordinate- and hydrogen-bond interactions, *Chem. Commun.* 899-900; (c) Burrows, A.D., Chan, C.W., Chowdhry, M.M., McGrady, J.E., and Mingos, D.M.P. (1995) Multidimensional crystal engineering of bifunctional metal-complexes containing complementary triple hydrogen bonds, *Chem. Soc. Rev.* **24**, 329-337.

66. Munakata, M., Wu, L-P., Yamamoto, M., Kuroda-Sowa, T., and Maekawa, M. (1996) Construction of three-dimensional supramolecular coordination copper(I) compounds with channel structures hosting a variety of anions by changing the hydrogen-bonding mode and distances, *J. Am. Chem. Soc.* **118**, 3117-3124.

67. (a) Braga, D. and Grepioni, F. (1999) Complementary hydrogen bonds and ionic interactions give access to the engineering of organometallic crystals, *J. Chem. Soc. Dalton Trans.* 1-8; (b) Braga, D., Grepioni, F., and Desiraju, G.R. (1998) Crystal engineering and organometallic architecture, *Chem. Rev.* **98**, 1375-1405.

68. (a) Chen, C.-N., Zhang, H.-X., Yu, K.B., Zheng, K.C., Cai, H., and Kang, B.S. (1998) Extended networks *via* hydrogen bond linkages of zig-zag coordination chains, *J. Chem.Soc. Dalton Trans.* 1133-1136; (b) Aakeröy, C.B., Beatty, A.M., and Helfrich, B.A. (1998) Two-fold interpenetration of 3-D nets assembled *via* three-coordinate silver(I) ions and amide-amide hydrogen bonds, *J. Chem. Soc. Dalton Trans.* 1943-1946; (c) Kumar, R.K., Balasubramanian, S., and Goldberg, I. (1998) Crystal engineering with tetraarylporphyrins, an exceptionally versatile building block for the design of multidimensional supramolecular structures, *Chem. Commun.* 1435-1436; (d) Cameron, B.R., Corrent, S.S., and Loeb, S.J. (1995) Transition metals as both host and guest: Second-sphere coordination between a Pt-azacrown ether host and a Pt-NH_3 guest, *Angew. Chem. Int. Ed. Engl.* **34**, 2689-2691; (e) Rivas, J.C.M. and Brammer, L. (1998) Supramolecular assembly of anion-channel and anion-layer structures of $[PtL_4]X_2$ (L=nicotinamide; X=Cl, or PF_6): surprisingly robust arene ring 'herringbone' motifs and adaptable amide-amide hydrogen bonding, *New J. Chem.* **22**, 1315-1318.

69. (a) Aakeröy, C. B. and Beatty, A. M. (1998) Low-dimensional architectures of silver(I) coordination compounds assembled *via* amide-amide hydrogen bonds, *Crystal Engineering* **1**, 39-49; (b) Aakeröy, C.B. and Beatty, A.M. (1998) Supramolecular assembly of low-dimensional silver(I) architectures *via* amide-amide hydrogen bonds, *Chem. Commun.* 1067-1068.

70. Aakeröy, C.B., Beatty, A.M., and Leinen, D.S. (1998) The oxime functionality: A versatile synthon for supramolecular assembly of metal-containing hydrogen-bonded architectures, *J. Am. Chem. Soc.* **120**, 7383-7384.

71. Aakeröy, C.B., Beatty, A.M., and Leinen, D.S. (1999) A new route to porous solids: Organic/inorganic hybrid materials assembled *via* hydrogen bonds, *Angew. Chem. Int. Ed. Engl.* in press.

UM00012733
NOVARTIS EXHIBIT 1017
Novartis v. Regents, IPR2023-01346
Page 1479 of 4460

This Page is Inserted by IFW Indexing and Scanning Operations and is not part of the Official Record

BEST AVAILABLE IMAGES

Defective images within this document are accurate representations of the original documents submitted by the applicant.

Defects in the images include but are not limited to the items checked:

- ☐ BLACK BORDERS
- ☐ IMAGE CUT OFF AT TOP, BOTTOM OR SIDES
- ☐ FADED TEXT OR DRAWING
- ☐ BLURRED OR ILLEGIBLE TEXT OR DRAWING
- ☐ SKEWED/SLANTED IMAGES
- ☐ COLOR OR BLACK AND WHITE PHOTOGRAPHS
- ☐ GRAY SCALE DOCUMENTS
- ☐ LINES OR MARKS ON ORIGINAL DOCUMENT
- ☐ REFERENCE(S) OR EXHIBIT(S) SUBMITTED ARE POOR QUALITY
- ☐ OTHER: _____

IMAGES ARE BEST AVAILABLE COPY.
As rescanning these documents will not correct the image problems checked, please do not report these problems to the IFW Image Problem Mailbox.

Hydrogen-bonded Layers of Hydrogentartrate Anions: Two-dimensional Building Blocks for Crystal Engineering

Christer B. Aakeröy,*[a]† and Peter B. Hitchcock[b]
[a] *Department of Chemistry, University of Minnesota, 207 Pleasant St. S.E., Minneapolis, MN 55455, USA*
[b] *School of Chemistry and Molecular Sciences, University of Sussex, Falmer, Brighton, UK BN1 9QJ*

An investigation of hydrogen-bond patterns in a family of ionic crystals has established the use of hydrogen bonding as a potential design strategy for crystal engineering of ionic materials. In 11 out of 12 crystal structures of anhydrous hydrogentartrate salts (data extracted from the Cambridge Structural Database), the anions were found to generate infinite two-dimensional sheets created by relatively short O—H···O hydrogen bonds. The regular occurrence of the infinite layer, even in the presence of widely differing cations, demonstrates the selectivity, strength and directionality of hydrogen bonds between ions in the solid state. The two-dimensional sheet was subsequently employed as a building block ('scaffolding') in the synthesis of a material with a three-dimensional hydrogen-bond network, 1*H*-imidazolium hydrogen L-tartrate (the X-ray single-crystal structure is reported), where the cation provides the anticipated cross-link between adjacent anionic layers. Each anionic network was also described using a notation based upon graph theory which simplifies the process of recognizing and communicating complex structural information.

Keywords: *Hydrogen bonding*; *Crystal engineering*; *Graph set*; *Hydrogentartrate*; *Crystal structure*

Ever since Pasteur carried out the first reported separation of crystalline enantiomers,[1] tartaric acid has held a firm place in the archives of ground-breaking chemical discoveries. 145 years later, it is possible that hydrogentartrate salts may play a key role in inspiring further development in one of the most exciting and challenging of current scientific disciplines: crystal engineering.[2]

Many elegant studies have illustrated that hydrogen bonding can be used as a versatile tool, with which molecular subunits can be joined together in a relatively predetermined way.[3–6] However, hydrogen bonding is also known to be energetically strong enough to have a profound effect on the spatial arrangement of ions in the solid state,[7] and it would therefore seem reasonable to use the strength and directionality of the hydrogen bond as an interionic synthetic route towards specific ionic aggregates and materials.[8,9]

Earlier work on some organic hydrogentartrates (the materials were prepared and investigated for their non-linear optical properties)[10] showed that their crystal structures incorporated a highly ordered, infinite layer of hydrogentartrate anions linked together by relatively short O—H···O interactions. This paper presents an extensive analysis of 12 crystal structures of hydrogentartrate salts with the purpose of establishing whether an infinite 2D anionic layer is a regular feature of these salts. Such aggregates could be used as structural building blocks (molecular 'scaffolding'), provided that they can be shown to possess structural and spatial consistency in the presence of chemically different counterions. This survey focuses on the anionic networks, since they form a point of reference throughout these materials and they are also expected to generate the most distinctive patterns, due to the availability of several hydrogen-bond donors and acceptors on each anion.

Potential applications for the design of novel materials with predictable structural features and properties can be found in almost every commercial and academic area concerned with macroscopic structure–property considerations, *e.g.* non-linear optics, shape-selective catalysis and pharmaceutical drug design.

Encoding Hydrogen-bond Patterns

An important aspect of crystal engineering pertains to the manner in which hydrogen-bond patterns are described. Etter *et al.* have developed a methodology[11] for classifying hydrogen-bond networks in, primarily, molecular solids. However, since the existing graph-set language is not always adequate for examining multi-dimensional aggregates with a high hydrogen-bond density (a consequence of the inherent difficulties with translating 3D information into scalar quantities), an additional descriptor,‡ based upon the terminology of Etter *et al.*, has been utilized as a means of specifically representing 2D hydrogen-bonded networks.

The original encoding[11] comprises a classification of patterns generated by specific hydrogen-bond types and by combinations of hydrogen bonds. Most patterns in organic molecular solids can be adequately described in terms of four principal motifs; chains (*C*), dimers (*D*), rings (*R*) and intramolecular hydrogen bonds (*S*).¶ Although this notation may not

† Permanent address: University of Sussex, School of Chemistry and Molecular Sciences, Falmer, Brighton, UK BN1 9QJ.

‡ The 2D descriptor utilized in this paper is employed as a means of facilitating a comparison and analysis of specific aggregate-types. The descriptor may have general applicability to a range of 2D structural types and this is currently being investigated. In the course of this investigation, certain modifications to the 2D descriptor may become necessary.

¶ A graph set is specified using the pattern designator (*G*), its degree (*n*) and the number of donors (*d*) and acceptors (*a*); $G_d^a(n)$. *G*, the descriptor referring to the pattern of hydrogen bonding, can be either *S* (intramolecular bond), *C* (infinite chain), *R* (intermolecular ring) or *D* (acyclic dimers and other finite structures) and the parameter *n* refers to the number of atoms in a ring, or the repeat unit of a chain. The set of ions/molecules to be analysed is called an array. Graph sets are assigned initially to motifs (patterns constructed by only one type of hydrogen bond), and then to the first-level network (a sequential listing of every motif). For example, if the array contains four different hydrogen-bond types, then the first-level graph set is a combination of four motifs. Higher-level networks are assigned by listing patterns generated by combinations of different hydrogen-bond types.

UM00012735
NOVARTIS EXHIBIT 1017
Novartis v. Regents, IPR2023-01346
Page 1481 of 4460

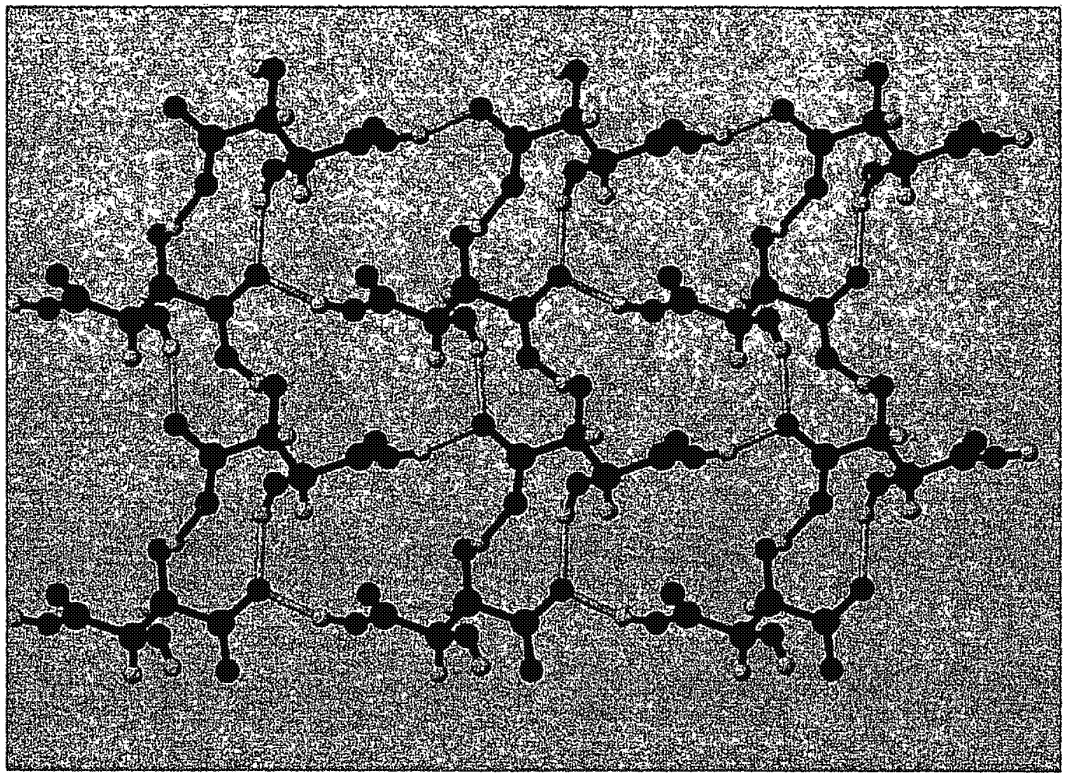


Plate 1 Anionic network of caesium hydrogen-L-tartrate; $N_{2D} = L\{R_3^3(11)R_4^3(17)\}$.[19] Covalent bonds, red; hydrogen bonds, yellow, green and white.

Table 1 Aggregate types and a graph-set description for the anionic networks in hydrogentartrate salts[a]

salt	aggregate type	graph set	r(O···O)/Å[b]	∠(O—H···O)/degrees
1	double chain	$N_1 = C_1^1(6)C_1^1(6)C_1^1(7)$	2.49	177
2	buckled layer	$N_{2D} = L\{R_2^2(11)R_4^2(17)\}$	2.559	178
3	buckled layer	$N_{2D} = L\{R_2^2(11)R_4^2(19)\}$	2.55	161
4	buckled layer	$N_{2D} = L\{R_2^2(7)R_4^2(21)\}$	2.51	174
5	buckled layer	$N_{2D} = L\{R_4^4(22)\}$	2.50	167
6	buckled layer	$N_{2D} = L\{R_4^4(22)\}$	2.49	179
7	flat layer	$N_{2D} = L\{R_3^3(12)R_3^3(16)\}$	2.438	163
8	buckled layer	$N_{2D} = L\{R_2^2(11)R_4^2(17)\}$	2.57	165
9	buckled layer	$N_{2D} = L\{R_2^2(11)R_4^2(19)\}$	2.54	168
10	flat layer	$N_{2D} = L\{R_4^4(22)\}$	2.498	168
11	buckled layer	$N_{2D} = L\{R_4^4(21)\}$	2.48	174
12	buckled layer	$N_{2D} = L\{R_2^2(11)R_4^2(17)\}$	2.558	173
13	flat layer	$N_{2D} = L\{R_3^3(12)R_3^3(16)\}$	2.50	167

[a]The search yielded structural data for (*a*) hydrogen-L-tartrates with the following cations; (–)-3-benzoyl-3-ethyl-1-methylpiperidinium (**1**),[13] rubidium (**2**),[14] *S*-(+)-*N*-methylamphetammonium (**3**),[15] 3-methylene-4-(prop-2-enyl)pyrrolidinium (**4**),[16] (–)-adrenalinium (**6**),[17] 3-hydroxypyridinium (**7**),[18] caesium (**8**),[19] *R*-(–)-*N*-methylamphetammonium (**9**),[15] (–)-1-phenylethylammonium (**10**),[20] piperazinium(2+) (**11**),[9] (*b*) ammonium hydrogen-D-tartrate (**12**),[21] and (*c*) (–)-1-phenylethylammonium hydrogen-*meso*-tartrate **13**.[22] [b]The hydrogen-bond interaction responsible for the head-to-tail linking of adjacent anions.

provide an unambiguous assignment of every structural arrangement, it is flexible enough to facilitate a systematic description of a wide range of hydrogen-bonded solids.[12]

The presence of hydrogen-bonded, infinite, 2D aggregates (sheets or layers) in crystal structures is not a unique phenomenon. Although a hydrogen-bonded sheet can be generated by the interconnection of very different (chemically and geometrically) building blocks, certain structural aspects of a sheet are amenable to a compact, yet informative, notation. One way of describing the topology of a hydrogen-bonded sheet is to identify the size, and the number, of unique hydrogen-bonded rings within the sheet. This paper will employ the following notation for characterizing such aggregates:

$$N_{2D} = L\{R_a^a(n)^{'}R_a^a(n)^{''}R_a^a(n)\ldots\}$$

UM00012736
NOVARTIS EXHIBIT 1017
Novartis v. Regents, IPR2023-01346
Page 1482 of 4460

where N_{2D} indicates a 2D network, L specifies it to be of a layered, or sheet-like, type, and the remaining variables are the same as those defined previously.

Plate 1 shows an example of how this notation is applied. Note that N_{2D} does not include intramolecular hydrogen bonds since such bonds are not instrumental in connecting adjacent molecules/ions into aggregates. Furthermore, only rings that do not contain smaller hydrogen-bonded rings as part of their structure are listed in this 2D descriptor.

Results and Discussion

Table 1 summarizes the observed aggregate types and a graph-set description for each structure, and it also contains infor-

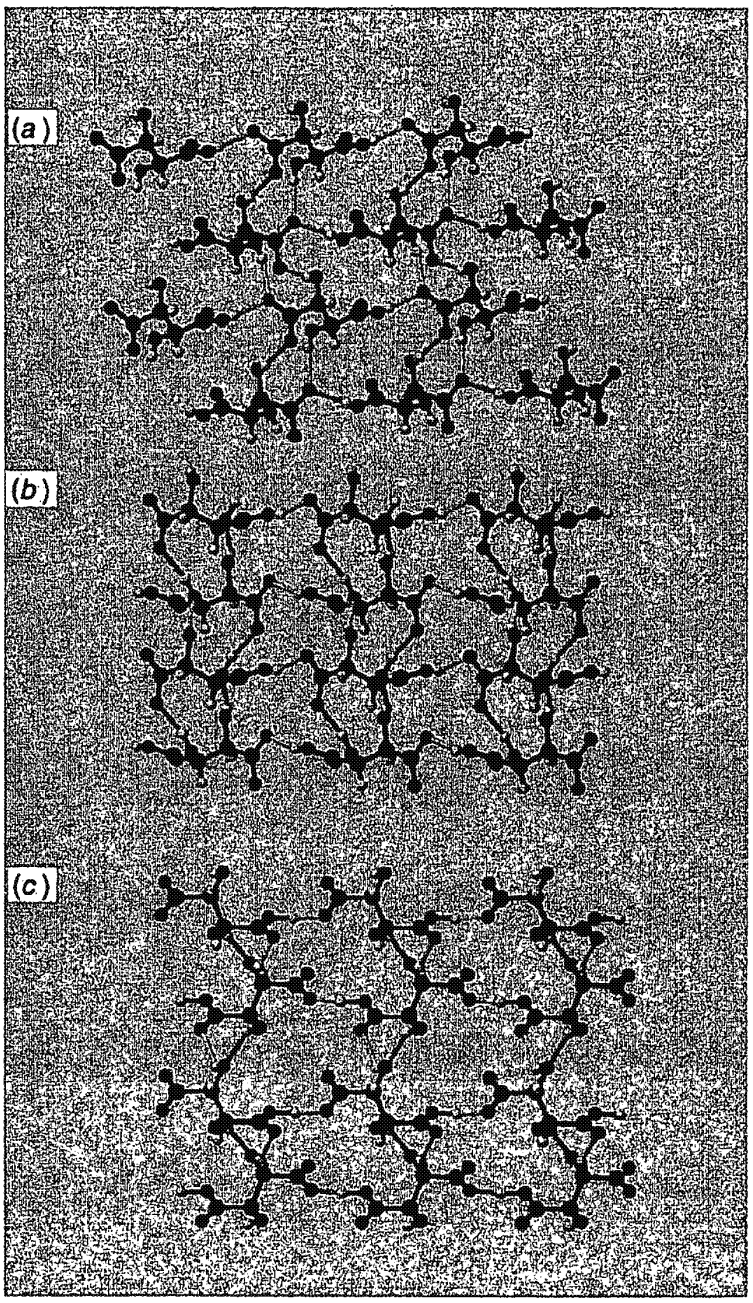


Plate 2 Anionic networks of (*a*) 2,[14] (*b*) 3,[15] and (*c*) 4.[16] The relevant graph sets are listed in Table 1. Covalent bonds, red; hydrogen bonds yellow, green and white.

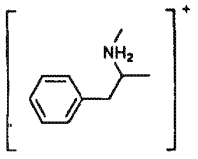
UM00012737
NOVARTIS EXHIBIT 1017
Novartis v. Regents, IPR2023-01346
Page 1483 of 4460

mation about the geometry of the O—H···O hydrogen bond (coloured yellow in Plate 1) which is responsible for the head-to-tail linking of adjacent anions into infinite chains. This interaction is present in every hydrogentartrate structure included in this survey.

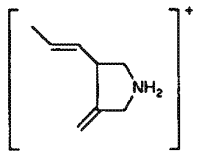
The most commonly occurring hydrogen-bonded aggregate in these salts is an infinite 2D anionic sheet; a structural feature exhibited by 11 of the 12 structures in this family. The sheet is generated by crosslinking of neighbouring chains and each chain is created by a O—H···O hydrogen bond linking anions in a 'head-to-tail' fashion. Adjacent chains are then cross-linked either by one O—H···O hydrogen bond, creating a network with a $N_{2D}=L\{R_2^2(n)\}$ graph set, or by two O—H···O hydrogen bonds, generating a network with a $N_{2D}=L\{R_2^2(n)'R_2^2(n)\}$ graph set. The average O···O distance for the 'head-to-tail' hydrogen bond is 2.51(4) Å with an average O—H···O bond angle of 170(6)°, indicating the presence of a strong, almost linear, hydrogen bond.

The anionic sheet is absent in only one crystal structure, (−)-3-benzoyl-3-ethyl-1-methylpiperidinium hydrogen-L-tartrate (**1**).[13] There does not seem to be a simple explanation for the observed structure of this compound; salts containing similar cations are currently being prepared with a view to establishing whether this is a structurally unique material.

The remarkable consistency of the infinite hydrogen-bonded sheet is illustrated by the fact that hydrogen-L-tartrate salts with very different (both chemically and geometrically) cations *e.g.* rubidium, *S*-(+)-*N*-methylamphetaminium and 3-methylene-4-(prop-2-enyl)pyrrolidinium, (in **2**,[14] **3**[15] and **4**[16]) display very similar anionic configurations, Plate 2. The cations of **3** and **4** are shown below. Consequently, hydrogentartrate anions may be employed as a means of incorporating a specific structural 2D feature into a crystalline material whilst, at the same time, imposing severe restrictions on the positional freedom of the cation.



cation of **3**



cation of **4**

Design of Novel Hydrogen-bonded Structures

Hypothesis

Having established that most of the materials in this diverse series are dominated by rigid, structurally consistent, anionic networks, a new hydrogentartrate salt 1*H*-imidazolium hydrogen-L-tartrate (**5**) was synthesized. The cation, 1*H*-imidazolium, was chosen in a deliberate attempt to provide a specific cross-link between adjacent sheets. The combination of hydrogen-bond donors at opposite ends of a small, rigid spacer, and a lack of hydrogen-bond acceptors (which could disrupt the anionic network), suggested that this cation would provide a cross-link for the anionic scaffolding, thereby creating a three-dimensional network. This hypothesis was tested by the subsequent preparation and crystallographic characterization of 1*H*-imidazolium hydrogen-L-tartrate.

Crystal Structure of 1H-Imidazolium Hydrogen-L-tartrate†

The cation and anion do not exhibit any unusual features (Fig. 1), with the anion displaying the expected zig-zag con-

† Fractional coordinates are listed in Table 2 and selected bond lengths and angles in Table 3.

Table 2 Final fractional coordinates (×10⁴ for C, N, O; ×10³ for H) and equivalent isotropic thermal factors for **5** with e.s.d.s in parentheses

	x	*y*	*z*	U_{eq}
O(1)	3609(2)	871(0)	8234(2)	37(1)
O(2)	2680(2)	−290(4)	5900(2)	42(1)
O(3)	−487(2)	−1436(4)	6469(2)	45(1)
O(4)	−482(2)	2684(3)	6592(2)	42(1)
O(5)	−1990(2)	305(4)	9624(2)	42(1)
O(6)	−3466(2)	1544(3)	7439(2)	38(1)
N(1)	5582(3)	581(4)	4076(3)	45(1)
N(2)	5986(3)	639(4)	1798(2)	42(1)
C(1)	2435(3)	68(4)	7155(2)	26(1)
C(2)	648(3)	−370(4)	7616(3)	29(1)
C(3)	−265(3)	1509(4)	7904(3)	28(1)
C(4)	−2054(3)	1083(4)	8378(3)	27(1)
C(5)	6739(3)	193(5)	3198(3)	42(1)
C(6)	4057(3)	1301(5)	3198(3)	40(1)
C(7)	4307(4)	1338(5)	1775(3)	43(1)
H(O1)	501(5)	118(8)	803(5)	
H(N1)	607(5)	57(8)	533(5)	
H(2)	90(5)	−116(8)	861(4)	
H(N2)	651(5)	57(8)	94(4)	
H(O3)	21(5)	−162(8)	584(5)	
H(3)	57(5)	223(9)	876(4)	
H(O4)	−146(5)	298(7)	648(4)	
H(5)	804(5)	−48(8)	362(5)	
H(6)	318(5)	176(7)	357(5)	
H(7)	358(5)	173(8)	90(5)	

U_{eq} is defined as one third of the trace of the orthogonalised U_{ij} tensor.

Table 3 Selected bond lengths (/Å) and angles (/degrees) for **5** with e.s.d.s in parentheses

bond lengths/Å			
O(1)–C(1)	1.303(2)	O(1)–H(O1)	1.13(4)
O(2)–C(1)	1.206(2)	O(3)–C(2)	1.413(3)
O(3)–H(O3)	1.86(4)	O(4)–C(3)	1.417(3)
O(4)–H(O4)	0.176(4)	O(5)–C(4)	1.236(3)
O(6)–C(4)	1.264(3)	N(1)–C(5)	1.319(4)
N(1)–C(6)	1.357(3)	N(1)–H(N1)	1.12(4)
N(2)–C(5)	1.311(3)	N(2)–C(7)	1.357(4)
N(2)–H(N2)	0.94(4)	C(1)–C(2)	1.522(3)
C(2)–C(3)	1.525(4)	C(2)–H(2)	1.03(4)
C(3)–C(4)	1.528(3)	C(3)–H(3)	1.02(4)
C(5)–H(5)	1.09(4)	C(6)–C(7)	1.331(4)
C(6)–H(6)	0.86(4)	C(7)–H(7)	0.91(4)
bond angles/degrees			
C(1)–O(1)–H(O1)	119(2)	C(2)–O(3)–H(O3)	101(3)
C(3)–O(4)–H(O4)	103(3)	C(5)–N(1)–C(6)	108.5(2)
C(5)–N(1)–H(N1)	119(2)	C(6)–N(1)–H(N1)	131(2)
C(5)–N(2)–C(7)	109.0(2)	C(2)–C(3)–C(4)	109.8(2)
C(7)–N(2)–H(N2)	124(2)	C(5)–N(2)–H(N2)	127(2)
O(1)–C(1)–C(2)	113.2(2)	O(1)–C(1)–O(2)	125.1(2)
O(3)–C(2)–C(1)	110.5(2)	O(2)–C(1)–C(2)	121.7(2)
O(3)–C(2)–H(2)	109(3)	O(3)–C(2)–C(3)	110.1(2)
C(1)–C(2)–H(2)	109(2)	C(1)–C(2)–C(3)	109.4(2)
O(4)–C(3)–C(2)	109.5(2)	C(3)–C(2)–H(2)	109(3)
O(4)–C(3)–H(3)	107(3)	O(4)–C(3)–C(4)	112.5(2)
C(2)–C(3)–H(3)	108(3)	C(4)–C(3)–H(3)	110(2)
O(5)–C(4)–O(6)	126.3(2)	O(5)–C(4)–C(3)	117.5(2)
O(6)–C(4)–C(3)	116.2(2)	N(1)–C(5)–N(2)	108.2(2)
N(1)–C(5)–H(5)	123(2)	N(2)–C(5)–H(5)	129(3)
N(1)–C(6)–C(7)	107.4(2)	N(1)–C(6)–H(6)	123(3)
C(7)–C(6)–H(6)	130(3)	N(2)–C(7)–C(6)	106.9(2)
N(2)–C(7)–H(7)	122(3)	C(6)–C(7)–H(7)	131(3)

UM00012738
NOVARTIS EXHIBIT 1017
Novartis v. Regents, IPR2023-01346
Page 1484 of 4460

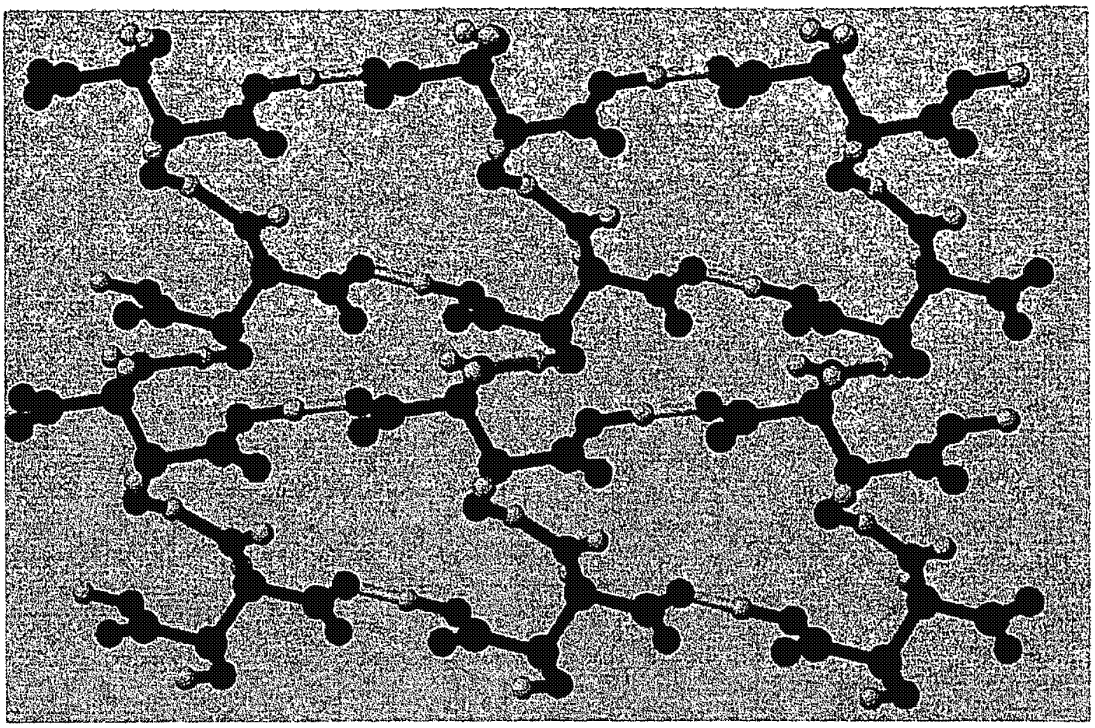


Plate 3 Infinite 2D sheet of anions, parallel to the *a*–*b* plane, in **5**. Covalent bonds, red; hydrogen bonds, yellow and green.

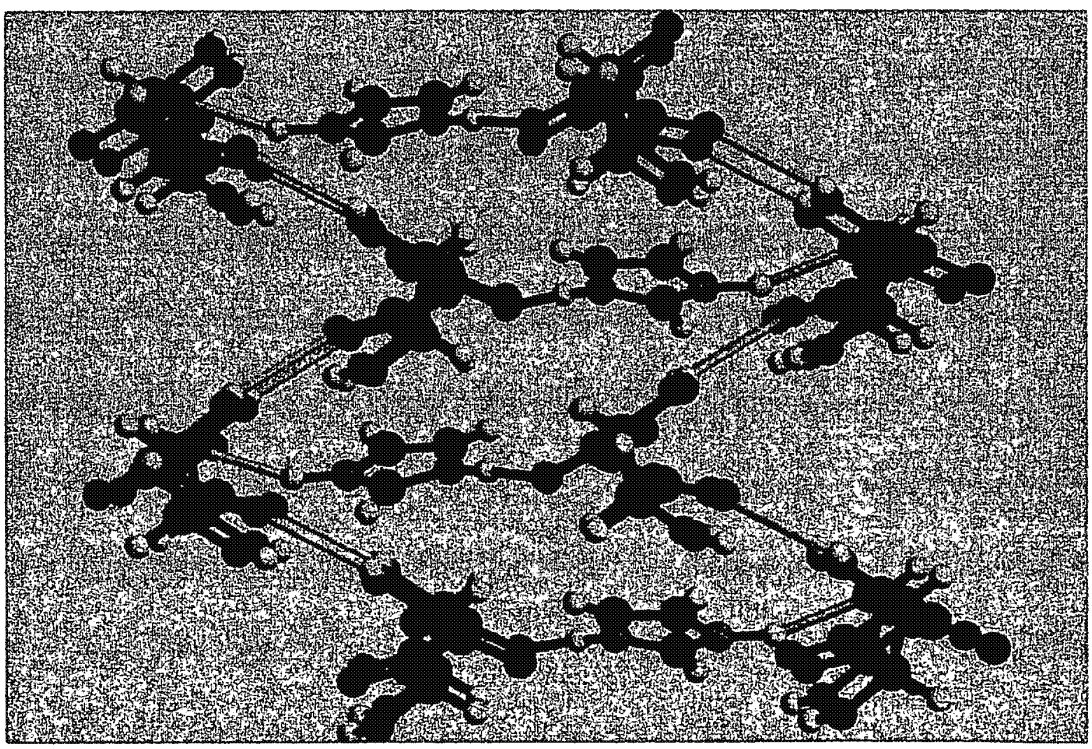


Plate 4 Cross-linking of adjacent anionic sheets by the 1*H*-imidazolium cation in **5**. Cation/anion layer parallel to the *a*–*c* plane. Covalent bonds, red; hydrogen bonds, green, pink and black.

UM00012739
NOVARTIS EXHIBIT 1017
Novartis v. Regents, IPR2023-01346
Page 1485 of 4460

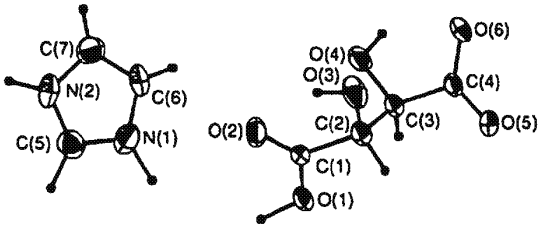


Fig. 1 ORTEP drawing (20%) showing the geometry and numbering scheme of the cation and anion of 5

figuration with a C—C—C—C torsion angle of almost 180°. The anions form infinite chains through a head-to-tail arrangement, in which anions from neighbouring unit cells are linked along the *a* axis *via* a short hydrogen bond *r*[O(1)···O(6)′] 2.503(2) Å, Table 4. These chains are then cross-linked in the *a*–*b* plane by ions related by the 2_1 screw axis parallel to *b*, *via* one hydrogen bond *r*[O(3)···O(4)″] 3.049(3) Å, to form an infinite 2D sheet (Plate 3) with the graph set $N_{2D}=L\{R_4^4(22)\}$, Table 1. In addition, there is an intramolecular hydrogen bond within the sheet, *r*[O(4)···O(6)] 2.645(3) Å, but as it does not provide a link between anions, it does not appear in the 2D descriptor (although it would be listed in a first-level graph set).

The imidazolium ion does, as intended, provide a cross-link between the anionic 'scaffolding' since each cation is engaged in two hydrogen bonds, *r*[N(2)···O(5)] 2.724(3) and *r*[N(1)···O(6)′] 3.040(3) Å, parallel to *c*, between adjacent anionic layers (Plate 4). This also results in an interlinked anion/cation layer in the *a*–*c* plane with layers located at $y\approx 0$ and $y\approx 0.5$.

Although it is impossible to predict, *a priori*, the exact arrangement of the cations within this salt, their spatial freedom has been severely restricted by the presence and geometry of the anionic sheets, thereby locking them into the structural framework in the anticipated fashion.

Summary

This study has demonstrated that hydrogentartrate anions can be employed as ionic building blocks in crystal engineering by virtue of their tendency to create rigid, 2D aggregates which restrict and direct the possible orientation of the cation in the solid state. This observation also highlights the strength and directionality of hydrogen bonds between ions. A novel salt, 1H-imidazolium hydrogen-L-tartrate, was then designed based upon the 2D anionic sheet. The cation provided the expected cross-link between adjacent sheets, thereby creating a 3D hydrogen-bonded network throughout the material. A language based upon graph theory[11] (with an additional 2D descriptor) has facilitated the classification and analysis of the complex hydrogen-bond patterns present in this series of differing hydrogentartrate salts.

The availability of structurally consistent hydrogen-bonded ionic aggregates, in combination with an increased awareness of how to restrict the spatial freedom of the counterion, will undoubtedly play a crucial role in the future engineering of ionic crystalline materials.

Experimental

Analysis of Literature Data

A search was made of the Cambridge Crystallographic Database (CSD, January 1992 Release) for organic and inorganic hydrogentartrate salts. The search was limited to structures of anhydrous hydrogentartrates reported after 1970, and only structures without disorder and where hydrogen atoms had been located were included. Salts containing transition metals were also excluded.

The relevant crystallographic data were the transferred to a Macintosh IIfx and a Silicon Graphics Workstation where software from CAChe Tektronix, Molecular Simulation Inc. (Cerius 3.2 and Quanta 3.3) and Biosym (Insight/Discover 2.10) was employed in the analysis of the patterns generated by the hydrogen bonds within these structures.

Preparation of 1H-Imidazolium Hydrogen-L-tartrate

An aqueous solution (20 cm^3) of 1*H*-imidazole (1.0 g; 15 mmol) was mixed with an aqueous solution (15 cm^3) of L-tartaric acid (2.2 g; 15 mmol). The solvent was evaporated by warming it on a hot plate until a white precipitate formed. The product was collected by filtration and recrystallized from water to produce clear, colourless crystals.‡ Found: C, 38.4; H, 4.7; N, 12.7%. Calculated for $C_7H_{10}N_2O_6$: C, 38.54; H, 4.62; N, 12.84%. m.p. 179–181 °C.

X-Ray Structure Determination

Crystal Data

$C_7H_{10}N_2O_6$, $M=218.2$, monoclinic, space group $P2_1$, $a=0.7569(1)$ nm, $b=0.6953(1)$ nm, $c=0.8993(2)$ nm, $\beta=101.55(1)°$, $U=0.4637$ nm^3, $Z=2$, $D_c=1.56$ g cm^{-3}, $F(000)=228$. Monochromatic Mo-Kα radiation, $\lambda=0.071069$ nm, $\mu=1.3$ cm^{-1}, $T=173$ K.

Data Collection

Data were collected on a crystal (0.4 mm × 0.2 mm × 0.2 mm), using an Enraf-Nonius CAD4 diffractometer fitted with a cold dinitrogen stream low-temperature attachment, in the θ–2θ mode, with $\Delta\theta=\{0.8+0.35\tan(\theta)\}°$ and a maximum scan time of 1 min.

‡ In order to verify that the chosen single crystal was representative of the bulk material, the X-ray powder diffraction pattern was simulated from the single-crystal data (using CERIUS 3.2 from Molecular Simulation Inc.) and compared with the experimental X-ray powder pattern, recorded on a bulk sample. The match between simulated and experimental pattern demonstrated that only one structural form of the salt was present.

Table 4 Geometry of the hydrogen bonds in 5 with e.s.d.s in parentheses[a]

D—H···O	*r*(D—H)/Å	*r*(H···O)/Å	*r*(D···O)/Å	∠(D—H···O)/degrees
O(1)—H(O1)···O(6)′	1.13(4)	1.38(4)	2.503(2)	167(4)
O(3)—H(O3)···O(4)″	0.86(4)	2.29(4)	3.049(3)	148(3)
O(4)—H(O4)···O(6)	0.76(4)	2.14(4)	2.645(3)	125(4)
N(1)—H(N1)···O(6)′	1.12(4)	1.98(4)	3.040(3)	158(4)
N(2)—H(N2)···O(5)‴	0.94(4)	1.80(4)	2.724(3)	166(3)

[a]Symmetry code: (′) $x+1, y, z$; (″) $-x, y-\frac{1}{2}, 1-z$; (‴) $x+1, y, z-1$.

UM00012740
NOVARTIS EXHIBIT 1017
Novartis v. Regents, IPR2023-01346
Page 1486 of 4460

Solution and Refinement of Structure

A total of 890 reflections were measured for $2<\theta$/degrees <25 and $+h+k\pm l$, and 841 unique reflections with $|F^2|>3\sigma(F^2)$ were used in the refinement, where $\sigma(F^2)=\{\sigma^2(I)+(0.04I)^2\}^{1/2}/Lp$. There was no crystal decay and no correction was made for absorption.

Non-hydrogen atoms were located by direct methods using SHELXS-86 and refined with anisotropic thermal parameters by full-matrix least-squares analysis. Hydrogen atoms were located on a difference map and their positions refined but thermal parameters were fixed at $B_{iso}=0.04\,nm^2$, with a weighting scheme of $w=1/\sigma^2(F)$. The refinement converged to give $R=0.041$, $R'=0.046$, $S=1.8$ with 165 variables. Programs from the Enraf-Nonius SDP-Plus package were run on a Micro VaxII computer.

Additional material available from the Cambridge Crystallographic Data Centre comprises thermal parameters.

Many thanks go to Prof. J. Bernstein (Ben-Gurion University of the Negev), Dr. J. C. MacDonald (Harvard University) and Prof. K. R. Seddon (The Queen's University of Belfast) for helpful suggestions and invaluable discussions. Generous financial support (C.B.A.) from The Royal Swedish Academy of Sciences and DRA (Fort Halstead) is gratefully acknowledged.

References

1 L. Pasteur, *Ann. Chim. Phys.*, 1848, **24**, 442.
2 G. R. Desiraju, *Crystal Engineering. The Design of Organic Solids*, Elsevier, Amsterdam, 1989; J. M. Lehn, *Angew. Chem. Int. Edn. Engl.*, 1988, **27**, 89; J. M. Lehn, *Angew. Chem. Int. Edn. Engl.*, 1990, **29**, 1304; G. M. Whitesides, J. P. Mathias and C. T. Seto, *Science*, 1991, **254**, 1312; V. Vögtle, *Supramolecular Chemistry*, Wiley, Chichester, England, 1991; M. C. Etter, *J. Phys. Chem.*, 1991, **95**, 4601.
3 F. Garcia-Tellado, S. J. Geib, S. Goswami and A. D. Hamilton, *J. Am. Chem. Soc.*, 1991, **113**, 9265.
4 X. Zhao, Y-L. Chang, F. W. Fowler and J. W. Lauher, *J. Am. Chem. Soc.*, 1990, **112**, 6627.
5 D. Simard, D. Su and J. D. Wuest, *J. Am. Chem. Soc.*, 1991, **113**, 4696.
6 G. T. Seto and G. M. Whitesides, *J. Am. Chem. Soc.*, 1990, **112**, 6409.
7 C. B. Aakeröy, M. Leslie and K. R. Seddon, *Struct. Chem.*, 1992, **3**, 63.
8 C. B. Aakeröy, P. B. Hitchcock and K. R. Seddon, *J. Chem. Soc., Chem. Commun.*, 1989, 1856; C. B. Aakeröy, G. S. Bahra, P. B. Hitchcock, Y. Patell and K. R. Seddon, *J. Chem. Soc. Chem. Commun.*, 1993, 152; C. B. Aakeröy, D. Phil. Thesis, University of Sussex, 1990.
9 R. Masse and J. Zyss, *J. Mol. Eng.*, 1991, **1**, 141; J. Zyss, J. Pecaut, J. P. Levy and R. Masse, *Acta Crystallogr., Sect. B*, 1993, **49**, 334.
10 C. B. Aakeröy, P. B. Hitchcock and K. R. Seddon, *J. Chem. Soc., Chem. Commun.*, 1992, 553.
11 M. C. Etter, J. C. MacDonald and J. Bernstein, *Acta Crystallogr., Sect. B*, 1990, **46**, 256; M. C. Etter, *Acc. Chem. Res.*, 1990, **23**, 120.
12 T. Steiner and W. Saenger, *J. Am. Chem. Soc.*, 1992, **114**, 10146; R. G. Ball and M. W. Baum, *J. Org. Chem.*, 1992, **57**, 801; S. Larsen and H. L. Dediego, *Acta Crystallogr., Sect. C*, 1993, **49**, 303.
13 J. R. Ruble, G. Hite and J. R. Soares, *Acta Crystallogr., Sect. B*, 1976, **32**, 136.
14 L. K. Templeton and D. H. Templeton, *Acta Crystallogr., Sect. C*, 1989, **45**, 675.
15 E. Fogassy, M. Acs, F. Faigl, K. Simon, J. Rohonczy and Z. Ecsery, *J. Chem. Soc., Chem. Commun.*, 1986, 1881.
16 W. Oppolzer, T. N. Birkinshaw and G. Bernardinelli, *Tetrahedron Lett.*, 1990, **31**, 6995.
17 D. Carlström, *Acta Crystallogr., Sect. B*, 1973, **29**, 161.
18 V. A. Tafenko, B. P. Bespalov and V. R. Gakel, *Zh. Strukt. Khim.*, 1990, **31**, 165.
19 L. K. Templeton and D. H. Templeton, *Acta Crystallogr., Sect. A*, 1978, **34**, 368.
20 E. Molins, C. Miravitlles, F. Lopez-Calahorra, J. Castells and J. Raventos, *Acta Crystallogr., Sect. C*, 1989, **45**, 104.
21 A. L. Spek, *Acta Crystallogr., Sect. C*, 1987, **43**, 1633.
22 J. Kroon, A. J. M. Duisenberg and A. F. Peerdeman, *Acta Crystallogr., Sect. C*, 1984, **40**, 645.

Paper 3/03632D; *Received* 25*th June*, 1993

UM00012741
NOVARTIS EXHIBIT 1017
Novartis v. Regents, IPR2023-01346
Page 1487 of 4460

This Page is Inserted by IFW Indexing and Scanning Operations and is not part of the Official Record

BEST AVAILABLE IMAGES

Defective images within this document are accurate representations of the original documents submitted by the applicant.

Defects in the images include but are not limited to the items checked:

- ☐ BLACK BORDERS
- ☐ IMAGE CUT OFF AT TOP, BOTTOM OR SIDES
- ☐ FADED TEXT OR DRAWING
- ☐ BLURRED OR ILLEGIBLE TEXT OR DRAWING
- ☐ SKEWED/SLANTED IMAGES
- ☐ COLOR OR BLACK AND WHITE PHOTOGRAPHS
- ☐ GRAY SCALE DOCUMENTS
- ☐ LINES OR MARKS ON ORIGINAL DOCUMENT
- ☐ REFERENCE(S) OR EXHIBIT(S) SUBMITTED ARE POOR QUALITY
- ☐ OTHER: _____

IMAGES ARE BEST AVAILABLE COPY.
As rescanning these documents will not correct the image problems checked, please do not report these problems to the IFW Image Problem Mailbox.

HYDROGEN-BONDING IN SOLIDS

Some Strategies and Aspects of Crystal Engineering

CHRISTER B. AAKERÖY
Department of Chemistry, Kansas State University, Manhattan, Kansas, 66506, USA.

1. Preamble

This Chapter provides a personal overview of some of the strategies, structures and successes that have appeared in the area of crystal engineering over the last fifteen years. Unfortunately, it is only possible to present but a small selection of the many elegant and imaginative efforts that have been made during this time, and I can only apologise to those names that I have been forced to omit (although you are neither forgotten, nor ignored!). For a more comprehensive coverage of the field, the reader is directed to several excellent books [1,2] and review articles [3,4,5,6,7,8,9,10].

The phrase 'crystal engineering', coined over twenty-five years ago by Gerhard Schmidt [11], provides a suitably evocative description of this genuinely multi-disciplinary field of chemistry. As the name implies, this is, indeed, hands-on practical chemistry which sometimes can be very frustrating. This can be appreciated by anyone who has spent months trying to find the unique solvent combination, or the perfect rate of evaporation, which finally produces those tiny crystals which, in turn, will prove that your ingenious (or fanciful, depending upon the point of view) design strategy works. On those memorable occasions when the crystal structure really did contain the motifs that you wanted (as opposed to those structures which would only submit to a humble rationalisation with the benefit of hindsight), then you were actually taking a small step towards that elusive pot of gold: the ability to predict the spatial arrangement of molecular and ionic building blocks in a three-dimensional crystalline material. In order to move closer to this goal, it is crucial that a careful design strategy is adopted prior to making a string of new materials. Commonly, such a strategy is derived from observed packing patterns of related molecular building blocks, and from an understanding of recognition mechanisms between different functional groups or moieties.

2. Motivation

The physical properties of any material (*e.g.* conductivity, density, colour, melting point, *etc.*) are determined by the crystal structure, *i.e.* the spatial arrangement of atoms, molecules

K. R. Seddon and M. Zaworotko (eds.), Crystal Engineering, 303–324.
© 1999 *Kluwer Academic Publishers. Printed in the Netherlands.*

UM00012743
NOVARTIS EXHIBIT 1017
Novartis v. Regents, IPR2023-01346
Page 1489 of 4460

or ions, of that particular material. This observation is most clearly illustrated by comparing the behaviour of diamond and graphite; the two solids contain exactly the same type of building blocks, carbon atoms, however, the three-dimensional arrangement of atoms in the two materials differ, which has dramatic consequences for their physical properties.

The history and development of solid-state chemistry have always been linked to, if not synonymous with, those of structural chemistry. New, and improved, methods of characterisation, *e.g.* diffraction and spectroscopy based upon synchrotron or neutron sources, coupled with better theoretical descriptions of the nature and behaviour of solid materials, have enabled us to envisage and develop practical devices of enormous commercial importance. Nevertheless, continuing progress in most technological areas is still hampered by a lack of materials with ideal performances and, unfortunately, we are still unable to anticipate the crystal structure of even the simplest of compounds, even if we have complete information about its chemical composition [12]. However, if we were to acquire the ability to control the structure of a solid, we would also be able to predict, and customise, its physical properties and reactivity. Consequently, the intentional design and synthesis of specific structural aggregates in the solid state, crystal engineering, is attracting considerable academic and commercial attention, since a successful incorporation of desirable structural units into a crystal may result in the development of novel materials with *cf.* improved electrical, optical or catalytic properties. Unfortunately, the task of controlling the assembly and orientation of individual molecules into one, two and, finally, three-dimensional architectures is extremely difficult, as molecules are capable of adopting a vast number of conformations in the crystal. In addition, since the crystal structure itself is the result of a very fine balance between all the intermolecular interactions that are present in the material, we need a detailed understanding of the competition between several fundamental intermolecular forces.

3. Background

The history of crystal engineering (as defined by the first occurrence of that term), only dates back about twenty-five years,[¶] but in the first decade, much of the foundation was laid, and many current strategies are directly related to those earlier studies. For example, Leiserowitz and co-workers were among the first to appreciate the importance of systematic and detailed examinations of structural data. Consequently, several of their papers described methodical analyses of structural behaviour and packing patterns within series of related compounds which, in turn, made it possible to identify hydrogen-bond preferences of certain functional groups. For example, primary monoamides [13] commonly display a ribbon-like motif (see Figure 1a) [14], whereas the diamides generate infinite layers (see Figure 1b) [15]. If one of the hydrogen-bond donors is removed, as in *N*-methylamides [16], the resulting motif is commonly an infinite chain. Much work was also done on carboxylic

---

¶ However, it is worth pointing out that many structural chemists, *e.g.* Hassel, Robertson and Kitaigorodsky, were actively doing crystal engineering long before the language of crystal engineering existed.

UM00012744
NOVARTIS EXHIBIT 1017
Novartis v. Regents, IPR2023-01346
Page 1490 of 4460

iearly illustrated by comparing
tain exactly the same type of
al arrangement of atoms in the
ıeir physical properties.
ry have always been linked to,
w, and improved, methods of
ıpon synchrotron or neutron
nature and behaviour of solid
actical devices of enormous
in most technological areas is
and, unfortunately, we are still
of compounds, even if we have
lowever, if we were to acquire
also be able to predict, and
ıtly, the intentional design and
ystal engineering, is attracting
ı successful incorporation of
ɔpment of novel materials with
unately, the task of controlling
one, two and, finally, three-
are capable of adopting a vast
ıe crystal structure itself is the
interactions that are present in
competition between several

rrence of that term), only dates
of the foundation was laid, and
ırlier studies. For example,
te the importance of systematic
everal of their papers described
atterns within series of related
ıydrogen-bond preferences of
ides [13] commonly display a
es generate infinite layers (see
ved, as in *N*-methylamides [16],
rk was also done on carboxylic

uctural chemists, *e.g.* Hassel,
crystal engineering long before

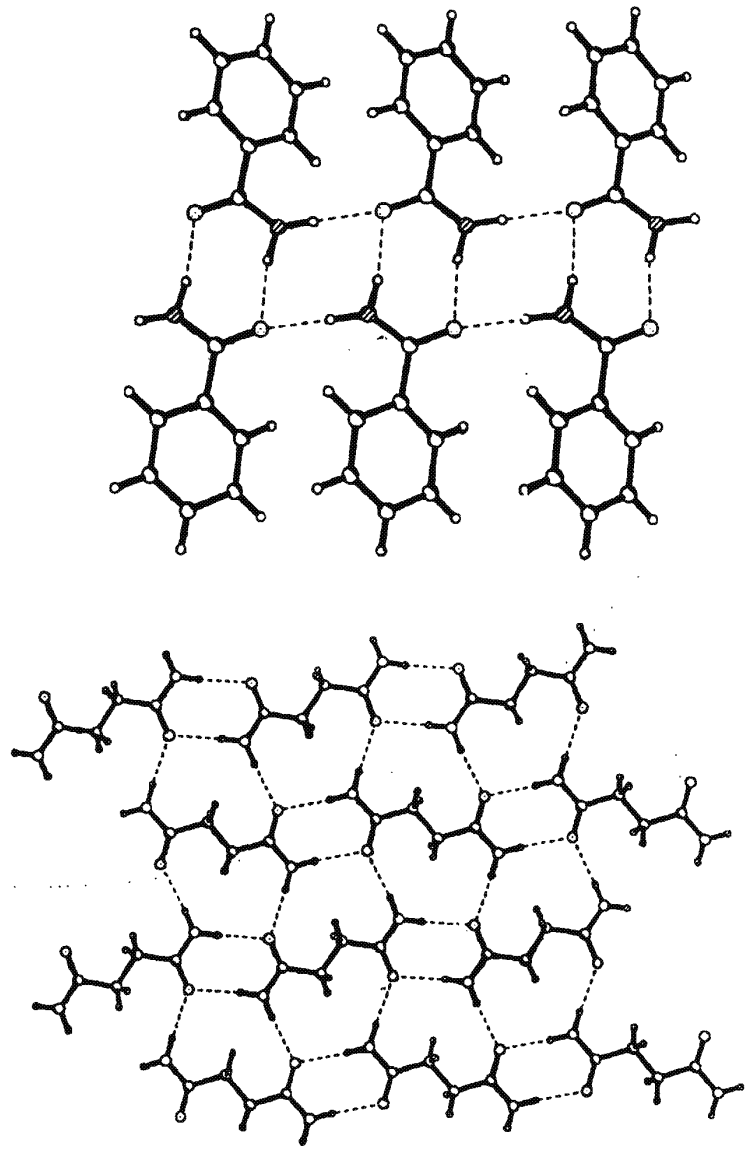


Figure 1. *(a; upper) A hydrogen-bonded ribbon in benzamide [14], and (b; lower) the infinite hydrogen-bonded layer in the crystal structure of succinamide [15].*

UM00012745
NOVARTIS EXHIBIT 1017
Novartis v. Regents, IPR2023-01346
Page 1491 of 4460

acids, and an abundance of structural evidence was presented which highlighted the typical dimeric arrangement for monocarboxylic acids [17], and the infinite chains commonly generated by dicarboxylic acids, Figure 2 [18].

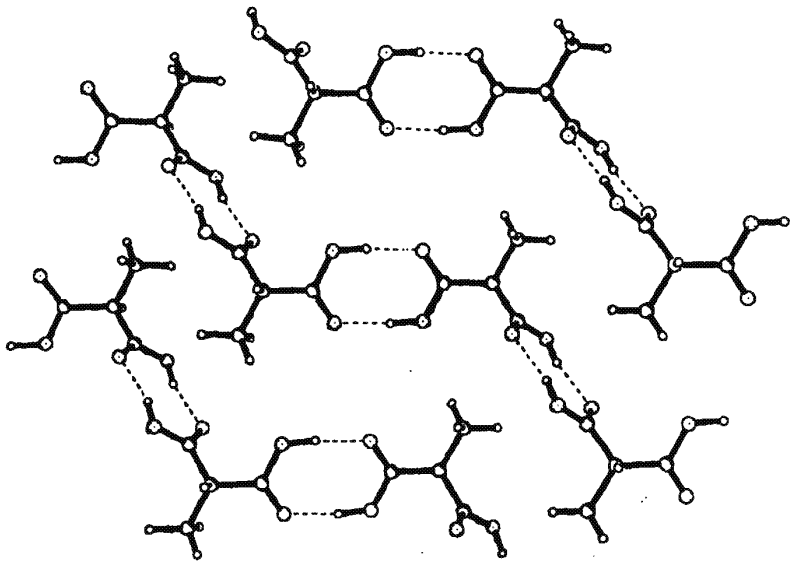


Figure 2. An infinite chain generated by head-to-head dimeric hydrogen-bond interactions in methylmalonic acid [18].

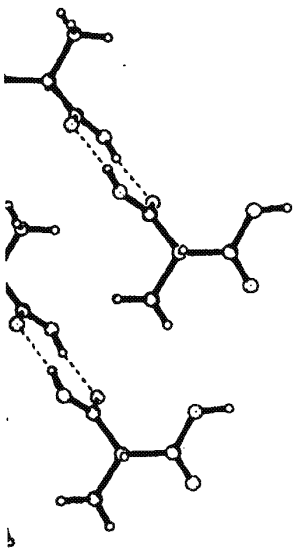
From an extensive study on *N*-acyl amino acids and other amide-acid compounds, Leiserowitz and coworkers were also able to show that the amide oxygen atom is usually a stronger hydrogen-bond acceptor than the carboxylic oxygen atom [19]. This meticulous approach, including the way in which structural information was collated and classified, set important new standards for how a specific crystal engineering project should be accomplished; many of the current strategies in this field can be traced back to the work carried out at the Weizmann Institute. For example, reference [17] has been cited over 270 times since it appeared in 1976.

With the growing realisation that hydrogen bonding can, and does, take place between a large number of donors and acceptors, so have other systematic studies of weaker, but still prevalent (and important!) hydrogen-bond interactions appeared in the literature. For example, the importance, and frequency, of C-H···O interactions have been described in detail by Desiraju [20]. It is clear that although such interactions are individually weaker than O-H···O and N-H···O forces, they are both long-range and directional and, thus, can play an important part in design strategies for new materials.

The case of C-H···O interactions is a good example of how attitudes can be changed, and how our understanding of intermolecular forces has improved in the light of

UM00012746
NOVARTIS EXHIBIT 1017
Novartis v. Regents, IPR2023-01346
Page 1492 of 4460

ted which highlighted the typical
d the infinite chains commonly



-head dimeric hydrogen-bond

nd other amide-acid compounds,
he amide oxygen atom is usually
ygen atom [19]. This meticulous
on was collated and classified, set
engineering project should be
can be traced back to the work
ence [17] has been cited over 270

nding can, and does, take place
ave other systematic studies of
ond interactions appeared in the
f C-H···O interactions have been
although such interactions are
, they are both long-range and
strategies for new materials.
ample of how attitudes can be
rces has improved in the light of

systematic examinations of structural data. When it was initially suggested that C-H···O hydrogen bonds may influence structure and packing [21,22], the idea was met with considerable scepticism [23]. Today, however, there is little argument about the existence of such hydrogen bonds and, instead, the debate is now more concerned with the strength and nature of such interactions. Subsequently, it has been demonstrated that the strength of a C-H···O interaction is related both to C-H carbon acidity [24] and to the basicity of the acceptor oxygen atom [25]. This behaviour has been verified in a systematic database study which identified a positive correlation between observed C···O distances and acidity of the C-H donor moiety [26].

While we are on the topic of systematic examinations of crystallographic data, it should be stated again that, in many instances, such studies would not have been possible to perform (within a reasonable time frame) without access to the structural information in the Cambridge Crystallographic Database [27]. Furthermore, the continued improvement in search algorithms, statistical features and display software, has generated one of the most efficient and valuable research tools in the area of crystal engineering. It is now a matter of routine to compare the appearance of a new crystal structure with all extant structural data for compounds with similar molecular formula, shape or substitution pattern. Clearly, analysing new structures against the backdrop of such information ought be carried out, as a matter of routine, in all aspects of structural and solid-state chemistry.

Another important consequence of systematic structural studies, is the emergence of reliable, 'standard', intermolecular-interaction patterns, which can be used both as a basis for molecular modelling/simulation of unknown structures, and as a 'reality-check' for calculations on existing systems. For example, the development of molecular-mechanics-based force fields is, to a large extent, dependent upon the existence of statistically verifiable, commonly observed, intermolecular geometries and packing patterns (for more information, see the chapter on molecular modelling in this volume, pp. 69-82).

3.1. CO-CRYSTALS AND GRAPH SETS: THE LEGACY OF M.C. ETTER [28]

The field of crystal engineering is to a large extent the field of intermolecular interactions and, in fact, crystal engineering can be thought of as intermolecular synthesis, as distinct from conventional covalent synthesis. Consequently, we need to acquire a detailed and comprehensive understanding of the balance between, and the structural effects of, various intermolecular forces. The selectivity, strength, and directionality of the hydrogen bond have contributed towards making it the most prominent of forces (or 'tools') in intermolecular synthesis, but competition between different hydrogen-bond donors and acceptors in a solid, can still generate vastly different spatial arrangements in a solid. An elegant way of probing the relative strength of competing hydrogen-bonds was pioneered by Etter and co-workers using co-crystallisation techniques [29,30,31]. In order to elucidate hydrogen-bond preferences for a specific type of molecule, the most relevant information can only be obtained if the target molecule is 'exposed' to different neighbours within a three-dimensional architecture. Furthermore, if the inherent chemistry of the molecule is disturbed by, for example, substitution or protonation/deprotonation, the observed structural behaviour is influenced by too many 'hard-to-assess' factors. Consequently, by incorporating the target molecule in a series of co-crystals (where it will remain a structural constant), it

UM00012747
NOVARTIS EXHIBIT 1017
Novartis v. Regents, IPR2023-01346
Page 1493 of 4460

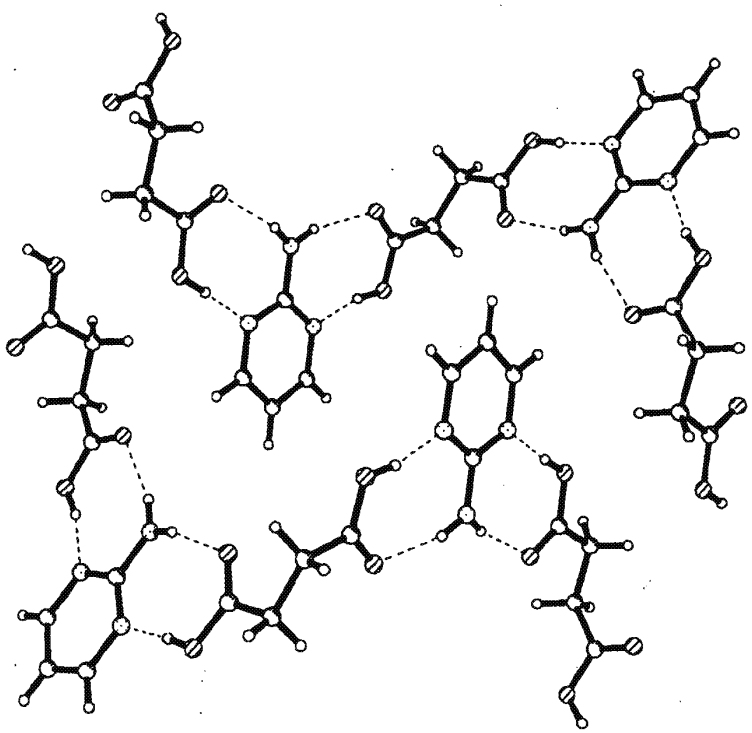
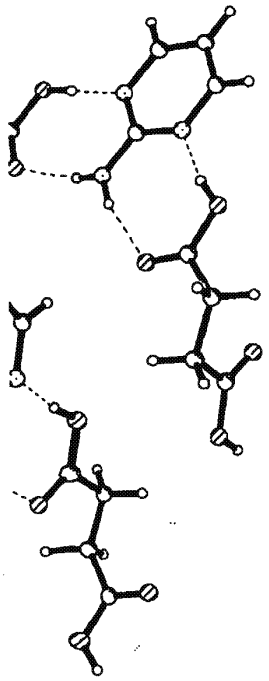


Figure 3. *Infinite ribbons in 2-aminopyrimidine succinic acid (1/1), an example of a molecular co-crystal [32].*

is possible to obtain unbiased information about preferred packing patterns and relative hydrogen strengths of various donors/acceptors.

Systematic studies on triphenylphosphine oxide [29] demonstrated how it could be used as a reliable co-crystallisation agent for many organic compounds which otherwise did not form good-quality crystals. Another high-impact study identified a good geometric 'fit' between 2-aminopyrimidine and dicarboxylic acids which produced cyclic dimeric motifs, resulting in infinite ribbons, see Figure 3 [32]. Through a careful analysis of existing structural data [27], coupled with their own crystal structures of key compounds, Etter and coworkers were able to formulate hydrogen-bond rules (or guidelines) for specific families of organic molecules, *e.g.* imides [31], nitroanilines [33], and diaryl ureas [30]. In addition, some general guidelines were also suggested:

UM00012748
NOVARTIS EXHIBIT 1017
Novartis v. Regents, IPR2023-01346
Page 1494 of 4460



nic acid (1/1), an example of a

j packing patterns and relative

9] demonstrated how it could be
ompounds which otherwise did
identified a good geometric 'fit'
produced cyclic dimeric motifs,
a careful analysis of existing
es of key compounds, Etter and
guidelines) for specific families
d diaryl ureas [30]. In addition,

- the best hydrogen-bond donor and the best hydrogen-bond acceptor form a hydrogen bond to one another.

- all good proton donors/proton acceptors will participate in hydrogen bonding.

Although it is possible to find examples of structures which do not obey these 'rules', they do represent conclusions which are consistent with a large amount of crystallographic data. Furthermore, the work of Etter and co-workers highlights the importance of systematic structural studies of closely related compounds. In addition, they also clearly demonstrated that it is not always necessary to investigate highly complex molecules which require considerable synthetic efforts. In fact, it is almost a prerequisite that the model system in question is relatively simple, otherwise it will be very time consuming, and difficult, to accumulate enough structural information.

Another important aspect of hydrogen bonding in solids, which was also addressed by Etter *et al.* [34], relates to the question of how all the existing hydrogen-bond motifs in a structure can be described in a consistent, and 'user-friendly' way. The proposed approach, based upon graph-theory, has come some way towards a 'language' for classifying hydrogen-bond patterns, and for identifying similarities or differences between complex hydrogen-bonded networks in organic crystals. The method has had some impact on the crystallographic and the organic solid-state communities alike, and recent clarifications and additions [35], are likely to make the methodology even more accessible.

3.2. ENCODING GRAPH SETS

The original encoding comprises a classification of patterns generated by specific hydrogen-bond types and by combinations of hydrogen bonds. It has been found that most patterns in organic molecular solids can be adequately described in terms of four principal *motifs*; chains (*C*), dimers (*D*), rings (*R*), and intramolecular hydrogen bonds (*S*). Although this notation may not provide an unambiguous assignment of every structural arrangement, it is flexible enough to facilitate a systematic description of a wide range of hydrogen-bonded solids. A measure of the impact that this nomenclature has had already, is provided by the fact that two of the early graph-set publications have received more than 200 citations by September 1996. In a recent publication by Bernstein *et al.*, some ambiguities in the original notation have been clarified, and the nomenclature has been placed on a slightly more rigorous footing. Even so, the appealing simplicity of this approach remains intact, and it is very likely that terms like, $R_2^2(8)$ (an eight-membered ring with two hydrogen-bond donors and two hydrogen-bond acceptors, *e.g.* the carboxylic head-to-head dimer), will become recognised, and applied, by a wider community.

4. Molecular solids

The last ten years have witnessed a huge increase in the number of publications which describe the use of hydrogen bonding as a means of building new, predictable, useful and/or aesthetically pleasing, molecular packing patterns.

UM00012749
NOVARTIS EXHIBIT 1017
Novartis v. Regents, IPR2023-01346
Page 1495 of 4460

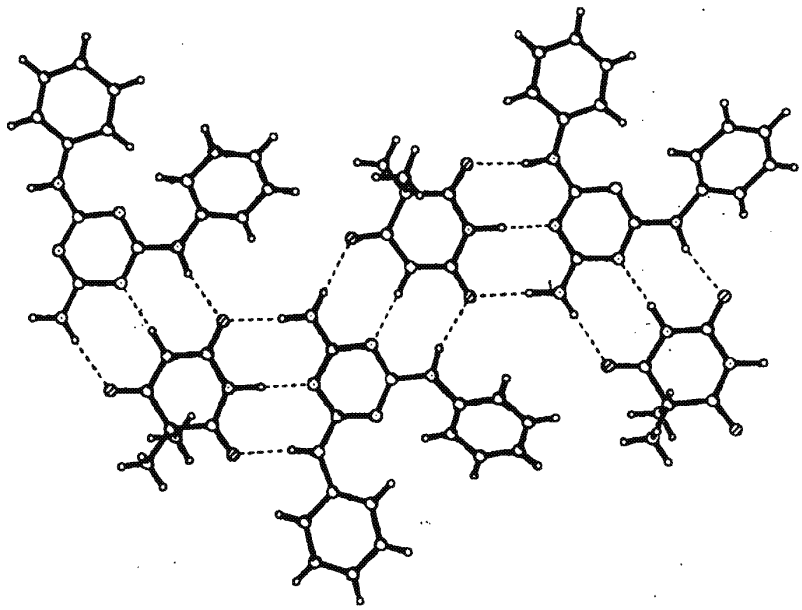


Figure 4. *An infinite ribbon resulting from the complementarity hydrogen-bond sites of barbituric acid and N,N'-diphenylmelamine [39].*

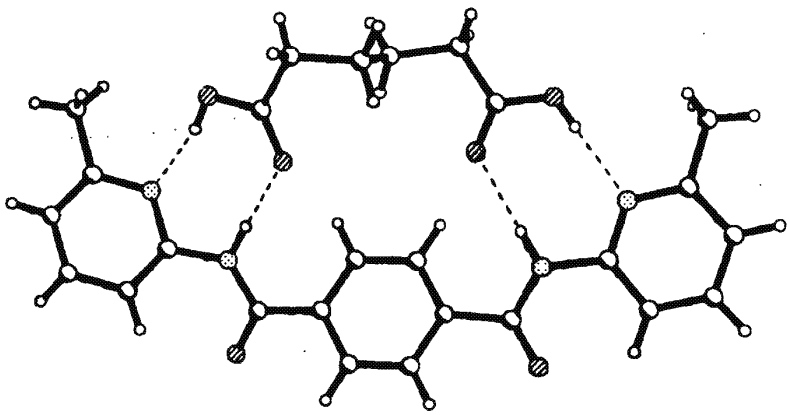
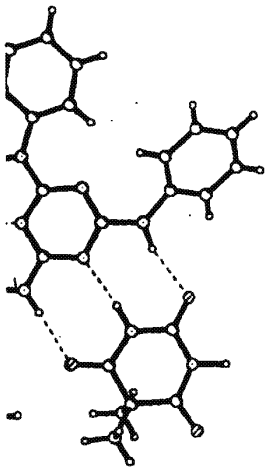
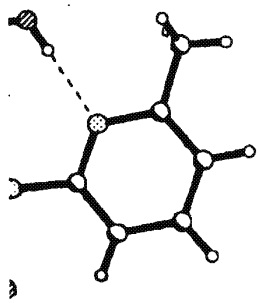


Figure 5. *A good geometric fit and complementary hydrogen bonds between a dicarboxylic acid and two aminopyridine moieties [41].*

UM00012750
NOVARTIS EXHIBIT 1017
Novartis v. Regents, IPR2023-01346
Page 1496 of 4460



ıentarity hydrogen-bond sites : [39].



hydrogen bonds between a ıties [41].

Whitesides and coworkers [36,37,38] have designed flexible architectures by combining melamine derivatives with barbituric acids or isocyanuric acids. The complementarity of the donors and acceptors of these molecules result in multiple hydrogen bonds which, in turn, drive the self-assembly of several types of motifs, *e.g.* 'tapes' and 'rosettes', see Figure 4 [39].

Hamilton and coworkers have exploited the complementarity of 2-aminopyridine and carboxylic moieties, Figure 5, in systems based upon 2-amino-6-methylpyridine [40], 2-aminopyridines [41], and various diacids. These components have a propensity to form infinite, hydrogen-bonded sheets, and this motif is also amenable to precise spatial variations through a suitable choice of spacer. They were also able to design self-assembling helices [42] based upon aminopyridine and diacids.

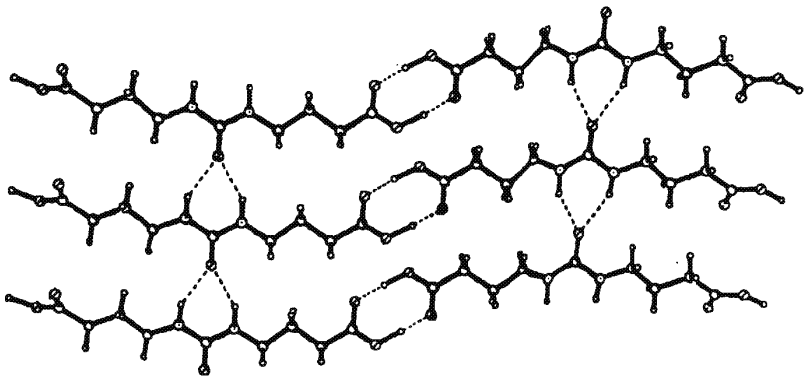


Figure 6. An infinite layer designed around the infinite chain of dicarboxylic acids, and the 1-D motif of the urea moiety [43].

Fowler, Lauher and coworkers [43,44] have devised strategies for designing hydrogen-bonded layers, based upon various dicarboxylic acid urea derivatives, see Figure 6. The infinite layers appear with reassuring regularity and, in addition, the precise distance between neighbouring units can be varied, which may have useful implications for photochemical solid-state reactions.

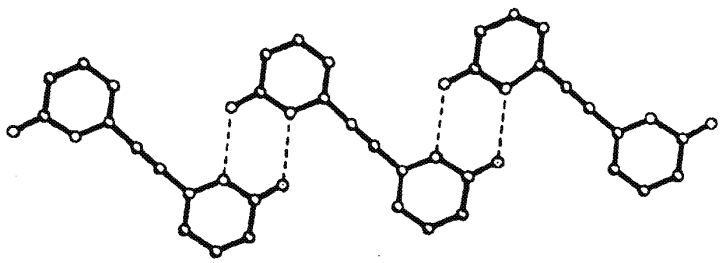


Figure 7. The infinite chain in a self-complementary trans-dipyridone [45].

UM00012751
NOVARTIS EXHIBIT 1017
Novartis v. Regents, IPR2023-01346
Page 1497 of 4460

Wuest and coworkers have employed the pronounced tendency of 2-pyridone to form a reliable dimeric motif, in the design of both chains [45], see Figure 7, and three-dimensional architectures which incorporate considerable cavities [46].

One of the most prolific, and inventive, contributors to the field of crystal engineering, Gautam Desiraju, has made extensive use of a variety of intermolecular forces in the design of an array of reliable, structural motifs. Notably, the successful use of unconventional (or weaker) hydrogen bonds, *e.g.* C-H···O and C-H···N, has led to a widespread appreciation of the importance of a collective of weaker interactions working in concert for the overall assembly of molecular building blocks into low-dimensional motifs. For example, six C-H···N hydrogen bonds create infinite layers of 1,3,5-tricyanobenzene molecules in a co-crystal with hexamethylbenzene [47], see Figure 8, and C-H···O interactions create a molecular sheet in the crystal structure of 3,4-methylenedioxycinnamic acid, see Figure 9 [48,49].

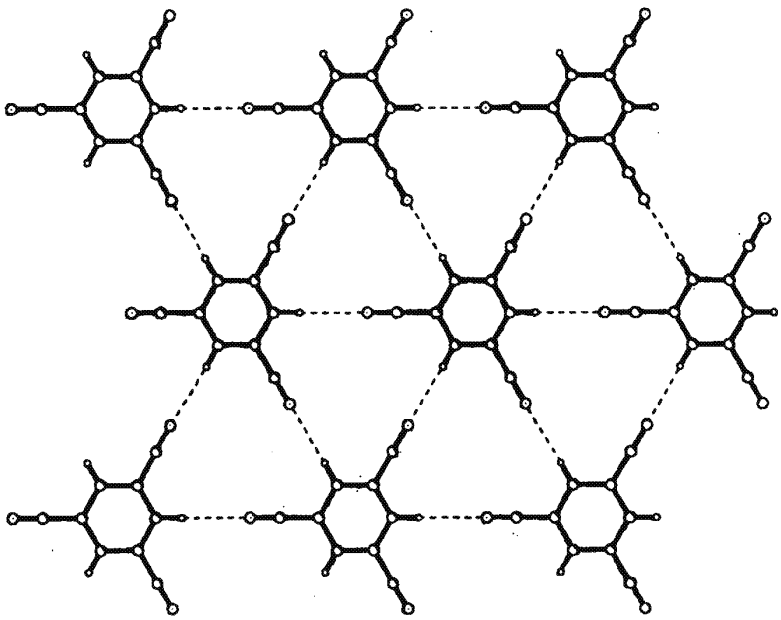


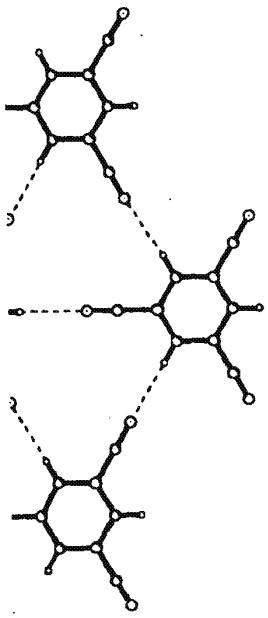
Figure 8. The infinite layer of 1,3,5-tricyanobenzene molecules in a co-crystal with hexamethylbenzene [47].

Ermer and coworkers [50] have utilised the complementarity of available hydrogen-bond donors and acceptors in 1:1 co-crystals of amines and alcohols. The recognition between hydroxy- and amino- groups has resulted in both two-dimensional and three-dimensional hydrogen-bonded networks.

These are but a few examples of the many structural motifs and design strategies based upon hydrogen-bond interactions, which have appeared lately. There are no signs that

UM00012752
NOVARTIS EXHIBIT 1017
Novartis v. Regents, IPR2023-01346
Page 1498 of 4460

nced tendency of 2-pyridone to
s [45], see Figure 7, and three-
cavities [46].
ibutors to the field of crystal
variety of intermolecular forces
Notably, the successful use of
·O and C-H···N, has led to a
of weaker interactions working
ks into low-dimensional motifs.
ayers of 1,3,5-tricyanobenzene
], see Figure 8, and C-H···O
of 3,4-methylenedioxycinnamic



molecules in a co-crystal with

nentarity of available hydrogen-
ind alcohols. The recognition
th two-dimensional and three-

ral motifs and design strategies
d lately. There are no signs that

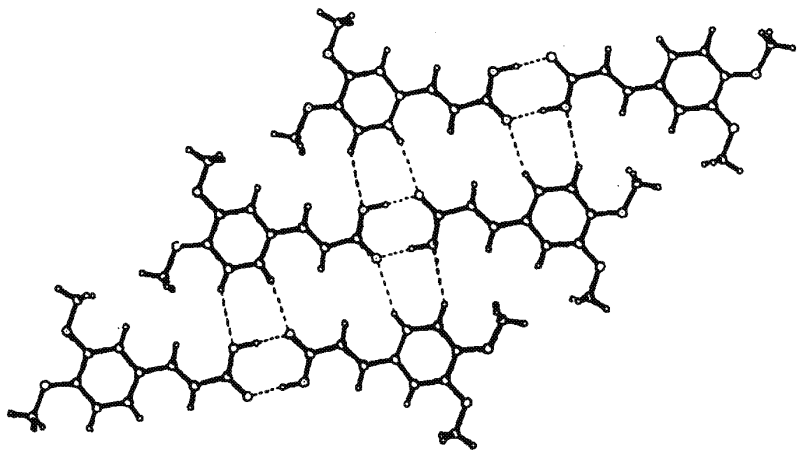


Figure 9. The importance of C-H···O interactions in 3,4-methoxycinnamic acid [49].

this evolution is slowing down. On the contrary, more and more groups are beginning to realise that maybe, they too, have actually been doing crystal engineering for some time, although their efforts and results may not have been discussed against the backdrop of such phrases.

5. Metal-containing compounds

So far, we have only examined hydrogen-bond interactions within a strict organic framework. However, recent literature shows a rapidly expanding body of publications which describe the use of hydrogen-bonds (and other intermolecular interactions) as a means of directing the assembly of inorganic components in three-dimensions. This expansion is likely to open several exciting avenues, since we now have access to metal complexes with their widely varying oxidation states and coordination geometries.

Systematic structural studies of metal-containing compounds, and of inorganic structures in general, have, in reality, a much longer history than the equivalent approach to organic solids. Some recent studies of molecular inorganic chemistry have also been carried out in the 'spirit' of crystal engineering, *i.e.* with the expressed objectives to investigate intermolecular forces and correlations between molecular functionality and packing [51,52,53,54,55]. This clearly demonstrates that both areas, organic and inorganic chemistry, can be seamlessly brought together in the domain of crystal engineering where, after all, intermolecular forces rule.

One of the most versatile and fruitful design strategies in metal-based crystal engineering employs metal cations, or complexes, as linking agents for organic molecules. The main focus in this field has been the deliberate synthesis of rigid three-dimensional structures with large internal channels and cavities. Robson and coworkers have designed

UM00012753

NOVARTIS EXHIBIT 1017
Novartis v. Regents, IPR2023-01346
Page 1499 of 4460

a variety of 3-D structures with hexagonal channels [56] and very large internal cavities, capable of harbouring a large number of solvent molecules [57]. A variety of self-assembled helical motifs, based upon relatively simple molecular monomers, have been devised by Hamilton [42], Lehn [58], and many others. For example, Lehn [58] has utilised the self-complementary hydrogen bonding in heterocyclics as a means of designing ladder architectures. Furthermore, some very elegant work has also involved the design and synthesis of both circular double helical structures [59], and supramolecular cages [60]. A more detailed description of this, and related work, can be found in the chapter by Hamilton in this volume (pp. 357-370).

The term 'coordination polymer' has recently become another 'household' name in crystal engineering [61], and a multitude of 2-D and 3-D aggregates have been described. For an in-depth discussion of such compounds, the reader is directed to the chapter by Zaworotko in this volume (pp. 383-408).

Finally, Mingos and coworkers have recently presented several different metal-containing structures which have been assembled through a combination of complementary hydrogen bonds between organic ligands, and coordinate-bond formation of due to the metal ion of choice [62,63].

It is quite likely that this particular niche in crystal engineering will experience the most rapid development over the next few years. There is clearly an abundance of structural information available on transition-metal complexes and organometallic systems, and in many cases, such structural information is now being re-examined with a view to understanding and identifying the role of intermolecular forces in the packing of such materials.

6. Ionic compounds

As has been outlined above, crystal engineering in the organic solid state has, so far, been mainly devoted to the design of molecular solids. However, research into the design and engineering of ***ionic materials*** [64,65,66] has been neglected for several reasons. Firstly, hydrogen bonding is seldom perceived to be energetically strong enough to have a deterministic effect on the geometry and structure of ionic solids. Secondly, molecular modelling, which has enjoyed considerable success in the study of organic and biomolecular systems, has not been geared towards exploring ionic solids and, thus, research on such systems has not benefited from the improved computational facilities that have become available in recent years. Nevertheless, the interest in organic and organic-inorganic salts is increasing, and many hydrogen-bonded anionic structures, *e.g.* hydrogentartrates [65,67,68], dihydrogenphosphates [69] and hydrogensulfates [70], have recently been shown to provide suitable 'scaffolding' for polarizable cations in new materials for nonlinear optics. Typically, the cation is incorporated between chains, or layers, of anions held together by hydrogen bonds, and the role of such anionic aggregates has been to provide structural stability and some influence over the packing of the anions. However, detailed control over the assembly and arrangement of ions in a solid material still proves to be an elusive goal, and further work is required in order to increase the choice of reliable two-dimensional

UM00012754
NOVARTIS EXHIBIT 1017
Novartis v. Regents, IPR2023-01346
Page 1500 of 4460

building blocks and, more importantly, to allow us to rationalize and predict structural arrangements of the ions ("subunits") within such materials.

6.1 RELIABLE 2-D MOTIFS BASED UPON HYDROGENMALATE AND HYDROGENTARTRATE ANIONS

A potentially useful strategy for designing and controlling the assembly of new organic salt can be based around a three-step approach. First of all, we need to identify building blocks with a propensity to form infinite 1-D motifs. This can simply be achieved by using dicarboxylic acids as a starting point. As outlined previously, dicarboxylic acids are inclined to form infinite chains through a sequence of dimeric head-to-head interactions between neighbouring molecules. Each link, the commonly occurring $R_2^2(8)$ motif, provides a reliable connector irrespective of the overall shape of the acid. If the acid is then deprotonated once, we are left with a carboxylate 'tail' (a strong hydrogen-bond acceptor), and a carboxylic 'head' (a good hydrogen-bond donor). These two moieties are very likely to participate in a strong, short O-H···O hydrogen bond which subsequently gives rise to an infinite anionic chain. This provides the first step, the 1-D motif, in the design strategy. Then, by choosing an acid with other hydrogen-bonding groups almost perpendicular to the chain, it maybe be possible to create an O···O 'cross-link' between neighbouring chains, thereby building up an

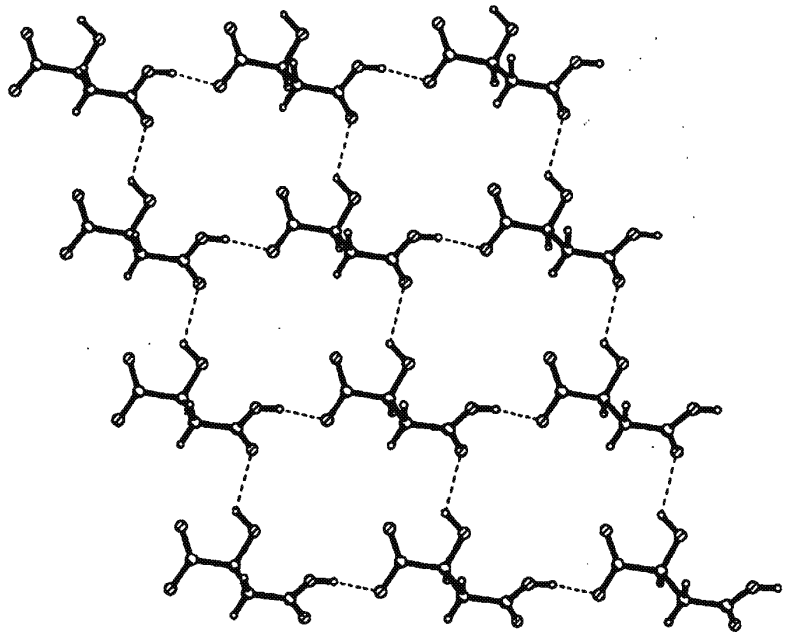


Figure 10. A face-on view of the infinite anionic layer in 4-(chlorobenzyl)ammonium hydrogen-l-malate [71].

UM00012755
NOVARTIS EXHIBIT 1017
Novartis v. Regents, IPR2023-01346
Page 1501 of 4460

infinite 2-D layer, such as that shown in Figure 10. Two building blocks which have provided ample evidence for the utility of this approach are the hydrogentartrate and hydrogenmalate anions [71,72], which both have the ability to create infinite anionic sheets. The reliability of this architecture is illustrated by the fact that the 2-D layer persists even in the presence of widely differing cations. The 2-D layers formed by hydrogenmalate and hydrogentartrate anions can be broadly classified into two types depending upon the relative orientation of chains within each layer. If the chains are arranged in a parallel fashion (which gives rise to a polar sheet), the layer is commonly very flat. However, if the chains are arranged in an anti-parallel manner, the sheet will have a buckled appearance, as in Figure 11. Consequently, the detailed shape of the anionic sheet, is determined by the specific nature of the cation, and the driving force behind this interaction is still being investigated.

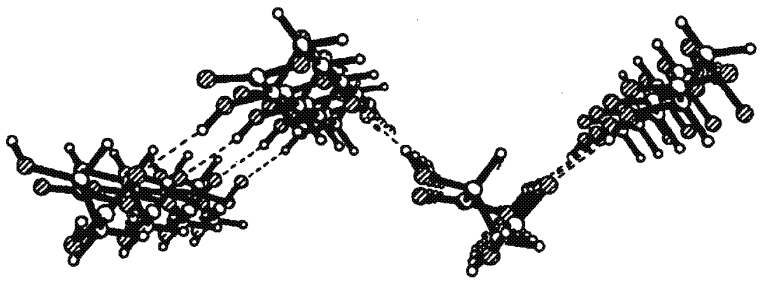


Figure 11. An edge-on view of the buckled anionic layer in benzimidazolium hydrogen-l-malate [72].

Having created a two-dimensional motif, the advantage of using ionic compounds now becomes very clear. Instead of having to build in yet another functionality in the original building block (which could, synthetically, be very difficult), the final step in the process, the link from 2-D to 3-D motifs is provided by the cation. The cation can now fill either of two roles in the construction of the 3-D structure. Either, the cation will act as an active bridge between adjacent layers, or it will simply act as a space filler between layers. The first route is easily achieved by choosing a cation with hydrogen-bond donors in appropriate positions, *e.g.* imidazolium or 3-hydroxypyridinium, each of which has two good hydrogen-bond donors at opposite ends of a rigid frame. Alternatively, a spacer can attach itself to one side only of the anionic layer, *e.g.* 4-methylbenzylammonium, or it may be completely lacking in hydrogen-bond capability, *e.g.* rubidium.

Now, since the anionic layer itself is both rigid and reliable, we have essentially reduced the problem of multiple degrees of freedom to a system where the interplanar distance is the only variable. This is to some extent an oversimplification, since we can see two different types of layers and different degrees of buckling within a layer. However, the major structural features are predetermined through a careful choice of ionic building block.

Another valuable consequence of using chiral building blocks for the sheet (although there is inherently no reason why such components should be selected), is the fact

UM00012756
NOVARTIS EXHIBIT 1017
Novartis v. Regents, IPR2023-01346
Page 1502 of 4460

that we can now begin to examine how the stereochemistry around a chiral centre will affect the detailed structure of the final crystalline material. For example we can simply compare the structures of a sequence of hydrogen-*L*-tartrates with the corresponding *meso*-analogues. Changing the absolute configuration corresponds to a very small chemical change, but it may have significant influence on the overall packing within the crystal structure.

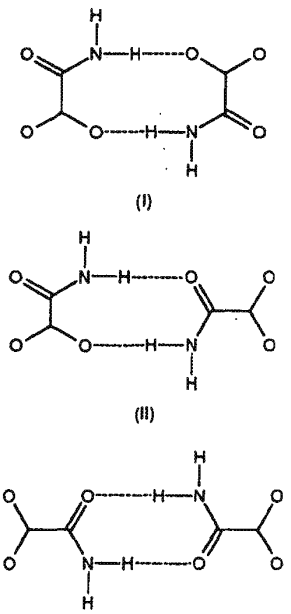
This work provides a useful illustration of how we can approach the central problem of crystal engineering by 'locking' individual components into an infinite network. This obviously reduces their positional freedom and, consequently, makes it considerably easier to make a well-informed 'guess' (or, if one is feeling generous, 'prediction') as to how the new material is going to assemble in the solid state.

There is obviously no reason for us to limit ourselves to the use of carboxylic/carboxylate complementarities in the design of new organic salts. Essentially any functional group which displays a propensity to form certain types of aggregates can be used, provided that the balance between different intermolecular forces (and their relative strength) is being considered.

6.2 A FLEXIBLE BUILDING BLOCK OF INFINITE ARCHITECTURES: THE OXAMATE ANION

What happens if our original building block is not providing us with consistency and reliability? Shall we throw it away and look for another starting point? Not necessarily. In order to learn more about the precise details of cation-anion interactions and the way in which such interactions may induce a certain type of anionic network, we also need to examine series of structures containing ions which can give rise to a few different, but well-defined, low-dimensional motifs.

With this in mind, we have recently examined a group of crystal structures where the common denominator is the oxamate anion, $[OOCCONH_2]^-$ [73]. This particular anion has a number of options available to it when it aggregates into a solid material. Hypothetically, this anion can generate anionic dimers (held together by two hydrogen bonds) in at least three different ways, as shown in Scheme 1. Obviously, there is a possibility that there will no anion-anion contacts in the structure, or that neighbouring anions are held together by only one hydrogen bond. However, the geometry and complementarity of the functional groups on this anion would favour a dimeric arrangement. So, in this case, we have one anion going in as a structural 'enquiry', and the outcome may be one of three hypothetical structural



Scheme 1

UM00012757
NOVARTIS EXHIBIT 1017
Novartis v. Regents, IPR2023-01346
Page 1503 of 4460

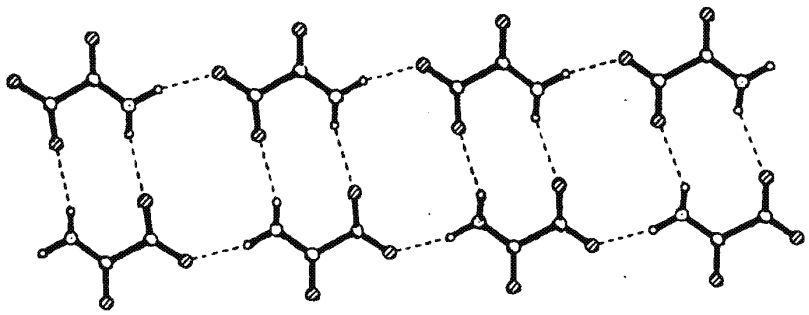


Figure 12. An infinite anionic ribbon in imidazolium oxamate [73].

'responses'. Having examined the structures of several oxamate salts, it was discovered that all three possible dimer units were, indeed, observed. The oxamate anion commonly creates either 1-D motifs (ribbons or ladders, Figure 12), or infinite 2-D sheets, Figure 13. Again, the final outcome is determined by specific cation-anion interactions, but at this stage we are, at least, able to identify some cation characteristics which would seem necessary for inducing

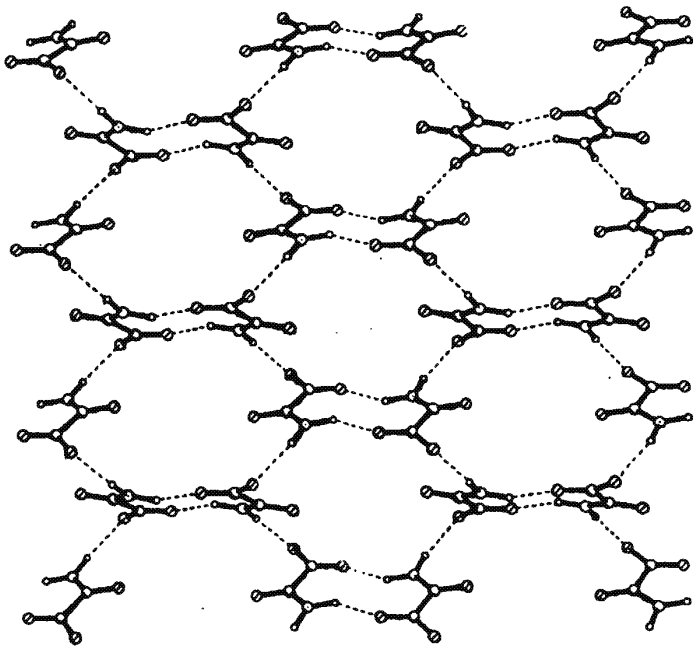


Figure 13. The 2-D anionic layer in 3-(chlorobenzyl)ammonium oxamate [73].

either 1-D or 2-D pa
ammonium cation, e
attached to the same
N-H···O interactions)
secondary or tertiary
be insufficient to brin
piperidinium oxamate
importance is the size
anionic regions, whic
e.g. the potassium io
formation of the infini
This model s
oxamate anion, can a
cation-anion interact
investigations are likel
forces determine the
synthetic efforts.

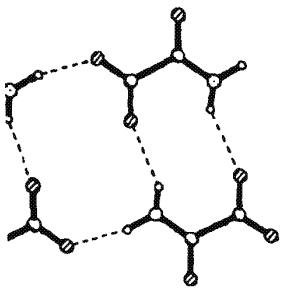
Acknowledgments

Financial support from
State University, is gr
sincere thank you to m
and Deirdre Hughes.

References

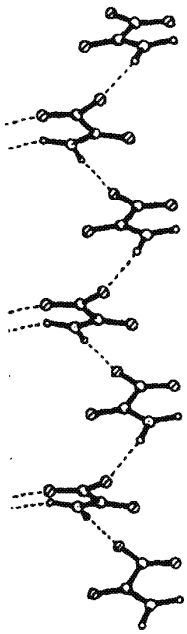
1. Desiraju, G.
Elsevier, Am
2. Desiraju, G.R.
Crystal as a
3. Mathias J.P.
Soc. Rev. **21**,
4. Aakeröy, C.
engineering,
5. Subramanian,
recent develo
357-401.
6. MacDonald, J
bonded tapes

UM00012758
NOVARTIS EXHIBIT 1017
Novartis v. Regents, IPR2023-01346
Page 1504 of 4460



amate [73].

ıate salts, it was discovered that
ɑmate anion commonly creates
: 2-D sheets, Figure 13. Again,
ɔactions, but at this stage we are,
ıuld seem necessary for inducing



ımonium oxamate [73].

either 1-D or 2-D patterns. For this family of compounds, it would seem that a primary ammonium cation, *e.g.* 4-chlorobenzylammonium, with three hydrogen-bond donors attached to the same point, is capable of bringing three anions close enough together (*via* N-H···O interactions) to encourage the formation of an infinite layer. On the other hand, secondary or tertiary amines are only able to form a bridge between two anions, which may be insufficient to bring about the formation of the infinite 2-D sheet. In those cases, *e.g.* piperidinium oxamate, the anions instead adopt a 1-D motif. Another factor that may be of importance is the size of the cation. Clearly, a large cation will increase the spacing between anionic regions, which tends to inhibit sheet formation. In contrast, if the cation is small, *e.g.* the potassium ion, the anions will be closer together which, in turn, facilitates the formation of the infinite anionic layer (as observed in potassium oxamate monohydrate).

This model system, built around the multi-functional (in hydrogen bonding terms) oxamate anion, can allow us to probe the relative importance and influence of various cation-anion interactions for resulting crystal structures. Such systematic structural investigations are likely to provide a source of reliable information about how intermolecular forces determine the crystal structure, and, thus, may provide useful guidance for future synthetic efforts.

Acknowledgments

Financial support from The Queen's University of Belfast, DRA Fort Halstead, and Kansas State University, is gratefully acknowledged. Furthermore, I would also like to extend a sincere thank you to my hardworking students/coworkers, Mark 'Woody' Nieuwenhuyzen and Deirdre Hughes.

References

1. Desiraju, G.R. (1989) *Crystal Engineering: The Design of Organic Solids*, Elsevier, Amsterdam.
2. Desiraju, G.R. (ed.)(1995) *Perspectives in Supramolecular Chemistry, Vol. 2, The Crystal as a Supramolecular Entity*, Wiley, Chichester.
3. Mathias J.P. and Stoddart, J.F. (1992) Constructing a molecular lego set *Chem. Soc. Rev.* **21**, 215-225.
4. Aakeröy, C.B. and Seddon, K.R. (1993) The hydrogen bond and crystal engineering, *Chem. Soc. Rev.*, **22**, 397-407.
5. Subramanian, S. and Zaworotko, M. (1994) Exploitation of the hydrogen bond: recent developments in the context of crystal engineering, *Coord. Chem. Rev.* **137**, 357-401.
6. MacDonald, J.C. and Whitesides, G.M. (1994) Solid-state structures of hydrogen-bonded tapes based on cyclic secondary diamides, *Chem. Rev.* **94**, 2383-2420.

UM00012759

NOVARTIS EXHIBIT 1017
Novartis v. Regents, IPR2023-01346
Page 1505 of 4460

7. Burrows, A.D., Chan, C-W., Chowdhry, M.M., McGrady, J.E., and Mingos, D.M.P. (1995) Multidimensional crystal engineering of bifunctional metal complexes containing complementary triple hydrogen bonds, *Chem. Soc. Rev.*, **24**, 329-339.

8. Lehn, J-M. (1990) Perspectives in supramolecular chemistry - From molecular recognition towards molecular information processing and self-organization, *Angew. Chem. Int. Ed. Engl.* **29**, 1304-1319.

9. Desiraju, G.R. (1995) Supramolecular synthons in crystal engineering - A new organic synthesis, *Angew. Chem. Int. Ed. Engl.* **34**, 2311-2327.

10. Braga, D. and Grepioni, F. (1996) Intermolecular interactions and supramolecular organization in organometallic solids, *Chem. Commun.*, 571-578.

11. Schmidt, G.M.J. (1971) Photodimerization in the solid state, *Pure Appl. Chem.* **27**, 647-678.

12. Maddox, J. (1988) Crystals from first principles, *Nature*. **335**, 201.

13. Leiserowitz, L. and Schmidt, G.M.J. (1969) Molecular packing modes. Part III. Primary amides, *J. Chem. Soc., A*, 2372-2382.

14. Blake, C.C.F. and Small, R.W.H. (1972) The crystal structure of benzamide, *Acta Cryst., Sect. B*, **28**, 2201-2206.

15. Davies, D.R. and Pasternak, R.A. (1956) The crystal structure of succinamide, *Acta Cryst.*, **9**, 334-338.

16. Leiserowitz, L. and Tuval, M. (1978) Molecular packing modes. *N*-methylamides, *Acta Cryst., Sect. B*, **34**, 1230-1247.

17. Leiserowitz, L. (1976) Molecular packing modes. Carboxylic acids, *Acta Cryst., Sect. B* **32**, 775-803.

18. Derissen, J.L. (1970) Crystal structure and conformation of methylmalonic acid *Acta Cryst., Sect. B*, **26**, 901-904.

19. Berkovitch-Yellin, Z., Ariel, S., and Leiserowitz, L. (1983) The comparative role of the proton-acceptor properties of amide and carboxylic groups in influencing crystal packing patterns- doubly *vs* singly hydrogen-bonded systems in *N*-acyl amino-acids and in other amide-acid crystals, *J. Am. Chem. Soc.* **105**, 765-767.

20. Desiraju, G.R. (1991) The C-H···O Hydrogen Bond in Crystals: What is it? *Acc. Chem. Res.*, **24**, 290-296.

21. Sutor, D.J. (1962) The C-H···O hydrogen bond in crystals, *Nature*, **195**, 68-69.

22. Sutor, D.J., (1963) Evidence for the existence of C-H···O bonds in crystals, *J. Chem. Soc.*, **1**, 1105-1110.

23. Donohue, J. (1968) in W.H. Freeman, A. Rich and N. Davidson, N, (eds.), *Structural Chemistry and Molecular Biology*, San Francisco, 1968, pp. 459-463.

24. Desiraju, G.R. (1989) Distance dependence of C-H···O interactions in some chloroalkyl compounds, *J. Chem. Soc., Chem. Commun.*, 179-180.

UM00012760
NOVARTIS EXHIBIT 1017
Novartis v. Regents, IPR2023-01346
Page 1506 of 4460

McGrady, J.E., and Mingos,
ering of bifunctional metal
n bonds, *Chem. Soc. Rev.*, **24**,

r chemistry - From molecular
essing and self-organization,

crystal engineering - A new
, 2311-2327.

teractions and supramolecular
nun., 571-578.

lid state, *Pure Appl. Chem.* **27**,

ature. **335**, 201.

ular packing modes. Part III.

l structure of benzamide, *Acta*

stal structure of succinamide,

king modes. *N*-methylamides,

Carboxylic acids, *Acta Cryst.*,

mation of methylmalonic acid

. (1983) The comparative role
rboxylic groups in influencing
gen-bonded systems in *N*-acyl
n. Chem. Soc. **105**, 765-767.

d in Crystals: What is it? *Acc.*

crystals, *Nature*, **195**, 68-69.

C-H···O bonds in crystals, *J.*

and N. Davidson, N, (eds.),
Francisco, 1968, pp. 459-463.

C-H···O interactions in some
nmun., 179-180.

25. Steiner, T. (1994) Effect of acceptor strength on C-H···O hydrogen-bond lengths as revealed by and quantified from crystallographic data, *J. Chem. Soc., Chem. Commun.*, 2341-2342.

26. Pedireddi, V.R. and Desiraju, G.R. (1992) A crystallographic scale of carbon acidity, *J. Chem. Soc., Chem. Commun.*, 988-990.

27. Allen, F.H. and Kennard, O. (1993) 3D search and research using the Cambridge Structural Database, *Chemical Design Automation News*, **8**, 30-37.

28. Etter, M.C. (1991) Hydrogen-bonds as design elements in organic chemistry, *J. Phys. Chem.*, **95**, 4601-4610.

29. Etter, M.C. and Baures, P.W. (1988) Triphenylphosphine oxide as a cocrystallization aid, *J. Am. Chem. Soc.* **110**, 639-640.

30. Etter, M.C., Urbanczyk-Lipkowska, Z., Zia-Ebrahimi, M., and Panunto, P.W. (1990) Hydrogen-bond directed cocrystallization and molecular recognition properties of diarylureas, *J. Am. Chem. Soc.* **110**, 8415-8426.

31. Etter, M.C. and Reutzel, S.M. (1991) Hydrogen-bond directed cocrystallization and molecular recognition properties of acyclic amides, *J. Am. Chem. Soc.* **113**, 2586-2598.

32. Etter, M.C., Adsmond, D.A., and Britton, D. (1990) 2-Aminopyrimidine succinic acid (1/1) cocrystal, *Acta Cryst., Sect. C*, **46**, 933-934.

33. Panunto, T.W., Urbanczyk-Lipkowska, Z., Johnson, R., and Etter, M.C. (1987) Hydrogen-bond formation in nitroanilines - the 1st step in designing acentric materials, *J. Am. Chem. Soc.*, **109**, 7786-7797.

34. Etter, M.C., MacDonald, J.C., and Bernstein, J. (1990) Graph-set analysis of hydrogen-bond patterns in organic crystals, *Acta Cryst., Sect. B* **46**, 256; Etter, M.C. (1990) Encoding and decoding hydrogen-bond patterns of organic compounds, *Acc. Chem Res.* **23**, 120-126.

35. Bernstein, J. Davies, R.E., Shimoni, L., and Chang, N.-L. (1995) Patterns in hydrogen bonding: Functionality and graph set analysis in crystals, *Angew. Chem. Int. Ed., Engl.*, **34**, 1555-1573.

36. Zerkowski, J.A., Seto, C.T., Wierda, D.A., and Whitesides, G.M. (1990) Design of organic structures in the solid state: Hydrogen-bonded molecular tapes, *J. Am. Chem. Soc.* **112**, 9025-9026.

37. Zerkowski, J.A., MacDonald, J.C., Seto, C.T., Wierda, D.A. and Whitesides, G.M. (1994) Design of organic structures in the solid state: Molecular tapes based on the network of hydrogen bonds present in the cyanuric acid-melamine complex, *J. Am. Chem. Soc.* **116**, 2382-2391.

38. Mathias, J.P., Simanek, E.E., Zerkowski, J.A., Seto, C.T., and Whitesides, G.M. (1994) Structural preferences of hydrogen-bonded networks in organic solution - the cyclic CA_3-M_3 "Rosette", *J. Am. Chem. Soc.* **116**, 4316-4325.

UM00012761
NOVARTIS EXHIBIT 1017
Novartis v. Regents, IPR2023-01346
Page 1507 of 4460

39. Zerkowski, J.A., MacDonald, J.C., and Whitesides, G.M. (1994) Investigations into the robustness of secondary and tertiary architecture of hydrogen-bonded crystalline tapes, *Chem. Mater.*, **6**, 1250-1257.

40. Garcia-Tellado, F., Goswami, S., Chang, C.K., Geib, S.J., and Hamilton, A.D. (1990) Molecular recognition - a remarkably simple receptor for the selective complexation of dicarboxylic acids, *J. Am. Chem. Soc.* **112**, 7393-7394.

41. Garcia-Tellado, F., Geib, S.J., Goswami, S., and Hamilton, A.D. (1991) Molecular recognition in the solid state: controlled assembly of hydrogen-bonded molecular sheets, *J. Am. Chem. Soc.* **113**, 9265-9269.

42. Geib, S.J., Vicent, C., Fan, E., and Hamilton, A.D. (1993) A self-assembling hydrogen-bonded helix, *Angew. Chem. Int. Ed. Engl.* **32**, 119-121.

43. Zhao, X., Chang, Y.-L., Fowler, F.W., and Lauher, J.W. (1990)An approach to the design of molecular solids - the ureylenedicarboxylic acids, *J. Am. Chem. Soc.*, **112**, 6627-6634.

44. Chang, Y.-L., West, M.-A., Fowler, F.W., and Lauher, J.W. (1993) An approach to the design of molecular solids. Strategies for controlling the assembly of molecules into two-dimensional layered structures, *J. Am. Chem. Soc.* **115**, 5991-6000.

45. Ducharme, Y. and Wuest, J.D. (1988) Use of hydrogen-bonds to control molecular aggregation - extensive. self-complementary arrays of donors and acceptors, *J. Org. Chem.* **53**, 5787-5789.

46. Simard, M., Su, M., and Wuest, J.D. (1991) Use of hydrogen-bonds to control molecular aggregation - self-assembly of 3-dimensional networks with large chambers, *J. Am. Chem. Soc.* **113**, 4696-4698.

47. Reddy, D.S., Goud, B.S., Panneerselvam, K., and Desiraju, G.R. (1993) C-H···N mediated hexagonal network in the crystal structure of the 1:1 molecular complex 1,3,5-tricyanobenzene-hexamethylbenzene, *J. Chem. Soc. Chem. Commun.* 663-664.

48. Sarma, J.A.R.P. and Desiraju, G.R. (1987) C-H···O interactions and the adoption of 4 Å short-axis crystal structures by oxygenated aromatic compounds, *J. Chem. Soc., Perkin Trans. II*, 1195-1202.

49. Desiraju, G.R., Calabrese, J.C., and Harlow, R.L. (1991) Pseudoinversion centers in space group $P\bar{1}$ and in a redetermination of the crystal structrue of 3,4-dimethoxycinnamic acid - A study of non-crystallographic symmetry, *Acta Cryst., Sect. B*, **47**, 77-86.

50. Ermer, O. and Eling, A. (1995) Molecular recognition among alcohols and amines - super-tetrahedral crystal architectures of linear diphenol-diamine complexes and aminophenols, *J. Chem. Soc., Perkin, Trans. II*, 925-944.

51. Orpen, A.G. (1993) Structural systematics in Molecular Inorganic Chemistry, *Chem. Soc. Rev.*, **22**, 191-197.

UM00012762
NOVARTIS EXHIBIT 1017
Novartis v. Regents, IPR2023-01346
Page 1508 of 4460

52. Brammer, L., Zhao, D., Ladipo, F.T., and Braddock-Wilking, J., (1995) Hydrogen bonds involving transition metal centres - A brief review, *Acta Cryst., Sect. B*, **51**, 632-640.

53. Biradha, K., Desiraju, G.R., Braga, D., and Grepioni, F. (1996), Hydrogen bonding in organometallic crystals. 3. Transition-metal complexes containing amido groups, *Organometallics*, **15**, 1284-1295.

54. Braga, D., Grepioni, F., Tedesco, E., Biradha, K., and Desiraju, G.R. (1996) Hydrogen bonding in organometallic crystals. 4. M-H···O hydrogen bonding interactions, *Organometallics*, **15**, 2692-2699.

55. Braga, D., Costa, A.L., Grepioni, F., Scaccianoce, L., and Tagliavini, E. (1996), OH···O and CH···O hydrogen bonding in hydrated crystals of paramagnetic $[(\eta^6\text{-}C_6H_6)_2Cr]^+$, *Organometallics*, **15**, 1084-1086.

56. Abrahams, B.F., Hoskins, B.F., Liu, J., Robson, R. (1991) The archetype for a new class of simple extended 3D honeycomb frameworks, *J. Am. Chem. Soc.*, **113**, 3045-3051.

57. Batten, S.R., Hoskins, B.F., and Robson, R. (1995) Two interpenetrating 3D networks which generate spacious sealed-off compartments enclosing of the order of twenty solvent molecules, *J. Am. Chem. Soc.*, **117**, 5385-5386.

58. Baxter, P.N.W., Hanan, G.S., and Lehn, J.-M. (1996) Inorganic arrays *via* multicomponent self assembly: the spontaneous generation of ladder architectures, *Chem. Commun.*, 2019-2020.

59. Hasenknopf, B., Lehn, J.-M., Knesiel, B.O., Baum, G., and Fenske, D. (1996) Self-assembly of circular double helicates, *Angew. Chem., Int. Ed. Engl.*, **35**, 1838-1840.

60. Drain, C.M., Fischer, R., Nolen, E.G., and Lehn, J.-M. (1993) Self-assembly of a bisporphyrin supramolecular cage induced by molecular recognition between complementary hydrogen bonding sites, *J. Chem. Soc., Chem. Commun.*, 243-245.

61. Subramanian, S. and Zaworotko, M. (1995) Porous solids by design: $[Zn(4,4'\text{-}bpy)_2(SiF_6)]_n.xDMF$, a single framework octahedral coordination polymer with large square channels, *Angew. Chem., Int. Ed. Engl.* **34**, 2127-2128.

62. Burrows, A.D., Mingos, D.M.P., White, A.J.P., and Williams, D.J. (1996) Molecular recognition of 2,6-diaminopyridine by platinum orotate complexes, *Chem. Commun.*, 148-151.

63. Chowdhry, M.M., Mingos, D.P.M., White, A.J.P., and Williams, D.J. (1996) Novel supramolecular self-assembly of a transition-metal-organo network based upon simultaneous coordinate- and hydrogen-bond formation, *Chem. Commun.*, 899-900.

64. Aakeröy, C.B., Bahra, G.S, Hitchcock, P.B., Patell, Y., and Seddon, K.R. (1993) Crystal engineering: Hydrogen-bonded salts of hydroxybenzoic acids for second harmonic generation, *J. Chem. Soc., Chem. Commun.*, 1993, 152-156.

UM00012763
NOVARTIS EXHIBIT 1017
Novartis v. Regents, IPR2023-01346
Page 1509 of 4460

65. Aakeröy, C.B., Hitchcock, P.B., and Seddon, K.R. (1992) Organic salts of *l*-tartaric acid: materials for second harmonic generation with a crystal structure governed by an anionic hydrogen-bonded network, *J. Chem. Soc., Chem. Commun.*, 553-555.

66. Pecaut, J. and Masse, R. (1993) Structure of *bis*(2-amino-5-nitropyridinium) dichromate as a step towards the design of efficient organic-inorganic nonlinear optical crystals, *Acta Cryst., Sect. B*, **49**, 277-282.

67. Aakeröy, C.B. and Hitchcock, P.B. (1993) Hydrogen-bonded layers of hydrogentartrate anions: Two-dimensional building blocks for crystal engineering *J. Mater. Chem.* **3**, 1129-1135.

68. (a) Zyss, J., Pecaut, J., Levy, J.P., and Masse, R. (1993) Synthesis and crystal structure of guanidinium *L*-monohydrogentartrate - encapsulation of an optically nonlinear octupolar cation, *Acta Cryst. Sect., B*, **49**, 334-342. (b) Dastidar, P., Row, T.N.G., Prasad, B.R., Subramanian, C.K., and Bhattacharya, S. (1993) Binary salts of substituted pyridines and *L*-tartaric acid as nonlinear optical organic materials: Crystal structure of *L*-tartaric acid-4-dimethylaminopyridine (1:1) dihydrate salt, *J. Chem. Soc., Perkin Trans. 2* **12**, 2419-2428. (c) Bhattacharya, S., Dastidar, P., and Row, T.N.G. (1994) Hydrogen-bond directed self-assembly of *D*-(+)-dibenzoyl tartaric acid and 4-aminopyridine: Optical nonlinearities and stoichiometry-dependent novel structural features, *Chem. Mat.*, **6**, 531-537. (d) Watanabe, O., Noritake, T., Hirose, Y., Okada, A., and Kurauchi, T. (1993) Synthesis, crystal-structure and nonlinear-optical properties of 2-amino-5-nitropyridine-*L*-(+)-tartrate, a new 2nd-harmonic-generation crystal, *J. Mat. Chem.* **3**, 1053-1057.

69. (a) Aakeröy, C.B., Hitchcock, P.B., Moyle, B.D. and Seddon, K.R. (1989) A novel class of salts for second harmonic generation, *J. Chem. Soc., Chem. Commun.* 1856-1859. (b) Masse, R. and Durif, A. (1990) Synthesis and crystal-structures of alpha-methyl alaninium dihydrogen monophosphate - an approach for the design and preparation of polar organic-inorganic materials, *Zeitschr. Krist.*, **190**, 19-32.

70. Pecaut, J., Le Fur, Y., and Masse, R. (1993) Crystal engineering and structural investigations of the 2-amino-5-nitropyridinium salts $[C_5H_6N_3O_2]^+$ $[HSO_4]^-$ and $[C_5H_6N_3O_2]^+$ $[H_2AsO_4]^-$ *Acta Cryst. Sect. B*, **49**, 535-541.

71. Aakeröy, C.B. and Nieuwenhuyzen, M. (1996) Hydrogen bonding in crystal engineering: 2-D layers of hydrogen L-malate anions, *J. Mol. Struct.*, **374**, 223-239.

72. Aakeröy, C.B. and Nieuwenhuyzen, M. (1994) Hydrogen-bonded layers of hydrogenmalate anions: A framework for crystal engineering, *J. Am. Chem. Soc.*, **116**, 10983-10991.

73. Aakeröy, C.B., Hughes, D.P., and Nieuwenhuyzen, M. (1996) The oxamate anion: A flexible building block of hydrogen-bonded architectures for crystal engineering, *J. Am. Chem. Soc.*, **118**, 10134-10140.

UM00012764
NOVARTIS EXHIBIT 1017
Novartis v. Regents, IPR2023-01346
Page 1510 of 4460

This Page is Inserted by IFW Indexing and Scanning Operations and is not part of the Official Record

BEST AVAILABLE IMAGES

Defective images within this document are accurate representations of the original documents submitted by the applicant.

Defects in the images include but are not limited to the items checked:

- ☐ BLACK BORDERS
- ☐ IMAGE CUT OFF AT TOP, BOTTOM OR SIDES
- ☐ FADED TEXT OR DRAWING
- ☐ BLURRED OR ILLEGIBLE TEXT OR DRAWING
- ☐ SKEWED/SLANTED IMAGES
- ☐ COLOR OR BLACK AND WHITE PHOTOGRAPHS
- ☐ GRAY SCALE DOCUMENTS
- ☐ LINES OR MARKS ON ORIGINAL DOCUMENT
- ☐ REFERENCE(S) OR EXHIBIT(S) SUBMITTED ARE POOR QUALITY
- ☐ OTHER: _____

IMAGES ARE BEST AVAILABLE COPY.
As rescanning these documents will not correct the image problems checked, please do not report these problems to the IFW Image Problem Mailbox.

Pergamon

Crystal Engineering, Vol. 1, No. 1, pp. 39–49, 1998
Copyright © 1998 Elsevier Science Ltd
Printed in the USA. All rights reserved
0025-5408/98 $19.00 + .00

PII S0025-5408(98)00033-6

LOW-DIMENSIONAL ARCHITECTURES OF SILVER COORDINATION COMPOUNDS ASSEMBLED *VIA* AMIDE-AMIDE HYDROGEN BONDS

C.B. Aakeröy* and A.M. Beatty
Department of Chemistry, Kansas State University, Manhattan, KS 66506, USA

(Refereed)
(Received November 12, 1997; Accepted January 17, 1998)

ABSTRACT

The syntheses and crystal structures of di(6-methylnicotinamide)silver(I) triflate (**1**), di(6-methylnicotinamide)silver(I) nitrate (**2**), and di(*iso*nicotinamide)silver(I) triflate dihydrate (**3**) are described. Despite the structural differences in their counter-anions, both **1** and **2** exhibit very similar hydrogen-bonded networks, where a ladder motif is formed through amide-amide hydrogen bonding interactions. The *para* position of the amide moiety in **3** promotes chain formation through amide-amide hydrogen bonds. These structures illustrate the robust hydrogen-bonding ability of the amide functionality, even in a potentially disruptive environment of metal ions, anions and water molecules. The influence of substituents on the nicotinamide ligand and the effect of varying anions in this system are discussed. © *1998 Elsevier Science Ltd*

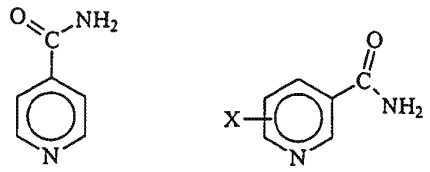
KEYWORDS: A. inorganic compounds, A. layered compounds, C. X-ray diffraction, D. crystal structure.

INTRODUCTION

Strategies for predicting and controlling the assembly of molecules and ions in the solid state have emanated from the two main synthetic branches of chemistry. Investigations of the assembly of *organic* molecules or ions through intermolecular interactions have led to the identification of a number of useful tools for supramolecular design, such as iodo-nitro, chloride-chloride, and π-π stacking interactions [1]. Arguably, the most extensively studied and most efficient intermolecular connector has proved to be the hydrogen bond. Functional groups such as carboxylic acids and amides consistently interact with each other *via*

*To whom correspondence should be addressed.

UM00012766
NOVARTIS EXHIBIT 1017
Novartis v. Regents, IPR2023-01346
Page 1512 of 4460



a. *iso*nicotinamide b. substituted nicotinamides, X= *e.g.* alkyl, halide, NO_2

SCHEME 1.
Possible variations of the model ligand, nicotinamide.

hydrogen bonds, resulting in the formation of 1-D, 2-D, and 3-D architectures [2]. Meanwhile, the assembly of *metal complexes* has been achieved primarily through the formation of "coordination polymers." The inherent coordination geometry of certain metal ions has been propagated into 3-D networks through covalent interactions with bidentate ligands such as 4,4′ bipyridine and piperazine [3]. Interest in these systems stems from the fact that ordered transition metals can provide access to magnetic, optical and conductive properties not readily available in organic molecular solids. A combination of the two aforementioned strategies, using ligands which can simultaneously coordinate metal ions *and* participate in strong hydrogen bonding interactions [4], may have the advantage of added flexibility, as hydrogen bonds may undergo conformational changes to accomodate for example different substituents and solvent molecules, with no drastic effect on the overall motif.

STRATEGY

There is considerable interest in the design of low-dimensional architectures, as their structures, and therefore properties, are anisotropic. Transition metal compounds are useful building blocks from a crystal engineering standpoint, because the coordination geometry about the metal center can be used to initiate and propagate a desired extended motif. With this in mind, we are examining a low-dimensional system which lends itself well to the systematic study of the structural changes that may be effected by variations in substituents or counterions.

Silver(I) is one of the few metal ions that commonly displays linear coordination geometries, AgL_2, and hence provides an appropriate model system [5]. The choice of ligand depends on two criteria: first, the ligand must provide a site that coordinates preferentially to the silver ion (e.g., the nitrogen atom in pyridine); and second, a functional group that forms strong hydrogen bonds to itself must also be present. The amide functionality is an appropriate intermolecular connector, because its supramolecular hydrogen bonding motifs are well characterized in molecular solids, and because silver(I) ions are unlikely to coordinate to either the carbonyl oxygen or amine nitrogen atoms in the presence of a pyridine nitrogen atom. Therefore nicotinamide, which satisfies both conditions, is an appropriate model ligand. This system is versatile, as the position of the amide moiety can be changed from *meta* (nicotinamide) to *para* (*iso*nicotinamide) (Scheme 1a). In addition, a range of substituents (e.g., Me, Cl, NO_2), can be attached to the pyridine ring (Scheme 1b), allowing the exploration of electronic and steric effects on the overall structure.

UM00012767
NOVARTIS EXHIBIT 1017
Novartis v. Regents, IPR2023-01346
Page 1513 of 4460

In order to investigate the influence of steric requirements and hydrogen bonding ability of the *counterion*, we are also incorporating a range of anions into a family of silver(I) complexes. To demonstrate this strategy, we recently reported the crystal structures of three dinicotinamidesilver(I) compounds [6] assembled *via* directional amide-amide hydrogen bonding interactions, and we now report the X-ray single crystal structures of three new compounds, $[(6\text{-}CH_3\text{-}3\text{-}CONH_2\text{-}C_5H_4N)_2Ag]^+[O_3SCF_3]^-$ **1**, $[(6\text{-}CH_3\text{-}3\text{-}CONH_2C_5H_4N)_2Ag]^+[NO_3]^-$ **2**, and $[(4\text{-}CONH_2\text{-}C_5H_4N)_2Ag]^+[O_3SCF_3]^-\cdot 2H_2O$ **3**, all of which exhibit one-dimensional architectures, propagated through amide-amide hydrogen bonds.

EXPERIMENTAL

Preparation of di(6-methylnicotinamide)silver(I) triflate (1). Silver triflate (0.09 g, 0.36 mmol) was dissolved in ~10 mL distilled water. To this solution was added 0.1 g (0.72 mmol) 6-methylnicotinamide dissolved in ~25 mL of a 1:1 EtOH:H_2O mixture. The solution was briefly stirred, the solvent was allowed to evaporate slowly at ambient temperature, and single crystals of **1** were formed as colorless rods (m.p. 198–202°C).

Preparation of di(6-methylnicotinamide)silver(I) nitrate (2). Silver nitrate (0.1 g, 0.59 mmol) was dissolved in ~15 mL distilled water. To this solution was added 0.24 g (1.77 mmol) 6-methylnicotinamide dissolved in ~30 mL of a 1:1 EtOH:H_2O mixture. The solution was briefly stirred, and the solvent was allowed to evaporate slowly at ambient temperature, yielding single crystals of **2** as colorless needles (m.p. 204–207°C).

Preparation of di(*iso*nicotinamide)silver(I) triflate dihydrate (3). Silver triflate (0.09 g, 0.36 mmol) was dissolved in ~10 mL distilled water. To this solution was added 0.09 g (0.72 mmol) isonicotinamide dissolved in ~20 mL of distilled water. The mixture was briefly stirred, and the solution was allowed to evaporate slowly at ambient temperature. Single crystals of **3** were formed as colorless prisms (m.p. 228–232°C).

X-ray Crystallography. Crystal data were collected using a Siemens P4 four-circle diffractometer with graphite monochromated Mo-Kα radiation. Hydrogen atom positions were located from difference Fourier maps except in **1**, where the positions of the aromatic hydrogen atoms were calculated; a riding model with fixed thermal parameters [u_{ij} = $1.2U_{ij}$(eq) for the atom to which they are bonded] was used for subsequent refinements. The weighting function applied was $w^{-1} = [\sigma^2(F_o^2) + (g_1P)^2 + (g_2P)]$ where $P = [F_o^2 + 2F_c^2]/3$. The SHELXTL PC and SHELXL-93 packages were used for data reduction and structure solution and refinement [7]. Table 1 provides crystallographic details for **1–3**.

RESULTS

The reaction of silver(I) triflate with two equivalents of 6-methylnicotinamide leads to the formation of di(6-methylnicotinamide)silver(I) triflate **1** (Fig. 1A), where the cationic complex contains a silver ion coordinated to two ligands in a near-linear fashion $\measuredangle L\text{-Ag-}L$, 176.1(2)°. As expected, the coordination to the silver ion is through the ring nitrogen atoms. The shortest silver-oxygen distance is between the silver ion and a nitrate oxygen atom, rAg(1)···O(2), 2.673(5)Å. The 1-D geometry of the complex cation is propagated in the solid

UM00012768
NOVARTIS EXHIBIT 1017
Novartis v. Regents, IPR2023-01346
Page 1514 of 4460

TABLE 1
Data Collection and Refinement for **1–3**

Crystal data	1	2	3
CCDC deposit number	CCDC-1290/1	CCDC-1290/2	CCDC-1290/3
Empirical formula	$C_{15}H_{16}N_4O_5SF_3Ag$	$C_{14}H_{16}N_5O_5Ag$	$C_{13}H_{16}N_4O_7SF_3Ag$
MW	529.25	442.19	537.23
Crystal size (mm)	0.48 × 0.40 × 0.18	0.36 × 0.14 × 0.10	0.40 × 0.38 × 0.32
Crystal system	triclinic	triclinic	triclinic
Space group	P-1	P-1	P-1
a (Å)	8.4093(4)	6.7247(4)	8.4410(4)
b (Å)	10.6016(10)	10.4425(7)	9.1064(5)
c (Å)	11.3768(7)	12.6145(7)	13.4948(6)
α (deg)	98.979(6)	106.354(5)	107.336(4)
β (deg)	92.340(4)	97.706(5)	98.908(3)
γ (deg)	111.430(5)	102.644(7)	97.506(4)
Volume (Å^3)	927.28(11)	811.05(9)	960.90(8)
Z	2	2	2
D_{calc} (g cm^{-3})	1.896	1.811	1.857
F(000)	528	444	536
μ(Mo-K$_\alpha$) (mm^{-1})	1.266	1.280	1.230
Temp (K)	173	173	173
θ–2θ scans; θ range (deg)	1.82–22.50	1.72–23.00	1.62–23.50
Reflns collected	2611	2443	3030
Unique reflns	2411	2219	2813
Observed reflns (I > 2σI)	2305	1952	2660
Data:parameter (obs. data)	8.80	8.64	10.2
R/R$_w^2$ (obs data)	0.0428/0.1449	0.0269/0.0610	0.0286/0.1010
R/R$_w^2$ (all data)	0.0491/0.1760	0.0353/0.0649	0.0347/0.1298
$\Delta\rho_{max/min}$ (e Å^{-3})	1.349/−1.880	0.373/−0.552	0.609/−0.989
S	1.208	1.055	1.232

state through amide-amide hydrogen bonds (Table 2), leading to infinite $C_1^1(12)$ chains [8]. Neighboring chains are linked through symmetry related hydrogen bonds, forming a "head-to-head" $R_2^2(8)$ motif. These two intermolecular interactions create an infinite ladder arrangement (Fig. 2). There are no further hydrogen bond interactions between adjacent cationic ladders. The anion acts as a cross-link between two cationic ladders *via* hydrogen bonds to the two remaining amide hydrogen atoms. Thus the triflate ion, which has oxygen atoms readily available as hydrogen bond acceptors, does not disrupt the formation of the intended ligand-ligand hydrogen bonds, and the amide functionalities propagate a linear assembly of the silver complexes.

The reaction of silver(I) nitrate with 6-methylnicotinamide leads to the formation of di(6-methylnicotinamide)silver(I) nitrate **2** (Fig. 1B), where the cationic complex is again formed by near-linear coordination of two ligands to silver(I), $\measuredangle$*L*-Ag-*L*, 171.0(1)°. The shortest silver-oxygen distance is between the silver ion and a nitrate oxygen atom,

UM00012769
NOVARTIS EXHIBIT 1017
Novartis v. Regents, IPR2023-01346
Page 1515 of 4460

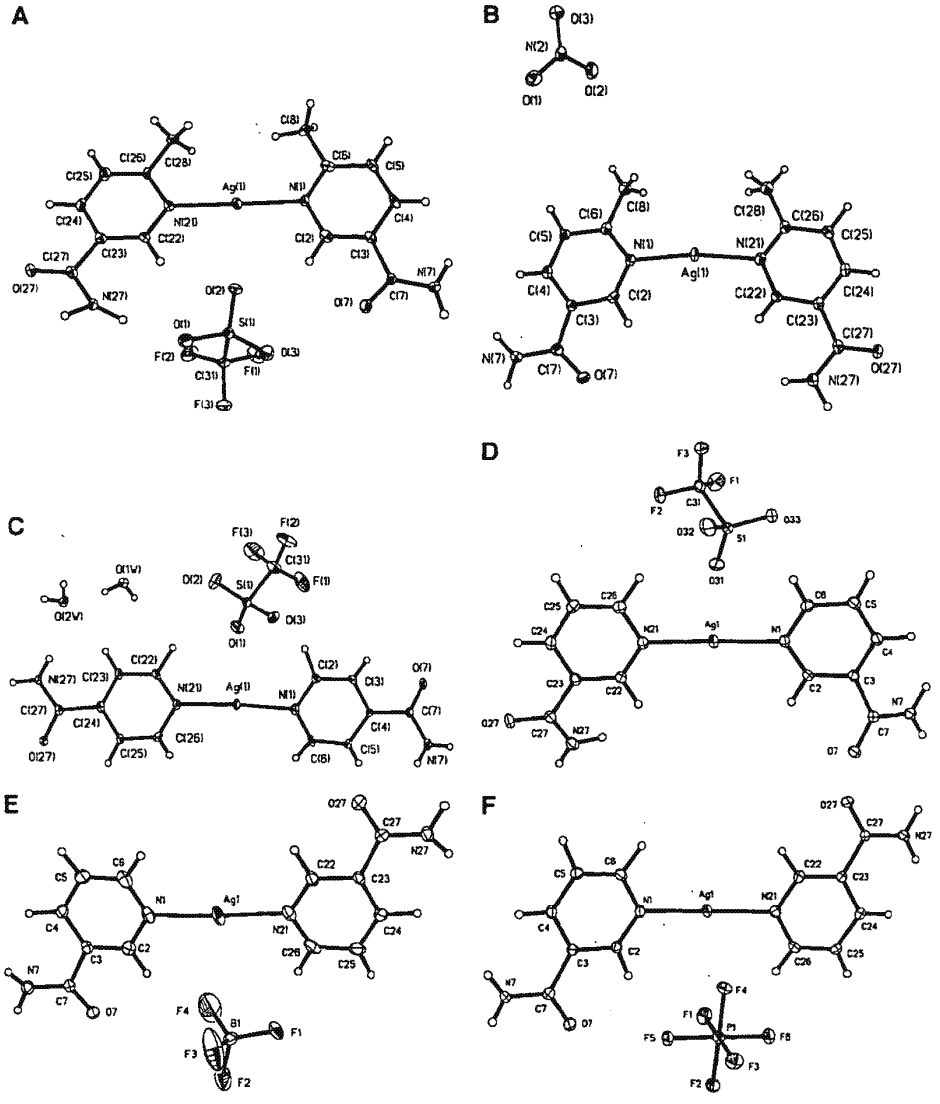


FIG. 1

A) Molecular structure and labeling scheme for **1** (30% thermal ellipsoids). *B*) Molecular structure and labeling scheme for **2** (30% thermal ellipsoids). *C*) Molecular structure and labeling scheme for **3** (30% thermal ellipsoids). *D*) Molecular structure and labeling scheme for **4** (30% thermal ellipsoids) [6]. *E*) Molecular structure and labeling scheme for **5** (30% thermal ellipsoids) [6]. *F*) Molecular structure and labeling scheme for **6** (30% thermal ellipsoids) [6].

*r*Ag(1)···O(3), 2.769(3)Å; as this distance is longer than the silver-oxygen distance observed in **1**, the bend in **2** is not attributed to a strong interaction between the silver ion and the nitrate anion. The amide-amide hydrogen bonding interactions of the ligand are nearly identical to **1** (Table 3), with a linear motif propagated in the solid state through amide-amide hydrogen

UM00012770
NOVARTIS EXHIBIT 1017
Novartis v. Regents, IPR2023-01346
Page 1516 of 4460

TABLE 2
Geometry of the Hydrogen Bonds in **1**

D-H—A	r(H—A) (Å)	r(D—A) (Å)	∠(D-H—A) (°)
N(7)-H(7A)—O(27)′	2.051(7)	2.929(7)	153.3(2)
N(7)-H(7B)—O(7)″	2.032(7)	2.902(7)	177.7(2)
N(27)-H(27A)—O(3)‴	2.369(7)	3.020(8)	126.4(2)
N(27)-H(27B)—O(1)	1.946(1)	2.939(8)	171.8(2)
C(5)-H(5)*—F(3)⁗	2.584	3.344(8)	136.3
C(25)-H(25)*—F(1)⁗′	2.571	3.474(9)	156.9

Symmetry codes: (′) $x, y-1, z-1$; (″) $-x+2, -y, -z-1$; (‴) $-x+2, -y+1, -z$; (⁗) $x, y+1, z$; (⁗′) $x, y, z-1$
*Non-amide hydrogen atoms were placed at idealized positions in **1**.

bonds, leading to infinite $C_1^1(12)$ chains. Neighboring chains are linked through symmetry related hydrogen bonds, forming a "head-to-head" $R_2^2(8)$ motif, which creates the infinite ladder arrangement, as exhibited in the triflate analog **1** (Fig. 3). There are no further hydrogen bond interactions between adjacent cationic ladders. The nitrate anion acts as a cross-link between two cationic ladders *via* hydrogen bonds to the two remaining amide hydrogen atoms, and the orientation of the nitrate oxygen atoms is virtually identical to that of the triflate oxygen atoms in **1**.

The reaction of silver(I) triflate with *iso*nicotinamide (4-pyridinecarboxamide) yields a linear complex, di(*iso*nicotinamide)silver(I) triflate dihydrate **3** (Fig. 1C). Intermolecular hydrogen bonds between the amide moieties (Table 4) extend the linear geometry of the complex, ∢*L*-Ag-*L*, 174.99(2)°, into a linear chain motif through two symmetry equivalent "head-to-head" $R_2^2(8)$ hydrogen bonds (Fig. 4). The chains are further linked through hydrogen bonding interactions with water and triflate oxygen atoms, which are arranged in channels between the chains, creating a three-dimensional hydrogen bonded network of cationic chains, triflate anions, and water molecules.

TABLE 3
Geometry of the Hydrogen Bonds in **2**

D-H—A	r(H—A) (Å)	r(D—A) (Å)	∠(D-H—A) (°)
N(7)-H(7A)—O(7)′	2.000(4)	2.890(4)	156.3(1)
N(7)-H(7B)—O(27)″	1.997(4)	2.930(4)	175.7(1)
N(27)-H(27A)—O(1)‴	2.052(4)	2.949(4)	159.2(1)
N(27)-H(27B)—O(2)⁗	2.087(4)	2.966(4)	172.7(1)
C(2)-H(2)—O(3)⁗	2.438(4)	3.220(4)	135.7(1)
C(22)-H(22)—O(3)⁗′	2.422(4)	3.218(4)	145.6(1)

Symmetry codes: (′) $-x, -y, -z$; (″) $1+x, 1+y, 1+z$; (‴) $1-x, -y, -1-z$; (⁗) $-1+x, y-1, z$

UM00012771
NOVARTIS EXHIBIT 1017
Novartis v. Regents, IPR2023-01346
Page 1517 of 4460

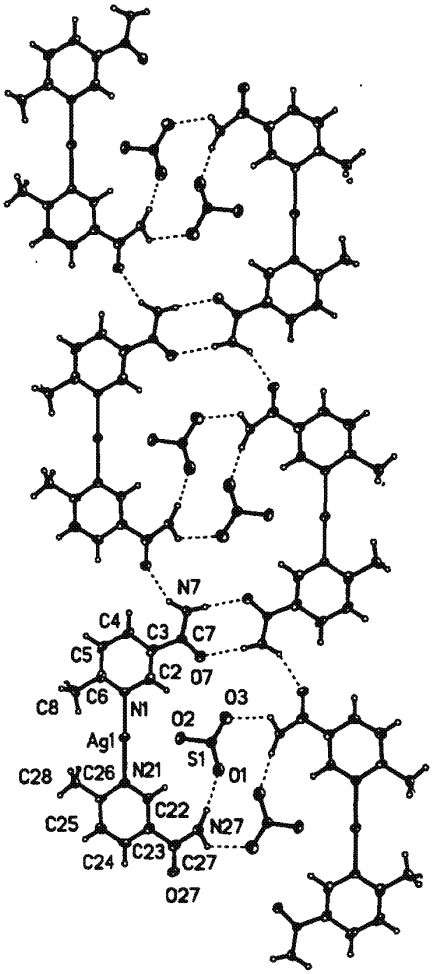


FIG. 2
The hydrogen-bonded ladder motif in **1**. The CF_3 portion of the triflate anion has been omitted for clarity.

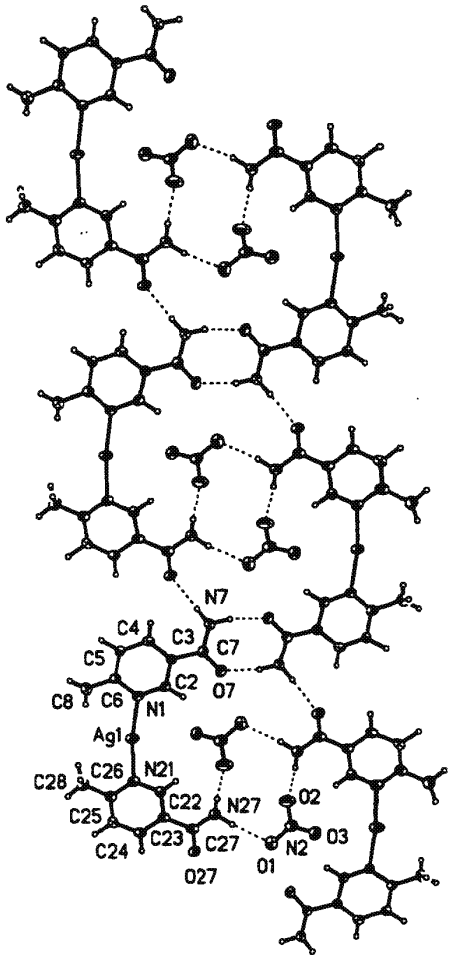


FIG. 3
The hydrogen-bonded ladder motif in **2**. The intermolecular interactions are very similar to those in 1.

DISCUSSION

We recently reported a structural study of dinicotinamidesilver(I) triflate **4** (Fig. 1D), dinicotinamidesilver(I) tetrafluoroborate **5** (Fig. 1E), and dinicotinamidesilver(I) hexafluorophosphate **6** (Fig. 1F), which were part of a systematic study of silver(I) complexes, where only the counterions were changed [6]. We found that "spherical" anions such as $[BF_4]^-$ and $[PF_6]^-$ gave rise to cationic sheets in **5** and **6** (Fig. 5). The sheets were formed by amide-amide hydrogen-bond interactions between linear silver(I) complexes, with the counterions sandwiched between cationic sheets, resulting in layered structures (Fig. 6). However, the previously reported structure of **4** (Fig. 7) is nearly the same as the structure of **1**

UM00012772
NOVARTIS EXHIBIT 1017
Novartis v. Regents, IPR2023-01346
Page 1518 of 4460

TABLE 4
Geometry of the Hydrogen Bonds in **3**

D-H—A	r(H—A) (Å)	r(D—A) (Å)	∠(D-H—A) (°)
N(7)-H(7B)—O(27)′	2.170(5)	2.965(5)	156.4(1)
N(7)-H(7A)—O(1W)″	2.109(6)	2.945(6)	158.1(2)
N(27)-H(27A)—O(2W)	2.195(5)	3.034(6)	163.4(1)
N(27)-H(27B)—O(7)‴	1.936(5)	2.872(5)	170.9(2)
O(1W)-H(2W)—O(27)⁗	2.052(5)	2.741(5)	153.2(1)
O(1W)-H(1W)—O(2W)	1.938(5)	2.793(5)	162.1(2)
O(2W)-H(3W)—O(1W)⁗′	1.943(5)	2.760(5)	140.9(2)
O(2W)-H(4W)—O(2)⁗′	2.010(5)	2.722(5)	153.0(2)
C(2)-H(2)—O(3)	2.451(6)	3.401(6)	135.5(1)
C(22)-H(22)—O(1)	2.468(6)	3.422(6)	139.9(2)

Symmetry codes: (′) $x-1, y, z+1$; (″) $x, y+1, z+1$; (‴) $x+1, y, z-1$; (⁗) $-x+1, -y+2, -z+2$; (⁗′) $-x+1, -y+1, -z+2$

(discussed above): the difference between the two compounds is a methyl substituent on the nicotinamide ligand in **4**. In both cases a *cis* conformation of the amide functionalities about the N-Ag-N axis means that the amide-amide interactions are confined to the observed one-dimensional network; both **1** and **4** display identical cationic ladder motifs. Consequently, the steric demand of the methyl group has virtually no effect on the overall assembly. Evidently, the amide-amide interactions are robust enough to accommodate small structural changes in the ligand.

It is instructive to examine the role of the anion by comparing **1** and **2**, as they differ only in the nature of the counterion: triflate vs. nitrate. While these anions have different spatial requirements, their hydrogen-bonding ability is similar. The two structures exhibit virtually identical amide-amide interactions, resulting in ladder arrangements of the linear complexes in both cases. The interaction of oxygen atoms of the triflate and nitrate counterions with the two available amide hydrogen atoms is nearly indistinguishable; hence the different *steric* requirements of the anions do not perturb the overall supramolecular assembly.

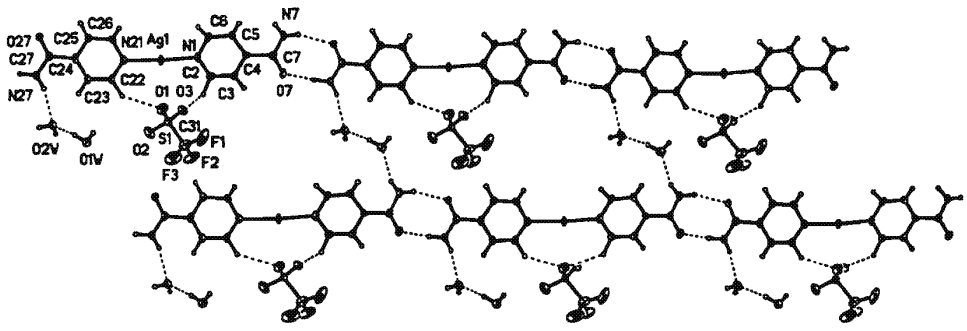


FIG. 4
The hydrogen-bonded chain motif in **3**. Adjacent chains are linked through hydrogen bonds to water molecules.

UM00012773
NOVARTIS EXHIBIT 1017
Novartis v. Regents, IPR2023-01346
Page 1519 of 4460

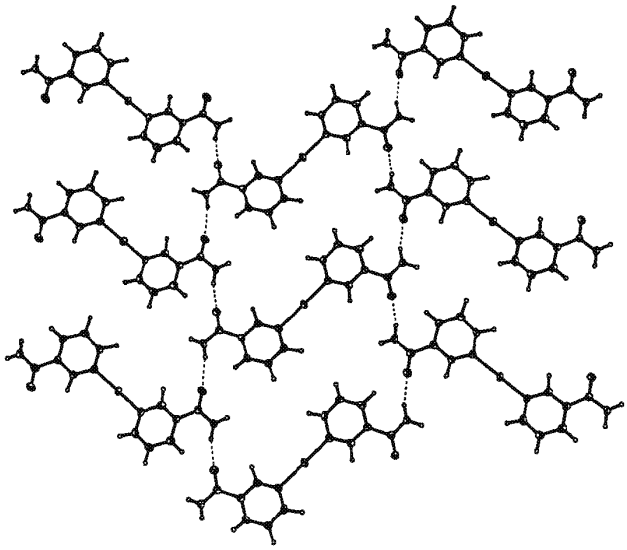


FIG. 5

The hydrogen-bonded cationic sheet observed in **6** (see ref. [6]). Compound **5** displays an identical network.

A comparison of **4** and **3**, where both compounds contain the triflate counterion, allows an analysis of the other variable in this system: the location of the amide functionality, *meta* vs. *para*. The ladder structure of **4** depends on the *cis* relationship of the two *meta* amide functionalities in nicotinamide, which is not possible for the *para* geometry of the *iso*nicotinamide ligand in **3**. While **3** exhibits the same head-to-head amide-amide hydrogen bonds observed in **1**, **2**, and **4**, the resulting linear arrangement cannot accommodate the ladder motif. The presence of water molecules hydrogen-bonded between the chains prevents inter-chain amide-amide hydrogen bonding in **3**, resulting in the observed one-dimensional motif, where the cationic chains are isolated by triflate-hydrate channels. It is important to note that the amide-amide hydrogen bonds persist in **3** even in competition with the water molecules.

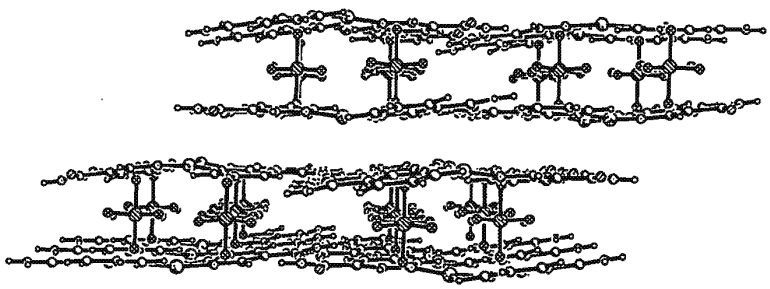


FIG. 6

Edge-on view of the layered structure of **6** (see ref. [6]). Hexafluorophosphate anions are sandwiched between cationic sheets. Compound **5** exhibits a similar structure.

UM00012774
NOVARTIS EXHIBIT 1017
Novartis v. Regents, IPR2023-01346
Page 1520 of 4460

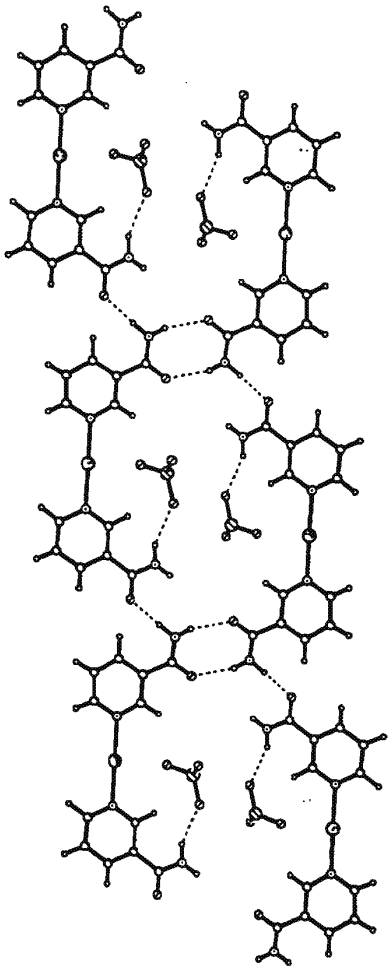


FIG. 7
The hydrogen-bonded ladder motif in **4** (see ref. [6]). The CF_3 portion of the triflate anion has been omitted for clarity.

CONCLUSION

The structural investigation of a series of the silver(I) nicotinamide complexes described here demonstrates that the amide functionality can be used as a tool for controlling the assembly of metal complexes. We have demonstrated that linear silver(I) complexes can be intermolecularly connected in a predictable manner, through careful choice of ligand and counterion. We have also shown that small changes in substituents on the pyridine ring may not have a great effect on the overall solid state structure of these compounds. Small variations in substituents or counterions may fine-tune the assemblies of these complexes, but hydrogen-bonding interactions between the amide moieties provide the dominating steering force for their supramolecular assembly.

UM00012775
NOVARTIS EXHIBIT 1017
Novartis v. Regents, IPR2023-01346
Page 1521 of 4460

ACKNOWLEDGMENTS

We acknowledge the financial support from Kansas State University and NSF-EPSCoR (OSR-9550487).

REFERENCES

1. G.R. Desiraju, *Crystal Engineering: The Design of Organic Solids*, Elsevier, Amsterdam, 1989; G.R. Desiraju, *Angew. Chem. Int. Ed. Engl.* **34**, 2311 (1995); C.B. Aakeröy, *Acta Crystallogr. Sect. B.* **53**, 569 (1997); M.J. Zaworotko, *Nature* **386**, 220 (1997); M.M. Conn and J. Rebek Jr., *Chem. Rev.* **97**, 1647 (1997).
2. S. Coe, J.J. Kane, T.L. Nguyen, L.M. Toledo, E. Wininger, F.W. Fowler, and J.W. Lauher, *J. Am. Chem. Soc.* **119**, 86 (1997); C.B. Aakeröy and M. Nieuwenhuyzen, *J. Am. Chem. Soc.* **116**, 10983 (1994); K.E. Schwiebert, D.N. Chin, J.C. MacDonald, and G.M. Whitesides, *J. Am. Chem. Soc.* **118**, 4018 (1996); R.E. Melendez, C.V. Krishnamohan, M.J. Zaworotko, C. Bauer, and R.D. Rogers, *Angew. Chem. Int. Ed. Engl.* **35**, 2213 (1996); O. Felix, M.W. Hosseini, A. de Cian, and J. Fischer, *Angew. Chem. Int. Ed. Engl.* **36**, 102 (1997); P. Brunet, M. Simard, and J.D. Wuest, *J. Am. Chem. Soc.* **119**, 2737 (1997); A. Marsh, M. Silvestri, and J.-M. Lehn, *Chem. Commun.* 1527 (1996); W.T.S. Huck, R. Hulst, P. Timmerman, F.C.J.M van Eggel, and D.N. Reinhoudt, *Angew. Chem. Int. Ed. Engl.* **36**, 1006 (1997).
3. J.-M. Lehn, *Angew. Chem. Int. Ed. Engl.* **29**, 1342 (1990); J.S. Miller, A.J. Epstein, and W.M. Reiff, *Acc. Chem. Res.* **21**, 114 (1988); S. Subramanian and M.J. Zaworotko, *Coord. Chem. Rev.* **137**, 357 (1994).
4. A.D. Burrows, C.-W. Chan, M.M. Chowdhry, J.E. McGrady, and D.M.P. Mingos, *Chem. Soc. Rev., Commun.* 329 (1995); A.D. Burrows, D.M.P. Mingos, A.J.P. White, and D.J. Williams, *Chem. Commun.* 97 (1996); L. Carlucci, G. Ciani, D.M. Proserpio, and A. Sironi, *J. Chem. Soc., Dalton Trans.* 1801 (1997); A. Hassan and S. Wang, *J. Chem. Soc., Dalton Trans.* 2009 (1997); C.M. Drain, K.C. Russel, and J.-M. Lehn, *Chem. Commun.* 337 (1996).
5. D. Venkataraman, S. Lee, J.S. Moore, P. Zhang, K.A. Hirsch, G.B. Gardner, A.C. Covey, and C.L. Prentice, *Chem. Mater.* **8**, 2030 (1996); L. Carlucci, G. Ciani, D.M. Proserpio, and A. Sironi, *J. Am. Chem. Soc.* **117**, 4562 (1995).
6. C.B. Aakeröy and A.M. Beatty, *Chem. Commun.*, submitted (1997).
7. G.M. Sheldrick, SHELXL-93, University of Göttingen.
8. For information about graph-set notation, see J. Bernstein, R.E. Davis, L. Shimoni, and N.-L Chang, *Angew. Chem. Int. Ed. Engl.* **34**, 1555 (1995); M.C. Etter, J.C. MacDonald, and J. Bernstein, *Acta Crystallogr. Sect. B* **46**, 256 (1990).

UM00012776
NOVARTIS EXHIBIT 1017
Novartis v. Regents, IPR2023-01346
Page 1522 of 4460

MOLECULAR MECHANICS AND CRYSTAL ENGINEERING

CHRISTER B. AAKERÖY
Department of Chemistry, Kansas State University, Manhattan, Kansas, 66506, USA.
ROBIN E. BOYETT
Division of Chemistry, University of Portsmouth, Portsmouth, PO1 2DT, UK.

1. Preamble

One of the main driving forces behind the evolution of molecular mechanics is the widespread and continuous interest in the structure of ***molecules***. The shape, size and conformation of molecules determine many of their properties (*e.g.* stability and reactivity) and, consequently, the ability to accurately predict the structure of a molecule may enable us to correctly anticipate many chemical characteristics of new or unknown molecular species. Central to the structure of any molecule is the nature and geometric features of a covalent bond, a concept which lends itself very well to a molecular-mechanics approach based upon a classical 'ball-and-spring' description.

In contrast, crystal engineering and supramolecular chemistry are concerned with the structure and properties of ***assemblies*** of molecules and with the way in which various intermolecular forces influence recognition processes. These intermolecular forces are often weak, and an accurate treatment of such interactions requires a good understanding and representation of many ill-defined concepts such as 'fractional-charge' and 'packing-forces'. With this in mind, it would seem that conventional molecular-mechanics calculations would have little to offer in terms of cultivating strategies and efforts in crystal engineering, even though they have been invaluable in studies of molecular geometries and properties. However, most modern force fields do not just examine molecular properties, but they are also likely to contain components and functions which deal explicitly with various intermolecular interactions.

More common ground also emerges when examining how molecular mechanics and crystal engineering have developed. Both these disciplines have relied on careful and systematic analyses of structural data: (i) in many force fields, equilibrium bond-lengths, bond-angles, *etc.*, are derived from extensive structural information for families of compounds or moieties, (ii) many design strategies in crystal engineering are based upon preferential packing preferences or hydrogen-bond patterns as identified from crystallographic data.

Many force fields have been shown to be very good at providing accurate predictions of geometries for a wide range of, notably, organic molecules. Consequently, it is generally accepted that covalent interactions (and their resulting geometries) can be

K. R. Seddon and M. Zaworotko (eds.). Crystal Engineering. 69–82.
© 1999 *Kluwer Academic Publishers. Printed in the Netherlands.*

UM00012777
NOVARTIS EXHIBIT 1017
Novartis v. Regents, IPR2023-01346
Page 1523 of 4460

estimated and predicted with a considerable degree of confidence using a force-field approach. However, intermolecular forces (the 'tools' of crystal engineering) are far more difficult to model with a classical mechanical approach. Indeed, as the central idea of a molecule described as a collection of 'balls-and-springs' cannot be immediately extended to weaker, sometimes non-directional, intermolecular forces, how can we apply molecular-mechanics methods to the challenges of crystal engineering? Unfortunately, the conformational flexibility of most molecules, coupled with the inherent spatial and positional freedom within a three-dimensional system, makes the task of calculating/predicting crystal structures and polymorphs a very tricky business indeed.

2. Molecular Mechanics: Basic Concepts

Before we discuss molecular mechanics in the context of crystal engineering and intermolecular synthesis, some basic principles involved will be outlined in the following section. For more comprehensive treatments, the reader is referred to several excellent reviews [1,2,3,4] and books [5,6] including the distinguished, 'benchmark', monograph by Burkert and Allinger [7].

2.1 POTENTIAL ENERGY FUNCTIONS AND FORCE FIELDS

Primarily, molecular mechanics, or force-field methods, attempt to formulate the multidimensional potential energy surface relating to all of the internal degrees of freedom in a gas-phase molecule. In order to do so, these methods treat a molecule as a collection of hard spherical atoms connected by harmonic forces; these forces attempt to restore the molecule to a low-energy structure if the molecule is deformed. The restoring forces can be represented by a potential energy function - the force field - which describes the contributions from various structural features to the energy of the molecule as a whole.

A molecule may be considered to have an ideal 'unstrained' configuration in which all of the bond lengths, bond angles and torsion angles, *etc.*, occupy their lowest available energy state. The difference in energy between a given molecular configuration and that of the ideal state is known as the steric energy, E. This energy may be found by the use of a force field, or Westheimer equation [8], where it is expressed as the sum of all the energy contributions from a number of arbitrary structural components, Equation (1).

$$E = \sum E_{stretch} + \sum E_{bend} + \sum E_{torsion} + \sum E_{non\text{-}bond} + \cdots \qquad (1)$$

The components in a force field vary from one molecular-mechanics method to another; the contributing energy functions generally represent the deformation of bond lengths, bond angles and internal rotations, in addition to non-bonded interactions such as van der Waals forces. The individual functions are analogous to the 'classical' equations of motion, and contain constants which are parameterised for each particular force field; ideally, these constants are weighted so that each function gives a balanced contribution to the whole, and so therefore no individual term dominates the calculation. The steric energy

UM00012778
NOVARTIS EXHIBIT 1017
Novartis v. Regents, IPR2023-01346
Page 1524 of 4460

confidence using a force-field
crystal engineering) are far more
Indeed, as the central idea of a
innot be immediately extended to
:s, how can we apply molecular-
gineering? Unfortunately, the
the inherent spatial and positional
k of calculating/predicting crystal

ext of crystal engineering and
will be outlined in the following
:r is referred to several excellent
ished, 'benchmark', monograph by

ORCE FIELDS

ods, attempt to formulate the
f the internal degrees of freedom
ls treat a molecule as a collection
iese forces attempt to restore the
ormed. The restoring forces can
rce field - which describes the
gy of the molecule as a whole.
instrained' configuration in which
tc., occupy their lowest available
olecular configuration and that of
rgy may be found by the use of a
:ssed as the sum of all the energy
onents, Equation (1).

$$\text{and} + \cdots \qquad (1)$$

molecular-mechanics method to
present the deformation of bond
non-bonded interactions such as
ous to the 'classical' equations of
l for each particular force field;
i gives a balanced contribution to
the calculation. The steric energy

is only a measure of the intramolecular strain for a given molecule; it therefore has a physical significance only when used to compare the energy of different molecular geometries with observable physical properties. Furthermore, it is very important to note that the individual component energy functions have no absolute meaning and should not be considered individually.

2.2 THE CONSTRUCTION OF FORCE FIELDS

Many different force fields are now available, and these attempt to reproduce the spectroscopic, thermochemical, or structural data for various sets of chemical compounds, and most are parameterised to calculate energy values corresponding to those of a vibrationally averaged molecule existing in the gas phase at 25 °C. Force fields are usually modified over long periods of time, new functions and types of parameter are incorporated as necessary; this is a result of researchers attempting to extend the predictions of particular methods to include problematical molecules in addition to those for which the method was initially optimised.

The construction of a typical valence force field will now be described. Valence force fields are those, that like MM2 [9] and CHARMm [10], consider all restoring forces to act along, or perpendicular to, covalent bonds [7].

2.3 BOND STRETCHING AND BOND BENDING

The energy of a chemical bond is assumed to be a function of its length: a bond will therefore have a 'natural' length which corresponds to its lowest energy state. Any stretching or compression of the bond will alter its energy, rather like that of a stretched spring, and the energy required to deform the bond by a particular distance may be found by applying Hooke's law. The contribution which bond stretching makes to the steric energy of a molecule is found from the sum of the energy functions pertaining to each individual bond, Equation (2), where k_s is the stretching force constant, and where l_o and l are the 'natural' and deformed bond lengths, respectively.

$$E_s = \sum_l \tfrac{1}{2} k_s (l - l_o)^2 \qquad (2)$$

The deformation of bond angles away from an optimum value may be treated in a similar way; the contribution of bending to the steric energy of a molecule being given by Equation (3), where k_b is the bending force constant, and where θ_o and θ represent a particular bond angle before and after deformation.

$$E_\theta = \sum_\theta \tfrac{1}{2} k_b (\theta - \theta_o)^2 \qquad (3)$$

The value of the force constant k_s is approximately ten times larger than that of k_b; this is a consequence of the fact that, in reality, the distortion of a molecule is manifested mostly by the bending, as opposed to the stretching, of bonds.

UM00012779
NOVARTIS EXHIBIT 1017
Novartis v. Regents, IPR2023-01346
Page 1525 of 4460

When bonds and bond angles are subjected to very large deformations, the potential functions described above may require modification. For example, cubic terms can be included in Equations (2) and (3) in order for them to obey Hooke's law, [11,12] or alternatively, Equations (2) and (3) may be replaced altogether by Morse functions, [13] which give a better approximation to the true potential curve, but are less easy to accommodate in a computational algorithm. Despite this problem, Morse functions are now quite commonly used in Urey-Bradley force fields [14].

2.4 CROSS-TERMS AND TORSIONAL TERMS

When a bond angle is decreasing, the bonds which constitute the angle are lengthened. Valence force fields take this phenomenon into account by 'cross-terms', the most commonly used being for stretch-bend interactions [15,16] which may be expressed by Equation (4), in which atoms i and j are bonded to a common atom, and have a bond angle θ, and the stretch-bend force constant k_{sb} has the effect of altering the bond lengths to suit the angle θ.

$$E_{s_b} = \sum_{\theta} \tfrac{1}{2} k_{sb}(ij) \left(\left(l - l_0\right)_i + \left(l - l_0\right)_j \right) \left(\theta - \theta_0\right) \qquad (4)$$

Some valence force fields also include stretch-stretch and bond angle bend-bend terms [17]. Urey-Bradley force fields [18] avoid the use of cross-terms by including a specific function for 1,3 (*i.e.* (*ij*)) interactions in addition to a term which considers the interactions between all other non-bonded atom pairs in a molecule [14,19].

Many force fields make a distinction between the in-plane and out-of-plane bending of bond angles [20,21], and some force fields make use of an additional torsion-bend term to account for ring puckering in cyclic molecules [12].

The free rotation about a chemical bond may be defined using a torsion (or dihedral) angle ω, Figure 1, where the bond BC is the axis of rotation [4].

The force field sums the energies of rotation over all non-terminal bonds in the molecule, commonly using an expression of the form of Equation (5) [22], in which V_1, V_2, *etc.*, are experimentally derived parameters.

$$E_{\omega} = \sum_{\omega} \tfrac{1}{2} \left[V_1(1+\cos(\omega)) + \tfrac{1}{2} V_2(1-\cos(2\omega)) + \ldots\ldots \right] \qquad (5)$$

The parameters which are employed in the description of torsion angles are probably the most difficult to parameterise, partly because the force constants involved in many torsion angles are considerably smaller than those which determine bond lengths and bond angles. Basically, Equation (5) attempts to describe the effects of different types of steric interactions on the torsional potential of a molecule [23]: Bowen and Allinger [24] ascribe the V_1 term to dipole-dipole and van der Waals interactions, V_2 (geometrically related to p orbitals) to conjugation, and V_3 steric (*i.e.* bonding/nonbonding orbital) interactions. The value of V_1 is such that the rotation about a single bond requires appreciably less energy than either bond stretching or bending. The Fourier series in the above expression is

UM00012780
NOVARTIS EXHIBIT 1017
Novartis v. Regents, IPR2023-01346
Page 1526 of 4460

arge deformations, the potential
: example, cubic terms can be
obey Hooke's law, [11,12] or
ether by Morse functions, [13]
l curve, but are less easy to
oblem, Morse functions are now

itute the angle are lengthened.
ross-terms', the most commonly
/ be expressed by Equation (4),
d have a bond angle θ, and the
ond lengths to suit the angle θ.

(4)

etch and bond angle bend-bend
of cross-terms by including a
to a term which considers the
nolecule [14,19].
-plane and out-of-plane bending
in additional torsion-bend term

e defined using a torsion (or
of rotation [4].
r all non-terminal bonds in the
ation (5) [22], in which V_1, V_2,

(5)

cription of torsion angles are
the force constants involved in
ch determine bond lengths and
he effects of different types of
23]: Bowen and Allinger [24]
tions, V_2 (geometrically related
nbonding orbital) interactions.
equires appreciably less energy
ies in the above expression is

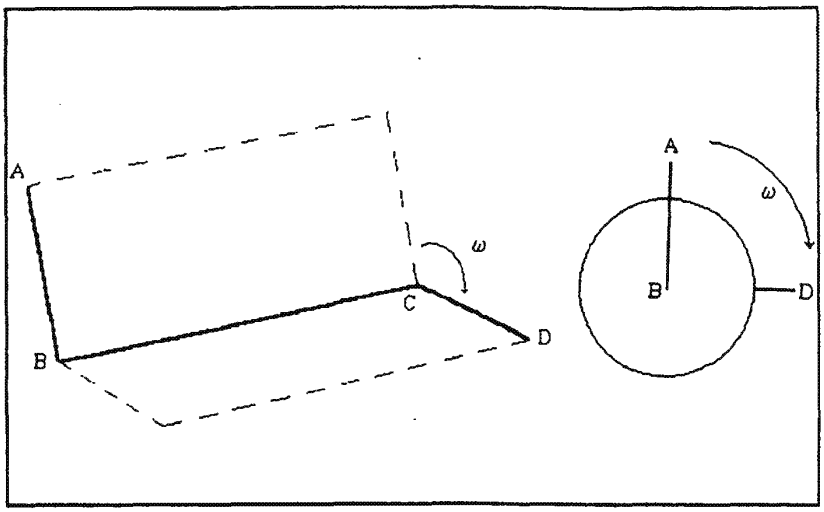


Figure 1 A torsion (or dihedral) angle.

generally truncated at the third term for application to most organic molecules, although some systems are adequately described using a single term function and the single parameter V_3. Some force fields also include an additional term to account for the effects of improper torsions. Such a function maintains the planarity of some molecules, and aids the accurate representation of the potential energy surface in the region adjacent to a minimum.

2.5 NON-BONDED INTERACTIONS

The component of a conventional force-field which is most relevant to research in, and development of, crystal engineering, pertains to the way in which intermolecular, non-covalent, interactions are described. A variety of functions have been used to determine the contribution that van der Waals interactions between non-bonded atoms make to the steric energy of a molecule; many of the earlier descriptions have been extensively reviewed elsewhere [25,26]. The total interactive potential between two non-bonded atoms separated by a distance r, is the sum of the energy contributions from an attractive term and a repulsive term. One commonly used function is the Lennard-Jones '6-12' potential, Equation (6),where the parameter ε defines the depth of the potential well, and r_0 corresponds to the lowest energy internuclear distance, usually defined as the sum of van der Waals radii of the two atoms.

UM00012781
NOVARTIS EXHIBIT 1017
Novartis v. Regents, IPR2023-01346
Page 1527 of 4460

$$E_V = \sum \varepsilon \left[\left(\frac{r_0}{r} \right)^{12} - 2 \left(\frac{r_0}{r} \right)^{6} \right] \qquad (6)$$

In this expression, the attractive potential is inversely proportional to the 6th power of their internuclear distance, and the repulsive potential inversely proportional to the 12th power. A 12th power repulsive term can become too steep at wide atomic separation, and 10th or 9th power terms are often used instead. The Allinger force fields incorporate a modified Buckingham-potential function, in which the repulsive term is exponential, this gives an improved representation of the effects of repulsion between electron clouds, Equation (7) [27].

$$E_V = \sum \varepsilon \left[- c_1 \left(\frac{r_0}{r} \right)^{6} + c_2 \exp \left(- c_3 \frac{r}{r_0} \right) \right] \qquad (7)$$

Here, the values c_1, c_2 and c_3 are identical for all atoms, whereas the parameters ε and r_0 depend upon the atom types involved.

The functions described above can only consider interactions between 1,4 pairs of non-bonded atoms. In valence force fields, the 1,3 non-bonded interactions are implicitly described by the $E_{stretch\text{-}bend}$ function. Additional terms may be included in some force fields to account for electrostatic interactions and hydrogen bonding, at both the inter- and intramolecular level. All parameters for non-bonded interactions rely on the interpolation of data derived from intermolecular forces into the description of intramolecular phenomena, they also require that all interactions are pairwise additive, regardless of the effects of the surrounding molecular environment.

3. Molecular Mechanics in Crystal Engineering: Any common ground?

A brief search of *Chemical Abstracts* for the period 1991-1996 shows that more than 3000 papers have been published where the phrase "molecular mechanics" has been present either in the title, or as a designated key word. Without a doubt, the vast majority of these papers have dealt with aspects of molecular geometries and/or properties. However, in a recent issue of *Chemical Reviews* (**1993**, *93*, No. 7), dedicated to molecular mechanics and modelling, many contributions describing calculations and simulations of chemical and physical interactions/behaviour beyond the molecule have been included. For example, articles describing interactions between molecules and surfaces [28], between surfaces and clusters [29], modelling of peptides in solution [30], as well as an illustration of a molecular mechanics approach to organic synthesis [31], were presented. This may indicate that although the focus has not shifted away from studies of isolated molecules, there is a growing interest in the behaviour of molecules within a 'real' physical medium, either liquid, or solid. Nevertheless, the editorial in the same issue emphasised the fact that "molecular

UM00012782
NOVARTIS EXHIBIT 1017
Novartis v. Regents, IPR2023-01346
Page 1528 of 4460

modelling has developed into a major tool for the understanding of molecules". This statement serves to underline the fact that molecular mechanics has primarily been driven by interest in molecular interactions and behaviour.

On the other hand, a thematic issue of *Chemistry of Materials* (1994, *6*, No. 8) devoted to structure and chemistry of the organic solid state, did not contain any contributions describing the use of molecular mechanics calculation in the context of crystal chemistry, molecular recognition or supramolecular strategies. It would seem, therefore, that theoreticians are moving their targets into the realm of crystal engineering and molecular recognition whereas many 'crystal engineers' have yet to embrace molecular mechanics as a typical weapon in their research armour.

Consequently, it seems as if we have to broaden our definition of what molecular mechanics is, or at least stress the importance of weaker forces for crystal packing and other 3-D phenomena, if we are to develop the common ground between classical modelling and crystal engineering. Clearly, we need to focus on the way in which intermolecular interactions are described and interpreted within a force-field.

This is not to say that classical modelling has not made important contributions to an improved understanding of crystal packing. For example, molecular mechanics methods have been used extensively in conjunction with Monte Carlo algorithms in the prediction of possible crystal structures of many organic compounds [32,33] and of hitherto undiscovered (but energetically feasible) polymorphs of existing compounds [34].

3.1 CRYSTAL PACKING: INTRODUCTION

Kitaigorodsky [35] has, arguably, been one of the most influential contributors to the understanding of crystal packing, and his principles of close packing neatly summarise the structural consequences of the balance between a variety of intermolecular forces within a crystalline lattice. Kitaigorodsky pioneered the idea that molecules strive to pack with maximum density (thus, minimising the free, 'empty', volume) and he was also able to formulate these observations within a mathematical framework. Using this approach, Kitaigorodsky made important contributions, and asked decisive questions about *e.g.* lattice dynamics, static crystals, imperfect crystals and phase transformations.

Other general guide lines (based upon extensive structural information) have also been suggested as a means for rationalising and possibly predicting crystal packing. For example, Donohue suggested that all acidic protons in a structure will participate in a hydrogen bond [36] and Etter made this idea more specific by stating that the best hydrogen-bond donors will interact with the best hydrogen-bond acceptors [37]. Similarly, observations regarding preferential packing of aromatic systems have lead to imaginative expressions like, 'herring-bone motif', 'sandwich structure', and 'honey-comb packing'. These general observations and 'guide-lines' are clearly very valuable when analysing a crystal structure, but if we want to make specific energy calculations, or predict likely packing motifs, we need to describe these intermolecular forces in a 'language' which can be encoded into a computer algorithm.

The principles of close packing have also provided an important backdrop for extensive discussions about possible correlation between crystallographic space group (frequency and type) and molecular shape and point group symmetry. This topic has

UM00012783
NOVARTIS EXHIBIT 1017
Novartis v. Regents, IPR2023-01346
Page 1529 of 4460

recently been discussed extensively by Brock and Dunitz, and they have been able to rationalise why certain molecules tend to show a pronounced preference for specific space groups and symmetry elements [38].

3.2 ATOM-ATOM POTENTIAL METHODS

The most commonly used methods for explaining and predicting crystal packing are energy-based techniques, often referred to as atom-atom potential methods. Much of the early development and validation work was carried out by Kitaigorodski [35] and Williams [39], but the general principles have been expanded upon and applied to a wide range of molecular and ionic solids during the last twenty years. For example, lattice energies and packing of carboxylic acids [40,41,42] and amides have been studied extensively [43].

Briefly, in the atom-atom potential approach the interaction energy of several polyatomic molecules/ions, is described in terms of a collection of two-centre analytical functions. Central to such an approach is the description of intermolecular interactions. These forces are commonly described using Lennard-Jones or Buckingham potentials (as outlined in Section 2.5). In addition (similar to most force-fields) an explicit electrostatic term is also introduced ($q_a q_b r_{ab}^{-1}$), despite the slow convergence of Coulombic lattice summations. It is also worth noting that, commonly, intramolecular interactions are neglected and that individual molecules are treated as rigid bodies.

Fitting of the parameters in the model potential can either be carried out against a potential-energy hypersurface calculated by some quantum-mechanical technique or, alternatively, they may be fitted against experimental crystallographic and/or thermodynamic data. Either way, the aim is to obtain the parameters of the potential which best reproduce the crystal properties of a solid material. In this way, force-fields have been developed for studying crystal packing and intermolecular forces in many 'families' of compounds *e.g.* carboxylic acids, amides, alcohols, and hydrocarbons, *etc.* A few examples of other families of compounds and individual molecules solids which have been studied in this way include polythienyls [44] and *N*-phenyl phthalimide [45].

Initially, the usefulness and quality of a force-field should always be measured by its ability to accurately describe the packing of a series of known structures. This is usually done by relaxing the structure, thus, allowing the potential model to describe the magnitude and direction of all the intermolecular interactions in the crystal. The new lattice parameters can then be compared with the starting point, and this will provide a measure of how much the theoretical description of non-bonded forces differs from the nature and effects of the 'true' intermolecular interactions.

3.3 DESCRIPTION OF CHARGE

Although atom-atom techniques have been very successful when describing the packing of hydrocarbons and other molecules with a relatively symmetric charge distribution, polar molecules within a crystalline lattice usually presents a much more complicated problem. Since electrostatic forces play a major role in determining the lattice energy (which is a measure of the balance between attractive and repulsive interactions) of a crystalline solid composed of polar molecules, it is essential that both the magnitude and the inherent

UM00012784
NOVARTIS EXHIBIT 1017
Novartis v. Regents, IPR2023-01346
Page 1530 of 4460

anisotropy of the charge distribution is described accurately [46]. For example, Leiserowitz and co-workers [47] used charges obtained from experimental density distributions (represented by higher-order moments) in a systematic study of the electrostatic contribution to the lattice energies in carboxylic acids. Often, an improved description of the charge distribution, obtained by replacing fractional point charges with more realistic distributed multipole model, makes a considerable difference to the outcome of the calculation [48], and it is clear that such models are necessary for an improved representation of weaker, but directional, intermolecular forces [49]. Information about how the asymmetric 'charge-cloud' is arranged around a polar molecule or moiety is available through an evaluation of the distributed multipole representation of an *ab initio* wavefunction for the molecule of interest. By using multipoles (*e.g.* dipoles and higher-order moments), it is possible to obtain a more realistic description of important molecular features like stereochemically active lone-pairs, which are likely to have significant influence on the resulting packing of individual components. For an in-depth discussion of multipole representations of multipole charges, see the recent review by Price [50].

Once the charge distribution is in place, the overall energy (as calculated using standard atom-atom potentials) can be minimised with respect to the unit cell dimensions. Commonly, the unit cell parameters are allowed to move freely, although the calculation can be restricted by keeping the space group fixed through the simulation.

3.4 EXPERIMENTAL DATA AND TOPOLOGICAL METHODS

A very promising approach to solving the structure of a compound which does not yield crystals suitable for single crystal X-ray diffraction work, involves the combination of molecular modelling and high-resolution powder diffraction data [51,52]. The starting point for such an approach is an optimised molecular geometry, which is then positioned within a specific unit cell, the values of which can be derived by indexing the powder diffraction pattern. Alternatively, it is possible to generate 'clusters' of molecules where the assembly is generated by applying the most commonly occurring symmetry operators to a starting molecule. Conventional atom-atom techniques can produce a number of possible packing arrangements which are then further refined using Rietveld methods.

The most widely used methods for predicting crystal packing are energy based, but other approaches have appeared which rely on molecular size, shape and topology have been successfully applied to studying the packing of molecular solids, notably hydrocarbons. Although these methods can hardly be classified as 'molecular mechanics', they are based upon a systematic analysis of structural data, in much the same way as a force field is parameterised. Furthermore, they have facilitated an understanding of possible correlations between molecular and crystal structure for certain compounds.

For example, Desiraju and Gavezzotti have shown that it is possible to make informed estimates ('predictions') about the crystal structure of fused hydrocarbons based upon the carbon-hydrogen ratio in each molecule [53].

UM00012785
NOVARTIS EXHIBIT 1017
Novartis v. Regents, IPR2023-01346
Page 1531 of 4460

3.5 *CODICIL*

Finally, it should be re-emphasised that there are several important questions in this area which are currently being addressed but where the answers still prove to be elusive. For example, we are still unable to provide a prediction of thermal properties, *e.g.* melting point, for a crystalline material, even if we have access to complete single-crystal data! We fare equally poorly when we want to predict if a material is going to be symmetric or non-centrosymmetric, a question which is of fundamental importance for the resulting properties. However, it is worth pointing out that recent work by Whitesell, Davis and co-workers [54] on correlations between molecular dipole moment and crystal structure, seems to have laid to rest the 'myth' that large molecular dipole moments inherently lead to centrosymmetric structures.

We have also little insight into when, and why, a certain material will incorporate solvent molecules into the lattice, and how many units will appear in the asymmetric unit cell.

Despite recent advances in the development of atom-atom potential methods, much work is still required if we are to obtain a better *a priori* understanding of crystal packing and of the properties associated with new, or unknown, crystalline material. However, it is equally obvious that it is imperative that we continue to pursue these goals if we are to gain control over the design and synthesis of new structural motifs and, subsequently, of new materials with improved physical properties.

Acknowledgements

Financial support from The Queen's University of Belfast, DRA Fort Halstead, and Kansas State University, is gratefully acknowledged.

References

1. Williams, J.E., Stang, P.J. and Schleyer, P.v.R. (1968) Physical organic chemistry: Quantitative conformational analysis; calculation methods, *Ann. Rev. Phys. Chem.*, **19**, 531-558.
2. Allinger, N.L. (1976) Calculation of molecular structure and energy by force-field methods, *Adv. Phys. Org. Chem.*, **13**, 1-82.
3. Ermer, O. (1976) Calculation of molecular properties using force fields. Applications in organic chemistry, *Struct. Bonding (Berlin)*, **27**, 161-202.
4. (a) Boyd, D.B. and Lipkowitz, K.B. (1982) Molecular mechanics: The method and its underlying philosophy, *J. Chem. Ed.*, **59**, 269. (b) Cox, P.J. (1982) Molecular mechanics - Illustrations of its applications, *J. Chem. Ed.*, **59**, 275.
5. Hinchliffe, A. (1994) *Modelling Molecular Structures*, Wiley, Chichester.
6. Comba, P. and. Hambley, T.W. (1995) *Molecular Modeling of Inorganic Compounds*, VCH, Weinheim.

UM00012786
NOVARTIS EXHIBIT 1017
Novartis v. Regents, IPR2023-01346
Page 1532 of 4460

7. Burkert, U. and Allinger, N.L. (1982), *Molecular mechanics, ACS Monograph 177*, American Chemical Society, Washington D.C.

8. (a) Westheimer, F.H. and Mayer, J.E. (1946) The theory of the racemization of optically active derivatives of biphenyl, *J. Chem. Phys.*, **14**, 733-738.
(b) Westheimer, F.H. (1947) A calculation of the energy of activation for the racemization of 2,2'-dibromo-4,4'-dicarboxydiphenyl, *J. Chem. Phys.*, **15**, 252-260.
(c) Reiger, M. and Westheimer, F.H. (1950) The calculation and determination of the buttressing effect for the racemization of 2,2',3,3'-tetraiodo-5,5'-dicarboxybiphenyl, *J. Am. Chem. Soc.*, **72**, 19-26.

9. Allinger, N.L., Yuh, Y.H., and Li, J.-H. (1989) Molecular Mechanics: The MM3 force field for hydrocarbons. 1. *J. Am. Chem. Soc.*, **111**, 8551-8566.

10. Brooks, R., Bruccoleri, R.E., Olafson, B.D., States, D.J., Swaminathan, S., and Karplus, M. (1983) CHARMm - a program for macromolecular energy minimizations and dynamics calculations, *J. Comput. Chem.*, **4**, 187-217.

11. Engler, E.M., Andose, J.A., and Schleyer, P.v.R. (1973) Critical evaluation of molecular mechanics, *J. Am. Chem. Soc.*, **95**, 8005-8025.

12. Wertz, D.H. and Allinger, N.L. (1974), *Tetrahedron*, **30**, 1579.

13. Hagler, A.T., Stern, P.S., Lifson, S., and Ariel, S. (1979) Urey-Bradley force field, valence force field, and ab initio study of intramolecular forces in tri-*tert*-butylmethane and isobutane, *J. Am. Chem. Soc.*, **101**, 813-819.

14. Fitzwater, S. and Bartell, L.S. (1976) Representation of molecular force fields. 2. A modified Urey-Bradley field and an examination of Allinger's gauche hydrogen hypothesis, *J. Am. Chem. Soc.*, **98**, 5107-5119.

15. Allinger, N.L., Tribble, M.T., Miller, M.T., and Wertz, D.H. (1971) Conformational analysis. LXIX. An improved force field for the calculation of the structures and energies of hydrocarbons, *J. Am. Chem. Soc.*, **93**, 1637-1648.

16. Ermer, O. (1974) *Tetrahedron*, **30**, 3103-3105.

17. Ermer, O. and Lifson, S. (1973) Consistent force field calculations. III. Conformations and heats of hydrogenation of nonconjugated olefins, *J. Am. Chem. Soc.*, **95**, 4121-4132.

18. Urey, H.C. and Bradley, C.A. (1931) *Phys. Rev.*, **38**, 1969.

19. Jacob, E.J., Thompson, H.B., and Bartell, L.S. (1967) Influence of nonbonded interactions on molecular geometry and energy: Calculations for hydrocarbons based on Urey-Bradley field, *J. Chem. Phys.*, **47**, 3736-3753.

20. Allinger, N.L., Tribble, M.T., and Miller, M.A. (1972) *Tetrahedron*, **28**, 1173-1202.

21. Winkler, F.K. and Dunitz, J.D. (1971) *J. Mol. Biol.*, **59**, 169-182.

UM00012787
NOVARTIS EXHIBIT 1017
Novartis v. Regents, IPR2023-01346
Page 1533 of 4460

22. Allinger, N.L. (1977) Conformational analysis. 130. MM2. A hydrocarbon force field utilizing V_1 and V_2 torsional terms. *J. Am. Chem. Soc.*, **99**, 8127-8134.

23. Radom, L., Hehre, W.J., and Pople, J.A. (1972) *J. Am. Chem. Soc.*, **94**, 2371-2381.

24. Bowen, J.P. and Allinger, N.L. (1991) in Lipkowitz and Boyd (eds.) *Reviews in computational chemistry*, Vol 2, VCH, New York, 81.

25. Fitts, D.D. (1966) Statistical mechanics: A study of intermolecular forces, *Ann. Rev. Phys. Chem.*, **17**, 59-80.

26. Buckingham, A.D. and Utting, B.D. (1970) Intermolecular forces, *Ann. Rev. Phys. Chem.*, **21**, 287-316.

27. (a) Hill, T.L. (1946) On steric effects, *J. Chem. Phys.*, **14**, 465. (b) Hill, T.L. (1948) Steric effects. I. Van der Waals potential energy curves, *J. Chem. Phys.*, **16**, 399-404.

28. Steele, W. (1993) Molecular interactions for physical adsorption, *Chem. Rev.*, **93**, 2355-2378.

29. Berry, R.S. (1993) Potential surfaces and dynamics: What clusters tell us, *Chem. Rev.* **93**, 2379-2394.

30. Brooks, C.L. and Case, D.A. (1993) Simulations of peptide conformational dynamics and thermodynamics, *Chem. Rev.* **93**, 2487-2502.

31. Lipkowitz K.B. and Peterson, M.A. (1993) Molecular mechanics in organic synthesis, *Chem. Rev.* **93**, 2463-2486.

32. (a) Perlstein, J. (1992) Molecular Self-Assemblies: Monte Carlo Predictions for the Structure of the One-Dimensional Translation Aggregate, *J. Am. Chem. Soc.* **114**, 1955-1963. (b) Perlstein, J. (1994) Molecular Self-Assemblies. 4 Using Kitaigorodskii's Aufbau Principle for Quantitatively Predicting the Packing Geometry of Semiflexible Organic Molecules in Translation Monolayer Aggregates, *J. Am. Chem. Soc.* **116**, 11420-11432.

33. Gdanitz, R.J., (1992) Prediction of molecular crystal structures by Monte Carlo simulated annealing without reference to diffraction data, *Chem. Phys. Letts.*, **190**, 391-396.

34. Karfunkel, H.R. and Gdanitz, R.J. (1992) *Ab initio* prediction of possible crystal structures for general organic molecules, *J. Comp. Chem.* **13**, 1171-1183.

35. (a) Kitaigorodsky, A.I.; *Organic Chemical Crystallography*, 1961, Consultants Bureau, New York; (b) Kitaigorodsky, A.I., *Molecular Crystals and Molecules*, 1973, Academic Press, New York.

36. Donohue, J. (1952) The hydrogen-bond in organic crystals, *J. Phys. Chem.*, **56**, 502-510.

37. Etter, M
compou

38. Brock, C
Mater.,

39. (a) Wi
crystallin
D.E. and

40. Lifson, S
Intermol
and the

41. Michopo
the cryst
72, 899-

42. Hagler, A
Proteins.
from Am

43. Momany
interacti
nonbond
potential

44. Gavezzo
polythier

45. Kendrick
mechanic
13, 408-

46. Willock,
realistic
Mol. Cry

47. Berkovit
of the
Experim

48. Wheatley
applied t

49. Willock,
of molec
Comp. C

50. Price, S.L
complex

UM00012788
NOVARTIS EXHIBIT 1017
Novartis v. Regents, IPR2023-01346
Page 1534 of 4460

.30. MM2. A hydrocarbon force
'hem. Soc., 99, 8127-8134.

) J. Am. Chem. Soc., 94, 2371-

witz and Boyd (eds.) *Reviews in*
'rk, 81.

ly of intermolecular forces, *Ann.*

nolecular forces, *Ann. Rev. Phys.*

n. Phys., 14, 465. (b) Hill, T.L.
nergy curves, *J. Chem. Phys.*, 16,

sical adsorption, *Chem. Rev.*, 93,

iics: What clusters tell us, *Chem.*

tions of peptide conformational
2487-2502.

Molecular mechanics in organic

lies: Monte Carlo Predictions for
on Aggregate, *J. Am. Chem. Soc.*
ecular Self-Assemblies. 4 Using
tatively Predicting the Packing
iles in Translation Monolayer
132.

crystal structures by Monte Carlo
ion data, *Chem. Phys. Letts.*, 190,

nitio prediction of possible crystal
mp. Chem. 13, 1171-1183.

ystallography, 1961, Consultants
olecular Crystals and Molecules,

anic crystals, *J. Phys. Chem.*, 56,

37. Etter, M.C. (1990) Encoding and decoding hydrogen-bond patterns of organic compounds, *Acc. Chem. Res.*, *23*, 120-126.

38. Brock, C.P. and Dunitz, J.D. (1994) Towards a grammar of crystal packing, *Chem. Mater.*, **6**, 1118-1127.

39. (a) Williams, D.E. (1967) Nonbonded potential parameters derived from crystalline aromatic hydrocarbons, *J. Chem. Phys.* **45**, 3770-3778. (b) Williams, D.E. and Starr, T.L. (1977) *Comput. Chem.* **1**, 173.

40. Lifson, S., Hagler, A.T., and Dauber, P. (1979) Consistent Force Field Studies of Intermolecular Forces in Hydrogen-Bonded Crystals 1. Carboxylic Acids, Amides, and the C=O···H Hydrogen bonds, *J. Am. Chem. Soc.* **101**, 5111-5121.

41. Michopoulos, Y., Adam, C.D., and Leslie, M. (1991) Atom-atom potentials and the crystal structure simulation of long linear chain carboxylic acids, *Mol. Phys.*, **72**, 899-909.

42. Hagler, A.T., Huler, E., and Lifson, S. (1973) Energy Functions for Peptides and Proteins. I. Derivation of a Consistent Force Field Including the Hydrogen Bond from Amide Crystals, *J. Am. Chem. Soc.* **96**, 5319-5327.

43. Momany, F.A., McGuire, R.F., Burgess, A.W., and Scheraga, H.A. (1975) Energy interactions in polypeptides. VII. Geometric parameters, partial atomic charges, nonbonded interactions, hydrogen bond interactions, and intrinsic torsional potentials for the naturally occurring amino acids, *J. Phys. Chem.* **79**, 2361-2381.

44. Gavezzotti, A. and Filippini, G. (1991) Crystal packing and lattice energies of polythienyls: calculations and predictions, *Synthetic Metals*, **40**, 257-266.

45. Kendrick, J., Robson, E., and McIntyre, S. (1992) *Ab initio* and molecular mechanics study of *N*-phenyl phthalimide and its crystal structure, *J. Comp. Chem.*, **13**, 408-413.

46. Willock, D.J., Leslie, M., Price, S.L., and Catlow, C.R.A. (1993) The need for realistic electrostatic models to predict the crystal structure of N.L.O. molecules, *Mol. Cryst. Liq. Cryst.* **235**, 217-224.

47. Berkovitch-Yellin, Z. and Leiserowitz, L. (1982) Atom-Atom Potential Analysis of the Packing Characteristics of Carboxylic Acids. A study Based on Experimental Electron Density Distributions, *J. Am. Chem. Soc.* **104**, 4052-4064.

48. Wheatley, R.J. and Price, S.L. (1990) A systematic intermolecular potential method applied to chlorine, *Molec. Phys.*, **71**, 1381-1404.

49. Willock, D.J., Price, S.L., Leslie, M., and Catlow, C.R.A. (1995) The relaxation of molecular crystal structures using a distributed multipole electrostatic model, *J. Comp. Chem.*, **16**, 628-647.

50. Price, S.L., (1996) Applications of realistic electrostatic modelling to molecules in complexes, solids and proteins, *J. Chem. Soc., Faraday Trans.*, **92**, 2997-3008.

UM00012789
NOVARTIS EXHIBIT 1017
Novartis v. Regents, IPR2023-01346
Page 1535 of 4460

51. Gavezzotti, A. and Filippini, G. (1996) Computer prediction of organic crystal structures using partial X-ray diffraction data, *J. Am. Chem. Soc.*, **118**, 7153-7157.

52. Fagan, P.G., Roberts, K.J., Docherty, R., Chorlton, A.P., Jones, W., and Potts, G.D. (1993) An *ab initio* approach to crystal structure determination using high resolution powder diffraction and computational chemistry techniques: Application to 6,13-dichlorotriphendioxazine, Daresbury Laboratory Report *DL/SCI/P896E*.

53. Desiraju, G.R., and Gavezzotti, A., (1989) From molecular to crystal structure: Polynuclear aromatic hydrocarbons, *J. Chem. Soc., Chem. Commun.*, 621-623.

54. Whitesell, J.K., Davis, R.E., Saunders, R.J., Wilson, R.J., and Feagins, J.P., (1991) Influence of molecular dipole interactions in the solid state, *J. Am. Chem. Soc.* **13**, 3267-3270.

UM00012790
NOVARTIS EXHIBIT 1017
Novartis v. Regents, IPR2023-01346
Page 1536 of 4460

This Page is Inserted by IFW Indexing and Scanning Operations and is not part of the Official Record

BEST AVAILABLE IMAGES

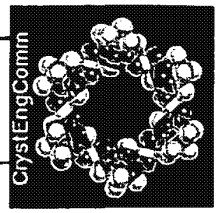
Defective images within this document are accurate representations of the original documents submitted by the applicant.

Defects in the images include but are not limited to the items checked:

- ☐ BLACK BORDERS
- ☐ IMAGE CUT OFF AT TOP, BOTTOM OR SIDES
- ☐ FADED TEXT OR DRAWING
- ☐ BLURRED OR ILLEGIBLE TEXT OR DRAWING
- ☐ SKEWED/SLANTED IMAGES
- ☐ COLOR OR BLACK AND WHITE PHOTOGRAPHS
- ☐ GRAY SCALE DOCUMENTS
- ☐ LINES OR MARKS ON ORIGINAL DOCUMENT
- ☐ REFERENCE(S) OR EXHIBIT(S) SUBMITTED ARE POOR QUALITY
- ☐ OTHER: _____

IMAGES ARE BEST AVAILABLE COPY.
As rescanning these documents will not correct the image problems checked, please do not report these problems to the IFW Image Problem Mailbox.

New building blocks for crystal engineering. Syntheses and crystal structures of oxime-substituted pyridines



Paper

Christer B. Aakeröy, Alicia M. Beatty and Destin S. Leinen

Department of Chemistry, Kansas State University, Manhattan, KS, 66506, USA. E-mail: aakeroy@ksu.edu

Received 26th July 2000, Accepted 5th September 2000
Published on the Web 18th September 2000

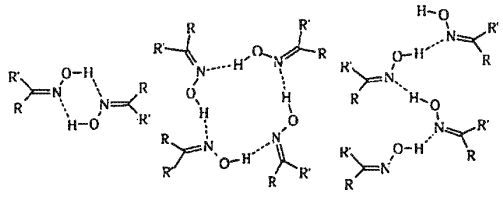
The syntheses and crystal structures of a family of oxime-substituted pyridine ligands [py-C(R)NOH, where R = H, Me, Ph, or NH_2] are presented. The compounds are all prepared in good yields by allowing a suitably substituted pyridine to react with hydroxylamine. Their solid-state structures show that the dominating hydrogen bond, a head-to-tail O–H···N interaction between the oxime O–H moiety and the pyridine nitrogen atom, is present in each of the seven reported cases. This intermolecular interaction generates infinite chains that are crosslinked into 2D or 3D assemblies by weaker C–H···N or C–H···O hydrogen bonds.

Introduction

The ability to predict and control the assembly of molecules and complex ions into extended ordered networks is an important goal in crystal engineering. Even though there are many inherent difficulties with using comparatively weak forces as primary synthetic tools, considerable progress has been made during the last decade.[1] In this context, the selectivity and directionality of the hydrogen bond have been instrumental in the preparation of distinctive structural aggregates,[2] and the use of hydrogen bonding as a steering force has emerged as the most important strategy in crystal engineering.[3] Despite recent advances, detailed control over the supramolecular assembly of molecules remains an elusive goal, and much more work is required to increase the choice of reliable building blocks of extended architectures held together by non-covalent forces.[4]

The oxime functionality is well known in organic synthesis,[5] analytical chemistry,[6] and coordination chemistry,[7–10] yet it has remained relatively unexplored as an intermolecular connector in crystal engineering.[11] However, recent work has shown how oxime pyridine derivatives can be utilized in the assembly of a variety of coordination complexes into extended networks.[12,13] By itself, the oxime moiety can, in the absence of other hydrogen bond donors/acceptors, generate several low-dimensional networks through hydrogen bonds. Adjacent moieties can form a head-to-head $R_2^2(6)$ motif (resulting in discrete dimers), or a catemeric motif that can lead to either discrete multi-molecular rings or infinite chains, Scheme 1.

From a crystal engineering perspective, the oxime moiety could be particularly appealing since it is electronically and sterically 'tunable'; *R* and *R'* can be modified to include a wide range of electron donors/acceptors or 'inert' spacers, and these functional groups are accessible through well-known synthetic methods.[14]



Scheme 1 Possible hydrogen bond motifs with oxime functionalities.

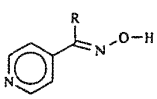
If the oxime functionality is attached to a moiety that can act as coordinating site for a metal ion, then a potential 'bridge' between coordination complexes and supramolecular assembly has been constructed, Scheme 2.

Previous data demonstrate that the oxime functionality does enable the assembly of silver(I) ions *via* the dimeric head-to-head interaction to infinite silver(I) chains that are further propagated into 2D sheets *via* C–H···O hydrogen bonds, Fig. 1.

The counter-ions are positioned between the cationic layers, and participate in weaker hydrogen bonds to the layer above and below. Structures of this type demonstrate that supramolecular synthesis using the oxime functionality can provide predictable structural arrangements where coordination complexes are directed into ordered networks by relatively weak forces working in concert. As part of this process, it is necessary to (i) synthesize and characterize a range of new ligands and (ii) to determine their solid-state behavior and hydrogen bond patterns in the absence of metal-ions. In this paper we present the syntheses of five oxime-substituted pyridine ligands, and the crystal structures of seven such compounds.

Experimental

Syn-2-aldoximepyridine, **1**, and 3-aldoximepyridine, **2**, and all starting materials were purchased from Aldrich and used as received without further purification. Melting points were determined using a Fisher-Johns Mel-Temp melting point apparatus and are uncorrected. ^{1}H NMR spectra were recorded on a Varian 400 MHz spectrometer. ^{13}C NMR spectra were recorded on a Varian 200 MHz spectrometer.



Scheme 2 Generic oxime-substituted pyridine ligand for crystal engineering of coordination complexes.

DOI: 10.1039/b006043g

This journal is © The Royal Society of Chemistry

UM00012792
NOVARTIS EXHIBIT 1017
Novartis v. Regents, IPR2023-01346
Page 1538 of 4460

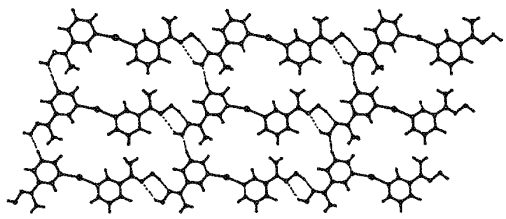


Fig. 1 Infinite cationic sheet in di(3-acetyloximepyridine)silver(I) hexafluorophosphate.

Crystallization of syn-2-aldoxime, 1, and 3-aldoximepyridine, 2

Slow evaporation of saturated solutions of **1** in 95% ethanol and **2** in absolute ethanol produced colorless rods and colorless needles, respectively, suitable for X-ray diffraction.

Synthesis of 3-acetyloximepyridine, 3

3-Acetylpyridine (4.00 g, 3.30 mmol) was dissolved in ethanol (30 ml) with stirring. $NH_2OH{\cdot}HCl$ (3.44 g, 4.95 mmol) in 30 ml distilled water and Na_2CO_3 (2.62 g, 24.8 mmol) in 50 ml distilled water were added to the ethanolic 3-acetylpyridine solution. The mixture was heated under reflux for 48 h. The resulting solution was concentrated under reduced pressure, producing a white precipitate. The vessel was cooled in an ice bath, and a white solid was collected *via* vacuum filtration. The precipitate was washed with small portions of cold water, and dried with an aspirator. Yield: 3.42 g (76%). Mp 118–120 °C. ^{1}H NMR: δ_H (400 MHz; DMSO-d_6) 2.15(3H, s), 7.37–7.40(1H, dd), 7.97–7.99(1H, d), 8.52–8.53(1H, d), 8.81(1H, s) and 11.45(1H, s). ^{13}C NMR: δ_C (200 MHz; DMSO-d_6) 11.4, 123.4, 132.4, 132.8, 146.5, 149.3 and 151.0. Colorless, irregular prisms suitable for X-ray diffraction were grown from a saturated solution of **3** in methylene chloride.

Synthesis of 4-acetyloximepyridine, 4

4-Acetylpyridine (4.00 g, 3.30 mmol) was dissolved in ethanol (30 ml) with stirring. $NH_2OH{\cdot}HCl$ (3.44 g, 4.95 mmol) in 30 ml distilled water and Na_2CO_3 (2.62 g, 24.8 mmol) in 50 ml distilled water were added to the ethanolic 4-acetylpyridine solution. The mixture was heated under reflux for 48 h. The resulting solution was concentrated under reduced pressure, producing a white precipitate. The vessel was cooled in an ice bath, and a white solid was collected *via* vacuum filtration. The precipitate was washed with small portions of cold water, and dried with an aspirator. Yield: 3.92 g (87%). Mp 157–158 °C. ^{1}H NMR: δ_H (400 MHz; DMSO-d_6) 2.13(3H, s), 7.57–7.58(2H, d), 8.54–8.56(2H, d) and 11.68(1H, s). ^{13}C NMR: δ_C (200 MHz; DMSO-d_6) 11.0, 119.8, 143.8, 149.7 and 151.4. Colorless, irregular prisms suitable for X-ray diffraction were grown from a saturated solution of **4** in methylene chloride.

Synthesis of 4-amidoximepyridine, 5

4-Cyanopyridine (2.00 g, 19.2 mmol) was dissolved in ethanol (20 ml) with stirring. $NH_2OH{\cdot}HCl$ (1.34 g, 19.2 mmol) in 10 ml distilled water and Na_2CO_3 (1.02 g, 9.61 mmol) in 25 ml distilled water were added to the ethanolic 4-cyanopyridine solution. The mixture was stirred overnight. The resulting brown solution was concentrated under reduced pressure, producing an off-white precipitate. The vessel was cooled in an ice bath, and an off-white precipitate was collected *via* vacuum filtration. The solid was washed with small portions of cold water, dried with an aspirator, and recrystallized from ethanol to yield off-white crystals. Yield: 1.41 g (54%). Mp 201–205 °C. ^{1}H NMR: δ_H (400 MHz; DMSO-d_6) 5.98(2H, s), 7.61–7.62(2H, d), 8.54–8.55(2H, d) and 10.04(1H, s). ^{13}C NMR: δ_C (200 MHz; DMSO-d_6) 119.5, 140.4, 148.7 and 149.5. Colorless prisms suitable for X-ray diffraction were grown from a saturated solution of **5** in absolute ethanol.

Synthesis of 4-benzoyloximepyridine, 6

4-Benzoylpyridine (4.00 g, 2.18 mmol) was dissolved in ethanol (40 ml) with stirring. $NH_2OH{\cdot}HCl$ (2.28 g, 3.27 mmol) in 20 ml distilled water and Na_2CO_3 (1.74 g, 16.4 mmol) in 45 ml distilled water were added to the ethanolic 4-benzoylpyridine solution. The mixture was stirred for 6 days to produce a white precipitate. The vessel was cooled in an ice bath, and a white solid collected *via* vacuum filtration. The precipitate was washed with small portions of cold water, and dried with an aspirator. Yield: 2.10 g (49%). Mp 184–188 °C. ^{1}H NMR: δ_H (400 MHz; DMSO-d_6) 7.29–7.31(2H, d), 7.38(5H, s), 8.68–8.69(2H, d) and 11.67(1H, s). ^{13}C NMR: δ_C (200 MHz; DMSO-d_6) 123.5, 126.6, 128.5, 129.2, 135.1, 141.2, 149.6 and 153.1. Colorless, rectangular prisms suitable for X-ray diffraction were grown from a saturated solution of **6** in methanol.

Synthesis of 3-benzoyloximepyridine, 7

3-Benzoylpyridine (2.00 g, 1.09 mmol) was dissolved in ethanol (25 ml) with stirring. $NH_2OH{\cdot}HCl$ (1.14 g, 1.64 mmol) in 20 ml distilled water and Na_2CO_3 (0.87 g, 8.19 mmol) in 40 ml distilled water were added to the ethanolic 3-benzoylpyridine solution. The mixture was heated under reflux for 48 h. Upon cooling to room temperature, a white precipitate appeared. The solution was concentrated under reduced pressure, then cooled in an ice bath. A white precipitate was collected *via* vacuum filtration, washed with small portions of cold water, and dried with an aspirator. Recrystallization from ethanol gave white crystals. Yield: 1.76 g (81%). Mp 154–157 °C. ^{1}H NMR: δ_H (400 MHz; DMSO-d_6) 7.37(5H, s), 7.46–7.50(1H, m), 7.69–7.72(1H, d), 8.47(1H, s), 8.58–8.60(1H, d) and 11.59(1H, s). ^{13}C NMR: δ_C (200 MHz; DMSO-d_6) single isomer: 123.4, 126.8, 128.4, 129.1, 129.2, 135.9, 136.6, 149.1, 149.2, and 152.6; mixture of isomers: 123.4, 126.8, 128.3, 128.5, 128.7, 128.8, 129.1, 129.2, 129.7, 132.4, 132.5, 134.3, 135.9, 136.6, 147.6, 149.1, 149.3, 149.5, 152.7, and 153.0. Colorless prisms suitable for X-ray diffraction were grown from a saturated solution of **7** in acetone.

X-ray crystallography

Crystal data for **1–7** were collected using a Siemens P4 four-circle diffractometer with graphite monochromated Mo-Kα ($\lambda = 0.71073$ Å) radiation at 173 K. Cell parameters were obtained from 35 accurately centered reflections in the 2θ range 10–28°. Data were collected using a θ–2θ scanning technique, and Lorentz and polarization corrections were applied. The structures were solved by direct methods, with non-hydrogen atoms found by successive full matrix least squares refinement on F^2 and refined with anisotropic thermal parameters. Hydrogen atom positions were located from difference Fourier maps, and a riding model with fixed thermal parameters [$u_{ij} = U_{ij}$(eq) for the atom to which they are bonded] was used for subsequent refinements. The weighting function applied was $w^{-1} = [\sigma^2(F_o^2) + (g_1P)^2 + (g_2P)]$ where $P = [F_o^2 + 2F_c^2]/3$. The SHELXTL PC and SHELXL-93 packages were used for data reduction and structure solution and refinement.[15] Tables 1–3 provide crystallographic details for **1–7**, and the molecular geometries and numbering schemes are shown in Fig. 2.

Results

There are two unique molecules in the asymmetric unit of **1**. The molecules, related by a 2_1 screw axis, form infinite 1D chains held together by hydrogen bonds. The predominant

UM00012793
NOVARTIS EXHIBIT 1017
Novartis v. Regents, IPR2023-01346
Page 1539 of 4460

Table 1 Crystal data and refinement for 1–3 [a]

Crystal data	1	2	3
Empirical formula	$C_6H_6N_2O$	$C_6H_6N_2O$	$C_7H_8N_2O$
M	122.13	122.13	136.15
Crystal size/mm^3	0.62 × 0.36 × 0.24	0.24 × 0.22 × 0.22	0.46 × 0.40 × 0.28
Crystal system	Monoclinic	Orthorhombic	Monoclinic
Space group	$P2(1)/c$	$Pna2(1)$	$C2/c$
a/Å	16.407(2)	19.014(2)	12.8175(9)
b/Å	8.4341(7)	3.8296(4)	9.627(2)
c/Å	9.0196(8)	8.1179(8)	11.420(1)
α/°	90	90	90
β/°	105.758(7)	90	91.918(6)
χ/°	90	90	90
V/Å^3	1201.2(2)	591.1(1)	1408.4(3)
Z	8	4	8
μ(Mo-Kα)/mm^{-1}	0.096	0.098	0.089
T/K	173(2)	173(2)	173(2)
Reflections collected	2253	1103	1090
Unique reflections	2102	815	1039
Observed reflections ($I > 2\sigma I$)	1399	639	893
R/R_w^2 (obs. data)	0.0481/0.1091	0.0446/0.0900	0.0418/0.1085
R/R_w^2 (all data)	0.0825/0.1248	0.0646/0.0982	0.0487/0.1135

[a]Click here for full crystallographic data (CCDC no. 1350/33).

Table 2 Crystal data and refinement for 4–6[a]

Crystal data	4	5	6
Empirical formula	$C_7H_8N_2O$	$C_6H_7N_3O$	$C_{12}H_{10}N_2O$
M	136.15	137.15	198.22
Crystal size/mm^3	0.42 × 0.38 × 0.34	0.65 × 0.54 × 0.36	0.40 × 0.20 × 0.20
Crystal system	Monoclinic	Orthorhombic	Monoclinic
Space group	$P2(1)/c$	$Pna2(1)$	$P2(1)/c$
a/Å	6.3502(7)	12.5433(6)	5.7943(6)
b/Å	14.296(1)	8.7821(9)	17.615(2)
c/Å	7.6172(7)	5.7857(4)	10.271(1)
α/°	90	90	90
β/°	91.622(5)	90	99.290(8)
χ/°	90	90	90
V/Å^3	691.2(1)	637.33(8)	1034.6(2)
Z	4	4	4
μ(Mo-Kα)/mm^{-1}	0.091	0.103	0.083
T/K	173(2)	173(2)	173(2)
Reflections collected	1717	803	2004
Unique reflections	1584	803	1817
Observed reflections ($I > 2\sigma I$)	1159	775	1251
R/R_w^2 (obs. data)	0.0521/0.1312	0.0286/0.0779	0.0507/0.1027
R/R_w^2 (all data)	0.0756/0.1454	0.0300/0.0786	0.0860/0.1169

[a]Click here for full crystallographic data (CCDC no. 1350/33).

hydrogen bond interaction assembling the chains is a head-to-tail O–H···N hydrogen bond involving the oxime O–H and the pyridine nitrogen atom [O7–N1 = 2.787(3) Å; O27–N21 = 2.785(3) Å], Fig. 3. There is also a C–H···N hydrogen bond involving the oxime C–H and the oxime nitrogen atom [C7–N7 = 3.274(3)Å; C(27)–N(27) = 3.283(3) Å]. The chains are arranged in an *anti*-parallel fashion and pack in a typical herringbone motif.

In the crystal structure of **2**, infinite 1D chains are assembled through a head-to-tail O–H···N hydrogen bond involving the oxime O–H and the pyridine nitrogen atom [O7–N1 = 2.717(3) Å]. Adjacent chains are related by a glide plane, and the two chains are linked through a C–H···O [C2–O7 = 3.450(3) Å] hydrogen bond to form a 1D ribbon, Fig. 4. The ribbons are arranged in a herringbone motif and are hydrogen bonded to neighboring ribbons *via* C–H···N [C5–N7 = 3.659(4) Å] interactions to produce an overall 3D hydrogen bonded structure. All the oxime moieties within a ribbon point in the same direction, and all the ribbons, in turn, are aligned in a parallel fashion.

In the structure of **3**, the molecules form infinite 1D chains assembled through a head-to-tail O–H···N hydrogen bond

Table 3 Crystal data and refinement for 7[a]

Crystal data	7
Empirical formula	$C_{12}H_{10}N_2O$
M	198.22
Crystal size/mm^3	0.50 × 0.25 × 0.06
Crystal system	Monoclinic
Space group	$P2(1)/n$
a/Å	5.649(1)
b/Å	12.737(2)
c/Å	14.507(2)
α/°	90
β/°	96.33(1)
χ/°	90
V/Å^3	1037.4(3)
Z	4
μ(Mo-Kα)/mm^{-1}	0.083
T/K	173(2)
Reflections collected	2614
Unique reflections	2382
Observed reflections ($I > 2\sigma I$)	1084
R/R_w^2 (obs. data)	0.0820/0.1795
R/R_w^2 (all data)	0.1842/0.2279

[a]Click here for full crystallographic data (CCDC no. 1350/33).

UM00012794
NOVARTIS EXHIBIT 1017
Novartis v. Regents, IPR2023-01346
Page 1540 of 4460

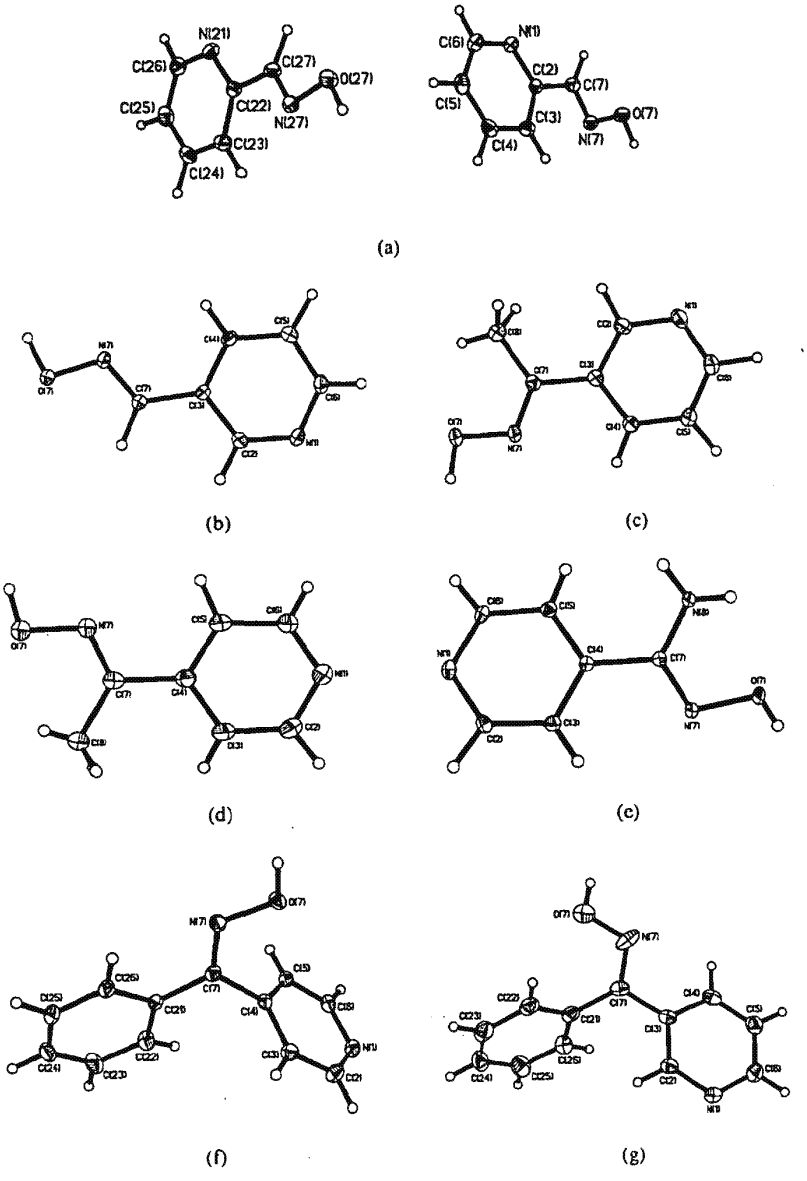


Fig. 2 Thermal ellipsoid plots of (a) 2-aldoximepyridine, 1; (b) 3-aldoximepyridine, 2; (c) 3-acetyloximepyridine, 3; (d) 4-acetyloximepyridine, 4; (e) 4-amidoximepyridine, 5; (f) 4-benzoyloximepyridine, 6; and (g) 3-benzoyloximepyridine, 7. Click images or compound numbers to access 3D representations.

involving the oxime O–H and the pyridine nitrogen atom [O7–N1 = 2.720(2) Å], Fig. 5. Additional C–H···N [C4–N7 = 3.481(2) Å] and C–H···O [C5–O7 = 3.246(2) Å] hydrogen bonds cross-link the 1D chains to produce a 3D hydrogen bonded infinite architecture.

The crystal structure of 4 contains infinite 1D molecular chains assembled through a head-to-tail O–H···N hydrogen bond involving the oxime O–H and the pyridine nitrogen atom [O7–N1 = 2.711(2) Å]. The molecules comprising the chains are related by a 2_1 screw axis. Neighboring chains run *anti*-parallel to each other, Fig. 6. The chains are cross-linked *via* C–H···O hydrogen bonds [C6–O7 = 3.360(2) Å] resulting in 2D sheets. These sheets, which lie in the *ac* plane, stack to produce a lamellar structure. There are no hydrogen bond interactions between sheets.

The crystal structure of 5 also contains infinite 1D chains assembled through a head-to-tail O–H···N hydrogen bond involving the oxime O–H and the pyridine nitrogen atom [O7–N1 = 2.745(2) Å]. The chains are cross-linked *via* C–H···N hydrogen bonds [C2–N8 = 3.682(2) Å] involving a pyridine C–H and the nitrogen atom of the amino group attached to the oxime functionality. This interaction results in the formation of

UM00012795
NOVARTIS EXHIBIT 1017
Novartis v. Regents, IPR2023-01346
Page 1541 of 4460

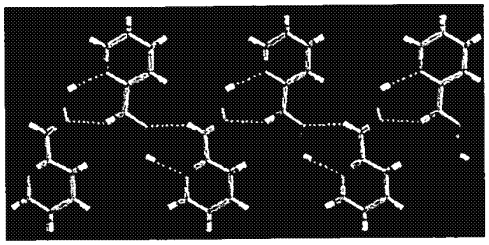


Fig. 3 Infinite chain of 2-aldoximepyridine, **1**. Click image or here to access 3D representation.

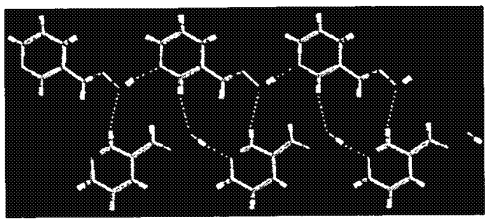


Fig. 4 Infinite ribbon of 3-aldoximepyridine, **2**. Click image or here to access 3D representation.

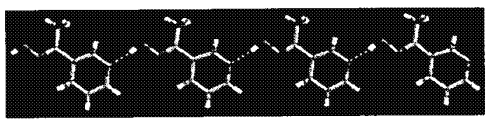


Fig. 5 Infinite 1D chain of 3-acetyloximepyridine, **3**. Click image or here to access 3D representation.

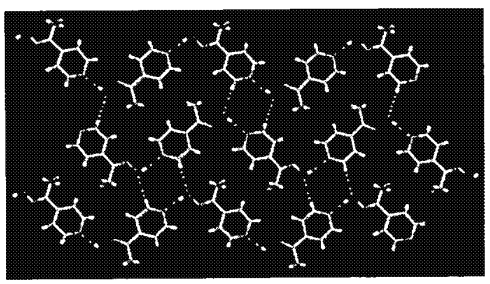


Fig. 6 Infinite sheets of 4-acetyloximepyridine, **4**. Click image or here to access 3D representation.

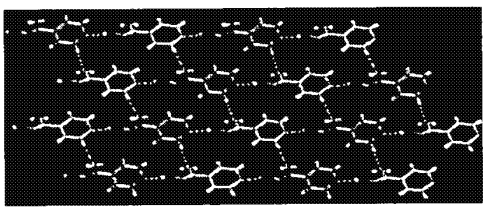


Fig. 7 Infinite 2D sheet in 4-amidoximepyridine, **5**. Click image or here to access 3D representation.

infinite 2D sheets, Fig. 7. The sheets have a corrugated appearance and stack together. The 2D sheets are propagated into a 3D structure by additional N–H···N hydrogen bonds between the amino N–H and the oxime nitrogen atom [N8–N7 = 3.090(2) Å]. The overall structure is a 3D hydrogen bonded architecture.

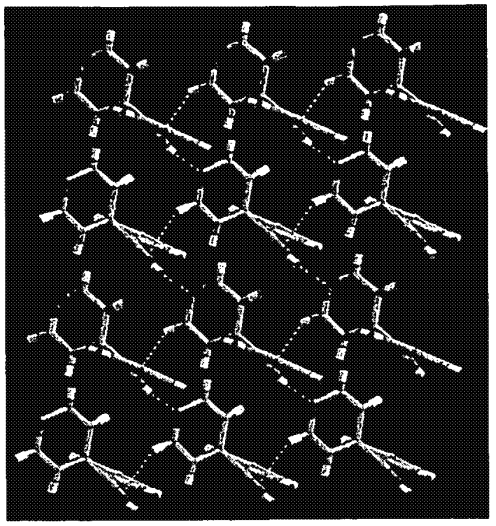


Fig. 8 Infinite 2D sheet in 4-benzoyloximepyridine, **6**. Click image or here to access 3D representation.

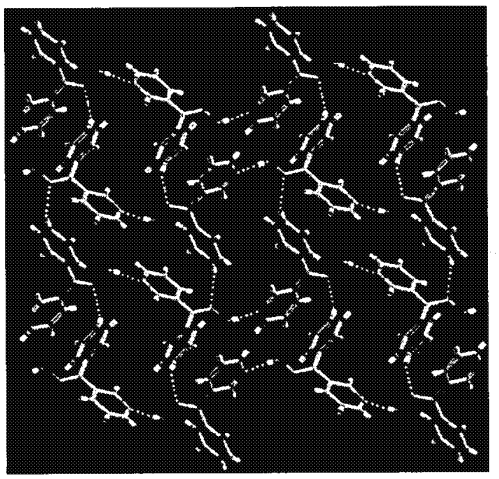


Fig. 9 Infinite 2D sheet in 3-benzoyloximepyridine, **7**. Click image or here to access 3D representation.

In **6**, the molecules form infinite 1D chains assembled through a head-to-tail O–H···N hydrogen bond involving the oxime O–H and the pyridine nitrogen atom [O7–N1 = 2.749(2) Å]. Molecules within each chain are related by a 2_1 screw axis. Neighboring chains run parallelly, and are cross-linked by C–H···O hydrogen bonds [C6–O7 = 3.278(3) Å] to generate infinite 2D sheets, Fig. 8. The phenyl rings protrude above and below the corrugated 2D sheets and interdigitate as a result of close-packing; however, there are no short aryl–aryl contacts or hydrogen bonding interactions between sheets.

Finally, in **7**, the molecules form infinite 1D chains assembled through a head-to-tail O–H···N hydrogen bond involving the oxime O–H and the pyridine nitrogen atom

UM00012796
NOVARTIS EXHIBIT 1017
Novartis v. Regents, IPR2023-01346
Page 1542 of 4460

[O(7)–N(1) = 2.737(4) Å]. The molecules within each chain are related by a 2_1 screw axis. The chains are cross-linked by C–H···N hydrogen bonds involving a phenyl C–H and the oxime nitrogen atom [C(24)–N(7) = 3.509(6) Å] to form infinite corrugated sheets, Fig. 9. The chains comprising each sheet run in an *anti*-parallel fashion. The corrugated sheets stack in a tongue-and-groove manner as a result of close packing; however, there are no hydrogen bonds between sheets.

Discussion

Compounds **3**–**7** were synthesized in moderate to good yields by allowing the appropriate substituted pyridine to react with hydroxylamine. The chemical shifts, splitting patterns, and integration in the ^{1}H-NMR spectra of **3**–**7** supported the identities of the desired compounds and no trace of starting material was observed in the spectra. The ^{1}H-NMR and ^{13}C-NMR spectra of the crude compounds revealed that **3**–**6** were isolated as single isomers, whereas **7** was isolated as a mixture of geometrical isomers. A single isomer of **7** was obtained by recrystallization from ethanol.

The crystal structures for **1**–**7** show that all the molecules have the *antiperiplanar* conformation, with C=N–O–H torsion angles in the range of 166–180°. This conformation is more stable than the *synplanar* conformation and is also required for hydrogen bond formation. In addition, all molecules, except **6**, display a configuration where the oxime O–H is *trans* to the pyridyl ring.

The dominating intermolecular interaction in all structures is a head-to-tail hydrogen bond from the oxime moiety to the pyridine nitrogen atom. Regardless of the R substituent of the oxime functionality (–H, $-CH_3$, $-NH_2$, or Ph), this interaction prevails and generates infinite 1D molecular chains in **1**–**7**. A search of the CSD[16] found other pyridineoxime derivatives[17] where the same head-to-tail hydrogen bond is present in each case. More recently, two other oxime-substituted pyridines were also reported to display the very same interaction.[18] This supports the conclusion that the pyridine nitrogen atom is a better hydrogen bond acceptor than the oxime nitrogen atom in these molecules.

While changing the nature of the *R* substituent does not affect the principle structural motif (*i.e.* chain formation) in **1**–**7**, it does play a role in determining the structural outcome. This secondary influence may be attributed more to steric, rather than electronic, factors. For example, 3-aldoximepyridine crystallizes in the orthorhombic space group $Pna2_1$, while 3-acetyloximepyridine crystallizes in the monoclinic space group $C2/c$.

We have shown that pyridineoximes form infinite 1D chains in the solid-state assembled *via* a head-to-tail O–H···N hydrogen bond between the oxime O–H and the pyridine nitrogen atom. Although many options for assembly are possible (Scheme 1), the primary motif (*i.e.* chain formation) remains intact and dominates the crystal structures of **1**–**7**. The O–H···N interaction not only reaffirms the notion of the best hydrogen bond donor pairing with the best acceptor,[19] but also demonstrates the ability of a stronger hydrogen bond to dictate the structural outcome over weaker C–H···A interactions.

We have previously demonstrated the utility of the pyridineoximes as 'building blocks' ideally suited for the supramolecular synthesis of inorganic–organic hybrid materials due to the consistency in their primary hydrogen bond interactions (*i.e.* dimer formation). This work opens avenues into the organic solid-state, as the persistence of the O–H···N hydrogen bond provides for the controlled and predictable assembly of compounds displaying both oxime and pyridyl moieties.

Acknowledgements

We are grateful for financial support from NSF (CHE-0078996) and Kansas State University.

References

1 (*a*) G. R. Desiraju, *Crystal Engineering: The Design of Organic Solids*, Elsevier, Amsterdam, 1989.; (*b*) J.-M. Lehn, *Supramolecular Chemistry*, VCH, Weinheim, 1995.; (*c*) C. B. Aakeröy, *Acta Crystallogr., Sect. B*, 1997, **B53**, 569; (*d*) *Perspectives in Supramolecular Chemistry, Vol. 2, The Crystal as a Supramolecular Entity*, ed. G. R. Desiraju, Wiley, Chichester, 1995.
2 (*a*) R. Thaimattam, D. S. Reddy, F. Xue, T. C. W. Mak, A. Nangia and G. R. Desiraju, *J. Chem. Soc., Perkin Trans.*, 1998, 1783; (*b*) P. R. Ashton, M. C. T. Fyfe, S. K. Hickingbottom, S. Menzer, J. F. Stoddart, A. J. P. White and D. J. Williams, *Chem. Eur. J.*, 1998, **4**, 577; (*c*) S. V. Kolotuchin and S. C. Zimmerman, *J. Am. Chem. Soc.*, 1998, **120**, 9092; (*d*) K. Kobayashi, T. Shirasaka, K. Yamaguchi, S. Sakamoto, E. Horn and N. Furukawa, *Chem. Commun.*, 2000, 41; (*e*) D. E. Lynch, S. Chatwin and S. Parsons, *Cryst. Eng.*, 1999, **2**, 137; (*f*) C. B. Aakeröy and M. Nieuwenhuyzen, *J. Am. Chem. Soc.*, 1994, **116**, 10983; (*g*) C. B. Aakeröy, D. P. Hughes and M. Nieuwenhuyzen, *J. Am. Chem. Soc.*, 1996, **118**, 10134; (*h*) J. A. Swift, A. M. Pivovar, A. M. Reynolds and M. D. Ward, *J. Am. Chem. Soc.*, 1998, **120**, 5887.
3 (*a*) V. A. Russell and M. D. Ward, *Chem. Mater.*, 1996, **8**, 1654; (*b*) C. B. Aakeröy and K. R. Seddon, *Chem. Soc. Rev.*, 1993, **22**, 397; (*c*) S. Subramanian and M. Zaworotko, *Coord. Chem. Rev.*, 1994, **137**, 357.
4 G. R. Desiraju, *Angew. Chem., Int. Ed. Engl.*, 1995, **34**, 2311.
5 J. P. Freeman, *Chem. Rev.*, 1973, **73**, 283.
6 N. M. Samus and A. V. Ablov, *Coord. Chem. Rev.*, 1979, **28**, 177.
7 V. Y. Kukushkin, D. Tudela and A. J. L. Pombeiro, *Coord. Chem. Rev.*, 1996, **156**, 333.
8 S. Kawata, S. Kitagawa, H. Machida, T. Nakamoto, M. Kondo, K. Katada, K. Kikuchi and I. Ikemoto, *Inorg. Chim. Acta*, 1995, **229**, 211.
9 V. Yu, T. Nishioka, D. Tudela, K. Isobe and A. J. L. Pombeiro, *Coord. Chem. Rev.*, 1996, **156**, 333.
10 K. Isobe and I. Kinoshita, *Inorg. Chem.*, 1997, **36**, 6157.
11 (*a*) F. J. Hoogesteger, L. W. Jenneskens, H. Kooijman, N. Veldman and A. J. Spek, *Tetrahedron*, 1996, **52**, 1773; (*b*) K. Y. Lau, A. Mayr and K.-K. Cheung, *Inorg. Chim. Acta*, 1999, **285**, 223; (*c*) A. W. Marsman, PhD Thesis, Utrecht University, 1999.; (*d*) L. Chertanova, C. Pascard and A. Sheremetev, *Acta Crystallogr., Sect. B*, 1994, **B50**, 708.
12 C. B. Aakeröy, A. M. Beatty and D. S. Leinen, *Angew. Chem., Int. Ed.*, 1999, **38**, 1815.
13 C. B. Aakeröy, A. M. Beatty and D. S. Leinen, *J. Am. Chem. Soc.*, 1998, **120**, 7383.
14 (*a*) T. Katagi, H. Kataoka, K. Takahashi, T. Fujioka, M. Kunitomo, Y. Yamaguchi, M. Fujiwara and T. Inoi, *Chem. Pharm. Bull.*, 1992, **40**, 2419; (*b*) T. Kato, Y. Goto and T. Chiba, *Yakugaku Zasshi*, 1967, **87**, 689; (*c*) H. Adkins, I. A. Wolff, A. Pavlic and E. Hutchinson, *J. Am. Chem. Soc.*, 1944, **66**, 1293; (*d*) E. Bernasek, *J. Org. Chem.*, 1957, **22**, 1263; (*e*) G. Massolini, M. Kitsos, C. Gandini and G. Caccialanza, *Pestic. Sci.*, 1989, **26**, 209; (*f*) G. Massolini, M. L. Carmellino and A. Baruffini, *Farmaco Ed. Sci.*, 1987, **42**, 117.
15 SHELXTL PC and SHELXL-93, G. M. Sheldrick, University of Göttingen, 1993.
16 Cambridge Structural Database, ver. 5.18; Cambridge Crystallographic Data Centre, 12 Union Road, Cambridge, England.
17 (*a*) M. Martínez-Ripoll and H. P. Lorentz, *Acta Crystallogr., Sect. B*, 1976, **B32**, 2322; (*b*) M. Martínez-Ripoll and H. P. Lorentz, *Acta Crystallogr., Sect. B*, 1976, **B32**, 2325; (*c*) J. M. Sorof, H. L. Carrell, J. P. Glusker, J. McLick and E. Kun, *Acta Crystallogr., Sect. C*, 1985, **C41**, 785; (*d*) Z. G. Aliev, V. G. Kartsev and L. O. Atovmyan, *Zh. Strukt. Khim.*, 1991, **32**, 113–3; (*e*) N. Okabe and M. Akita, *Acta Crystallogr., Sect. C*, 1997, **C53**, 1324; (*f*) T. Taga, A. Uchiyama, K. Machida and T. Miyasaka, *Acta Crystallogr., Sect. C*, 1990, **C46**, 2241.
18 (*a*) M. Mazik, D. Bläser and R. Boese, *Tetrahedron Lett.*, 1999, **40**, 4783; (*b*) M. Mazik, D. Bläser and R. Boese, *Tetrahedron*, 1999, **55**, 7835.
19 M. C. Etter, *J. Phys. Chem.*, 1991, **95**, 4601.

UM00012797
NOVARTIS EXHIBIT 1017
Novartis v. Regents, IPR2023-01346
Page 1543 of 4460

Measurement: A Mettler FP82 hot stage, controlled by a Mettler FP80 Processor, was used to control the temperature. The temperature was lowered from 2 °C above the clearing point to room temperature at a rate of 0.1 °C/min. The transition temperatures characterizing two LC materials are shown in Table 2 [12]. Though PCH5 crystallizes at 30 °C, it can be readily supercooled to room temperature and the experiment was performed in this supercooled nematic state. The LC texture was observed using a polarizing microscope. The intensity of the light propagating through the sample cell between two crossed polarizers was measured by a photodiode situated in the image plane of the microscope. Absorption spectra in the UV–visible region using polarized light were measured by a Perkin-Elmer Lambda 9 Spectrophotometer.

Received: February 3, 1993
Final version: Feburary 26, 1993

[1] J. C. Wittman, P. Smith, *Nature* **1991**, *352*, 414.
[2] D. W. Berreman, *Phys. Rev. Lett.* **1972**, *28*, 1683.
[3] D. C. Flanders, D. C. Shaver, H. I. Smith, *Appl. Phys. Lett.* **1978**, *32*, 597.
[4] M. Nakamura, M. Ura, *J. Appl. Phys.* **1981**, *52*, 210.
[5] J. Cheng, G. D. Boyd, *Appl. Phys. Lett.* **1979**, *35*, 444.
[6] J. M. Geary, J. W. Goodby, A. R. Kmetz, J. S. Patel, *J. Appl. Phys.* **1987**, *62*, 4100.
[7] H. Ikeno, A. Oh-saki, M. Nitta, N. Ozaki, Y. Yokoyama, K. Nakaya, S. Kobayashi, *Jpn. J. Appl. Phys.* **1988**, *27*, L475.
[8] Y. Nishikata, A. Morikawa, Y. Takiguchi, A. Kanemoto, M. Kakimoto, Y. Imai, *Jpn. J. Appl. Phys.* **1988**, *27*, L1163.
[9] G. Duda, G. Wegner, *Makromol. Chem., Rapid Commun.* **1988**, *9*, 495. J. Michl, E. W. Thulstrup *Spectroscopy with Polarized Light*, VCH, New York **1986**, p. 395.
[10] G. Duda, A. J. Schouten, T. Arndt, G. Lieser, G. F. Schmidt, C. Bubeck, G. Wegner, *Thin Solid Films* **1988**, *159*, 221.
[11] S. Schwiegk, T. Vahlenkamp, Y. Xu, G. Wegner, *Macromolecules* **1992**, *25*, 2513.
[12] T. Sauer, T. Arndt, D. N. Batchelder, A. A. Kalachev, G. Wegner, *Thin Solid Films* **1990**, *187*, 357.
[13] H. Ichinose, M. Suzuki, T. Goto, *Mol. Cryst. Liq. Cryst.* **1991**, *203*, 25.

Novel Colorless Composite Materials for Nonlinear Optics**

By *Christer B. Aakeröy, Nazar E. Azoz, Munteser Kadim, Kenneth R. Seddon,** and *Lynne Trowbridge*

The field of nonlinear optics (NLO) has been the subject of intense research activity in recent years,[1–5] and a large proportion of the many publications that appear regularly are concerned with the development of novel nonlinear optical materials, notably those capable of second harmonic generation (SHG). We have recently demonstrated[6] that it is possible to synthesize *yellow* nonlinear optical composites by growing well-aligned microcrystals of 3-nitroaniline (the guest) from a melt in a polymer matrix (the host) using a thermal-gradient zone-melting (TGZM) technique. In this technique, molten crystals of the guest material contained within a thermally softened polymeric host are induced to crystallize in a well-aligned manner by passage over a sharp temperature gradient. We have now devised a method for the preparation of *colorless* SHG-active composites, whereby the guest crystals are deposited from solution rather than from the melt, and aligned within the polymer matrix by inducing evaporation of the solvent along a thermal gradient. Preparation of the composite is therefore carried out under milder conditions, as it does not require excessive heating of either component. Controlling factors, which can be varied greatly by changing solvent, include the solubilities of the guest and the host in the chosen solvent-system, and the crystal-habit of the guest.

The composites prepared by the TGZM technique[6] are transparent and low-scattering, with excellent chemical and temporal stability. This approach, although extremely promising, does place some constraints on the guest which will provide the nonlinear response. For example, many SHG-active materials will either melt at temperatures considerably above the decomposition point of the host (e.g. $LiNbO_3$), or decompose prior to melting (e.g. 4-(*N*-pyrrolidino)-3-(*N*-ethanamido)-nitrobenzene (PAN),[7] or salts such as piperidinium dihydrogenphosphate[8]), which would preclude their incorporation into composites formed by the TGZM method. Furthermore, in order to maximize the optical band width, a colorless composite is desirable; the films made by the TGZM method, to date, have all been yellow.[6] Finally, it is most important to be able to prepare SHG-active composites which are stable at elevated temperatures, 200–300 °C, as this will significantly reduce the assembly costs of an integrated optical device.[9] Clearly, in order to improve and extend the methods by which SHG-active guests could be incorporated into a polymer matrix, it was highly desirable to develop alternatives to the TGZM method.

Our developing studies on hydrogen-bonded salts[8, 10, 11] have demonstrated that hydrogen bonds between ions are strong enough to exercise a controlling function in the structural organization and packing of ions within a crystalline material.[12] Moreover, we have also shown that it is possible to use the organic cations to carry the high optical polarizability, and the hydrogen-bonding inorganic[8] (or organic[10]) anions to provide thermal and structural stability. Our philosophy has recently been adopted by Zyss and co-workers[13] for the design of a related material for nonlinear optics; this crystalline salt, 2-amino-5-nitropyridinium dihydrogenphosphate, showed significant SHG-activity.[13]

The goal of obtaining colorless SHG-active composites was thus achieved by aligning microcrystals of a recently developed colorless material, benzylammonium dihydrogenphosphate (BADP), $[PhCH_2NH_3][H_2PO_4]$[8] within a series of different polymers. This material could not be used as a guest using the TGZM technique; it either decomposed or produced films of poor optical quality.

The composites were prepared from aqueous solutions of BADP, and polymer (poly(ethylene oxide) {PEO}, poly-

[*] Prof. K. R. Seddon
School of Chemistry, The Queen's University of Belfast
Belfast, BT9 5AG (Northern Ireland)
Dr. C. B. Aakeröy, Dr. N. E. Azoz, Dr. M. Kadim, L. Trowbridge
School of Chemistry and Molecular Sciences, University of Sussex
Falmer, Brighton, BN1 9QJ (UK)

[**] We are indebted to the Venture Research Unit (BP) for generous financial support, the Iraqi Government and DRA (Fort Halstead) for studentships (N.E.A., M.K., and L.T.).

© VCH Verlagsgesellschaft mbH, W-6940 Weinheim, 1993
0935-9648/93/0505-0364 $ 5.00+.25/0

UM00012798
NOVARTIS EXHIBIT 1017
Novartis v. Regents, IPR2023-01346
Page 1544 of 4460

ADVANCED MATERIALS

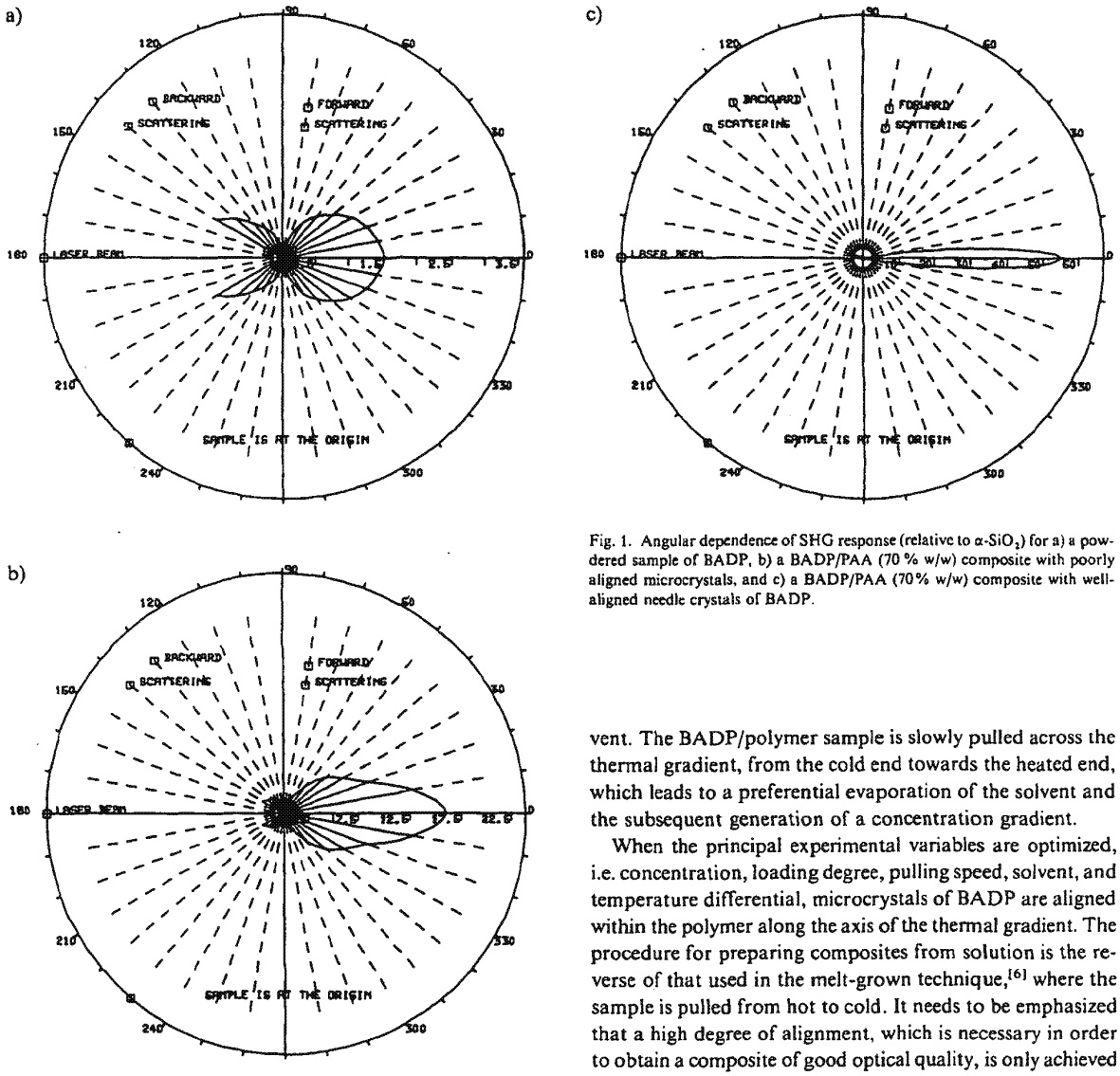


Fig. 1. Angular dependence of SHG response (relative to α-SiO_2) for a) a powdered sample of BADP, b) a BADP/PAA (70 % w/w) composite with poorly aligned microcrystals, and c) a BADP/PAA (70% w/w) composite with well-aligned needle crystals of BADP.

(acrylamide) {PAA}, or poly(vinylpyrrolidone) {PVP}), with varying loading degrees (50–90 wt.-% of guest). The solutions were placed in a sonic bath to remove air bubbles and to ensure that both BADP and polymer were completely dissolved. Thin films, 30–60 μm, were cast by dipping a carefully cleaned microscope slide into the solution. The slide was then placed in the sample-channel in a thermal-gradient apparatus (as described in[6]).

The thermal gradient, the magnitude of which is determined by the guest/host system, must be optimized for each specific guest/host combination. However, the heated end is always maintained at a temperature below the melting point of both guest and host, and well below the boiling point of the solvent. The BADP/polymer sample is slowly pulled across the thermal gradient, from the cold end towards the heated end, which leads to a preferential evaporation of the solvent and the subsequent generation of a concentration gradient.

When the principal experimental variables are optimized, i.e. concentration, loading degree, pulling speed, solvent, and temperature differential, microcrystals of BADP are aligned within the polymer along the axis of the thermal gradient. The procedure for preparing composites from solution is the reverse of that used in the melt-grown technique,[6] where the sample is pulled from hot to cold. It needs to be emphasized that a high degree of alignment, which is necessary in order to obtain a composite of good optical quality, is only achieved if all the experimental variables are very carefully controlled and optimized.

By using this solution-based method, we have been able to incorporate microcrystals of BADP in an aligned fashion, and with a high loading degree (> 85 wt.-%), into a variety of host polymers, to produce colorless, transparent, low-scattering, SHG-active composites with excellent temporal stability; this last property is particularly important with respect to optical devices. These composites have shown no measurable decay in SHG-activity over a period of two years. Furthermore, the composites do not appear to be prone to optical damage, even after prolonged exposures to the fundamental light (1064 nm) from a Nd:YAG laser (ca. 10 mJ cm^{-2}).

The alignment of the guest crystals within the polymer matrix is the dominating factor in terms of eliminating light scattering from the composite. This is clearly illustrated in

UM00012799
NOVARTIS EXHIBIT 1017
Novartis v. Regents, IPR2023-01346
Page 1545 of 4460

Figures 1a–c, which show the angular distribution of the second harmonic (SH) intensity as a function of the alignment of the guest particles. These measurements were carried out on BADP/PAA composites by detecting the green 532-nm light arising from frequency doubling of the incident 1064 nm light from a Nd:YAG laser.

In Figure 1a, the medium is a powdered microcrystalline sample of BADP (sample size approx 150–180 μm), without polymer, and the angular scattering distribution exhibits a "figure-of-eight" which is characteristic of randomly distributed microcrystals.[14] Figure 1b shows a partially aligned composite (70 wt.-% BADP/PAA) and, as seen, there is very little back-scattering from the sample. Finally, Figure 1c shows a well-aligned BADP/PAA composite (70 wt.-% BADP/PAA). In this case, the angular distribution of the SH is very narrow and most of the SH flux is confined to a narrow cone (ca. 5°) in the forward direction. The magnitude of the SH response in the forward direction has also increased significantly (from 1.5 to 55 times α-SiO_2) compared with the powdered sample. This behavior applies to the whole range of composites that have been prepared.

Since the light scattering is minimized, and optical homogeneity is improved by matching the average value of the refractive index of the guest with that of the host in a direction normal to that of the plane of the film, it is possible to enhance the SHG intensity of the composite in the forward direction by a suitable choice of polymer. The best refractive index match between guest and host in these systems is achieved if microcrystals of BADP ($n = 1.553(3)$, $\lambda = 532$ nm[15]) are grown in a matrix of PVP ($n = 1.558(1)$, $\lambda = 633$ nm[15]).

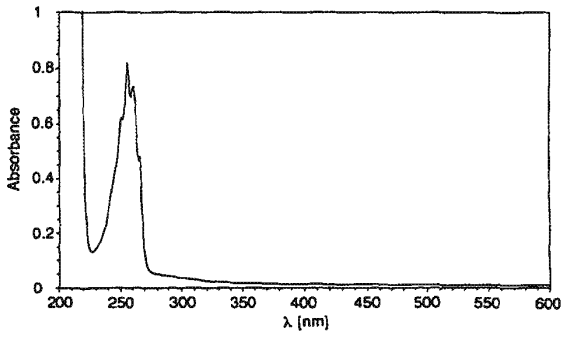


Fig. 2. The electronic absorption spectrum of benzylammonium dihydrogenphosphate in water.

crystals.[8] The last factor is an essential requirement for obtaining an alignment of the SHG-active crystals within the polymer matrix (disc-like crystals do not align very easily).

The work of Miyata and co-workers[16] on 4-nitroaniline has demonstrated that it is possible to produce a new polymorph by inducing crystal growth within a polymer matrix. This possibility was investigated in the BADP/PAA system by recording X-ray diffraction patterns on several composites with varying composition. The experimental patterns were then compared (a) with each other, (b) with polycrystalline BADP, and (c) with the simulated X-ray diffraction pattern based upon single crystal data[8] (using the CERIUS 3.1 package). The excellent match between experimental and simulated patterns (see Fig. 3) showed that BADP retained its original structure, even in the presence of the polymer, during the crystallization process. Furthermore, the alignment of the microcrystals did, as expected, coincide with the long axis, c, of the needle, and the morphology of the crystal is dominated by the {100} face, perpendicular to the growth direction. The increased importance of the {100} face BADP crystals aligned within a PAA polymer is also illustrated by

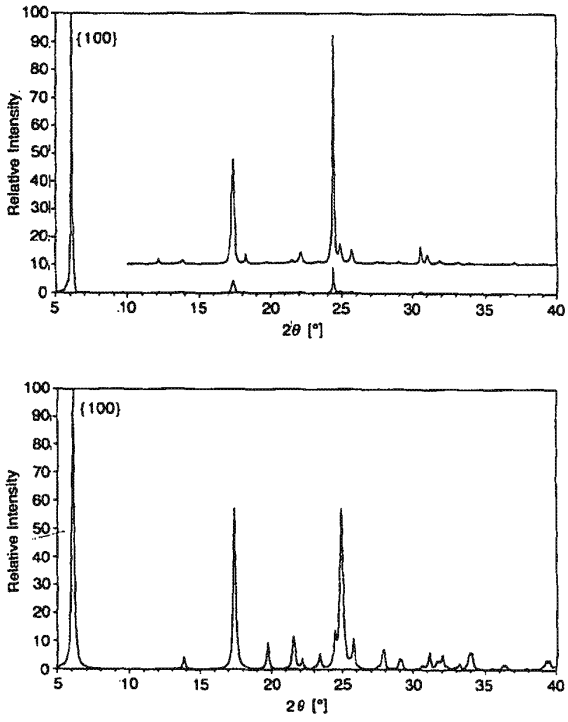


Fig. 3. a) The experimental X-ray diffraction pattern of a BADP/PAA (70% w/w) well-aligned composite, with an expansion (×9) inset. b) The simulated (CERIUS 3.1) X-ray diffraction pattern of BADP randomly-oriented microcrystals (based upon single crystal data) [8].

© VCH Verlagsgesellschaft mbH, W-6940 Weinheim, 1993

0935-9648/93/0505-0366 $ 5.00+.25/0 Adv. Mater. 1993, 5, No. 5

UM00012800
NOVARTIS EXHIBIT 1017
Novartis v. Regents, IPR2023-01346
Page 1546 of 4460

ADVANCED MATERIALS

the X-ray diffraction pattern where the d_{100} peak shows a dramatically enhanced intensity.

Of the limited number of polymers investigated here, PVP is the most appropriate host for a BADP composite, not only for its well-matched refractive index, but also because of its solubility properties and its high melting point (>300 °C). This means that a BADP/PVP composite will remain stable at temperatures which approach those used in realistic assembly, and at peak working levels.[9]

The technique described here does not rely on water as a solvent. An organic solvent (e.g. toluene, dichloromethane, propanone, *N,N*-dimethylmethanamide, etc.), may also be used, which makes it possible to incorporate SHG-active molecular solids (e.g. 4-(*N,N*-dimethylamino)-3-(*N*-ethanamido)-3-nitrobenzene {DAN}[17]), as guest materials.[18]

The SHG-active composites described in this communication exhibit many useful chemical and physical properties and, as such, they represent an important new addition to the field of nonlinear optics. The nonlinear optical properties provided by microcrystals of BADP, in combination with the durability and strength of the polymer matrix make these, and related composites, prime candidates for incorporation into optoelectronic devices (see, for example, [9]). In addition, by using the solution-based method described herein, it is possible to synthesize SHG-active composites using a wide variety of guests and hosts, thereby extending the flexibility of the resulting composite.

Received: March 6, 1992
Final version: February 18, 1993

[1] *Nonlinear Optical Properties of Organic Molecules and Crystals* (Eds: D. S. Chemla, J. Zyss), Academic Press, New York **1987**, Vols. 1 and 2.
[2] *Nonlinear Optical Properties of Organic and Polymeric Materials* (Ed: D. J. Williams), Am. Chem. Soc., Washington **1983**, Vol. 233.
[3] *Molecular and Polymeric Optoelectronic Materials: Fundamentals and Applications* (Ed: G. Khanarian), SPIE, San Diego **1986**, Vol. 682.
[4] *Nonlinear Optical Properties of Materials* (Ed: G. Khanarian), SPIE, Washington **1988**, Vol. 971.
[5] *Materials for Nonlinear Optics* (Eds: S. R. Marder, J. E. Sohn, G. D. Stucky), Am. Chem. Soc., Washington **1991**, Vol. 455.
[6] N. Azoz, P. D. Calvert, M. Kadim, A. J. McCaffery, K. R. Seddon, *Nature* **1990**, *344*, 49–51.
[7] R. J. Twieg, K. Jain, in [2], pp. 57–80.
[8] C. B. Aakeröy, P. B. Hitchcock, B. D. Moyle, K. R. Seddon, *J. Chem. Soc., Chem. Commun.* **1989**, 1856–1859.
[9] R. Lytel, G. F. Lipscomb, E. S. Binkley, J. T. Kenney, A. J. Ticknor, in [5], pp. 103–112.
[10] C. B. Aakeröy, P. B. Hitchcock, K. R. Seddon, *J. Chem. Soc., Chem. Commun.* **1992**, 553–555.
[11] C. B. Aakeröy, G. S. Bahra, P. B. Hitchcock, Y. Patell, K. R. Seddon, *J. Chem. Soc., Chem. Commun.* **1993**, 152–156.
[12] C. B. Aakeröy, M. Leslie, K. R. Seddon, *Struct. Chem.* **1992**, *3*, 63–65.
[13] R. Masse, J. Zyss, *Mol. Eng.* **1991**, *1*, 141–152. Z. Kotler, R. Hierle, D. Josse, J. Zyss, R. Masse, *J. Opt. Soc. Am. B* **1992**, *9*, 534–547.
[14] S. K. Kurtz, T. T. Perry, *J. Appl. Phys.* **1968**, *39*, 3798–3813.
[15] M. Kadim, A. J. McCaffery, K. R. Seddon, unpublished results.
[16] T. Watanabe, K. Yoshinaga, D. Fichou, S. Miyata, *J. Chem. Soc., Chem. Commun.* **1988**, 250–251.
[17] R. J. Twieg, C. W. Dirk, *IBM Research Report* RJ-5329, **1986**.
[18] N. Azoz, J. H. B. Ramsey, K. R. Seddon, unpublished results (1991).

Molecular Accessibility in Interpenetrating Organometallic Polymer Networks (IOPNs): An ESR Evaluation**

By *Benedetto Corain,** *Carlo Corvaja, Silvano Lora, Giancarlo Palma*, and *Marco Zecca*

We have recently proposed in this journal a novel synthetic pathway to metallo-organic macromolecular composites,[1,2] which might embody, in principle, a novel strategy for the preparation of supported metal catalysts.[3] The proposal is based on the generation of a cross-linked organometallic copolymer inside the macro- and microporous domains[4] of organic and inorganic supports.

In previously described model experiments[1,2] we have generated a polyvinylferrocene (VF)/dimethylacrylamide (DMAA)/methylenebisacrylamide (MBAA, 4 mol-%) network ("guest" component, **G**), Figure 1, inside the microporous domains of a poly-DMAA/MBAA (4 mol-%) matrix, **I**, ("host" component) (composite **I**–Fe). In this material,

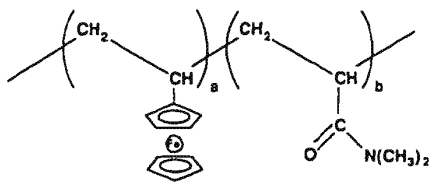


Fig. 1. Schematic representation of the guest organometallic copolymer dispersed inside matrix **I**.

expected to be a model metallorganic (macro)molecular composite, the organometallic units were found to be homogeneously distributed throughout the entire bulk volume of the composite particles and to maintain their original molecular structure after polymerization of the pendant vinyl group.[11]

If these materials are to be proposed as models of supported metal catalysts, the overall accessibility of the metal center to the reagents and a negligeable retention of the products inside the polymer network must also be accomplished. In connection with these further requirements, ISEC (Inverse Steric Exclusion Chromatography)[15,6] analysis gave us encouraging results[2] and ESR spectroscopy of convenient paramagnetic probes did appear a suitable and quite inde-

[*] Prof. B. Corain, Dr. M. Zecca
Centro Studio Stabilità e Reattività Composti Coordinazione, C.N.R., c/o Dipartimento di Chimica Inorganica Metallorganica Analitica, University of Padova
via Marzolo 1, I-35131 Padova (Italy)
Prof. C. Corvaja, Prof. G. Palma
Dipartimento di Chimica Fisica, University of Padova
via Loredan 2, I-35131 Padova (Italy)
Dr. S. Lora
Istituto Fotochimica Radiazioni d'Alta Energia, C.N.R.
via Romea 4, I-35020 Legnaro (Italy)

[**] This work was partially supported by Centro per lo Studio degli Stati Radicalici ed Eccitati, C.N.R., Progetto Finalizzato Chimica Fine II, C.N.R., Rome and by MURST (40%), Rome.

 © VCH Verlagsgesellschaft mbH, W-6940 Weinheim, 1993 0935-9648/93/0505-0367 $ 5.00+.25/0

UM00012801
NOVARTIS EXHIBIT 1017
Novartis v. Regents, IPR2023-01346
Page 1547 of 4460

Pergamon

Tetrahedron 56 (2000) 6693–6699

TETRAHEDRON

Organic Assemblies of 2-pyridones with Dicarboxylic Acids

Christer B. Aakeröy,[a,*] Alicia M. Beatty,[a] Mark Nieuwenhuyzen[b] and Min Zou[a]

[a]*Department of Chemistry, Kansas State University, Manhattan, KS, 66506, USA*
[b]*School of Chemistry, The Queen's University, Belfast BT9 5AG, Ireland, UK*

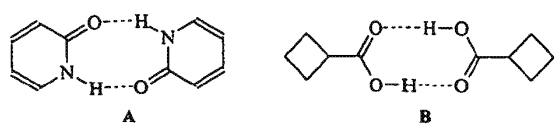
Received 21 December 1999; accepted 25 January 2000

Abstract—The syntheses and crystal structures of four cocrystals; 2-pyridone fumaric acid (2/1), 2-pyridone *meso*-2,3-dibromosuccinic acid (2/1), 5-chloro-2-pyridone adipic acid (2/1) and 6-methyl-2-pyridone (*S*)-malic acid (2/1), are reported. The competition between two self- and mutually-complementary hydrogen-bond moieties (carboxylic acid and 2-pyridone) are examined and compared with results obtained from an earlier study of 2-pyridone and unsubstituted aliphatic dicarboxylic acids. © 2000 Elsevier Science Ltd. All rights reserved.

Introduction

Molecular assembly is a vital aspect of crystal engineering, an area of considerable and widespread attention.[1–4] The primary goal in this field is to control the way in which individual molecules are brought together into extended architectures in the solid state, allowing us to affect solid state reactivity, and to design new functional materials. The synthetic tools available for the construction of such assemblies are non-covalent forces, many of which are poorly understood and difficult to calculate and measure. Consequently, controlling the chemical reactivity and properties of a solid through precise control over its crystal structure is a formidable task. The good news is that many assemblies and structural patterns have been constructed through intermolecular interactions, and the use of molecules or ions (instead of atoms) as building blocks of ordered networks has become an important synthetic strategy in chemistry and materials science.[5] However, crystal engineering is still in its infancy and thus it is necessary to assemble structural information, to identify recurring packing motifs and to correlate these with intermolecular interactions.[6] Many intermolecular connectors rely on the complementarity of various hydrogen-bonding moieties. Examples of such connectors include carboxylic acid/2-aminopyridine,[7] carboxylic acid/urea,[8] amides/acids,[9] carboxylic acid/oxime, and hydroxyl/amino.[10] The robustness and reliability of the self-complementary 2-pyridone moiety, Scheme 1A, have also been utilized for crystal engineering: Wuest and co-workers have constructed both low-dimensional[11] and diamondoid[12] assemblies based upon intermolecular hydrogen bonds between neighboring 2-pyridone moieties.

Although 2-pyridone moieties are known to form rigid dimers in the solid-state, the crystal structure of 2-pyridone[13] actually displays a catemer motif (infinite chains), indicating that it is possible to obtain alternative intermolecular arrangements despite the prevalence of 2-pyridone head-to-head dimers. Historically, probably the most well-known hydrogen-bond motif is the carboxylic acid head-to-head dimer,[14] Scheme 1B, which has been utilized extensively in crystal engineering both in the organic and the inorganic/organic solid state. Recent database studies have revealed, however, that carboxylic acids do engage in a variety of intermolecular hydrogen bonds and the self-complementary $R_2^2(8)$[15] motif is not as reliable as initially thought.[16] An earlier study of five co-crystals of 2-pyridone and some aliphatic dicarboxylic acids showed that each crystal structure contained planar dimers of 2-pyridone bridged by a dicarboxylic acid via a combination of O–H···O and C–H···O hydrogen bonds, resulting in infinite 1-D ribbons.[17] In order to further examine competition between complementary intermolecular forces we have determined the crystal structures of four cocrystals; 2-pyridone fumaric acid (2/1) **1**, 2-pyridone *meso*-2,3-dibromosuccinic acid (2/1) **2**, 5-chloro-2-pyridone adipic acid (2/1) **3** and 6-methyl-2-pyridone (*S*)-malic acid (2/1) **4**. These structures allow an examination of possible changes in packing patterns that may appear due to substituents on the 2-pyridone and/or acid moieties (**2–4**), or due to increased rigidity of the acid backbone (**1**).



A B

Scheme 1. (A) Hydrogen-bonded dimer formed by two 2-pyridone moieties; (B) head-to-head dimer of two carboxylic acid moieties.

Keywords: 2-pyridones; dicarboxylic acids; hydrogen bonded ribbon.
* Corresponding author. Tel.: +1-913-532-6096; fax: +1-913-532-6666; e-mail: aakeroy@ksu.edu

0040-4020/00/$ - see front matter © 2000 Elsevier Science Ltd. All rights reserved.
PII: S0040-4020(00)00488-9

UM00012802
NOVARTIS EXHIBIT 1017
Novartis v. Regents, IPR2023-01346
Page 1548 of 4460

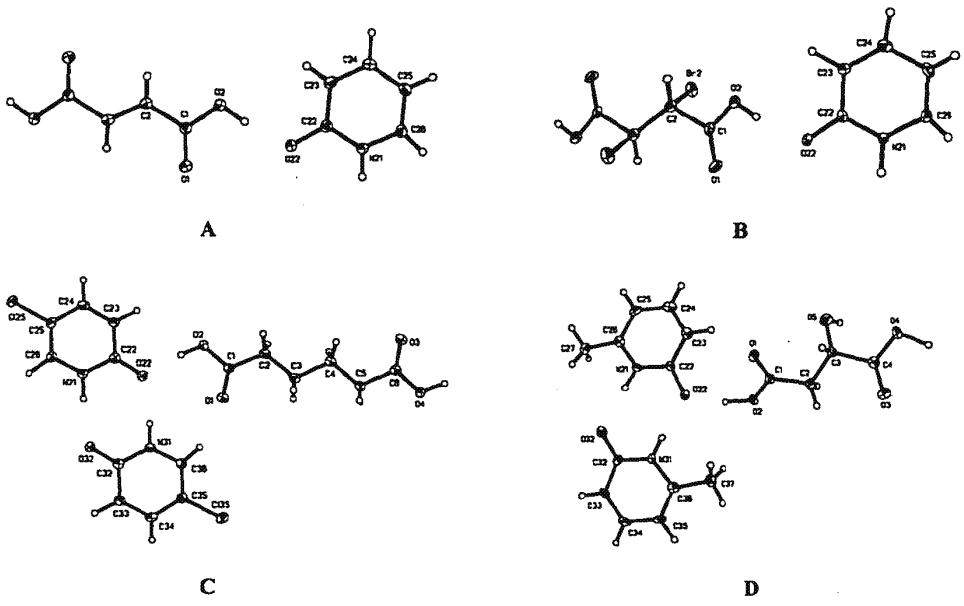


Figure 1. Molecular structure (30% ellipsoids) and labeling scheme (asymmetric unit only) for **1**–**4** (**A**–**D**, respectively).

Results

The reactions of 2-pyridone with fumaric acid and 2,3-dibromosuccinic acid, and the reaction of 5-chloro-2-pyridone with adipic acid and 6-methyl-2-pyridone with malic acid, result in co-crystals containing two pyridone molecules for each molecule of dicarboxylic acid. Structures **1** and **2** contain a dicarboxylic acid located on an inversion center, leading to an asymmetric unit consisting of one pyridone molecule and one half of a dicarboxylic acid. In **3** and **4** the asymmetric unit contains two pyridone molecules and one dicarboxylic acid. As expected, the pyridone (not the pyrid*ol*) tautomer is present in all structures, as evidenced by the exocyclic C–O bond distance (1.260–1.271 Å), which is considerably shorter than the C–O(H) bond distances noted in 6-chloro-2-hydroxypyridine (1.35 Å)[19] and 3-hydroxypyridine (1.32 Å).[20] Further support for the pyridone tautomer is provided by the location of the hydrogen atom on the pyridine nitrogen from a difference map in **1**–**3**.

In **1**, the two carboxylic acid moieties and the alkene unit of the acid backbone are coplanar, resulting in an overall planar conformation of fumaric acid. The 2-pyridone molecules form dimers via two symmetry-related N–H···O hydrogen bonds. Fumaric acid molecules link neighboring dimers through O–H···O and C–H···O hydrogen bonds, Fig. 2. These interactions lead to infinite dimer···acid···dimer···acid chains. Pyridone dimers and fumaric acid molecules within chains are co-planar, resulting in a flat one-dimensional ribbon. The ribbons are stacked parallel to each other in layers, and neighboring layers are related by ~80° rotation. There are no strong hydrogen bonds between neighboring chains in each layer or between adjacent layers.

In **2**, the molecular conformation of 2,3-dibromosuccinic acid is antiperiplanar with a 180° torsion angle of the carbon backbone. The near-planar carboxylic acid moieties are twisted slightly out of the plane of the carbon backbone, with torsion angle ∠[O(1)–C(1)–C(2)–C(2A)] = 25.7°. The 2-pyridone molecules assemble into dimers via symmetry-related N–H···O hydrogen bonds. As in **1**, the acid molecules link adjacent pyridone dimers together into infinite chains through two hydrogen bonds, O–H···O and C–H···O, Fig. 3. Pyridone dimers and the backbone of

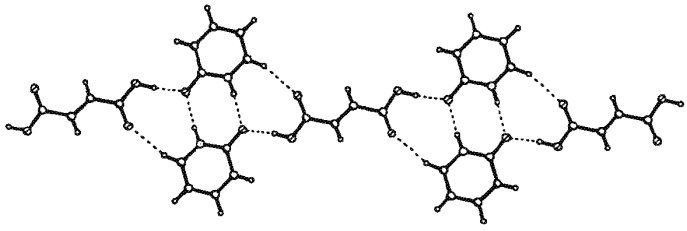


Figure 2. Hydrogen-bonded ribbon in **1**, with alternating fumaric acid molecules and 2-pyridone dimers.

UM00012803
NOVARTIS EXHIBIT 1017
Novartis v. Regents, IPR2023-01346
Page 1549 of 4460

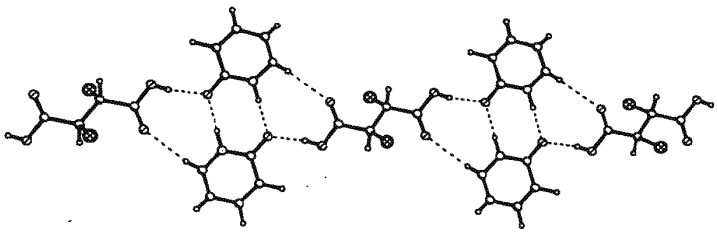


Figure 3. Hydrogen-bonded ribbon in **2**, where bromine atoms are above and below the plane of the ribbon.

2,3-dibromosuccinic acid molecules within chains are in the same plane resulting in a flat one-dimensional ribbon. Similar to **1**, these ribbons are stacked parallel in layers, and adjacent layers are nearly perpendicular, rotated by ~85°. As in **1**, there are no strong hydrogen bonds between neighboring ribbons.

The crystal structure of **3** is the only layered structure; the 5-chloro-2-pyridone dimers are formed via two equivalent N–H···O hydrogen bonds, and adipic acid molecules link these dimers (as in **1** and **2**) through two hydrogen bonds, O–H···O and C–H···O, into infinite ribbons, Fig. 4. However, these ribbons are further linked by C–H···O hydrogen bonds, Fig. 5, thereby generating an infinite layer. Adipic acid adopts an antiperiplanar conformation with a torsion angle of the carbon backbone close to 180°. The near-planar carboxylic moieties are slightly twisted out of the plane of the carbon backbone, with a torsion angle $\angle$[O(1)–C(1)–C(2)–C(3)] = 10.7°.

Compound **4** contains the expected 6-methyl-2-pyridone dimer formed via two complementary N–H···O hydrogen bonds, which are bridged by malic acid molecules to form ribbons similar to those in **1**–**3**. While the presence of the

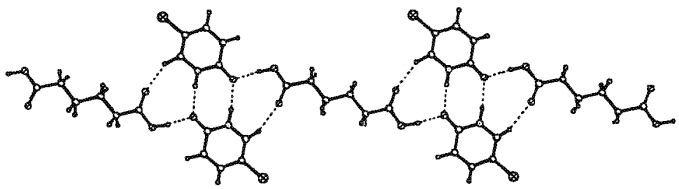


Figure 4. Hydrogen-bonded ribbon in **3**, exhibiting the same 1-D motif as in **1** and **2**.

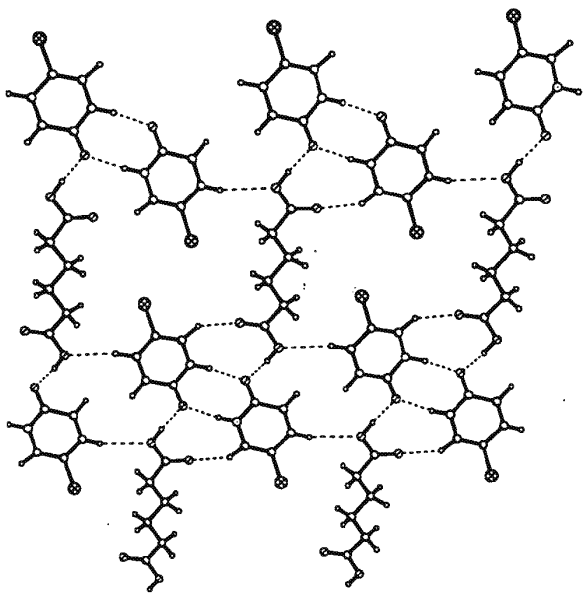


Figure 5. C–H···O hydrogen bonds link adjacent chains in **3**, forming a planar layer.

UM00012804
NOVARTIS EXHIBIT 1017
Novartis v. Regents, IPR2023-01346
Page 1550 of 4460

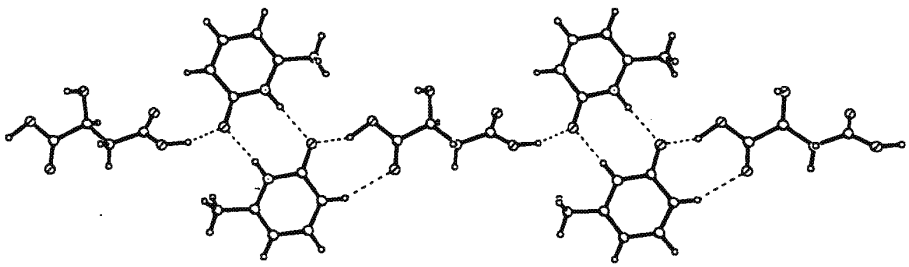


Figure 6. Hydrogen-bonded ribbon in 4; the C–H···O hydrogen bonds no longer bridge the pyridone dimers.

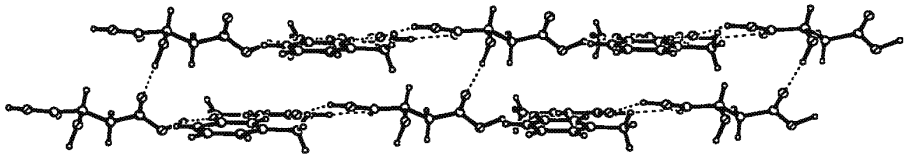


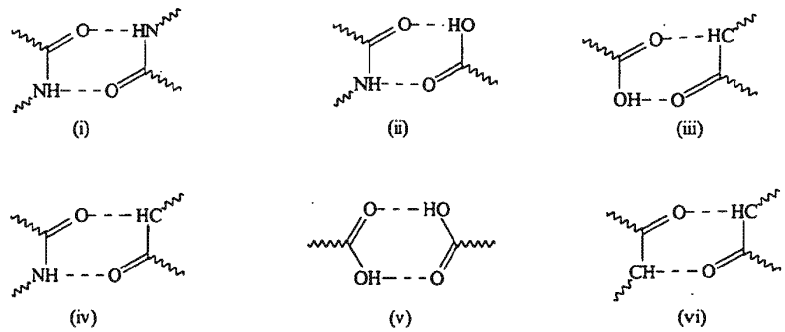
Figure 7. O–H···O hydrogen bonds link ribbons into infinite layers in 4.

pyridyl methyl group does not allow the formation of the same C–H···O hydrogen bond seen previously in **1–3**, the carbonyl group does link via a C–H···O hydrogen bond to the *same* pyridyl moiety, rather than across the pyridone dimer, Fig. 6. The ribbons are stacked to form layers, and the adjacent layers are oriented nearly perpendicular to each other, as in **1** and **2**. An additional hydrogen bond is formed between parallel ribbons: one of the carbonyl oxygen atoms is rotated out of the acid-pyridone plane to accept a hydrogen bond from the malic acid's hydroxyl group, Fig. 7. Thus these O–H···O hydrogen bonds link the ribbons to form a 2-D hydrogen bonded layer of ribbons.

Discussion

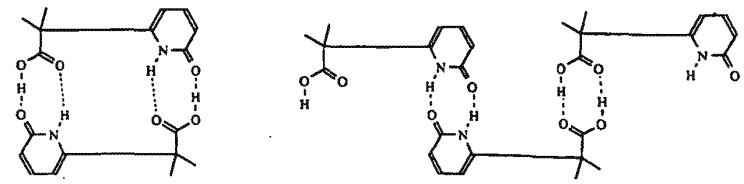
An integral part of useful intermolecular design is the ability to predict the structural outcome of a competition between two self-complementary moieties that can also form heteromeric dimers. The carboxylic acid and 2-pyridone groups represent two such moieties: both are known to form homomeric dimers, but they also have the potential to interact with each other. Thus the functional groups present in these molecules have the potential to engage in a range of possible $R_2^2(8)$ motifs, Scheme 2.

In an earlier study, the crystal structures of five co-crystals between 2-pyridone (un-substituted) and some aliphatic dicarboxylic acids (also un-substituted) revealed that the 1-D ribbon motif (formed by 2-pyridone dimers bridged by dicarboxylic acids) occurred in all cases. Likewise, regardless of substituents present on the 2-pyridone ring and on the acids, the four crystal structures **1–4** in the present study exhibit the same basic 1-D ribbon—the same 'supermolecule'. The self-complementarity of the 2-pyridone motif is not disrupted by the presence of a carboxylic acid moiety. The ribbon is generated by two strong hydrogen-bond interactions, N–H···O and O–H···O, both of which lie in the plane containing the two lone pairs of the amide oxygen atom. Within this plane, the H···O=C angles are very close to 120° in all four cases which demonstrates the directional preference of X–H···O (X=N, O) (contacts are directed towards the location of oxygen's two lone pairs). This geometric preference is in accordance with an earlier study of X-H···O (X=N,O) interactions



Scheme 2. Possible $R_2^2(8)$ motifs within co-crystals **1–4**.

UM00012805
NOVARTIS EXHIBIT 1017
Novartis v. Regents, IPR2023-01346
Page 1551 of 4460



Scheme 3. (A) Schematic representation of the molecular dimers 2,2-dimethyl-4-(2-oxo-1*H*-6-pyridyl)-3-butynoic acid.[25]; (B) hypothetical alternative motif of 2,2-dimethyl-4-(2-oxo-1*H*-6-pyridyl)-3-butynoic acid.

involving carbonyl oxygen atoms.[21] The recurrence of the acid-carbonyl hydrogen bond, O–H···O=C, should not be surprising, as it has been shown that in co-crystals of carboxylic acids and amides (2-pyridone can be considered a cyclic amide) the acid O–H tends to hydrogen bond to the amide oxygen atom.[22]

A search of the CSD[23] uncovered 59 non-ionic organic molecules or co-crystals that contain the 2-pyridone moiety. Of these, 47 structures (80%) exhibit pyridone–pyridone interactions (5 structures, including 2-pyridone itself, form catameric motifs, and 42, contain pyridone dimers). Eight co-crystals contain both a carboxylic acid and a 2-pyridone moiety.[24] Four of the structures exhibit the pyridone dimer with acids hydrogen bonded to the pyridone carbonyl oxygen atom (as in **1–4**), two show pyridone–pyridone dimers without additional hydrogen bonding to the acid, and two of these, for example 2,2-dimethyl-4-(2-oxo-1*H*-6-pyridyl)-3-butynoic acid[25] (**I**, Scheme 3) give an acid-pyridone heteromeric dimer (ii, Scheme 2). The structure of **I** contains dimers held together by two pyridone-acid interactions, Scheme 3A. However, the formation of molecular dimers connected by two homomeric interactions is precluded due to the positioning of the pyridone moiety, so this option is not available (although it is possible to envisage chains of molecules, Scheme 3B).

The results of the CSD search indicate that the 2-pyridone self-complementary interaction is a particularly reliable motif, and often persists even in the presence of other good hydrogen bond donors and acceptors. In fact, the dominant feature of the materials in the present study is the reliability of the 2-pyridone dimer irrespective of the nature of the co-crystalizing acid; i.e. the presence of substituents on either the acid or the pyridone ring does not perturb the formation of this dimer. However the choice of acid can affect how these dimers are arranged in the lattice with respect to each other, either herringbone as in **1**,**2** and **4** or coplanar as in **3**. This observation is consistent with that of the previous study on the unsubstituted system.

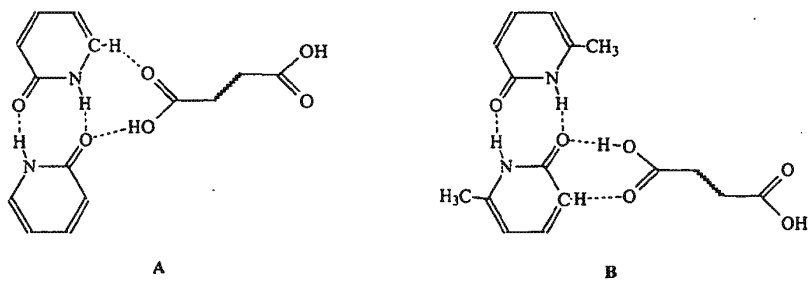
While the positioning of the substituents does not affect the formation of the dimer, it can be used to subtly modify the bridging motif of the acid group. In **4**, a methyl substituent in the six position precludes the formation of the usual hydrogen bonded chain, Scheme 4A. Instead the acid hydrogen bonds with the C–H moiety adjacent to the C=O moiety, Scheme 4B. Furthermore, substituents on the acid moiety do not affect the formation of the dimer···acid··· dimer···acid chains in **2** and **4**. Also in **4**, the chains are linked into layers via an O–H···O hydrogen bond from the hydroxyl group of the (*S*)-malic acid molecules to the carbonyl oxygen atoms of (*S*)-malic acid molecules in the chains below thereby stabilizing the layers.

Apparantly a combination of the size of the acid and substituents on the acid and/or the pyridone ring can be used to alternate between the layered structure observed in **3** (which is also observed with the 2-pyridone oxalic acid 2/1 co-crystal in the previous study[17]) and the dominant motif, the perpendicular layers observed in **1**, **2** and **4**.

Experimental

Preparation of 2-pyridone fumaric acid (2/1), 1

2-Pyridone (0.20 g, 2.22 mmol) and fumaric acid (0.26 g, 2.22 mmol) were dissolved together in a hot water–ethanol (1:1) mixture (50 ml). Colorless, rectangular prism-like crystals were formed after four weeks upon evaporation of the solvent (mp 217–219°C).



Scheme 4. Schematic of two possible hydrogen-bonding motifs for 2-pyridone dimers and dicarboxylic acids.

UM00012806
NOVARTIS EXHIBIT 1017
Novartis v. Regents, IPR2023-01346
Page 1552 of 4460

Table 1. Data collection and refinement for 1–4

Crystal data	1	2	3	4
Empirical formula	$C_7H_7NO_3$	$C_7H_7NO_3Br$	$C_{16}H_{18}N_2O_6Cl_2$	$C_{16}H_{20}N_2O_7$
CCDC deposit no.				
MW	153.14	233.05	405.22	352.34
Crystal size (mm)	0.4×0.2× 0.2	0.58×0.46×0.45	0.46×0.44×0.28	0.44×0.16×0.14
Crystal system	Monoclinic	Monoclinic	Triclinic	Orthorhombic
Space group	P2(1)/n	P2(1)/c	P-1	P2(1)2(1)2(1)
a (Å)	8.636 (1)	12.220 (2)	8.031 (1)	5.187 (1)
b (Å)	5.0337 (5)	4.854 (2)	10.503 (2)	9.727 (1)
c (Å)	16.473 (1)	14.367 (3)	12.269 (1)	32.812 (5)
α (°)	90	90	65.64 (1)	90
β (°)	96.135 (6)	103.10 (1)	83.53 (1)	90
γ (°)	90	90	77.62 (1)	90
Volume (Å^3)	712.0 (1)	830.0 (4)	920.5 (2)	1655.5 (4)
Z	4	4	2	4
D_{calc} (g cm^{-3})	1.429	1.865	1.462	1.414
F(000)	320	460	420	744
μ, Mo-K_α (mm^{-1})	0.113	4.917	0.388	0.112
Temperature (K)	173 (2)	173 (2)	173 (2)	153 (2)
Goodness of fit	1.053	1.171	1.012	1.044
R/R_w^2 (obs. data)	0.0313/0.0813	0.0250/0.0635	0.0331/0.1136	0.0678/0.1348
R/R_w^2 (all data)	0.0395/0.0875	0.0275/0.0648	0.0420/0.1248	0.1501/0.1699

Preparation of 2-pyridone meso-2,3-dibromosuccinic acid (2/1), 2

2-Pyridone (0.10 g, 1.05 mmol) was dissolved in a hot water–ethanol (1:1) mixture (50 ml) together with *meso*-2,3-dibromosuccinic acid (0.29 g, 1.05 mmol). Rectangular prism-like, colorless crystals were formed after three weeks upon evaporation of the solvent (mp 163–165°C).

Preparation of 5-chloro-2-pyridone adipic acid (2/1), 3

5-Chloro-2-pyridone (0.20 g, 2.22 mmol) and adipic acid (0.23 g, 2.22 mmol) were dissolved together in a hot water–ethanol (1:1) mixture (50 cm^3). Rectangular prism-like crystals were obtained after four weeks upon evaporation of the solvent (mp 125–127°C).

Preparation of 6-methyl-2-pyridone (*S*)-malic acid (2/1), 4

Malic acid (0.355 g: 2.65 mM) and 6-methyl-2-pyridone (0.294 g; 2.69 mM) were dissolved in hot ethanol (30 cm^3). The solution was allowed to cool, whereupon a white solid was formed. The solid was collected and recrystallised from ethanol (40 cm^3). Colorless needle-like crystals appeared upon slow evaporation of the solvent.

X-Ray crystallography

Crystal data were collected using a Siemens P4 four-circle diffractometer with graphite monochromated Mo-Kα radiation. Hydrogen-atom positions were located from difference Fourier maps, except for **4**, in which non-acid or -hydroxy hydrogen atoms were placed at calculated positions, and a riding model with fixed thermal parameters [u_{ij}=1.2U_{ij}(eq) for the atom to which they are bonded] was used for subsequent refinements. The SHELXTL PC and SHELXL-93 packages were used for data reduction and structure solution and refinement.[18] Table 1 contains crystallographic details and Fig. 1 displays labeling schemes and thermal ellipsoids for **1–4**.

Acknowledgements

We acknowledge financial support from NSF-EPSCoR (OSR-9550487), DuPont, and Kansas State University.

References

1. Desiraju, G. R. *Crystal Engineering: The Design of Organic Solids*, Elsevier: Amsterdam, 1989.
2. Lehn, J.-M. *Supramolecular Chemistry*, VCH: Weinheim, 1995.
3. Aakeröy, C. B. *Acta Crystallogr.* **1997**, *B53*, 569.
4. *Perspectives in Supramolecular Chemistry*, Desiraju, G. R., Ed.; Wiley: Chichester, 1995; Vol. 2.
5. Crystal engineering: From molecules and crystals to materials, A NATO Advanced Study Institute and a Euroconference, Erice, Italy, 1999.
6. Lehn, J.-M. *Angew. Chem. Int. Ed. Engl.* **1990**, *29*, 1304.
7. Garcia-Tellado, F.; Geib, S. J.; Goswami, S.; Hamilton, A. D. *J. Am. Chem. Soc.* **1991**, *113*, 265; Fan, E.; Vincent, C.; Geib, S. J.; Hamilton, A. D. *Chem. Mater.* **1994**, *6*, 1113.
8. Coe, S.; Kane, J. J.; Nguyen, T. L.; Toledo, L. M.; Wininger, E.; Fowler, F. F.; Lauher, J. W. *J. Am. Chem. Soc.* **1997**, *119*, 119.
9. Palmore, G. T. R.; McBride, M. T. *Chem. Commun.* **1998**, 145.
10. Ermer, O.; Eling, A. *J. Chem. Soc. Perkin Trans. 2* **1994**, 925.
11. Ducharme, Y.; Wuest, J. D. *J. Org. Chem.* **1988**, *53*, 5787.
12. Simard, M.; Su, D.; Wuest, J. D. *J. Am. Chem. Soc.* **1991**, *113*, 4696.
13. Penfold, B. R. *Acta Crystallogr.* **1953**, *6*, 591.
14. Leiserowitz, L. *Acta Crystallogr.* **1976**, *B32*, 775.
15. For information about graph-set notation, see Etter, M. C.; MacDonald, J. C.; Bernstein, J. *Acta Crystallogr.*, **1990**, *B46* 256.
16. Bernstein, J.; Davis, R. E. private communication.
17. Aakeröy, C. B.; Beatty, A. M.; Zou, M. *Cryst. Eng.* **1998**, *1*, 225.
18. Sheldrick, G. M. SHELXL-93, University of Göttingen.
19. Kvick, A.; Olovsson, I. *Ark. Kemi* **1969**, *30*, 71.
20. Ohms, U.; Guth, H.; Treutmann, W. *Kristallogr.* **1982**, *99*, 159.
21. Murray-Rust, P.; Glusker, J. P. *J. Am. Chem. Soc.* **1984**, *106*, 1018.

UM00012807
NOVARTIS EXHIBIT 1017
Novartis v. Regents, IPR2023-01346
Page 1553 of 4460

22. Bernstein, J.; Etter, M. C.; Leiserowitz, L. In *Structure Correlation*, Burgi, H.-B., Dunitz, J. D., Eds.; VCH: Weinheim, 1994; Vol. 2, p 431.
23. Allen, F. H.; Kennard, O. *Chemical Design and Automation News* **1993**, *8*, 3137 (CSD version 5.17).
24. CSD reference codes: POVFIP, RAGJIS, TAFCUY, VOCHIE, VOJFAB, VOJFEF, YINJOU, YINJUA.
25. Walsh, P. L.; Maverick, E.; Chiefari, J.; Lightner, D. A. *J. Am. Chem. Soc.* **1997**, *119*, 3802.

UM00012808
NOVARTIS EXHIBIT 1017
Novartis v. Regents, IPR2023-01346
Page 1554 of 4460

ELSEVIER

Journal of Molecular Structure 474 (1999) 91–101

Journal of
MOLECULAR
STRUCTURE

Pitfalls in the supramolecular assembly of silver(I) coordination compounds

Christer B. Aakeröy*, Alicia M. Beatty

Department of Chemistry, Kansas State University, Manhattan, KS 66506, USA

Received 17 December 1997; received in revised form 5 May 1998; accepted 5 May 1998

Abstract

The syntheses and crystal structures of (6-methylnicotinic acid) (6- methylnicotinato)silver(I), di (6-methylnicotinic acid) silver(I) nitrate, (2-chloro-6-methylnicotinato) silver(I), di (2-chloro-6-methylnicotinic acid) silver(I) nitrate, and (2-methylnicotinic acid) (2-methylnicotinato) silver(I) are described. These coordination complexes were synthesized under the same conditions and with very similar ligands but their resulting structures are quite different, in part due to the degree of protonation of the nicotinic acid ligand(s). The structures vary from coordination polymers to hydrogen-bonded coordination dimers, to linear structures linked by anion–carboxylic acid hydrogen bonds. This study illustrates some of the difficulties involved in predicting hydrogen-bonded networks in transition-metal systems which contain carboxylic acid moieties and coordinatively unsaturated metal ions. © 1998 Elsevier Science B.V. All rights reserved.

Keywords: Coordination polymers; Crystal engineering; Hydrogen bonding; Nicotinic acid; Silver complexes

1. Introduction

The predictable and controlled assembly of molecules and ions in the solid state is one of the primary goals of crystal engineering, and the last decade has seen the arrival of several useful tools for synthesizing supramolecular assemblies [1–5]. The hydrogen bond is arguably the most effective intermolecular connector, and hydrogen-bonded motifs such as carboxylic acid dimers and amide–amide ribbons have been utilized in the design of extended assemblies in organic molecular solids [6–17]. More recently, intermolecular assembly of metal complexes via hydrogen bonding has gained attention, where, rather than forming the more common coordination polymers using covalent interactions [18–25], neighboring metal complexes are connected and oriented through ligand–ligand hydrogen bonds [26–28]. For example, Mingos has used molecular recognition strategies to connect neighboring transition-metal complexes as well as to link metal complexes to organic molecules using complementary hydrogen-bonding groups [29,30].

Recently we employed various nicotinamide ligands in the assembly of silver(I) complexes, where the pyridine nitrogen atom provides a coordinate covalent interaction with the silver ion. The geometry encoded in these linear silver(I) complexes was then propagated in a predictable manner via amide–amide hydrogen bonds between neighboring cations [31–33]. The presence of substituents on the pyridine ring did not have a great effect on the overall

* Corresponding author. Tel.: 00 1 913 532 6096; Fax: 00 1 913 532 6666; e-mail: aakeroy@ksu.edu.

0022-2860/98/$ - see front matter © 1998 Elsevier Science B.V. All rights reserved.
PII: S0022-2860(98)00563-8

UM00012809
NOVARTIS EXHIBIT 1017
Novartis v. Regents, IPR2023-01346

structure, but the nature of the counterion could significantly influence the assembly and orientation of the cationic motifs.

Now we wish to examine whether nicotinic acid, the carboxylic acid analog of nicotinamide, can be used as a reliable connector in the assembly of transition-metal complexes. Carboxylic acid and carboxylate moieties have a well-known ability to generate hydrogen-bonded motifs in organic molecular and ionic solids [34]. Therefore, a potential advantage of a nicotinic acid–nicotinate ligand system would be that a carboxylate moiety can eliminate the need for a counterion in metal complexes, thereby avoiding the structural interference induced by the chemical and steric demands of a counterion. A possible disadvantage of these ligands is that the carboxylate moiety may compete with the pyridine nitrogen atom for the metal center, which would interfere with the design strategy. There is a precedent for using analogs of nicotinic acid in metal complexes: the structure of a silver(I)-*iso*-nicotinic acid complex has been reported [35], where (*iso*-nicotinic acid)-(*iso*-nicotinato) silver(I) tetrahydrate forms a linear complex, with two ligands coordinated through the pyridine nitrogen atoms to silver(I). The complex has no counterion; rather, one of the ligands has lost a proton, and exists as the *iso*-nicotinate. Therefore, an intermolecular hydrogen bond (between the carboxylic acid unit of one complex and the carboxylate unit of a neighboring complex) results in an infinite chain of silver complexes. In contrast, (nicotinato) silver(I) is a coordination polymer in which the pyridine nitrogen atom and both carboxylate oxygen atoms are coordinated to silver ions, resulting in polymeric sheets [36].

We want to establish whether we can reliably use the carboxylic acid as an intermolecular connector in metal complexes, and to probe this in some detail by attaching substituents on the pyridine ring. To this end, we obtained the X-ray single crystal structures of five new silver(I) complexes: (6-methylnicotinic acid) (6- methylnicotinato) silver(I), **1**; di (6-methylnicotinic acid) silver(I) nitrate, **2**; (2-chloro-6-methylnicotinato) silver(I), **3**; di (2-chloro-6-methylnicotinic acid) silver(I) nitrate, **4**; and (2- methylnicotinic acid) (2-methylnicotinato) silver(I), **5**.

2. Experimental

2.1. Preparation of (6-methylnicotinic acid) (6-methylnicotinato) silver(I), 1, and di (6-methylnicotinic acid) silver(I) nitrate, 2

Silver nitrate (0.10 g, 0.59 mmol) was dissolved in 20 ml of a 1:1 ethanol:water mixture. To this solution was added 0.16 g (1.2 mmol) 6-methylnicotinic acid dissolved in 40 ml of a 1:1 ethanol:water mixture. The solution was briefly stirred, the solvent was allowed to evaporate slowly at ambient temperature, and single crystals of **1** were formed in solution as colorless prisms. The solvent was then allowed to evaporate to dryness at ambient temperature, and single crystals of **2** were formed as colorless prisms.

2.2. Preparation of (2-chloro-6-methylnicotinato) silver(I), 3, and di (2-chloro-6-methylnicotinic acid) silver(I) nitrate, 4

Silver nitrate (0.10 g, 0.59 mmol) was dissolved in 20 ml of a 1:1 ethanol:water mixture. To this solution was added 0.20 g (1.2 mmol) 2-chloro-6-methylnicotinic acid dissolved in 40 ml of a 1:1 ethanol water mixture. The solution was briefly stirred, the solvent was allowed to evaporate slowly at ambient temperature, and single crystals of **3** were formed in solution as colorless prisms. The solvent was then allowed to evaporate to dryness at ambient temperature, yielding single crystals of **4** as colorless rods.

2.3. Preparation of (2-methylnicotinic acid) (2-methylnicotinato) silver(I), 5

Silver nitrate (0.10 g, 0.59 mmol) was dissolved in 20 ml of a 1:1 ethanol:water mixture. To this solution was added 0.16 g (1.2 mmol) 2-methylnicotinic acid dissolved in 40 ml of a 1:1 ethanol:water mixture. The mixture was briefly stirred, and the solution was allowed to evaporate slowly at ambient temperature. Single crystals of **5** were formed in solution as colorless prisms.

2.4. X-ray crystallography

Single-crystal diffraction data were collected using a Siemens P4 four-circle diffractometer with graphite monochromated Mo–Kα (λ = 0.71073 Å) radiation.

UM00012810
NOVARTIS EXHIBIT 1017
Novartis v. Regents, IPR2023-01346
Page 1556 of 4460

Table 1
Data collection and refinement for **1–5**

Crystal data	1	2	3	4	5
Empirical formula	$C_{14}H_{13}N_2O_4Ag$	$C_{14}H_{14}N_3O_7Ag$	$C_7H_5NO_3ClAg$	$C_{14}H_{12}N_3O_7Cl_2Ag$	$C_{14}H_{13}N_2O_4Ag$
M_w	381.13	444.15	278.44	513.04	381.13
Crystal size (mm)	0.43 × 0.24 × 0.18	0.40 × 0.37 × 0.29	0.42 × 0.18 × 0.10	0.48 × 0.36 × 0.36	0.42 × 0.34 × 0.28
Crystal system	monoclinic	monoclinic	monoclinic	monoclinic	triclinic
Space group	*C*2	*C*2/*c*	*C*2/*c*	*C*2/*c*	*P*-1
a (Å)	11.484(2)	14.054(2)	12.856(1)	8.4333(5)	8.068(7)
b (Å)	10.367(1)	7.666(1)	11.419(1)	13.525(1)	8.093(1)
c (Å)	11.488(2)	16.499(2)	10.877(1)	15.533(9)	11.353(1)
α (deg)					73.909(7)
β (deg)	95.16(1)	111.775(7)	90.560(1)	99.714(3)	72.926(6)
γ (deg)					70.746(6)
Volume (Å^3)	1362.3(3)	1650.8(4)	1596.7(2)	1746.3(2)	655.5(1)
Z	4	8	8	8	2
D_{calc} (g cm^{-1})	1.858	1.787	2.317	1.951	1.931
F(000)	760	888	1072	1016	380
μ(Mo–K$_α$) (mm^{-1})	1.497	1.264	2.809	1.505	1.555
Temperature (K)	173	173	173	173	173
θ range (deg.)	1.78–22.49	2.66–23.50	2.39–22.50	2.66–22.48	1.92–25.00
Range h	− 12 to 1	− 15 to 0	− 13 to 13	− 1 to 9	− 1 to 9
Range k	− 11 to 1	0 to 8	− 12 to 1	− 14 to 1	− 9 to 9
Range l	− 12 to 12	− 17 to 18	− 11 to 1	− 16 to 16	− 13 to 13
Reflections collected	1266	1274	1383	1575	2843
Unique reflections	1077	1217	1039	1148	2309
Observed reflections ($I > 2σI$)	1049	1149	954	1100	2209
Observed data:parameter	5.5	9.99	8.67	8.80	11.6
Refinement	full-matrix least squares on F^2	full-matrix least squares on F^2	full-matrix least squares on F^2	full-matrix least squares on F^2	full-matrix least squares on F^2
R/R_w^2 (obs data)	0.0190/0.0529	0.0233/0.0571	0.0464/0.1357	0.0194/0.0511	0.0224/0.0574
R/R_w^2 (all data)	0.0201/0.0536	0.0257/0.0584	0.0544/0.1556	0.0204/0.0517	0.0238/0.0582
$Δρ_{max/min}$ (eÅ^{-3})	0.365/ − 0.334	0.436/ − 0.470	1.837/ − 1.463	0.416/ − 0.316	0.674/ − 0.786
S	1.138	1.060	1.330	1.265	1.175
Weighting function variables	$g_1 = 0.0345$ $g_2 = 2.1056$	$g_1 = 0.0332$ $g_2 = 3.5710$	$g_1 = 0.000$ $g_2 = 115.2909$	$g_1 = 0.0239$ $g_2 = 2.6770$	$g_1 = 0.0276$ $g_2 = 0.7221$

UM00012811

NOVARTIS EXHIBIT 1017
Novartis v. Regents, IPR2023-01346
Page 1557 of 4460

Table 2
Atomic coordinates (× 10^4) and equivalent isotropic displacement parameters (Å × 10^3) for **1**

	x	y	z	U(eq)
Ag(1)	14 680(1)	5015(1)	7867(1)	28(1)
N(1)	14 153(4)	6965(1)	8361(4)	19(1)
N(21)	15 751(4)	3533(5)	7079(4)	21(1)
O(7A)	11 918(4)	9302(5)	10914(4)	39(1)
O(7B)	12 794(4)	7464(5)	11535(3)	29(1)
O(27A)	17 105(4)	2210(4)	3480(3)	28(1)
O(27B)	16 845(4)	4312(4)	3810(3)	28(1)
C(2)	13 677(5)	7128(6)	9380(5)	21(1)
C(3)	13 183(5)	8284(6)	9691(5)	19(1)
C(4)	13 195(5)	9306(6)	8915(5)	24(1)
C(5)	13 706(5)	9153(6)	7877(5)	23(1)
C(6)	14 165(5)	7966(6)	7619(5)	22(1)
C(7)	12 584(5)	8382(6)	10812(5)	23(1)
C(8)	14 694(6)	7727(7)	6474(5)	30(2)
C(22)	16 114(4)	3779(6)	6001(5)	20(1)
C(23)	16 535(5)	2826(6)	5314(5)	18(1)
C(24)	16 621(5)	1591(6)	5749(5)	26(1)
C(25)	16 311(5)	1344(6)	6851(5)	26(2)
C(26)	15 861(5)	2319(6)	7500(5)	20(1)
C(27)	16 852(5)	3178(6)	4110(5)	20(1)
C(28)	15 451(5)	2090(7)	8672(5)	26(1)
H(27)	17 290(4)	2355(4)	2638(3)	34
H(2)	13 648(5)	6277(6)	9767(5)	25
H(4)	12 858(5)	10 039(6)	9166(5)	29
H(5)	13 667(5)	10 017(6)	7187(5)	28
H(8A)	14 264(6)	6964(7)	5993(5)	36
H(8B)	14 637(6)	8470(7)	6001(5)	36
H(8C)	15 385(6)	7441(7)	6801(5)	36
H(22)	15 943(4)	4996(6)	5823(5)	24
H(24)	17 015(5)	942(6)	5427(5)	31
H(25)	16 499(5)	519(6)	7210(5)	32
H(28A)	15 870(5)	1386(7)	9010(5)	32
H(28B)	14 792(5)	1976(7)	8790(5)	32
H(28C)	15 536(5)	2931(7)	9195(5)	32

Crystal stabilities were monitored by measuring three standard reflections after every 97 reflections, with no significant decay observed. Cell parameters were obtained from 35 accurately centered reflections in the 2θ range 10–25. Data were collected using a θ–2θ scanning technique, Lorentz, polarization and Psi-scan absorption corrections were applied. The structures were solved using Patterson methods, with the remaining non-hydrogen atoms found by successive full-matrix least-squares refinement on F^2 and refined with anisotropic thermal parameters. Hydrogen atom positions were located from difference Fourier maps; and a riding model with fixed thermal parameters

Table 3
Atomic coordinates (× 10^4) and equivalent isotropic displacement parameters (Å × 10^3) for **2**

	x	y	z	U(eq)
Ag(1)	0	6497(1)	2500	24(1)
N(1)	455(2)	6617(3)	3903(2)	21(1)
N(2)	5000	2542(5)	7500	27(1)
O(7B)	3254(2)	4437(3)	5439(1)	39(1)
O(7A)	3035(2)	5345(3)	6642(1)	38(1)
O(1)	4176(2)	1774(3)	7330(2)	34(1)
O(2)	5000	4209(4)	7500	41(1)
C(2)	1353(2)	5896(4)	4401(2)	22(1)
C(3)	1727(2)	5941(4)	5301(2)	21(1)
C(4)	1136(2)	6748(4)	5707(2)	24(1)
C(5)	206(2)	7458(4)	5198(2)	24(1)
C(6)	− 123(2)	7396(4)	4295(2)	21(1)
C(7)	2742(2)	5141(4)	5789(2)	25(1)
C(8)	− 1126(2)	8164(4)	3719(2)	32(1)
H(7)	3594(2)	4931(3)	6902(1)	45
H(2)	1791(2)	5333(4)	4079(2)	26
H(4)	1411(2)	6700(4)	6335(2)	28
H(5)	− 214(2)	8055(4)	5439(2)	29
H(8A)	− 1602(2)	8544(4)	4008(2)	38
H(8B)	− 999(2)	9165(4)	3388(2)	38
H(8C)	− 1373(2)	7277(4)	3295(2)	38

Table 4
Atomic coordinates (× 10^4) and equivalent isotropic displacement parameters (Å × 10^3) for **3**

	x	y	z	U(eq)
Ag(1)	4491(1)	5776(1)	1317(1)	21(1)
Cl(1)	2083(3)	2471(3)	2264(3)	29(1)
N(1)	927(8)	2710(9)	4187(10)	20(3)
O(7A)	3911(7)	5075(9)	4267(9)	28(2)
O(7B)	3393(7)	4575(8)	2385(8)	23(2)
C(2)	1746(10)	3180(11)	3624(12)	17(3)
C(3)	2312(10)	4131(11)	4062(12)	17(3)
C(4)	1942(10)	4628(12)	5162(12)	22(3)
C(5)	1050(11)	4187(12)	5682(13)	25(3)
C(6)	557(10)	3210(12)	5199(13)	22(3)
C(7)	3306(10)	4607(12)	3517(13)	20(3)
C(8)	− 361(11)	2663(14)	5780(14)	32(4)
H(4)	2309(10)	5268(12)	5539(12)	27
H(5)	759(11)	4566(12)	6387(13)	30
H(8A)	− 581(11)	1997(14)	5306(14)	38
H(8B)	− 176(11)	2416(14)	6597(14)	38
H(8C)	− 918(11)	3221(14)	5818(14)	38

UM00012812
NOVARTIS EXHIBIT 1017
Novartis v. Regents, IPR2023-01346
Page 1558 of 4460

Table 5
Atomic coordinates (× 10^4) and equivalent isotropic displacement parameters (Å × 10^3) for 4

	x	y	z	U(eq)
Ag(1)	10 000	1285(1)	7500	27(1)
Cl(1)	7416(1)	1164(1)	8696(1)	30(1)
N(1)	10 497(3)	1191(2)	8930(1)	21(1)
N(2)	5000	1385(2)	12500	26(1)
O(7A)	8550(3)	1252(2)	11 616(1)	36(1)
O(7B)	6667(2)	1444(2)	10 439(1)	35(1)
O(1)	5000	483(2)	12500	52(1)
O(2)	6281(2)	1868(2)	12 499(1)	32(1)
C(2)	9269(3)	1222(2)	9369(2)	22(1)
C(3)	9436(3)	1260(2)	10 271(2)	21(1)
C(4)	11 016(3)	1255(2)	10 728(2)	25(1)
C(5)	12 303(3)	1221(2)	10 280(2)	27(1)
C(6)	12 020(3)	1196(2)	9383(2)	24(1)
C(7)	8062(3)	1329(2)	10 766(2)	24(1)
C(8)	13 342(3)	1168(2)	8853(2)	31(1)
H(7)	7792(3)	1340(2)	11 909(1)	43
H(4)	11 189(3)	1224(2)	11 396(2)	30
H(5)	13 424(3)	1246(2)	10 608(2)	32
H(8A)	13 308(3)	1793(2)	8392(2)	38
H(8B)	13 352(3)	593(2)	8492(2)	38
H(8C)	14 136(3)	1237(2)	9092(2)	38

Table 6
Atomic coordinates (× 10^4) and equivalent isotropic displacement parameters (Å × 10^3) for 5

	x	y	z	U(eq)
Ag(1)	3496(1)	1496(1)	2693(1)	29(1)
N(1)	2228(3)	− 678(3)	3503(2)	19(1)
N(21)	5358(3)	3138(3)	1723(2)	16(1)
O(7A)	− 3235(2)	− 2169(3)	5179(2)	27(1)
O(7B)	− 2441(2)	− 1864(3)	3111(2)	22(1)
O(27A)	9991(2)	2308(2)	− 1251(2)	21(1)
O(27B)	9052(3)	5211(3)	− 2063(2)	29(1)
C(2)	575(3)	− 631(3)	3422(2)	15(1)
C(3)	− 278(3)	− 1920(3)	4206(2)	15(1)
C(4)	576(3)	− 3221(3)	5093(2)	19(1)
C(5)	2297(4)	− 3292(3)	5128(2)	23(1)
C(6)	3078(3)	− 1999(4)	4317(2)	23(1)
C(7)	− 2128(3)	− 1970(3)	4180(2)	17(1)
C(8)	− 279(4)	897(3)	2489(2)	21(1)
C(22)	6559(3)	2890(3)	636(2)	15(1)
C(23)	7602(3)	4093(3)	10(2)	14(1)
C(24)	7392(3)	5534(3)	533(2)	19(1)
C(25)	6204(3)	5722(3)	1678(2)	20(1)
C(26)	5206(3)	4513(3)	2237(2)	20(1)
C(27)	8957(3)	3903(3)	− 1216(2)	17(1)
C(28)	6699(3)	1291(3)	150(2)	20(1)
H(27)	11 056(2)	2055(2)	− 1992(2)	25
H(4)	− 50(3)	− 4035(3)	5597(2)	23
H(5)	2832(4)	− 4166(3)	5817(2)	28
H(6)	4241(3)	− 1952(4)	4424(2)	27
H(8A)	164(4)	613(3)	1605(2)	25
H(8B)	− 1608(4)	1202(3)	2795(2)	25
H(8C)	5(4)	1949(3)	2405(2)	25
H(24)	8112(3)	6485(3)	− 11(2)	22
H(25)	6007(3)	6728(3)	1977(2)	24
H(26)	4342(3)	4606(3)	3020(2)	24
H(28A)	7761(3)	289(3)	384(2)	24
H(28B)	6892(3)	1584(3)	− 819(2)	24
H(28C)	5617(3)	859(3)	576(2)	24

[u_{ij} = $1.2U_{ij}$(eq) for the atom to which they are bonded] was used for subsequent refinements. The weighting function applied was $w^{-1} = [\sigma^2(F_o^2) + (g_1P)^2 + (g_2P)]$ where $P = (F_o^2 + 2F_c^2)/3$. The SHELXTL PC and SHELXL-93 packages were used for data reduction and structure solution and refinement [37], and the crystallographic details for compounds **1–5** are listed in Table 1. Fractional atomic coordinates for compounds **1–5**1 are listed in Tables 2–6, respectively.

3. Results

The reaction of silver(I) nitrate with two equivalents of 6-methylnicotinic acid leads to the formation of (6-methylnicotinic acid) (6-methylnicotinato) silver(I), **1** (Fig. 1), where the coordination around the silver ion is approximately linear; ∠N(1)–Ag(1)–N(2I), 156.9°. The asymmetric unit contains one (6-methylnicotinic acid) (6- methylnicotinato) silver(I) complex. With two oxygen atoms in close proximity (≈ 2.5 Å), the silver ion is perhaps most accurately described as being four-coordinate (Table 7, Fig. 1). In addition to the coordinate covalent bonds, an O–H...O hydrogen bond exists between neighboring carboxylic acid and carboxylate units [*r*H(27)...O(7B), 1.445(5) Å; *r*O(27A)...O(7B), 2.451(5) Å; ∠O(27A)-H(27)...O(7B), 167.9(2)°] (Fig. 2). Although the interaction leads to an infinite chain, the structure is dominated by the Ag–N, Ag–O interactions, forming a coordination polymer that extends in three dimensions.

Further evaporation of the solution which yielded **1** results in the formation of single crystals of di (6-methylnicotinic acid) silver(I) nitrate **2** (Fig. 3), where the cationic complex contains a silver ion

UM00012813
NOVARTIS EXHIBIT 1017
Novartis v. Regents, IPR2023-01346
Page 1559 of 4460

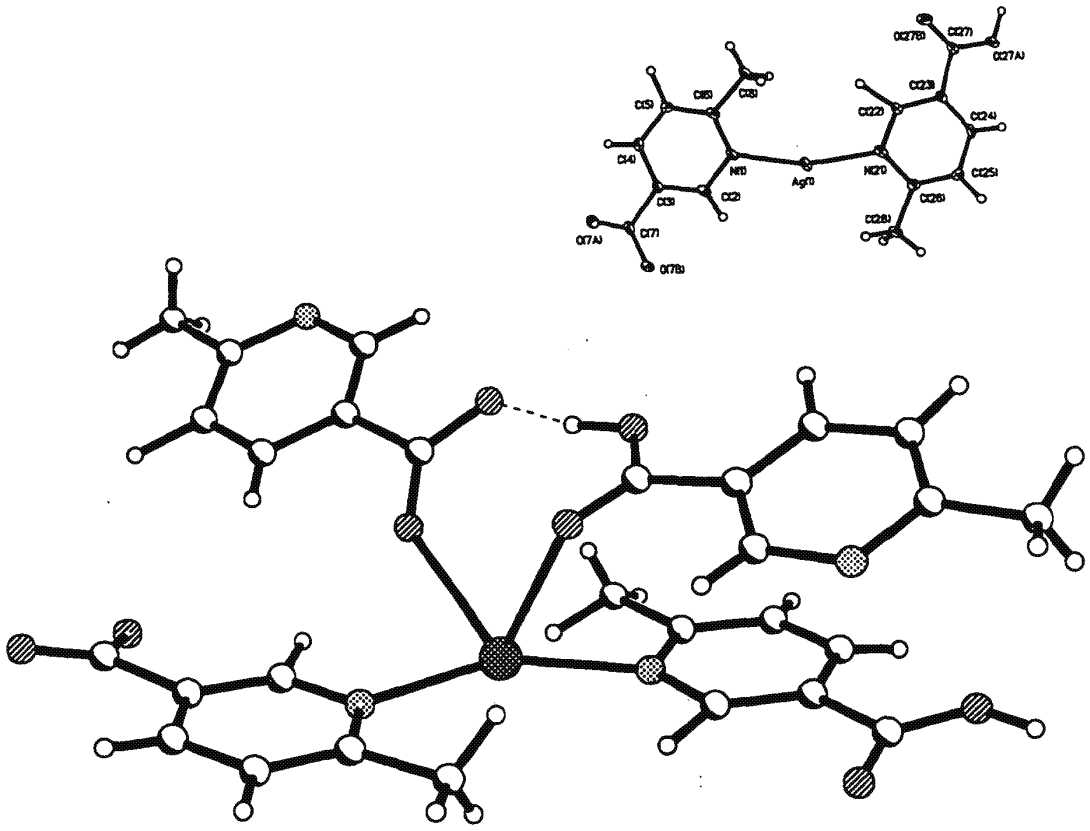


Fig. 1. The coordination geometry about the silver ion in the coordination polymer in **1**. The inset shows the asymmetric unit of **1** with labeling scheme.

Table 7
283Selected bond lengths (Å) and angles (°) for **1**[a]

Ag(1)–N(1)	2.199(5)
Ag(1)–N(21)	2.213(5)
Ag(1)–O(7A)	2.517(4)
Ag(1)–O(27B)	2.590(4)
N(1)–Ag(1)–N(21)	156.9(2)
N(1)–Ag(1)–O(7A)′	84.0(2)
N(21)–Ag(1)–O(7A)′	118.9(2)
N(1)–Ag(1)–O(27B)″	105.5(2)
N(21)–Ag(1)–O(27B)″	82.2(1)
O(7A)′–Ag(1)–O(27B)″	29381.6(1)

[a] Symmetry code: (′)$x + 5/2, y - 1/2, -z + 2$; (″) $-x + 3, -y, -z + 1$.

coordinated to two ligands through the pyridyl nitrogen atoms in a near-linear fashion [rAg(1)–N(1), 2.163(2) Å; ∠N(1)–Ag(1)–N(1A), 175.1(1)°]. The asymmetric unit contains one-half of the complex (one 6-methylnicotinic acid coordinated to silver, and one-half of the nitrate anion). The shortest silver-oxygen distance is > 2.7 Å. The 1-D geometry of the complex cation is propagated in the solid state through two symmetry-related O–H...O hydrogen bonds [rH(7)...O(2), 1.934(2) Å; rO(7A)...O(2), 2.736(2) Å; ∠O(7A)-H(7)...O(2), 172.9(1)°] between the acid hydroxyl group and an oxygen atom of the nitrate counterion, leading to an infinite chain linked through nitrate ions (Fig. 3).

In the structure of (2-chloro-6-methylnicotinato)

UM00012814
NOVARTIS EXHIBIT 1017
Novartis v. Regents, IPR2023-01346
Page 1560 of 4460

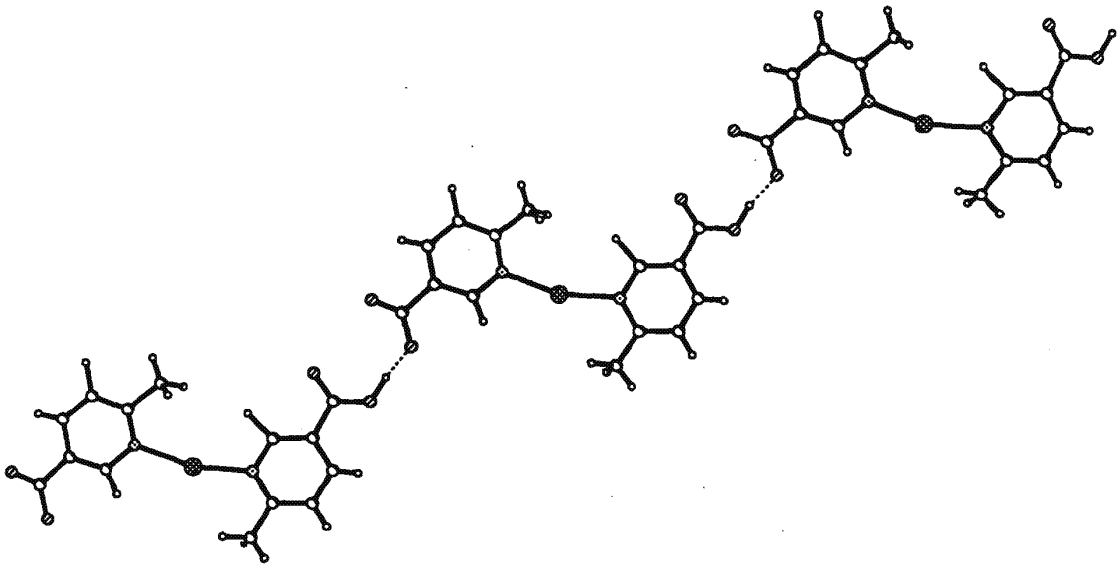


Fig. 2. The linear motif formed by hydrogen-bonding interactions in 1. Ag–O interactions with nearby cations have been omitted for clarity.

silver(I), 3 (Fig. 4), the silver ion is coordinated to three carboxylate oxygen atoms and one pyridine nitrogen atom, resulting in a distorted tetrahedral arrangement (Table 8). The asymmetric unit contains one 2-chloro-6-methyl nicotinate ligand coordinated to silver; the tetrahedral coordination is generated through symmetry-related ligands. The bridging carboxylate units lead to a short Ag–Ag distance of

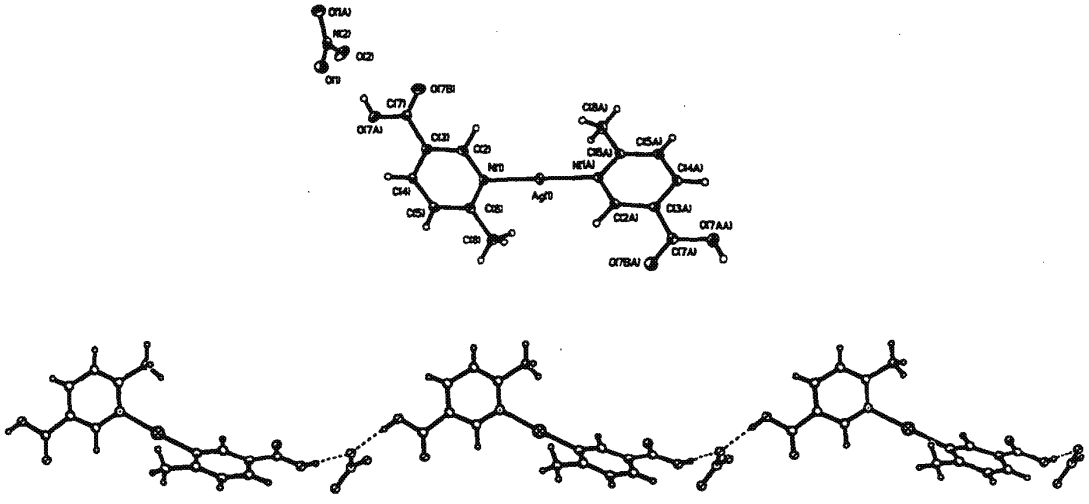


Fig. 3. The chain formed by carboxylic acid–nitrate hydrogen bonds in 2. The inset is the linear cation and associated anion with the labeling scheme.

UM00012815
NOVARTIS EXHIBIT 1017
Novartis v. Regents, IPR2023-01346
Page 1561 of 4460

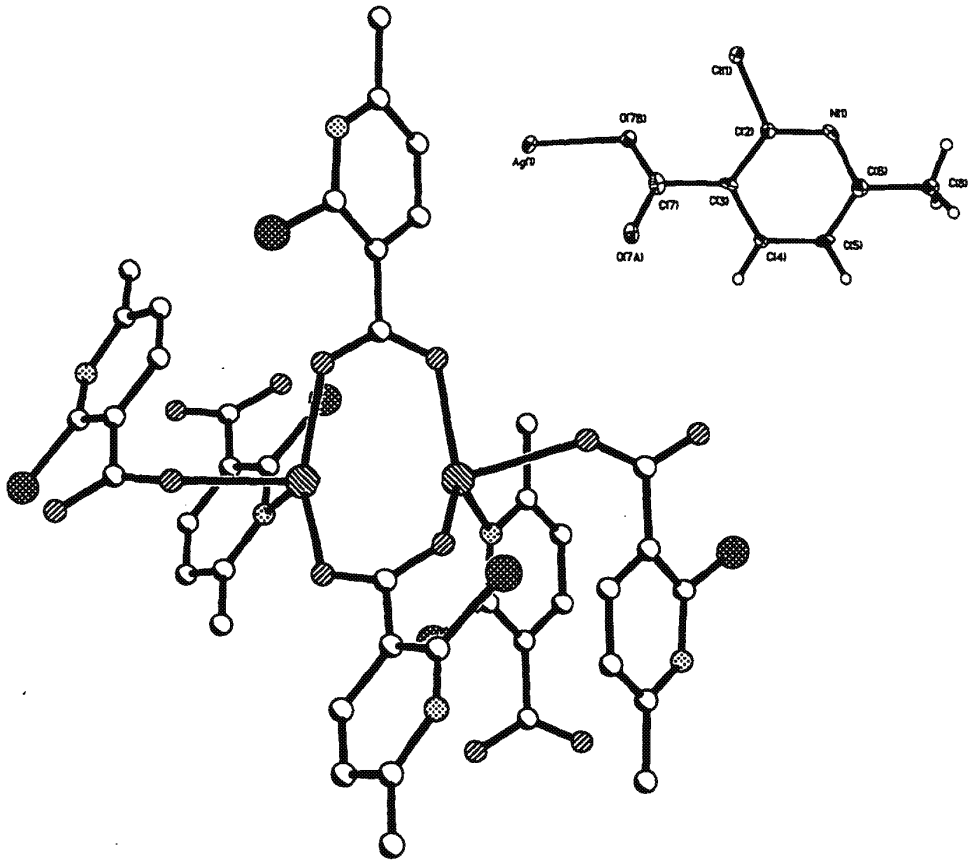


Fig. 4. The bridging carboxylate interactions in the coordination polymer in **3**. Hydrogen atoms have been omitted for clarity. The inset is the asymmetric unit of **3** with labeling scheme.

Table 8
Selected bond lengths (Å) and angles (°) for **3**[a]

Ag(1)–N(1)″	2.34(1)
Ag(1)–O(7B)	2.29(9)
Ag(1)–O(7A)′	2.300(9)
Ag(1)–O(7A)‴′	2.54(1)
O(7B)–Ag(1)–O(7A)′	119.2(4)
O(7B)–Ag(1)–N(1)″	122.9(4)
O(7A)′–Ag(1)–N(1)″	117.9(4)
O(7B)–Ag(1)–O(7A)‴′	92.2(3)
O(7A)′–Ag(1)–O(7A)‴′	83.1(3)
N(1)″–Ag(1)–O(7A)‴′	95.2(4)

[a] Symmetry code: (′) $-x+1,y,-z+1/2$; (″) $-x+1/2,y+1/2,-z+1/2$; (‴′)$x,-y+1,z-1/2$.

2.875(2) Å (Fig. 4). The coordination polymer extends in three dimensions, and there are no acid–acid hydrogen bonds, as the carboxylic acid moiety is fully deprotonated.

Further evaporation of the solution which yielded **3** results in the formation of single crystals of di (2-chloro-6-methylnicotinic acid) silver(I) nitrate, **4** (Fig. 5), where the ligands coordinate through the pyridine nitrogen atoms to the silver ion, [*r*Ag-N, 2.194(2) Å; ∠(N1)-Ag-(N1A), 173.3(1)°. The asymmetric unit contains one-half of the cation and one-half of the anion, as in **2**. The shortest silver-oxygen distance is > 2.7 Å. The 1D geometry of the complex cation is propagated by symmetry-related O–H...O

UM00012816
NOVARTIS EXHIBIT 1017
Novartis v. Regents, IPR2023-01346
Page 1562 of 4460

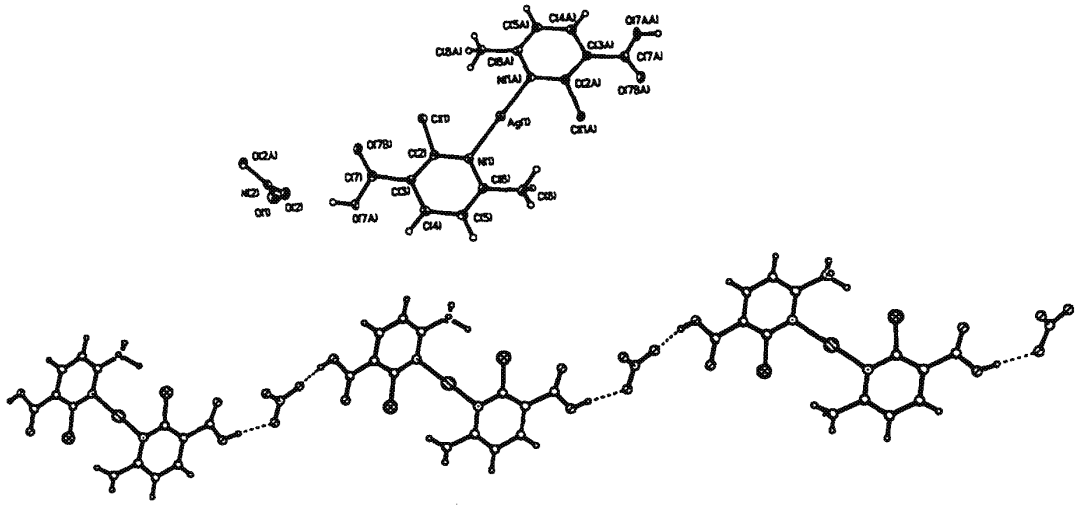


Fig. 5. The chain formed by carboxylic acid–nitrate hydrogen bonds in **4**. The inset is the linear cation and associated anion with labeling scheme.

hydrogen bonds [*r*H(7)...O(2), 1.835(3) Å; *r*O(7A)...O(2), 2.668(3) Å; ∠O(7A)-H(7)...O(2), 165.08(9)°] leading to an infinite chain linked through nitrate ions similar to that in **2** (Fig. 5).

The reaction of silver(I) nitrate with two equivalents of 2-methylnicotinic acid leads to the formation of (2-methylnicotinic acid) (2-methylnicotinato) silver(I), **5** (Fig. 6), where the asymmetric unit contains one (2-methylnicotinic acid) (2-methylnicotinato) silver(I) subunit. The coordinate covalent bonds (Table 9) result in a dimeric species, where two nicotinate ligands bridge two silver(I) ions. Although the coordination geometry around silver is no longer linear, these dimers are assembled into an extended 1D motif by O–H...O hydrogen bonds [*r*H(27)...O(7B), 1.430(2) Å; *r*O(27A)...O(7B), 2.448(2) Å; ∠O(27A)-H(27)...O(7B), 173.8(1)°] between neighboring ligands (Fig. 6).

4. Discussion

An examination of the structures **1**–**5** in the context of predictable supramolecular assemblies demonstrates that, under the reaction conditions used in this study, exceptions are the rule. In fact, in two of the reactions, two different complexes were isolated (**1**,**2** and **3**,**4**). Only **1** displays an obvious similarity to the aforementioned structure of (*iso*-nicotinic acid) (*iso*-nicotinato) silver(I), in which chains are formed through intermolecular carboxylic acid–carboxylate hydrogen bonds. Despite this similarity, the structure of **1** is dominated by coordinate-covalent interactions, and is best described as a three-dimensional coordination polymer.

Recurring patterns in this series of compounds are not readily apparent. For example, the molecular structure of **1** and **5** differ only in the position of the methyl substituent on the aromatic ring. However, this small change leads to very different structures, including differences in coordination geometry. The structure of **3** further illustrates the lack of recognizable patterns; the bridging carboxylate motif present in **3** is absent in **1** and **5**. It is also important to note that the hydrogen bonding distance between O(7B) and O(27A) is short in **1** and **5** (≈ 2.45 Å), which is reflected in the carboxylate C–O distances [C(7)–O(7A), 1.235(8) Å; C(7)–O(7B), 1.271(8) Å for **1**; [C(7)–O(7A), 1.229(3) Å; C(7)–O(7B), 1.285(3) Å for **5**.] Even though this is a short O–O contact, the carboxylate and carboxylic acid moieties are crystallographically inequivalent, and the hydrogen atom was located on the carboxylic acid moiety.

In **2** and **4**, where the nitrate counterion is present,

UM00012817
NOVARTIS EXHIBIT 1017
Novartis v. Regents, IPR2023-01346
Page 1563 of 4460

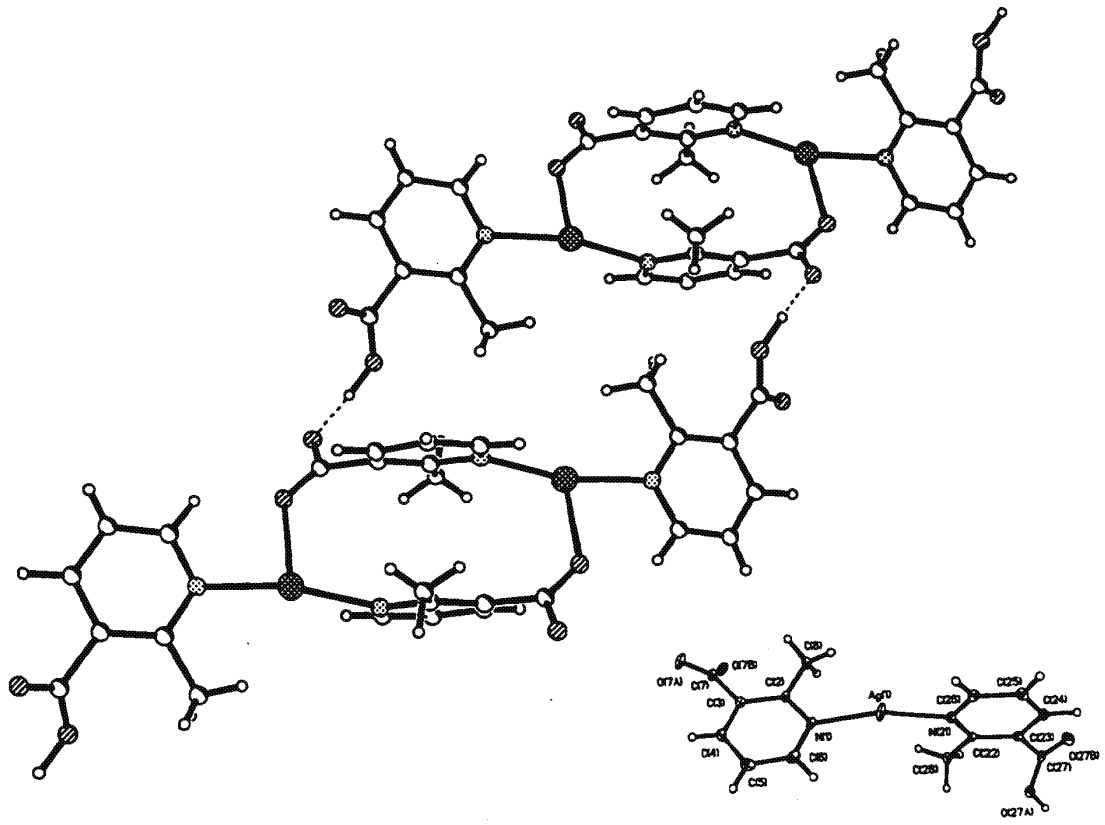


Fig. 6. The nicotinate ligands bridge silver ions, and hydrogen bonds between dimers form an extended one-dimensional motif in **5**. The inset is the asymmetric unit of **5** with labeling scheme.

the anion participates in hydrogen bonding interactions between neighboring complexes, interfering with ligand–ligand interactions. The fact that these complexes contain fully protonated ligands can be attributed to the increased acidity of the reaction mixture after the precipitation of **1** and **3**, respectively. The major difference between the structures of **2** and **4** appears to be the torsion angle about silver, where the two pyridyl rings in **4** are essentially coplanar [C(2)–N(1)–Ag(1)–N(1A) = 1.71°], but are twisted with respect to each other in **2** [C(2)–N(1)–N(1A)–C(6A) = 59.4°]. This result is surprising, considering that the nicotinic acid groups in **2** have only one bulky substituent (6-methyl), while those in **4** are di-substituted (2-chloro, 6-methyl).

Table 9
Selected bond lengths (Å) and angles (°) for 5[a]ross-ref refid = "tblfn3" >

Ag(1)–N(1)	2.17(2)
Ag(1)–N(21)	2.184(2)
Ag(1)–O(7A)′	2.556(2)
N(1)–Ag(1)–N(21)	165.49(8)
N(1)–Ag(1)–O(7A)′	94.16(7)
N(21)–Ag(1)–O(7A)′	92.23(7)

[a] Symmetry code: (′) $-x, -y, -z+1$.

5. Conclusion

The five very different structures described above demonstrate that we cannot always translate the prin-

UM00012818
NOVARTIS EXHIBIT 1017
Novartis v. Regents, IPR2023-01346
Page 1564 of 4460

ciples of organic molecular solids to the assembly of coordination complexes. Difficulties arise due to the formation of the carboxylate anion, which in some cases competes successfully (and unpredictably) for metal coordination sites. Thus, while the role of protonated carboxylates may be identified easily (linear hydrogen-bonding motifs in **2** and **4**), the oxygen atoms of non-protonated carboxylate moieties and the pyridine nitrogen atoms compete unpredictably for coordination to the metal ion, resulting in a mixture of bridging and non-bridging coordination environments. Therefore, in order to implement a reliable strategy for the supramolecular assembly of coordination complexes via carboxylic acid hydrogen bonds, we must carefully control the acidity of the reaction mixture, so that we have a consistent set of functional groups for intermolecular interaction. Once consistent ligand-based intermolecular connectors are present, we may further facilitate ligand-ligand interactions by using more non-coordinating anions such as tetrafluoroborate or hexafluorophosphate [38] (in place of hydrogen-bonding nitrate as in **2** and **4**.) The unpredictable system described in this paper contrasts with the silver(I) coordination complexes of nicotinamide, where the amide functionality proved to be a reliable connector for supramolecular assemblies [31–33].

Acknowledgements

We acknowledge the financial support from Kansas State University and NSF-EPSCoR (OSR-9550487).

References

[1] J.-M. Lehn, Angew. Chem. Int. Ed. Engl. 29 (1990) 1304.
[2] G.R. Desiraju, Crystal Engineering: The Design of Organic Solids, Elsevier, Amsterdam, 1989.
[3] G.R. Desiraju, Angew. Chem. Int. Ed. Engl. 34 (1995) 2311.
[4] C.B. Aakeröy, Acta Crystallogr. Sect. B. 53 (1997) 569.
[5] M.J. Zaworotko, Nature 386 (1997) 220.
[6] S. Coe, J.J. Kane, T.L. Nguyen, L.M. Toledo, E. Wininger, F.W. Fowler, J.W. Lauher, J. Am. Chem. Soc. 119 (1997) 86.
[7] C.B. Aakeröy, M. Nieuwenhuyzen, J. Am. Chem. Soc. 116 (1994) 10983.
[8] R.E. Melendez, C.V. Krishnamohan, M.J. Zaworotko, C. Bauer, R.D. Rogers, Angew. Chem. Int. Ed. Engl. 35 (1996) 2213.
[9] O. Felix, M.W. Hosseini, A. deCian, J. Fischer, Angew. Chem. Int. Ed. Engl. 36 (1997) 102.
[10] P. Brunet, M. Simard, J.D. Wuest, J. Am. Chem. Soc. 119 (1997) 2737.
[11] A. Marsh, M. Silvestri, J.-M. Lehn, Chem. Commun. (1996) 1527.
[12] C.B. Aakeröy, P.B. Hitchcock, J. Mater. Chem. 3 (1993) 1129.
[13] C.B. Aakeröy, P.B. Hitchcock, K.R. Seddon, J. Chem. Soc. Chem. Commun. (1992) 553.
[14] J. Zyss, J. Pecaut, J.P. Levy, R. Masse, Acta Crystallogr. Sect. B, 49 (1993) 334.
[15] S. Bhattacharaya, P. Dastidar, T.N.G. Row, Chem. Mater. 6 (1994) 531.
[16] O. Watanabe, T. Noritake, Y. Hirose, A. Okada, T. Kurauchi, J. Mat. Chem. 23 (1993) 321.
[17] S. Hanessian, M. Simard, S. Roelens, J. Am. Chem. Soc. 117 (1995) 7630.
[18] R. Robson, B.F. Abrahams, S.R. Batten, R.W. Gable, B.F. Hoskins, J. Liu, Supramolecular Architectures, ACS Publication, Washington, DC, 1992, pp. 256–273.
[19] O.M. Yaghi, G. Li, H. Li, Nature 378 (1995) 703.
[20] A.J. Blake, N.R. Champness, S.S.M. Chung, W.-S. Li, M. Schröder, Chem. Commun. (1997) 1005.
[21] S. Subramanian, M.J. Zaworotko, Angew. Chem. Int. Ed. Engl. 34 (1995) 2127.
[22] E.C. Constable, Chem. Commun. (1997) 1073.
[23] M. Fujita, Y.J. Kwon, S. Washizu, K. Ogura, J. Am. Chem. Soc. 116 (1994) 1151.
[24] D. Venkataraman, S. Lee, J.S. Moore, P. Zhang, K.A. Hirsch, G.B. Gardner, A.C. Covey, C.L. Prentice, Chem. Mater. 8 (1996) 2030.
[25] L. Carlucci, G. Ciani, D.M. Proserpio, A. Sironi, J. Am. Chem. Soc. 117 (1995) 4562.
[26] L. Carlucci, G. Ciani, D.M. Proserpio, A. Sironi, J. Chem. Soc. Dalton Trans. (1997) 1801.
[27] A. Hassan, S. Wang, J. Chem. Soc. Dalton Trans. (1997) 2009.
[28] C.M. Drain, K.C. Russel, J.-M. Lehn, Chem. Commun. (1996) 337.
[29] A.D. Burrows, C.-W. Chan, M.M. Chowdhry, J.E. McGrady, D.M.P. Mingos, Chem. Soc. Rev. Commun. (1995) 329.
[30] A.D. Burrows, D.M.P. Mingos, A.J.P. White, D.J. Williams, Chem. Commun. (1996) 97.
[31] C.B. Aakeröy, A.M. Beatty, Chem. Commun. (1998) 1067.
[32] C.B. Aakeröy, A.M. Beatty, Cryst. Engng 1 (1998) 3.
[33] C.B. Aakeröy, A.M. Beatty, B.A. Helfrich, J. Chem. Soc. Dalton Trans. (1998) 1943.
[34] L. Leiserowitz, M. Tuval, Acta Crystallogr. Sect. B, 34 (1978) 1230.
[35] F. Jaber, F. Charbonnier, R. Faure, M. Petit-Ramel, Z. Kristallogr. 209 (1994) 536.
[36] G. Smith, A.N. Reddy, K.A. Byriel, C.H.L. Kennard, Polyhedron 13 (1994) 2425.
[37] G.M. Sheldrick, SHELXL-93, University of Göttingen.
[38] C.B. Aakeröy, A.M. Beatty, D.S. Leinen, J. Am. Chem. Soc. 120 (1998) 7383.

UM00012819
NOVARTIS EXHIBIT 1017
Novartis v. Regents, IPR2023-01346
Page 1565 of 4460